Graves under the microscope:

micromorphological study of sediments

in archaeological burials

Sabina Ghislandi

Doctor of Philosophy

University of York

Archaeology

March 2016

ABSTRACT

The InterArChive project investigated the sediment of the grave fills of archaeological burials. This study applied micromorphological analysis, scanning electron microscopy-energy dispersive spectroscopy (SEM-EDS) and image analysis on sediments of seventeen graves spanning from 4th C BC - 15th C AD and three experimental piglet burials (2009-2013). A new standardized and rapid method was developed for the measurement of porosity.

The grave types comprised wooden coffin, absence of coffin and chamber tombs. The sediments were sandy clay soils, variably affected by water-logged conditions, from temperate oceanic climates; sandy loam soil and limestone and sandstone deposits in Mediterranean climates.

The microstructure of the backfill, features produced by the decomposition of the corpse and interactions with the surrounding sediment, secondary products related to the environmental conditions in the grave, degree of weathering of bone fragments in the different contexts, preservation of organic components from the graves and biological activity during and after the corpse decomposition were investigated.

The results showed that corpse decomposition within the soil produced characteristic microstructures and features according to the type of soil and climate. Neoformed minerals, such as vivianite, siderite and leucophosphite formed in water-logged soils and anaerobic conditions. Amorphous phosphates were preserved only in water-logged soils. In all environments examined redoximorphic pedofeatures formed in the area around the skeleton in the absence of a coffin or in the layers above the skeleton in the presence of a coffin. Organic components and bone fragments were rarely preserved, especially in limestone and sandstone deposits from warm climates. Fungal and mesofauna activities were better represented in aerobic conditions and Mediterranean climate. Changes in porosity and segregation of mineral grains showed downward movement of soil particles and fluids from the layers above the skeleton and they highlighted the role of the coffin as barrier to this movement.

CONTENTS

LIST OF FIGURES

LIST OF TABLES

LIST OF ACCOMPANYING MATERIAL

Supplementary Data (DVD):

- Micromorphological analysis (.pdf)

- Mosaics (.ppt)

- SEM-EDS analysis (.xls)

- Chapter 4: Image analysis graphs (.ppt)

- Chapter 5: Graphs (.ppt)

- Chapter 5: Microscope pictures (.jpg)

ACKNOWLEDGEMENTS

I would like to thank all of the members of the InterArChive project, Professor Don Brothwell, Dr. Maria Raimonda Usai and, above all, Professor Brendan Keely.

Thank you to the York Archaeological Trust and the Dutch Cultural Heritage Agency for providing the information regarding the excavations of Hungate and Borgharen.

Thank you to Professor Giovanni Boschian, who introduced me to the world of soil micromorphology and continues to be my mentor.

Special thanks to Maurizio, who shared with me rain and wind during these years.

DECLARATION OF ORIGINALITY

I certify that, to the best of my knowledge, the content of this thesis is product of my own work. I declare that the assistance received in preparing this thesis and sources have been acknowledged and referenced.

This thesis has not been submitted for any other degree or purposes.

xxx

Chapter 1. INTRODUCTION

"Nil sumus et fuimus. Mortals, respice, lector,

in nihil a nihilo quam cito recidimus"

(Roman epitaph. Toynbee 1996, 34)

Archaeology and forensic science were the first to develop studies in the scientific analysis of graves, while soil science was left behind. Soils, however, have received more attention in recent times as resources of physical evidence of taphonomic processes (Tibbett and Carter 2008) and new studies involving sediment analysis were applied to archaeological burial contexts (Macphail et al. 1998; Huckleberry et al. 2003; Angelucci 2008; Ern et al. 2010; Aspöck 2011; O'Connor et al. 2011; Karkanas et al. 2012; Ern et al. 2010; Ern et al. 2012; Ern and Trombino 2013; Zangarini et al. 2014).

The InterArChive project developed in this new research environment, proposing a multidisciplinary approach involving micromorphology of soils, inorganic geochemistry and trace organic chemical analysis for the study of archaeological graves (Usai et al. 2014).

1.1 THE INTERARCHIVE PROJECT

The InterArChive project was developed between 2009 and 2015 by the Departments of Archaeology and Chemistry of the University of York, in collaboration with the Biological and Environmental Science School of the University of Stirling. It was supported by an Advanced Researcher Grant from the European Research Council (ERC).

The team comprised: Prof. Don Brothwell, Dr. Raimonda Usai, Carol Lang, Helen Williams, Annika Burns, Sabina Ghislandi, Fabio Serchisu, Allan Hall, Andrew Jones, David Broughton, Harry Wyn Williams and Emma Tong. (Department of Archaeology); Prof. Brendan Keely, Dr. Matt Pickering, Kimberley Green, Adam Pinder and Scott Hicks (Department of Chemistry) and Dr. Clare Wilson (Biological and Environmental Science School).

The InterArChive project was an experimental study testing, for the first time, the combined application of soil micromorphology, inorganic geochemistry and trace organic chemical analysis, applied to samples of sediments collected in the proximity of skeletons in archaeological burial contexts.

The object of the investigation was the sediment of the grave fill, especially from the areas in contact with the skeleton. Thus, the focus was not on human remains or grave goods, but on the microscopic evidence sealed within the ground.

The overall aim was to improve the quality and quantity of the information recovered from graves, exploiting the soil physical and chemical characteristics in which the skeleton was entombed, recovering evidence of corpse decomposition, grave construction, burial rituals and, when possible, information about diet, drug-use and cause of death (Usai et al. 2014).

Samples for micromorphological and chemical analysis were collected, in collaboration with local archaeological groups, from 31 sites across Scandinavia, Europe and North Africa, from the Neolithic to the twentieth Century, and selecting a variety of soil contexts (Usai et al. 2014). In addition to these sites, ten experimental burials of stillborn piglets were performed in 2009 at five locations in North Yorkshire and were excavated and sampled between the summers of 2012 and 2013.

The application of the innovative approach to the study of burial context required a new and pertinent procedure of sampling, which was developed in a complementary manner that recognised the capabilities of the micromorphology and chemistry approaches (Chapter 3, Sections 3.1 and 3.2).

1.2 THE PRESENT RESEARCH

The present research started in 2012 and concerned the micromorphological analysis of sediments of seventeen graves spanning from 4th C BC - 15th C AD, plus three experimental piglet burials, buried in 2009 and excavated in 2012 (Chapter 3, Section 3.3). The research was developed within the InterArChive project, thus it shared the same purpose of increasing the quality and quantity of information from grave sediments at a microscopic level.

Forensic studies have demonstrated that the decomposition of a corpse within the soil environment is influenced by several factors, mainly: temperature, moisture, soil type, associated materials, decomposer adaptation and trauma (Carter and Tibbett 2008, 38; Chapter 2, Section 2.2.4). Hence, the evidence produced by the interaction between these factors, the corpse and the soil was sought in this research.

The aim of the study was to detect and understand the changes that occurred in the burial sediments over time and their relationship to the presence of the grave and to natural and anthropic post-depositional processes. A further objective was to assess how soil composition and climatic conditions influenced the burial sediments.

Figure 1.1 illustrates the complexity of these relationships and the variables analysed in this research. Five archaeological cemeteries were selected for the study, including 3 types of graves, 5 types of soil and 2 different climatic conditions, to expand the variables of analysis (Table 1.1; Chapter 3, Section 3.3).
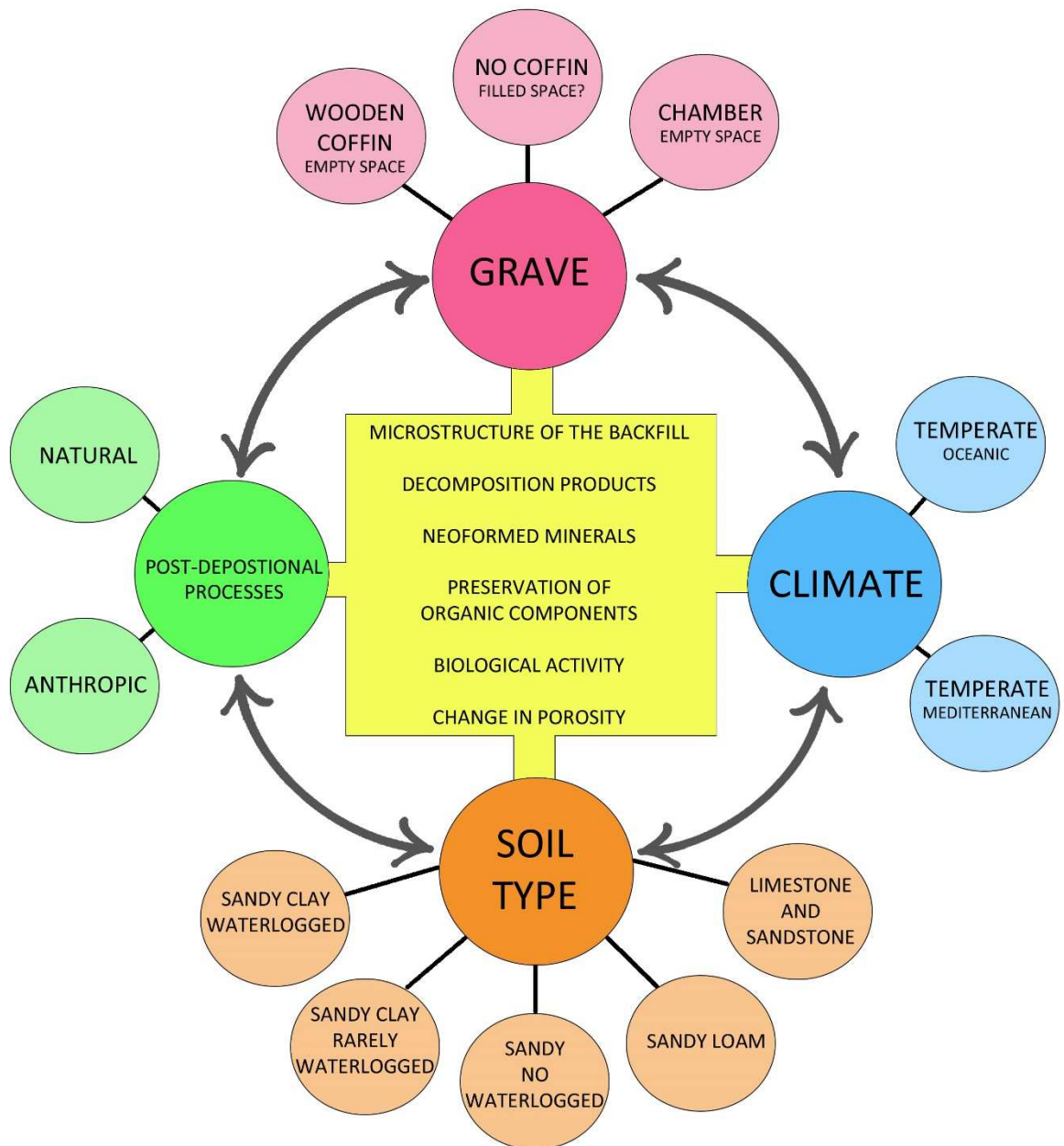
Figure 1. 1: Aims and questions of this research. How did grave characteristics, soil type, climate and post-depositional processes influence burial sediments? This research investigated the possible microstructures of backfills, the decomposition products, the neoformed minerals, the preservation conditions of organic components, the biological activity and the porosity within the burial sediments.

The grave contexts were:

- chamber tomb: empty space around the corpse and filling of the area of entrance of the grave (Pill'e Matta: Punic and Roman periods);
- wooden coffin: empty space at the beginning of corpse decomposition and successive (undefined timing) filling of the space with the collapse of the coffin (Hungate: Roman and Anglo-Scandinavian periods; Borgharen: Medieval period);
- in contact with the ground, possibly covered by a plank with rapid infill (Haymarket: Medieval period);
- in contact with the ground at the bottom level, delimited and covered by stone plaques (Rossio do Carmo: Moorish period).

Different types of soil characterized the cemeteries as summarized in Figure 1.1. and Table 1.1:

- sandy clay soil in a water-logged environment (Hungate);
- sandy clay (mostly clay) soil in rarely water-logged environment (Haymarket);
- sandy soil in non-waterlogged environment (Borgharen);
- limestone and sandstone in a dry and alkaline environment (Pill'e Matta);
- sandy loam soil affected by intense erosion (Rossio do Carmo).

Two distinct climatic conditions were represented by the locations of the cemeteries:

- temperate oceanic (Hungate, Haymarket and Borgharen);
- temperate Mediterranean (Rossio do Carmo and Pill'e Matta).

In addition, as mentioned above, three experimental piglet burials were analysed in this research, as reference material to compare with the archaeological sites (Table 1.1).

The burial contexts were:

- wooden coffin, which was filled with sediment at the moment of the burial, to simulate advanced breaching of the coffin and to facilitate the decomposition of the piglet in a short period of time (3 years);
- in contact with the ground.

Two different type of soils characterized the experiment:

- limestone;
- sandy clay, water-logged.

The experimental burials were all excavated in areas affected by temperate oceanic climate.

SITE	PERIOD	GRAVE TYPE	SOIL TYPE	MAIN POST DEPOSITIONAL PROCESSES	CLIMATE
Hungate	Roman and Anglo-Scandinavian	Wooden coffin	Sandy clay, water-logged	Natural water-logged Flooding for the King's Fish Pool City dump Industrial activities	Temperate oceanic
Haymarket	Medieval	No coffin (?) or wooden plank	Sandy clay, rarely water-logged	Rarely water-logged (2-4 m above Hungate) Church and urban area	Temperate oceanic
Borgharen	Medieval	Wooden coffin	Sandy, no water-logged	Agricultural area Possible flooding from the Meuse (the site is in a deep valley)	Temperate oceanic
Rossio do Carmo	Moorish	Chamber/ no coffin	Sandy loam	Erosion/ desertification Urban site	Temperate Mediterranean
Pill'e Matta	Punic and Roman	Chamber	Limestone and sandstone	Collapse of the vaults Industrial activities	Temperate Mediterranean
Piglet 2	2009-2012	Wooden coffin, filled with sediment	Limestone	-	Temperate oceanic
Piglet 6	2009-2012	No coffin	Sandy clay, water-logged	Water-logged	Temperate oceanic
Piglet 7	2009-2012	Wooden coffin, filled with sediment	Sandy clay, water-logged	Water-logged	Temperate oceanic

Table1. 1: Main characteristics related to period, grave type, soil type, post-depositional processes and climate of the archaeological cemeteries and experimental burials analysed in this research.

1.2.1 RATIONALE OF RESEARCH

The first rationale of this research was to identify possible features produced by the decomposition of the corpse within the soil and how the nature of such features differs among different environments and soil types. For this purpose, the five types of soil offered a variance

from intense water-logged and cold condition to dry and warm environment. The differences between graves enabled observation of the role of the coffin in the formation of specific features. They were classified as (Figure 1.1):

- products from the interaction of corpse decomposition and surrounding sediment, such as vivianite and amorphous phosphate. These features were identified in burial contexts in previous studies (Ern et al. 2010; Ern et al. 2012; Ern and Trombino 2013; Zangarini et al. 2014; Chapter 2, Section 2.1.2; Chapter 6, Section 6.4.2);
- secondary products related to environmental conditions of the grave: redoximorphic pedofeatures, siderite and secondary calcium carbonate (Chapter 6, Sections 6.4.1, 6.4.4 and 6.4.6);
- preservation of bone fragments and difference of preservation in different contexts (Chapter 6, Section 6.3.2);
- preservation of organic components from the graves: coffin and, possibly, other materials (Chapter 6, Section 6.3.1);
- biological activity during and after the corpse decomposition: mesofauna and fungi (Chapter 6, Sections 6.3.3 and 6.3.4).

The second rationale was the understanding of the processes forming the grave infill, the movement of soil particles and fluids in the grave and the role of the coffin and corpse decomposition in this movement. In addition, the fabric microstructure and the porosity were examined to understand the presence or absence of coffin and its decay rate. These aims were attempted by the analysis of the fabric microstructure through microscopy (Chapter 6, Section 6.1.) and the measurement of frequency of porosity in the samples through the image analysis (Chapter 4 and Chapter 6, Section 6.2).

The third rationale was the validation of the methods of sampling and analysis applied to burial sediments and their possible application in future studies by different groups of workers. The method of sampling, already tested in different archaeological environments by previous studies (Courty 1989, 40-42; Vepraskas 1990, 9-13; Goldberg and Macphail 2003), was applied for the first time to burial sediments. It was standardized for all of the graves, collecting the samples in the same anatomical locations and in the layers above the skeleton (Chapter 3, Section 3.1). The first aim was to establish if the samples were collected in locations which provide useful information regarding the decomposition within the soil. The second aim was to produce information which could increase the knowledge of the processes related to the burials, which were not detectable by macroscopic analysis. The third aim was to create a method applicable to other funerary contexts by different groups of research. This project, with the innovative application of micromorphology to the study of burial sediments, has the potential to contribute to the

knowledge of the environment of the grave and to detect microscopic evidences related to the history of the cemetery, suppling answers to the archaeologists (Chapter 7, Section 7.3).

Specific hypotheses were investigated in the research:

- the movement of soil particles and fluids, the fabric microstructure and the soil porosity change according to the presence or absence of coffin;
- in presence of coffin, the fabric microstructure changes according to rapid or slow breaching of the coffin;
- moving soil particles are entrapped in some anatomical locations of the skeleton, possibly skull and pelvis;
- the decomposition of a corpse within the soil promotes the formation of specific indicators;
- the frequency of these indicators changes according to the presence or absence of coffin;
- the type and frequency of these indicators change according to the type of soil and climate;
- traces of micro- and mesofauna are detectable even if the corpse skeletonized within the soil and they can increase the information related to the environment;
- organic components could preserve and give information regarding coffin and other materials.

1.2.2 METHODOLOGIES APPLIED

The burials were investigated through micromorphological analysis (Chapter 2, Sections 2.1 and 2.3.1-2.3.3; Chapter 3, Section 3.4.1), image analysis (Chapter 2, Section 2.3.4; Chapter 3, Section 3.4.3; Chapter 4) and scanning electron microscopy-energy dispersive spectroscopy (SEM-EDS) (Chapter 2, Section 2.3.5; Chapter 3, Section 3.4.4).

Micromorphology is based on microscopic level description and interpretation of components, structures and fabrics, and their relations in space and time, within 30 μm thin sections produced from undisturbed soil samples. The principal aim is the identification of the processes responsible for the formation or transformation of soil and of specific features (Bullock et al. 1985, 9; Courty et al. 1989, xvii; Vepraskas 1990, 1; Stoops 2003, 5). Micromorphological analysis was the main method used in the analysis of the grave sediments in this research. It offered the opportunity to observe the microstructure of the fabric, the presence of indicators such as neoformed minerals and the characteristics of microscopic remains, such as organic components or traces of micro-

and meso-fauna activities. Micromorphology was the appropriate method of investigation for the morphology of the burial sediments at a microscopic level.

Image analysis is a quantitative method for analysing features of thin sections using digital images. These features are separated and measured from their background and from other features (Vepraskas 1990, 97). One application of image analysis is the measurement of soil porosity, which was applied in this research. Porosity in the samples was measured as a percentage of the area occupied by voids, through the processing of digital images of the samples (Chapter 4). The frequency of porosity within the samples was recorded to detect differences between the anatomical location of the skeleton and between the area of the skeleton and the layers above it, to identify possible variations in porosity within the burial sediments and to detect if these variations were influenced by characteristics of the grave. It was of interest in this research to investigate the movement of soil particles and fluids within the grave, to detect eventual patterns of the soil porosity within the graves and the layers above, investigating the role of the skeleton and coffin as possible barriers to this movement (Chapter 4, Section 4.4). In addition, the frequency of porosity recorded by image analysis was compared with the morphology of the voids observed in the same samples by micromorphology, to investigate in which cases the variance of porosity was caused by biological activities of micro and meso-fauna (Chapter 6, Section 6.2). This research developed a new approach for the image analysis of grave soils. The aim was to provide an automated, standardized and rapid method of measurement of porosity, which can be easily learnt and applied by other researchers (Chapter 4).

SEM-EDS analysis was applied to provide micro-chemical data of primary and post-depositional components, whose interpretation was uncertain through the micromorphological analysis (Chapter 5, Sections 5.1.4, 5.3.4 and 5.5.4). The data, representing the weight (%) of chemical elements, were elaborated in box-plots. The elemental composition and its variation provided information to understand the origin of pedofeatures and the variation of fine material within the sediments of some graves. This method was used to implement the micromorphological analysis.

In accordance with the idea stated by Vepraskas (1990, 39) and Goldberg and Macphail (2006, 355), that micromorphological description and interpretation should to be separated as much as possible, this thesis presents the results of image analysis in Chapter 4 and of micromorphology and SEM-EDS in Chapter 5, while Chapter 6 is dedicated to their discussion and interpretation.

Chapter 2. RESEARCH CONTEXT: MICROMORPHOLOGY OF SOIL, ARCHAEOTHANATOLOGY AND FORENSIC SOIL SCIENCE

The present research was focused on micromorphological analysis to test, within the InterArChive project, which observations and interpretations contribute effectively to the understanding of burial contexts. The general micromorphological methods were supplemented by image analysis and SEM-EDS to provide semi-automated analysis of porosity and elemental chemical measurements, respectively, as introduced in Chapter 1. The approach necessarily required knowledge of the basis of micromorphology and the mode of operation of the petrographic microscope, as well as an understanding of the characteristics of mineral and organic components in thin sections. Moreover, notions regarding the soil properties were important for the interpretation of the mineral and organic features observed, which form and react according to the soil characteristics. Practical knowledge and experience in the techniques of image analysis and SEM-EDS were acquired during the course of the research and required engagement with the principles of the techniques in addition to practical and technical learning.

The object of the analysis was the examination of grave sediments. Thus, understanding of processes involved in the decomposition of the corpse, forensic taphonomy and funerary archaeology was required.

As stated in Chapter 1, the InterArChive project involved an innovative approach, hence no other directly relevant studies concerning the application of micromorphology and sediment analysis to examine the relationship between the grave contents and the surrounding soils were available. Nevertheless, a limited number of studies relating to sedimentological analysis in grave contexts have been published in the last two decades.

This chapter provides a literature context to the research presented in the thesis. Thus, it presents a review of micromorphological literature concerning the background to its application to soils and sediments. In addition, applications of forensic science to burial environments are considered together with relevant studies utilising image analysis or SEM-EDS.

2.1 MICROMORPHOLOGY OF SOILS AND SEDIMENTS

Micromorphology of soil and sediments is the main methodology applied to the investigation of burials in this research and it is explained in this section. The first part focuses on the definitions

and brief history of this technique (Section 2.1.1), while the second part provides an overview of the sedimentary studies applied to burial contexts (Section 2.1.2).

2.1.1 DEFINITION AND HISTORY

Micromorphology is a key method of study employed in soil science. It is based on microscopic level description and interpretation of components, structures and fabrics, and their relations in space and time, within undisturbed soil samples. Studies are typically conducted on 30 μm thick slides of consolidated soil samples. The principal aim is the identification of the processes responsible for the formation or transformation of soil and of specific features (Bullock et al. 1985, 9; Courty et al. 1989, xvii; Vepraskas 1990, 1; Stoops 2003, 5). Prior to the application of geoarchaeological methods the typical approach in archaeology involved description of findings and their spatial arrangement from contexts without much consideration of the soils or sediments in which the finds were embedded. As a consequence, important information for the reconstruction of the history of sites was irretrievably lost (Karkanas and Goldberg 2008).

Born as a technique employed in pedology in the 1930s, the application of soil micromorphology to archaeology started in the 1950s with several different purposes for its application to understand: the nature of the soil before construction of a site in order to enhance palaeoenvironmental interpretation; the nature and origin of the different sediments (detrital, chemical, biochemical, organic and pyroclastic), anthropogenic features (remains of human occupation, materials used, effects of land use practices on soils) and post-depositional processes (humification, bioturbation, erosion and sedimentation, diagenesis and pedogenesis) (Davidson et al. 1992) that affected the site. This introduction of micromorphology was parallel to the reconsideration of the impact of human activities and natural factors on the formation of archaeological soils and sediments specifically at the level of mineral and organic components (Courty 1992). Since its introduction, soil micromorphology has played an important role in studies of different historical periods and archaeological situations. It was employed in the study of deposits containing burnt remains, in human constructions such as tells, in the analysis of living floors and occupational debris, in the investigation of pastoral activities and land management practices and, more recently, in urban deposits (Karkanas and Goldberg 2008). One example of micromorphological research applied to archaeological contexts, and successful in the analysis of site formation processes and traces of activities, emerged from a NERC project in which core domestic and ritual contexts of three early urban sites in the Near East were investigated (Matthews et al. 1997). According to those researchers, the main contributions from micromorphology were the simultaneous analysis of sediments, artefacts and bioarchaeological components to provide information on their depositional and contextual relationships and,

hence, develop sociocultural and environmental understanding (Matthews et al. 1997). To achieve these outcomes, the researchers integrated micromorphological observations with microstratigraphy, staining techniques and SEM-EDS analysis (Matthews et al. 1997). Thus, micromorphology is an important method of analysis to understand site formation processes and to reconstruct palaeoenvironments. Despite the fact that micromorphology provides semi-quantitative data, Goldberg and Macphail (2006, 359-361) noted that this characteristic does not make micromorphology unreliable and that these analyses are the essential first step in the identification and interpretation of the soil structure and features. Notably, the integration with other techniques can support a more complete understanding. According to Karkanas and Goldberg (2008), this is particularly true for anthropogenic processes related to urban sites. The suggestion of the authors was to combine the micromorphological data with other instrumental techniques to identify previously unrecognizable microscopic features and, supplemented by observations from others disciplines, to improve interpretations. However, it is important to remember that SEM-EDS is complementary to, and cannot substitute the role of, standard micromorphological analysis. Soil micromorphology has to be performed as a first step of analysis: investigators need to know and understand what they are examining through SEM-EDS analysis (Goldberg and Macphail 2003, 359-361).

The first scholar who used magnifying instruments in a systematic way to study soils was W.L. Kubiena, who received the international recognition of "founding father of micropedology" after the publication of his manual *Micropedology* in 1938 (Stoops 2003, 6). This was the first book dedicated to micromorphology, in which Kubiena explained that micromorphology was essential to understanding how the components of soils were interacting and not only which were the basic soil components (Vepraskas 1990, 1). Moreover, Kubiena defined some essential basis of soil fabric analysis. Fabric's skeleton (sic) was defined as being composed of immovable individual particles, not subjected to changes, while fabric's plasma (sic) was identified as being the part of the soil that was easily moved and redeposited, or changed in composition or shape. The composition of fabric's skeleton and plasma comprised what were termed elementary fabric types. Eight types were identified and applied in Kubiena's analysis. However, his descriptions were based on a limited set of features and, for this reason, the creation of a universally applicable terminology for soil features was not achieved (Vepraskas 1990, 2; Stoops 2003, 6).

In the 1960s the use of micromorphology expanded to a number of countries and new approaches were developed. In 1964, R. Brewer published *Fabric and Mineral Analysis of Soils*, developing the first systematic and understandable protocol for descriptions in soil microscopy, particularly important in pioneering the development of the concept of pedological features (Stoops 2003, 7). Brewer adopted the concept of fabric of Kubiena, but he focused more on voids

and distinct features. Unfortunately, Brewer's classification concentrated on mineral soil components and rarely on organic materials (Vepraskas 1990, 3). In a paper published a few years later, Brewer argued that there were two levels of interpretation of micromorphological data. The first and more common level was related to the general processes occurred within the soil, such as illuviation or crystallization, while the second concerned the understanding of the chemical and physical processes related to the micromorphological features. He stated that many features in thin section were not readily interpretable, because the properties or the behaviour of the constituents were not well known or because they were not identifiable with enough accuracy. Brewer favoured a morphological approach to a genetic one, in order to facilitate the comprehension and classification of the features based on the characteristics that can be observed and defined (Brewer 1972).

Questions related to the use of terminology stimulated the formation of the International Working Group on Soil Micromorphology in 1969 under the sponsorship of the International Society of Soil Science. In 1979, the Working Group published a dictionary called *Glossary of Soil Micromorphology*, where common terms for micromorphology were defined in different languages (Vepraskas 1990, 4).

The most important works in the 1980s were *Micromorphology of soils* by FitzPatrick (1984) and *Handbook for soil thin section description* by Bullock et al. (1985). FitzPatrick's publication was more intended to be a tool for students and workers to aid their study and analysis and to introduce the techniques, descriptions and applications of micromorphology to other fields. The book comprised the description of soil structure, voids and several types of pedological features, describing both organic and mineral components. In addition, example illustrations were included to enhance the descriptions. By contrast, the volume of Bullock evolved from the concepts of Brewer (1964) and Kubiena (1938), creating a detailed and comprehensive system of classification, with a very well developed terminology. Bullock provided a correction to the Brewer system, giving the right emphasis to the description more than interpretation. He also considered organic components and substituted the terms on fabric's skeleton and plasma with the concept of c/f ratio to make the description more effective (Vepraskas 1990, 5; Stoops 2003, 7). An important publication concerning the techniques used to make thin sections was *Thin section preparation of soils and sediments* by C. P. Murphy (1986) (Vepraskas 1990, 5).

Finally, a review of the evolution of concepts and terminologies was recently presented by Stoops (2003) and a very well detailed manual for the interpretation of features was edited by Stoops, Marcelino and Mees (2010).

2.1.2 MICROMORPHOLOGICAL AND SEDIMENTARY STUDIES APPLIED TO BURIALS

Investigation of soil and sediments in burial contexts is innovative and quite new in the archaeological research. The InterArChive project, as already stated, pioneered the application of the methodologies illustrated above, in association with trace organic chemistry, to graves from a wide range of historical periods and geological characteristics. Few works of the project have been published so far (Usai et al. 2014; Pickering et al. 2014, 237-245) and others are in preparation for the year 2016. The former was an overview of the project, which presented aims, sites of analysis and methodologies applied. The second regarded the results from the organic residue analysis, complemented by micromorphological analysis, of the Viking mass grave on Ridgeway Hill, Weymouth. Analysis of thin sections, from samples collected in the proximity of the skull (× 2), pelvis (× 2) and heel (× 1), from four different skeletons, showed surface disturbance or poor cohesion in the upper part of the samples, with evidence of pedoturbation in all the slides. The frequent organic matter characterizing the slides was identified by organic chemical analysis as products of plant waxes and roots (Pickering et al. 2014, 237-245).

A preliminary report from the InterArChive project regarding the micromorphology of two prehistoric ritual burials from Yemen was presented at the EGU General Assembly in 2010 (Usai et al. 2010). Samples were taken for micromorphology, SEM-EDS, X-ray diffraction, gas chromatography/ mass spectrometry. Observations from microscopy indicated that the burial matrix contained plant, hair and seed fragments. Microprobe did not reveal any special significance, while chemical analyses revealed high levels of uric acid in the deposits containing organic fragments (Usai et al. 2010).

The few studies involving sediment analysis applied to archaeological burial contexts are discussed in this section (Macphail et al. 1998; Huckleberry et al. 2003; Angelucci 2008; Ern et al. 2010; Aspöck 2011; O'Connor et al. 2011; Karkanas et al. 2012; Ern et al. 2010; Ern et al. 2012; Ern and Trombino 2013; Zangarini et al. 2014). Their case studies are systematically classified in Table 2.1.

AUTHOR/S AND DATE	ENVIRONMENTAL CONDITIONS	TYPE OF BURIAL	KEY OBSERVATIONS	IMPLICATIONS	METHODS APPLIED	MARKERS
Macphail et al. 1998	Turf deposit. Temperate oceanic climate. Northwest London	Chamber with cremated remains	Analysis on turf deposit. Post-depositional effects: partial replacement or coating of organic matter by Fe and Mn	Preservation of pseudomorphic organic fabrics and identification of layers of cattle dung	Micromorphology; diatoms; SEM-EDS; microprobe	Identification of organic fabrics
Huckleberry et al. 2003	Streambank, receded as result of seasonally high water and wave activity. Kennewick, Washington	Skeleton found in the streambank	Observation of peds cemented within the cranium and of thin sections from the streambank	The sediment in the cranium derived from the burial site and it was not introduced along the shore	Micromorphology; granulometry; XRD; thermogravimetry; trace-elements analysis	Characteristics of the peds and correlation with the surrounding soil
O'Connor et al. 2011	Water-logging sediment. Temperate oceanic climate. Heslington East, York	Skull with brain in a pit	Observation of peds within the skull and of the bone structure	No translocation of decomposition products took place through voids or fabric. Bacterial or fungal activities were not present in the bone	Micromorphology of sediment, bone and soft tissue; 3D photography and laser; high-resolution laser scanning, CT and MRI scanning; SEM; DNA; brain neurochemistry; tissue and sediment chemistry	Pedofeatures related to water and liquid translocation. Bone preservation: traces from bacteria and fungi
Angelucci 2008	Shallow depression in alkaline rock, filled with organic sediment. Temperate Mediterranean climate. Encosta de Sant'Ana.	Roman ustrinum	1) good preservation of ash; 2) distribution of the red zone; 3) thickness of the organic infilling; 4) bones with traces of different degrees of heat; 5) presence of reworked mudbrick in the infilling	1) the ustrinum was quickly buried after its last use. Climate and rock type had a role in the preservation; 2) the ustrinum was used for several bodies; 3) the inner interface of the ustrinum exceeded 600°C; 4) the ustrinum was renovated at least one and it was not carefully cleaned after use	Micromorphology	Preservation of the weatherable components in relation to climate and soil. Bone preservation and characteristics. Link between macroscopic and microscopic data. Documentation of the stratigraphy

AUTHOR/S AND DATE	ENVIRONMENTAL CONDITIONS	TYPE OF BURIAL	KEY OBSERVATIONS	IMPLICATIONS	METHODS APPLIED	MARKERS
Karkanas et al. 2012	Alkaline rocks. Temperate Mediterranean climate. Mycene.	Mycenean dromoi	1) sorted gravel pockets with reverse or normal grading, generally parallel to the slope; 2) extensive planar erosional surfaces and abrupt change of compaction; 3) constructed plaster floors	1) grain flow and debris fall processes related to the action of shovelling; 2) reopening of the grave; 3) reopening of the grave	Micromorphology; soil flotation; archaeobotanical, phytolith and organic residue analyses	Nature of the infill in the grave. Identification of possible reopening
Aspöck 2011	Temperate oceanic climate. North Europe.	Merovingian reopened graves	1) dark organic rich pits within the grave fill; 2) dislocation of the bones	1) organic material probably originated through mixing of the surface with the disturbed area of the fill or because the pit was left open; 2) if parts of the skeleton were still in connection, the grave was open short time after the burial	Macroscopical analysis. The author was interested in developing microscopic approach	Observation of possible features indicating reopening of the grave
Ern et al. 2010, 2012; Ern and Trombino 2013; Zangarini et al. 2014	Different types of soils and different times of burial.	Experimental burials of pigs and piglets	1) concentration of metal oxides in the form of violet-blue colorations in XPL; 2) magnesium phosphate crystallizations; 3) significant sulfur levels	1) related to specific chemical burial conditions 2) related to decomposition of bones and soft tissues buried from 7 to 103 weeks; 3) transport and fixation of soft tissue decomposition fluids over 7 weeks	Micromorphology; SEM-EDS; grain size analysis; pH in H_2O and KCl; total nitrogen and organic carbon; quantification of available phosphorous; determination of cation exchange capacity and base saturation; volatile fatty-acids analyses	Identification of permanence indicators of the remains in the soils

Table 2. 1: Summary of the case studies involving sediment analysis in archaeological graves

One of the first micromorphological works on funerary sites was the investigation of the "turf-filled" funerary shaft at St. Albans, northwest of London (Macphail et al. 1998). However, the study was performed on the deposit above the burial and it was not related to the human remains. The site was discovered during the excavations of former gardens on the upper slope of the river valley for housing development, and it was constituted by a rectangular enclosure of 2 ha, delimited by a ditch of 3 m depth and a shaft 3 m deep and 8 m square in the middle of it. The sides of the shaft were delimited by wooden walls and the floor was planked. A chamber of 3 x 4 m in the middle of the floor was identified as mortuary chamber and burial of cremated remains of an Iron Age chieftain. In addition, three human skeletons were found in the east side of the entrance, covered with sand and gravel (Macphail et al. 1989). According to the archaeological data, the chamber was demolished in the past, after the placement of the ashes and remains in the grave. It was later covered with layers of materials, which were macroscopically identified as turves. The analysis of these sediments involved micromorphology, diatoms, SEM-EDS and microprobe. The results highlighted the presence of five microfabric types in each sample. Post depositional effects were identified as partial replacement or coating of organic matter by iron and manganese, favouring the pseudomorphic preservation of organic fabrics and the identification of layers of cattle dung. This last recognition, in addition to the presence of trampling structures, suggested the use of turves from pasture or cattle stocking areas (Macphail et al. 1989).

The first sedimentological analysis in relation to human remains was conducted in 2003, to determine the provenience of a skeleton found in Kennewick, Washington (Huckleberry et al. 2003). The skeleton appeared from a streambank, which had receded as a result of seasonally high water levels and wave activity. To define the original burial location, sediments adhering to the bones, stratigraphy and geomorphology of Columbia Park were analysed. The sediments on the skeletal remains were preserved as a result of the presence of secondary calcite and silica cements, and intact peds of 1 cm in diameter were present inside the cranium. The analyses performed included micromorphology, granulometry, XRD, thermogravimetry and trace-elements analysis (Huckleberry et al. 2003). Micromorphology was done on one of the peds from the cranium and compared with the thin sections of peds from the streambank. The observations of composition and texture confirmed that the cranium was filled with sediment derived from the burial site and it was not introduced along the shore after the exhumation of the skeleton. Analyses of the other samples indicated that the sediment cemented on the bones was equivalent to the deposits of the upper part of lithostratigraphic Unit 2 at Columbia Park, except for the dark sediment from the pelvis, rich in organic matter and similar to the one in the shoreline. This

sediment was probably incorporated after the erosion of the skeleton from the streambank (Huckleberry et al. 2003).

Micromorphological analysis of sediment from the inside of a cranium were applied, with several other analyses (3D photography and laser scanning, high-resolution laser scanning, CT and MRI scanning, SEM, DNA, brain neurochemistry, tissue and sediment chemistry, bone and soft tissue thin sections), to the examination of the prehistoric human brain discovered in Heslington, York, in 2008 (O'Connor et al. 2011). The brain, which appeared as a resilient yellow mass at the moment of discovery, was found in a pit within a dark-stained human cranium with articulated mandible. The micromorphological results indicated that little movement of water occurred in the cranium and nearly no translocation of decomposition products took place through voids or fabric. Thin section from the bone showed that the bone was well preserved, except for some structural cracks, and that microbial, bacterial or fungal activities were not present. The good preservation of the brain was suggested to be conditional on the same circumstances that predispose the formation of adipocere (O'Connor et al. 2011).

Micromorphological analysis was applied to a Roman age incineration feature by Angelucci (2008). Although this was not a case of inhumated remains, the study fitted perfectly in the context of examination of burial practices. The object of research was an *ustrinum* located in the urban site of Encosta de Sant'Ana. *Ustrinum* designates a funerary construction used for the incineration of corpses in the ancient Roman world, from which the burnt remains were collected after the funeral pyre and buried elsewhere (Angelucci 2008). Ancient Roman authors described some of the rituals related to the *ustrina*, affirming that it was common to collect only small portions of the remains, as the symbolical representative part (Angelucci 2008). The burial under analysis was composed by several structural elements: the perimeter, which was defined by an oval and elongated ridge, the internal part, which was modelled as a shallow depression cut into the Miocene bedrock, the filling of the depression composed by organic sediment and the reddened belt, characterizing the base of the internal part and the sides of the ridge. The excavation was organized in diagonally opposite squares, to permit the observation of the boundary between the archaeological feature and the bedrock. The sediment was systematically sampled for micromorphology (Angelucci 2008). The micromorphological evidence confirmed that the feature hosted fires, that bones were burned over it and that the burnt remains were residually accumulated and consequently partially removed. The good preservation of weatherable components, such as ash, suggested that the *ustrinum* was quickly buried after its last use and that the alkaline bedrock and the Mediterranean climate helped in the preservation of the feature (Angelucci 2008). From the distribution of the reddened zone and the thickness of the organic infilling, Angelucci deduced that the *ustrinum* was used for the cremation of various

bodies and, by the presence of different degrees of heat treatment of bones, that the inner interface of the *ustrinum* exceeded 600°C (Angelucci 2008). The presence of a reworked mud-brick like fragment in the infilling indicated that the *ustrinum* was renovated at least once and the characteristics of the infillings showed that it was not carefully cleaned after use (Angelucci 2008). This work was a good example of examination of a burial context through micromorphological analysis. All the microscopic observations were, in fact, linked to the macroscopic data, the sampling was focused on the *ustrinum* and on the bedrock and documentation of the stratigraphy of the feature was fully presented. In addition, historical information from literary sources was considered and combined with the archaeological data.

Attention to the processes of backfilling and re-opening of the graves was given to the Mycenaean chambers tombs (Karkanas et al. 2012) and Early Medieval inhumations in Brunn am Gebirge, Austria, and Winnall II, England (Aspök 2011).

In the work of Karkanas et al. (2012), micromorphological samples were taken from the stratigraphy of four dromos (entrance corridor of the tomb) to recover information for the understanding of the mortuary practices. It is known that chamber tombs with multiple burials were re-opened several times in the past to allow the deposition of corpses, but few excavations reported data regarding stratigraphy and context, impeding the understanding of activities such as the opening and closing of the entrance corridors and the time in which the dromoi were completely filled (Karkanas et al. 2012). A new excavation strategy was created for this purpose, in addition to soil flotation, archaeobotanical analysis, phytolith analysis and organic residue analysis (Karkanas et al. 2012). Undisturbed soil samples were collected in all stratigraphic interfaces that had previously been documented *in situ* by photography and drawing. The soil was consolidated by spraying repeatedly with a dilute sodium silicate solution and, once hardened, the blocks were jacketed with gypsum cloth to secure them as undisturbed samples and cut out with a sharp tool. Baulks along and across the dromos and inside the chamber were left to provide checks during the excavation and to make accurate stratigraphic drawings (Karkanas el al. 2012). Micromorphological observations helped to identify the location, the number and the slope of re-openings. In particular, sorted gravel pockets with reverse or normal grading, generally parallel to the slope, were associated to grain flow and debris fall processes in relation to the formation of small piles during shovelling of debris in the tombs. The features related to the re-opening were extensive planar erosional surfaces, sometimes associated with a basal line feature and an abrupt change in degree of compaction. The presence of constructed plastered floors, related to the phases of opening and re-opening of the tombs, and the sedimentological evidence suggested that the dromoi stayed open for a short period after each opening.

During the Merovingian period in Europe, re-opening of graves was a common practice related to grave-robbery. In most cases, grave goods were removed and the skeleton displaced. For this reason, this practice was considered a disturbance in the study of cemeteries (Aspöck 2011). On the contrary, the aim of the research started by Aspöck was to create a taphonomy-based approach to the study of re-opened graves, based on the reconstruction of natural and anthropic processes involved. Re-opened graves were characterized by dark organic rich pits visible under the top soil and located within the grave fill. The organic material probably originated through mixing of the surface with the disturbed area of the fill or because the pit was left open and gradually filled by sediments coming from the top layer (Aspöck 2011). Different levels of disarticulation of skeletons indicated that the re-opening could happen in different moments after the entombment. If the grave was opened very soon after burial, the skeleton was partially pulled out or lying in an unusual position. If the corpse was already partially disarticulated, some parts of the corpse were disintegrated upon moving, while others were dislocated in composition. If the skeleton was fully skeletonized, but still in an empty space, a mix of bones and grave goods was spread all over the bottom of the grave. Finally, if the corpse was fully skeletonized and the grave structure had collapse, only few bones and grave goods were found (Aspöck 2011). The project is still in development (Grave Reopening Research: www.reopenedgraves.edu) and the author was interested to involve micromorphological analysis for the identification and interpretation of features related to the re-opening activities (personal communication).

An interdisciplinary team of the University of Milano and University of Bicocca, formed by soil scientists and forensic pathologists, has been working on a project on forensic geopedology in recent years. Presentation of the project and very preliminary results were introduced at the EGU General Assembly and, unfortunately, only published abstracts were available (Ern et al. 2010; Ern et al. 2012; Ern and Trombino 2013; Zangarini et al. 2014). The team is working on several sets of experimental burials of pigs and piglets in different soil types and for different times of burial, in order to get new evidence on environmental behaviour related to the burial, focusing on pedological and micropedological aspects (Ern et al. 2012). The analyses applied were: grain size analysis, determination of pH in H_2O and KCl, total nitrogen and organic carbon analyses, quantification of available phosphorous, determination of cation exchange capacity and base saturation, analyses of volatile fatty acids, SEM-EDS and petrographic optical microscope analyses and thin sections descriptions (Ern and Trombino 2013). Micromorphological and SEM-EDS analyses were performed on bone tissue of buried remains. The results showed: unusual concentration of metal oxides in the form of violet-blue colorations in XPL, which seemed related to specific chemical burial conditions; magnesium phosphate crystallizations, usually noticed in bones buried from 7 to 103 weeks, and possibly related to decomposition of bones and soft

tissues; presence of significant sulfur levels in bones buried for over 7 weeks, which seemed to be related to the transport and fixation of soft tissue decomposition fluids (Zangarini et al. 2014). Phosphatic features mainly related to the grain size of the impregnated soil particles and weather conditions of exhumation, while time-since-burial was marginally effective (Ern et al. 2012). The presence of vivianite, an iron hydrate phosphate, was interpreted as a possible marker of the presence of buried remains in the soil (Ern et al. 2010). The members of the project stated that the results obtained so far showed that micromorphological techniques, in association with spatial resolved chemical analyses, allowed the identification of permanence indicators of the remains in the soils, for example metal oxide concentrations, and time-dependent markers of decomposition, such as sulfurus levels and magnesium phosphates, in order to determine the post-mortem-interval and time-since-burial (Zangarini et al. 2014).

In conclusion to this section, it is possible to affirm that micromorphology of soil and sediments had an early relevance to archaeological studies, while it was applied to burial contexts only in the last two decades. These last studies involved the analysis of the sediments in funerary settings, such as the shaft at St. Albans (Macphail et al. 1989), the *ustrinum* at Encosta de Sant'Ana (Angelucci 2008) and the chamber tombs in Mycenae (Karkanas et al. 2012), looking at the type of infill and the depositional processes involved in its formation. In other cases, micromorphological analysis was applied to the bones or to the sediments calcified on the bones themselves, such as the skeleton in Kennewick (Huckleberry et al. 2003), or very exceptionally on soft tissue, such as the brain from Heslington (O'Connor et al. 2011). These previous works represented the basis for comparison with the analysis of the sediments within the graves, the processes involved in their formation and the observation of the condition of bone fragments. The research developed by the University of Milan and University of Bicocca (Ern et al. 2010; Ern et al. 2012; Ern and Trombino 2013; Zangarini et al. 2014) was focused on the soil behaviour in relation to the burial and to the decomposition reactions. It offered a comparison for permanent indicators of the remains in the soils, such as neoformed mineral and phosphates. Finally, the Grave Reopening Research (Aspöck 2011) represents the increasing interest for the application of micromorphology to grave sediments, to which the InterArChive project is attempting to give an answer.

2.2 ARCHAEOTHANATOLOGY AND FORENSIC SOIL SCIENCE

The analysis of burial sediments at the microscopic level requires the understanding of the grave environment at a macroscopic level. Since the grave includes the skeleton and sediments, it is important to have knowledge of both of them. This section considers the information regarding the application of funerary archaeology (Section 2.2.1) and its connection with forensic science

(Section 2.2.2). Section 2.2.3 introduces to the soil properties, while Section 2.2.4 is dedicated to the phases of corpse decomposition and to factors influencing the decomposition within the soil.

2.2.1 INTRODUCTION TO ARCHAEOTHANATOLOGY

Archaeothanatology is the discipline that reconstructs the attitudes of ancient populations towards death, analysing the human skeleton and the actions related to the care and treatment of the corpse (Duday 2009, 6). It belongs to the sphere of archaeology and, particularly, to that of funerary archaeology. It was developed in France in the early 1980s as an approach to burial study including archaeology, biology, study of bones, decomposition of the corpse and products of decomposition (Duday 2009, 3). The innovation of this discipline was to place the interred corpse at the centre of interest of the grave, since "the dead body is the *raison d'être* for the tomb" and the focus of the activities related to the burial (Duday 2009, 6).

The first point to note is that the skeleton was originally a corpse, which went through phases of decomposition and skeletonization (Duday 2009, 7-13). Secondly, it is important to distinguish different types of funerary deposit, which can be isolated or in cemeteries, single or multiple, or with more than one corpse within a pit. Differences can be applied to the structure and typology of the grave, which can be located in a natural or artificial structure, such as cave or hypogeum, or in the ground, with or without coffin or other type of structure (Duday 2009, 13). In addition, it is important to distinguish between primary and secondary burials. In the first case, the corpse is buried in the same place where the funeral ceremony and the decomposition take place. In the second case, the body is temporarily buried in a place where the decomposition occurs; when the corpse is skeletonized the bones are transferred to another grave (Duday 2009, 14).

If the corpse was deposited in a primary burial, the remains are not generally disturbed and the skeleton is found roughly in its original position and anatomical connections are preserved (Duday 2009, 14). When the decomposition happens in an empty space, for example inside a coffin or in a chamber tomb, the bones undergo movements caused by gravity and absence of material able to maintain them in their correct anatomical relationship. The head turns on one side because of the spherical shape of the cranium and the dissociation of the cervical vertebrae. The vertebral column is slightly displaced, the ribs are flattened because the thoracic volume is absent and the patellae fall outside the knees; the bones of fingers are still in place, but not interconnected (Duday 2009, 32-38). In case of decomposition in filled space, the soft tissues are progressively replaced by sediments, whose role of support prevents the falling of bones, maintaining their connection (Duday 2009, 38-40).

If the dry bones were deposited in secondary burial, they are not in anatomical connection and not all the bones are present. However, the evidence in this situation is more difficult to interpret,

particularly in the distinction between intentional or unintentional acts (Duday 2009, 89-92). The term reduction describes the practice of moving the bones of a skeleton within the container in which it was buried, to locate a new corpse. In the case of reduction extending outside the confines of the container the bones of the first inhumation are heaped on the lid and if the lid collapses, the bones fall inside the container over the more recent remains which have been placed in the space, causing a stratigraphic inversion (Duday 2009, 72-72).

During the decomposition of a corpse, the original soft tissues are replaced by the fill of the burial. When filling is delayed, there is a gradual pressure from the sediments, which leads to closure of the intersegmental angles of the body. However, this does not happen when the joints are extended or lightly flexed. The process of filling of the grave can occur in three different ways: force of gravity, generally with sandy, ashy or very fine sediments; increase in volume of clay wet by decomposition fluids and disturbance caused by activity of mesofauna (Duday 2009, 52-57).

2.2.2 ARCHAEOLOGY AND FORENSIC SCIENCE

The complexity of burial deposits requires specific techniques and precautions during excavation of the bones, grave goods and sediment and also demands careful documentation of the processes and activities involved. Protocols have been elaborated over time and applied to different burial contexts. The basic requirements include the use of very small tools to expose the bones, which should not be left uncovered for too long to avoid damage from atmospheric conditions (Roberts 2009, 74-75). The skeleton can be removed from the soil only after a complete documentation, which includes photographs, drawings and completion of skeleton record sheets. All the bones and teeth have to be carefully extracted and placed in different labelled containers to avoid any damage. Sediments and stratigraphy have to be documented too, and samples of soil are collected for further analysis (Roberts 2009, 76-80).

Archaeological techniques for the excavation of burials started to be applied to crime scene investigations in the 1970s. According to Morse et al. (1976), the presence of an archaeologist in the forensic team was beneficial or, as an alternative, the team had to be trained in the use of archaeological techniques, because archaeological methodology could help to detect clandestine burials and to acquire all the possible information on the activities related to them (Morse et al. 1976). However, the introduction of archaeological techniques was not rapidly applied in forensic studies. In the 1990s Spennemann and Franke (1995) advocated the use of these approaches, presenting the results from a data-controlled case study from Mejatto Island (Spennemann and Franke 1995). Their procedure was characterized by four main factors: site clearance, exhumation, documentation and sampling. The first phase of the investigation concerned the creation of map and planimetry of the cemetery and the clearance of the vegetation, gravel

coverage and grave markers from the area of the identified graves. Subsequently, the excavation of the graves was performed dividing the fill in several layers, which were fully documented. Samples were collected above and underneath the body and in the surrounding soil (Spennemann and Franke 1995).

Nowadays archaeological techniques are fully employed in forensic researches, to locate and recover human remains and related evidences. The aim is the legal acquiring of data that can be useful to detect a connection between suspect, victim and crime, as well as the possible use in future legal proceedings. The main contributions of archaeology in forensic science are: using of systematic, controlled and adaptable approach; increasing of the accuracy in the collection and preservation of skeletal remains; understanding of the depositional and post-depositional processes that occurred in the grave; preventing post-mortem damage to skeletal remains and recording of environmental data which can be analysed by entomologists, botanists and other specialists (Dupras et al. 2006, 105).

The collection of such different environmental data reflects the multidisciplinary nature of forensic science, and more precisely of forensic soil science, which is more focused on the disturbed and moved soils. Thus, archaeology is not the only discipline used by this science, which also includes pedology, geochemistry, mineralogy, molecular biology and geophysics (Fitzpatrick 2008, 6).

2.2.3 FORENSIC SOIL SCIENCE AND PEDOLOGY: BASIC CONCEPTS ON SOIL

Forensic soil science is the branch of forensic science that uses methods of pedology for the understanding of human decomposition processes, burial site location and questions relating to soil taphonomy (Fitzpatrick 2008, 2).

Pedology is an area of soil science concerned with the dynamics and development of soil. It recognizes static aspects of soils related to the study of constituents and properties of soil, and dynamic aspects, associated with the pedogenesis and formation of profiles. These two conditions cannot be separated, since they are complementary (Duchaufour 1998, 1-2).

Soil is a three-dimensional natural body resulted from both destructive and synthetic forces, which is not static but is resilient to perturbations (Brady 1974, 8). It is located in the uppermost layers of the earth crust and it is characterized by different organizations of mineral and organic components, water and air (Catt 1990, 2).

Mineral components are variable in size and composition within a soil. They are represented by rock fragments, derived from the weathering of parent material and generally of coarse size, and minerals such as quartz and feldspars, which can be coarse or very fine, such as colloidal clay

particles. Minerals can be primary or secondary. In the first case, they are minerals which have persisted in the soil with little change in composition, for example quartz mineral grains. In the second case, secondary minerals are formed by the weathering of other less resistant minerals and they are more present in the fine materials (Brady 1974, 13-14).

Organic components in soil include partially decayed and partially intact plant and animal residues, which are continually altered by soil organisms and may be replenished by addition of fresh inputs. Organic matter is differentiated into original tissue and its partially decomposed equivalent and humus. Original tissue includes fresh roots and materials which are intensively attacked by soil organisms. Humus is the colloidal and more resistant product of this decomposition, black or brown in colour, and more capable of holding water than is clay. Despite the general low percentage of organic matter in soil, this component has an important role, in the formation of granules and aggregates, providing phosphorous, sulfur and nitrogen, increasing the capability of soil to retain water and supplying the main source of energy to soil microorganisms. (Brady 1974, 14-15).

Soil water is held within the soil pores with different levels of strength, according to the quantity of water present and pore size. Solutions containing dissolved salts supply nutrients to plants (Brady 1974, 15-16).

Soil air is related to soil water, because the air moves into soil pores that are not occupied by water. Soil air is variable, it has higher moisture content than the atmosphere and the content of carbon dioxide is higher while the one of oxygen is lower than the levels in the atmosphere (Brady 1974, 16).

Thus, soil water and soil air occupy the soil pores, which constitute the void space in a soil. Their origin can be related to the activity of soil biota, or to other factors such as cracking or packing. Generally voids larger than 0.075 mm are formed by roots and biota between sand grains and peds and they conduct water and air rapidly, while voids smaller than 30 µm are more typical in clayey soils and they can retain water for long periods (Shaetzl and Anderson 2009, 17).

Soil formation occurs on stable land surfaces through interaction of atmospheric and biological forces. These factors relate to different parent materials in different topographic situations and over different chronological times, contributing to the diversification of soils. These processes include: weathering of minerals by reaction with water, oxygen and carbon dioxide; superficial disturbance caused by desiccation, root penetration, tree-fall, animal borrowing, shrinking and swelling of clays, frost and human activities; incorporation of decomposing organic remains; movement of materials in solution or of solid particles in suspension (Catt 1990, 2).

The term of soil profile designates the sequence of horizons between the land surfaces and the uppermost material unaffected by soil-forming processes. Each soil profile is the result of the interaction of five factors. The first is the climate, which contributes to the breakdown of the parent material and affects the velocity of soil processes. The second is the fauna living on and within the soil: plant, animals and humans. Their influence is caused by the need for water and nutrients, their role in the decomposition of waste materials and the movement of soil materials. The third is the topography, because the location of the soil can affect the consequences of climatic factors. The fourth is the parent material, or rather the mineralogical and physical characteristics of the materials. The fifth is the length of time related to the pedogenesis (Catt 1990, 2; Fitzpatrick 2008, 8).

Different types of soil horizons have been classified through a system of notation, which attributes a letter to each specific horizon. Master horizons could have descriptive suffixes in lower-case letters, providing additional information, while transitional horizons are designated with two capital letters (Shaetzl and Anderson 2009, 36). O horizons are generally at the top of a soil profile; they are composed of organic materials and decomposing debris. A horizons are usually situated under the O horizon and they are composed by mineral and organic particles, such as coatings of humus, isolated fragments of organic matter, dead plant and animal fragments, faecal pellets, seeds, pollen grains and opal phytoliths. E horizons are light-coloured mineral horizons, which have lost organic matter or clay/oxides/iron/aluminium, due to downward translocation of these substances by filtrating water. B horizons are dominantly mineral, but can also contain organic accumulations from the upper or lateral organic-rich horizons. B horizons can possibly contain traces of illuviation or translocation of materials by percolating water, or deposition of materials by dessication, adsorption, filtering or precipitation. C horizons are located between the solum and bedrock and they constitute the soil parent material. They can be affected by weathering, alteration by pedogenic processes or having illuvial deposits (Shaetzl and Anderson 2009, 36-51).

The main types of soil are Entisols, Vertisols, Inceptisols, Mollisols, Alfisols, Ultisols, Spodosols, Aridisols and Histosols. Entisols are not fully developed soil, because they are too young or because material has been rapidly removed by erosion. They are composed of mineral or organic horizons, developed on slightly altered parent material. Vertisols are rich in clay, which produces shrinking and swelling movements related to seasonal humidity. Inceptisols are composed of an A horizon and a weakly developed B horizon. They often form in the rolling parts of the landscape and in the foothills of mountains. Mollisols are rich in humus, dark-coloured and with extensive earthworm activity. Alfisols have high amounts of translocated clay and chemical nutrients, but little humus. Ultisols have a horizon containing significant amounts of translocated clay (argillic

horizon) but low chemical bases. Spodosols are characterized by sandy parent materials, and are generally rich in aluminium, organics matter and sometimes iron/aluminium sesquioxides; all translocated into their B horizons. Aridisols are dry and have a low content of organic components. Histosols are formed by organic material and support bog, swamp and marsh conditions (Rapp and Hill 2006, 41-42).

In forensic soil analyses, it is important to collect soil samples from the crime scene and to be able to compare them. The samples are generally described looking at six fundamental characteristics: colour, depth changes in consistency, texture, structure, segregations/coarse fragments, abundance of roots in the different layers (Fitzpatrick 2008, 11-12).

Soil colour is defined on dry and moist samples using Munsell Soil Colour Charts, which define colour on the coordinates of hue, value and chroma. The colour of soil is influenced by the presence of iron oxides and organic matter. Red and yellow colours indicate oxidizing conditions, while dark grey and blue shades are caused by reducing, water-logged or wet conditions. The mixture of red or yellow matrix and dark grey or bluish areas indicates periodic conditions of water saturation (Fitzpatrick 2008, 13-14).

Soil consistency means the strength and coherence of a soil, determined by manipulating the sample in the hand and establishing how much force is required to break or distort the sample. Consistency can be designated as loose, soft, firm, very hard and rigid. It is influenced by soil texture, mechanical compaction, organic matter components, cementing agents and the presence of water (Fitzpatrick 2008, 14).

Soil texture indicates the percentage of sand, silt and clay composing the sample. This characteristic can affect the capacity of water retention, the compaction and the erodibility of soil. In the first case, water and nutrients are more rapidly drained in soil containing coarse-grained sands, because of the presence of large pores. Conversely, soils rich in clay have good capacity to retain water. Compaction can affect both root growth and water movement and sandy soils are more inclined to subsurface compaction than finer soils. Fine sand grains are easily eroded and transported by wind, while coarser grains are heavier. Clay, instead, is light but difficult to transport because of binding to other particles. The coarse fragments can provide indications on the extent of weathering, comminution processes and lithology, observing their shape, which is defined by sphericity and roundness. (Fitzpatrick 2008, 15; Shaetzl and Anderson 2009, 9-13).

Soil structure defines how the soil particles are arranged and bound together. Soil structure can be characterized by pedality (presence of peds), or it can be structureless, massive or with slickensides. In case of pedality, the structure is characterized by the presence of peds, or rather

aggregates with strong internal cohesion and whose sizes increase with depth. Wet-dry or freeze-thaw cycles, root and faunal activities are the possible factors responsible for the formation of peds. Slickensides are shiny planes of weakness along which movement occurs in shrink-swell medium-to-heavy clay soils, typical of wet and dry expansive clays (Fitzpatrick 2008, 20; Shaetzl and Anderson 2009, 18).

Segregation designates the accumulation of distinct mineral particles, which occur in the soil with different sizes, shapes and forms. The most common are iron oxides, calcium carbonate and gypsum (Fitzpatrick 2008, 20-21).

Soil is usually used in forensic science as an associative evidence and it is treated as a passive medium. On the contrary, soil is dynamic and can respond rapidly to environmental changes, such as pollution and disturbance. Analysing the soil processes related to cadaver decomposition it is possible to have more and better information as detailed below (Carter and Tibbett 2008, 29-30).

2.2.4 CORPSE DECOMPOSITION WITHIN SOIL

The decomposition of corpses can be affected by environmental, climatic and anthropogenic factors. Their analysis can permit the identification of cause and time of death and the location of the corpse during the decomposition. This section discusses the different processes of decomposition (autolysis, putrefaction and decay); their association and relationship with the presence of insects, plants and fungi; the influence of temperature, of the position in the site (deposition on the surface or buried, with or without coffin) and effects of additional material (clothes or metal objects) on the rate of decomposition.

A cadaver contains both enteric and dermal microbial communities, between 60%-80% water, high concentrations of lipid and protein and has a narrow C:N ratio. The decomposition of the corpse follows three processes: autolysis, putrefaction and decay. *Autolysis* corresponds to the destruction of cells; it can start a few minutes after death and is affected by temperature and moisture. *Putrefaction* takes place with the creation of an anaerobic environment, in which carbohydrates, lipids and proteins are transformed in organic acids and gases, resulting in colour change, odour and bloating of the cadaver. At this point, the skin is often broken and oxygen is reintegrated inside the cadaver. *Decay* starts with the beginning of aerobic metabolism and it is characterized by rapid breakdown (Carter and Tibbett 2008, 31).

Insects and scavengers play a major role in the decomposition of the corpse. In particular, insects can arrive a few minutes after death: blowflies and flesh flies are the first and maggot activity can represent the most important factor in the removal of soft tissues. Scavengers typically have more impact when insects and microprobes are less active (Carter and Tibbett 2008, 33).

The immediate area around the corpse is affected during decomposition and is characterized by changes in the succession of insects, plants and fungi, as well as variation in concentration of chemical compounds. Six stages have been detected for the cadaver decomposition (Carter and Tibbett 2008, 33-34). The first two are the *fresh* and *bloated stages*, which occur from the moment of death to the breaking of skin. Blowflies and flesh flies arrive at these stages to deposit their eggs; in parallel, the activity of microbes increases. The build-up of gases associated with putrefaction increases pressure and causes fluids to exit from natural openings and flow into the soil. When the skin ruptures, more areas are available for colonisation by fly larvae and aerobic microbial activity (Carter and Tibbett 2008, 35). The third stage, *active decay,* corresponds to the greatest mass loss due to the release of cadaveric fluids into the soil. This stage ends with the migration of maggots (Carter and Tibbett 2008, 35-36). In these first stages, fungi, such as zygomycetes, dueteromycetes and ascomycetes appear in response to the high concentrations of ammonia (Carter and Tibbett 2008, 37). The last three stages, *advanced decay*, *dry* and *remains,* are slower than the previous stages, probably owing to the lower abundances and more refractory nature of the remaining cadaveric materials. The surface of the grave soil related to maggot activity is characterized by dead vegetation. This factor has been interpreted as being caused by the decomposition fluids or the excretion of antibiotics by maggots. Advanced decay is related to the increase in the concentration of soil nitrogen. The other nutrients contained in the fluids are phosphorous, potassium, calcium and magnesium. Advanced decay probably ends when plant growth recommences (Carter and Tibbett 2008, 36). These last stages of decomposition are associated with a decreased presence of Collembola and Acari. Moreover, fungal fruiting bodies form in response to organic N and high concentrations of ammonium and nitrate (Carter and Tibbett 2008, 37).

The main factors influencing the decomposition of a corpse are: temperature, moisture, soil type, associated materials, decomposer adaptation and trauma. Differences in these influences has been observed for exposed and buried corpses (Carter and Tibbett 2008, 38).

In the case of a corpse deposited on the soil surface, temperature affects the processes of autolysis and putrefaction and the insect activity. If temperature increases, a consequent increase in the rate of decomposition ensues. In parallel, low temperature slows the progression of decomposition. Notably, putrefaction stops below 4°C, because the decomposer activity is arrested and desiccation in favoured (Carter and Tibbett 2008, 38-39). Moisture influences the decomposition: extremely dry environments cause desiccation, which inhibits microbial activity, whereas extremely wet environments promote adipocere formation (Carter and Tibbett 2008, 39). Traumas can induce an exposed corpse to faster decomposition, attracting insects to open

wounds, while the presence of clothing increase the rate of decomposition because it offers protected areas for maggots (Carter and Tibbett 2008, 40).

In the case of a corpse buried within the soil, the rate of decomposition is generally considered to be slowed. A rise in temperature produces an increase of the rate of decomposition, but slower than in exposed cadavers. Soil moisture can influence the decomposition as it affects the metabolism of decomposer organisms. However, this effect can be modified by the soil texture: sandy soils with low moisture contents support desiccation, because gases and moisture can move freely within the soil fabric, while clayey soils, holding water, inhibit cadaver breakdown (Carter and Tibbett 2008, 41-42). The content of moisture in the grave soil is one of the main environmental variables affecting the decomposition of the corpse within the soil. Precisely, it could affect and modify the relationship between temperature and decomposition (Carter et al. 2010). Corpse decomposition has an effect on pH: in the first phase, there is the formation of an alkaline environment, which is followed to the formation of acidic conditions. Moreover, in acid soils plants produce tannins which decrease microbial activity, slowing the decomposition (Carter and Tibbett 2008, 42-43). The presence of clothes preserves and decreases the decomposition, preventing the action of meso- and microfauna. A clothed corpse in a moist, free-drain soil forms adipocere, which preserves it from breakdown (Carter and Tibbett 2008, 42-43). In addition, the cloths in natural fibres are better preserved compares with the same textiles buried directly in soil, without being in contact with a corpse. This has been explained as being caused by the corpse containing bacteria, which are not able to degrade cellulose, and by the presence of lipid decomposition products, which have an effect of preservation (Lowe et al. 2013). On the contrary, the presence of plant material accelerates the decomposition, probably for the introduction of additional microbial flora and the augment of C:N ratio, which promotes microbial activity. Materials such as textiles, leather and wood can be preserved by the concentration of metal ions, caused by the presence of metal objects within the burial. In addition, the rate of corpse decomposition is subject to the quantity and how often cadaveric material is added to the soil (Carter and Tibbett 2008, 43). The presence of modern coffin alters the rate of decomposition, because liquefaction of soft tissue proceeds until only a semifluid mass remains. This type of decomposition is rapid and it is attributed to the retention of water in the coffin, slightly aerobic environment and short periods between the death and burial (Forbes 2008, 215-216).

During the process of decomposition of a cadaver, under specific conditions, the formation of adipocere can occur. Adipocere (from adipo = fat and cere = wax) is a greyish-white, soft, cream-like substance, formed by the alteration of soft tissue, becoming a solid and resistant mass over time (Fiedler and Graw 2003). The principal processes leading to the formation of adipocere are hydrolysis and hydrogenation, which produce saturated fatty acids. Adipocere formation can take

place in any site where fatty tissue or lipids are present in the body prior to death. This product has been observed in lead-lined coffins, peat bogs, ice glaciers and submerged locations; all characterized by anaerobic conditions (Forbes 2008, 210). The range of moist soil textures can be variable, but in saturated or waterlogged soils adipocere forms rapidly. Warm temperatures are favourable, as well as mildly alkaline pH, while highly alkaline environments prohibit the formation of adipocere. The absence of coffin helps a rapid formation, because of anaerobic conditions. However, adipocere was also observed in coffins due to the initial phase of aerobic conditions being superseded by anaerobic conditions within the coffin. Adipocere is not a final product and can decompose to the free fatty acids (Forbes 2008, 211-212).

The skeletonization of the cadaver occurs when there is the complete disintegration of soft tissues. In anaerobic environments, such as is prevalent in graves, it is a slow process. The organic collagen of bone is eliminated by the activity of bacterial collagenases, while the inorganic phase is altered through the loss of mineral hydroxyapatite by inorganic chemical weathering. These losses make the bone structure weaker (Forbes 2008, 213-214).

As mentioned above, invertebrate fauna plays an important role in the rupture of the corpse. Forensic entomology is the area of forensic science which analyses the interaction between insects and cadavers. Insects are the first organisms reaching the corpse after death and their succession can be used to define the post-mortem interval. Different odours emitted by the body during the phases of decomposition can attract different insects, so insect taxa reflect the physical changes in the body (Dadour and Harvey 2008, 109-110). Flies (Diptera) and beetles (Coleoptera) are the most frequent insects observed in the area of cadavers. Blowflies (Diptera: Calliphoridae) are the first to arrive after death, to deposit eggs or live larvae in the areas of orifices or wounds. The larvae secrete enzymes and bacteria, consuming the soft tissues. Once the larvae have finished with the process of feeding, they pupate in soil, in clothing or under surrounding objects. After a period of metamorphosis, the adult fly appears and the empty pupal cases remain in the soil, even for many years (Dadour and Harvey 2008, 112). A short time after the arrival of blowflies, other insects arrive on the corpse: flesh flies (Diptera: Sarcophagidae), carrion flies (Diptera: Muscidae), predaceous beetles such as rove beetles (Coleoptera: Staphylinidae), carrion beetles (Silphidae), clown beetles (Histeridae), skin beetles (Dermestidae) and checkered beetles (Cleridae) (Dadour and Harvey 2008, 112). Beetles arrive during the fresh stage and they increase during the bloat stage (Dadour and Harvey 2008, 117).

Mites (Acari) are associated with soil under the corpse in late decomposition stages. However, some *Necrophorus* species can be present in the early stages, transported by flies to the areas of cadaver. In the group of soil-dwelling mites, the Cunaxidae are predatory and live in the soil under the remains, feeding on insects and larvae. The Winterschmidtiidae and Acaridae can be observed

at the end of decay, feeding on fungi and detritus. Bornemissza consume the remaining skin and aid the process of skeletonization (Dadour and Harvey 2008, 114-115).

Spiders (Araneae) can be found around a cadaver as general predators, but their arrival is not related to any specific phase of decomposition. Millipedes are found under the corpse, feeding on plant material, during the dry stage of decomposition. Springtails (Collembola) are plant feeding too and they can be attracted by the seepage of fluids. Ants (Hymenoptera) are often associated with carrion, but their presence is not predictable (Dadour and Harvey 2008, 115-116).

When a corpse is buried, the activity of insects is inhibited. However, blowfly and flesh fly have been observed on carrion buried ca. 30 cm under the surface. Adult flies were noted moving through surface soil cracks to reach the corpse or depositing eggs on the surface following rain. In addition, insects can be introduced within the burial if the entombment is delayed (Dadour and Harvey 2008, 118-119).

In conclusion, archaeological techniques and methods, forensic concepts and pedology are strictly interconnected in the analysis of burials. Knowledge of soil properties and corpse decomposition is critical for the detection and interpretation of features through microscopic analysis.

2.3 REVIEW OF THE METHODOLOGIES APPLIED TO THIS RESEARCH

The application of micromorphology requires knowledge of sampling methods and sample processing (Section 2.3.1), the principles of light microscopy for the identification of mineral and organic components in the samples (Section 2.3.2) and procedures in sample description and analysis (Section 2.3.3). In addition, definition and application of image analysis and SEM-EDS analysis are illustrated (Sections 2.3.4 and 2.3.5). These analyses were, in fact, applied in this research to enhance the micromorphological analysis.

2.3.1 APPROCHES TO SAMPLING AND SAMPLE PROCESSING

Essential to the success of micromorphology is the examination of undisturbed soil samples, from which the 30 μm thin sections are produced. The samples must be undisturbed in order to preserve the original spatial arrangement between the components, structures and fabric. Hence, sampling is a critical part of all of micromorphological studies and good outcome of the study are entirely dependent on the quality of the sampling. It is essential that all the samples represent the soil material as it exists in the field, but at the same time, the dimension of the samples can be a limitation. For this reason, it is very important to consider some aspects before

collection: the purpose of the investigation; site selection and supplementary data; size of the samples and thin sections; orientation of samples; number of replicate samples needed; time of sampling; collection method; documentation; transport and storage of the samples (Vepraskas 1990, 8). Replicate samples are collected to enable statistical analysis of data and thereby have a better representation of the soil characteristics (Vepraskas 1990, 10).

Two sampling strategies can be applied to different situations: systematic sampling, when an entire stratigraphic sequence needs to be analysed, and selective sampling, when the aim is to resolve a specific problem. The former considers collecting the samples from a column, generally without any gaps, to detect all the variations within the section. The second is focused on the structure or layer to analyse. Samples are generally collected from vertical surfaces, but there are situations in which a different approach has to be formulated (Courty 1989, 40-42). Vertically oriented samples are useful for the observation of horizon boundaries, bedding planes or void systems, while horizontally oriented are applied to studies on clay illuviation, water movement and root growth (Vepraskas 1990, 10). In addition, bulk samples should be collected to conduct chemical and mineralogical analysis (Courty 1989, 42; Vepraskas 1990, 9).

Samples are collected with rigid containers to prevent the collapse of the sediments, which are often loosely to poorly cemented. The most widely used containers are the so-called Kubiena tins, made of three parts in metal: one side and two removable lids. Their size can be variable and made on request, depending on the requirements for the study. The side, which forms a rectangular frame, is inserted in the sediment and carefully removed with the help of a knife or trowel, first having replaced the front lid. The sample is then cut flat and covered with the back lid. All this operation has to be done in a very gentle way, avoiding any possible disturbance (Vepraskas 1990, 12-13; Courty 1989, 42-43). The Kubiena box is then annotated with orientation, depth, number of sample and site and, successively, wrapped with tissue paper, aluminium foil or plastic wrap (Vepraskas 1990, 13; Courty 1989, 42; Goldberg and Macphail 2003). Other techniques of sampling can be applied, depending on the nature of the soil. For example, if the sediment contains coarse inclusions, plastic semi flexible down-pipe can be used as core. In cases where the sediment is loose, is possible to coat and stabilize the outer surface with a solution of sodium silicate before removal. In other situations, when poorly sorted mixtures of rockfall are mixed with finer interstitial material, plaster jacketing can provide the solution, hardening one side of the sample in place and then applying the plaster on the internal side, once the sample has been extracted (Goldberg and Macphail 2003). It is essential to document the sampling with photographs, sketches and notes, otherwise some information can be irretrievably lost (Vepraskas 1990, 14; Courty 1989, 42; Goldberg and Macphail 2003).

The processing of the samples requires three fundamental steps: drying the sample, impregnating it with resin and grinding it to the standard thickness of 30 μm. Samples have to be dry, because water does not mix with any type of resin. They can be dry through air or oven-drying, acetone replacement or freeze-drying. In the first case, samples are left at room temperature with adequate ventilation or in an oven set at 40° or less. The time required is between 5 and 8 weeks for air drying, while it is faster with the use of an oven. However, some alterations may occur within the structure of the sample, for example shrinkage, formation of cracks, clay particle rearrangement and fracture, void closure, crystallization of soluble minerals and increased oxidation of organic matter (Vepraskas 1990, 16; Fitzpatrick 1993, 2). Acetone replacement achieves the removal of water by submerging the sample in an acetone bath, causing the diffusion of the water out of the soil and its replacement with acetone. The acetone has to be replaced every 3 to 7 days with fresh acetone and the process is complete when no water is found in the acetone, generally between 2 and 8 weeks. Calcium chloride has to be placed in the same box, to trap the water, and replaced as often as the acetone. This method minimizes shrinkage and crack formation and polyester resin mixes well with acetone. However, the acetone replacement can produce shrinkage of tissues that were hydrated at the time of collection, such as roots (Vepraskas 1990, 18; Fitzpatrick 1993, 2-3). Freeze-drying utilizes liquid Freon 12. Samples are dipped into the freon, quickly freezing the water at a temperature of about -158°C. The formation of large crystals is prevented and the possibilities of cracking are reduced. The frozen sample is transferred to an ice condensator, which removes the ice by sublimation within about one week. The negative aspects are the expense of the equipment, the formation of cracks in the centre of samples thicker than 2 cm and the role of Freon 12 in damaging the ozone layer (Vepraskas 1990, 19).

Once completely dry, samples can be impregnated with a resin chosen from among several options: unsaturated polyester resin, epoxy and methyl methacrylate. Polyester resins are viscous and not suited to small soil voids, because they not seep quickly. Thus, they have to be diluted with acetone or styrene to have a complete impregnation of the material. Epoxy resins do not mix with acetone, so they cannot be used to impregnate samples dried by acetone replacement. Methacrylate is less viscous than polyester, but it shrinks on hardening and it is unstable in an electron beam (Vepraskas 1990, 20-21).

The resin is prepared stirring a hardener in the solution and leaving it under a low vacuum until the air bubbles have escaped. The sample is placed in a container and the resin is poured down the side of the sample until the lower quarter is submerged. In this way, the resin enters from the bottom of the sample by capillary rise, letting the air escape. After 30 minutes, the process is repeated and the sample is submerged. The samples are placed in a vacuum chamber for one

night and then in a ventilated fume cupboard for about three days. The process requires about 6 weeks for the acetone to evaporate completely and the sample to harden. The samples are then placed in an oven and cured at 40°C for 2 to 3 days (Vepraskas 1990, 21).

Once cool the samples are cut down their length with a diamond saw and re-impregnated on the surface if cracks or pores are present. When the surface is completely dry, the sections are ground on the cut side until it is flat and smooth. The grinding is generally done with progressively finer powders and papers, by machine and by hand, with the use of oil. Water is generally avoided, because it can cause the expansion of clay minerals and the dissolution of soluble materials. The prepared side of the slide is glued to a clean glass slide and left to cure with pressure applied using a special press. The mounted glass and slide are place in a special jig and sawn to a thickness of 1-2 mm. The slide is then ground to a thickness of 40 μm using mechanical grinder or hand-grinding, while the final thickness of 30 μm is obtained by hand grinding with diamond plates and powders. Quartz has to become white in colour when examined using a polarizing microscope with XPL. The last step is to polish the surface to a mirror-like finish or to overlay it with a cover slip (Courty 1998, 59-61; Vepraskas 1990, 22; FitzPatrick 1993, 4-6).

2.3.2 PRINCIPLES OF LIGHT MICROSCOPY

Thin sections are examined with a petrographic microscope or polarizing light microscope. The microscope has a circular stage that can be rotated around 360°, a slot to insert special plates into the light path for the identification of minerals and two filters, a polarizer and an analyser, both made of a material that polarizes light. The polarizer is fixed, while the analyser can be moved. Light waves from the light source of the microscope, as the ordinary light waves, vibrate in all directions perpendicular to the direction of propagation of the light ray. The polarizer absorbs most of the light, but transmits the light in one specific plane, illuminating the sample. The analyser is orientated to transmit light waves vibrating at 90° to those which passed through the polarizer. When the analyser is in the light path, it absorbs all of the transmitted light and the field of view of the microscope is dark (Vepraskas 1990, 24).

The appearance of a mineral under crossed polarizers depends on the refractive index of the mineral; the ratio of the velocity of light in a vacuum to its velocity in the mineral. Minerals can have up to three indices of refraction, depending on the types and arrangement of the atoms of which they are composed. *Isotropic* materials have one index of refraction and they appear black in colour under crossed polarizers, even when rotating the stage, because all plane polarized light transmitted through the material is absorbed by the analyser. In fact, the light waves move through these materials with the same velocity, because the atoms or molecules are randomly or equivalently distributed and the vibration direction of polarizer and analyser are perpendicular to

each other. This is the case of glasses and plastic resins (Vepraskas 1990, 28; Stoops 2003, 150). *Anisotropic* minerals are crystalline, with atoms arranged in rigid three dimensional pattern and have two or three indices of refraction which affect the light transmission. When one wave length of plane polarized light is transmitted through anisotropic materials, the light beam is divided in two perpendicular rays, which travel at different velocity through the material. As consequence, when the rays exit the minerals, one of them exits with a phase difference, dependent on the difference of the refractive indices and thickness of the mineral. The two rays interact when the analyser is in use. The numerical value of the difference between the highest and lowest refractive index, called *birefringence*, is useful for the identification of minerals. Anisotropic minerals go in *extinction*, or rather become non-birefringent in four positions at intervals of 90°, when the vibration direction of the mineral is parallel to that of the polarizer or analysed (Vepraskas 1990, 28-30; Stoops 2003, 152).

The optical, crystallographic and morphological properties of the features in thin sections can be observed and detected in transmitted light, allowing their identification. Colour, pleochroism and relief can be seen using plane polarized light, while interference colours and extinction angles are determined with crossed polarizers (Vepraskas 1990, 30).

Colour and *pleochroism*: minerals in thin section have characteristic colour or range of colours or they can be colourless. Pleochroism indicates the change of colour in some minerals, which became slightly coloured if they were transparent, or darker, when the stage is rotated in plane polarized light (Vepraskas 1990, 31; FitzPatrick 1993, 10).

Relief: indicates how well a material can be distinguished from the surrounding materials. It can be observed as a black line, especially in minerals, and it is determined by the amount of difference between the refractive indices of the material and the surroundings. The relief can be high, moderate or low (Vepraskas 1990, 31; FitzPatrick 1993, 12).

Interference colours: are the colours of anisotropic minerals illuminated under crossed polarizers, exhibiting the rainbow colours of Newton's scale. They depend on birefringence, thickness and crystallographic orientation of the mineral. The range from black to the first violet is called *first order*, from the first violet to the second violet is called *second order*, and so up to white which is *high order white* contrasting with the white of the first order, which is named *low order white* (Vepraskas 1990, 31; Fitzpatrick 1993, 14-15).

Extinction angle was explained above. In addition, cleavage and twinning can be useful for the identification of minerals. *Cleavage* indicates the planes in which some minerals separate. T*winning* is the intergrowth of two or more single crystals of the same material, which appear as

single grain in plane polarized light and with different areas between crossed polars (Vepraskas 1990, 32; FitzPatrick 1993, 16).

The properties described above are effective in the description and identification of minerals. The same properties are less relevant to the characterisation of organic components. These can include plant and animals' debris in various stages of decomposition, so their identification can be difficult. The parameters comprise size, shape, internal structure, colour, opacity, birefringence and fluorescence (Vepraskas 1990, 35). Colour can vary from yellow, red, brown and black and generally become darker with increasing stage of decomposition. Opacity characterizes many organic components and can be caused by the thickness of the material, the level of decomposition or material having been burnt. The general aspect for organic remains is amorphous and for this reason they can be confused with oxide minerals of iron or manganese. Birefringence and interference colours can appear in the cases of cellulose and insect remains. However, they disappear with the increase of decomposition. Fluorescence is produced by cellulose and lignin when the material is exposed to ultraviolet light and it can be useful in detecting incompletely decomposed organic matter (Vepraskas 1990, 36).

2.3.3 APPROACH TO DESCRIPTION OF THIN SECTION

In the analysis of thin sections, it is important to understand the problems associated with the observation of three-dimensional objects in two dimensions. According to Stoops (2003, 11), it is possible to deduce a body's three-dimensional shape from one two-dimensional section only when there are enough similar shaped bodies with random orientation. As example, some possible sections of a cube can include shapes of triangles, squares, rectangles, pentagons and hexagons. Moreover, the size is statistically smaller than the actual size of the grains, and objects in contact can appear as they are not touching each other (Stoops 2003, 11).

Furthermore, it is important to maintain the contact between the observation at macro scale and the one at micro scale, as well as encouraging the use of both optical microscopy and electron microscopy (Vepraskas 1990, 39). The observation of thin sections should be done at different scales of magnification before any description, to connect the feature observable at low magnification with its internal composition, detectable at higher magnification (Courty 1989, 70).

Different descriptive methods have been established over the years (Bullock et al. 1985; Courty 1989; FitzPatrick 1993; Stoops 2003).

2.3.4 IMAGE ANALYSIS

Image analysis is a quantitative method for analysing features of thin sections using digital images. These features are separated and measured from their background and from other features (Vepraskas 1990, 97) and the methods applied are variable and dependent on the samples and on the equipment supplied.

The basic equipment includes microscope, camera, computer and image-processing software. The images are scanned through the microscope with the camera, stored and analysed with the computer (Bui 1991). The selection of the features within the image is based on the presence of individual picture points or pixels, which compose the image itself (FitzPatrick 1993, 29). Each pixel is characterized by a specific code, RGB (red/green/blue) in most of the software, which indicates value, hue and saturation of the colour. The characterization with RGB code allows the selection of some pixels rather than others.

The image analysis started to be used in the 1970s due to the introduction of computerized applications, such as the analyser Quantimet 720, and it was of immediate interest for the measurement of soil porosity (Murphy et al. 1977a; Murphy et al. 1977b). At the beginning of this technique, photographs were used in place of scanned images and they were in grey scale instead of colours (FitzPatrick 1993, 29). The issue of isolation of voids, to permit their quantification, was recognised since the initial development of this analysis (Murphy el al. 1977a). In thin sections, under PPL, voids and many mineral grains, such as quartz, are colourless. Under XPL voids are isotropic, because filled by resin, which is isotropic, while anisotropic minerals go in extinction in four positions at intervals of 90° (Vepraskas 1990, 28-30; Stoops 2003, 150-152; Section 2.1.3). This means that, rotating the stage of the microscope, there are four positions in which mineral grains can be recorded as voids. Two solutions were proposed in the 1970s to distinguish the voids from the mineral components. The first was adding fluorescent dyes to the polyester resin before impregnating the sample. The image acquired under UV light was characterized by fluorescent pore space and non-birefringent mineral grains (Murphy et al. 1977a; FitzPatrick 1993, 22). The second solution implied the use of high contrast photographs taken with an automatic developer or printer. With the use of under-exposed photographs, it was possible to differentiate between transparent voids and less transparent minerals, which were of grey colour (Murphy et al. 1977a). In addition, the use of Quantimet analyser permitted to magnify the images and to proceed to a more rapid analysis (Murphy et al. 1977b). The ANOPOR system, a computer program for the automatic recognition and measurement of soil, was developed in the 1980s in association to the use of the Quantimet 720. The ANOPOR was able to recognize only channels, planar voids and vughs, excluding the high interconnected pores, thereby limiting its potential for

application in the analysis of soils (Ringrose-Voase and Bullock 1984). However, the parameters used by the ANOPOR offered objective and consistent descriptions of the pore structure. Hence, this system was considered useful if integrated with measurements taken at several scales (Ringrose-Voase 1987). Improvements in the image analysis systems were developed since the end of the 1980s, with the creation of different systems and better qualities of video, software and hardware. In some cases, image analysis systems were integrated with SEM-EDS, combining elemental, spatial and spectral data of different soil features. In addition, the image analysis software systems became more user-friendly (Protz et al. 1987). This development entailed the creation of less expensive software-base image analysers, which were not always considered appropriate for the analysis of complex structures such as soil pores (Thompson et al. 1992). The availability of different software produced the creation and application of several protocols and methods of the image analysis. However, in these protocols, the final measurement was always standardized and based on mathematical morphology and stereological principles (Bryant and Davidson 1996).

According to Thompson et al. (1992), it is necessary to observe some procedures to obtain accurate results. Firstly, it is important to determine the suitable number of samples and images to analyse, to select the representative area of the sample and to decide the more appropriate magnification. Secondly, it is important to develop a standardize protocol suitable for the samples and the equipment available, to obtain adequate images and to proceed automatically in the analysis, controlling as many variables as possible. Moreover, it is important to relate the data to the soil behaviour.

The image analysis was applied in recent years to archaeological researches for the study of old cultivated soils (Bryant and Davidson 1996), historic landscape management (Adderley et al. 2006) and changes in soil produced by excremental features (Bui 1991; Bruneau et al. 2004). The results confirmed the image analysis as useful methodology for the quantification and identification of different soil features, such as peds, turf and faecal pellets, in addition to the study of voids. Particularly for the identification of these features, the use of high resolution image mosaics in colour and the notation of micropedofeatures by the Munsell colour terminology were essential. The manufacture of the slides was also considered very important and the consistency in the thickness of the samples was fundamental for the comparison between the slides, based on the colour properties (Adderley et al. 2002).

2.3.5 SEM-EDS AND MICROPROBE ANALYSIS

Scanning electron microscopy in association with SEM-EDS and microprobe analysis can be employed to detect individual element distributions within a sample.

In SEM, the beam of high energy electrons hits the surface of the sample and provoke the emission of secondary electrons. A detector captures the electrons to form an image of the specimen, which can be recorded as a photograph (FitzPatrick 1993, 32). The images produced are grey scale with high definition and three-dimensional view in the case of three-dimensional samples (Goldberg and Macphail 2006, 363). The X-rays are formed when the beam of electrons hits the specimen and the energy or the wavelength of the X-rays can be detected by a wavelength dispersive detector, which gives the elemental composition of the specimen. The concentrations of individual elements can be measures in transects, at discreet points or across the thin section to produce an element map of the specimen (FitzPatrick 1993, 32-33). The electron beam can be focused to 1-2 μm across the specimen, analysing the composition of specific grains. The results are presented as spectra in which energies correspond to different elements, or as relative abundance plots of different elements (Goldberg and Macphail 2006, 365).

Backscattered electrons can be used as complement to secondary electron images, because they readily reveal variations in composition within the sample. The backscattered electrons are caused by an elastic contact with the electron beam and their energy of emission is proportional to the atomic number of the element. Thus, the higher the atomic number is, the brighter is the image (Goldberg and Macphail 2006, 363).

The SEM, with or without the use of microprobe, has been utilized for the analysis of aggregates, grains and unconsolidated sediments. In some cases, portions of thin sections were cut from samples and removed from the resin to allow the analysis (Courty 1989, 50-51). More recently previously polished uncovered thin sections have been utilised (Goldberg and Macphail 2006, 362). However, during the SEM-EDS analysis the resin, which impregnates the sample, is included in the measurements, causing an increase of the levels of C and O.

The use of SEM-EDS analyses allows multi-element soil investigations, which have been applied recently to archaeological contexts. These studies showed that different functional areas in human sites are characterised by different chemical signatures (Wilson et al. 2008). Thus, multi-element analysis of the soils of six small farms, abandoned between the late 1800s and 1940 highlighted the distinction of different areas in relation to their different functions (Wilson et al. 2008). The farms were chosen in areas with different geological characteristics and different background of element concentrations, with different soils within and outside the area of the

farms. The authors attributed a lack of correlation between the element concentrations of background soils those within the farms, to anthropogenic activities. In addition, despite the differences between the sites, the functional areas were characterized by similar concentration of Ca, P, Ba, Pb, Cu, Sr and Zn. Comparable concentration levels were observed in archaeological structures, such as Roman and Paleo-Indian settlements, ancient and modern house floors and areas of cultivation analysed in previous multi-element studies (Wilson et al. 2008). This research demonstrated that soil element concentrations in archaeological sites can be correlated with patterns of archaeological activities and, as affirmed by Wilson et al. (2008), multi-element analysis can be become a new instrument for the interpretation of functions on archaeological sites.

This chapter has presented an overview of the methodologies relevant to this research and on the basic information regarding the context of analyses: soil and graves. Emphasis was given to the first researches attempted in this new field, which connects mostly with micromorphology of soils, archaeology and forensic science.

Arising from this knowledge, the methods and materials of analysis evaluated and applied in the InterArChive project, and in this research, are presented in Chapter 3.

Chapter 3. MATERIALS AND METHODS

Chapter 1 introduced to the main objectives of the InterArChive project, which were to develop and test systematic approaches of sampling and laboratory procedures for archaeological graves, exploiting the physical and chemical characteristics of the soil around the skeletal remains to increase the quality and quantity of information. In addition, Chapter 1 presented the rationale for this research and introduced the case studies and the methodologies applied. The definition, history and application of the methodologies in previous studies were presented in Chapter 2.

The materials analysed and the sampling strategy applied by the InterArChive project, on the basis of previous studies, are introduced in the first section of this chapter, including information regarding the production of the thin sections. The second part of the chapter is dedicated to the materials selected for this research and the methods used in their analysis.

3.1 MATERIALS AND SAMPLING STRATEGY OF THE INTERARCHIVE PROJECT

Archaeological inhumations from 31 sites across Scandinavia, Europe and North Africa, from Neolithic to Twenty Century, were the objects of research of the InterArChive project (Appendices 1.1 and 1.2 for the complete list of the sites). The selection and sampling of these sites, conducted between 2009 and 2012 by the InterArChive team, was conditional upon graves preservation, logistic procedures and interest/availability from archaeologists who were managing the excavations. This selection comprised different types of soil and burial practices, with the purpose of investigating a wide range of case studies and multiple geoarchaeological variables. In addition to these sites, ten stillborn piglets were buried in 2009 in five locations of the North Yorkshire, to produce reference materials. The experimental burials were excavated and sampled between the summers of 2012 and 2013.

The InterArChive project developed two different and interconnected standard methods of sampling for soil micromorphology and organic chemistry. These sampling protocols were fully applied to several graves, except for problematic situations such as disturbed inhumations or unavailability of soil profile for the controls. Two sampling record sheets, one for the archaeological graves and the other for the piglet burials, were created to facilitate systematic annotations during the collection of the samples and favouring the correlation between micromorphological and chemical samplings (Appendices 1.3 and 1.4).

Micromorphology of soils, as introduced in Chapter 2, Section 2.1, analyses undisturbed soil samples, which are processed through sequential stages to obtain 30 µm thin sections. The most common method of sampling consists of the use of a Kubiena tin, or another type of container, inserted into the soil profile (Chapter 2, Section 2.3.1). However, the sampling strategy can be variable, depending on the purpose of the research: systematic sampling is applied to identify all of the small variations and to retrace the geological, pedological and archaeological history of the sequence, while selective sampling is applied to answer to specific questions (Bullock et al. 1985, 11-13; Courty et al. 1989, 40-43; Stoops 2003, 8-9; Chapter 2, Section 2.3.1). The sampling elaborated by the InterArChive team was selective and adapted to the burial context. The samples were taken within the fill of the grave and in the sediments related to the cut of the grave or in the surrounding area. The protocol did not consider the documentation of the soil profile in which the graves were cut, which would have been important for the interpretation of the data; in addition, reports from archaeologists were not always available. The sampling strategy, as illustrated in Figure 3.1.a, was structured along horizontal layers within the regions of the skeleton, while it was conceived on a vertical dimension within the infill above the skeletal remains (controls).

According to the aim of creating a standardize sampling method of the grave sediments, applicable to further studies (third rationale explained in Chapter 1, Section 1.2), three locations surrounding the skeleton were selected: the area of the skull (labelled in the record sheet as position 1), the area of the pelvis (2) and the area of the feet (3 – left foot; 4 – right foot). Two controls (C2 and C3) were collected in the grave fill above the skeleton. C3, the deepest, was generally taken in the layer in proximity to the skeleton, when the skull started to be visible during the excavation. The fills have the greatest similarity to the matrix that is in contact with the skeletal remains, hence the differences between C2 and C3 and the samples around the remains best reflected the impacts of the burials on the matrix composition and structure. Control C1 was located outside the space of the grave, not exclusively in the proximity of the burial (Figure 3.1).

Three different sizes of Kubiena tins were utilised to collect the samples, depending on the space available within the grave. The use of the largest size was preferred, when possible.

- Type A: 83 x 50 x 32 mm;
- type B: 60 x 35 x 25 mm;
- type C: 80 x 55 x 40 mm.

According to the skeleton sampling record sheet (Appendices 1.3 and 1.4), the relationship between the location of the Kubiena tins and skeletal remains was annotated as levels *x, y* or *z*. These letters indicate three levels of sampling in relation to the bones and they do not represent spatial coordinates.

- *x* level: above the bones;

- *y* level: at the same level of the bones;

- *z* level: below the bones.
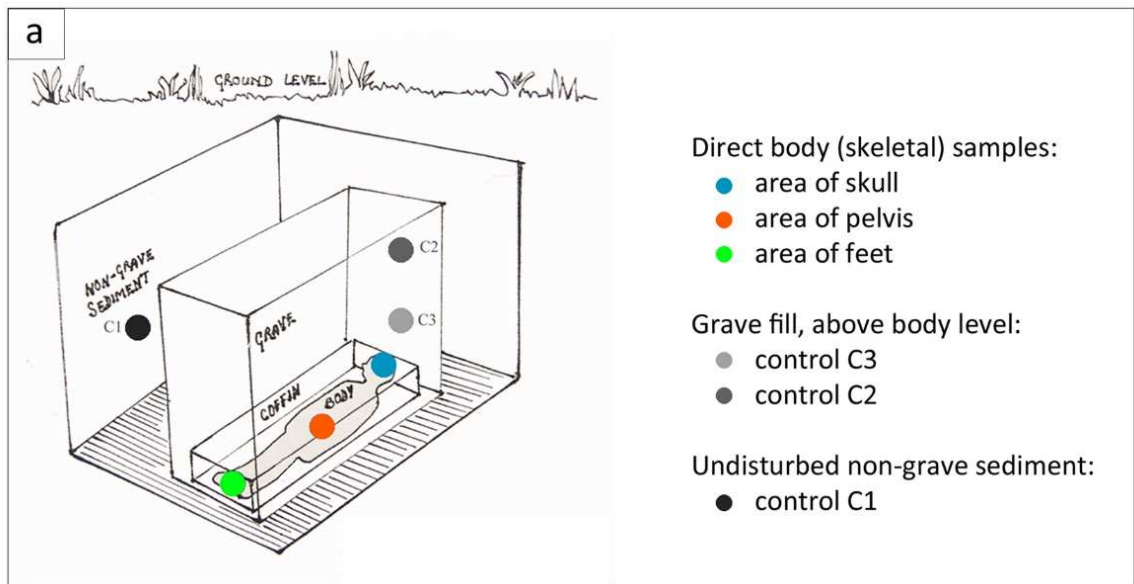
Figure 3.1: a) Sampling strategy of the InterArChive project. Samples were collected in direct contact with the skeleton in the area of the skull (blue), in the area of the pelvis (orange) and in the area of the feet (green). Controls were taken in the grave filling, above the skeletal remains level: C3 (light grey) and C2 (middle grey), and outside the infill, in non-grave sediments: C1 (dark grey). Examples of the sampling: b) C1 in Syningthwaite Priory, UK; c) C2 in Hofstadir, IS; d) C3 in Hungate, UK; e) C3 in Hofstadir, IS; f) sample from the area of the skull in Edinburgh, UK; g) sample from the area of the skull in La Compaene, FR; h) sample from the area of the pelvis in Hofstadir, IS; i) sample from the area of the feet in Thessaloniki, GR.

Each tin was annotated on both the lids with waterproof marker, indicating: orientation (up and North direction), body location, code of the site, number of skeleton or grave and side in contact with bones. The up direction was reported also on the other four surfaces of the tin. This information was important during the analysis and interpretation of data, because it gave details related to movement of soil particles and formation of coatings (see Glossary). The tin was photographed in loco, removed carefully from the sediment with a trowel, closed with the second lid and elastic bands and wrapped with plastic film. This procedure preserved the humidity and, consequently, the organic components within the sample until the phases of processing in the lab (Section 3.2), avoiding the formation of mould. In some cases, loose samples were taken in the proximity of the tins and conserved in plastic bags, in case of further analyses such as granulometry or pH levels.

The sampling record sheet included information such as: site code, skeleton or grave number, identification number of grave cut and of filling, North arrow, presence of coffin and, if possible, age of burial, sex of the inhumated, adult, sub-adult or infant. Additional fields referred to: schematic drawing of the burial, extra samples, comments, date of the recording, name of the person responsible for completing the sheet and number of pictures taken on the site. Regarding the photographical documentation, a general view of the grave was important possibly, before removing the Kubiena tins. Moreover, detailed photographs of the area surrounding each sample were encouraged.

3.2 SLIDES PRODUCTION

The samples were stored in fridges in the Mary Cudworth Lab of the Department of Archaeology, waiting to be processed by the project technician. Different methods of drying were reviewed in Chapter 2 (Section 2.3.1). In this project, the samples were dried through acetone replacement in the fume cupboard, to better preserve the high content of organic matter and to avoid possible distortions of the void structures. This phase could take several weeks, depending on the amount of water in the sediment. Once dried, the samples were impregnated by draining polyester resin through the interconnected porous and let them set (Chapter 2, Section 2.1.2; Vepraskas 1990, 16-21; FitzPatrick 1993, 2-3). Subsequently, the blocks were cut in two directions with the Delta Petrocut machine, as shown in Figure 3.2:

- longitudinal section to exploit the wider surface;
- orthogonal section to the first one, on the side closed to the skeleton, to have a section of the sediment in the proximity of the bones.

Once the section was cut, the surface of the block was polished and mounted with epoxy resin on a glass slide of dimensions 11 x 7.5 cm and ca. 0.2 cm in thickness and allowed to dry. When completely set, a thin layer was cut with the Delta Petrocut and ground to a thickness of 30 μm with the Logitech LP50 and polished with the Motopol 2000 grider/polisher and the Vector polisher (Chapter 2, Section 2.3.1; Courty 1998, 59-61; Vepraskas 1990, 22; FitzPatrick 1993, 4-6). The slides were not covered with a coverslip to allow SEM-EDS analysis.
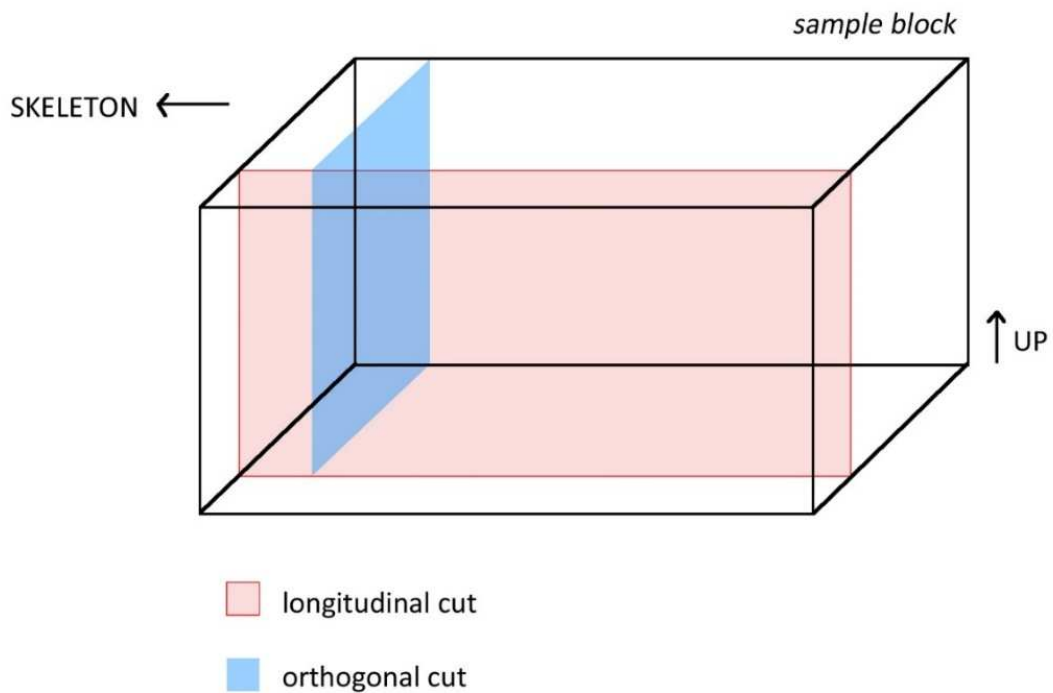
Figure 3.2: Exemplifying representation of the method used to cut the impregnated blocks. The longitudinal cut and the obtained surface are indicated in pink, while the orthogonal cut and its surface are coloured in blue.

3.3 SELECTION OF THE SITES

Five archaeological sites and three experimental burials were selected for the studies reported in this research: Hungate (Chapter 5, Section 5.1), Haymarket (Chapter 5, Section 5.2), Borgharen (Chapter 5, Section 5.3), Rossio do Carmo (Chapter 5, Section 5.4), Pill'e Matta (Chapter 5, Section 5.5) and the experimental piglet burials from Hovingham (piglet 2) and Heslington East (piglets 6 and 7) (Chapter 5, Section 5.6), listed in Appendices 1.1 and 1.2. The details related to period, grave type, soil type and climate of each site are presented in Table 1.1 (Chapter 1), and specific information is provided in Chapter 5, in the relevant sections. Micromorphological analysis, image analysis and SEM-EDS were applied to the samples of these sites. The slides, a total of 270, and the methods applied to each slide are listed in Appendix 1.6. In addition, nine other sites were chosen exclusively for the image analysis experiment (Appendices 1.1, numbers and names in italics, and

1.6). As explained in Chapter 4, the additional sites were included with the aim of increasing the range of the samples and variables from different sites and hence, performing a more complete experiment.

The selection of the sites and of individual graves was dependent on a number of different factors:

1) interest and coherence with the rationales of this research, described in Chapter 1, Section 1.2. The first rationale was to identify possible features produced by the decomposition of the corpse within the soil and how the nature of such features differs among different environments and soil types. To this end, the five types of soil offered a variance from intense water-logged and cold condition to dry and warm environment. Different sites were examined to assess the degree of variability among the sites and to assess the role of the coffin in the formation of soil microfeatures. The second rational was the understanding of the processes forming the grave infill, the movement of soil particles and fluids in the grave, the role of coffin and corpse decomposition in this movement. The third rationale was the assessment of a standardized method for the micromorphological analysis of burial sediments;

2) availability of information related to the sampling and archaeological excavations, because, as illustrated in Table 3.3, record sheets, photographs and reports from the archaeologists were missing or not accessible in some cases;

3) the graves with complete standard sampling in all of the anatomical locations were favoured. Occasionally it was not possible to take all of the samples requested by the protocol, because of the condition of some grave (e.g. missing part of the skeleton);

4) good quality of the manufacture of the thin sections. Some slides had the wrong thickness or they were partially damaged during the phases of production. For this reason, graves with good quality of slides were preferred. However, in the case of Haymarket, most of the slides were damaged due to poor preparation procedures (Appendix 1.5);

5) requirement from the InterArChive project to examine all of the sites, assigning different case studies to the five members of the team responsible for the micromorphological analysis.

All the case studies, except for Haymarket and the experimental piglets, were excavated and sampled before the author joined the project in 2012. Some of the case studies had already been analysed. Considering the remaining sites available (factor 5 above), and the quantity and quality of accessible information (factor 2 above), the author selected 5 case studies and 3 experimental piglet burials according to the rationales of this research (factor 1 above).

Considering the first and the second rationales, it was fundamental to select different types of soils, and graves (Table 3.1). In addition, the cemetery of Haymarket was chosen also for its proximity with Hungate, to investigate differences and similarities between the two of them, while Rossio do Carmo and Pill'e Matta aroused interest for the peculiarity of their burial practices and for the investigation of the organic matter preservation in different conditions. The choice of the experimental burials was subject to the selection of the case studies, because the purpose of the experimental burials was to procure reference material to compare with the archaeological burials. Piglets 6 and 7 were deposited in sandy soil, becoming comparable with Hungate, Haymarket and Borgharen; while piglet 2 was buried in limestone, being a good example for Pill'e Matta.

SITE	1° RATIONALE		2° RATIONALE
Hungate	Sandy clay soil	Water-logged	Wooden coffin
Haymarket	Sandy clay soil	Rarely water-logged	No coffin/ wooden plank (?)
Borgharen	Sandy soil	No water-logged	Wooden coffin
Rossio do Carmo	Sandy loam soil	Dry	No coffin/ schist plaques
Pill'e Matta	Limestone and sandstone	Dry	Chamber
Piglet 2	Limestone	-	Coffin
Piglet 6	Sandy clay soil	Water-logged	No coffin
Piglet 7	Sandy clay soil	Water-logged	Wooden coffin

Table 3. 1: Summary of the characteristics of the case studies in relation to the rationales of this research. Different types of soil were important to investigate the first rationale, while different types of graves for the second rationale.
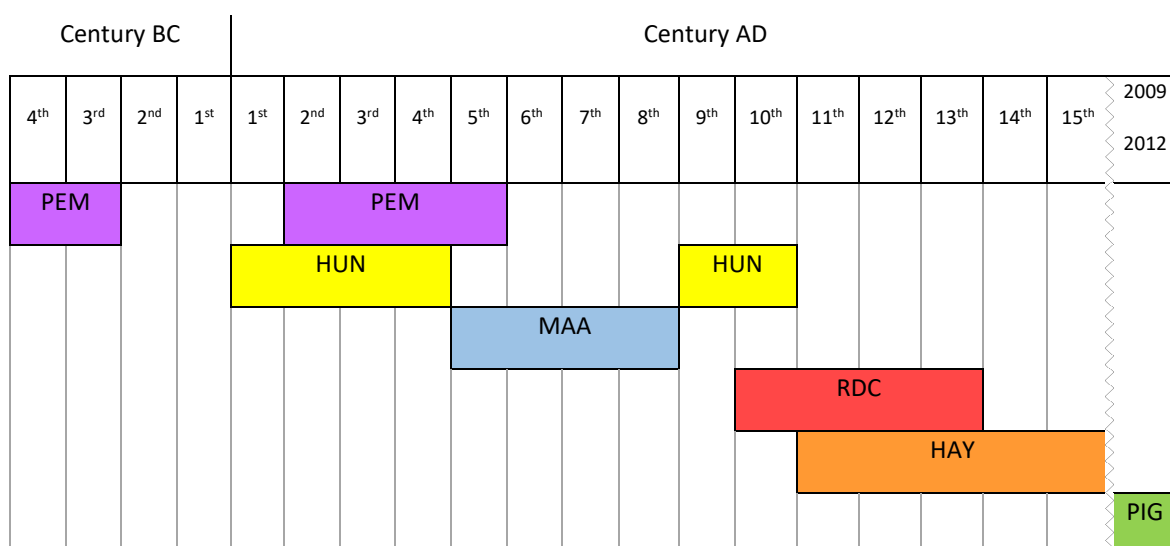
Table 3.2: Archaeological sites sampled and analysed in this research, organised according to their chronology. The abbreviations are the ones used during the sampling and adopted by the project: PEM= Pill'e Matta; HUN= Hungate; MAA= Borgharen; RDC= Rossio do Carmo; HAY= Haymarket and PIG= piglets.

The cemeteries selected in this research dated to different periods, as shown in Table 3.2, but this was not considered an over-riding criterion for the selection of the sites. However, it was considered as possible relevant factor for the observation of post-depositional processes in the analysis and discussion of the data (Chapter 6).

Once the sites were chosen, the selection of the graves (listed in Table 3.3) was dependant to the availability of complete sampling (factor 3 above) and to the quality of the slides (factor 4 above). However, in some cases, it was not possible to have a complete documentation, as shown in Table 3.3.

SITE	GRAVE	RECORD SHEET	PHOTOGRAPHS	INFORMATION FROM ARCHAEOLOGISTS
Hungate	51349/51351	✓	✓	✓
	51350/51364	✓	✓	✓
	52253	✓	N/A	✓
	53700	✓	✓	✓
	54077	✓	✓	✓
	54296	✓	✓	✓
	54931/54909	✓	N/A	✓
Haymarket	83012	✓	N/A	N/A
	84700	✓	N/A	N/A
	84779	✓	N/A	N/A
	84851	✓	N/A	N/A
Rossio do Carmo	395	✓	✓	N/A
Borgharen	15	✓	✓	✓
Pill'e Matta	237	N/A	✓	N/A
	238	N/A	✓	N/A
	268	N/A	N/A	N/A
	2680	N/A	N/A	N/A
Heslington East	6	✓	✓	N/A
	7	✓	✓	N/A
Hovingham	2	✓	✓	N/A

Table 3.3: List of the sites and graves analysed through micromorphology for this research. The tick indicates the availability of record sheets, photographies and site information from the archaeologists.

Inconsistent sampling and poor preservation characterized some of the samples in Borgharen, Rossio do Carmo and Pill'e Matta. In some graves of these and the other sites, pictures and notes were not taken and, in addition, in a few cases, data that were originally recorded, such us orientation of the tin, were omitted and lost by the technician responsible for preparation of the thin section slides processing (Haymarket and piglet burials). The cemeteries were sampled between 2009 and 2012, while the piglets were excavated in the summer months of 2012 and 2013. The author participated to the sampling of the experimental burials and of two graves in Haymarket (not analysed in this research), which was the last archaeological site to have been sampled when she joined the project in 2012. The InterArChive team provided most of the information related to the graves, which were used and included in this research. However, some information was lacking and it was not possible to obtain it. A summary of the information related to all of the slides is shown in Appendix 1.5, indicating when available: accurate location of the sample and not only of the body position (for example which was the exact position of the tin in relation to the skeleton, generally visible through a picture or a sketch), orientation of the slide (up), relation with the bones (which side of the sample was in contact with them), quality of the manufacture of the slide (0= less than 50% of the slide was visible and analysable; 1= more than 50% of the slide was visible; 2= 100% of the slide was visible).

Over the period of the InterArChive project, different technicians were involved in the production of the slides; there were considerable differences in the quality of slide manufacture.

- Borgharen and Rossio do Carmo: David Broughton;
- Hungate: Annika Burns;
- Pill'e Matta: Annika Burns, Harry Wyn Williams and Emma Tong;
- Haymarket: Emma Tong;
- Heslington East and Hovingham: Emma Tong (processing and production of slides) and Annika Burns (production of slides).

Considering the opportunity to examine a large number of slides, combined with an extensive sampling in Hungate and Haymarket, all of the slides made from these two sites, and not exclusively the ones from the graves listed in Table 3.3, were observed in order to increase the understanding of the selected graves.

3.4 METHODS

Thin sections were analysed through three methods: micromorphology of soils, image analysis and SEM-EDS. The former was applied to the selected graves from Hungate, Haymarket, Borgharen, Rossio do Carmo and Pill'e Matta (152 slides). As mentioned at the end of Section 3.3, micromorphological observations for specific features were implemented on all of the available slides from Hungate and Haymarket (83 slides). In addition, the slides analysed through micromorphology were digitized, creating photo-mosaics (158 slides). Image analysis was applied to all of the selected graves and to other 9 sites sampled by the team, in order to increase the data for the experiment described in Chapter 4 (144 slides). SEM-EDS was applied to some of the samples of Hungate, Borgharen and Pill'e Matta, to provide micro-chemical data of fine material and inorganic pedofeatures of uncertain interpretation (20 slides). The complete list of the slides and the related methods applied are consultable in Appendix 1.6, while a scheme of the process of research is shown in Figure 3.3 at the end of this chapter.

3.4.1 MICROMORPHOLOGY OF SOILS

Micromorphology was selected as main method of investigation of the burial sediments at the microscopic level. It offered the opportunity to observe the microstructure of the fabric, the presence of indicators such as neoformed minerals and the characteristics of microscopic remains, such as organic components or traces of micro and mesofauna activities (rationales 1 and 2, Chapter 1).

Thin sections were analysed with the standard petrographic microscope Axio Lab.A1 Zeiss and the AxioVision Imaging System software, using plane polarized light (PPL), cross polarized light (XPL), oblique incident light (OIL) and, in a few cases, fluorescence microscopy. Plane polarized light (PPL) allowed the identification of mineral properties, such as colour and pleochroism (the change in colour with rotation of the microscope stage), crystal form, shape, refractive index and relief. Under cross polarized light (XPL), it was possible to distinguish isotropic minerals from anisotropic. The first transmit PPL, but are in extinction under in XPL, such as glass. The second transmit light in some orientation under XPL but go in extinction at point as the stage of the microscope is rotated through 360°. Oblique incident light (OIL) is based on the principle that absorption or reflection of emitted light varies according to the type of magnification that is illuminated. It was used to identify opaque and quasi-opaque minerals and to distinguish small fragments of charcoal from Fe/Mn nodules (Vepraskas 1990, 24-36; FitzPatrick 1993, 10-15; Stoops 2003, 152). Finally, fluorescence microscopy is based on the property of several substances to emit secondary luminous energy of higher wavelength when they are excited by primary energy of short wavelength, such as green light, blue light, ultra-violet light and infra-red light. It was applied to detect accumulation of

phosphate and organic components (Courty, Goldberg and MacPhail 1989, 44-50; Vepraskas 1990, 24-37; Stoops 2003, 20-27). The objective used were: 2.5x, 5x, 10x, 20x and 40x.

The standard methods proposed by Stoops (2003) and Bullock et al. (1985) were adopted for the description of the slides. However, inorganic components with organic origin and the anthropogenic materials were classified differently (see the following section and Appendix 1.7). The percentages of fine material, peds, voids, mineral and organic components, pedofeatures and anthropogenic material were recorded as semi-quantitatively measurements and, for this reason, the graphs in Chapter 5 are displayed with an error bar of 5%.

In this research, the report of micromorphological analysis was organized in tables, considering the standard methods, the requirements of the project and the protocols applied by the other members of the team. The organization of data in tables permitted a clear and immediate understanding of the characteristics of the samples and gave the potential to compare the data between graves and sites. The structure of the table is shown in Appendix 1.7, while all of the reports are included in the Supplementary Data (DVD, Micromorphological analysis) attached to this thesis. The table was structured in five sections:

1) The first section of the table contained the information regarding the grave and the sample:
    - slide number: the unique number given to each thin section, followed by the abbreviation of the site;
    - body position: the region of the body which the sample was taken from;
    - orientation: if present, the direction of the up of the sample and its relationship with the skeleton and the location of the bones;
    - location: number of the grave, name of the site and city or village of the site;
    - slide area and percentage of the slide: if the slide was characterized by areas with different coarse/fine distribution patterns, number of the area in progression (ex. 1-2-3) and percentage of the covered area;
    - c/f limit (coarse/fine fabric unit limit): established at 50 µm by the InterArChive team.

    On the right of the table, a schematic representation of the skeleton (human or swine) was coloured to highlight the body region from which the sample was collected.

2) The second section included:
    - elements of fabric: the spatial arrangements of the soil components, in detail the type of coarse/fine related distribution, sorting of the coarse material, basic distribution, basic orientation, referred distribution and referred orientation;

- fine material: characteristics of the fine material regarding limpidity, b-fabric, abundance, PPL colour and XPL colour;
- peds: characteristics of the aggregates regarding type, abundance, size, accommodation and development;
- voids: characteristics of the soil pores regarding type, abundance, size and surface.

3) The third section concerned coarse material, divided in mineral and organic components:
- mineral components: type, frequency, size, shape, weathering, PPL colour and XPL colour. This group included mineral grains and foraminifera. These last were part of the eroded rock and they differentiated from the shells of mesofauna;
- organic components: type, frequency, size, shape, surface, weathering, PPL colour and XPL colour. This group included organic matter, inorganic components whose origin was organic or related to an organic possessor (bones or shells) and post-depositional organic material, such as roots and fungi. In the case of piglets, roots were included in the sediments during the burial, and possibly it happened the same in other graves. The choice to include the inorganic components with organic origin was to delineate a distinction from the mineral components which were part of the soil texture.

4) The fourth section inspected the pedofeatures, or rather features resulting from a change in composition or fabric of the groundmass, or that do not enclose groundmass material (Stoops 2003, 102-103) and anthropogenic material, as exotic component. This group was described by type, frequency, size, shape, surface, weathering, PPL colour, XPL colour, distribution, orientation, b-fabric and ID name.

5) The fifth section offered the chance to annotate notes and information, which were not contained in the previous entries.

A glossary at the end of the thesis explains the main technical terms used in the description of the slides.

The observation of the thin sections through the petrographic microscope and their analysis and description, completing the table explained above, were followed by the elaboration of histograms to compare the data within individual graves and among the graves from the same site, or from different sites. The results are illustrated in Chapter 5. The discussion and interpretation of the results are presented in Chapter 6.

3.4.2 PHOTO-MOSAICS AND MAPPING

All of the slides selected for the micromorphology, and a few more, were digitized through the AxioVision Imaging System software and the Axio Scope.A1 Zeiss microscope, provided with a mechanical stage and connected to a computer and camera. The photo-mosaic was the digitized

photographic reproduction of the entire slide, or of an area, composed by several pictures taken in sequence at high magnification. This method offered the opportunity of recording all of the slides in detail and readily observing them without recourse to the microscope. In addition, the photo-mosaics were annotated with the location of the most interesting features. Finally, the photo-mosaics were used for the SEM-EDS analysis (Section 3.4.4).

In the present research, all of the photo-mosaics were taken with an objective of 5x and a resolution of 150 pixels, to have enough details, but at the same time to not generate excessive sized images and, hence to prevent the computer crashing. The photo-mosaics were annotated with a scale bar and saved as .zvi (AxioVision file), to have a copy in the original format that contains full detail, .jpg for the use of images in the thesis and .tiff for the use with SEM-EDS. A second phase of annotation, regarding the most interesting features, was performed with Adobe Photoshop, which is a faster software with which to graphically elaborate than AxioVision, enabling the creation of maps from the slides. These maps were used in the interpretative process. All of the maps/photo-mosaics have been included in the Supplementary Data (DVD, folder "Mosaics") attached to this thesis.

3.4.3 IMAGE ANALYSIS

Image analysis is a quantitative method to analyse features of thin sections using digital images (Chapter 2, Section 2.2; Murphy et al. 1977a, 1997b; Vepraskas 1990, 97; Bui 1991; FitzPatrick 1993, 22-29; Stoops 2003, 150-152). It was applied in this research to measure the porosity of the samples and in the attempt to identify changes in the frequency of the voids, in relation to anatomical locations and to the different depth of the grave fill. It was of interest in this research to investigate the movement of soil particles and fluids within the grave, to detect eventual patterns of soil porosity within the graves and the layers above, investigating the role of the skeleton and coffin as possible barriers to this movement (Chapter 1, Section 1.2; Chapter 4, Section 4.4). Selected areas of the thin sections were captured as photo-mosaics, processed to isolate the voids from the rest of the groundmass and their frequency was measured. Hence, the Axio Scope.A1 with the AxioVision Imaging System software were used for this analysis. The protocol of the image analysis applied by the other members of the InterArChive project was not considered convincing in this research. For this reason, an experiment was carried out on 144 slides, to examine the level of accuracy of the old method and to find a possible correction. The experiment is carefully explained in Chapter 4. In addition, the frequency of porosity recorded by image analysis was compared with morphology, size and other characteristics such as infillings of the voids observed in the same samples by micromorphological analysis, to investigate in which cases the variance of porosity was caused by biological activity due to the actions of micro and meso-fauna (Chapter 6, Section 6.2).

3.4.4 SEM-EDS

SEM-EDS analyses (Chapter 2, Section 2.3) were employed with an EVO MA 15 Zeiss scanning electron microscope with workflow automation and INCA Software in the University of Stirling, to provide micro-chemical data of fine material and inorganic pedofeatures of uncertain interpretation (Courty 1989, 50-51; FitzPatrick 1993, 32-33; Goldberg and Macphail 2006, 363-365). The data, representing the weight (%) of chemical elements, were presented in box-plots and the variation of the chemical elements provided information to detect the origin of the pedofeatures or the elemental composition differences in the fine material.

The scanning electron microscope and the working area were composed of: the vacuum chamber of the microscope, where the sample was inserted and analysed; a screen where to follow backscattered images from the camera; a controller to move the stage inside the chamber; a screen where to display the photo-mosaic of the slide; and a screen and connected computer to work with INCA software and process the information and the analyses.

The slides were not covered by a coverslip to permit the analysis. Three copper triangles (ca. 0.5 mm of side) were located on each slide to equip the sample of three not equivocal coordinates, which were "anchored" to the triangles in the photo-mosaic. The latter worked as guide to move through the sample and select the area to analyse. The analyses were carried out selecting a region of interest and proceeding in the measurements forming line profiles or maps of the specimen. Calibration was achieved through the analysis of standard cobalt every two hours and standard dolomite at the beginning of each session.

In conclusion, the process of sampling and analysis applied in this research is summarised in Figure 3.3. The first step was the sampling of undisturbed soil samples from the burial sediments (Section 3.1). It was performed in the first stage of the InterArChive project, between 2009 and 2012. The author sampled two graves from Haymarket (83015 and 84579), which were not analysed in this research because the slides were not processed by the technician, and the experimental burials of piglets 1, 5-10. The second step was the slide production, described in Section 3.2. This was performed by the technicians. The author helped with the production of slides from the burial of piglet 2. The third step was the selection of the case studies and of the graves by the author, on the base of the rationales and criteria explained in Section 3.3. The fourth step was the analysis of the samples, which could be divided in four work-packages according to the different methodologies (Chapter 5). All of the photomosaics presented in this research (Supplementary Data, Mosaics), the micromorphological analyses, the creation of the table for the recording (Appendix 1.7), the image analysis experiment and all of the measurements, and the SEM-EDS analysis were performed by

the author. The pictures and all of the material presented in this thesis, excluding when explicitly acknowledged, were produced by the author. The fifth step involved the integration of the data from the different analyses, their discussion and interpretation (Chapter 6).
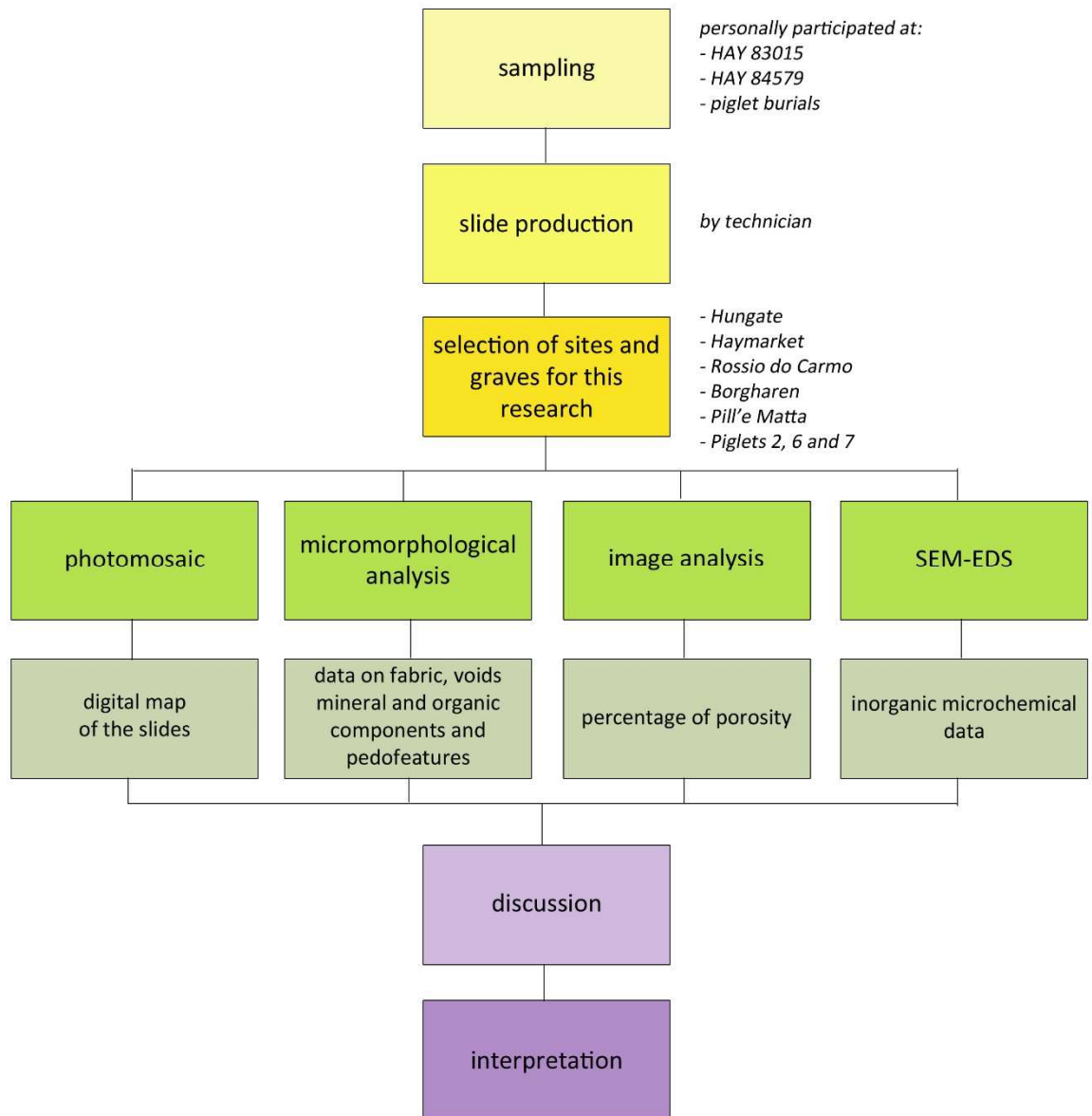
Figure 3.3: Illustration of the methodological process applied to this research.

Chapter 4. IMAGE ANALYSIS EXPERIMENT

Image analysis is a quantitative method for analysing features of thin sections using digital images. As introduced in Chapter 3, Section 3.4.3, this method was applied in this research to measure the porosity of the samples and in an attempt to identify differences in the frequency of the voids in relation to body location and from the backfill within the grave to the surface.

Different ways can be used to measure porosity, as reviewed in Chapter 2, Section 2.3.4, depending on the manufacture of the slides and the type of equipment. One method, nominated A in this chapter, was developed by the InterArChive team during the early stages of the project and applied to slides from some of the sites studied in the project (Lang 2014).

During the application of Method A, this author noted inaccuracies in the process to obtain the results. To determine if these inaccuracies were relevant, Method A was tested and, simultaneously, two variations of the method were applied and examined (Methods B and C). The original view was that the inaccuracies were caused by the wrong choice of angles between the polarizer and analyser, so changes to the angles were applied. The validity of methods A, B and C was assessed by comparison with a fourth Method, D, which relied on the use of Adobe Photoshop software. The results from Methods A, B and C were found to be inconsistent. A new Method, called E and based on different procedures, was created and tested on the same slides. Furthermore, Method E was also evaluated by comparison with Method D. Method E, applied for the first time in this research, was determined to be accurate and appropriate for the manufacture of slides and the type of equipment available.

The methods and tests were applied to 144 slides, including slides from the archaeological case studies selected for this research and slides from another 9 sites sampled by the InterArChive team (Appendix 1.6). The additional sites were included with the aim of increasing the range of the samples and variables from different sites and hence, performing a more complete test. Methods A, B, C and D were applied to the exact same position in each slide (Appendix 2.1). Method E was performed later, so the areas selected were not exactly coincident with the previous ones. However, the same regions of the slides were examined and the dimensions over which the measurements were performed conformed to the analyses performed using Methods A, B and C. Method D was applied a second time to the new areas selected for Method E (Appendix 2.2).

The differences between the methods, the results obtained and the inaccuracies identified are explained and discussed in this chapter. Once the suitability of the Method E was confirmed it was

applied to the experimental piglet burials and to grave 83012 from Haymarket, the slides from which had not been ready at the time of the development of the image analysis approach. The results obtained in each of the case studies is presented in this chapter, whereas the discussion relating to the possible significance of differences in porosity is included in Chapter 6 and integrated with the micromorphological and SEM-EDS results (Chapter 5).

4.1 BASIS FOR THE APPLICATION OF IMAGE ANALYSIS

The equipment used for the image analysis included: Axio Scope.A1 Zeiss microscope, AxioVision Imaging System software and, separately, Adobe Photoshop software. The objects of the investigation were the same slides used for micromorphological and SEM-EDS analysis. The full extent of the area examined for each thin section was photographed using the method applied for the mosaics, as described in Chapter 3, Section 3.4.2. The selection of the area was determined in order to examine heterogeneous and highly representative portions of the thin sections. Thus, the dimensions of the areas were variable, but included between 1717 x 1243 and 2970 x 1848 pixels with a resolution of 150 pixel/inch.

Porosity in the thin sections was measured as a percentage of the area occupied by voids. Working with digital images allowed the isolation of voids from the rest of the features through establishment of a threshold. The composition of the pictures from defined units, pixels, permitted selection on the base of the RGB code of pixels, i.e. by differences in colour. The aim was to select the pixels within the mosaic that made up the voids and measure them using the AxioVision Imaging System software. This type of software did not permit the differentiation between different void types of different origin.

As explained in Chapter 2 Section 2.3.4, among the different methods applied to image analysis, the best results on voids have been obtained on samples impregnated with resin mixed with fluorescent dye and photographed under UV light illumination: the pores fluoresce and the mineral grains stay non-birefringent (FitzPatrick 1993, 22). However, the resin impregnated blocks prepared for the InterArChive project were impregnated with polyester resin without any dye (Chapter 3, Section 3.2), so a different solution had to be considered. It is well established that assessing porosity from pictures obtained under circular or plane polarized light, or between crossed polars, can be problematic, producing over-estimation caused by the characteristics of mineral grains. Voids are transparent in PPL and isotropic in XPL, but the same happens for some minerals, especially quartz, when they exhibit basal sections in PPL or they are in extinction in XPL (FitzPatrick 1993, 22). The solution is offered by combining several images of the same area, photographed with different types of illumination (FitzPatrick 1993, 29-30). Thus, the question in this research was

to define the right combination of images to obtain results with very small errors. The second important point was to elaborate a standardized method, in which the interference of the operator was reduced as much as possible, to diminish the consequent error and to favour the rapidity of analysis.

4.2 TESTING THE INTERARCHIVE PROTOCOL FOR IMAGE ANALYSIS

4.2.1 METHOD A

Method A was elaborated and applied by some members of the InterArChive team at the beginning of the project, as mentioned in the Introduction to this chapter.

The method is illustrated in Figure 4.1 and explained below. It can be summarized in four principal steps: recording three mosaic images, thresholding the voids, combining the mosaic images and measurement of porosity.

Mosaics of the same area were taken under three different angles of cross-polarized light:

- polarizer at 0° and analyser at 30° (Figure 4.2.a);

- polarizer at 0° and analyser at 60° (Figure 4.2.b);

- polarizer at 0° and analyser at 90° (Figure 4.3.c).

Voids were separated from the other features in each mosaic with the threshold function: all the pixels with the same RGB code were highlighted at the same time with a click of the mouse on them. Once all the areas related to voids were thresholded, the new pictures were saved. Pictures were in black and white, where white represents the voids and black all the other features (Figure 4.2.d-f).

It was noticeable that the threshold in each picture also included mineral grains and, on few occasions, bone fragments. Moreover, the voids were not always completely incorporated within the selection. Light colouration in the fine material was also affected and, in a few cases, added to the area identified as pore space. In addition, the use of a mosaic obtained with the analyser at 90° was considered superfluous in many cases. In fact, in many of the mosaics obtained, the fine material was so dark that it was quite difficult to distinguish it from the voids and, as a consequence, the selection of voids was done only on very small areas, to avoid erroneous choices. Hence, the use of this mosaic and its selection did not bring any new information regarding the presence of voids. Moreover, it was observed that some mosaics taken at 90° cross-polarized light were subject to problems relating to the light source: they appeared with boundaries of each single photograph, composing the mosaic, in lighter colour (Figure 4.2.c). As a result, the mosaic showed an internal

grid of lighter pixels, which adversely influenced the selection of pixels (Figure 4.2.f). This aspect affected all the process, integrating incorrect information to the final picture, to the threshold and, finally, to the measurement of porosity. Lastly, relatively little difference in thresholded areas was observed in the mosaics taken at 30° and 60° cross-polarized light, making one of the two effectively redundant.

In conclusion, careful visual comparison between the slide under PPL and the final black and white mosaic of the selected area, highlighted discrepancies: not all pores were isolated (white areas), while some mineral grains were selected as pores. Since the white areas (pores and some mineral grains in this case) were measured as voids by the software, the inclusion of the minerals and the exclusion of some voids affected the final result. This visual observation was confirmed by the results of the test applied on Method A (Section 4.2.4).

The composition of the three new black and white pictures was made using the software processing function -arithmetical add. One picture was added each time and the final image was in grey scale, where white represented the area of voids, black the non-void area in common to all three pictures and grey the area of non-intersection, or rather the area selected as void in one or two mosaics and as non-void in the other one or two mosaics (Figure 4.2.g-h). This process was completed to solve the inclusion of mineral grains, bone fragments and fine material. However, by attentive observation, it was evident that some mineral grains, as well as other features, remained included as voids. It was clearly visible that the area isolated as pore space was higher than the true value. The idea behind this protocol was that combining the three thresholded mosaics through the mathematical add logarithm and converting the final picture to a binary image, the grey areas would have been integrated with the black ones. On the contrary, they were integrated with the white areas, becoming voids even if they were not.

According to Lang's thesis (2014), the binary image has to be processed, changing the definition of the pixels (Processing – Morphology – Grey open – Change cross 4 – Ok). However, with or without this procedure, the measurements gave the same results, so it was considered as a redundant manipulation.

The final step was to start the measurement and calculate the percentage of void space (Figure 4.2.i).

As stated, the area of voids was higher than the real one and, looking at the final binary image, this was obvious by naked eye. However, to avoid empirical considerations and to establish the range of the error, the measurements were conducted on 144 slides (results in Appendix 2.3 and below in Section 4.2.4) and controlled with Method D, explained below in Section 4.2.3.
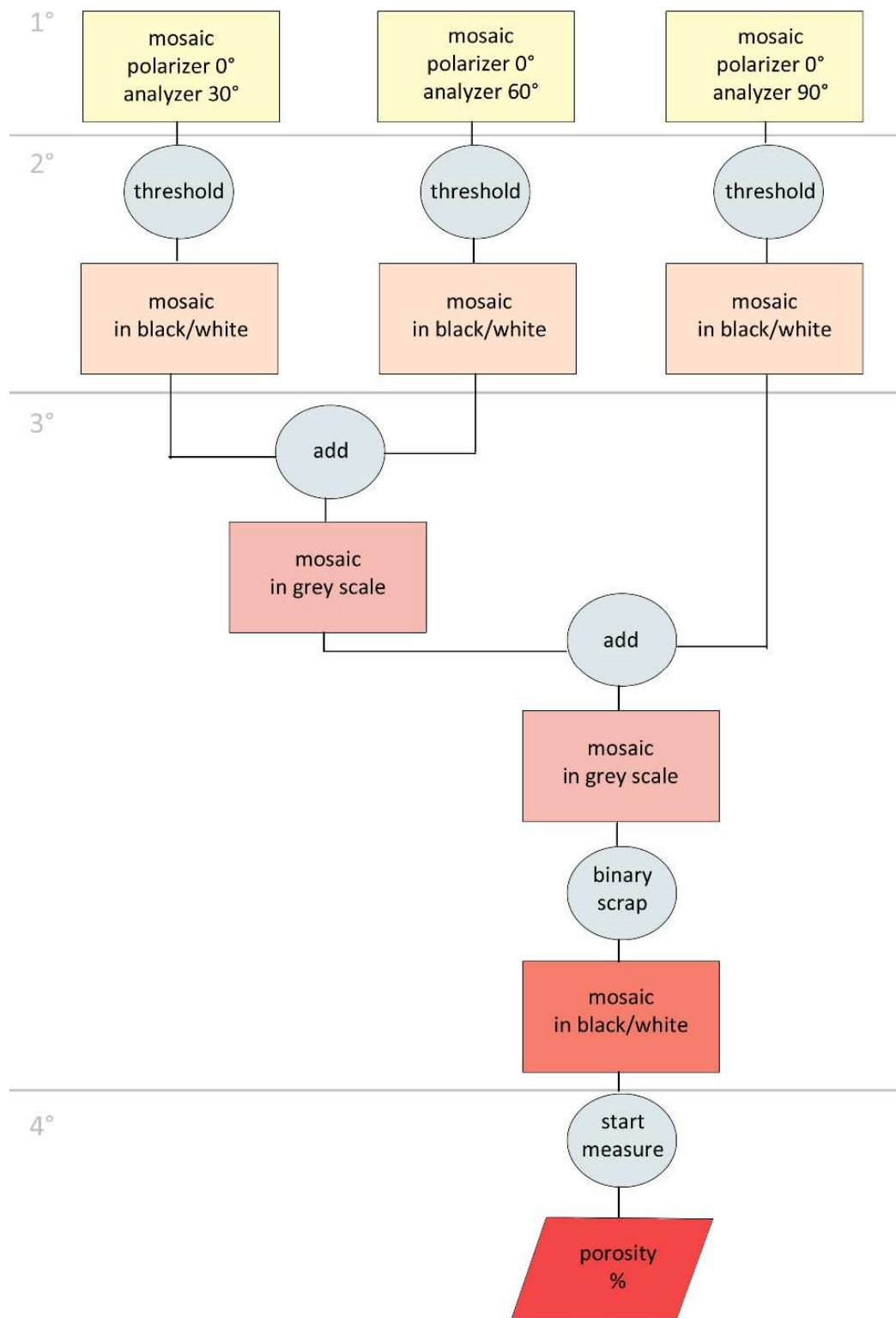
Figure 4.1: Image analysis of soil porosity. Scheme illustrating the procedural steps applied in Method A. Three mosaics of the same area were taken under different angles between analyser and polarizer. The new images in black and white were generated by mathematical addition, creating a new mosaic in grey scale. After the binary scrap process, the porosity was measured on the white areas.
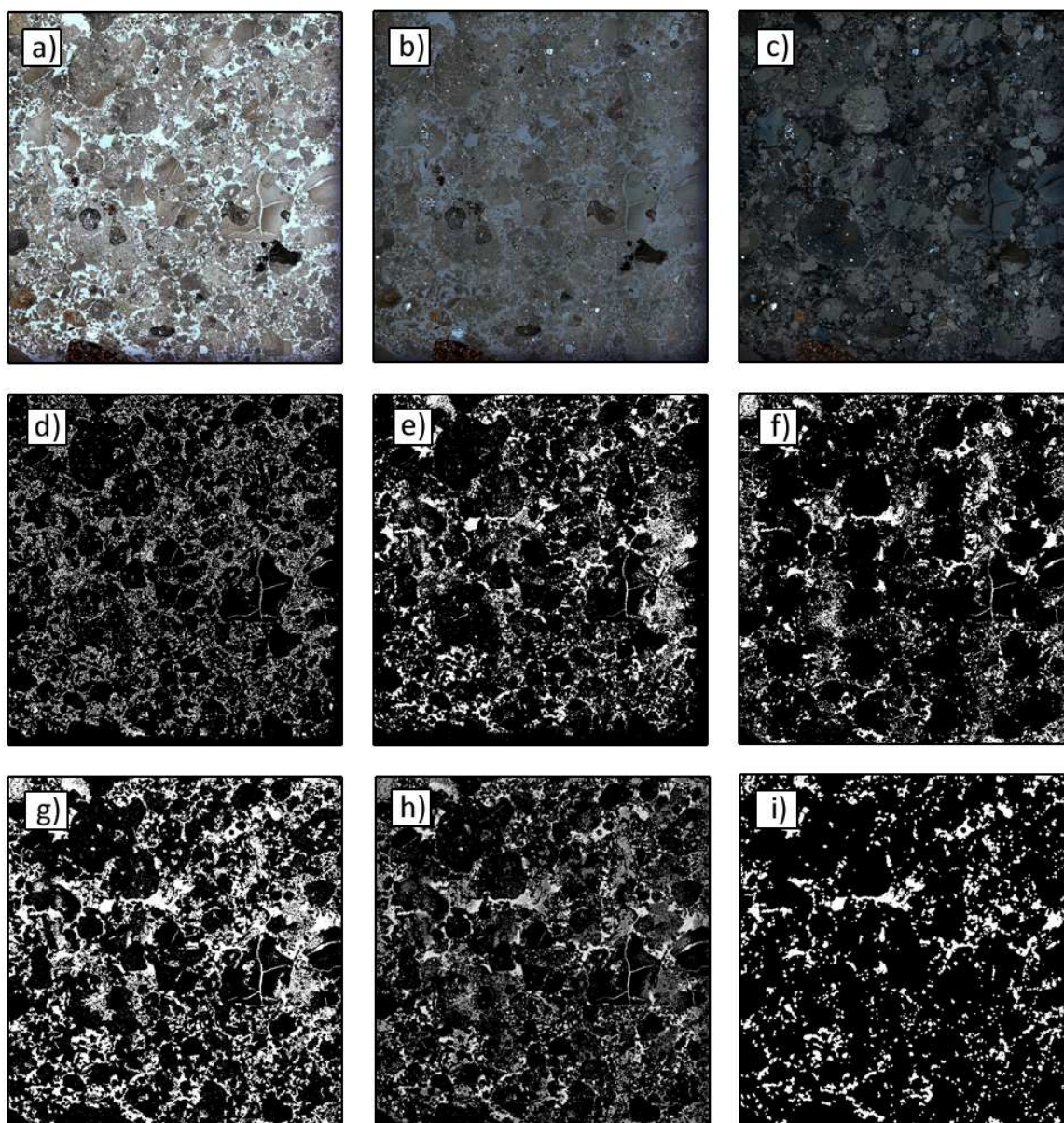
Figure 4.2: Examples of images obtained through the application of Method A. a) mosaic with polarizer at 0° and analyser at 30°; b) mosaic with polarizer at 0° and analyser at 60°; c) mosaic with polarizer at 0° and analyser at 90°; d) binary image from the threshold of mosaic (a); e) binary image from the threshold of mosaic (b); f) binary image from the threshold of image (c); g) grey scale image from the addition of figure (d) to (e); h grey scale image from the addition of figure (g) to (f); i) binary image from the binary scrap of image (h). Image (i) is the one used for the measurement of pores.

4.2.2 METHODS B AND C

During the first attempts of image analysis, it was recognised that Method A was an inaccurate approach. It was hypothesized that the error was caused by the erroneous choice of angles between the polarizer and analyser. Consequently, changes to these angles was considered, with the aim of detecting all of the mineral grains. Moreover, the explanation regarding the choice of the angles 30°-60°-90° was not provided by the members of project using Method A. Methods B and C followed the same steps as Method A (Figure 4.1).

Three different angles between polarizer and analyser were selected for Method B:

- polarizer at 0° and analyser at 0°;

- polarizer at 0° and analyser at 45°;

- polarizer at 0° and analyser at 90°.

In method C only two mosaics were taken, instead of three, to verify if the mosaic with polarizer at 0° and analyser at 45° was superfluous for the recording of data:

- polarizer at 0° and analyser at 0°;

- polarizer at 0° and analyser at 90°.

The process to combine the figures and to measure the porosity was exactly the same as that used for Method A and it was applied to all 144 slides, on the same areas that were analysed using of Method A (results in Appendix 2.3 and below in Section 4.2.4).

4.2.3 METHOD D

Method D was developed as a control method: it offered the opportunity to control the selection of each void. However, it was not used as the method for the image analysis because it was time-consuming and not suited to use in a standardized approach. Moreover, the operator had a major role in the selection of voids, while one of the aims of this experiment was to establish an automated method.

Method D was divided into three steps:

1) acquisition of the mosaic in PPL;
2) selection of the area of voids by Photoshop;
3) measurement of porosity by AxioVision software.

The main difference of the threshold operation between AxioVision and Photoshop was the possibility, in the second case, to select contiguous pixels with the "magic wand" tool. Consequently, the pixels with the same RGB code were not highlighted at the same moment, but only the pixels contiguous with the chosen ones. Thus, the author had the opportunity to select single voids by selecting the exact RGB code, thus excluding mineral grains or other features. The selection was possible because the mosaics were taken with sufficiently high resolution to magnify the image and detect each single grain or small pore. Moreover, the samples were previously observed with the petrographic microscope, to acquire confidence in the differentiation of the features for each sample.

Once all of the pores were selected, their area was filled with a contrasting colour, generally red or green, because these colours were unlikely to be present within the slides (Figures 4.3.b and 4.3.e). All the red or green pixels were thresholded at the same time and their inverted selection allowed simultaneous selection of all the non-pore features. This area was filled with black. The red pixels of the voids were then filled with white by substitution (Figures 4.3.c and 4.3.f). This last step was necessary, because when a picture was thresholded with AxioVision, the area of voids was highlighted in red. Thus, it was important to have a white base, to check the complete selection of the area. The selection with Photoshop was time-consuming, because it required an attentive examination of the mosaic at high definition, to reduce at minimum the possibility to exclude a void or to include a mineral grain.

The final pictures (Figure 4.3.c and 4.3.f) were already binary, hence it was possible to open them with AxioVision, do the threshold on the white areas and apply the software option - start measurement.

This type of measurement was conduct on all the 144 slides, on the same areas of Methods A, B and C and the results are presented in Appendix 2.3.
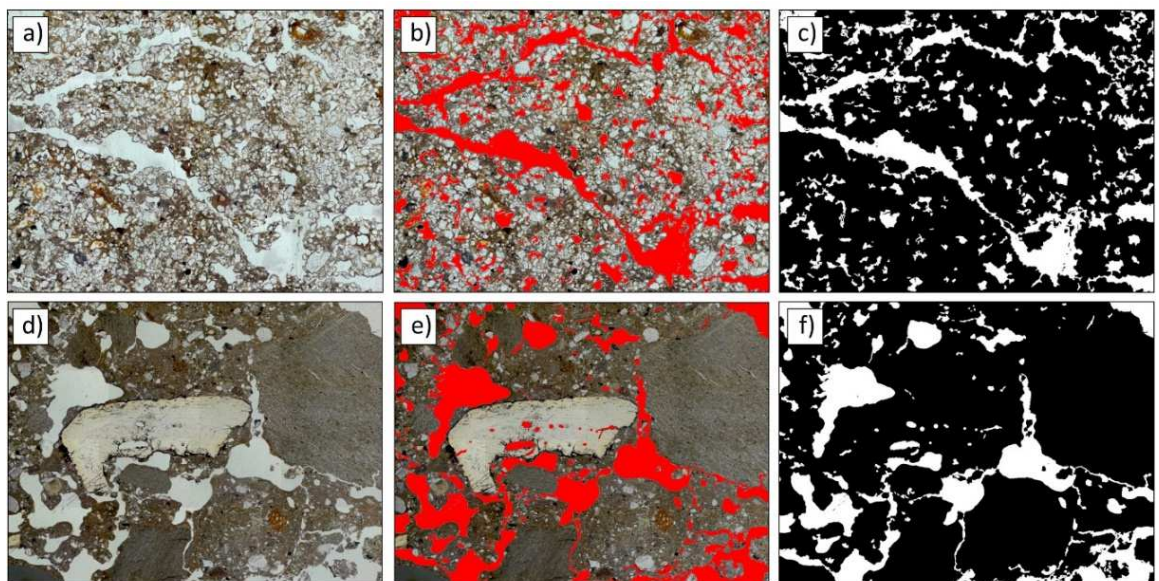
Figure 4.3: Examples of images obtained through the application of Method D. a,d) mosaic taken with polarizer at 0° and without analyser; b,e) selection of the area of voids with the "magic wand" tool and filling of the area in red; c,f) final image in which the area of voids is white and the area of soil and other components is black.

4.2.4 RESULTS FROM METHODS A, B, C AND D

Results from the application of Methods A, B, C and D are presented in Appendix 2.1 and in the graphical form (Figure 4.4).
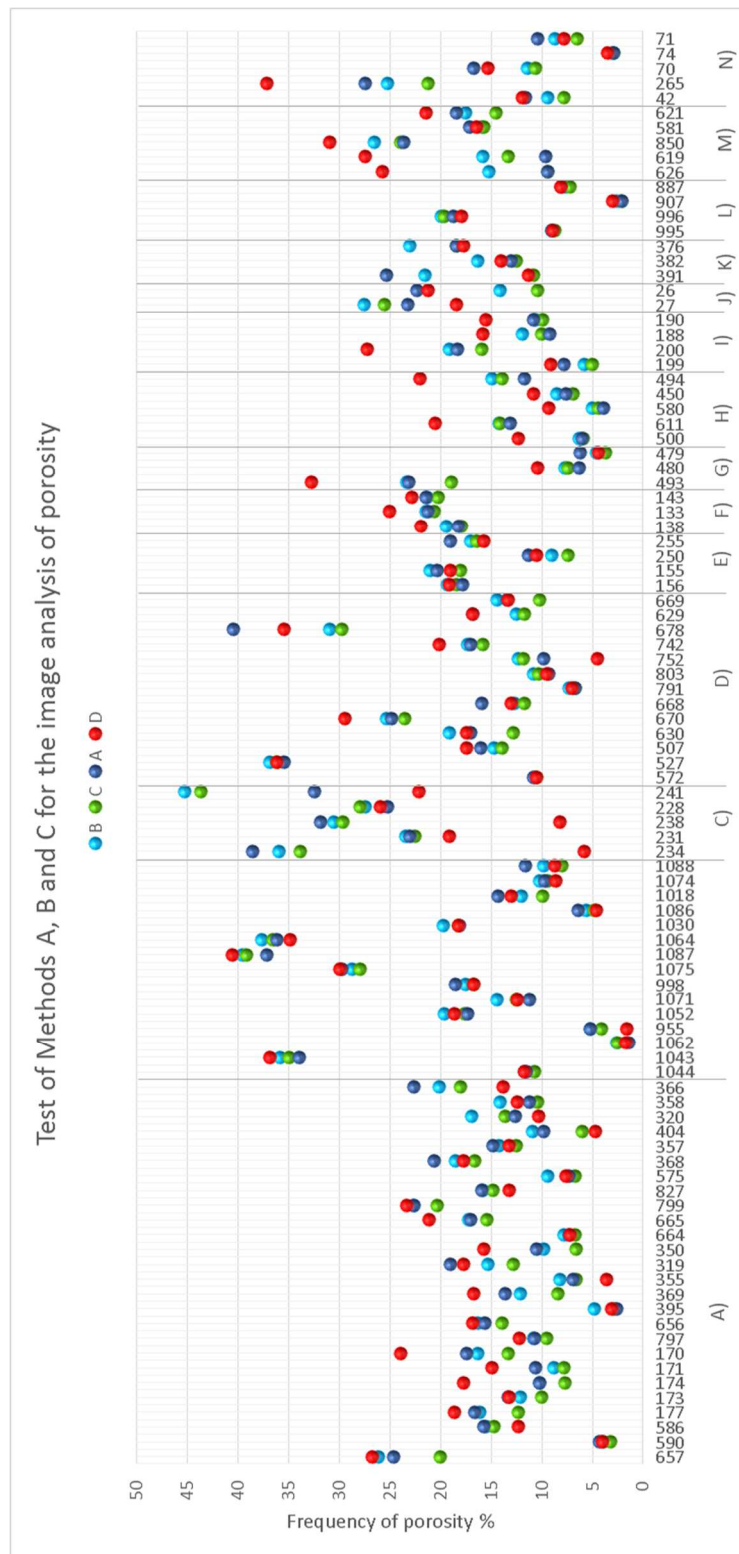
Figure 4.4: Results of the application of Methods A (blue), B (light blue), C (green) and the control D (red). On the x-axis are reported the number of the slides analysed, separated in archaeological sites: A) Hungate; B) Haymarket; C) Rossio do Carmo; D) Pill'e Matta; E) Borgharen; F) Thessaloniki; G) St. Thomas Osbaldwick; H) Catalhöyük; I) Heslington East; J) Edinburgh; K) Al Khiday; L) Sala; M) Hofstadir; N) Syningthwaite Priory.

Figure 4.4 showed a highly variable situation in which some results were accurate and close to the results of Method D (red), while some others were very different. This situation was characteristic of all of the three Methods A, B and C and no trend was detectable in the graph. Differences between the results obtained with Method D and the results with A, B and C were measured, to evaluate the distance between the results. The variance of 3% was arbitrarily chosen to separate accurate ($\leq$ 3%) and inaccurate ($\geq$ 3%) results. It was judged that a variation of 3% in the porosity was not influential. Using the distance approach inaccurate results were listed according to decreasing magnitude of the error (Tables 2.3, 2.4 and 2.5 in Appendix 2).

Method A: 38 slides (26.3% of the total) gave results with variance $\geq$ 3% compared with the results of Method D. Within these results, 7 were $\geq$ 10%, 14 were between 5% and 10% and 17 were $\leq$ 5% (Appendix 2.3).

Method B: 40 slides (27.7% of the total) had results with variance $\geq$ 3% compared with to results of method D. Within these results, 7 were $\geq$ 10%, 16 were between 5% and 10% and 17 were $\leq$ 5% (Appendix 2.4).

Method C: 49 slides (34% of total) had results with variance $\geq$ 3% compared with results of Method D. Within these results, 11 were $\geq$10%, 18 were between 5% and 10% and 20 were $\leq$ 5 % (Appendix 2.3).

Thus, Methods A and B gave very similar results, whereas Method C was the least accurate, with a higher number of erroneous measurements. Comparing the list of results, Methods A, B and C had in common 26 slides affected by the variance of $\geq$ 3% (Appendix 2.6). Hence, especially in these cases, the erroneous results could have been related to some characteristics of the slides, for which the methods were not appropriate. However, further observations of these slides were not performed, because the percentage of inaccurate results was so high (26.3-34%) that all the three methods were not considered reliable for the measurement of porosity.

In particular, it was observed that changing the angles between the polarizer and analyser did not lead to an improvement in the accuracy of the results. The error was attributed firstly to the process applied in the methods and possibly to the selection of angles.

A new method, based on a different processing approach, was then elaborated in this research.

4.3 TESTING THE METHOD DEVELOPED IN THIS RESEARCH

4.3.1 METHOD E

Method E was based on two principal aims:

- finding a sequence of image processing capable of highlighting all the mineral grains. In particular, the basic idea was to obtain an image in which the mineral components appeared coloured and not white, or rather with colours that differ from the area of pores.
- taking the appropriate number of mosaic images, under the right angles, to capture all the mineral grains when not in extinction.

Firstly, it was considered that, when the analyser is inserted into the microscope and the stage is rotated, anisotropic minerals go in extinction in four positions at intervals of 90°, while isotropic minerals stay continuously black (Vepraskas 1990, 28-30; Stoops 2003, 152; Chapter 2, Section 2.1.3). Consequently, it was observed that, to detect all the anisotropic minerals when they are not in extinction, it was necessary to take different mosaics at different rotation positions of the stage and of the sample. However, AxioScope was equipped with a rectangular and motorised stage, which could not rotate (Chapter 3, Section 3.4.2). Hence, it was essential to rotate polarizer and analyser at the same time, maintaining an angle of 90° between the two of them. After observation at the microscope and several tests, the author established that it was possible to detect all the anisotropic minerals under XPL with the combinations of two angles:

- polarizer at 0° and analyser at 90°;
- polarizer at 45° and analyser at 135°.

A third mosaic was used as base for the elaboration of the images:

- polarizer at 0° and analyser not inserted.

Method E was conceived for the selection of anisotropic minerals. Unfortunately, it was not possible to find a solution for the segregation of white isotropic minerals with the supplied equipment. However, the slides were observed firstly with the petrographic microscope and isotropic minerals were not identified. If these minerals were present, they probably occupied less than 1% of the slides. In addition, charred opaque material was detected and recorded with the mosaic taken in plane polarized light, excluding the possibility to identify the charred plants as isotropic minerals.

The method is illustrated in Figure 4.5 and an example of the mosaics through the various stages in the process is shown in Figure 4.6.
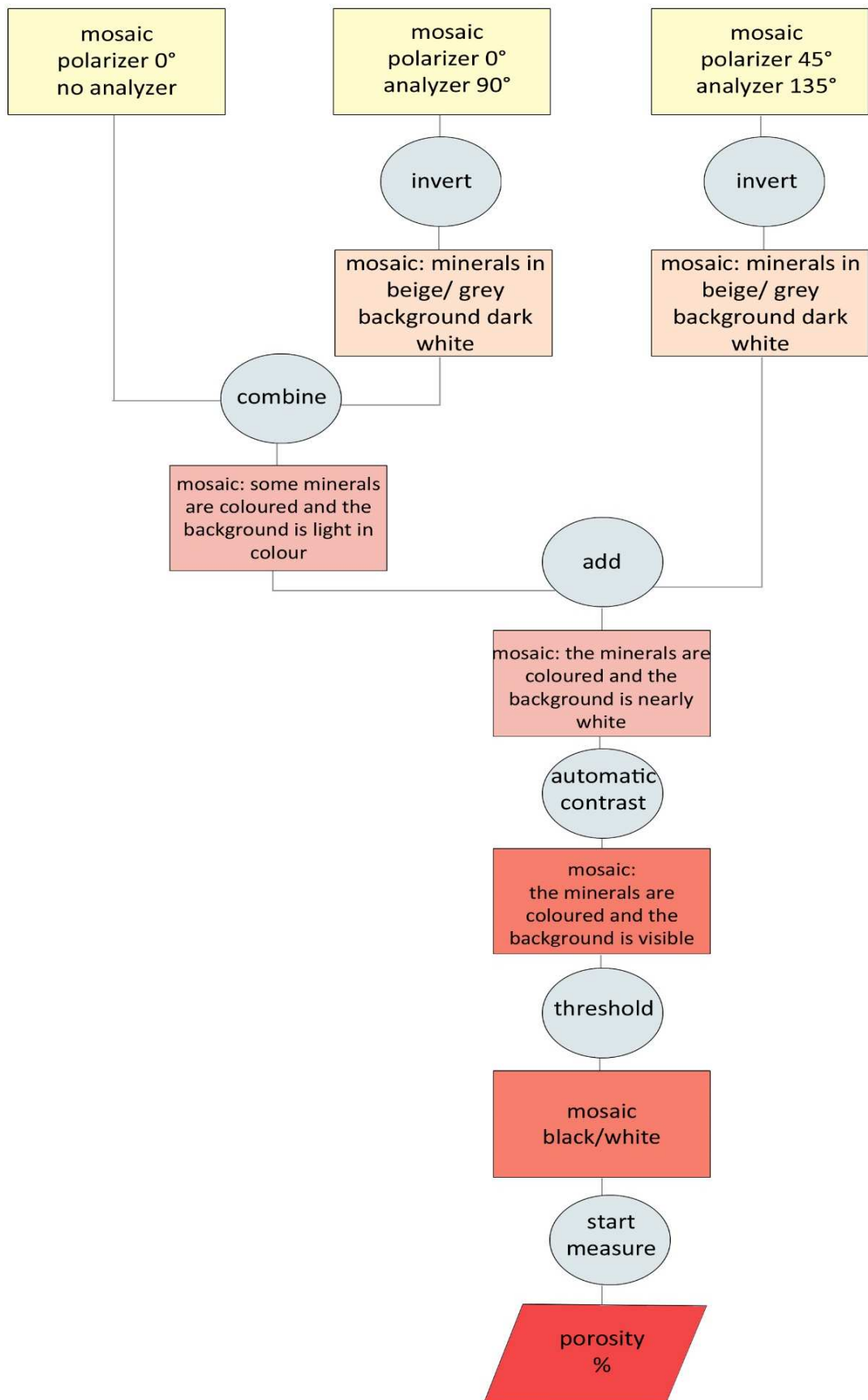
Figure 4.5: Scheme for the image analysis of soil porosity using Method E Three mosaics of the same area were taken under different angles between analyser and polarizer. The new images were inverted and combined to obtain a mosaic in which all the mineral grains were coloured. The threshold was easily applied on the white areas representing only the void space. The final mosaic was black/white and the porosity was measured on the white areas.

Three mosaics were taken at the angles mentioned above:

- polarizer at 0° and analyser not inserted (Figure 4.6.a);
- polarizer at 0° and analyser at 90° (Figure 4.6.b);
- polarizer at 45° and analyser at 135° (Figure 4.6.c).

The mosaics obtained with the analyser inserted had non-birefringent background and the mineral grains in colour, with shades from white to dark blue. These two mosaics were inverted to obtain images in negative (Processing – Adjust – Invert – Ok), where the mineral grains turned to shades between beige and grey, while the background was dark white (Figures 4.6.d and 4.6.e).

The mosaic taken under plane polarized light was used as the base to construct the final picture. This mosaic was combined with the other two (Processing – Arithmetic – Combine). This operation was preferred to the "Arithmetic – Add" used in Methods A, B and C, because it united the mosaics without applying an intersection. Distinct from the approach outlined earlier in Section 4.2.1, the software operation Add was used to combine the mosaics.

The resulting image, from the operation of combine, had very low contrast. This was due to the features being masked by the two layers of dark white background (Figure 4.6.f). The contrast was adjusted automatically (Processing – Adjust – Contrast – Automatic), obtaining a final mosaic characterized by white voids and coloured mineral grains (Figure 4.6.g).

Before moving to the following operations, the mosaic had to be saved as .jpg, otherwise the threshold was not retained. The mosaic was thresholded with the quick selection of all of the white and uniform pixels (Processing – Segmentation – Threshold interactive), producing a mosaic in black and white (Figure 4.6.h). Finally, the automatic measurement was accomplished (Measure – Automatic measurement – Start measurement).

The operations for Method E were more rapid than those applied in Methods A, B and C. Moreover, the final mosaic before the threshold had uniform white void areas, produced by the combination of the mosaics. Hence, the selection of the pixels characterizing voids was more rapid and simple, and minimized the need for intervention by the operator. It was observed that, compared with Methods A, B and C, the threshold was efficacious because it was applied to the final mosaic. Thus, it implicated the application at the beginning in the introduction of erroneous selections from the start of the method. On the contrary, the application at the end was performed on mosaics where the white pixels were exclusively related to void area.
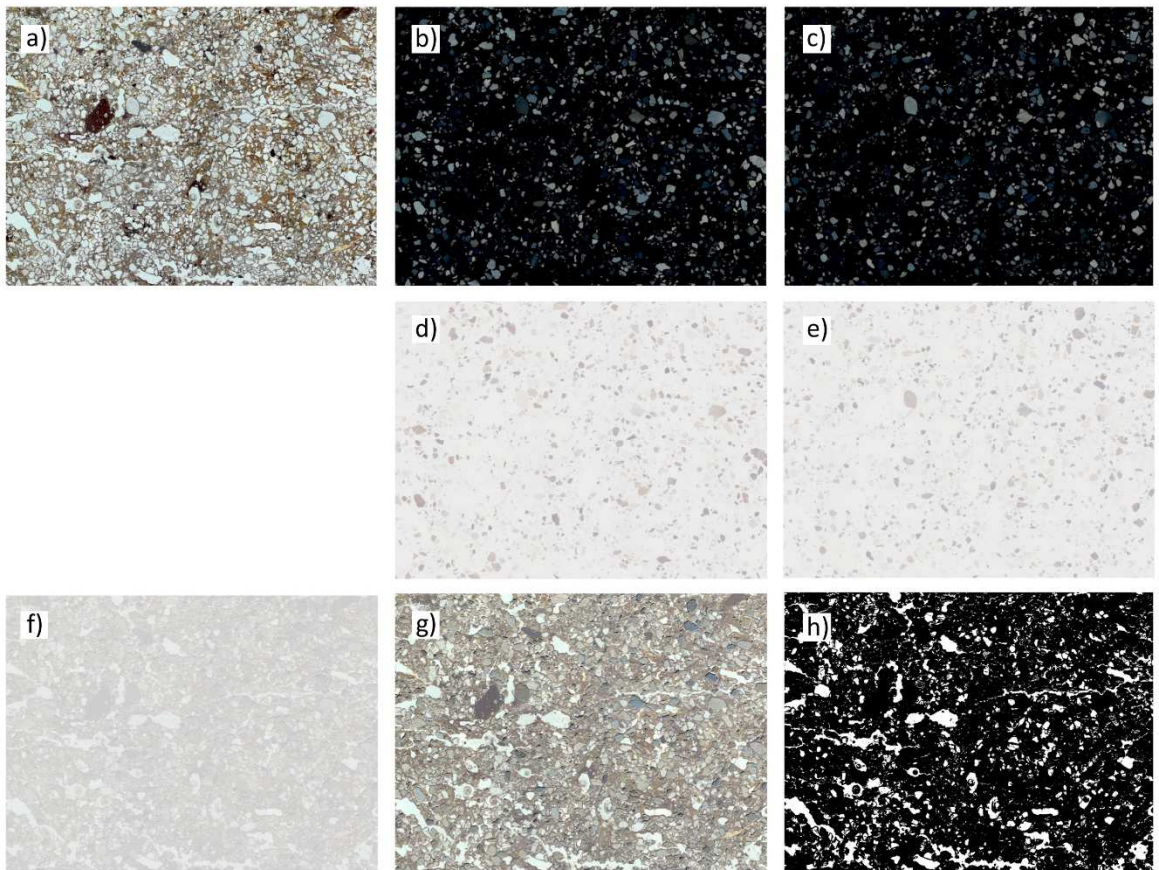
Figure 4.6: Examples of images obtained through the application of Method E. a) mosaic taken with polarizer at 0°; b) mosaic taken with polarizer at 0° and analyser at 90°; c) mosaic taken with polarizer at 45° and analyser at 135°; d) inverted mosaic form (b); e) inverted mosaic from (c); f) mosaic from the combination of (a), (d) and (e); g) mosaic with adjusted contrast from (f); h) threshold image from (g).

4.3.2 RESULTS FROM METHODS E AND D

Method E was applied on the same 144 slides as the previous methods, and it was tested with the application of Method D on the same areas of selection as were used for Methods A, B and C. The results are presented in Appendix 2.2 and graphically below (Figure 4.7).
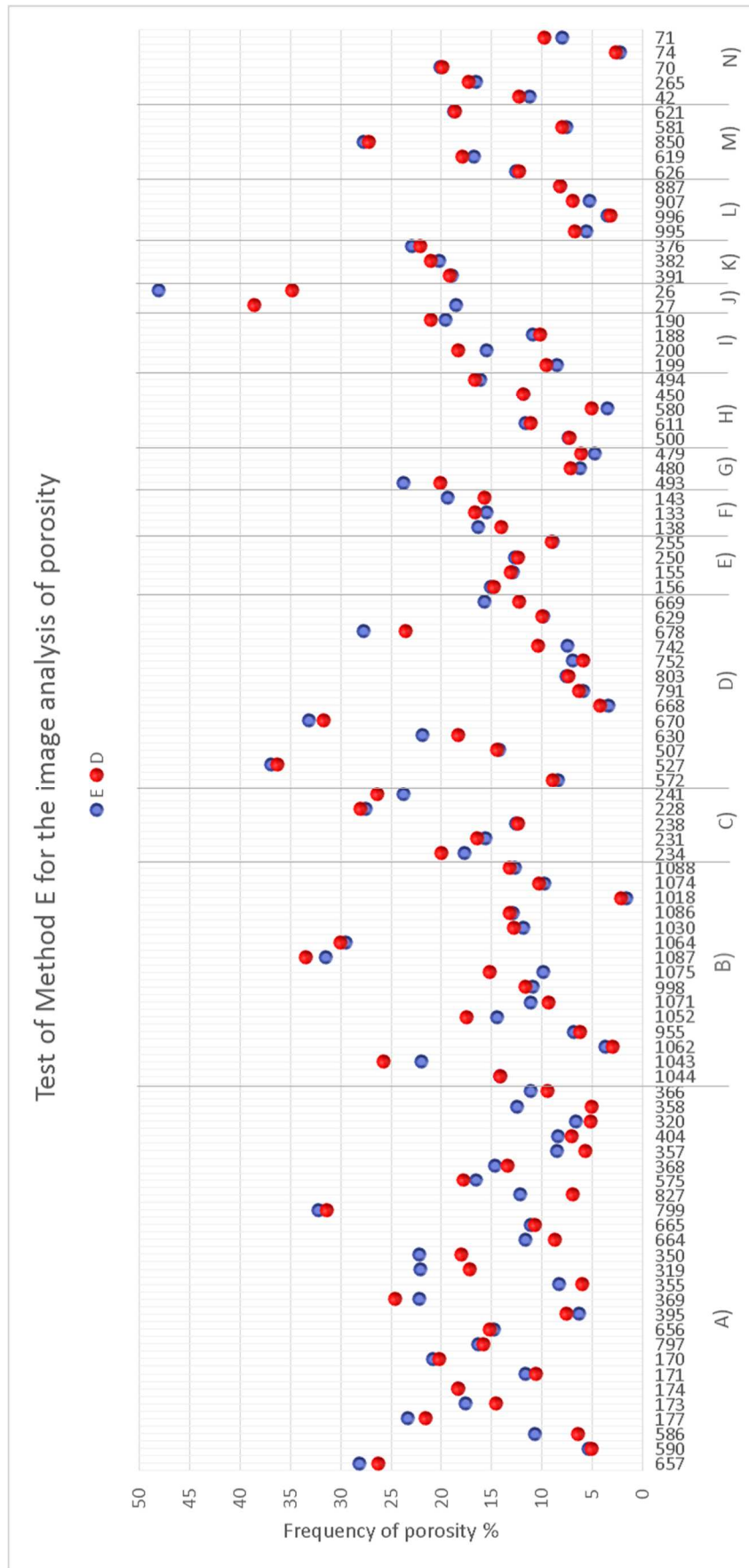
Figure 4.7: Results of the application of Methods E (blue) and the control D (red). On the x-axis are reported the slide number for the slides analysed, separated according to archaeological sites: A) Hungate; B) Haymarket; C) Rossio do Carmo; D) Pill'e Matta; E) Borgharen; F) Thessaloniki; G) St. Thomas Osbaldwick; H) Catalhöyük; I) Heslington East; J) Edinburgh; K) Al Khiday; L) Sala; M) Hofstadir; N) Syningthwaite Priory.

Figure 4.7 shows that most of the results of Method E were coincident with, or similar to, those of Method D. However, some slides had very distant results. As for the previous methods, difference between the results obtained with Method D and the results with E were measured, to evaluate the distance between the results. The inaccurate results (≥ 3%) were listed according to decreasing order of error (Appendix 2.7).

15 slides (10.4%) had a variance ≥ 3% compared with the results of Method D. Within these results, 2 were ≥ 10%, 3 were between 5% and 10% and 10 were ≤ 5%.

It was confirmed that Method E gave more accurate results on soil porosity than Methods A, B and C. However, 10.4% of the results, and particularly 3.4% of them with a variance ≥ 5%, were inaccurate. The slides with inaccurate results were subjected to further observation to detect if the problem was caused by the characteristics of the slides themselves.

The list of the slides with variance ≥ 3% was compared with the ones of Methods A, B and C (Appendix 2.8). Four slides had inaccurate results in common.

- slide 27, grave 1046 from Edinburgh;
- slide 350, grave 52253 from Hungate;
- slide 678, grave 2680 from Pill'e Matta;
- slide 493, grave 6 from St. Thomas Osbaldwick.

Samples from Edinburgh, Hungate and St. Thomas Osbaldwick were very sandy and, especially in the first two cases, many grains were internally fragmented, likely due to the operation of cutting and grinding of the slide. The sample from Pill'e Matta was characterized by very fine pores between the packing voids and possibly these were not thresholded.

Considering the results from Method E with variance ≥ 5% (Appendix 2.7), the problematic slides were:

- slide 27, grave 1046 from Edinburgh;
- slide 26, grave 1046 from Edinburgh;
- slide 358, grave 51349/51351 from Hungate;
- slide 1075, grave 84851 from Haymarket;
- slide 575, grave 54296 from Hungate.

Equally, in these cases, the slides were very sandy and the mineral grains were mostly fragmented (Figure 4.8). It seems that the fragmentation of the minerals caused less intense colours in XPL and this affected the selection of these components during the processing of the mosaics. Consequently, Method E could be considered accurate and efficient in terms of time and automatic procedures for the measurement of soil porosity with the equipment used in the study. In addition,

it was noted that the selection of the slides was extremely important, because damaged slides could introduce erroneous results.
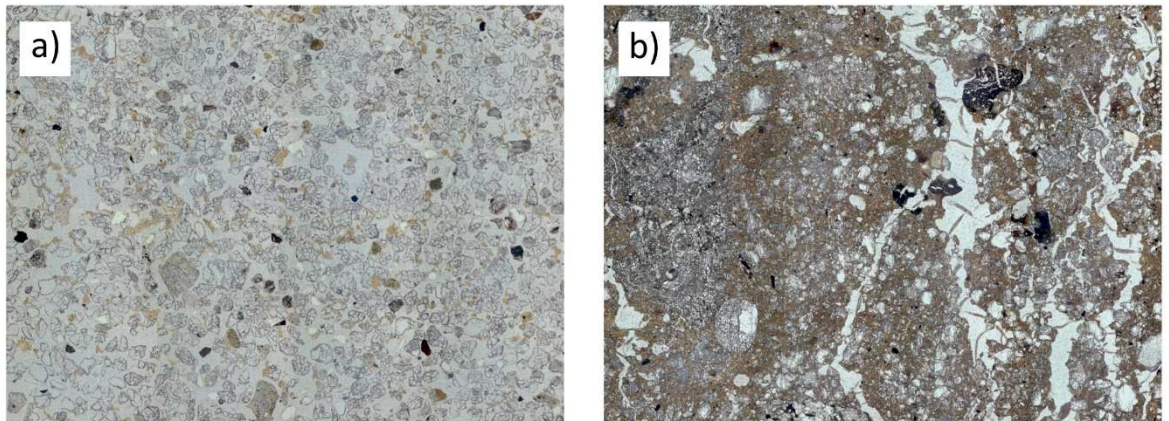
Figure 4.8: Examples of slides with fragmented mineral grains. a) Slide 26, grave 1046 from Edinburgh; b) Slide 1075, grave 84851 from Haymarket.

4.4 IMAGE ANALYSIS APPLIED TO THE CASE STUDIES

In this research, Method E was applied to the image analysis of soil porosity. The aim was to observe the presence of differences in soil porosity within the burial, to assess differences between the area of the skeleton and the layers above the remains. It was of interest in this research to investigate the movement of soil particles and fluids within the grave, to detect eventual patterns of soil porosity within the graves and the layers above, investigating the role of the skeleton and coffin as possible barriers to this movement. For these reasons, the measurement of porosity was taken in three anatomical positions (skull, pelvis and feet) and in the areas of controls. In addition, to test and cross-refer the results, the measurement was taken in different context types, such as different sediments and different grave types (wooden coffin, absence of coffin and chamber). The results from the case studies were compared to the results from the experimental burials of piglets to have a clear comparison regarding the variance of porosity in relation to the presence of the coffin.

The results from the case studies analysed in this research are presented in Appendix 2.9 and summarized in Figure 4.9. The absence of control samples or the incomplete sampling of some graves did not allow a whole reconstruction of the porosity. On the other hand, an intense sampling, such as that for grave 83012 from Haymarket and of the experimental burials of piglets (Figure 4.10), gave the opportunity to explore the variations of porosity in detail.

Porosity within the graves was variable and four main tendencies were observed (Figure 4.9):

1) porosity increased from the area of the skull to the area of the pelvis and from the C2 to the C3 (grave 54296 from Hungate);

2) porosity increased from the area of the feet to the area of the skull (graves: 51349/51351 from Hungate, 84851 from Haymarket, 15 from Borgharen and 395 from Rossio do Carmo). Increasing from the area of the C1 to the C2 (graves 15 from Borgharen and 395 from Rossio do Carmo). It increased from the C1 to the C2 and then decreased to the C3 (grave 51349/51351 from Hungate).

3) porosity increased from the area of the skull to the area of the pelvis and it decreased from the area of the pelvis to the area of the feet (graves: 52253 from Hungate, 84770 and 84779 from Haymarket, 237, 238 and 268 from Pill'e Matta). Porosity increased from the C2 to the C3 (graves 52253 from Hungate and 84779 from Haymarket) and it increased from the C3 to the C2 and to the area of the feet (grave 84700 from Haymarket).

4) porosity increased from the area of the pelvis to the areas of the skull and of the feet (graves 51350/51364 from Hungate and US2680 from Pill'e Matta). It increased from the C3 to the C2 and to the area of the skull (grave 51350/51364 from Hungate).
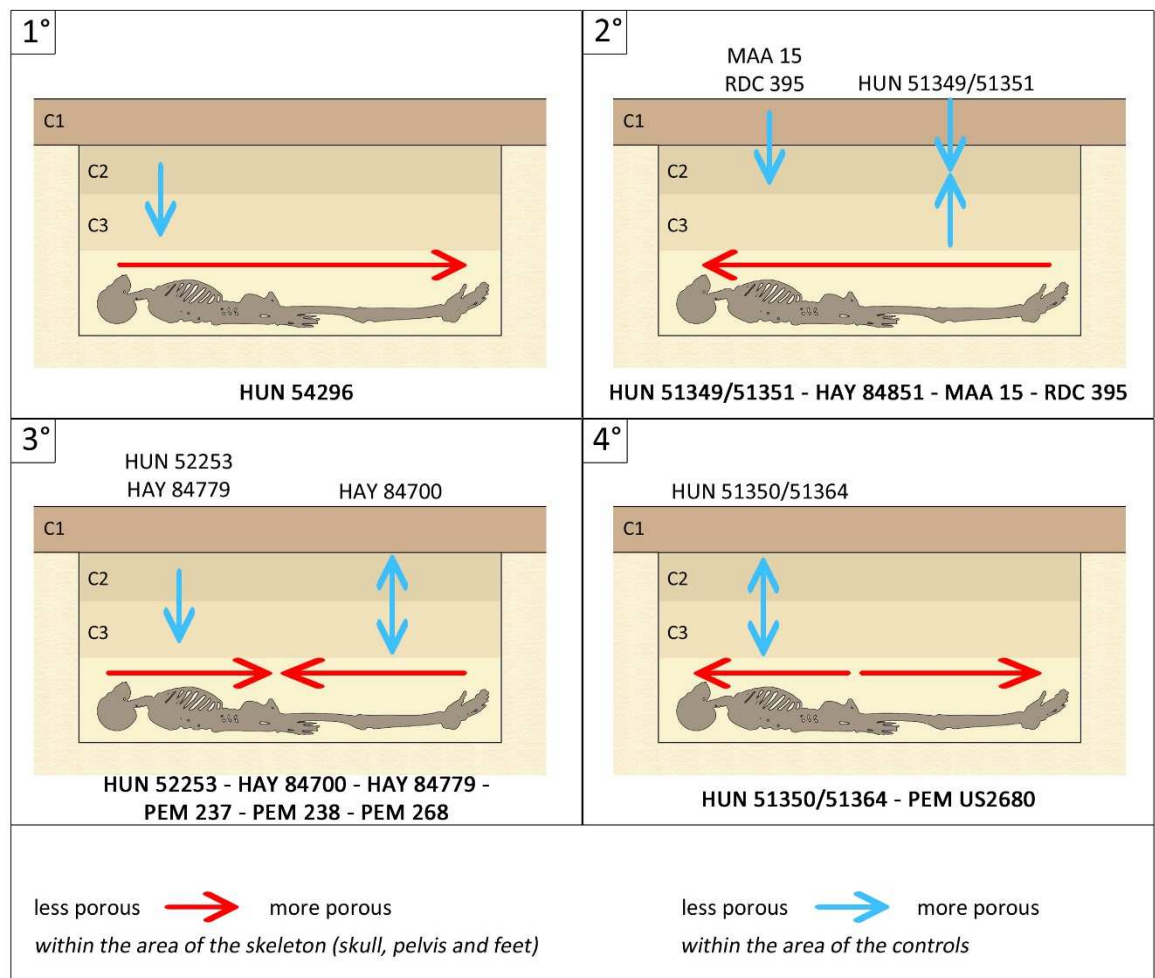
Figure 4.9: Tendencies of soil porosity registered within the graves with image analysis (Method E).

The intense sampling in Haymarket 83012 and piglet burial 2, 6 and 7 showed that the variation of porosity was more complex if observed in detail (Figure 4.10).

- Haymarket 83012: the porosity increased from the area of the skull to the area of the pelvis. The area of the skull was less porous in the layers at the same level as the bones (y) and the same was apparent in the area of the pelvis. On the other hand, the area of the feet was more porous in level y than level z. The areas on the sides of the pelvis had porosity similar to the area of the feet, except for one sample, which was less porous. Samples from the areas of controls were more porous and the porosity increase from the side of the skull to the side of the feet was evident here too (Figure 4.10.a).
- piglet burial 2: samples from the areas surrounding piglet 2 were highly porous, especially below the skull and in the gut area. The areas of the feet and of the muslin bag had approximately the same amount of voids as the controls (Figure 4.10.b).
- piglet burial 6: sample from the area of the skull was more porous in level z, while the area surrounding the piglet did not present great variation in porosity. The level y of the area of the skull and the area of the pelvis were the least porous. It seems that the porosity decreased from the area of the burial to the surface (Figure 4.10.c).
- piglet burial 7: level z of the area surrounding the piglet was less porous than level y. The porosity decreased from the area of the burial to the surface (Figure 4.10.d).
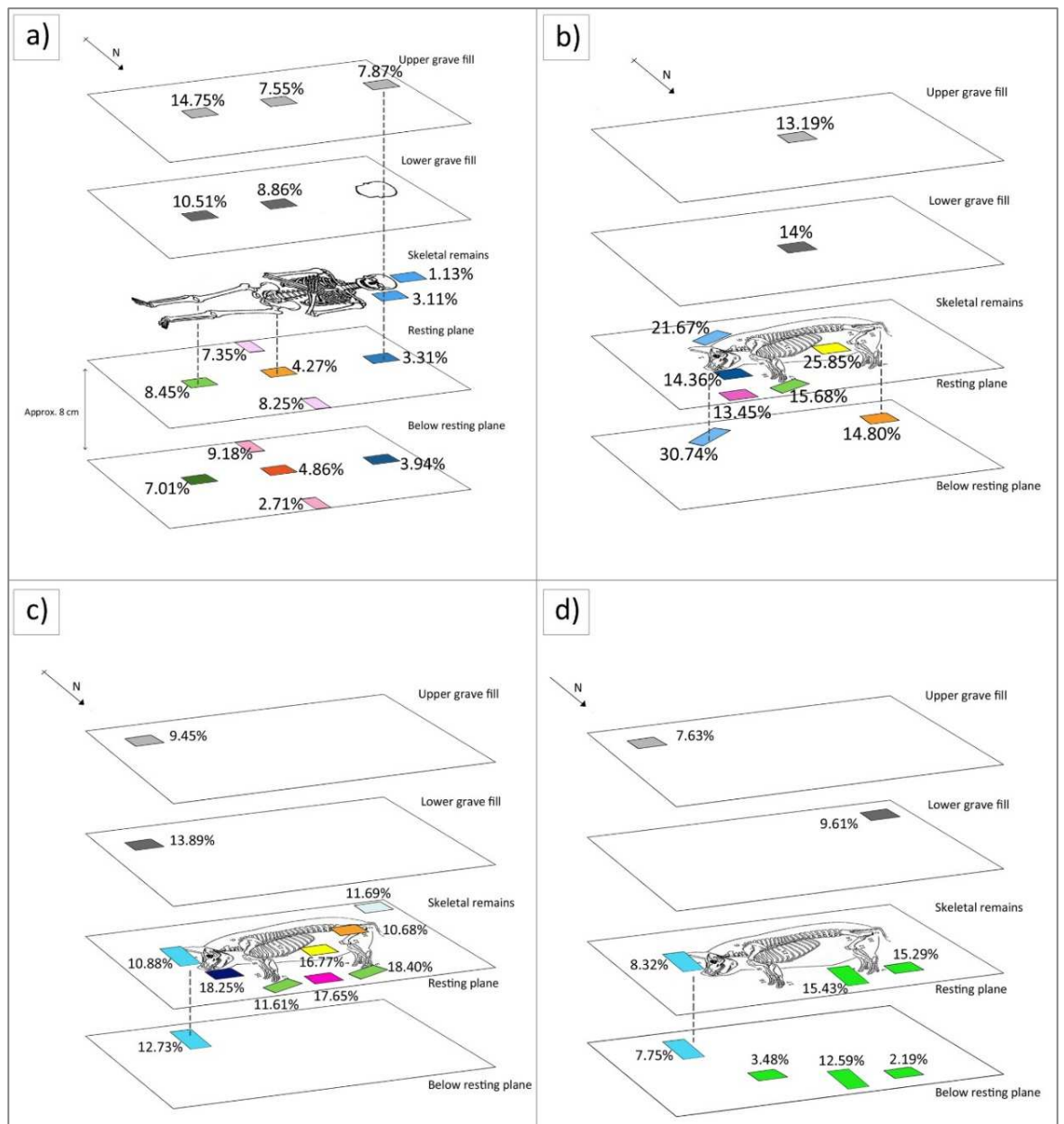
Figure 4.10: Tendencies of soil porosity registered within the grave with image analysis (Method E). a) grave 83012 from Haymarket; b) piglet burial 2 from Hovingham; c) piglet burial 6 from Heslington East; d) piglet burial 7 from Heslington East. The images are available in the Supplementary Data (DVD, folder Chapter 4 – Image analysis graph.

Chapter 5. CASE STUDIES

The case studies, analysed during this research and introduced in Chapter 3.3, are explicated in this chapter. The contents are structured around four main points (information regarding the site, description of the graves, micromorphological results and SEM-EDS results) and applied to each case study to facilitate comparison among the graves and between the cemeteries.

For each case study the following were produced:

-        information regarding the geology and the archaeology of the site, if available, and map with the location of the site, as well as plan of the cemetery. Unfortunately, this last information was available only for Borgharen and, in the case of Pill'e Matta, the only map available was from the publication of 2005 (Secci 2005, 4-5), not updated with the new graves excavated and sampled in 2009;

-        descriptions of graves focused on skeleton remains, grave fill, grave profile and surrounding sediments. The information came from the archaeologists who excavated the sites and from the notes of the InterArChive team during the sampling. However, as explained case by case, this information was rarely provided by the archaeologists, owing partly to differences in timescale for delivering outcomes and compounded by lack of explicit agreement between the two parties. In addition, the notes from the sampling concerned the sampling more than the characteristics of the grave. As consequence, in many situations, nothing or nearly nothing was known about the geoarchaeology of the site, the sediments of the fill and of the surrounding area. As noted in Chapter 3.3, the author sampled only two of the archaeological graves, in Haymarket, and the experimental burials, having joined the project in 2012 after completion of much of the sampling programme. The availability of photographs helped to compensate for absence during sampling, though photographs were not always taken. The material and information available for each grave are indicated in Table 3.2, Chapter 3.

Graves are represented graphically in this chapter with a photograph from the excavation, where available, and the location of the samples (Kubiena tins drawn as rectangles). On the right of the picture, is a schematic of a skeleton showing the list of the slides analysed through micromorphology and on the left, or around the picture, the mosaics of the thin sections of the grave soil samples are illustrated in all the figures in the thesis. The same colours are used to correlate anatomical positions of samples, slides and the resulting mosaics;

-       micromorphological results are organized grave by grave and follow the same order for each thin section: elements of fabric and peds, voids, mineral components and organic components (for the meaning of technical words, see Glossary at the end of the thesis). The results are graphically illustrated through histograms, having the same colour coding as used for the illustrations of the graves as mentioned above. This approach to presentation of the data, with features reported in alphabetic order, facilitates the comparison among the graves of the same cemetery and among different cemeteries. Electronic copies of all of the graphs, as power point presentations, have been included in the Supplementary Data (DVD) to visualize all histograms relating to one single grave at the same time. All of the micromorphological record sheets, with the features in alphabetic order, the mosaics of the thin sections presented with key and annotations and the data from SEM-EDS analysis have all been included in the Supplementary Data;

-       SEM-EDS results, presented in box-plots.

At the end of each section in the chapter, a selection of pictures, taken using a petrographic microscope and AxioVision imaging software, are included, to illustrate the features described in the result sections. They are located at the end of the sections as they are selected as representative examples of all of the graves of each case study. However, references within the text are also included. Copies of all of the photographs are included in the Supplementary Data, to give the opportunity to refer to them at higher resolution.

Considering Figure 1.1, the case studies are presented following a specific order which concerns type of soil, climate and type of grave. The first site is Hungate (Section 5.1), characterized by sandy clay water-logged sediments. The second is Haymarket (Section 5.2), characterized by sandy clay, rarely water-logged sediments. The third is Borgharen (Section 5.3), characterized by sandy and not water-logged sediments. All three sites were affected by temperate oceanic climate. The deposition of the corpse was in wooden coffin (Hungate and Borgharen) or in contact with soil (or possibly covered by a wooden plank, Haymarket). The fourth case study is Rossio do Carmo (Section 5.4), characterized by sandy loam soil and the fifth is Pill'e Matta (Section 5.5), whose graves were excavated in limestone and sandstone deposits. The last two sites were affected by temperate Mediterranean climate. Chamber tombs were typical in Pill'e Matta, while the grave in Rossio do Carmo could be considered a type in between the ones of Hungate, Haymarket and Borgharen and the ones of Pill'e Matta. The corpse in Rossio do Carmo was, in fact, deposed without coffin, but the walls of the burial and the top were covered with schist plates. The bottom of the grave was excavated in the rock, with a thin layer of sediment. The experimental burials of piglets are presented at the end of this chapter in numerical order (Section 5.6), as reference material for the case studies. Particularly, the results from Piglet 2 were compared with Pill'e Matta and the results from Piglets 6 and 7 with Hungate and Haymarket. In each case study, the graves are introduced

following, firstly, their chronological order, such as the period of the grave, and, secondly, the numerical order (number/code of the grave).

5.1 HUNGATE (UK). Roman and Anglo-Scandinavian cemetery, 1st-4th C AD and 9th-10th C AD

Hungate was the biggest archaeological excavation in the centre of the city of York, encompassed a Roman cemetery and Anglo-Scandinavian burials, delimited at the east by the River Foss (Figure 5.1). Evaluation excavations commenced in 2000 with boreholes and test pits (Evans 2007), and York Archaeological Trust developed an extensive excavation of the area from 2006 to 2012.

The InterArChive team was involved for the sampling of Roman and Anglo-Scandinavian graves in 2010. The results of seven graves are presented in this research.
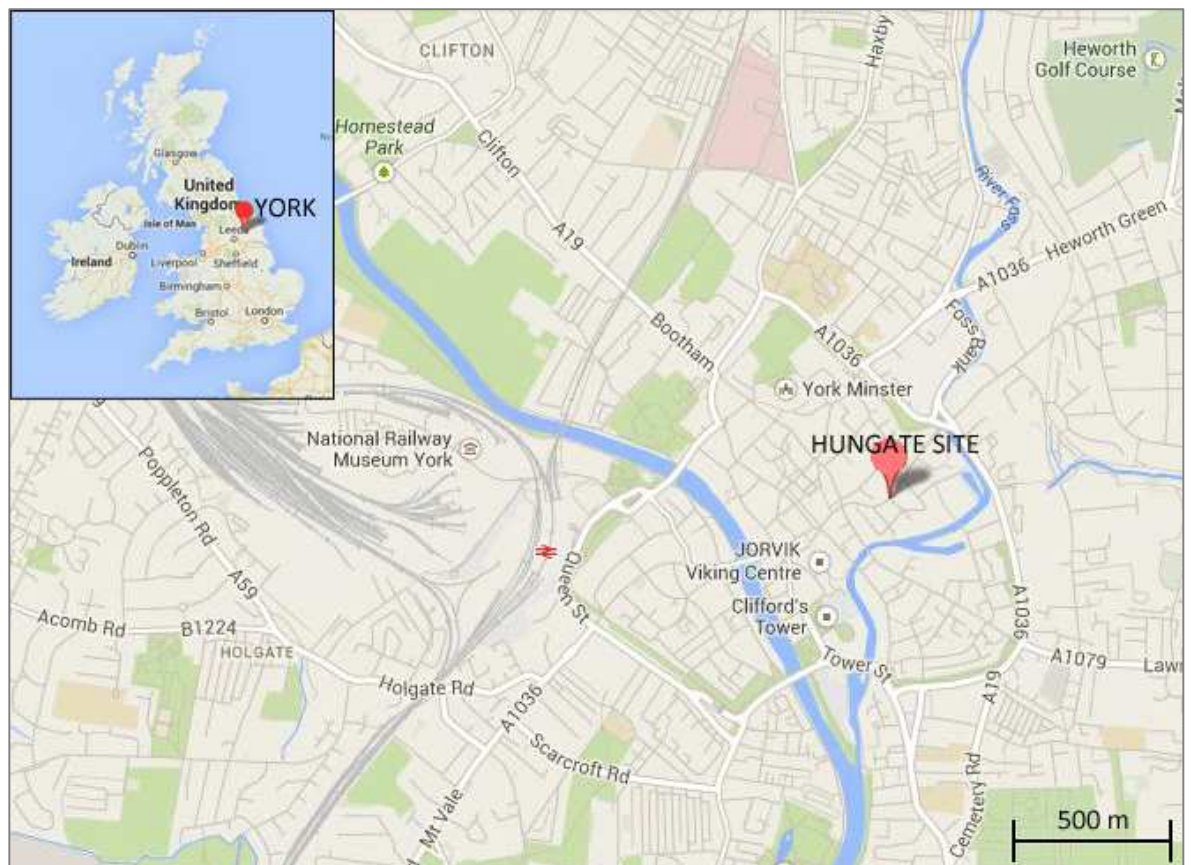
*Figure 5.1: Map with the location of Hungate in the centre of the city of York. Graphically modified from Google Maps ©
2014.*

5.1.1 THE SITE

The area developed on a natural slope, which drops from the city centre to the River Foss. Owing to its geomorphology, the area is subject to periodic flooding (Figure 5.2). The drift geology of the site was characterized by boulder clay with pockets of alluvium, sand and gravel (Evans 2007).

The archaeological deposit was quite shallow in the area of Dundas Street, but deeper in the direction of the River Foss and Garden Place, reaching 6m in depth. The archaeological strata included well stratified and preserved waterlogged organic remains, from the Roman period to the Post-Medieval age.

Figure 5.2: Map of the area of Hungate (greenish grey) denoting the elevation of the site above the sea level. The natural slope in Hungate was visible from the corner of the excavation between The Stonebow and Dundas Street (yellow dot – 14.268 m a.s.l.) to the River Foss (11-10 m a.s.l.). Graphically modified from Google Maps ©2015.

A civilian settlement was in place during the Roman period, while the area was used as a trade zone during the Anglo-Scandinavian period, because of the proximity to the River Foss. Part of the site was deliberately flooded in the 11th C AD for the construction of a ditch around York Castle and a shallow lake, known as the 'King's Fishpool', was created between Layerthorpe and the Foss Bridge (Hall 1996, 39-40) (Figure 5.3). The area was then gradually filled with refuse and river silts during the Late Medieval age (Macnab 1999, as cited in Evans 2007). During the occupation of a Carmelite Friary in the 13th C AD, the site was occupied by a church and a cemetery. In the 16th C AD, the King's

Fishpool was used as public refuse dump and in the 18th C AD the River Foss was canalized and the area was developed for heavy industry (Macnab 1999, as cited in Evans 2007).
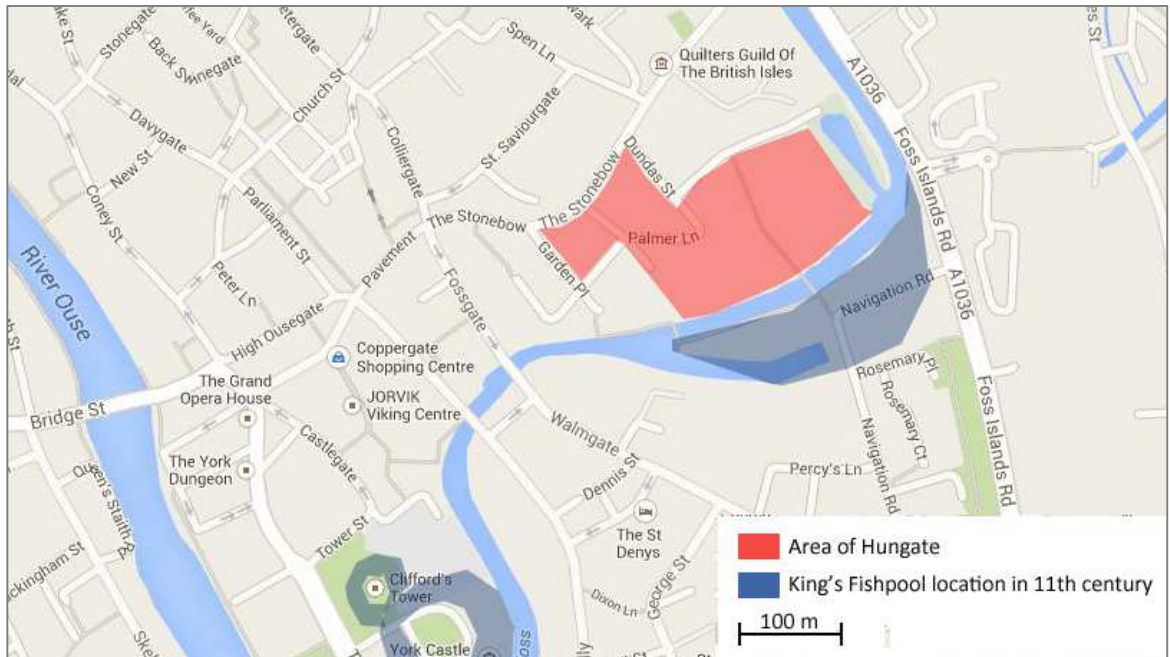
Figure 5.3: Map showing the location of the King's Fishpool in 16th c. in relation to River Foss and the area of Hungate. Graphically modified from Google Maps ©2014.

5.1.2 THE GRAVES

Seven graves were selected for this research (Table 5.1):

- Six Roman: 51350/51364, 51349/51351, 52253, 54077, 54296 and 54931/54909;

- One Anglo-Scandinavian: 53700.

In addition, the slides available from the remaining graves were examined in order to increase the information available regarding specific pedofeatures and hence facilitate the understanding of the significance of those features (Chapter 3.4 and Appendix 1.6).

Record sheets and information from YAT were available for all seven graves and they were used to develop the description that follow. Photographs were taken only for five graves (Table 3.2, Chapter 3). Information regarding orientation, relation with bones and accurate location were mostly complete (Appendix 1.5).

Unfortunately, it was not possible to obtain a map of the cemetery with the spatial arrangement of the graves, which would have been useful for the interpretation of the pedofeatures. Moreover, in the absence of a control C1 that was valid for all the graves, the C1 sample used was collected above

grave 51349/51351. The IADB database was not available for consultation during the period of research (www.iadb.org.uk).

GRAVE	DATE	TYPE	SKELETON INFORMATION and grave-goods	SOIL TYPE	CLIMATE
51350/51364	Roman, 3rd C AD	Wooden coffin; Adjacent to a cesspit	Adult; NE-SW oriented, skull to W and turned right; Right arm across the chest; Left arm partially missing	Sandy clay	Temperate oceanic
51349/51351	Roman, 3rd C AD	Wooden coffin	Adult; NE-SW oriented; Poor preservation of the skeleton; Grave goods: copper bracelet, jet bracelet, bead necklace, jet necklace, iron remains	Sandy clay	Temperate oceanic
52253	N/A	Wooden coffin	Juvenile skeleton; Pot with carbonaceous material	Sandy clay	Temperate oceanic
54077	Roman	Wooden coffin	Juvenile skeleton, poorly preserved	Sandy clay	Temperate oceanic
54296	Roman, 3rd-4th C AD	Wooden coffin	Adult; Well preserved	Sandy clay	Temperate oceanic
54931/54909	N/A	N/A	N/A	Sandy clay	Temperate oceanic
53700	Anglo-Scandinavian, 9th-10th C AD	Wooden coffin; Eight large stones surrounded the burial	Male adult	Sandy clay	Temperate oceanic

Table 5. 1: Summary of the available information regarding the graves in Hungate.

GRAVE 51350/51364

Grave 51350/51364 (Figure 5.4) was dated to the Roman period, probably 3rd C AD, and was situated in the SE corner of the site. The corpse had been placed in a wooden coffin and coffin nails were found near the skull during excavation. The stain of the coffin was a mid-grey colour, soft and silty; the archaeologists interpreted its dimension as 1.87 x 0.47 x 0.25 m. The skeleton was oriented NE-SW, with the skull to the West and turned to the right. The right arm was placed across on the chest, and the left was partially missing; the iliac blades were degraded. The cut of the grave was rectangular, with vertical sides and dimensions of 2.28 x 0.70 x 0.68 m. The grave was adjacent to a cesspit, located to the North of the grave. The backfill material was sandy clay and silt, with a firm consistency and mottled mid orange, light yellowish brown and mid grey colours. Pebbles and charcoal fragments were occasionally present. Evidence of bioturbation was visible in the layer above the grave, as consequence of agricultural use.
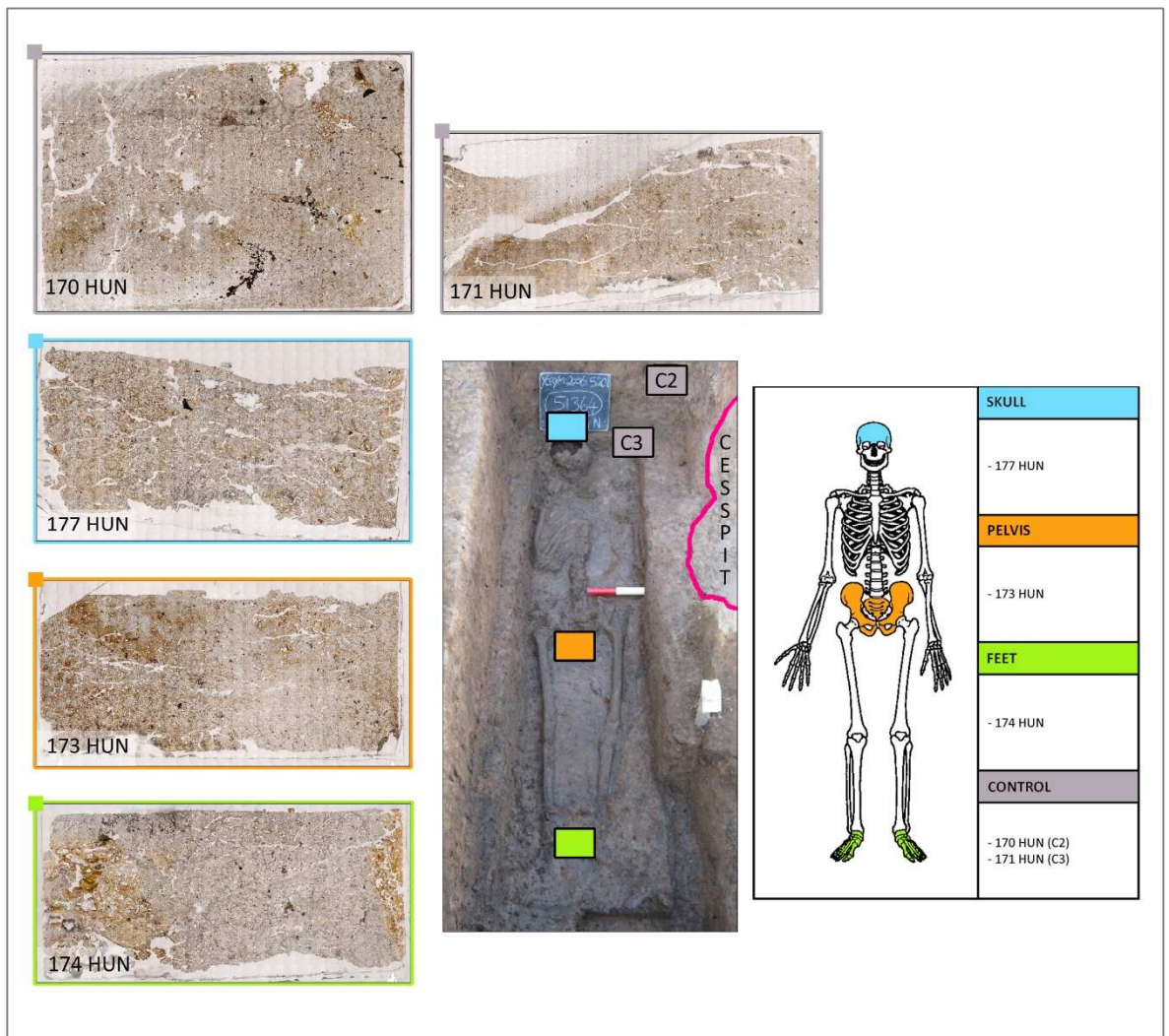
Figure 5.4: Grave 51350/51364. In the centre, photograph of the grave and location of the samples. The pink line indicates the limit of the cesspit. On the right, list of the slides in relation to their anatomical location. On the left and top, mosaics of the slides. See the text for descriptions.

GRAVE 51349/51351

Grave 51349/51351 (Figure 5.5) was dated to the Roman period, probably 3rd C AD. The corpse had been placed supine in a wooden coffin, of which nails and stain remained. The skeleton condition was poor, but several grave goods were preserved: one copper bracelet, one jet bracelet, one bead necklace, one jet necklace, one object in iron, iron remains from shoes and a casket. The skeleton was oriented NE-SW, matching the cut of the grave which had rectangular shape, vertical sides and flat base. The dimensions of the grave cut were 2.12 x 0.72 x 0.75 m and the grave was probably associated with a group of burials present in the same area and arranged with the same orientation. The backfill was mid grey, soft and silty, probably contaminated by hydrocarbon from a 20th C AD petrol station, and exhibited a stain from the coffin.
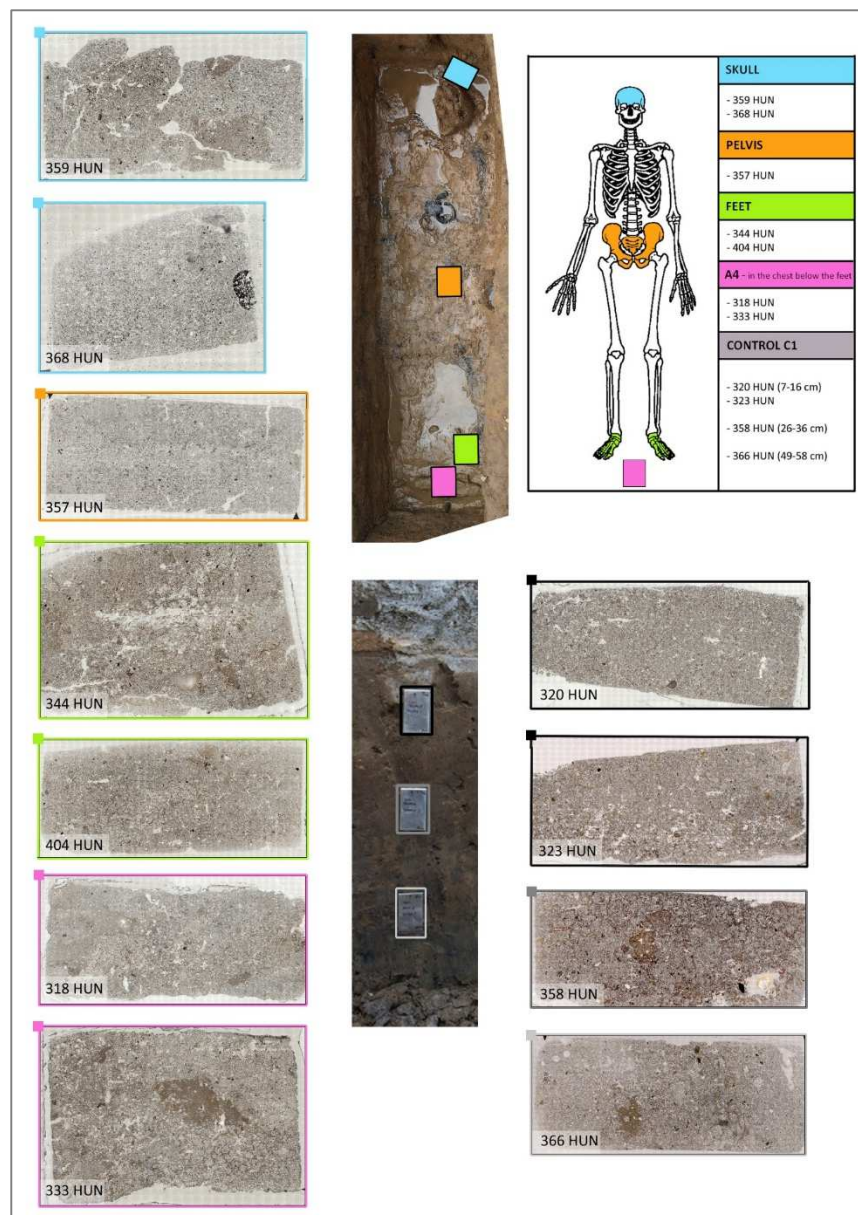
Figure 5.5: Grave 51349/51351. In the centre, photographs of the grave and soil profile, with location of the samples. On the top right, list of the slides in relation to their anatomical location. On the left and right, mosaics of the slides. See the text for descriptions.

GRAVE 52253

Grave 52253 (Figure 5.6) contained poorly preserved remains of a juvenile skeleton buried in a wooden coffin, the presence of which was indicated by nails and a grey stain. The sub-rectangular grave cut was 110 x 95 x 70 cm and truncated to the N-W by the cut of a pit. The grave cut was characterized by steep sides, possibly with a small step at 30 cm from the base. The layer below the cut comprised clayey sand of brownish orange colour and was highly compacted. Occasional charcoal flecks and pebbles were present. A pot containing carbonaceous material was found at the SE end of the burial. Fragments of other pot remains were found during the excavation.
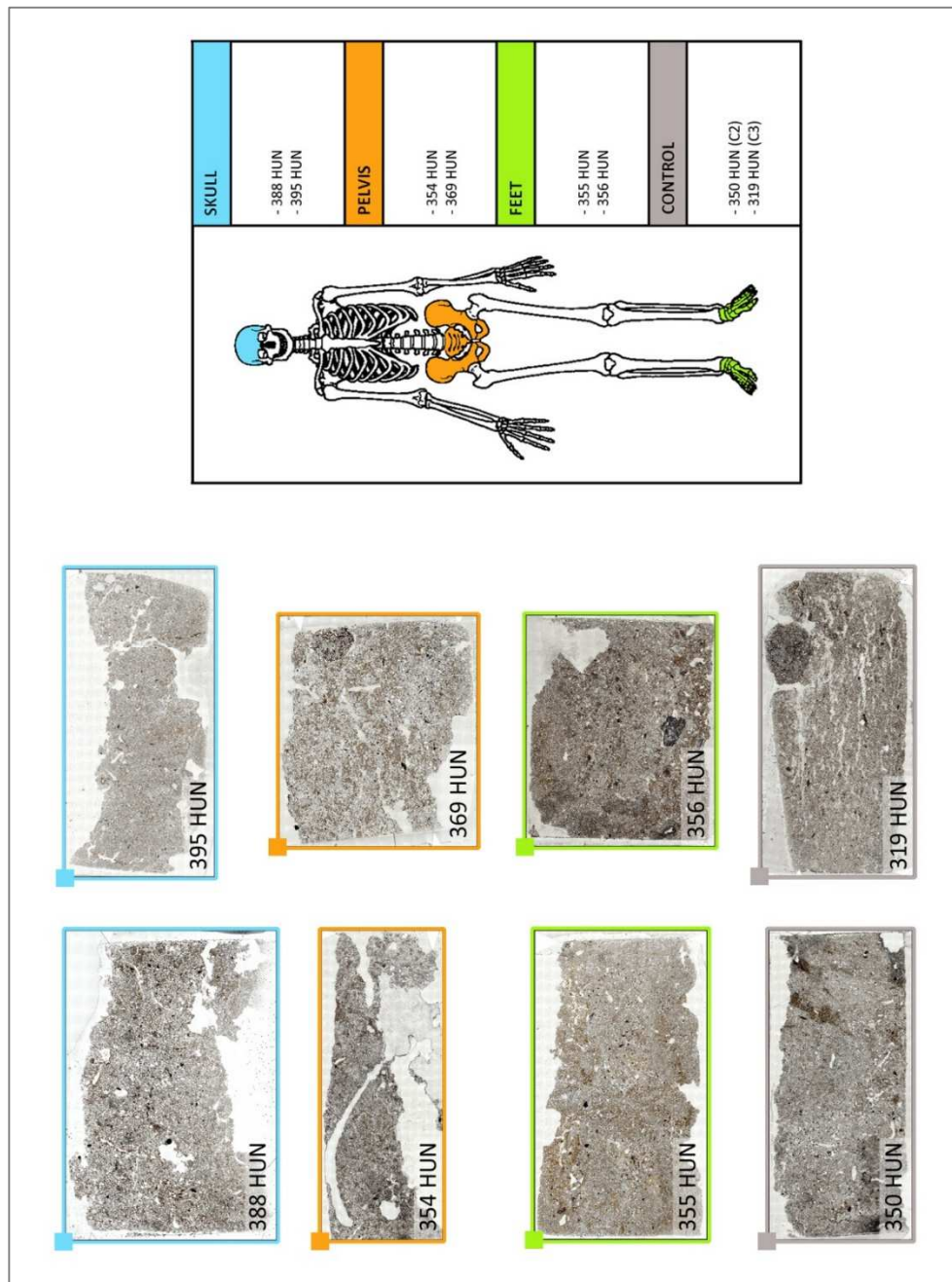
Figure 5.6: Grave 52253. No photographs of the grave were available. On the right, list of the slides in relation to their anatomical location. On the left, mosaics of the slides. See the text for descriptions.

GRAVE 54077

Grave 54077 (Figure 5.7) was dated to the Roman period. It contained the poorly preserved skeleton of a child that had been interred in a wooden coffin, of which iron nails remained. The skeleton was 92 cm long and it was oriented NW-SE. No grave goods were found. The cut of the grave was 140 x 74 x 33 cm in size, with vertical sides and a sharp break at the top and bottom. The layer below the skeleton was composed of firm mid brownish grey silty sand. A section of the deposit was friable, containing clay, and it was described by the archaeologists as remains of a coffin. Moderate iron stains and a band of friable grey clay were present, while charcoal fragments and subangular pebbles were occasional.
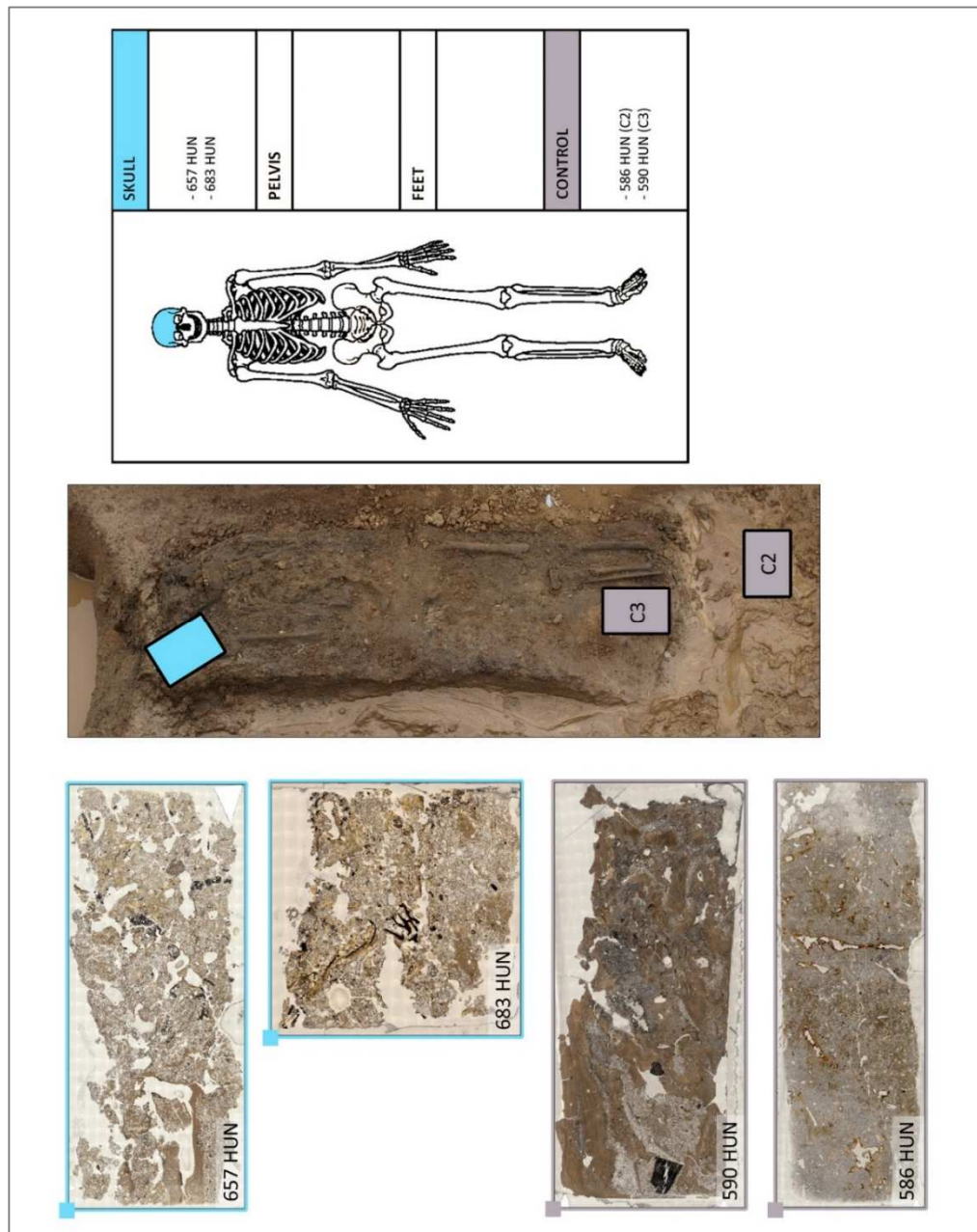
Figure 5.7: Grave 54077. In the centre, photographs of the grave and location of the samples. On the right, list of the slides in relation to their anatomical location. On the left, mosaics of the slides. See the text for descriptions.

GRAVE 54296

Grave 54296 was dated to the Roman period, probably 3rd- 4th C AD (Figure 5.8). It contained well preserved skeletal remains that had been placed in a coffin, of which iron nails were found. Hobnail shoes were found in the area of the feet. The grave cut was rectangular, oriented NW-SE, of dimensions 215 x 45 x 55 cm and with sharp sides. The layer below the skeleton was friable and composed of mid grey brown silty sand.
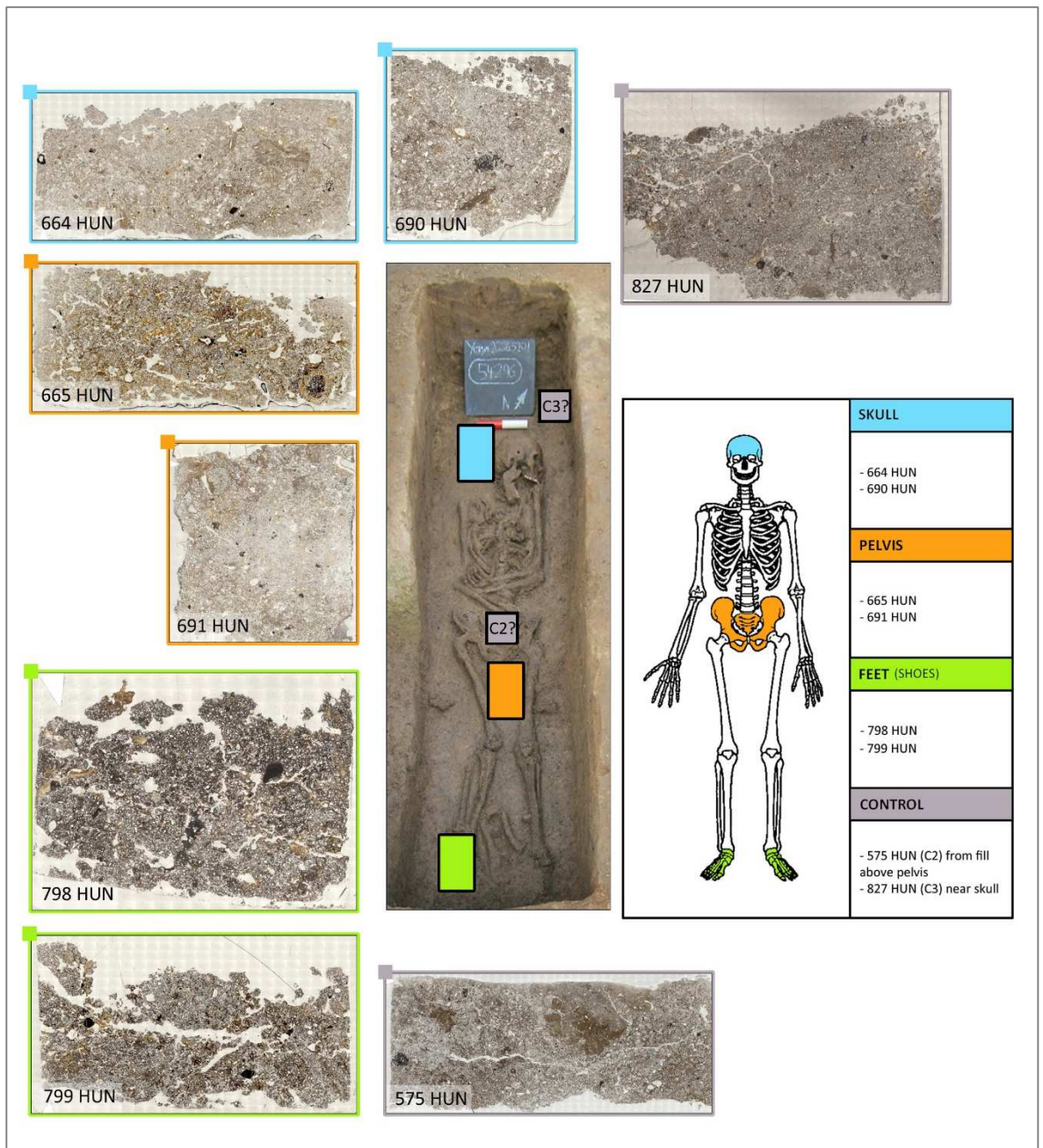
Figure 5.8: Grave 54296. In the centre, photographs of the grave and location of the samples. On the right, list of the slides in relation to their anatomical location. On the top, left and bottom, mosaics of the slides. See the text for descriptions.

GRAVE 54931/54909

No information was available for this grave (Figure 5.9).
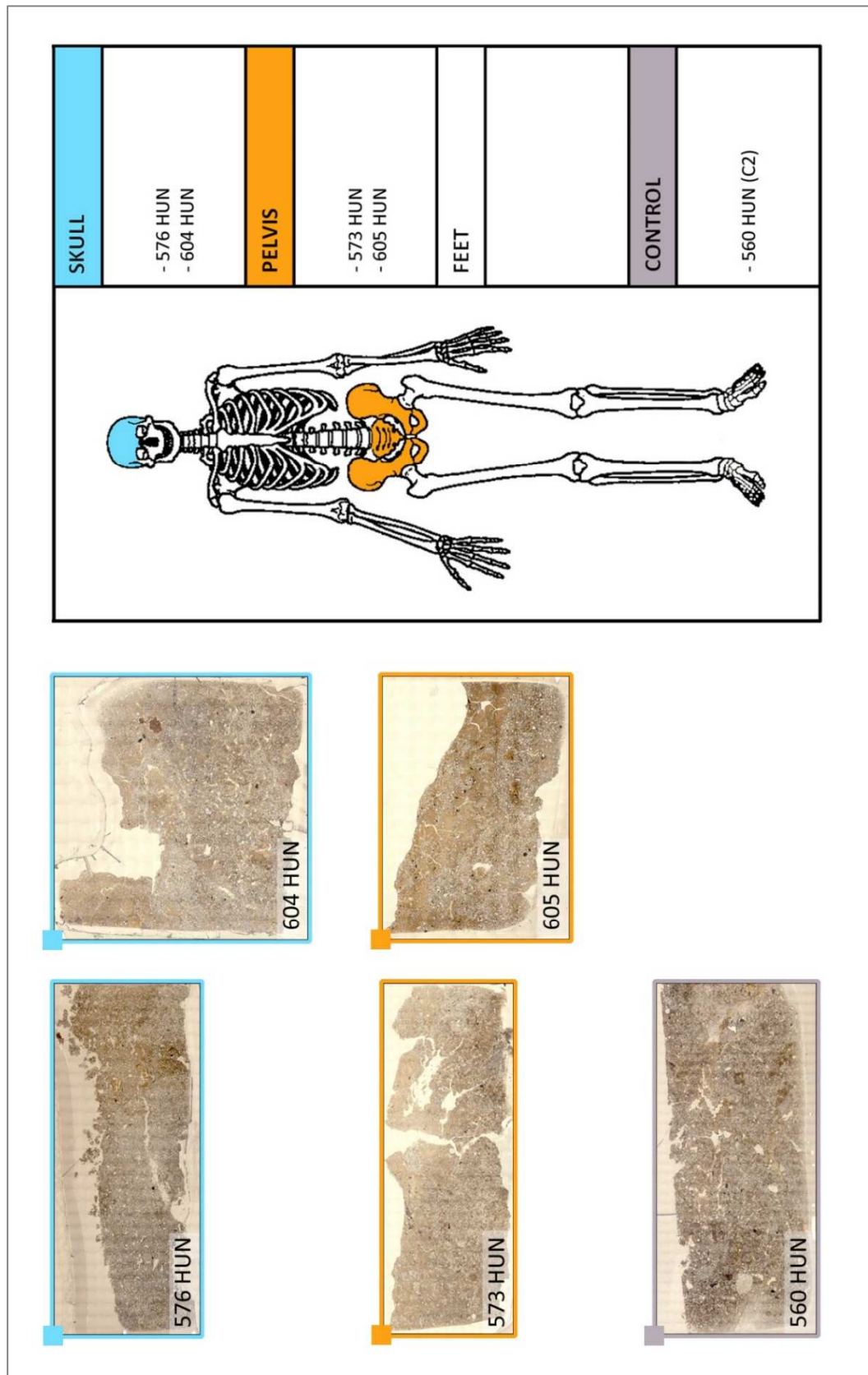
Figure 5.9: Grave 54931/54909. No photographs were available for this the grave. On the right, list of the slides in relation to their anatomical location. On the left, mosaics of the slides. See the text for descriptions.

GRAVE 53700

Grave 53700 (Figure 5.10) was dated to the Anglo-Scandinavian period by the presence of Viking age pottery in the fill. The subject was a male adult, that had been placed in a wooden coffin, traces of the lid of which were still visible in the sampling regions near the chest, pelvis and legs at the time of excavation. The skeleton was oriented West-East, with the head toward the West. Eight large stones surrounded the burial.
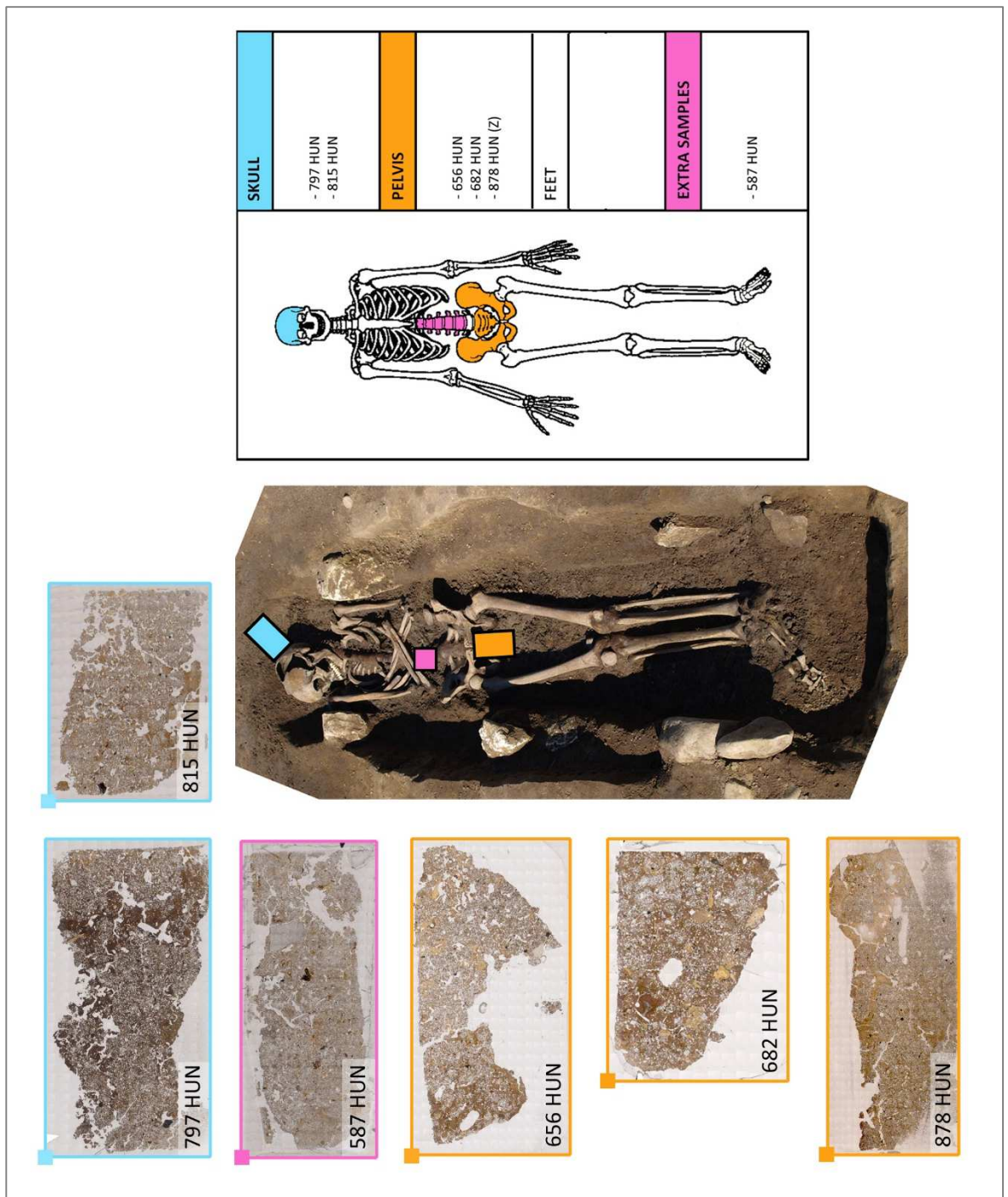
Figure 5.10: Grave 53700. In the centre, photographs of the grave, with location of the samples. On the top right, list of the slides in relation to their anatomical location. On the left and top, mosaics of the slides. See the text for descriptions.

5.1.3 MICROMORPHOLOGICAL RESULTS

GRAVE 51350/51364

ELEMENTS OF FABRIC AND PEDS

The fabric in grave 51350/51364 exhibited two principal c/f related distributions, accompanied by several intermediate distributions. Areas were principally porphyric and poorly/moderately sorted or chitonic and moderately/well sorted. These two distributions were either strongly separated or intermingled (Supplementary Data, folder "Mosaics"). Porphyric areas were brown/light brown/yellowish brown in PPL and brown/yellow or isotropic in XPL, with dotted limpidity and speckled b-fabric. Porphyric areas occupied between 10-30% of the samples. Chitonic areas were yellowish or reddish brown in PPL and orange/yellow or isotropic in XPL, with speckled or parallel striated b-fabric. Samples from this grave were apedal.

VOIDS

Five types of void were identified in grave 51350/51364: chambers, channels, modified complex, packing and planar (Figure 5.11).

Figure 5.11: Abundance of different types of void in relation to their anatomical location within grave 51350/51364. Chambers were more abundant in the area of the feet, channels and planar voids in the region of the skull and modified complex voids and packing voids in the control C2.

Chambers were quite common in the area of the feet (8%), few in the areas of the skull and C3 (5%) and very few in the area of the pelvis (2%). Their size was between 500-2000 µm and the surface was undulating. Channels were equally present in all of the samples (5%), but more common in the area of the skull (8%).Modified complex voids, characterized by curved and pointed surfaces, were observed only in the areas of the skull and pelvis (5%) and in the control C2 (8%). The percentage of packing voids increased from the area of the skull to the control C2, but they were not detected in the area of the pelvis. Planar voids, of thickness 100-1500 µm, were more abundant in the area of the skull (15%) than the pelvis, feet (5%) and C3 (8%).

MINERAL COMPONENTS

As shown in Figure 5.12, mineral components were mostly quartz (45-55%) that was sub-angular and not weathered. Very few fragments of quartzite were observed in the areas of the feet (2%) and C2 (5%). Rare grains of biotite were identified in the area of the skull (2%).
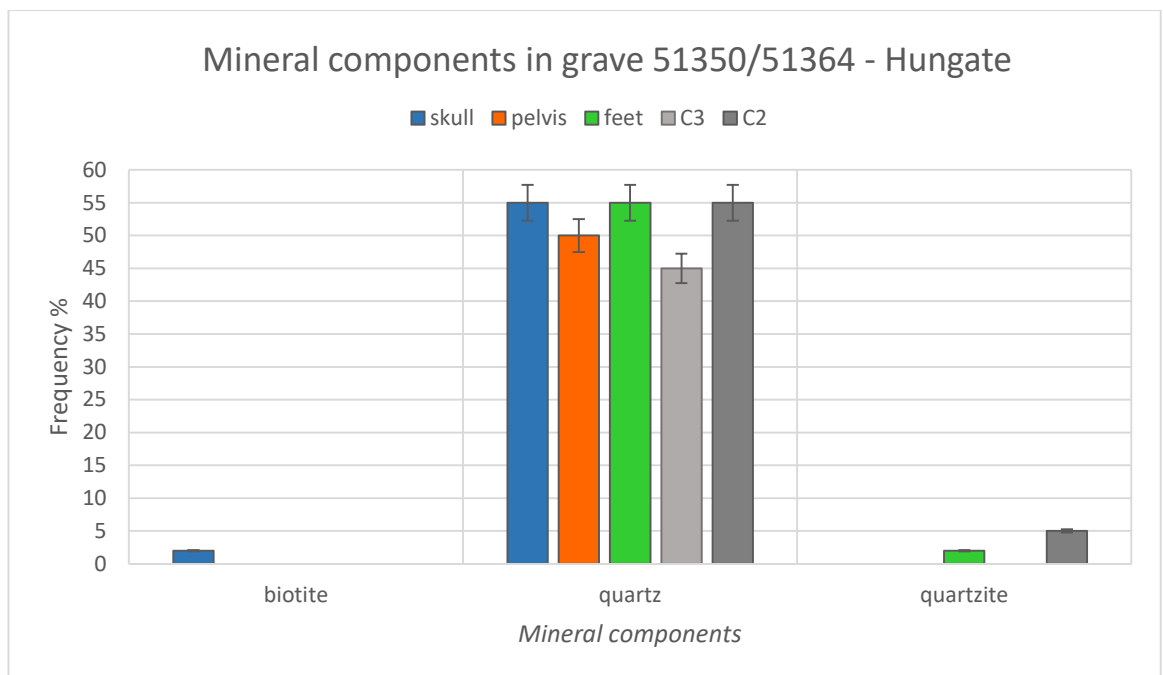
Figure 5.12: Frequency of mineral components in relation to their anatomical location within grave 51350/51364. Quartz was dominant in all of the samples.

ORGANIC COMPONENTS

Organic components were not frequent in grave 51350/51364 (Figure 5.13). Fragments of humified plant structures were detected in all of the samples (2%), except for the control C3. The plant remains were weathered of partially weathered, brown/black in PPL and isotropic in XPL; their size ranged between 50-2000 µm. Some of the coarser fragments were identified as parts of angiosperm by the presence of vessels.

Bone fragments were frequent in the area of the feet (20%). The right and left sides of the slide both included coarse pieces of bones (maximum length, 15 mm), three in total. These fragments were weathered: the histological structure was not visible and the surface had cracks and looked phosphatized (Figure 5.41.f). The colours were yellow in PPL and black with a few beige sub-rounded zones. The voids of the original spongy structure were partially filled with laminated coatings and the structure itself was embedded with ultrafine crystallitic fabric (Figure 5.45). Bone fragments from the area of the pelvis were smaller (100-1000 µm), very few (2%) and partially weathered.
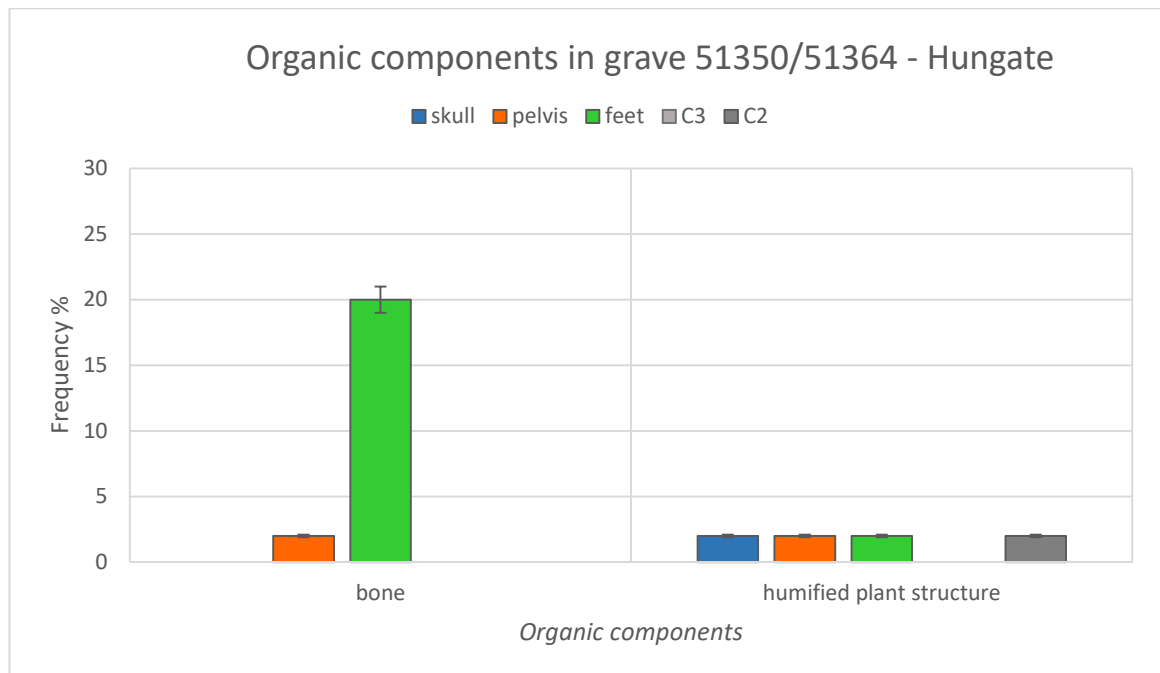
Figure 5.13: Frequency of organic components in relation to their anatomical location within grave 51350/51364. Bone fragments were frequent in the area of the feet, while humified plant structures were very few but represented in most of the samples.

PEDOFEATURES

The main pedofeatures identified in grave 51350/51364 were: brown organic coatings around voids, clay quasicoatings or coatings, clay textural impregnations, Fe/Mn nodules, coatings of goethite in voids, phosphatic coatings and spherulites with and without b-fabric (Figure 5.14).

The most frequent pedofeature was that of round spherulites. Two types were distinguished: the first was orange in PPL and orange/red in XPL, with cross striated b-fabric (Figure 5.44), the second was yellow in PPL and yellow/brown in XPL, without b-fabric (Figure 5.43). In the C3, the colour was more brown and the spherulites were located around voids and mineral grains, but not as densely accumulated. By contrast, in the samples collected next to the skeleton, the spherulites formed dense aggregations around voids and into the groundmass, between mineral grains. However, in

the area of the feet, several spherulites were trapped within coatings around the pores of bone fragments. Orange spherulites were more frequent in the areas of the feet and C3 (15%), common in around the skull (8%) and few around the pelvis (5%). The diameter of the spherulites was 5-12 µm in the areas of the skull, pelvis and C3. In the area of the feet, the spherulites were smaller: 4-10 µm for the spherulites among mineral grains and 2-5 µm for the ones in the coatings. Yellow spherulites were identified in the areas of the skull (5%), pelvis (15%) and feet (5%). The diameter was between 5-20 µm and some spherulites were characterized by an internal line, separating the spherule into two different layers.
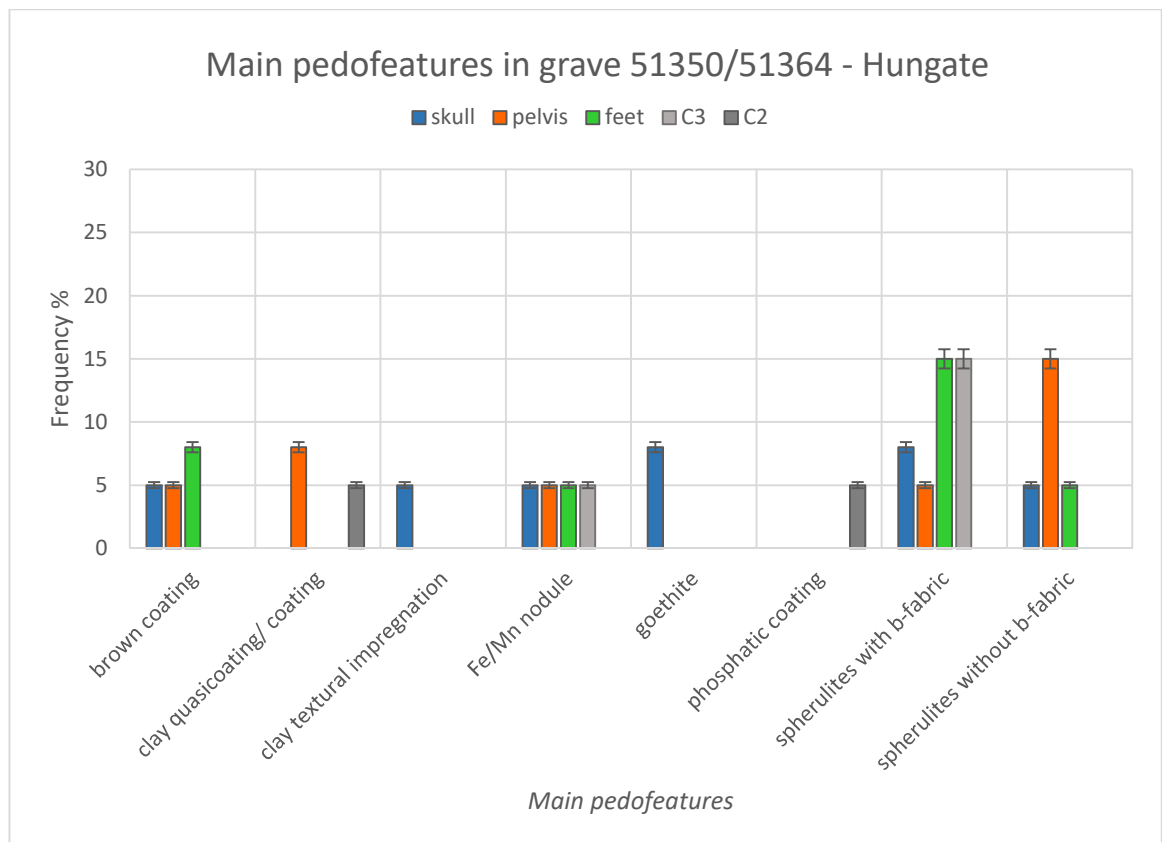
Figure 5.14: Frequency of the main pedofeatures in relation to their anatomical location within grave 51350/51364. Two types of spherulites, with or without b-fabric, were observed in the samples. Goethite was common only in the area of the skull, while few phosphatic coatings were present in control C2.

Phosphatic coatings around voids were observed only in control C2 (5%); the colour was yellow in PPL and isotropic in XPL, with undulating shape. This pedofeatures was peculiar for the presence of different layers, some Fe rich impregnated, which appeared reddish brown in PPL and red in XPL (Figure 5.46.c-d). In some cases, phosphates had the aspect of weathered granules as loose discontinuous infillings in voids.

Loose discontinuous or dense incomplete infillings of goethite in voids were identified in the area of the skull (8%). The goethite was characterized by fan-like crystals, orange/red colour in PPL and reddish brown or isotropic in XPL and with parallel striated b-fabric (Figure 5.51.a-d). Sub-angular/sub-rounded Fe/Mn nodules, 50-500 µm, were observed in all of the samples (5%), except for control C2. Another type of coating was represented by a thin dark brown layer around voids, probably having organic origin. These coatings were common in the area of the feet (8%) and few in the areas of the skull and pelvis (5%). Few examples of external quasicoatings of clay around voids were observed in the area of the pelvis (8%) and C2 (5%), while clay textural impregnations were noted in the area of the skull.

GRAVE 51349/51351

ELEMENTS OF FABRIC AND PEDS

The fabric in grave 51349/51351 exhibited chitonic/porphyric c/f related distribution and was moderately or poorly sorted. The fine material was light brown, sometimes more orange brown, in PPL and yellow/brown in XPL, with dotted limpidity and speckled or undifferentiated b-fabric. The amount of fine material was generally 20-40%, while coarse material was more abundant. Furthermore, some slides, from the samples collected within the skeleton layer, included small isolated areas in which fine material was more abundant (40-45%), more orange in PPL and with limpid or dotted limpidity; the b-fabric was speckled or parallel striated. All of the samples were apedal.

VOIDS

Four types of void were identified in grave 51349/51351: chambers, channels, modified complex and packing (Figure 5.15). Chambers were more abundant in the controls (8%) and decreasing in the areas of the skull, feet and the wooden chest located between the feet (5%). Very few chambers were seen in the area of the pelvis (2%). Channels were more abundant in the area of the skull (5-15%) and in the region of the pelvis and controls C2 and C1 (8%). Few channels were observed in the areas of the feet, the wooden chest located between the feet and control C3 (5%). Modified complex voids were rare, occurring only in the vicinity of the wooden chest (2%). By contrast, packing voids were the most frequent voids, especially in the areas of the pelvis and feet (25%). They reached 15% in all the other samples.
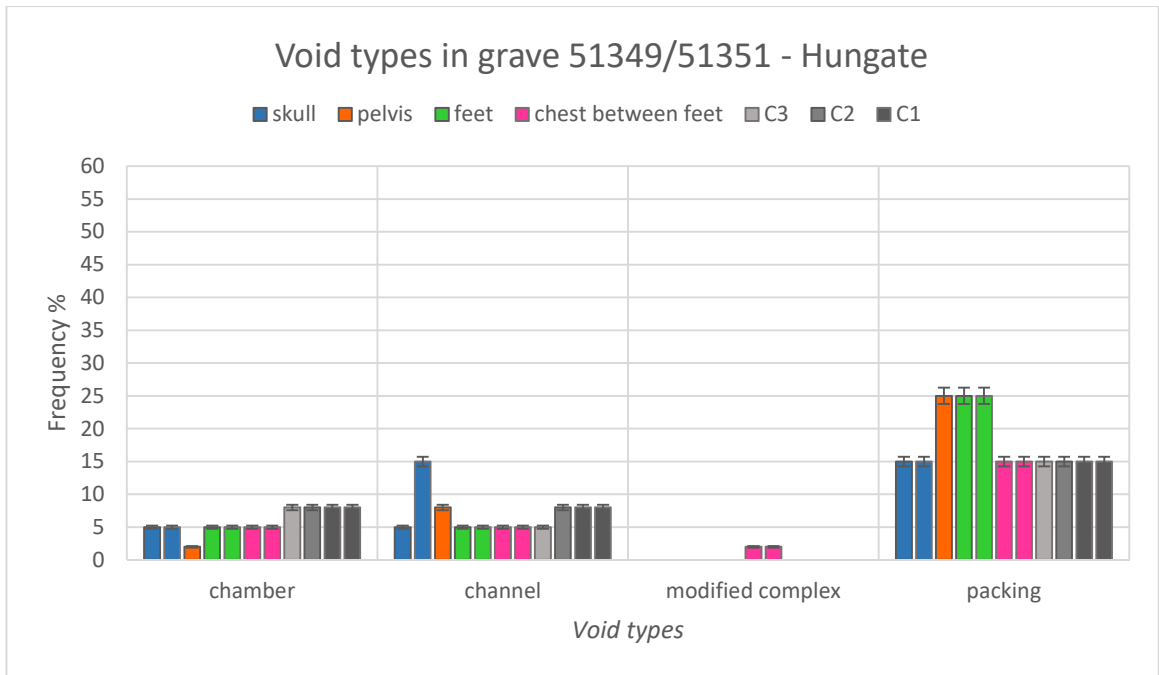
Figure 5.15: Abundance of different types of void in relation to their anatomical location within grave 51349/51351. Packing voids were the most common, while modified complex voids occurred only in the area of the chest between the feet.

MINERAL COMPONENTS

Seven types of mineral component were identified in grave 51349/51351: flint, glauconite, mica, plagioclase, pyroxene, quartz and quartzite fragments (Figure 5.16).
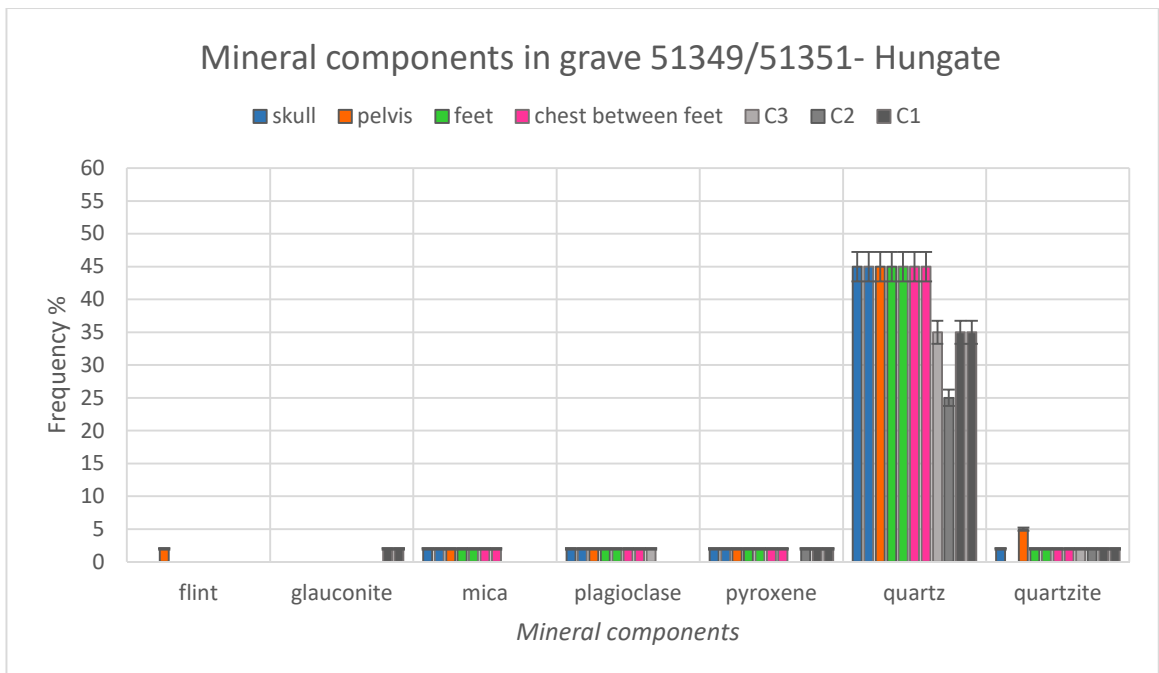
Figure 5.16: Frequency of mineral components in relation to their anatomical location within grave 51349/51351. Quartz was the dominant mineral.

Quartz was the most frequent mineral component: 45% in the skeleton layer and 25-35% in the control samples. The shape was angular or sub-rounded, the size was between 50-500 μm around the skeleton and 50-1000 μm in the controls and the grains were not highly weathered. Very few other mineral components were identified: quartzite fragments (2-5%), pyroxene (2%), plagioclase (2%, absent from C2 and C1), mica (2%) only in the area of skeleton, glauconite (2%) in the C1 and flint (2%) in the area of the pelvis. These mineral grains had angular shape, sometimes sub-rounded. Glauconite was always sub-rounded.

ORGANIC COMPONENTS

Organic components were not frequent in grave 51349/51351, particularly in the area of the skeleton where only humified plant structures (2%) and charcoal (2% in the area of the skull) were observed (Figure 5.17). Samples from controls, instead, contained fragment of bones and roots (2% in C1), rubified plant structure (2% in C2) and sclerotia (2% in C3 and C1). Humified plant structures were more abundant (2-8%) and fragments of charcoal were identified in C1. Some coarser fragments of humified plant structures (up to 2000 μm) were identified as fragments of angiosperm and some others of gymnosperm in the area of C1.
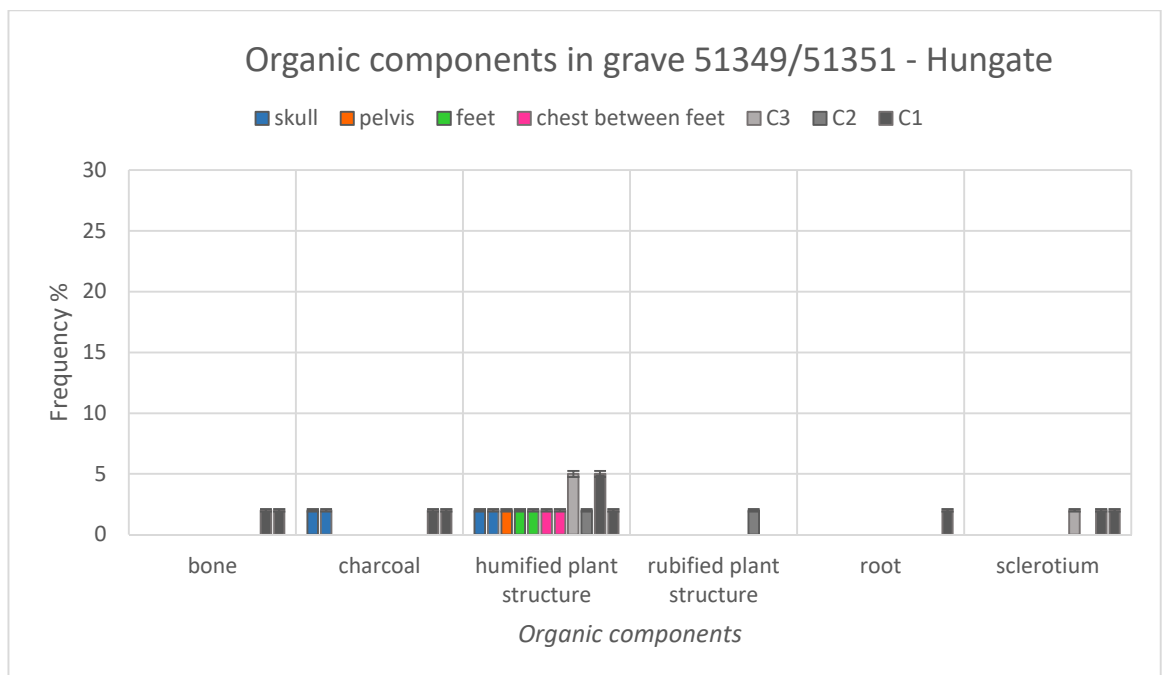
Figure 5.17: Frequency of organic components in relation to their anatomical location within grave 51349/51351. Very few organic components were represented in the samples, mostly humified plant structures.

PEDOFEATURES

Seven main types of pedofeature were observed in grave 51349/51351: clay coatings, Fe/Mn nodules, amorphous phosphates, redox strong impregnations, secondary radial crystals, spherulites with b-fabric and vivianite (Figure 5.18).

Redox impregnations, secondary radial crystals, spherulites and vivianite were in association with each other in some cases:

- Spherulites and redox impregnations in the areas of the skull and feet. In these cases, some spherulites were amorphous;
- Spherulites and vivianite in the areas of the pelvis, feet and wooden chest. Sometimes the vivianite crystals developed around the spherulites;
- Spherulites and vivianite crystals with secondary radial crystals or redox impregnations in the control C3.

Spherulites were the most frequent pedofeature: 15% in the areas of the feet and wooden chest between them, 8% in the areas of the pelvis and controls C3 and C2, 5% in the area of the skull and 2% in C1. They were located in the groundmass surrounding mineral grains as aggregations or as coatings around voids. The colour was orange in PPL and red/orange in XPL, with crossed b-fabric (excluded the examples mentioned above). The size was slightly different in the samples: 5-20 μm in all areas and 3-10 μm in the region of the pelvis.

Vivianite was observed in all of the samples (5-8%), excluding the areas of the skull, C2 and C1. Radial crystals grew within the groundmass, sometimes including quartz grains or spherulites (Figures 5.47.g-h and 5.48). The size of vivianite was between 500-1300 μm and the crystals were not weathered. The colour was blue/green/pale yellow pleochroic in PPL and blue/green/yellow/pink pleochroic in XPL. Secondary radial crystals looked like complete or incomplete dense infillings in voids. In the case of complete infillings, the crystal grain had crossed b-fabric and they were self-limited and showed a distinctive black line of limitation. Consequently, the infilling looked like it was cracked (Figure 5.49.c-d). In case of the incomplete infillings the crystal grains had rounded or sub-rounded shape when not in proximity with other crystals of the same composition (Figure 5.49.e-f). The size of each grain was between 50-500 μm. Amorphous phosphates were located in the control samples C2 and C1 (5%). They emerged as dense incomplete infillings in voids, as nodules or as strong impregnation within the groundmass. The size was between 500-1000 μm, the colours yellow in PPL and isotropic in XPL, without b-fabric.

Strong redox impregnations were observed in the controls (5%) and in the sample of the wooden chest (2-5%). The colour was variably red or black in PPL and the size between 700-2000 μm (Figure 5.50.e). Fe/Mn nodules were constant in the grave: 5% in the region of the skeleton and C3, 2% in the controls C2 and C1.

Clay coatings (or infillings in few cases) presented differences among the samples (Figure 5.50.c-d):

- Limpid clay coatings around voids, exhibiting parallel striated b-fabric, dark yellow colour in PPL and yellow/orange or isotropic in XPL. Observed in the areas of the skull and pelvis;

- Limpid laminated clay coatings around voids or laminated clay as strong impregnation around mineral grains. Parallel striated or striated b-fabric, dark yellow colour in PPL and yellow/orange or isotropic in XPL. Observed in the areas of the skull, feet and in the chest between feet.

- Limpid clay discontinuous infilling in voids in C2 and dense complete infilling in C3, with speckled or parallel striated b-fabric.
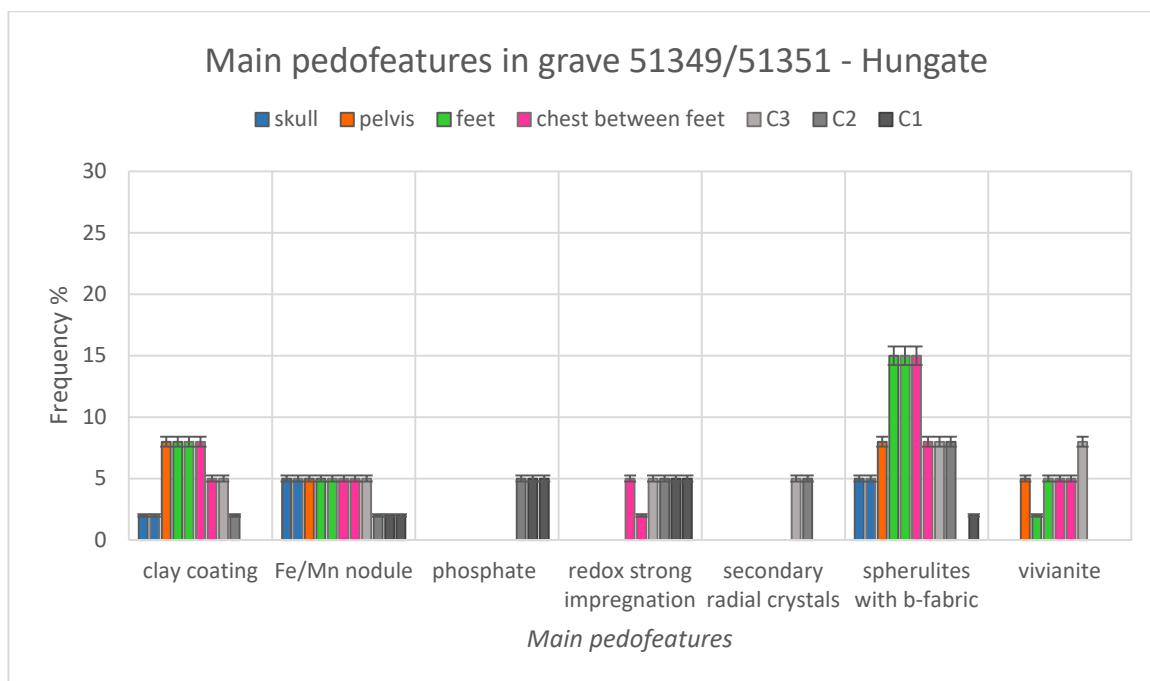
Figure 5.18: Frequency of the main pedofeatures in relation to their anatomical location within grave 51349/51351. Spherulites were observed in all of the samples from the area of the skeleton and in the controls. Vivianite was present in all of the samples excluding the region of the skull and controls C2 and C1. Phosphatic pedofeatures occurred only in controls C2 and C3.

GRAVE 52253

ELEMENTS OF FABRIC AND PEDS

The fabric in grave 52253 was characterized by chitonic/porphyric c/f related distribution and good or moderate sorting. Fine material was yellowish brown to brown in PPL and yellow/orange/brown in XPL, with speckled or striated b-fabric and dotted or limpid limpidity. The samples were quite homogenous and the amount of fine material was between 20-40%, though a few areas richer in fine material were observed in the area of the feet (40-60%, top of slide 356) and in control C2 (50-60%). All of the samples were apedal.

VOIDS

Five types of void were identified in grave 52253: chambers, channels, modified complex, packing and planar (Figure 5.19). Chambers were few in all of the samples (2-5%) and channels were slightly more abundant (2-8%), particularly in the area of the skull. Very few modified complex voids were observed in the same area, while they were common in the control C2 (8%). Packing voids were the most abundant in the layer of the skeleton (8-15%), few in C3 and common in C2 (8%). Planar voids were observed in C3 (15%), but the surface of these voids was not well delimited and it seemed that they originated, at least partially, during the manufacture of the slide.
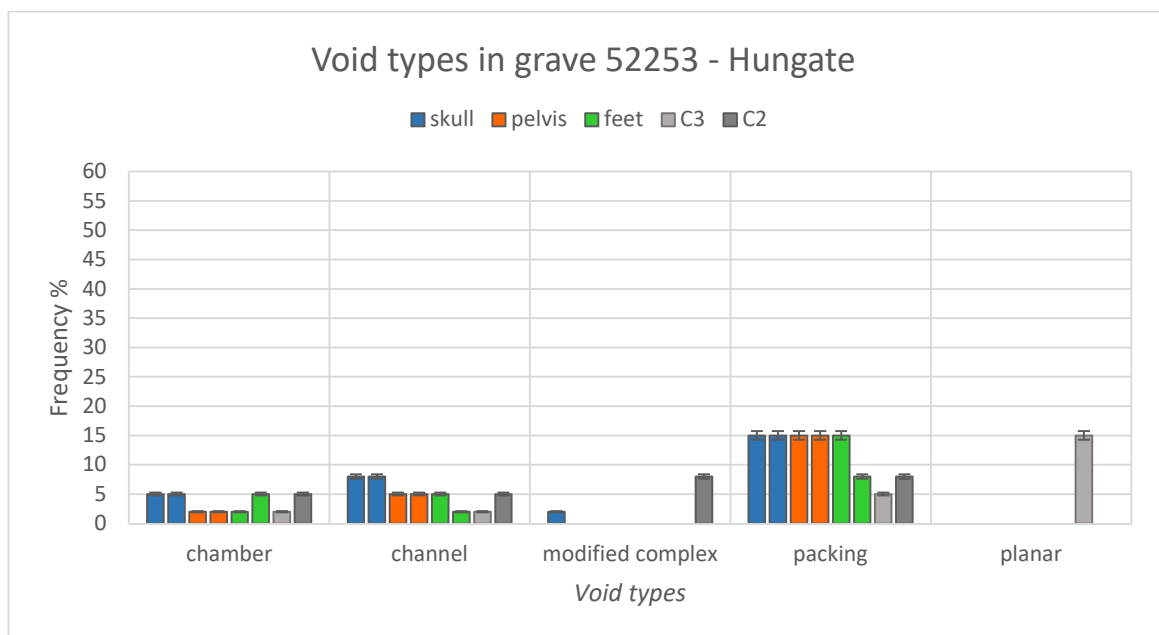
Figure 5.19: Abundance of different types of void in relation to their anatomical location within grave 52253. Packing voids were common in all of the samples, channel and chambers were more represented in the area of the skull and modified complex voids were detected only in the area of the skull and C3.

MINERAL COMPONENTS

Samples from grave 52253 were mainly composed of quartz grains: 45% in the areas of the skull and pelvis, 35% in the areas of the feet and controls (Figure 5.20). Very few examples of plagioclase, pyroxene and quartzite were observed in the samples (2%), while the presence of mica (2%) was detected only in the area of the feet (2%). The shape of the minerals was angular or sub-rounded.
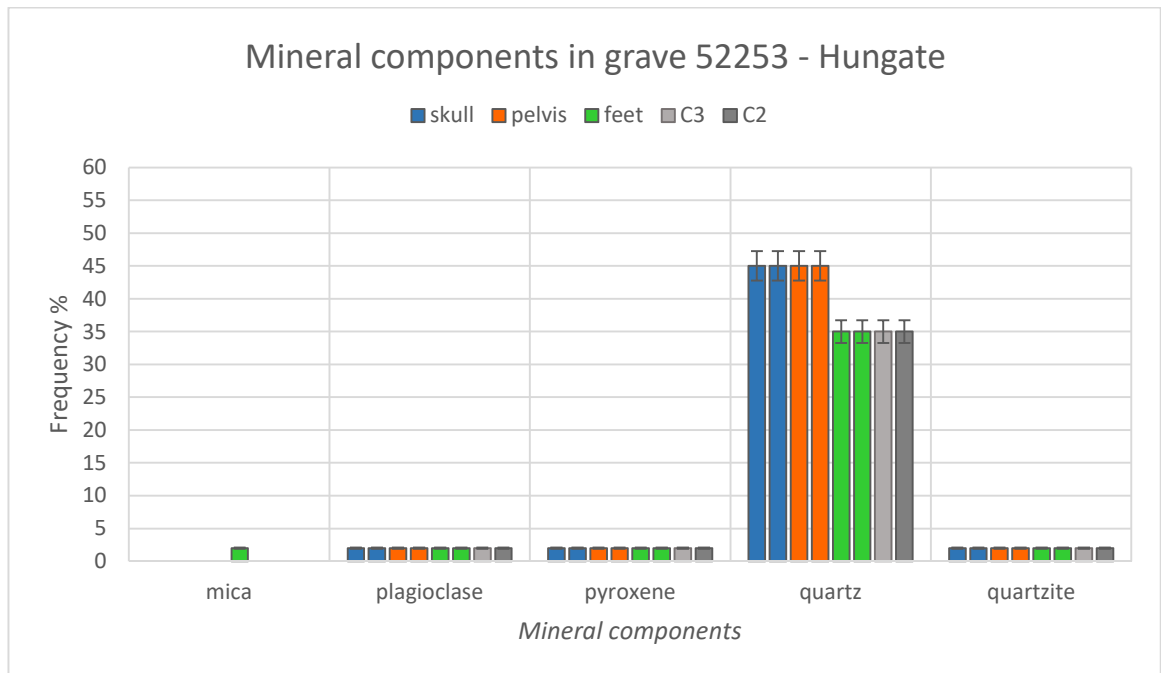
Figure 5.20: Frequency of mineral components in relation to their anatomical location within grave 52253. Quartz was the dominant component in all of the samples.

ORGANIC COMPONENTS

Organic components were rarely represented in grave 52253 (Figure 5.21). Fragments of humified plant structure were observed in all of the samples, between 2-5%. The coarser fragments were identified as angiosperm by the presence of vessels. Bone fragments were very few in the areas of the skull and pelvis (2%) and few in the area of the feet (2-5%). Coarse fragments (300-1000 µm) from the feet were sub-rounded in shape, light yellow in PPL and isotropic in XPL. They had not b-fabric and the histological structure was scarcely visible.
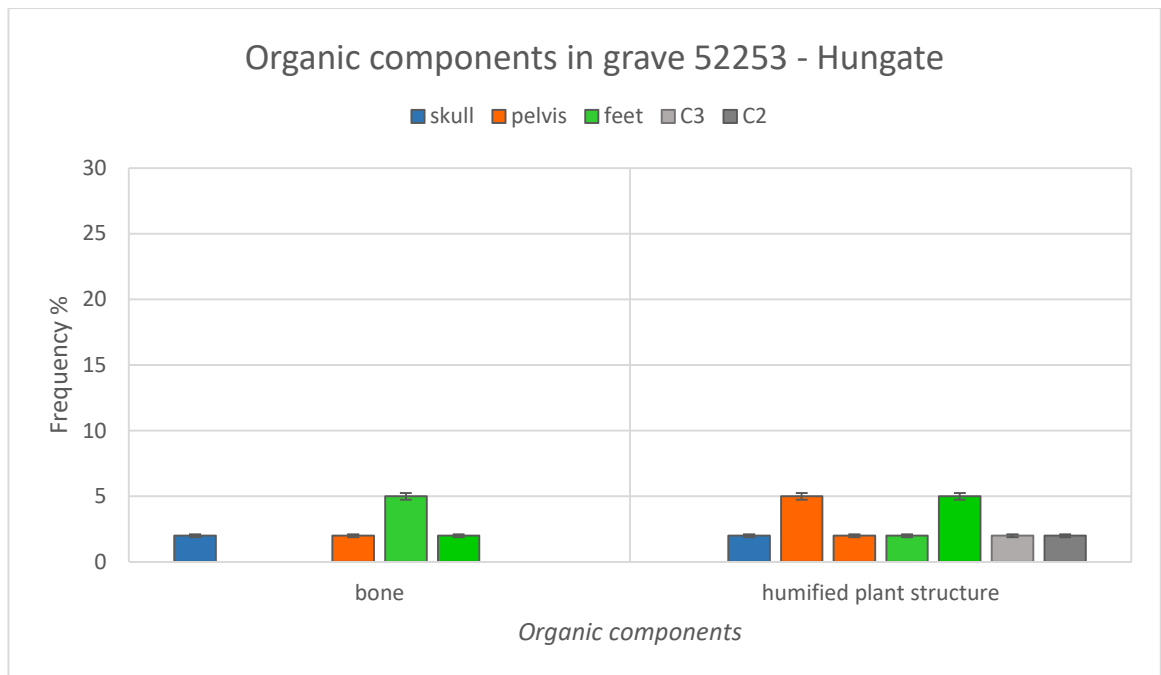
Figure 5.21: Frequency of organic components in relation to their anatomical location within grave 52253. Bone fragments and humified plant structures were few.

PEDOFEATURES

Six main types of pedofeature were detected in grave 52253: black redox impregnations, red redox impregnations, clay infillings or coatings, Fe/Mn nodules, spherulites with b-fabric and secondary radial crystals (Figure 5.22).

Spherulites were frequent in the area of the skull (8-15%), as loose discontinuous infillings in vertical voids or around mineral grains. In slide 395, spherulites were in association with CaCO$_3$ crystals as coating/dense complete infilling in voids. In this case, spherulites occupied the first layer of coating, while the CaCO$_3$ occupied the internal and subsequent part of the void. Spherulites were orange in PPL and red or isotropic in XPL, with crossed b-fabric and size between 5-10 μm. In slide 395, few spherulites were light yellow in PPL.

Secondary radial crystals were observed only in the area of the skull (5%). As mentioned above, they formed coatings around voids, generally vertical channels, or dense incomplete infillings. The crystals had sub-rounded shape and crossed b-fabric, similar to the ones in grave 51349/51351, but they were less developed. They were white/light yellow in PPL and pink/green in XPL. In addition, some of the infillings had internal laminations of Fe or Mn. In one case, the channel was completely filled by an external area of radial crystals and an internal area of Mn (Figure 5.49.g-h).

Black redox impregnations were observed in the areas of the pelvis (5%), C3 (5%) and C2 (8%), while red redox impregnations were found in the areas of the pelvis (8%), feet (5%) and C3 (5%). Fe/Mn

were equally represented in all of the samples (5%). The size was between 50-500 μm and the shape was sub-angular/sub-rounded. Limpid clay laminated infillings were detected in vertical voids in the areas of the skull and feet (2-5%). The colour was yellow in PPL with Fe or organic matter inclusions. The b-fabric was parallel striated.
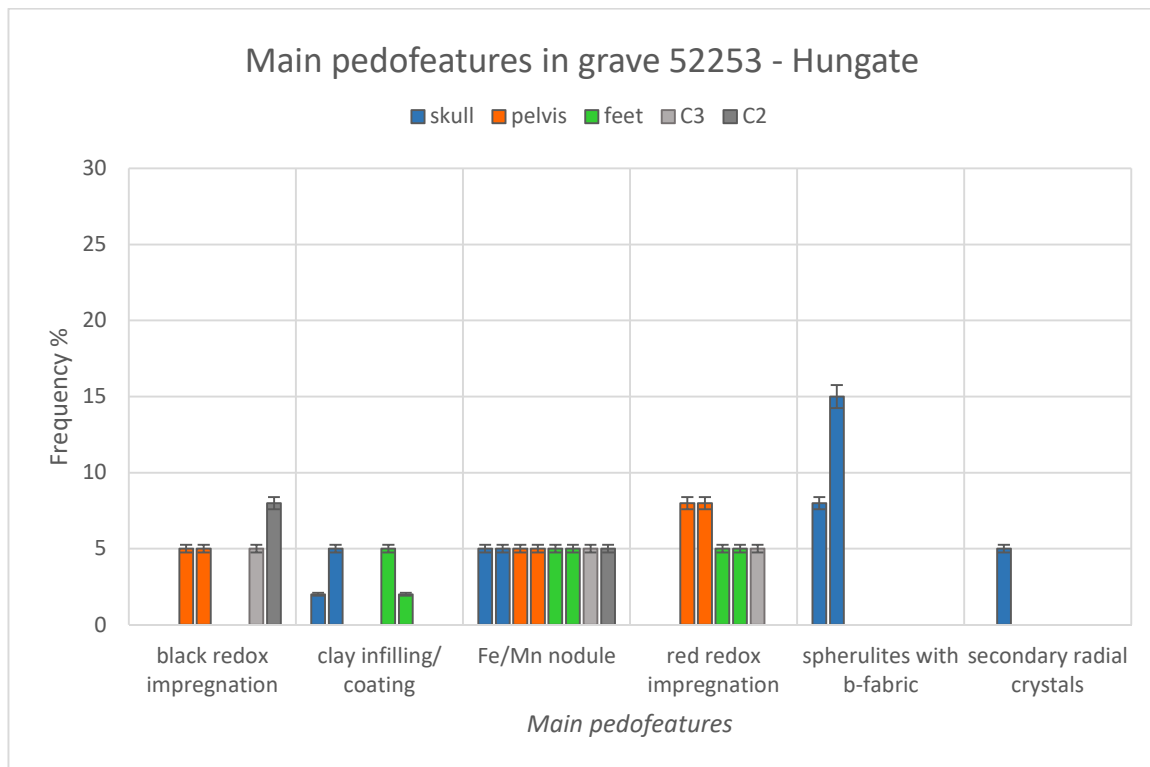
Figure 5.22: Frequency of the main pedofeatures in relation to their anatomical location within grave 52253. Spherulites were present only in the area of the skull, as well as secondary radial crystals.

GRAVE 54077

ELEMENTS OF FABRIC AND PEDS

Samples from grave 54077 did not present the same characteristics in fabric and microstructure. The area of the skull was characterized by chitonic/porphyric c/f related distribution and moderate sorting. Moreover, the microstructure was quite spongy in appearance owing to the prevalence of voids (30-40%). Sample C3 was characterized by two different types of fabric, very well defined (Supplementary Data, folder "Mosaics"). Type A (60-70%) exhibited monic c/f related distribution and was perfectly sorted, while type B (30-40%) was porphyric, well sorted and resembled an inclusion of type A. Sample C2 was porphyric, moderately sorted and with quite massive microstructure. The fine material was yellowish brown in PPL, yellow/brown in XPL, with dotted limpidity and speckled b-fabric in all of the samples. No peds were recognized.

VOIDS

Four types of void were observed in grave 54077: chambers, channels, modified complex and packing (Figure 5.23). Samples from the areas of the skull were more porous (30-40%) than controls C3 (5-10% type A and 2-5% type B) and C2 (20%). Furthermore, voids in the area of the skull were highly interconnected and reached 10000 μm in size. Chambers were few in the area of the skull (5%) and very few in C3 (2%). The channels and the modified complex voids were more abundant: 15% in the area of the skull, 5% in C3 and 8% in C2. Few packing voids were observed in the area of the skull and C2 (5%) and very few in C3 (2%).

Figure 5.23: Abundance of different types of voids in relation to their anatomical location within grave 54077. Modified complex voids and channels were common in the area of the skull and less frequent in the controls. Packing voids and chambers were few.

MINERAL COMPONENTS

Five types of mineral grain were identified in grave 54077: calcite, plagioclase, pyroxene, quartz and quartzite fragments (Figure 5.24). Quartz was the dominant mineral: 30% in the area of the skull and C3, 35% in C2. In the first case, the size was between 50-1300 μm, while in the controls the grains were smaller, between 50-500 μm. Quartzite was observed only in the area of the skull (2%), calcite in C3 (2%), pyroxene in both of them (2%) and plagioclase in all of the samples (2%).
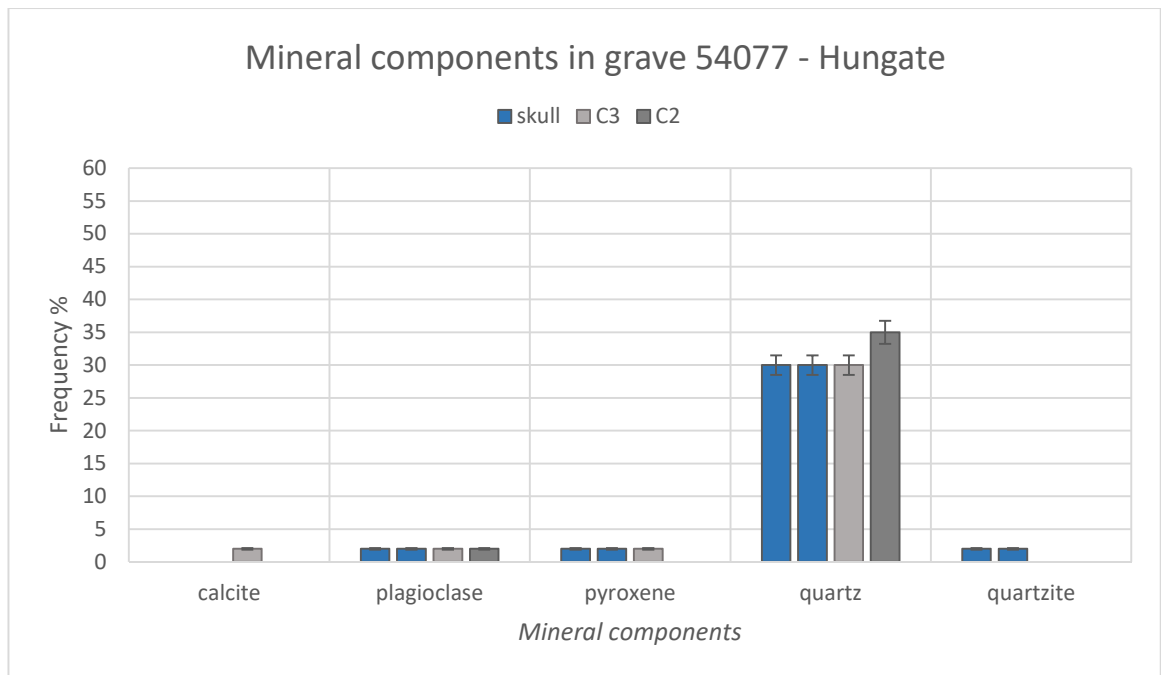
Figure 5.24: Frequency of mineral components in relation to their anatomical location within grave 54077. Quartz was dominant in all of the samples.

ORGANIC COMPONENTS

Four types of organic components were observed in grave 54077: calcified fragment of bones, humified plant structures, rubified bone fragment and white plant structures (Figure 5.25). Most of these remains came from the area of the skull, while few humified plant structures were detectable in the controls.

The humified plant structures from the area of the skull (15%) were the most interesting and well preserved organic remains from the graves of Hungate (Figure 5.42). The fragments were up to 4000 µm in size and were identified as gymnosperm wood. Very well preserved fragments showed orthogonal tracheids of thickness 10-15 µm, dark brown in PPL and isotropic in XPL. Other fragments were more or less weathered and it was possible to observe different stages of decomposition, from the initial breaking of the tracheids to nearly amorphous organic matter. Some of these fragments were embedded within phosphates.

Two fragments of bones were observed: the first was white in PPL and isotropic in XPL, with low first order birefringence. It was weathered and identified as having been calcined. The second was reddish brown in PPL and isotropic in XPL, without birefringence. This fragment was identified as rubified bone. A few unidentified white plant structures with subrounded shape were observed in the area of the skull.

Figure 5.25: Frequency of organic components in relation to their anatomical location within grave 54077. Humified plant structures were common in the area of the skull.

PEDOFEATURES

Seven main pedofeatures were identified in grave 54077: clay coatings, Fe/Mn nodules, amorphous phosphates associated with vivianite, red spherulites infillings, amorphous phosphates associate with secondary $CaCO_3$ crystals, red redox hypocoatings and red redox impregnations (Figure 5.26).

Amorphous phosphates were detected only in the area of the skull, in association with vivianite (15%) and secondary radial crystals (2%). Moreover, as noted above, many phosphates included fragments of wood (Supplementary Data, folder "Mosaics"). The phosphates appeared as coatings around voids, nodules and as strong impregnations in the fine material if associated with vivianite, or as coatings if associated with secondary radial crystals. Their colour was yellow in PPL and isotropic in XPL. Vivianite crystals were generally rounded or sub-rounded in shape, with radial crystals and often concatenated among them. Vivianite was often located in proximity to fragments of wood. The colour of vivianite was green/blue in PPL and green/blue/pink in XPL (Figure 5.47.a, c-f). Coatings of secondary radial crystals were associated with phosphates exhibiting two modes: external coatings around phosphatic amorphous nodules or coatings around voids with subsequent coatings of amorphous phosphate.

Thick limpid clay coatings (100-1200 μm) coated the horizontal surfaces of voids. The colour was yellowish brown in PPL and yellow/brown in XPL, the b-fabric was striated and the surface was smooth. Thin laminations were visible within the coatings (Figure 5.50.a-b).

With the exception of the 2% of red redox impregnations within the area of the skull, redox pedofeatures were exclusive to the control samples. Red redox impregnations were more abundant in C3 and C2 (5%) and frequent red redox hypocoating surrounded the voids in C2. Some of the same voids were also partially filled by red spherulites. These seemed different from the ones described in the previous graves. They were 5 μm size, red in PPL and XPL, without b-fabric (Figure 5.50.g). Fe/Mn nodules were observed in all of the samples (2%), especially in C2 (5%). The size was between 50-300 μm in the controls and 50-100 μm in the area of the skull.

Figure 5.26: Frequency of the main pedofeatures in relation to their anatomical location within graves 54077. Phosphates were present only in the area of the skull, associate with vivianite or secondary CaCO₃ coatings.

GRAVE 54296

ELEMENTS OF FABRIC AND PEDS

The fabric was characterized by chitonic/porphyric c/f related distribution and good/moderate sorting. Few zones in the area of the skull (5-10%) and in C2 (20-30%) demarcated by porphyric c/f related distribution, moderate sorting and the increase of fine material (70-85%). By contrast, the amount of fine material in the rest of the slide was between 20-30% in the area of the skull, 30-40% in the area of the feet and 40-50% in the C3. The fine material was yellowish brown in PPL and

yellow/brown in XPL, with dotted limpidity and speckled b-fabric. Fine material in the porphyric zone of control C2 was reddish brown in PPL and red/yellow in XPL. All of the samples were apedal.

VOIDS

Four types of void were observed in grave 54296: chambers, channels, modified complex and packing (Figure 5.27). Chambers were very few in all of the samples (2%), while channels were more abundant (8%) especially in control C2 (15%). Modified complex voids were frequent in the area of the pelvis (8-15%), few in the areas of the skull and feet (5%) and very few in the controls (2%). Packing voids were common in the area of the skull (8%), very few in C2 (2%) and few in the remaining samples (5%).
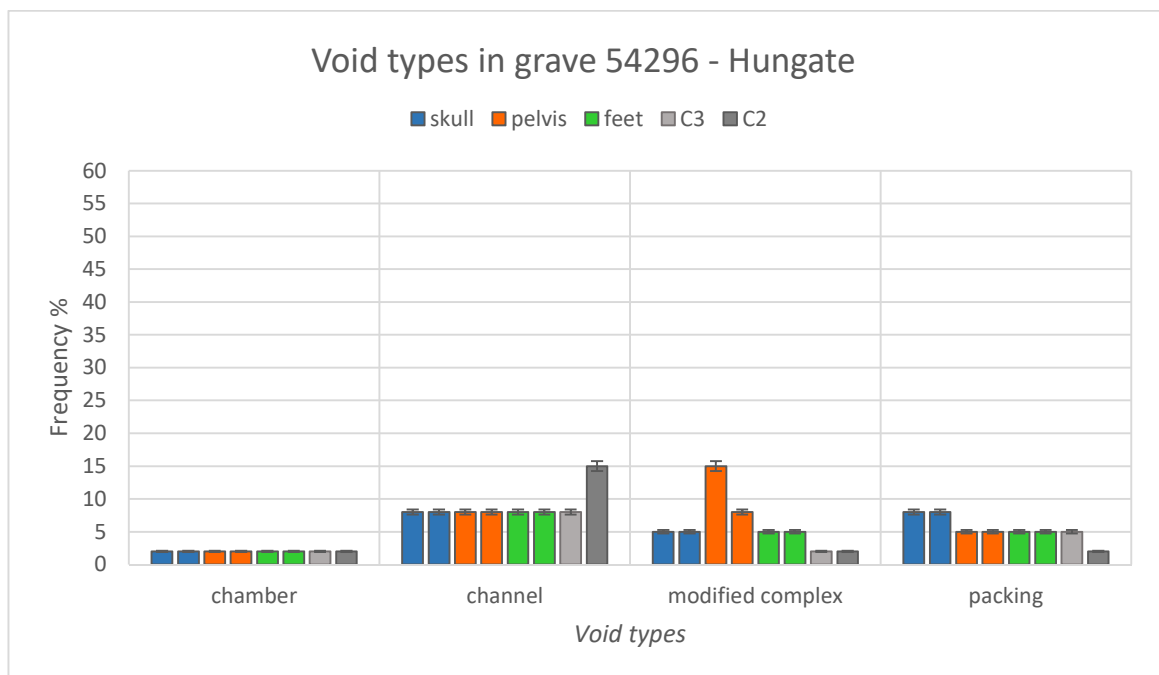
Figure 5.27: Abundance of different types of void in relation to their anatomical location within grave 54296. Modified complex were present in all of the samples and more abundant in the area of the pelvis. Channels were the most frequent voids, especially in C2.

MINERAL COMPONENTS

Four types of mineral component were identified in grave 54296: calcite, plagioclase, pyroxene, quartz and quartzite fragments (Figure 5.28). Quartz was most frequent: 40% in the area of the skull, 35-40% in the area of the pelvis, 30% in the area of the feet, 15% in C3 and 25% in C2. The size was generally between 50-700 µm, but the grains were smaller (50-200 µm) in the separated zones. Quartzite (100-700 µm) and pyroxene (50-300 µm) were very few in all of the samples, as well as pyroxene (50-300 µm), which was not detected in C2.
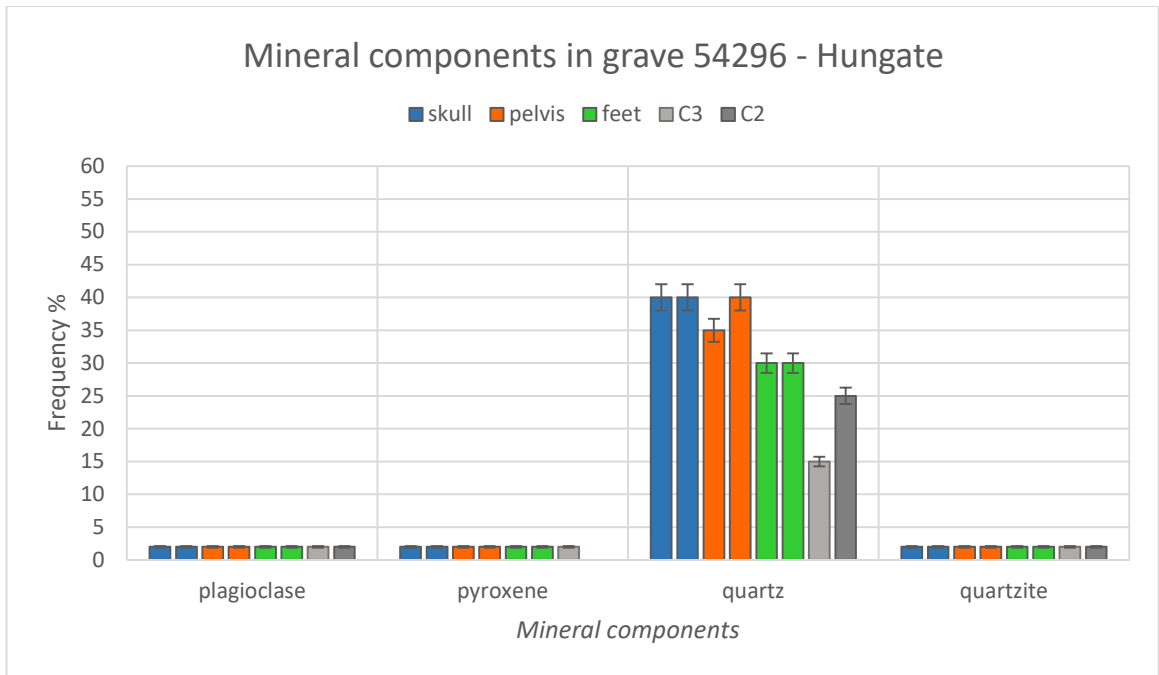
Figure 5.28: Frequency of mineral components in relation to their anatomical location within grave 54296. Quartz was the dominant mineral.

ORGANIC COMPONENTS

Humified plant structures were the only organic components observed in grave 54296, with low frequency in all of the samples (2-5%) (Figure 5.29).
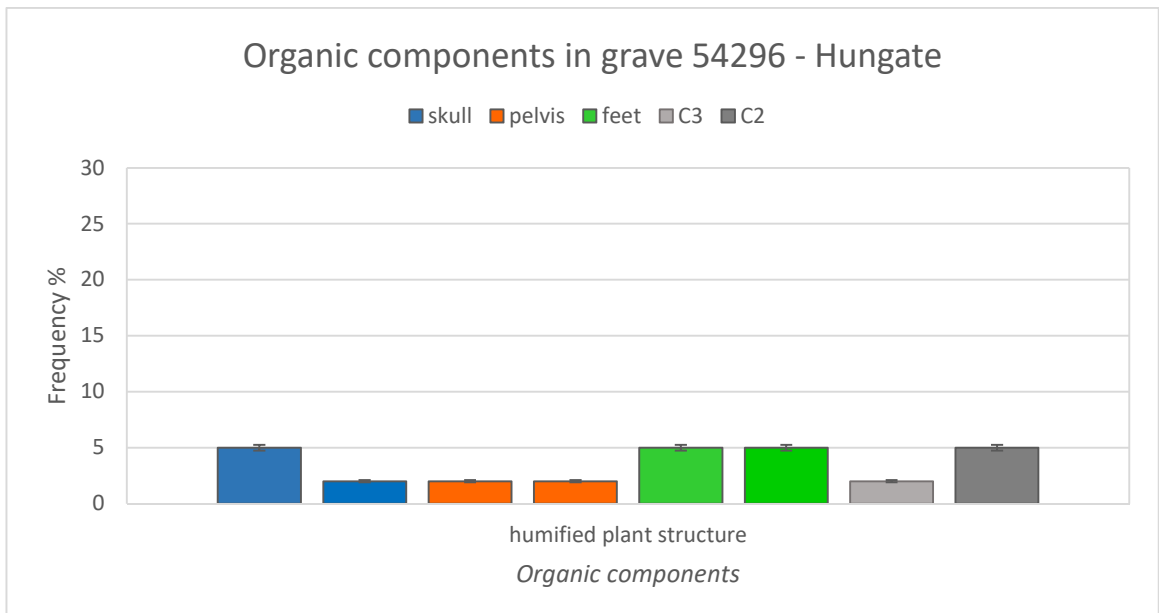
Figure 5.29: Frequency of organic components in relation to their anatomical location within grave 54296. Humified plant structure was the only type observed and was not abundant (2-5%).

PEDOFEATURES

The main types of pedofeature in grave 54296 were: black/red redox impregnations, clay coatings, Fe/Mn nodules, amorphous phosphates, phosphates associated with vivianite, coatings of secondary radial crystals and worm-derived calcium carbonate granules (Figure 5.30).
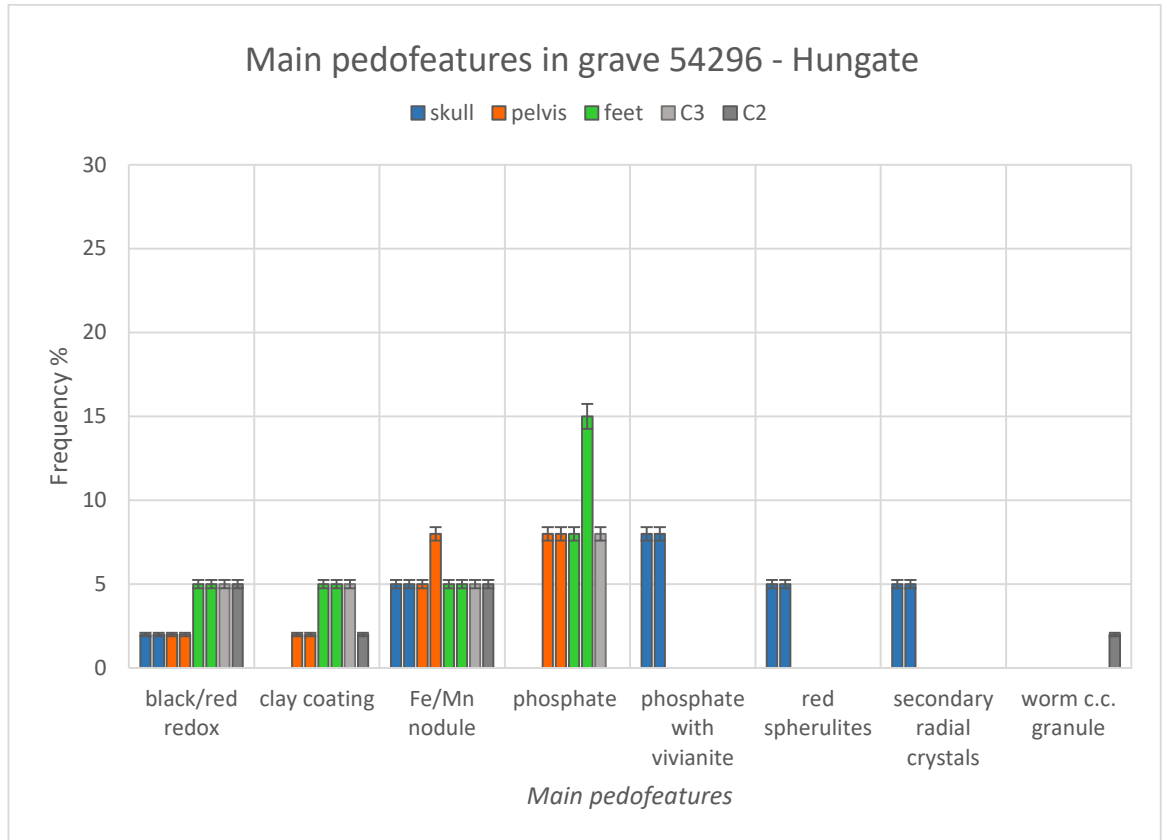
Figure 5.30: Frequency of the main pedofeatures in relation to their anatomical location within grave 54296. Phosphates were observed in all of the samples and they were associated with vivianite in the area of the skull. Red spherulites and secondary radial crystals were present only in the area of the skull.

Phosphates were the most common pedofeatures (Figure 5.46.a-b,g): 8-15% in the area of the feet, 8% in the region of the pelvis and in C3. Amorphous phosphates were associated with vivianite crystals in the area of the skull (8%). The crystals of vivianite had different layers of development, generally radial but not well developed and many with small crystals. Consequently, the amorphous phosphates were characterized by some small blue/green areas (Figure 5.47.b). The phosphates associated with vivianite occurred mainly as coatings around voids, but were also detected as nodules or infillings within voids. Some phosphatic coatings had Fe rich laminations or were associated with very small red spherulites (3-5 μm) having crossed b-fabric. The spherulites were observed only in the area of the skull (5%) and were arranged as external coatings around the phosphatic coatings.

Coatings of secondary radial crystals, observed only in the area of the skull (5%), were mostly associated with the phosphatic coatings and occurred frequently with the red spherulites. They were generally external coatings to both these pedofeatures. The crystals had crossed b-fabric, similar to the ones observed in graves 51349/51351 and 52253. Small rounded nodules of Mn were often in contact with them, as in grave 52253 (Figure 5.49.a-b). Fe/Mn nodules (50-300 µm) were few in all of the samples (5%) and slightly more abundant in the area of the pelvis (5-8%). Black or red redox strong impregnations were very few in the regions of the skull and pelvis (2%) and few in the areas of the feet and controls (5%) (Figure 5.50.f).

Clay coatings around voids, generally at the bottom of them, were identified in all of the samples, except the skull. They were more frequent in the area of the feet and C3, where they were thickest (up to 200 µm). The colour was yellowish brown in PPL, with speckled b-fabric. One single worm-derived calcium carbonate granule (250-800 µm), sub-rounded and with radial crystals, was present in control C2.

GRAVE 54931/54909

ELEMENTS OF FABRIC AND PEDS

The fabric exhibited porphyric c/f related distribution with moderate sorting. All of the samples from the layer of the skeleton had some zones (A) richer in fine material (50-70%). Type A occupied 25-50% of the slides and were characterized by fine material, orange-light brown in PPL and brown/yellow in XPL. The limpidity was dotted or limpid and the b-fabric was speckled or parallel striated. The fine material in the area of the pelvis was less orange in colour and the b-fabric was speckled or crystallitic. Fine material of type B was less abundant (20-50%), yellowish light brown or more brown in PPL and brown/yellow in XPL, with dotted limpidity and speckled b-fabric. Sample C2 only exhibited characteristics of type B. All of the samples were apedal.

VOIDS

Three types of void were observed in grave 54931/54909: chambers, channels and packing (Figure 5.31). Chambers were more frequent in the control C2 (15%), common in the area of the pelvis (8%) and few in the area of the skull (5%). Channels were common in the areas of the pelvis and C2 (8%) and few in the area of the skull (5%). Packing voids were equally present in all of the slides (8%).
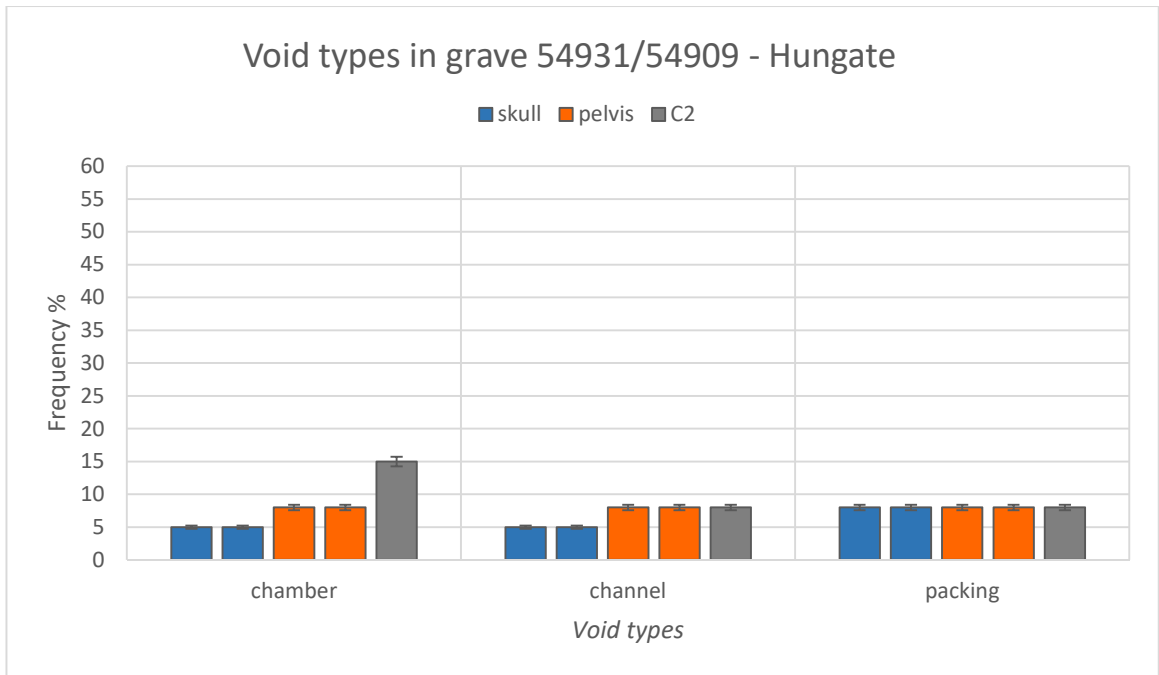
Figure 5.31: Abundance of different types of void in relation to their anatomical location within grave 54931/54909. Great differences among the samples were not observed, but control C2 had more chambers.

MINERAL COMPONENTS

Four types of mineral component were identified in grave 54931/54909: calcite, pyroxene, quartz and quartzite (Figure 5.32).
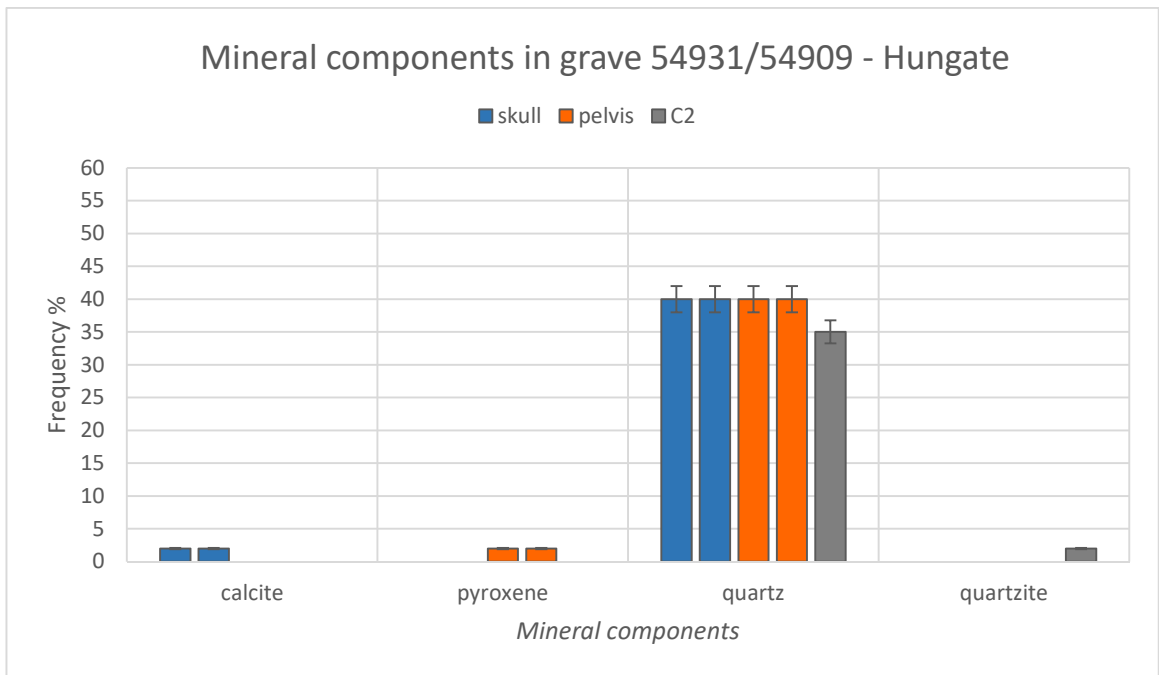
Figure 5.32: Frequency of mineral components in relation to their anatomical location within grave 54931/54909. Quartz was dominant in all of the samples.

Quartz (50-1000 μm) was dominant in all of the slides (35-40%). Very few grains of calcite were observed in the area of the skull, very few pyroxene grains were present in the area of the pelvis and very few quartzite grains in control C2.

ORGANIC COMPONENTS

Four types of organic component were identified in grave 54931/54909: amorphous organic matter, bone fragments, humified plant structure and sclerotia (Figure 5.33).
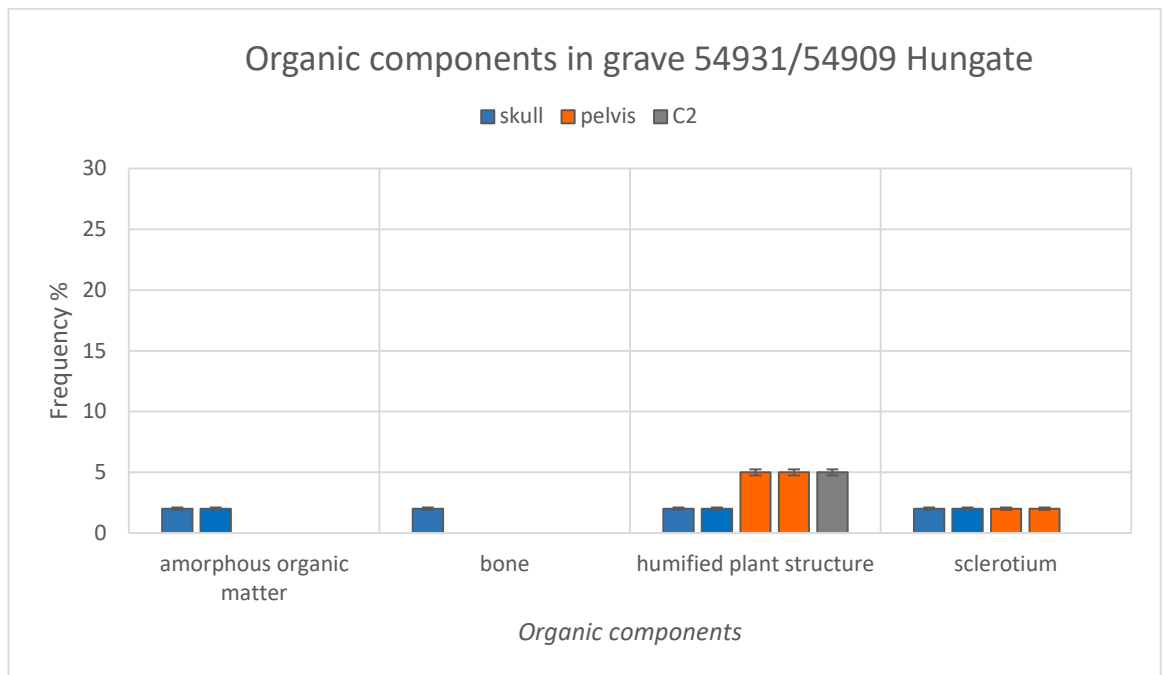
Figure 5.33: Frequency of organic components in relation to their anatomical location. Few humified plant structures and very few amorphous organic matter, bone fragments and sclerotia were observed.

Fragments of amorphous organic matter (50-200 μm) and bones (100-200 μm) were present in the area of the skull (2%). Bone fragments were orange in PPL and reddish brown in XPL, not weathered and with circular shape and thickness around 10 μm. Humified plant structures were very few in the area of the skull (2%) and few in the region of the pelvis and control C2 (5%). They were partially weathered though some fragments from the area of the pelvis had quite well preserved tracheids. These fragment looked like the pieces of wood from grave 54077. Partially weathered sclerotia (100-200 μm) were observed in the areas of the skull and pelvis (2%).

PEDOFEATURES

Six main types of pedofeature were identified in grave 54931/54909: Fe/Mn nodules, Fe rich amorphous phosphates, limpid clay impregnations and coatings, secondary radial crystals, amorphous phosphates and vivianite (Figure 5.34).

Amorphous phosphates were detected in all of the slides: they were frequent in the area of C2 (15%), common in the area of the pelvis (2-10%) and few in the area of the skull (5%). Phosphates had different forms in relation to anatomical position: coatings and infillings within voids in C2, nodules and coatings around voids in the area of the pelvis and Fe rich nodules or with granular aspect in the area of the skull. In this last case, the spherulites, comprising the internal part of the phosphate and smaller than 5 μm, appeared similar to phosphatized fungal bodies and hyphae.

Secondary radial crystals occurred in the areas of the skull and C2, as coatings around phosphatic coatings. Vivianite crystals (100-400 μm) were present in the area of the skull (2%), within the amorphous phosphatic pedofeatures. Limpid clay impregnations and coatings around voids were few in all of the samples (5%).

Fe/Mn nodules were very few in the area of the skull (2%) and few in the areas of the pelvis and C2 (5%). An unidentified pedofeature from the area of the pelvis comprised a bundle of rectangular structures (135-500 x 11-26 μm), yellowish brown in PPL and red/orange in XPL. Some of these structures had internal granular fabric, while others had rough surfaces and were surrounded by very thin tubular structures of the same colour and aspect (Figure 5.51.e-h).
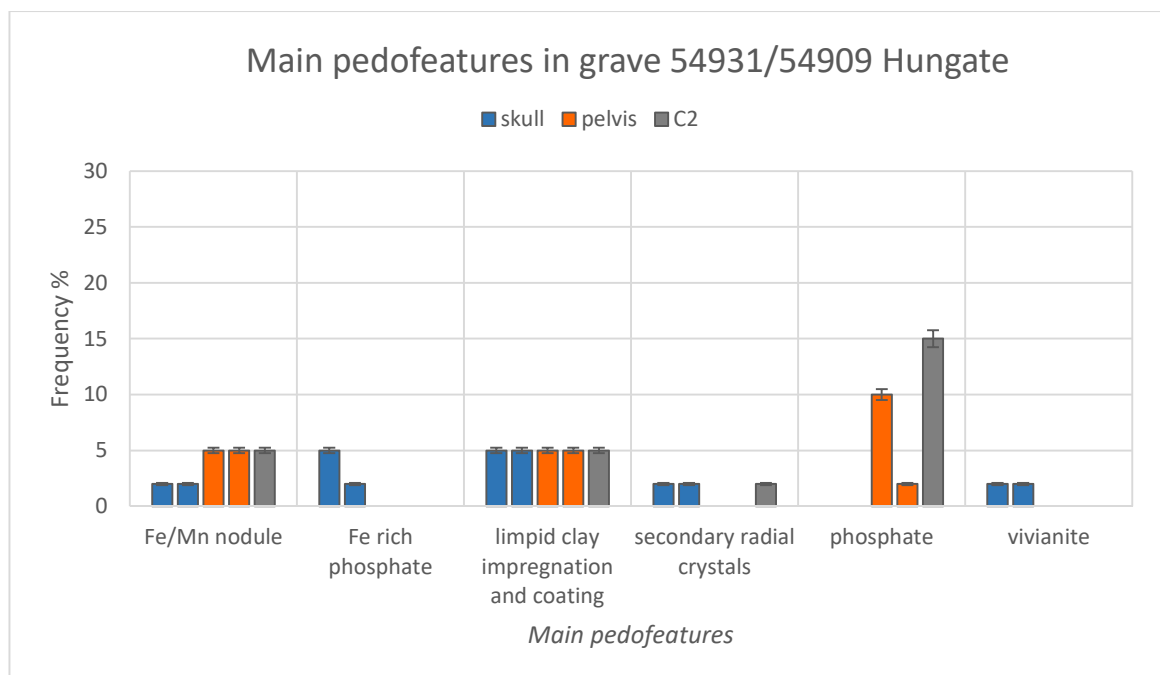
Figure 5.34: Frequency of the main pedofeatures in relation to their anatomical location within grave 54931/54909. Phosphates were observed in the areas of the pelvis and C2, while vivianite and $CaCO_3$ were present in the area of the skull.

GRAVE 53700

ELEMENTS OF FABRIC AND PEDS

Each sample from grave 53700 was characterized by two different types: A (50-85%) and B (20-50%), proportions depending on the slides. Type A had close porphyric c/f related distribution and good sorting. The fine material was 10-40%, yellowish brown/brown in PPL and reddish brown or yellow/brown in XPL, with dotted limpidity and speckled b-fabric. Type B was open porphyric and well sorted. The fine material was more abundant (60-80%), reddish brown or yellowish brown in PPL and yellow/brown in XPL, with dotted limpidity and speckled or parallel striated b-fabric. The sample from the area of the vertebrae had a third type (10%), C, characterized by chitonic c/f related distribution, good sorting and highly distinct from A and B types. The colour was yellow/orange in PPL and yellow or isotropic in XPL, with limpid or dotted limpidity and parallel striated b-fabric. Samples from the areas of the skull and pelvis had spongy appearing microstructures. Granular peds (5-10%) were observed in the sample from the area of the vertebrae: fine in size, unaccommodated and weakly developed.

VOIDS

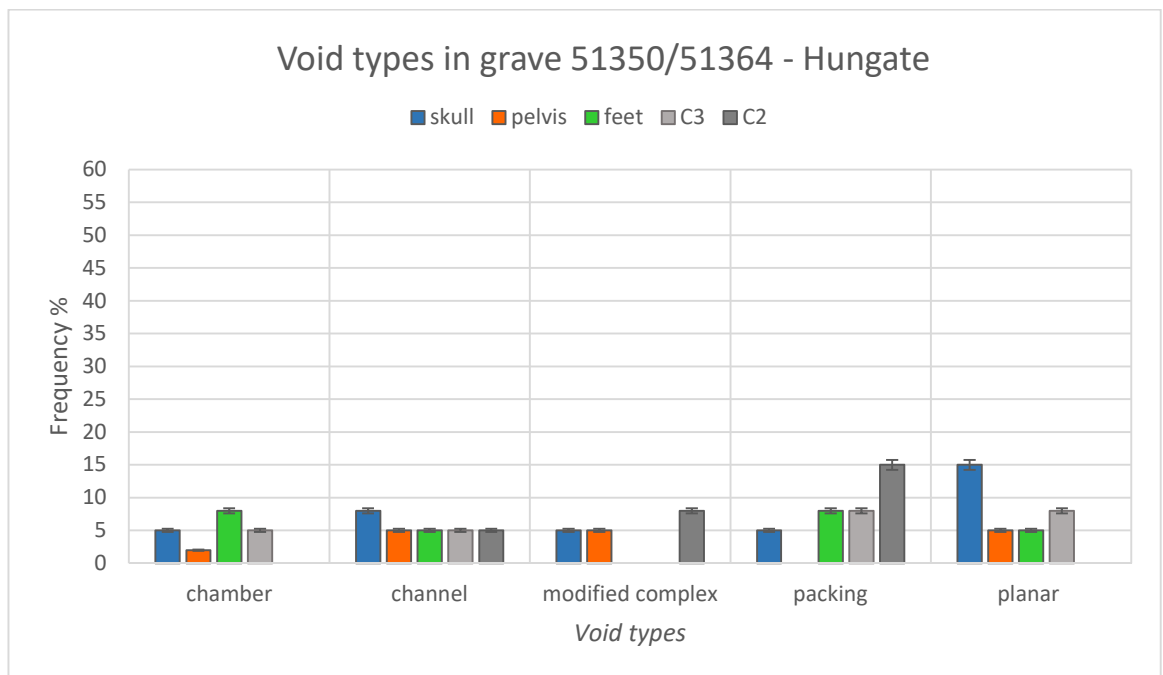Four types of void characterized grave 53700: chambers, channels, modified complex and packing (Figure 5.35).

Figure 5.35: Abundance of different types of void in relation to their anatomical location within grave 53700. Modified complex were frequent in the area of the skull and common in the areas of the pelvis and vertebrae, while chambers and channels were common especially in the area of the pelvis.

Chambers were common in the area of the pelvis (8-15%) and very few in the area of the skull (2%). Channels were common in the area of the pelvis (8-15%) and in the area of vertebrae (10%). Modified complex were frequent in the areas of the skull (8-25%) and vertebrae and common in one slide from the area of the pelvis (8%). Packing voids were observed in the areas of the skull (8%), pelvis (5%) and vertebrae (15%).

MINERAL COMPONENTS

Three types of mineral component were identified in grave 53700: flint, quartz and quartzite (Figure 5.36). Quartz was dominant in all of the samples (30-50%), while quartzite was present only in the areas of the pelvis (2%) and vertebrae (5%) and flint in the area of the pelvis (2%).

Figure 5.36: Frequency of mineral components in relation to their anatomical location within grave 53700. Quartz was dominant in all of the samples.

ORGANIC COMPONENTS

Six types of organic component were observed in grave 53700: amorphous organic matter, bone fragments, fungal hyphae, humified plant structures, roots and sclerotia (Figure 5.37). Very few amorphous organic matter was observed in the area of the skull (2%), while humified plant structures (200-2000 µm) were identified in all of the samples (2-5%) (Figure 5.41.c-d). Very few fragments were characterized by vessels and ascribable to the angiosperms. One trace of gymnosperm wood was represented by the imprint of a fragment into the fine material in the area of the pelvis (level *z*). From the same sample, a fraction of humified plant (>2000 µm) comprising

four fragments oriented parallel to the resting plane, was characterized by circular/angular brown cells with infilling of fine material. The colour was light brown in PPL and brown or isotropic in XPL.

Bone fragments were more frequent in the area of the pelvis (2-5%). They were partially weathered and, in one case, black stains were visible on the structure (Figure 5.41.e). A phosphatized fragment of bone attacked by fungal hyphae was observed in the sample taken in the level *z* of the pelvis. Fungal hyphae were also present in the groundmass of the same sample. Sclerotia (20-200 μm) were observed in the area of the skull and pelvis (2%).

Very few roots were identified in the area of the pelvis. They were orange in PPL and partially white in the internal section in XPL (Figure 5.41.a-b). A round feature, probably organic, was observed in the area of the skull. It had sub-round shape, 150-250 μm size and exhibited an internal granular structure and thin external layer (10-15 μm). The granular area was partially fragmented and yellow and brown in PPL and reddish brown in XPL; the external layer was yellow in PPL and isotropic in XPL. It comprised rectangular cells, visible only with SEM (Figure 5.41.g-h).
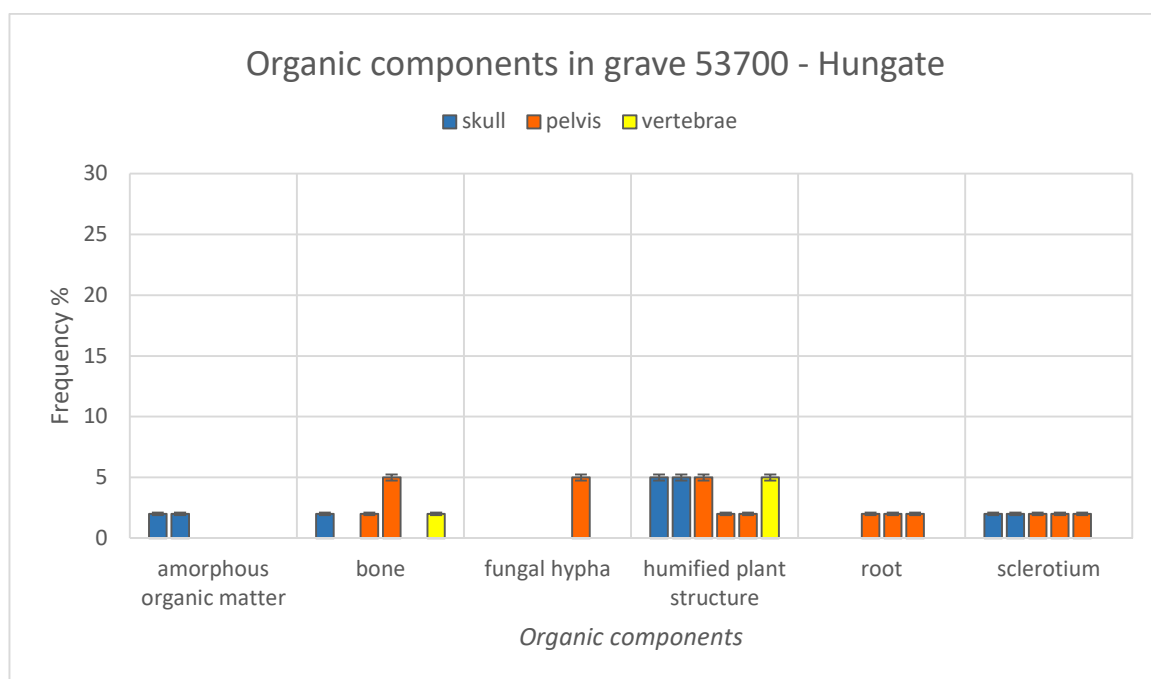
Figure 5.37: Frequency of organic components in relation to their anatomical location within grave 53700. Traces of fungal activity were found in the areas of the pelvis and skull.

PEDOFEATURES

Five main types of pedofeature were identified in grave 53700: clay coatings, Fe/Mn nodules, phosphates, red redox pedofeatures and vivianite (Figure 5.38).

Amorphous phosphates were present in all of the samples and were more frequent in the area of the pelvis (5-20%). They occurred as coatings within voids, nodules and strong impregnations in the

fine material (Figure 5.46.h). The colour was light yellow or yellow in PPL and isotropic in XPL. Some phosphates had crystallitic layers (Figure 5.46.e) and in a few cases in the area of the pelvis, they were weathered, having granular aspect similar to coalescent excremental features (Figure 5.46.f). Few subrounded amorphous phosphates appeared as coatings around spherical Mn nodules in the areas of the skull and pelvis. One example of vivianite (100-150 µm) was identified in the area of the pelvis. Few red redox impregnations were observed in the areas of the pelvis, excepting level *z*, and vertebrae (5%), but not in the area of the skull. Fe/Mn nodules were common in the area of the skull (2-8%) and few in the other samples.

Clay coatings around mineral grains were very few in the area of the skull (2%) and few in the area of the pelvis (5%), not including level *z*. Most of the pedofeatures and the coarse organic components in the level *z* of the area of the pelvis were oriented parallel to the resting plane.
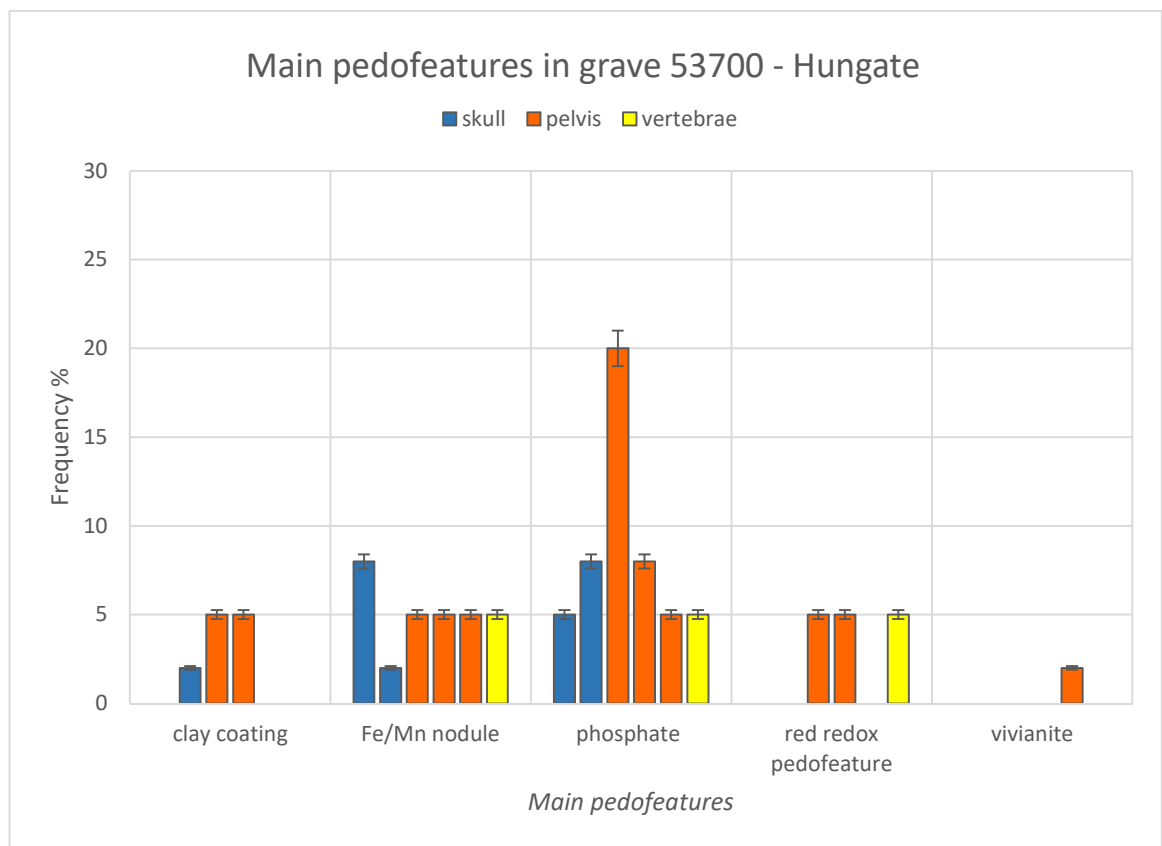
Figure 5.38: Frequency of the main pedofeatures in relation to their anatomical location within grave 53700. Amorphous phosphates were present in all of the samples and were more abundant in the area of the pelvis. Vivianite was observed only in the area of the pelvis.

ADDITIONAL SLIDES

Other graves from Hungate that were not chosen for this research were also sampled by the InterArChive team. Slides from some of these graves were utilized to compare pedofeatures, their frequency and relationship with those examined in this study (Appendix 1.6). In particular, amorphous phosphates, orange spherulites, vivianite and goethite were considered (Figure 5.39).

Amorphous phosphates were present in most of the slides, between 2-16%. They were not detected in: one slide from control C2 and a coffin stain from grave 54264, controls C3 from graves 54166 and 54104, control C2 and the area of the pelvis from grave 51330, some of the slides from the areas of the skull, pelvis and feet from grave 51326.

Phosphates were associated with orange spherulites in 33 slides and were quite common in more than half of those slides (2-25%). All the spherulites were characterized by crossed b-fabric; spherulites such as the yellow ones without b-fabric (*cf* grave 51350/51364) were not present.

Vivianite features were very few (2-5%) in six slides: from the area of the pelvis of grave 54907 (phosphates and spherulites), from the areas of stain and skull of grave 54273 (phosphates), from control C2 of grave 54264 (phosphates and siderite), from the area of the skull of grave 54166 (phosphates) and from the control C3 of grave 54090.

Goethite was identified in only two slides: from the area of coffin stain of grave 54264 (spherulites) and from the control C2 of grave 51326 (phosphates).
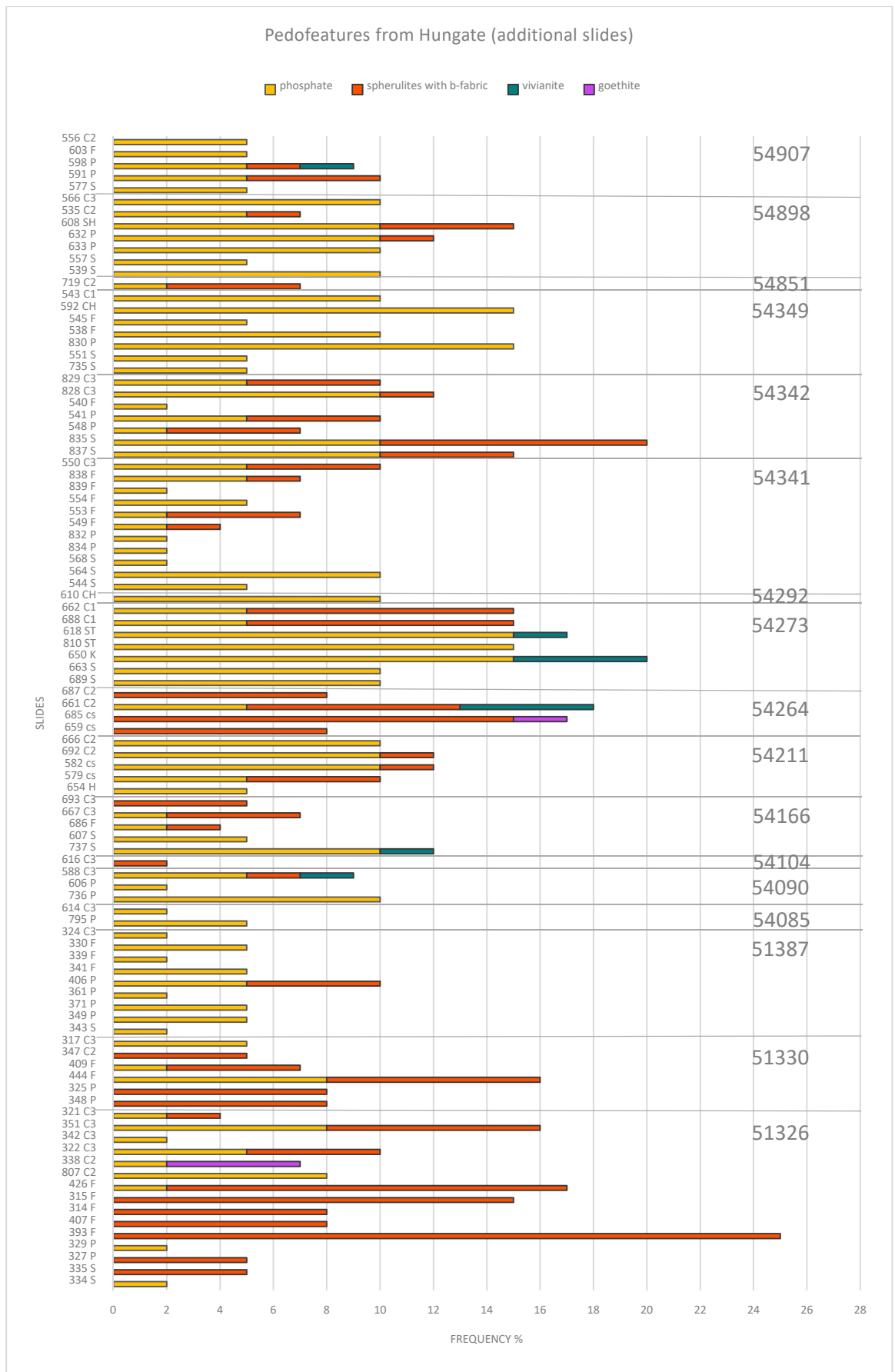
Figure 5.39: Frequency of the main pedofeatures in the additional slides from Hungate. On the right, the numbers of the graves. On the left, the number of the slides: S=skull, P=pelvis, F=feet, H=hand, ST= stain, CH= chest, SH=shoulder, K= knees, cs=coffin stain.

5.1.4 SEM-EDS RESULTS

SEM-EDS analyses were applied to detect the composition of the spherulites and to support interpretation of the difference between those with b-fabric and those without. Several measurements were taken across the spherulites and fine material from grave 51350/51364 and the weight (%) of several chemical elements was recorded.

The data presented in the box-plot (Figure 5.40) are un-normalized and the measurements of O and C were excluded owing to the presence of the resin in which the samples were consolidated. Hence, the data on the remaining elements are overestimated, but this choice was preferred to underestimation to facilitate visualisation of the components. The elements Al, Si, P, K, Ca and Fe were considered as they exhibited high variability and concentration. Components with less than 0.1% of weight were excluded from the box-plot.

Al, Si and K are abundant in the fine material and progressively less abundant in the spherulites without b-fabric and more so in the ones with b-fabric. The opposite trend occurs with Ca, Fe and P, which are more abundant in the orange spherulites, decreasing in the yellow ones further in the fine material.
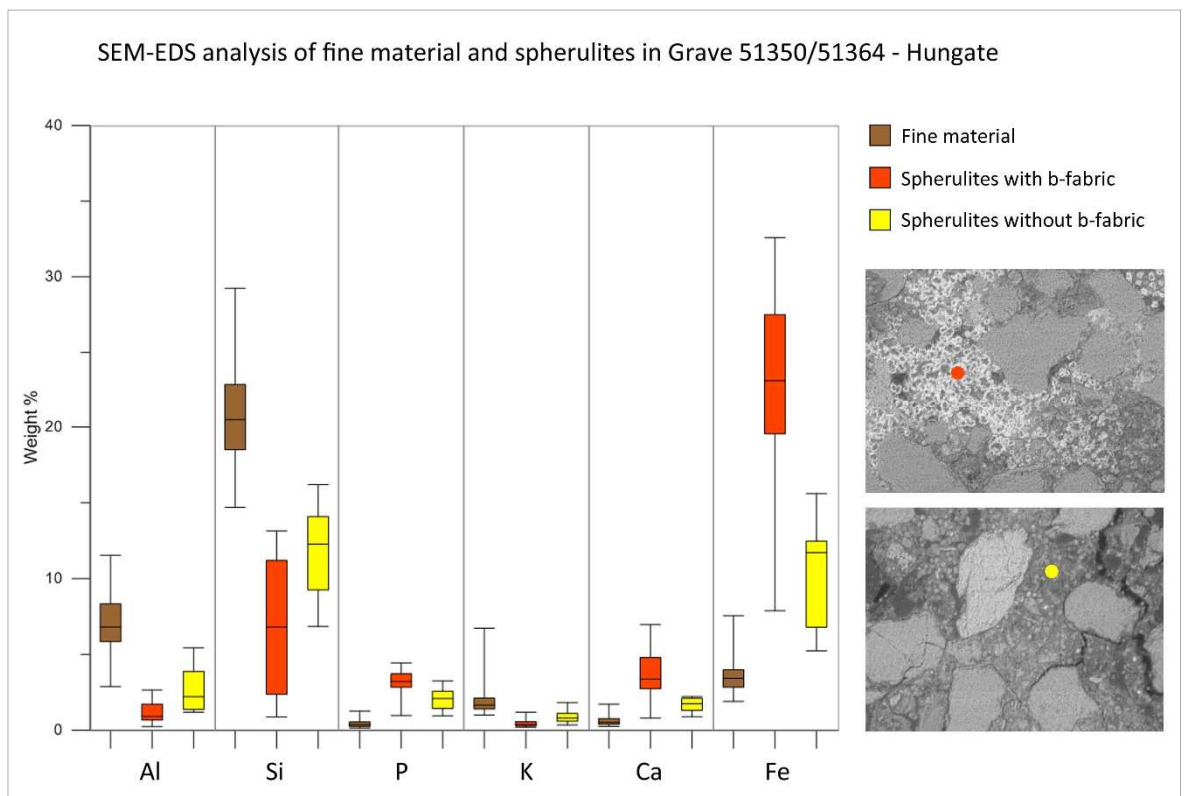
Figure 5.40: Box-plot showing the results of SEM-EDS analysis on spherulites, with and without b-fabric, and fine material in grave 51350/51364. On the right, under the legend, two photographs from SEM showing the two types of spherulites. The oranges were very bright, while the yellows were not easy to visualize.

The following figures were selected as representative of the features described in Section 5.1.3:

- Figure 5.41: organic components;

- Figure 5.42: gymnosperm wood from grave 54077;

- Figure 5.43: spherulites without b-fabric from grave 51350/51364;

- Figure 5.44: spherulites with b-fabric from grave 51350/51364;

- Figure 5.45: spherulites with b-fabric from grave 51350/51364;

- Figure 5.46: amorphous phosphates;

- Figure 5.47: vivianite and amorphous phosphates;

- Figure 5.48: vivianite;

- Figure 5.49: secondary radial crystals;

- Figure 5.50: pedofeatures (clay coating, clay infilling, red redox impregnation, infilling of red Fe nodules);

- Figure 5.51: pedofeatures (goethite fan-like infilling from grave 51350/51364 and undetected pedofeatures from grave 54931/54909).
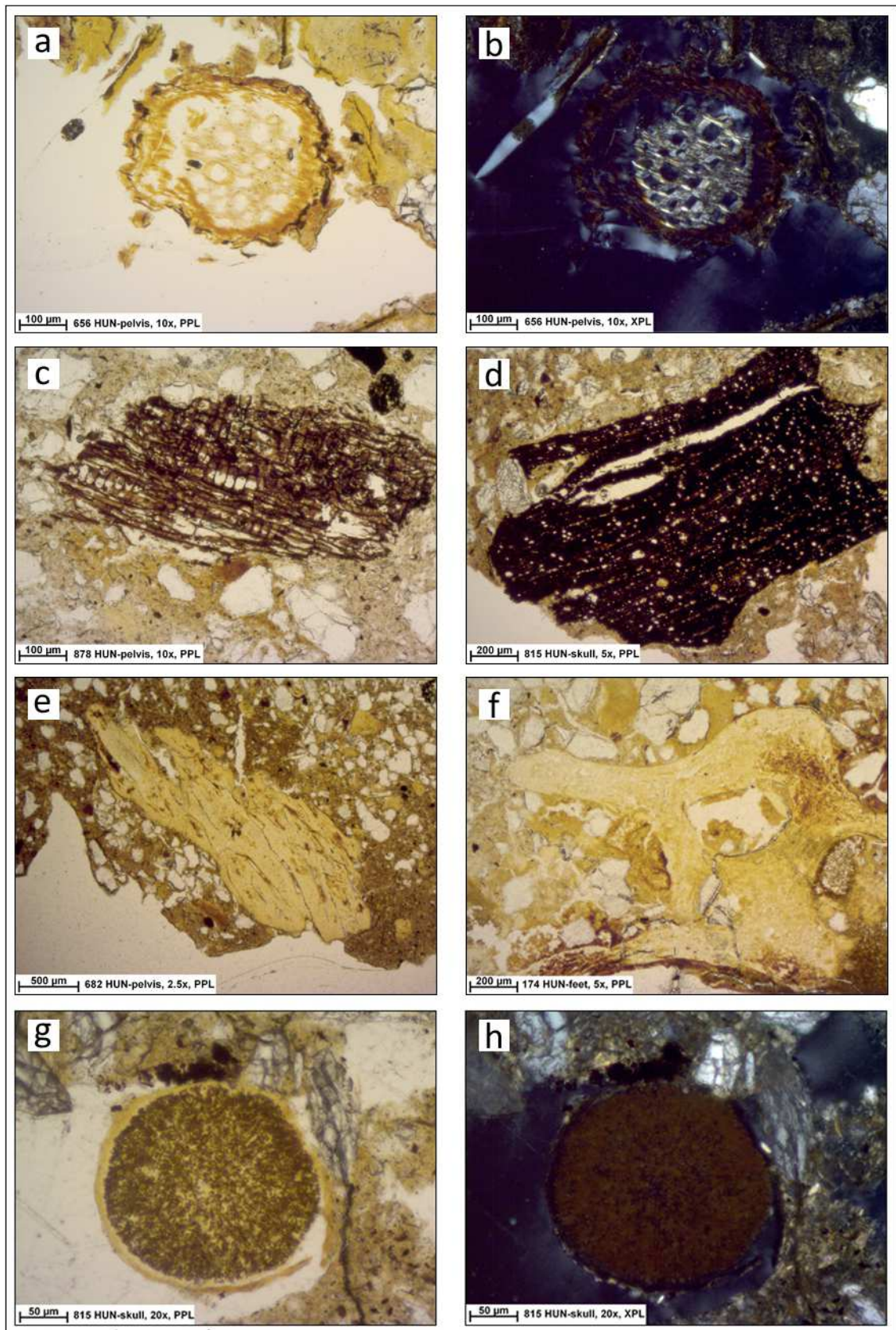
Figure 5.41: Organic components in Hungate: a-b) root from the area of the pelvis in grave 53700 in PPL (a) and XPL (b); c) humified plant structure from the area of the pelvis in grave 53700; d) humified plant structure from the area of the skull in grave 53700; e) fragment of bone with black stains from the area of the pelvis in grave 53700; f) fragment of weathered bone from the area of the feet in grave 51350/51364; g-h) organic remain from the area of the skull in grave 53700 in PPL (g) and XPL (h).

121
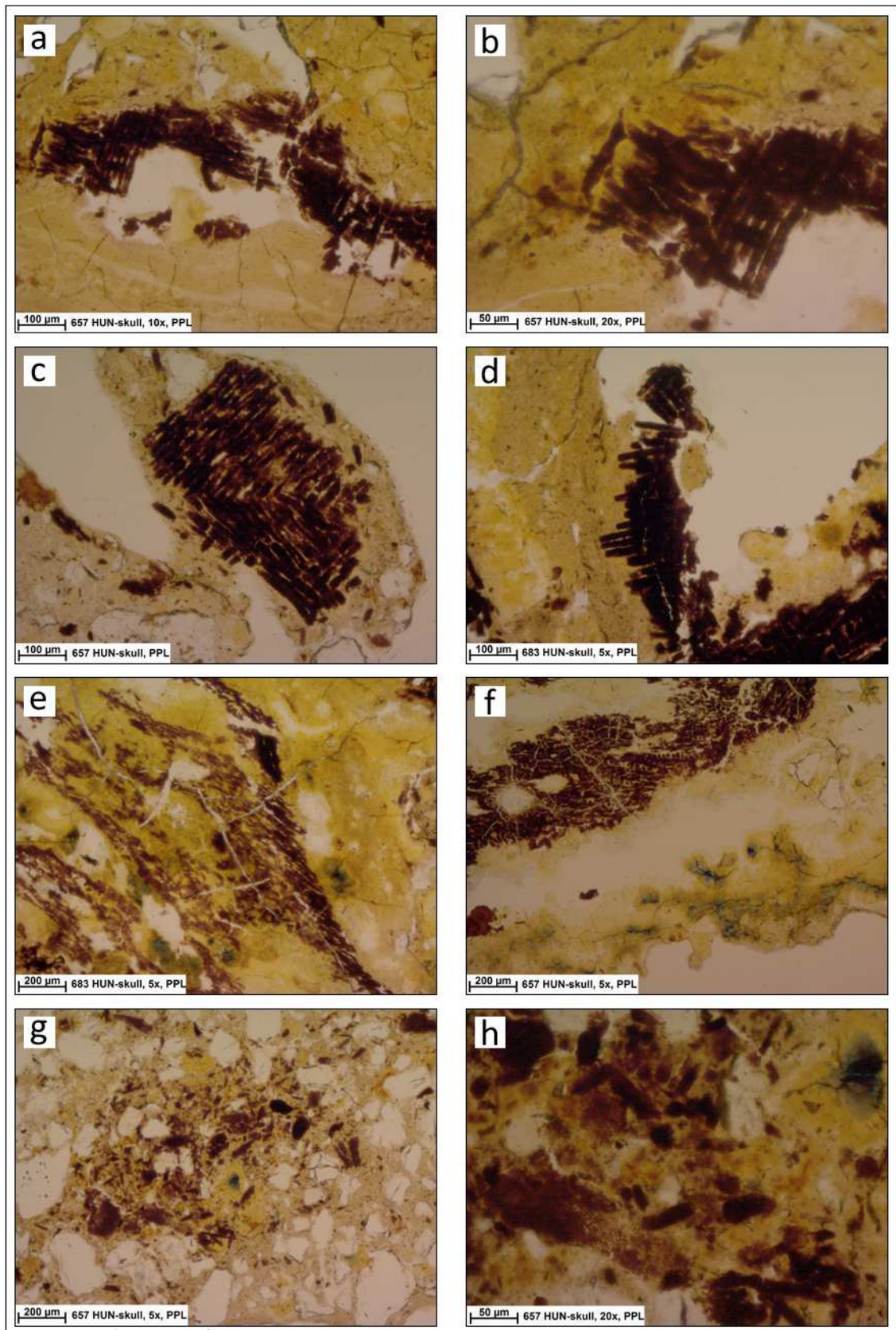
Figure 5.42: Gymnosperm wood from grave 54077. a-b-c-d) very well preserved fragments of wood; e-f) partially weathered fragments of wood; g-h) highly weathered fragments of wood.
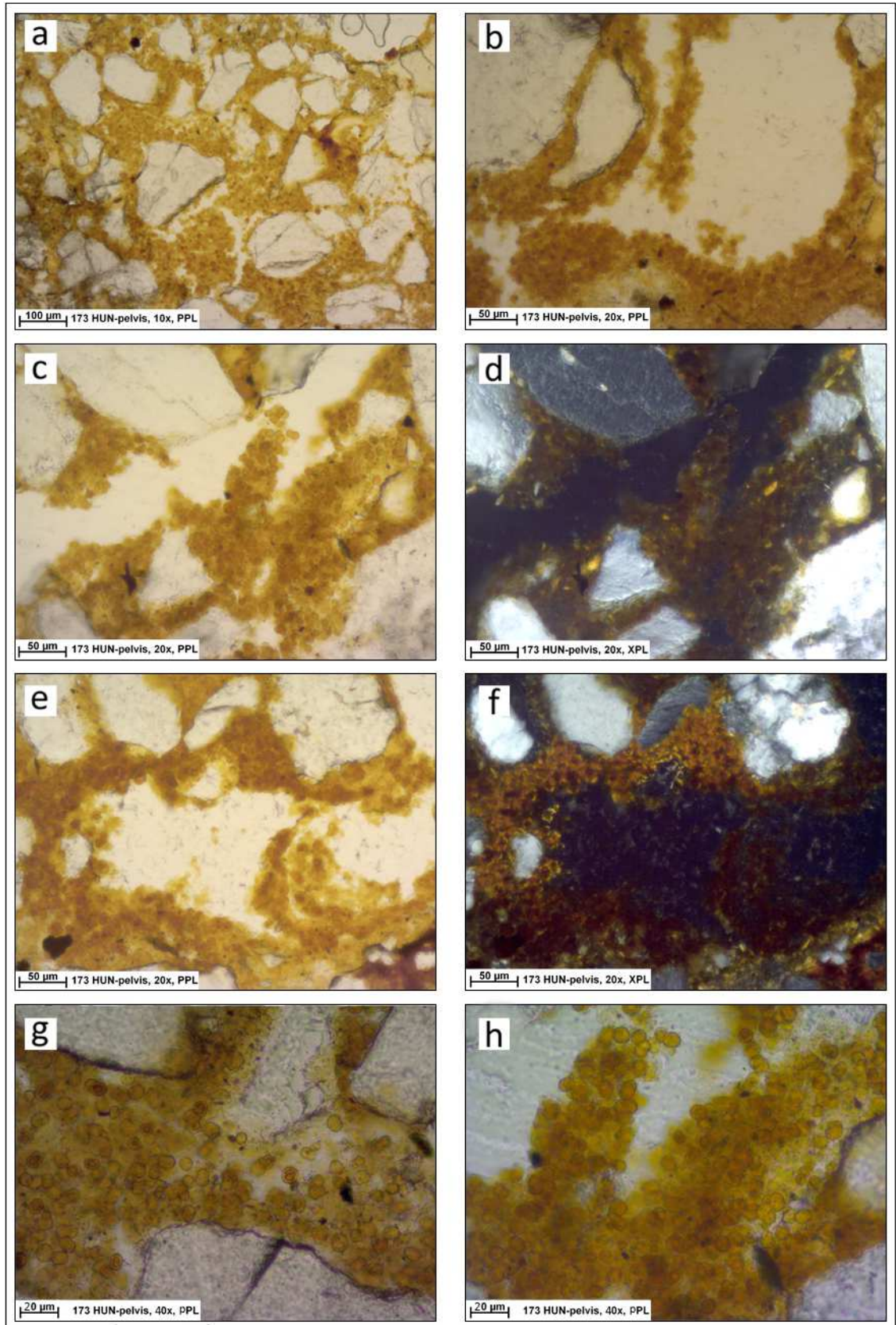
Figure 5.43: Spherulites without b-fabric from the area of the skull in grave 51350/51364. a-b-c-d) spherulites within the groundmass; e-f) the spherulites in the top of the coating had crossed b-fabric (f), while the spherulites in the bottom were amorphous; g-h) detail of the spherulites, some of them had an internal layer.
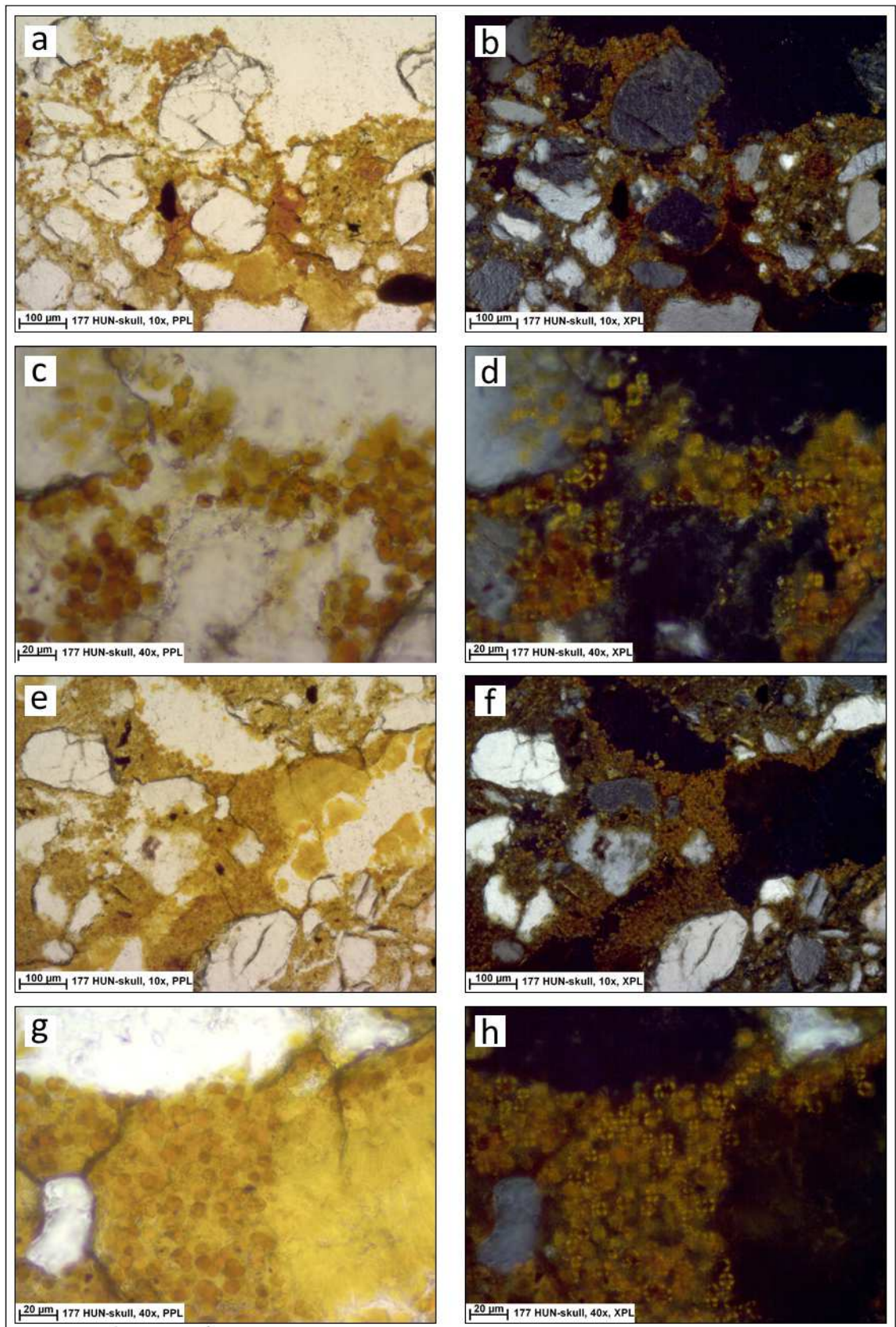
Figure 5.44: Spherulites with b-fabric from the area of the skull in grave 51350/51364. a-b) spherulites within the groundmass; c-d) detail of the spherulites; e-f) spherulites in the groundmass associated with amorphous phosphates, isotropic in XPL (f); g-h) detail of the spherulites and amorphous phosphates.
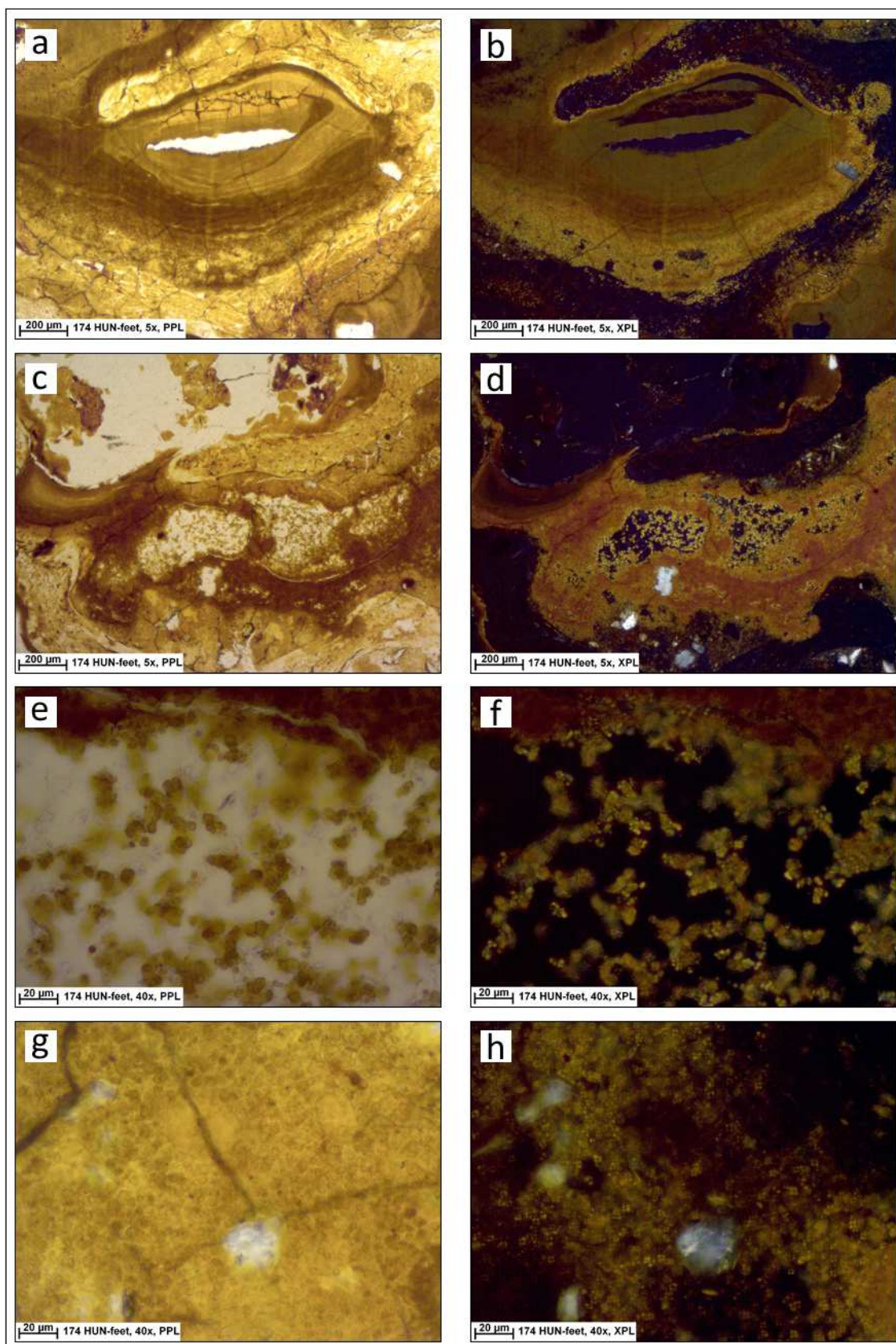
Figure 5.45: Spherulites with b-fabric from the area of the feet in grave 51350/51364. a-b-c-d) phosphatic and probably fine material-rich coatings around voids within weathered bone structure. The coatings are layered and contain very small spherulites; e-f) detail of the spherulites from the central area of the void; g-h) detail of the spherulites within the coating.
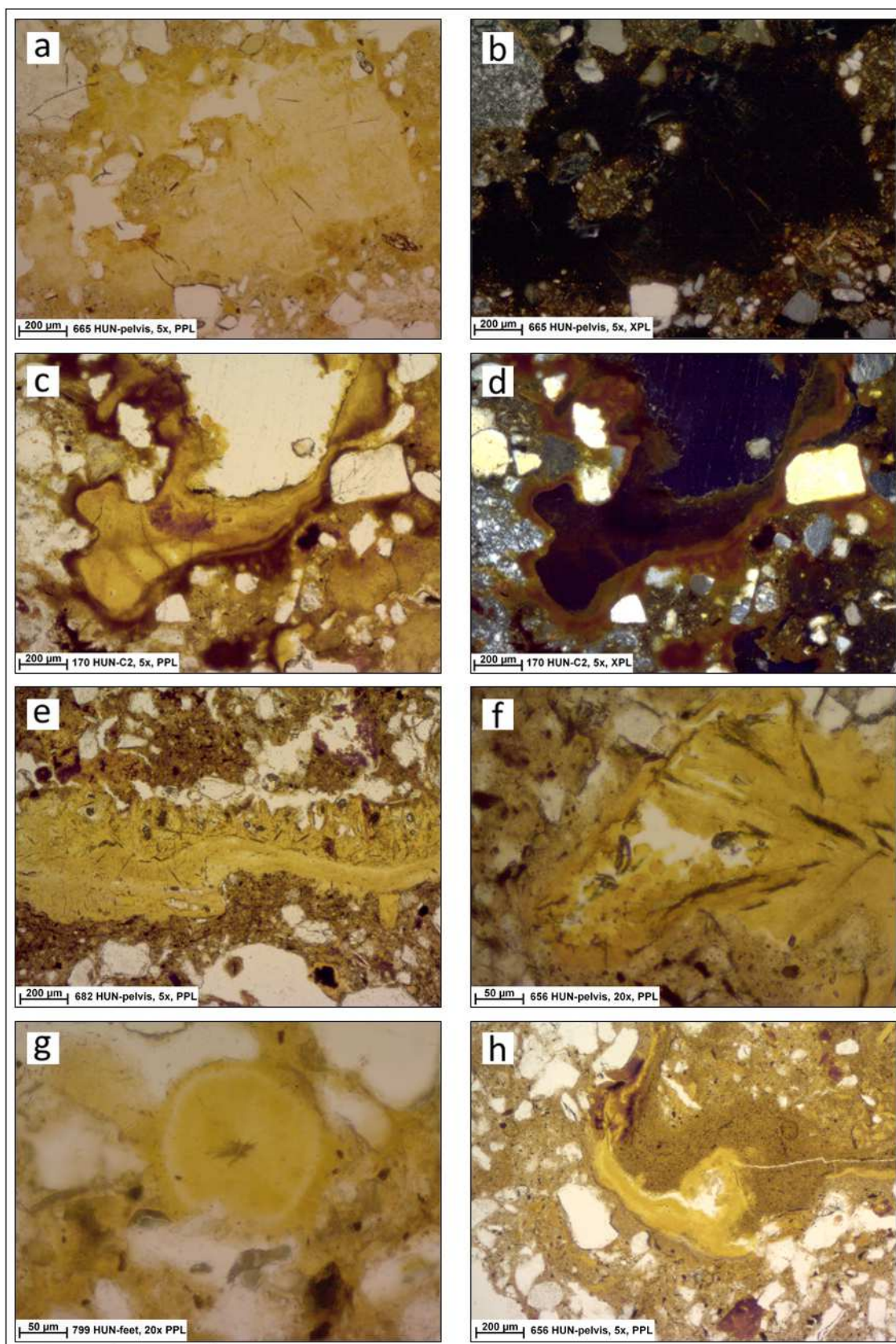
Figure 5.46: Amorphous phosphates in Hungate. a-b) amorphous phosphate within the groundmass from the area of the pelvis in grave 54296 in PPL(a) and XPL (b); c-d) coating of amorphous phosphate with iron rich layers from the control C2 in grave 51350/51364 in PPL (c) and XPL (d); e) amorphous phosphate with slightly crystallitic structure on the top layer from the area of the pelvis in grave 53700; f) amorphous phosphates with granular weathered zone from the area of the pelvis in grave 53700; g) sub-rounded nodule of amorphous phosphate from the area of the feet in grave 54296; h) coating/infilling of amorphous phosphate from the area of the pelvis in grave 53700.
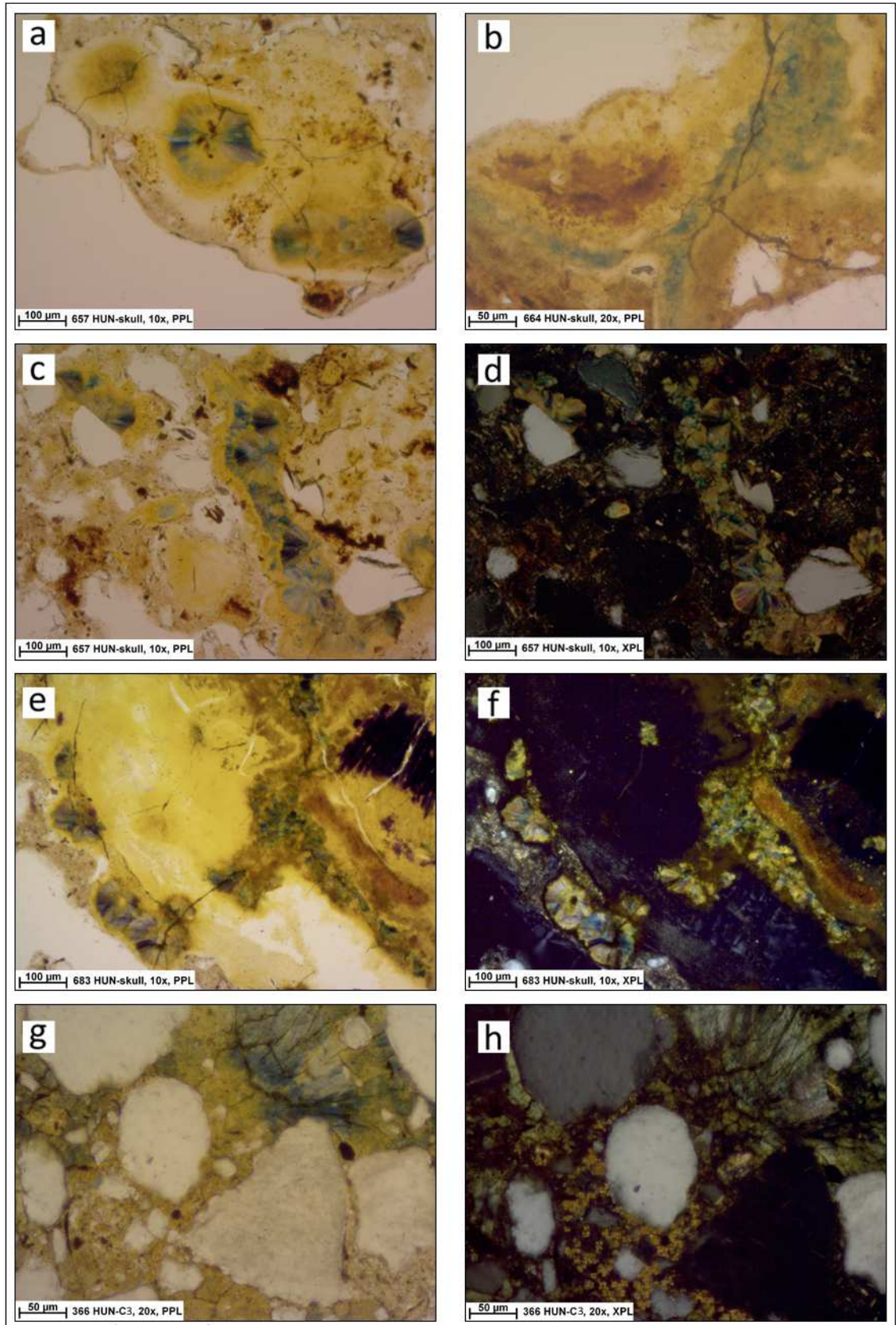
Figure 5.47: Vivianite and amorphous phosphates in Hungate. a) amorphous phosphatic area with sub-rounded and radial crystals of vivianite from the area of the skull in grave 54077; b) amorphous phosphate with greenish blue areas of vivianite from the area of the skull in grave 54296; c-d) phosphatic area with sub-rounded and radial crystals of vivianite in chain from the area of the skull in grave 54077 in PPL (c) and XPL (d); e-f) phosphatic area with sub-rounded and radial crystals of vivianite in chain from the area of the skull in grave 54077 in PPL (e) and XPL (f); g-h) crystals of vivianite associated with spherulites within the groundmass from the control C3 in grave 51349/51351.

127
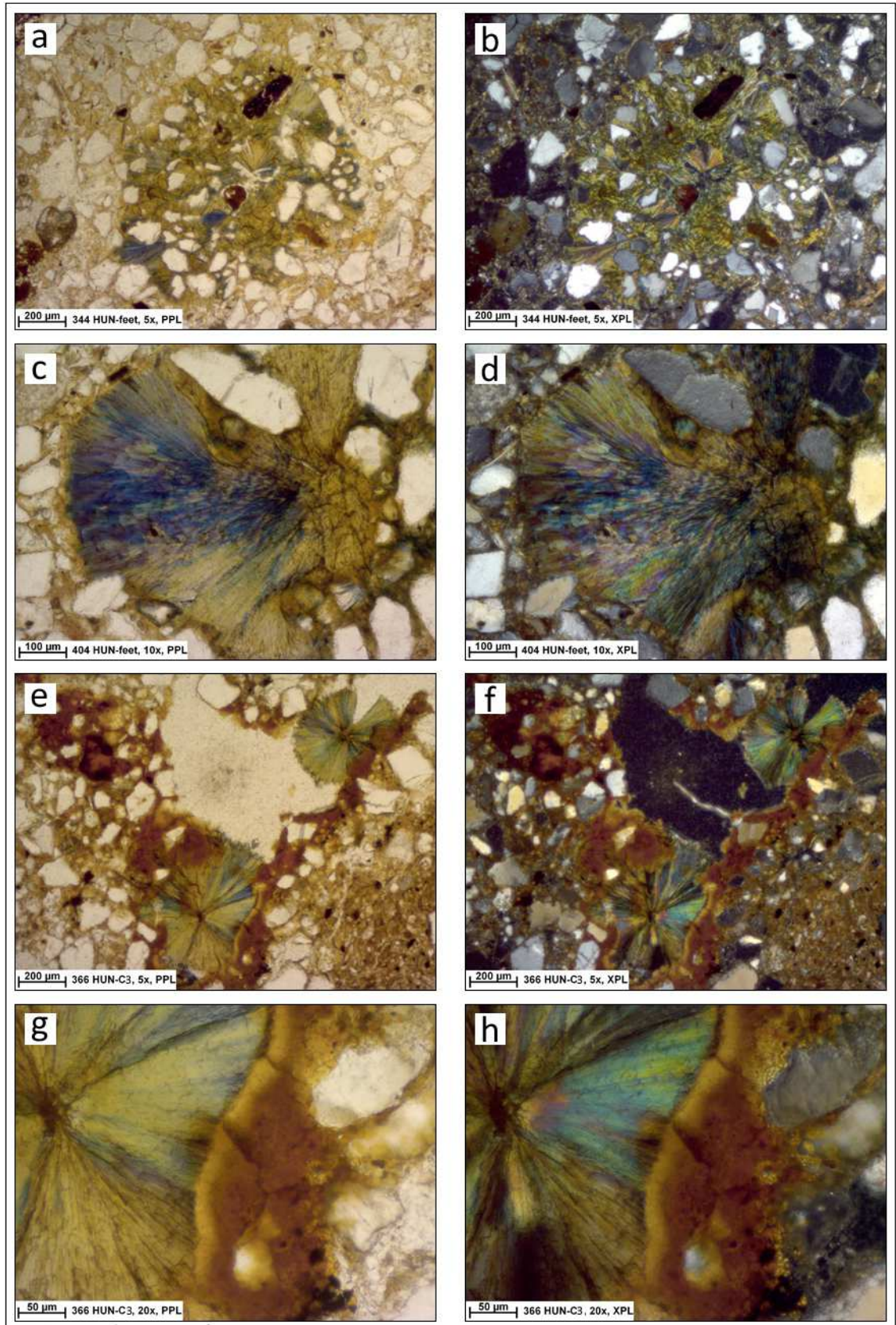
Figure 5.48: Vivianite in Hungate. a-b) Crystals of vivianite inter-grown within the groundmass and including mineral grains from the area of the feet in grave 51349/51351 in PPL (a) and XPL (b); c-d) radial crystals of vivianite from the area of the feet in grave 51349/51351 in PPL (c) and XPL (d); e-f) radial and sub-rounded crystals of vivianite within a void and associated to reddish brown coating with few very fine spherulites from the control C3 in grave 51349/51351 in PPL (e) and XPL (f); g-h) detail of the vivianite at the bottom of figures (e) and (f) in PPL (g) and XPL (h).
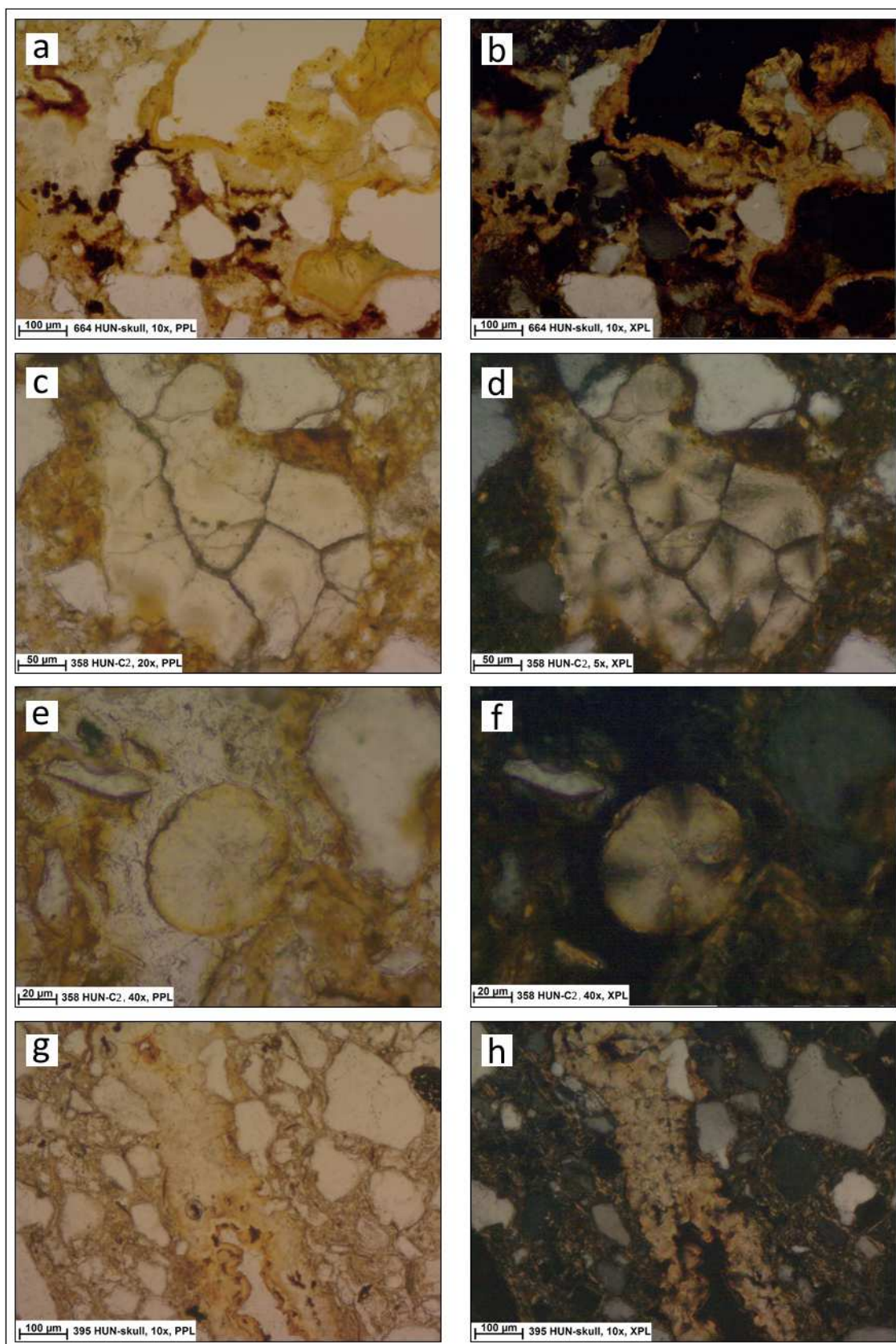
Figure 5.49: Secondary radial crystals in Hungate. a-b) area characterized by amorphous phosphatic coatings with Fe rich layers on the right, Mn inclusions in the centre and secondary radial crystals on the left from the area of the skull in grave 54296 in PPL (a) and XPL (b); c-d) infilling of crystals with radial structure and crossed b-fabric from the control C2 in grave 51349/51351 in PPL (c) and in XPL (d); e-f) sub-rounded crystal with crossed b-fabric from the control C2 in grave 51349/51351 in PPL (e) and XPL (f); g-h) infilling of sub-rounded and radial crystals in channel from the area of the skull in grave 52253 in PPL (g) and XPL (h).
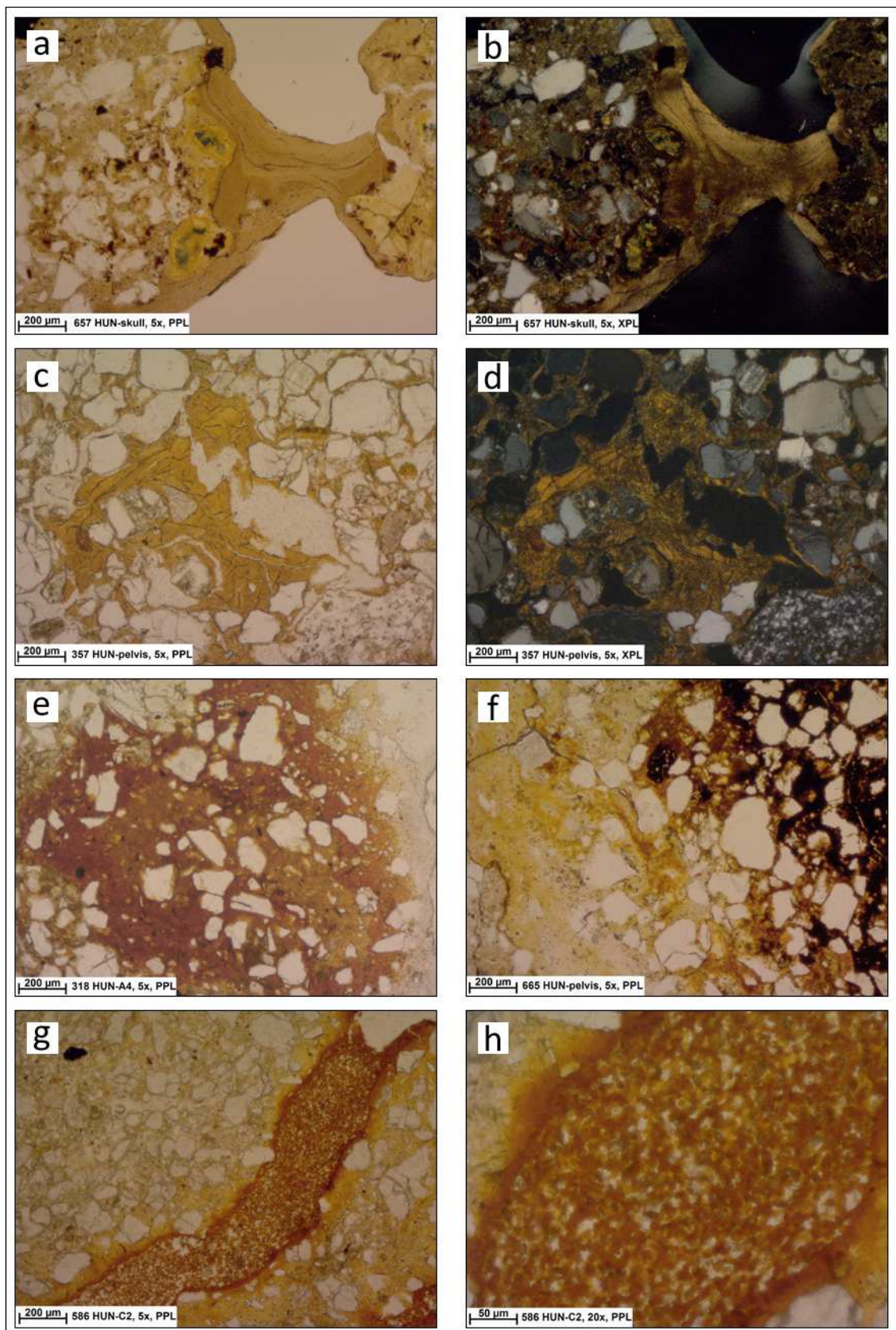
Figure 5.50: Pedofeatures in Hungate. a-b) clay coating with parallel striated b-fabric from the area of the skull in grave 54077 in PPL (a) and XPL (b); c-d) clay infilling with parallel striated or speckled b-fabric from the area of the pelvis in grave 51349/51351 in PPL (c) and XPL (d); e) red redox impregnation from the area of the chest below the feet in grave 51349/51351; f) black redox impregnation on the right and amorphous phosphate on the left from the area of the pelvis in grave 54296; g) infilling of small red Fe nodules in channel from the control C2 in grave 54077; h) detail of figure (g).
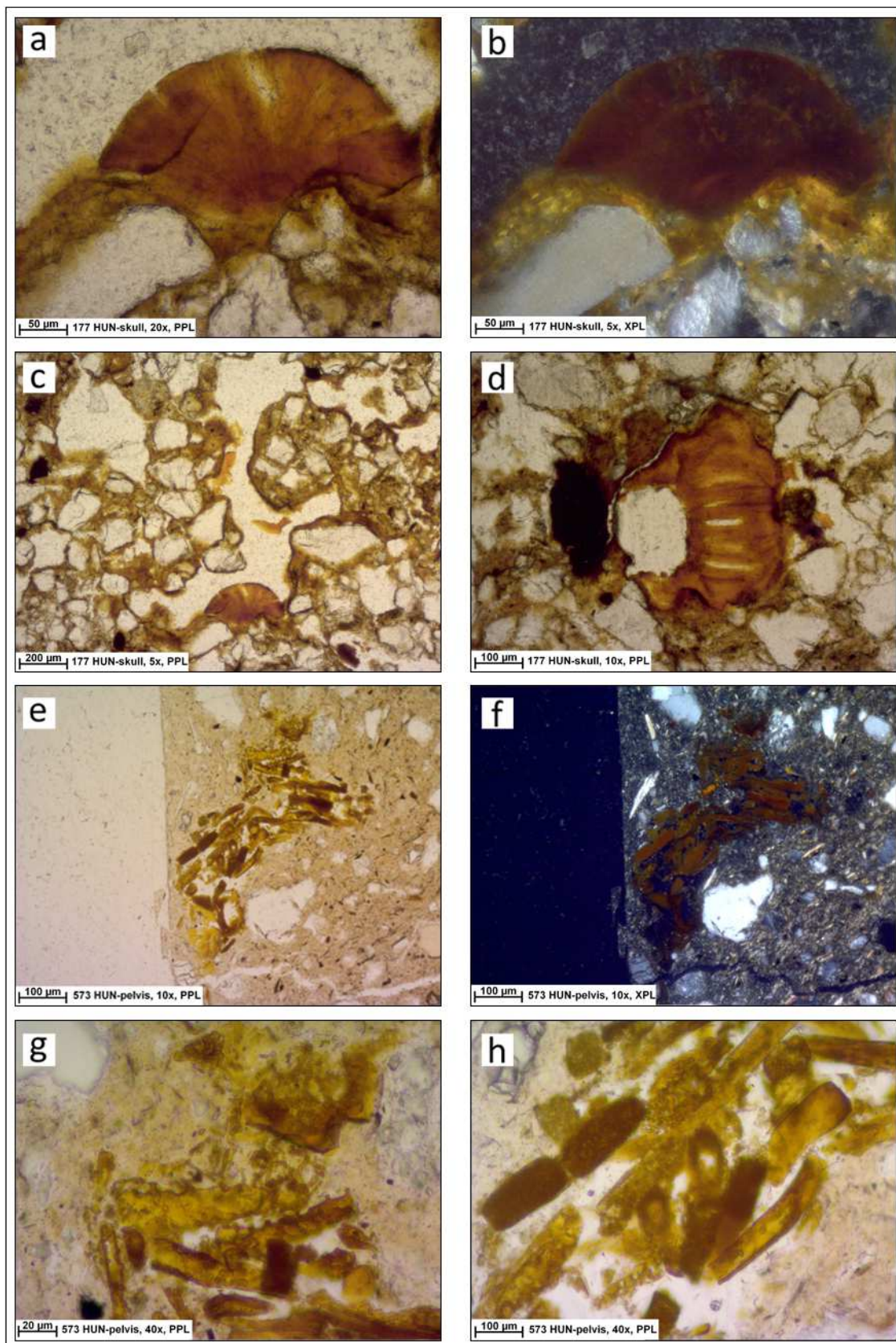
Figure 5.51: Pedofeatures in Hungate. a-b) goethite fan-like crystals on the wall of void from the area of the skull in grave 51350/51364 in PPL (a) and XPL (b); c) enlargement of figure (a); d) infilling of goethite in chamber from the area of the skull in grave 51350/51364; e-f) unidentified pedofeatures, probably with organic origin, from the area of the pelvis in grave 54931/54909 in PPL (e) and XPL (f); g-h) details of figure (e).

5.2 HAYMARKET (UK). Medieval cemetery, 11th-15th C AD

The site of Haymarket was located in the city centre of York, inside the city walls, next to the area of Hungate (Figures 5.52 and 5.53).

The archaeological area was discovered during excavations in the late 1980s, when the location of Church of All Saints in Peasholme Green was identified. Archaeological discoveries continued in 2012, during a new investigation by York Archaeological Trust, started after the demolition of a hostel in that area (Reeves 2013). The InterArChive team participated to the sampling of nine graves in 2012.

Figure 5.52:Map with the location of Haymarket in the city centre of York. Graphically modified from Google Maps ©2014.

5.2.1 THE SITE

All Saints Church was founded in 11th-12th C AD and it was in use until the late 16th C AD. It was officially closed in 1549 by an Act of Parliament. Consequently, the church was partly demolished and some roof tiles and stones were employed in other buildings in the city in 1586. It seemed that some of ruins were still visible in the early 18th C AD (Reeves 2013).

132

Recent excavations, developed by YAT, focused on the church area and the surrounding graveyard. The research showed that the church was built in two phases and that East and West ends of the buildings had stronger supporting structures. Some evidence of medieval vernacular buildings and two very large medieval stone buildings were identified in the proximity of the church. Finally, the discovery of a large Roman defensive ditch, possible clay extraction pits and a post-Roman terracing deposit suggested that the archaeological levels below the church and the graveyard were probably associated with the deposit of Hungate (Reeves 2013). Consequently, as shown in Figure 5.54, All Saints Church and the graveyard were at a higher elevation and possibly the sediments were rarely water-logged.
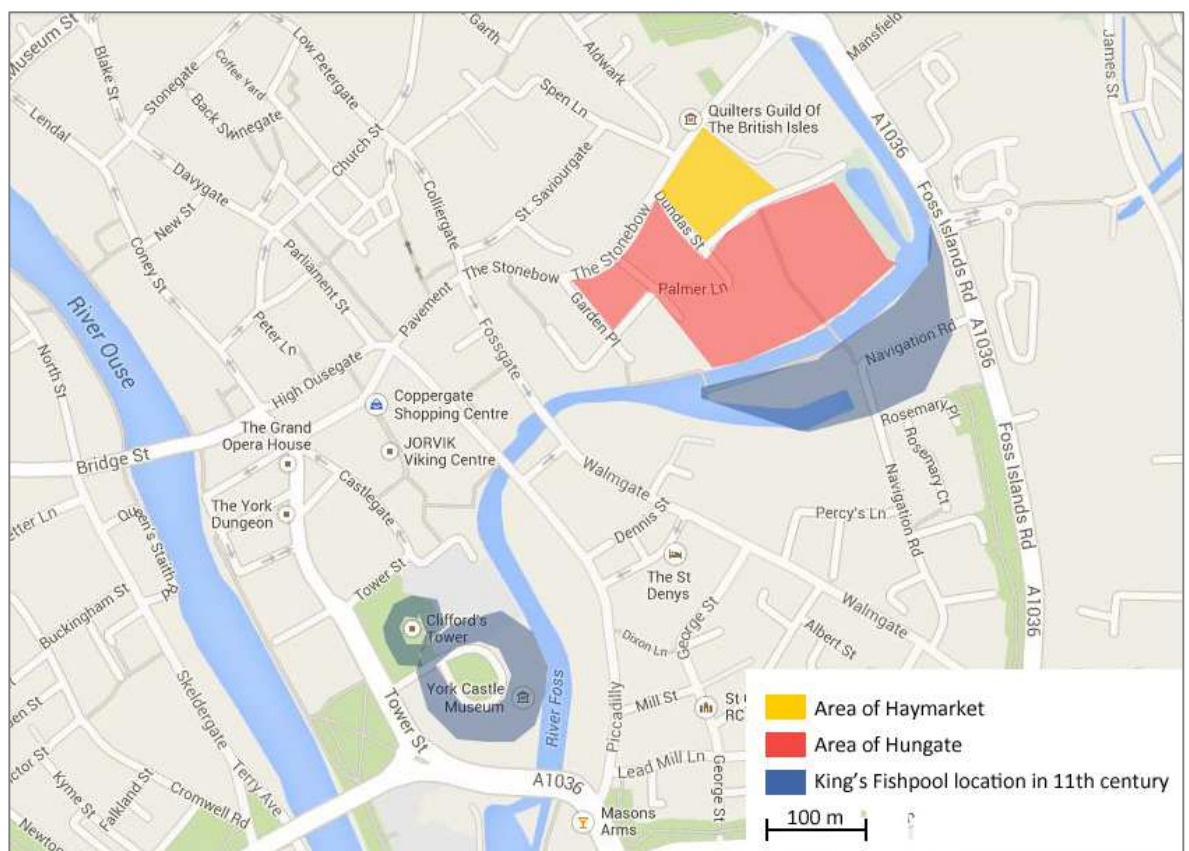
Figure 5.53: Map showing the two areas of Hungate and Haymarket in York. Graphically modified from Google © 2014.
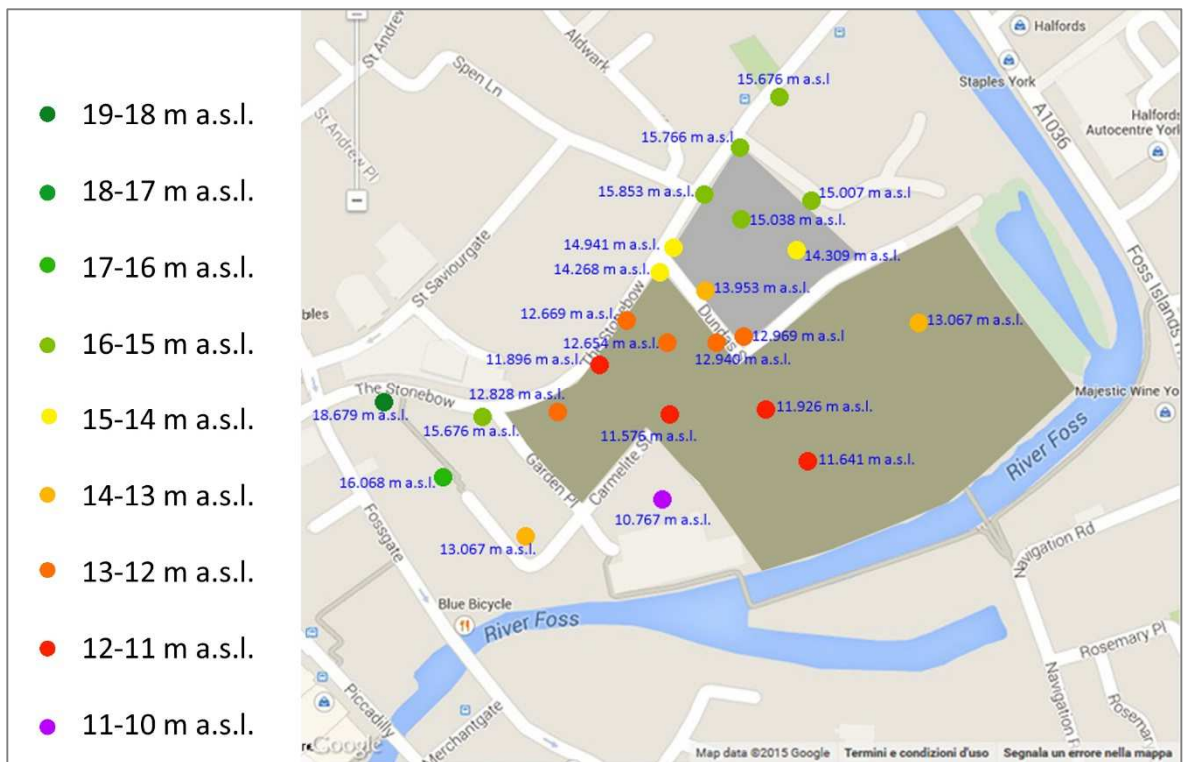
Figure 5.54: Map of the area of Hungate (greenish grey) and Haymarket (bluish grey) and measurement of their elevation above sea level. The natural slope in Hungate was visible from the corner between The Stonebow and Dundas Street (yellow dot – 14.268 m a.s.l.) to the River Foss (11-10 m a.s.l.). Graphically modified from Google Maps ©2015.

5.2.2 THE GRAVES

Four graves were selected for this research: 83012, 84700, 84779 and 84851 (Table 5.2). 27 additional slides from the other graves were investigated with regard to the pedofeatures (Appendix 1.6). No macroscopic information was available from YAT and few were recorded in the data sheets; pictures of the graves were obtained (Chapter 3, Table 3.2).

The quality of some of the slides was compromised owing to problems in their manufacture: some had uneven thickness and others were too thin. As a result, the organic matter was difficult to identify in thick regions and coarse components were completely fragmented and the fine material removed in thin areas (Appendix 1.5).

GRAVE	DATE	TYPE	SKELETON INFORMATION and grave-goods	SOIL TYPE	CLIMATE
83012	Medieval, 11th-15th C AD	N/A	Adult; The feet were missing due to a service trench	Sandy clay	Temperate oceanic
84700	Medieval, 11th-15th C AD	N/A	Adult; Hands under the pelvis and skull turned left	Sandy clay	Temperate oceanic
84779	Medieval, 11th-15th C AD	N/A	Adult; Upright feet with long root hair	Sandy clay	Temperate oceanic
84851	Medieval, 11th-15th C AD	N/A	Juvenile skeleton; hands under the pelvis	Sandy clay	Temperate oceanic

Table 5. 2: Summary of the available information regarding the graves in Haymarket.

GRAVE 83012

Grave 83012 (Figure 5.55) was subjected to an intense sampling, concerning not only the areas surrounding the skeleton (levels Y and Z), but also below the resting plane and the grave fill above the remains. In the absence of pictures, a schematic 3D representation is shown in Figure 5.56. The feet were missing due to a service trench cutting across the grave; the knees were sampled as an alternative to the foot position.
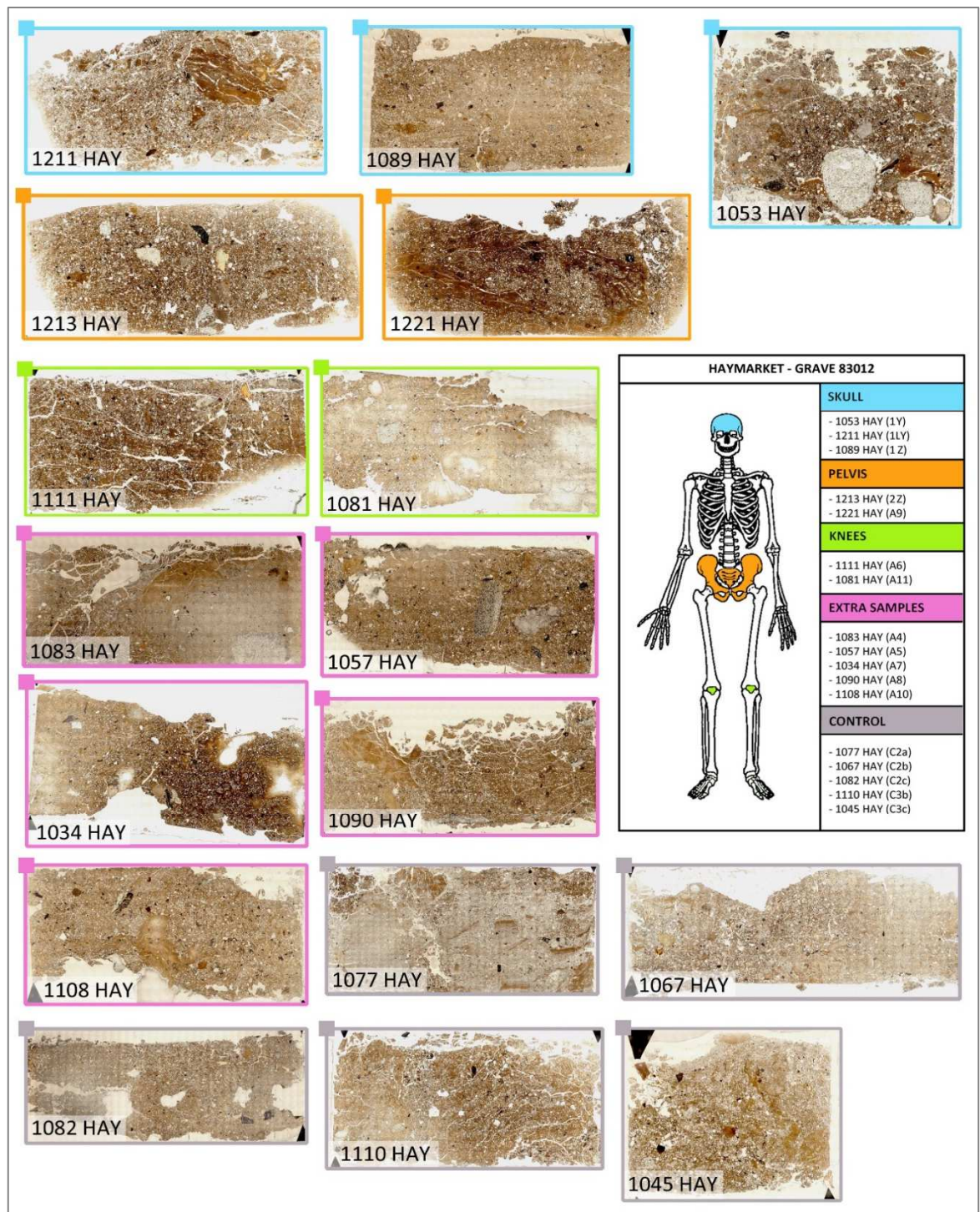
Figure 5.55: Grave 83012. On the right, list of the slides in relation to their anatomical location. On the top, left and bottom, mosaics of the slides. See the text for descriptions.
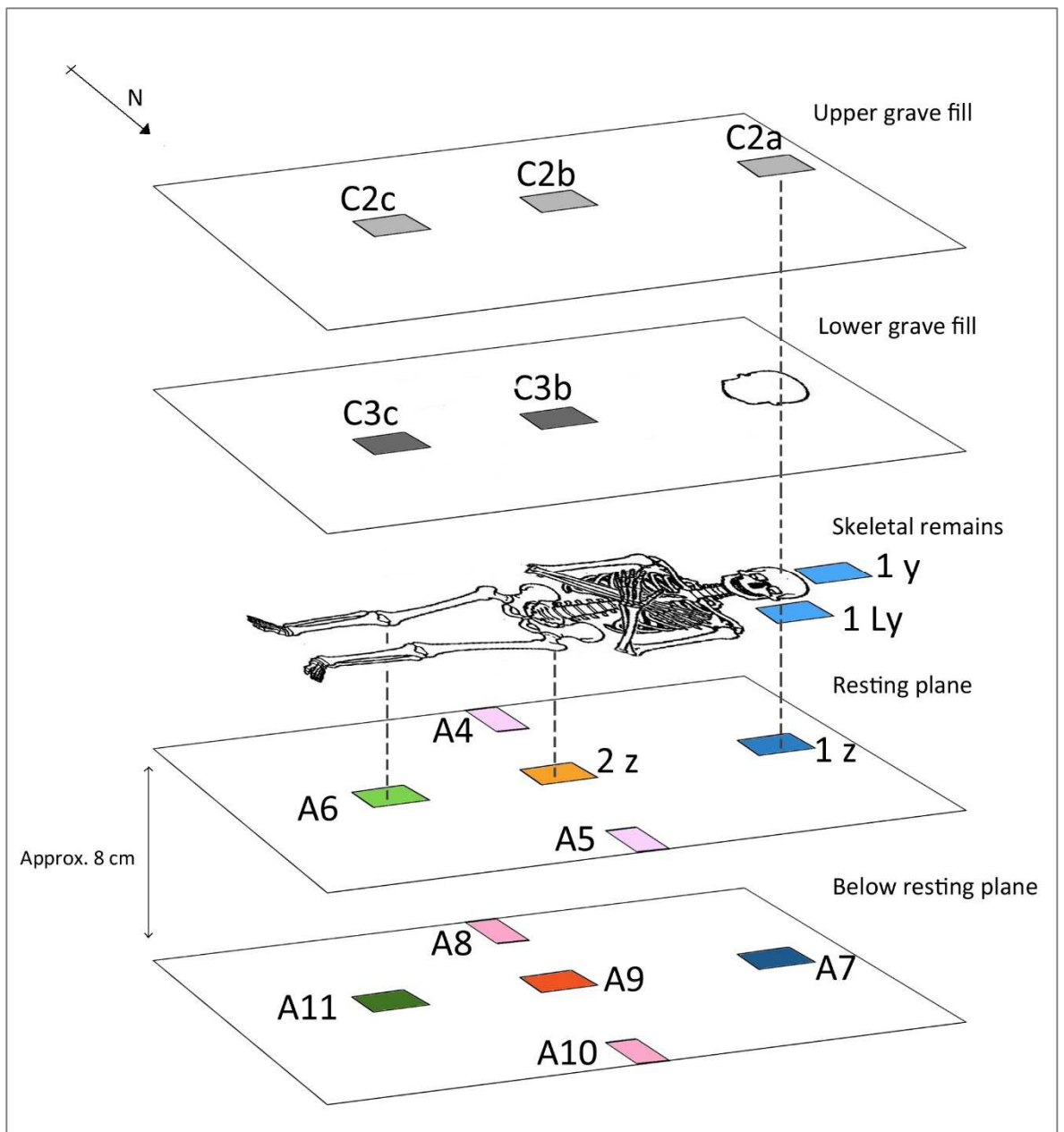
Figure 5.56: 3D representation of the sampling of grave 83012, with location of all of the samples.

GRAVE 84700

The skeleton of grave 84700 (Figure 5.57) had the hands under the pelvis and the skull turned to the left. The sample from the area of the skull was collected next to the occipital bone.
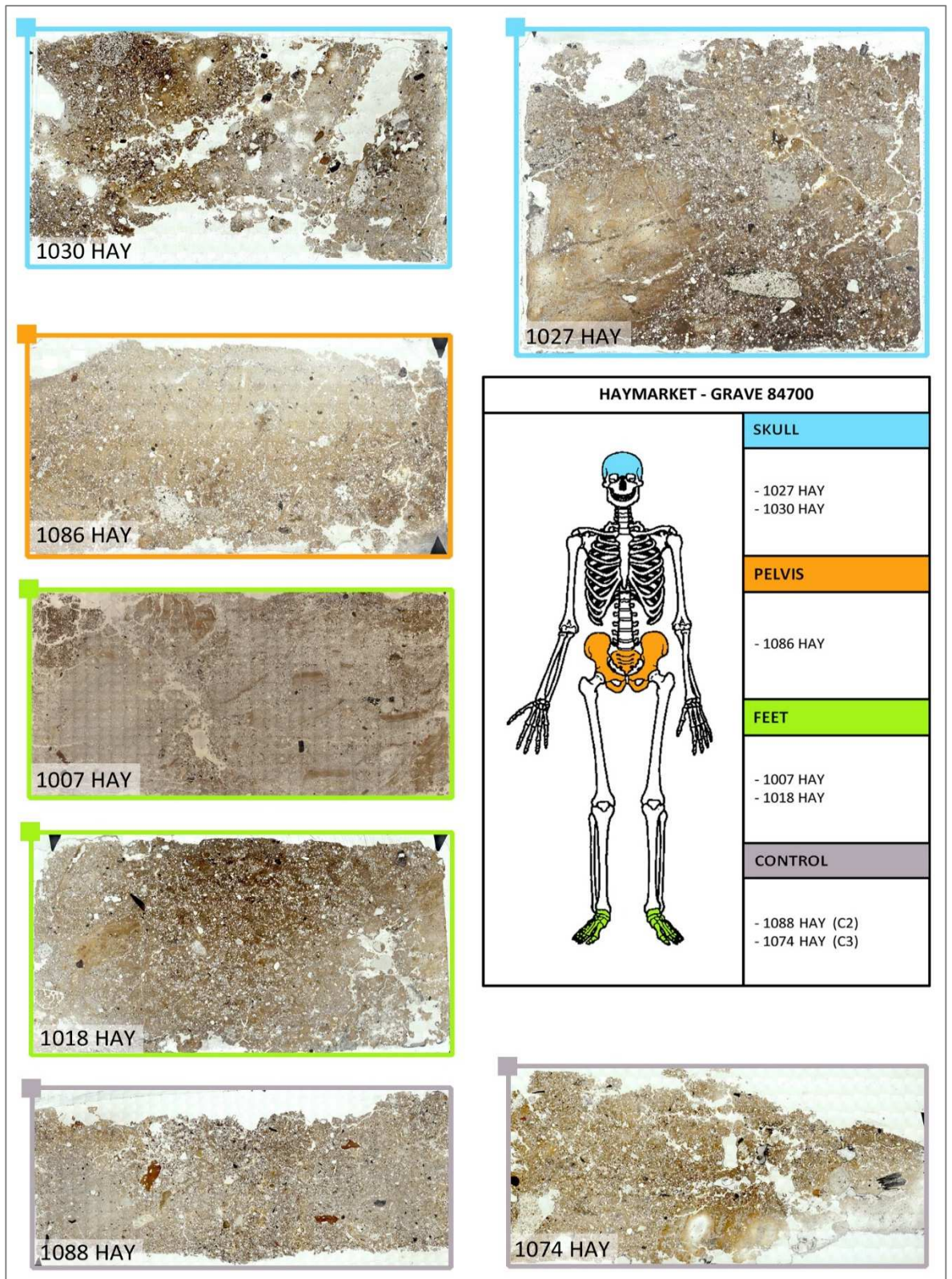
Figure 5.57: Grave 84700. On the right, list of the slides in relation to their anatomical location. On the top, left and bottom, mosaics of the slides. See the text for descriptions.

GRAVE 84779

Grave cut 84779 (Figure 5.58) was defined by the change in texture, from clay rich sediment inside the grave to more friable sandy sediment outside the grave. Substantial amounts of white roots matter with long root hairs was found in the sediment around the feet, which were upright. Fragments of charcoal of 2-3 cm were observed in the area of the skull, while several flints of 7-9 cm were situated next to the right shoulder, at the edge of the grave. An animal mandible was found to the left of the iliac crest.
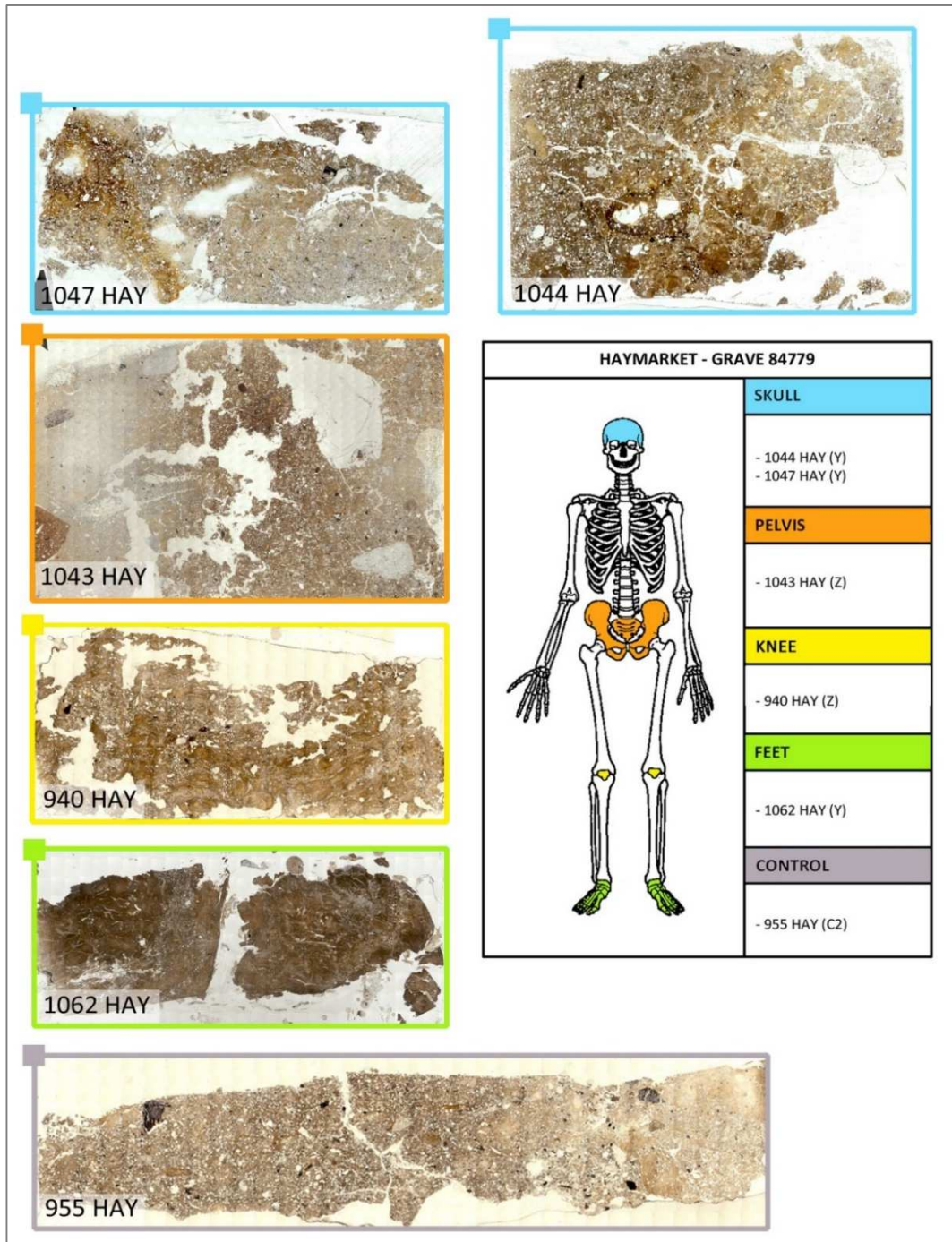
Figure 5.58: Grave 84779. On the right, list of the slides in relation to their anatomical location. On the top, left and bottom, mosaics of the slides. See the text for descriptions.

GRAVE 84851

Grave 84851 (Figure 5.59) contained a complete and articulated skeleton of a sub-adult or infant, having the hands under the pelvis. The skull was crushed during the excavation.
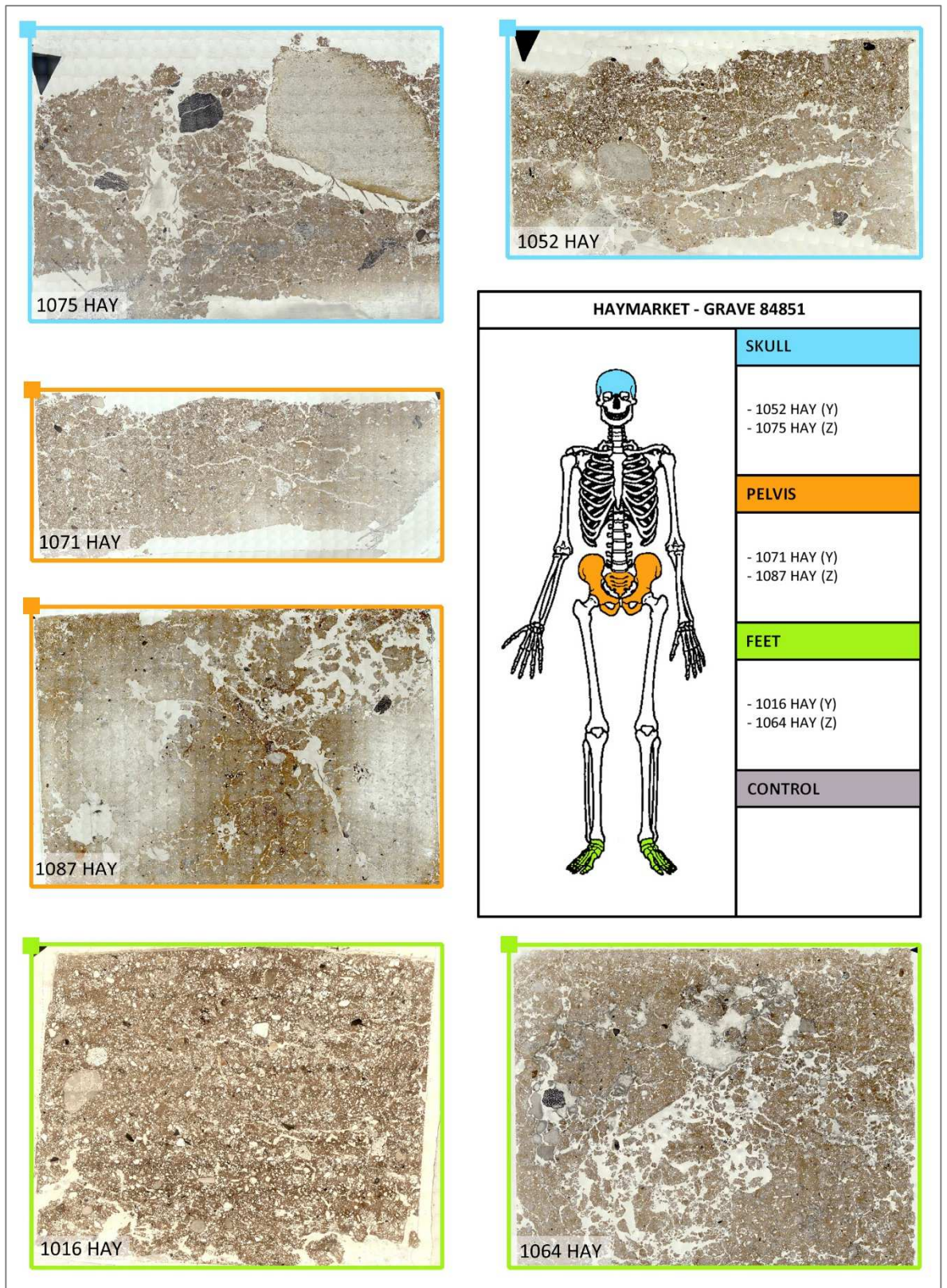
Figure 5.59: Grave 84851. On the right, list of the slides in relation to their anatomical location. On the top, left and bottom, mosaics of the slides. See the text for descriptions.

5.2.3 MICROMORPHOLOGICAL RESULTS

GRAVE 83012

ELEMENTS OF FABRIC AND PEDS

The fabric in grave 83012 was differentiated as three distinct types, A, B and C. Type A was characterized by double/single spaced porphyric c/f related distribution and moderate sorting. The fine material was light brown in PPL and yellow/brown in XPL, with dotted limpidity and speckled b-fabric. The abundance of fine material was between 40-75%, depending on the samples. This type was dominant in most of the samples (60-100%), excluding the sample from the side of the skull (10-20%), control C3 C (10-20%) and control C2 A (5%). Type B was characterized by chitonic/close spaced porphyric c/f related distribution and moderate sorting. The fine material was brown in PPL and orange-brown in XPL, with dotted limpidity and speckled b-fabric. The abundance of fine material was between 10-75%, depending on the samples. This type was dominant in the sample from the side of the skull (50-70%), in control C3 C (40-60%) and control C2 A (75%). Type C was monic/open porphyric c/f related distribution and well sorting, with very small mineral grains. Fine material was orange-brown in PPL and orange/brown in XPL, with limpid or dotted limpidity and speckled or slightly parallel striated b-fabric. Abundance of fine material was between 70-95%, depending on the samples. This type occupied between 5-40% of the slides and was not observed in samples A11 and C3 B. All of the samples were apedal.

VOIDS

Five types of void were observed in grave 83012: chambers, channels, cracks, modified complex voids and packing voids (Figure 5.60).

Channels were present in all of the samples, between 2-15%. They were common in the areas around the skeleton and in the controls and less abundant in the extra samples, except for A4. By contrast, cracks were more abundant in the extra samples (5-15%) than in the controls or the areas around skeleton. In fact, they were observed only in the area of the pelvis (2%) and control C3 (2-8%). Chambers were rare (2-5%), detected in the area of the skull, pelvis, sample A5 and control C3. Modified complex voids were few (5%) in the area of the skull, A6, A9, A10 and control C3 and more common in A4 and control C2 (Figure 5.78.h). Packing voids were detected in the controls (5-25%) and in the area of the skull (5%).
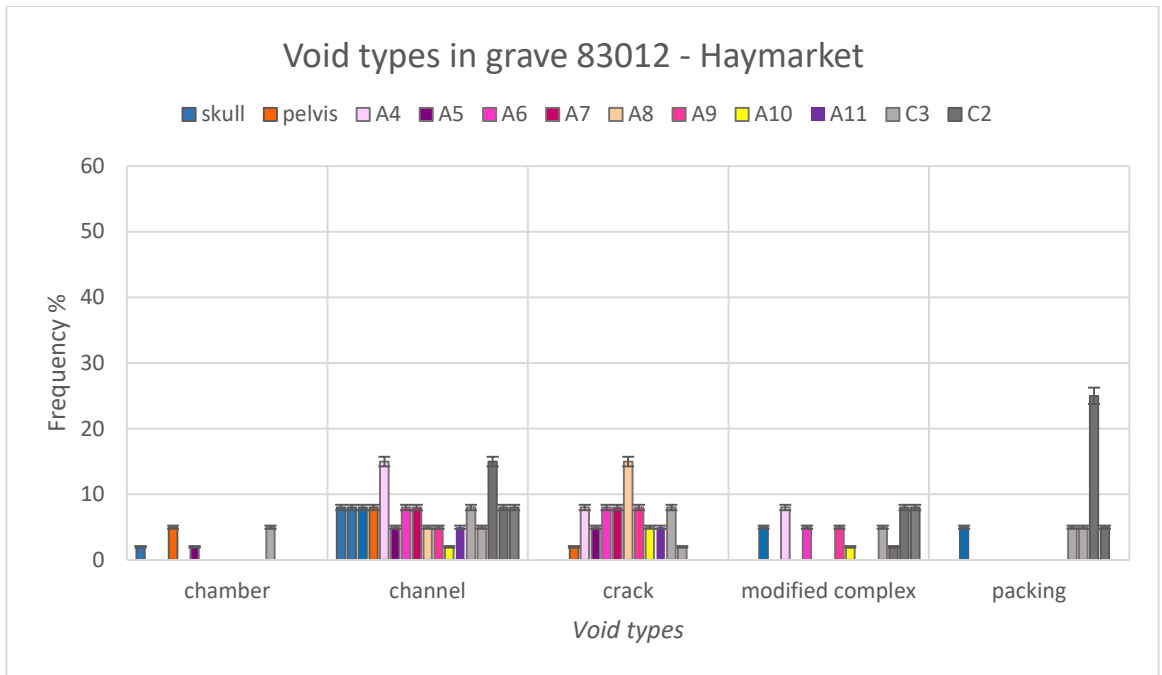
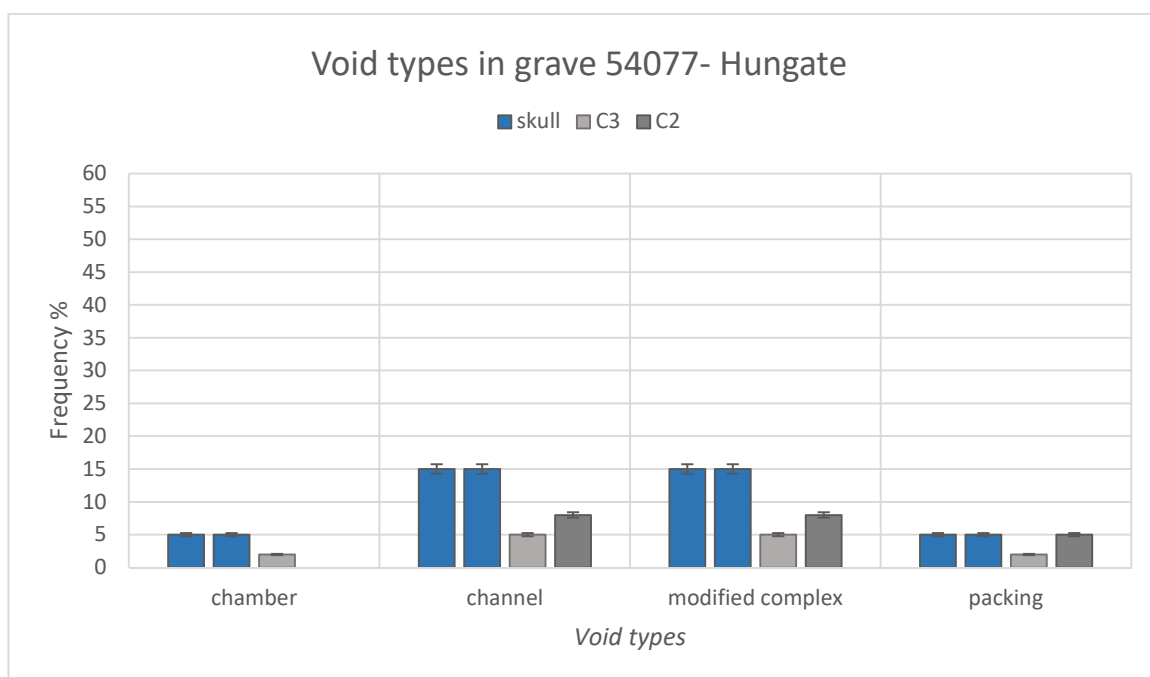*Figure 5.60: Abundance of different types of void in relation to their anatomical location within grave 83012. Channels were the most common and packing voids were present only in the controls and in the area of the skull.*

MINERAL COMPONENTS

Five types of mineral component were identified in grave 83012: calcite, mica, plagioclase, quartz and quartzite (Figure 5.61).
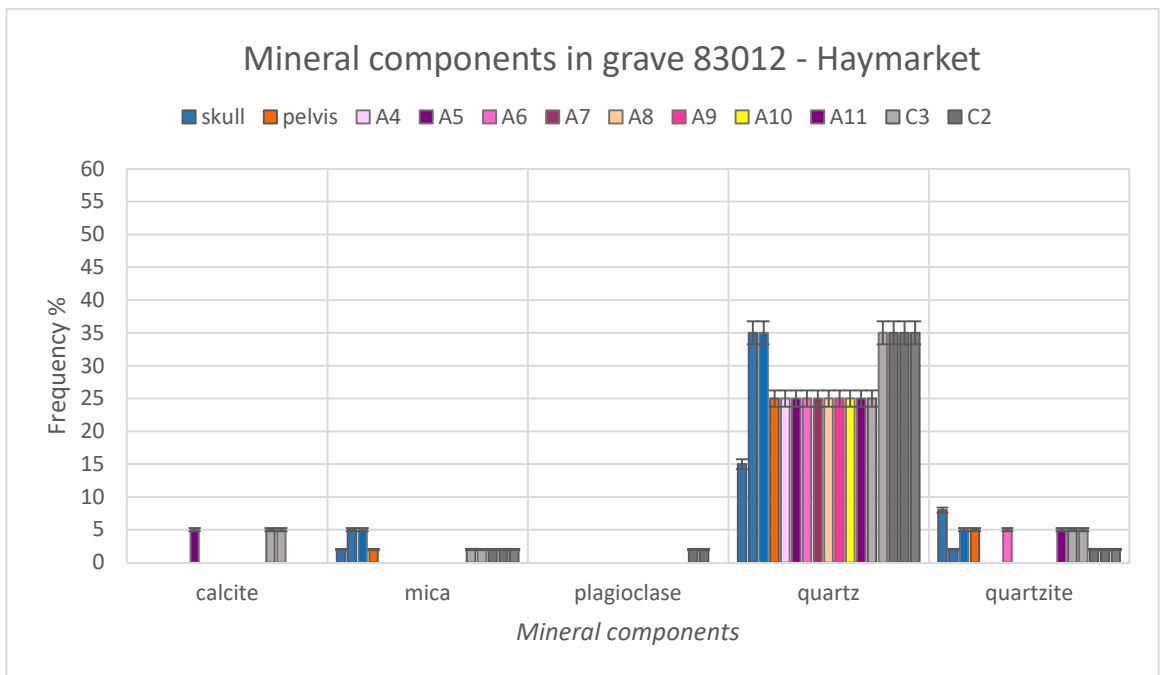
Figure 5.61: Frequency of mineral components in relation to their anatomical location within grave 83012. Quartz was the most frequent mineral in all of the samples.

Quartz (50-700 μm) was frequent in all of the samples, between 15-35%. The shape was angular/sub-rounded and it was not weathered. Quartzite fragments were few, present in the areas of the skull (2-8%), pelvis (5%), A6 and A11 (5%), control C3 (5%) and control C2 (2%). Plagioclase was observed only in the control C2 (2%), while mica was present in the areas of the skull, pelvis and controls (2-5%). Few fragments of calcite were identified in A5 and control C3 (5%).

ORGANIC COMPONENTS

Four types of organic component were detected in grave 83012: bone fragments, charcoal, humified structure and sclerotia (Figure 5.62).
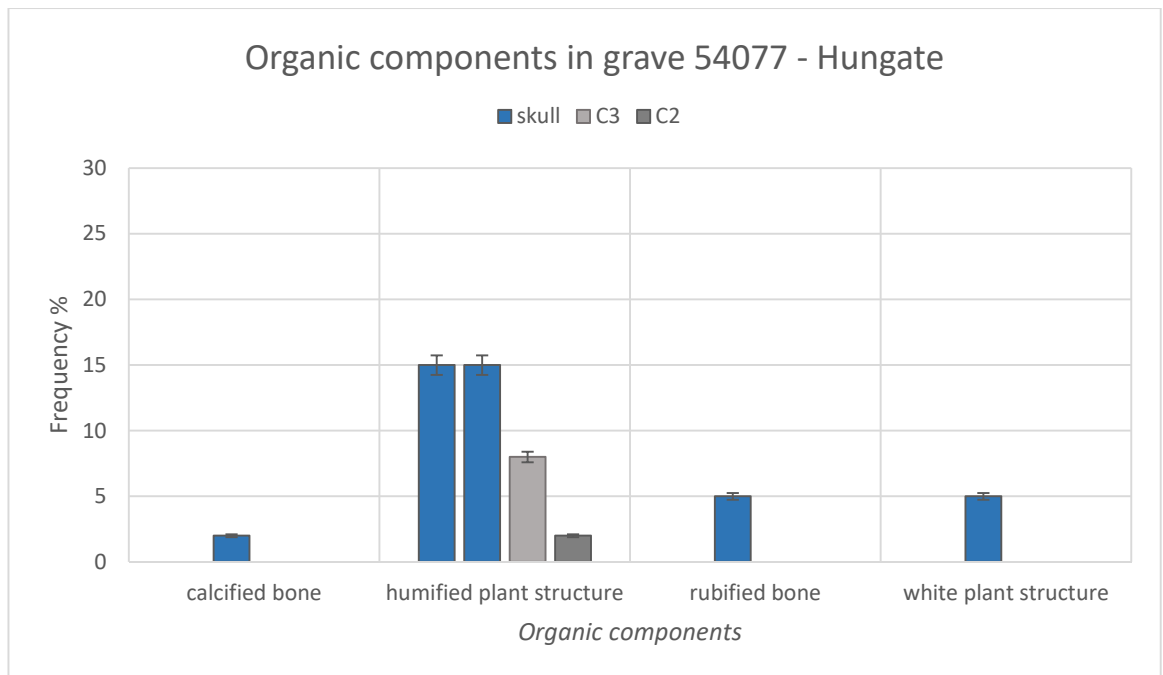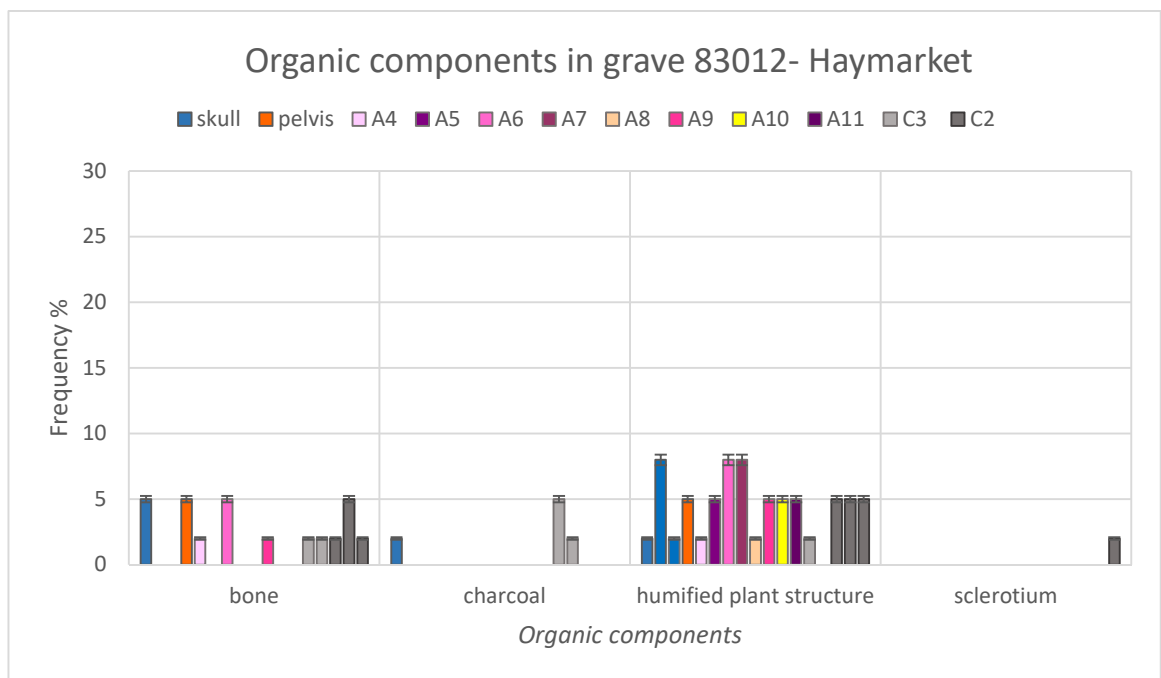

Figure 5.62: Frequency of organic components in relation to their anatomical location within grave 83012. Few humified plant structures were observed in most of the samples, while bone fragments were not always present.

Bone fragments were found in the area of the skull (5%), pelvis (5%), A4 (2%), A6 (5%), A9 (2%) and in the controls (2-5%). They were generally light yellow in PPL and low order grey birefringent or isotropic in XPL and partially weathered. Two specific types of weathering were observed on the bones: one coarse fragment (2000-3000 μm) from the area of the skull had part of the surface dark brown in colour and it was probably burnt. The histological structure was still visible, but not clear. However, that area of the slide had inclusions of dust in the resin. Another fragment of bone (2500 μm), from sample A6, had stains along vertical cracks parallel to its length (Figure 5.77.a). The cracks were filled with dark brown granules, with irregular surface and size between 2-20 μm (Figure 5.77.b). The stains developed along perpendicular lines from the cracks and were black or brown in PPL and red in XPL (Figure 5.77.d), with comb shape. In several cases the stains traced very fine cracks giving a dendritic appearance (Figure 5.77.c).

Very few fragments of charcoal were observed in the area of the skull (2%) and control C3 (2-5%). They were of sizes between 100-1500 µm, sub-angular shape and were partially weathered. Humified plant structures were present in all of the samples and were more abundant in the area of the skull and samples A6 and A7 (8%). They were between 100-4000 µm, sub-angular or sub-rounded shape and exhibited different levels of weathering (Figure 5.78.f). Very few sclerotia (380 µm) were detect in the control C2 (2%).

PEDOFEATURES

The main pedofeatures from grave 83012 were: black/red redox impregnations, clay coatings, soil micro-fauna faecal pellets, Fe/Mn nodules, amorphous phosphates, associated with vivianite and CaCO$_3$ in some cases, secondary CaCO$_3$ crystals and worm-derived calcium carbonate granules (Figure 5.63).
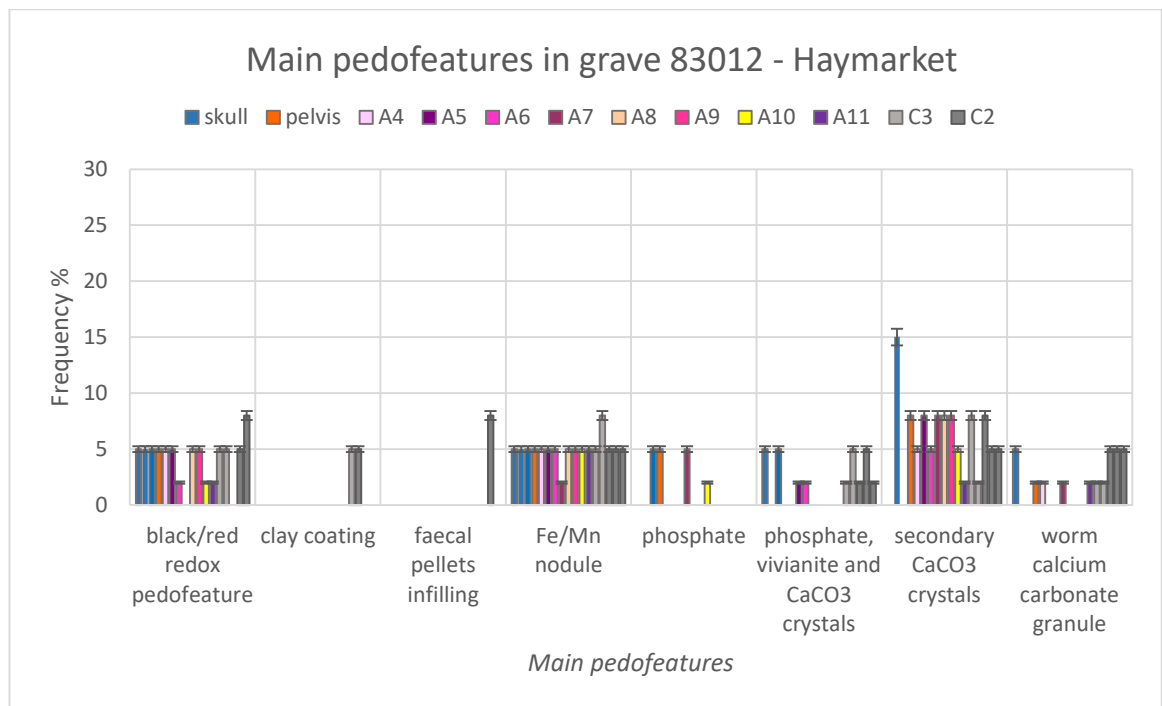
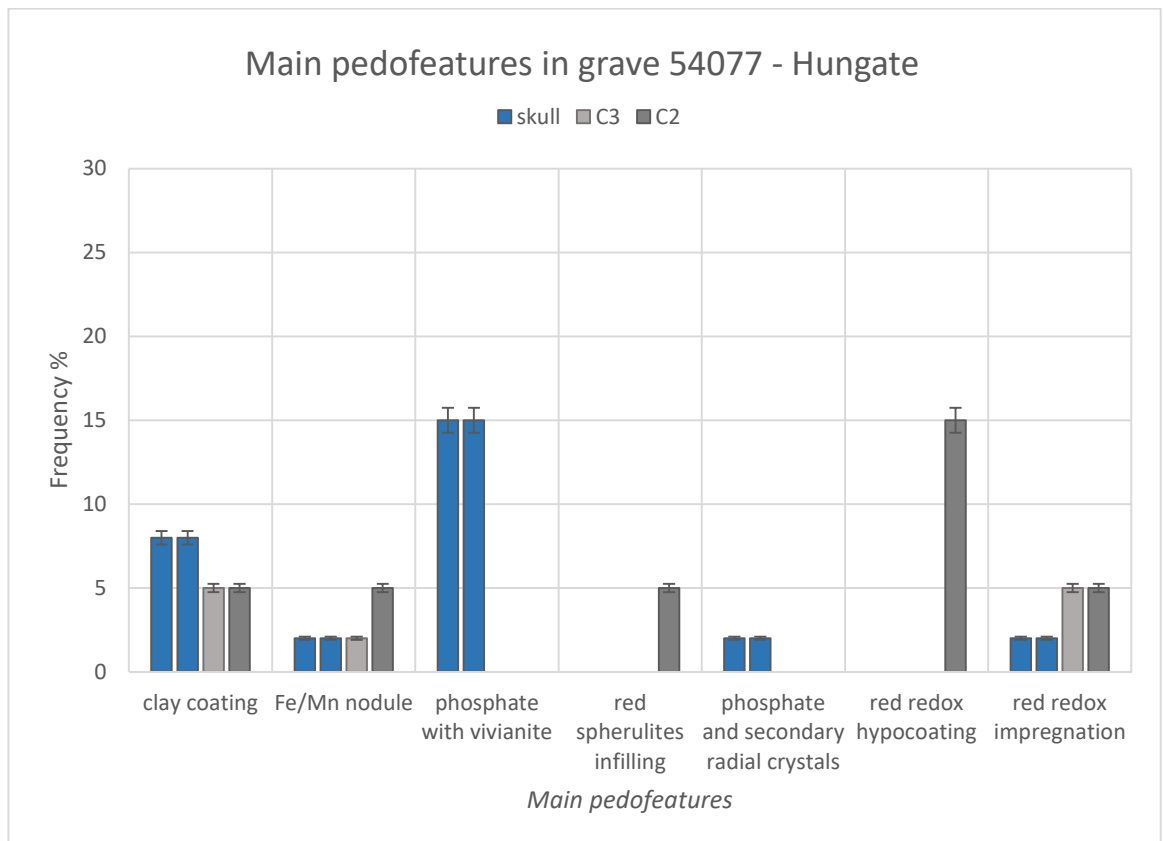*Figure 5.63: Frequency of the main pedofeatures in relation to their anatomical location within grave 83012. Phosphates were few, sometimes associated with vivianite and secondary CaCO$_3$ crystals. Worm-derived calcium carbonate granules were more frequent in the controls.*

Few amorphous phosphates were observed in the areas of the skull, pelvis, controls and A5, A6, A7 and A9 samples (2-5%). They occurred as nodules (200-1200 µm), coatings or strong impregnations within the groundmass, enclosing mineral components (Figure 5.79.b). In the areas of the controls, skull, A5 and A6, they were associated with vivianite and secondary CaCO$_3$ crystals. Vivianite, when embedded within phosphates, had small crystals, the boundaries of which were not easy to define. It looked like blue or green strong impregnations into the amorphous phosphates (Figure 5.79.a).

In one case from sample A6, vivianite was not associate with amorphous phosphate, had sub-rounded shape, size between 100-400 µm and radial well developed crystals (Figure 5.79.h).

$CaCO_3$ crystals, when associated with amorphous phosphates and vivianite, were organized as micritic thin layers or occurred as spherical crystals with crossed b-fabric and sizes between 20-50 µm. The spherulites were isolated or developed in chain. Secondary $CaCO_3$ crystals appeared also as quasicoatings around soil pores in nearly all of the samples (2-15%). Crystals from the layer on the void wall were generally coarser (20 µm) and with more intense b-fabric. The second layer had micritic aspect (Figure 5.81.c-d). Redox inclusions of Fe/Mn sub-rounded nodules within the quasicoatings were common (Figure 5.81.a-b). From sample A9, redoximorphic areas (300-1500 µm) had internal $CaCO_3$ crystals with radial development and first order birefringence.

Black/red redox pedofeatures were few in all of the samples (2-5%), except for A7 where they were not observed. They were slightly more frequent in control C2 (5-8%). Fe/Mn nodules were detected in all of the samples (2-5%) and were more frequent in control C3 (5-8%). Dusty clay coatings around voids were observed only in controls C3 and C2 (5%).

Soil micro-fauna faecal pellets as loose discontinuous infillings within modified complex voids were detected in control C2 B. The size was between 100-200 µm, sub-rounded shape, smooth surface, yellowish brown in PPL and brown with yellow speckles in XPL, with speckled b-fabric. Worm-derived calcium carbonate granules were observed in all the controls (2-5%), in the area of the pelvis, in samples A4, A7 and A11 (2%). The shape was sub-rounded, size between 300-2000 µm, with radial crystals grey in PPL and pink/green in XPL and crystallitic b-fabric. Some granules were partially weathered, while others were perfectly preserved.

GRAVE 84700

ELEMENTS OF FABRIC AND PEDS

The fabric in grave 84700 was differentiated into three distinct types, A, B and C. Type A was dominant in all of the samples (60-100%) and characterized by porphyric c/f related distribution and poor sorting. The fine material was brown in PPL and yellow/brown in XPL, with dotted limpidity and speckled or crystallitic b-fabric. The abundance of fine material was between 50-70%, depending on the samples. Type B was present in the area of the skull (20%), feet (20-30%) and control C3 (5-10%). It was characterized by double/single c/f related distribution and moderate sorting. The fine material was brown in PPL and yellow/brown in XPL, with dotted limpidity and speckled b-fabric. The abundance of fine material was between 60-80%. Type C was present in the areas of the skull (15-40%) and feet (5-10%). It was characterized by open porphyric c/f related

distribution and poor sorting. The fine material was light brown in PPL and pink/yellow/dark grey in XPL, with dotted limpidity and crystallitic b-fabric. The abundance of fine material was between 60-85%. Very fine to fine granular peds were observed in the area of skeleton (2-5%), control C3 (2%) and control C2 (5-10%).

VOIDS

Four types of void were observed in grave 84700: chambers, channels, modified complex voids and packing voids (Figure 5.64).
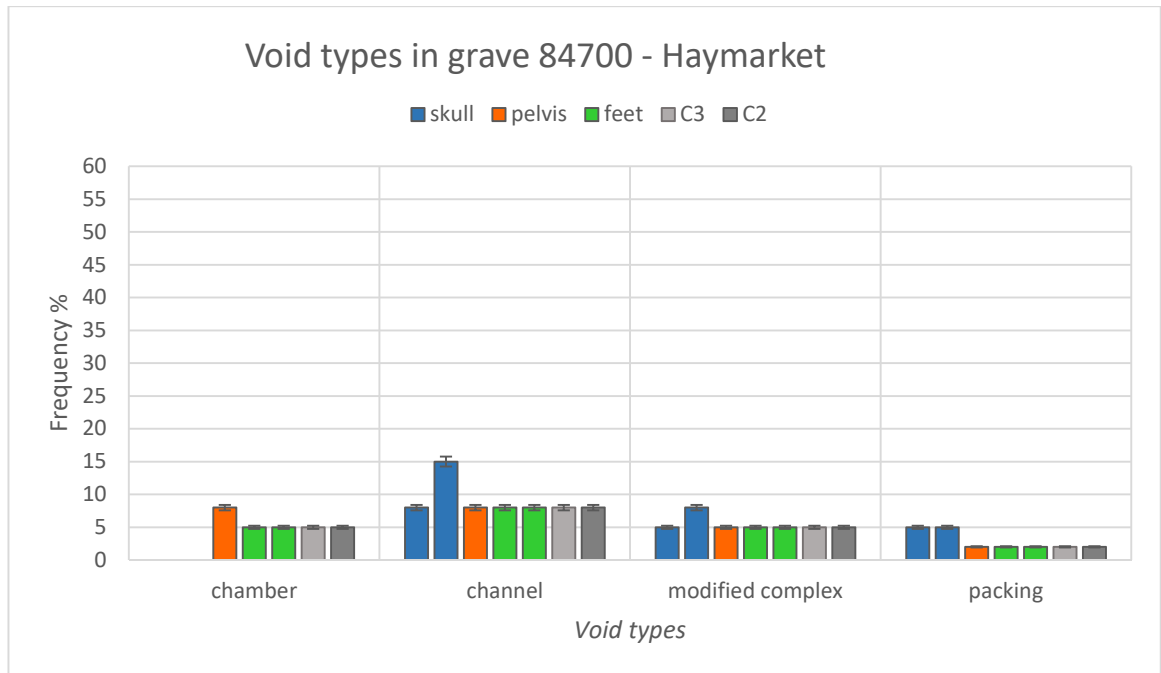
Figure 5.64: Abundance of different types of void in relation to their anatomical location within grave 84700. Channels were common and modified complex few, both observed in all of the samples.

Chambers were present in all of the samples (5%), except for the region of the skull. They were more abundant in the area of the pelvis (8%). Channels were frequent in the area of the skull (8-15%), where they reached 4000 µm in thickness, and were common in the rest of the samples (8%). Modified complex voids (Figure 5.78.g) were few in all of the samples (5%) and more abundant in the area of the skull (8%). Packing voids were few in the area of the skull (5%) and very few in the others (2%). The slides showed quite dense microstructure, apart from the area of the skull.

MINERAL COMPONENTS

Six types of mineral component were identified in grave 84700: chert, flint, mica, microcline, quartz and quartzite (Figure 5.65). Quartz was the most frequent mineral (15%) in all of the slides, followed by quartzite fragments (2-5%). Quartz dimensions were between 50-1000 µm, while quartzite reached 0.6 mm. Mica (5-300 µm) and microcline (300-700 µm) were very few in all of the samples (2%). Some fragments of flint (400-1500 µm) were observed in the controls (2%), while chert (130 µm-1 cm) was present in all the areas around the skeleton (2-5%) and in C3.
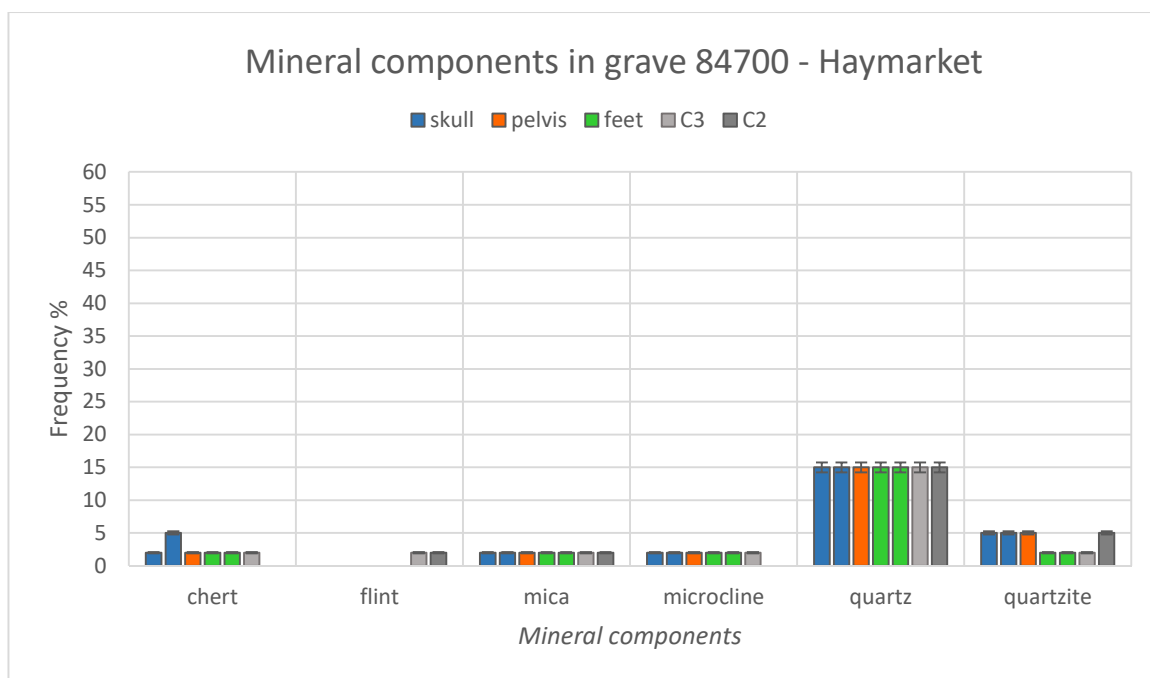
Figure 5.65: Frequency of mineral components in relation to their anatomical location within grave 84700. Quartz was the most frequent mineral in all of the samples.

ORGANIC COMPONENTS

Organic components identified in grave 84700 were: amorphous organic matter, bone fragments, charcoal, humified plant structures, sclerotia and possible worm remains (Figure 5.66). Amorphous organic matter (2-5%) and humified plant structures (5%) were present in all of the samples. The latter were characterized by different levels of weathering and their size was between 100-2300 µm. Bone fragments were light yellow in PPL and low order grey birefringent in XPL; the cellular structure was still visible in many cases (Figure 5.77.g-h). A weathered fragment of bone (600 µm) was affected by black/brown stains with granular aspect filling cracks in the bone. Fragments of partially weathered charcoal were observed in all of the samples (2-5%). Their shape was sub-angular and size was between 50-900 µm.

147

Sclerotia were detected in the areas of the skull, pelvis and control C2 (2%). Most were sub-rounded and ranging between 200-300 μm. Less frequent elongated fragments (200-600 μm) with sub-rectangular shape were present in the area of the skull. Possible remains of a worm were observed in the area of the skull, partially infilled by resin. The feature was of sub-rectangular shape, 750 μm long and 35-55 μm wide and showed divisions, resembling the segments of a worm.
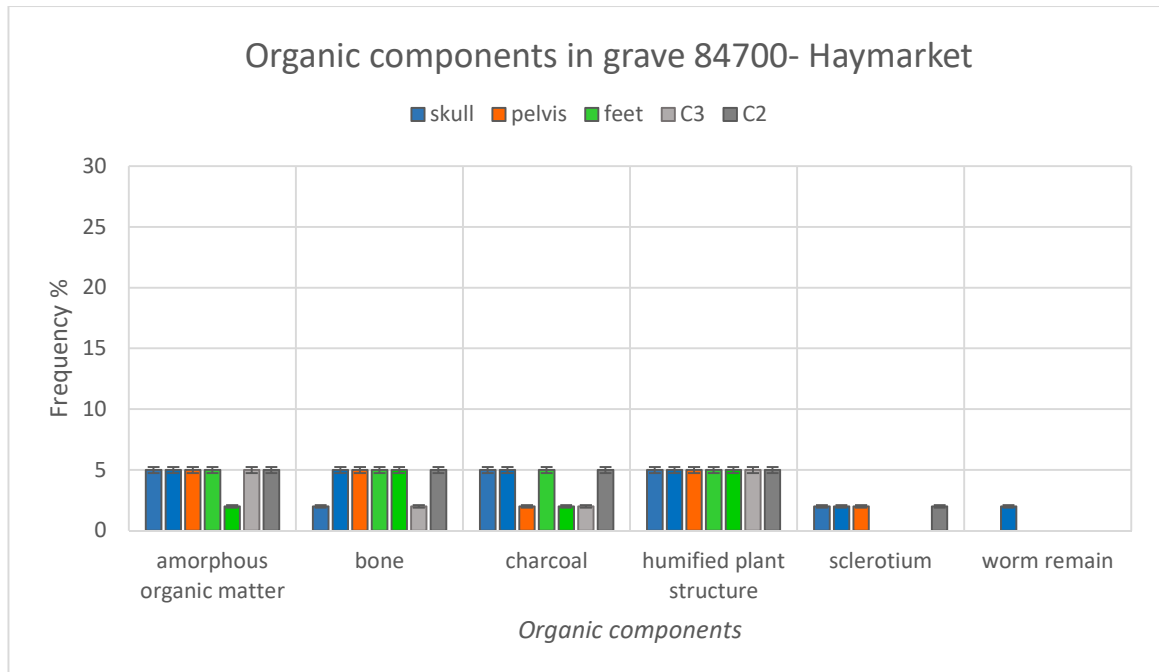
Figure 5.66: Frequency of organic components in relation to their anatomical location within grave 84700. Amorphous organic matter, bone fragments, charcoal and humified plant structures were present in all of the samples (2-5%).

PEDOFEATURES AND ANTHROPOGENIC MATERIAL

The main pedofeatures and anthropogenic materials in grave 84700 were: brick fragments, brown coatings around voids, Fe nodules, Fe/Mn nodules, amorphous phosphates, secondary $CaCO_3$ crystals, vivianite and worm-derived calcium carbonate granules (Figure 5.67). Amorphous phosphates were common in the areas of the skull and control C2 (8%). In the former, phosphates appeared as very thin and pellicular yellow coatings around voids, often characterized by two or three distinct sub-rounded layers (Figure 5.79.c-d). In the second, they were represented by thick coatings around voids or as discontinuous infillings in voids. Vivianite occurred as small crystals within the phosphates (2%) in the area of the skull and control C3, and as radial crystals (100-500 μm) intergrown within the groundmass. Secondary $CaCO_3$ was not associated with phosphates. In the areas of the skull (5%) and the feet (5%) it occurred as micritic impregnations. In the control secondary $CaCO_3$ crystals were characterized by spherulitic shape and crossed b-fabric (2%), developed on the surface of a fragment of bone. Fe nodules were observed in the areas of the pelvis (5%), feet (5%) and control C3 (2%). The size was between 35-300 μm, the shape rounded or sub-

rounded and the colour orange/red in PPL and XPL. Fe/Mn nodules were detected in all of the samples (2%), with higher frequency in the area of the skull (5%). The size was between 100-500 µm, the shape was sub-angular or sub-rounded and the colour reddish black in PPL and isotropic in XPL.

Very few fragments of brick were present in the areas of the pelvis (2%), feet and control C2 (5%). Brown coatings of spherules occurred around some voids in the area of the feet (2%). Their thickness was 15-30 µm and the spherules (5-15 µm) were brown in PPL and isotropic in XPL. Worm-derived calcium carbonate granules were identified in all of the samples (2%), being more frequent in the areas of the skull and control C2 (5%). They were between 100-1200 µm in size, sub-rounded in shape, light grey in PPL and pink/green in XPL. Some were very well preserved and the radial crystals were easy to detect, while others were weathered and some parts were missing.

Figure 5.67: Frequency of the main pedofeatures and anthropogenic material in relation to their anatomical location within grave 84700. Phosphates were common in the areas of the skull and C3. Worm-derived calcium carbonate granules were present in all of the samples.

GRAVE 84779

ELEMENTS OF FABRIC AND PEDS

The fabric in grave 84779 was differentiated in five types, A, B, D, E and F. Type C, observed in grave 84700, was not detected. Type A was frequent or dominant in all of the samples (30-85%), except for the area of the feet, where it was not observed. It was characterized by single/double spaced porphyric c/f related distribution and poor sorting. Fine material was yellowish brown in PPL and orange/brown in XPL, with dotted limpidity and speckled b-fabric. The abundance of fine material was between 40-70%, depending on the samples. Type B was present in control C2 (15%). It was characterized by open porphyric and moderate sorting. The fine material was yellowish light brown in PPL and yellow/orange in XPL, with dotted limpidity and intense speckled b-fabric. The abundance of fine material was between 70-85%. Type D was common in the areas of the knees and feet (35-60%). It was characterized by fine monic c/f related distribution and good sorting. Fine material was yellowish brown in PPL and yellow/orange in XPL, with dotted limpidity and parallel striated or speckled b-fabric. The abundance of fine material was between 70-95%, depending on the samples. Type E was common in the areas of the knees and feet (35-40%). It was characterized by close porphyric c/f related distribution, with very small mineral grains, and good sorting. The fine material was yellowish brown in PPL and yellow/orange in XPL, with dotted limpidity and speckled b-fabric. The abundance of fine material was between 40-75%. Type F was common in the area of the skull (20-60%). It was characterized by single or double spaced porphyric c/f related distribution and poor sorting. The fine material was orange-yellow in PPL and orange/yellow in XPL, with dotted limpidity and speckled b-fabric. It corresponded to the zone with higher amount of amorphous phosphates. The abundance of fine material was between 65-78%. Very fine granular peds (2%) were observed in the control C2.

VOIDS

Five types of void were identified in grave 84779: chambers, channels, cracks, modified complex voids and packing voids (Figure 5.68). Few chambers were present in the areas surrounding the skeleton and they were absent from the control. Channels were frequent in the areas of the pelvis, knees and C2 (15%), few in the area of the skull (5%) and very few in the area of the feet (2%). Cracks were common in the area of the feet (8%) and very few in the control (2%). By contrast, modified complex voids were very few in the area of the feet and few in the C2 (5%). Packing voids were slightly more abundant in the area of the skull (5-10%), than areas of the pelvis, knees and C2 (5%); they were absent in the area of the feet.
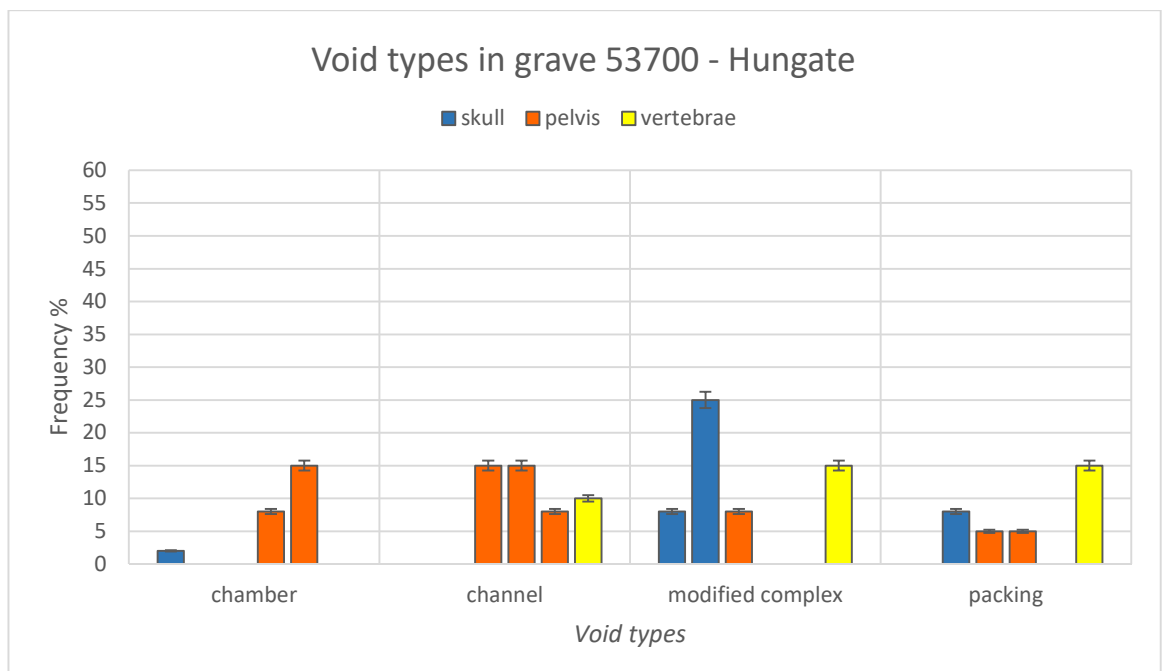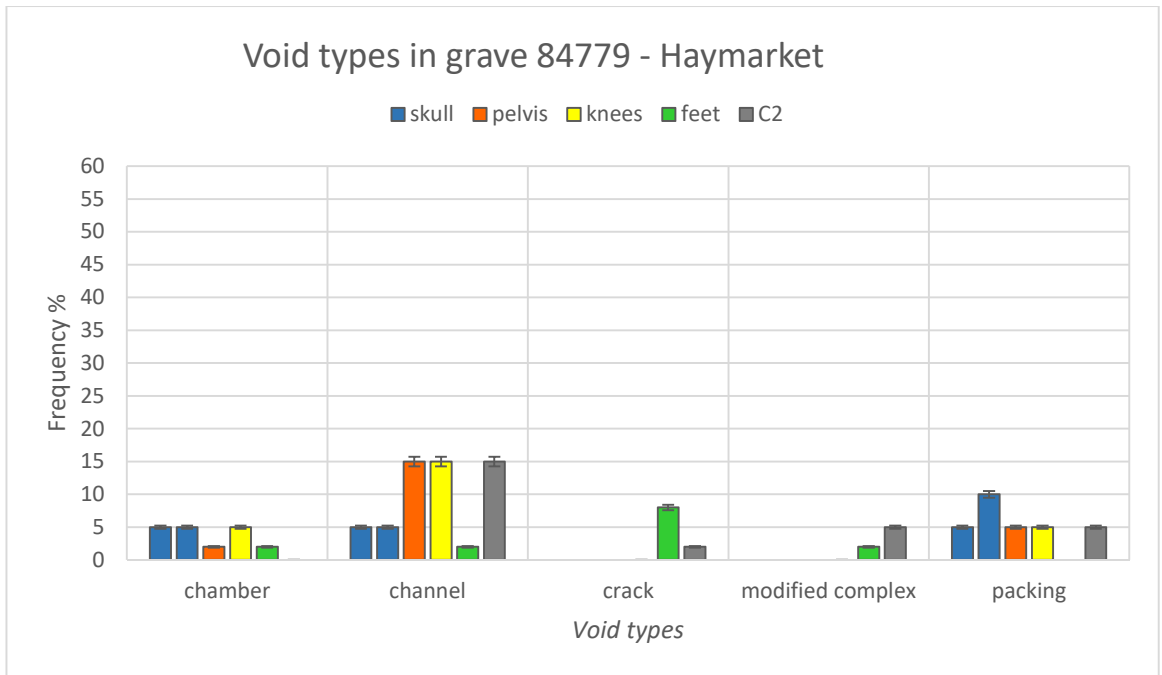
Figure 5.68: Abundance of different types of void in relation to their anatomical location within grave 84779. Modified complex voids were very few in the area of the feet and few in the control C2. Channels were frequent in the areas of the pelvis, knees and C2.

MINERAL COMPONENTS

Mineral components identified within grave 84779 were: calcite, flint, mica, microcline, plagioclase, pyroxene, quartz and quartzite (Figure 5.69).
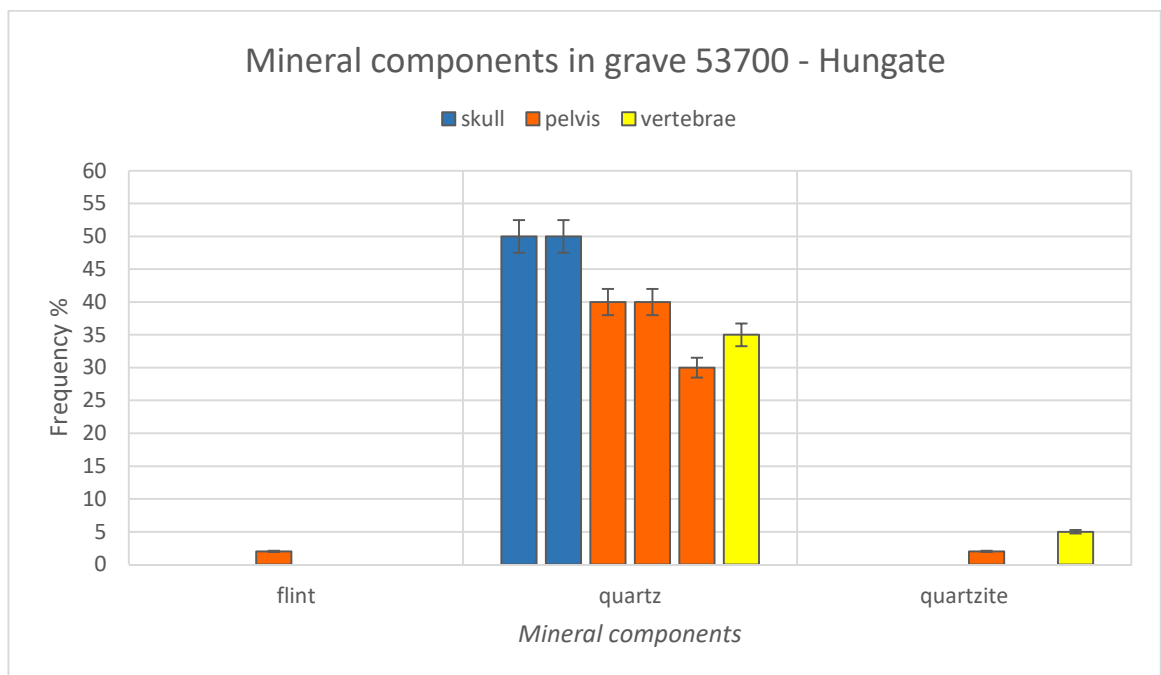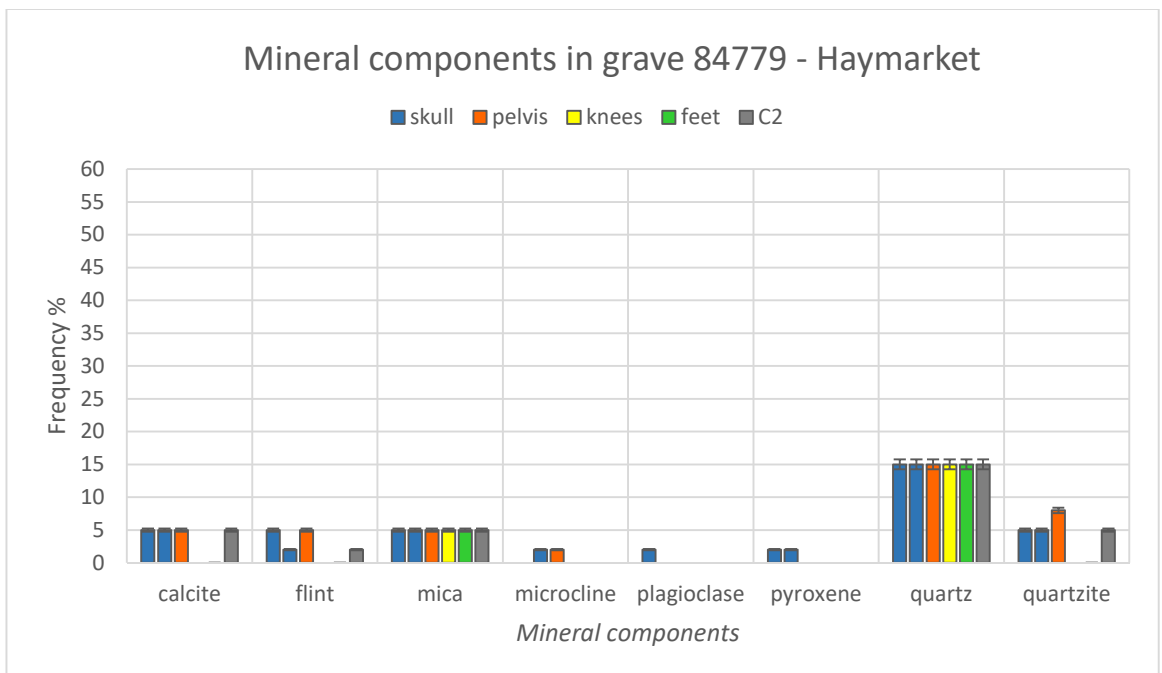

Figure 5.69: Frequency of mineral components in relation to their anatomical location within grave 84779. Quartz was frequent in all of the samples.

Quartz (50-1200 μm) was frequent in all of the samples (15%), while quartzite was few in the areas of the skull, pelvis and C2 (5-8%). Very few grains of pyroxene (100-200 μm), plagioclase (200-300 μm) and microcline (200-300 μm) were identified in the area of the skull; microcline was also present in the area of the pelvis. Mica (100-200 μm) was few, and present in all of the samples (5%), while calcite (200-1800 μm) and flint were recognized only in the areas of the skull, pelvis and C2 (2-5%).

ORGANIC COMPONENTS

Six types of organic component were identified in grave 84779: amorphous organic matter, bone fragments, charcoal, fungal spores, humified plant structures and sclerotia (Figure 5.70).

Amorphous organic matter was few (5%) in the areas of the skull, pelvis and control C2; very few (2%) in the areas of knees and feet. Bone fragments (200 μm – 1.5 cm) were more abundant in the area of the pelvis (5%) than the areas of the skull and knees (2%), while they were absent in the areas of the feet and control C2. Their colour was yellow or light yellow in PPL and low order grey birefringent in XPL. They had different levels of weathering. A coarse fragment on the right side of slide 1043 was typified by a spongy appearance typical of trabecular bone and presence of grey maculae within its structure; the background colour was white in PPL and isotropic in XPL. Rare brownish grey short lines were visible in XPL around the maculae (Figure 5.77.e-f). Fragments of charcoal (30-1100 μm) were observed in the control C2 (Figure 5.78.b). Most of them were concentrated in the right side of the slide (Supplementary Data, folder "Mosaics", Haymarket 84779). Fungal activity was detected in the area of the skull, with a fungal spore (10-32 μm) and sclerotia (70-80 μm) (Figure 5.78.a). The fungal spore was round in shape, brown purple in PPL and brownish or isotropic in XPL. Humified plant structures were few in the areas of the skull, pelvis and C2 (5%), very few in the area of knees (2%) and absent in the area of the feet. Some fragments were more dark brown in colour, while others were more orange-brown. The structures were not always the same and they probably derived from different plants. One coarse fragment (4 mm) from the control C2 had vessels characteristics of angiosperm wood. It was partially weathered and some zones were crossed by channels of biological origin (Figure 5.78 c-d). The wood fragment was diffuse- to semi-ring-porous, the pores were solitary or in radial groups or in radial rows of 2 to 3 multiples, and the growth ring boundaries were more or less distinct. The rays were difficult to distinguish between homogeneous or heterogeneous because weathered, therefore the fragment could be identified as Populus sp. or Salix sp. (www.woodid.net).
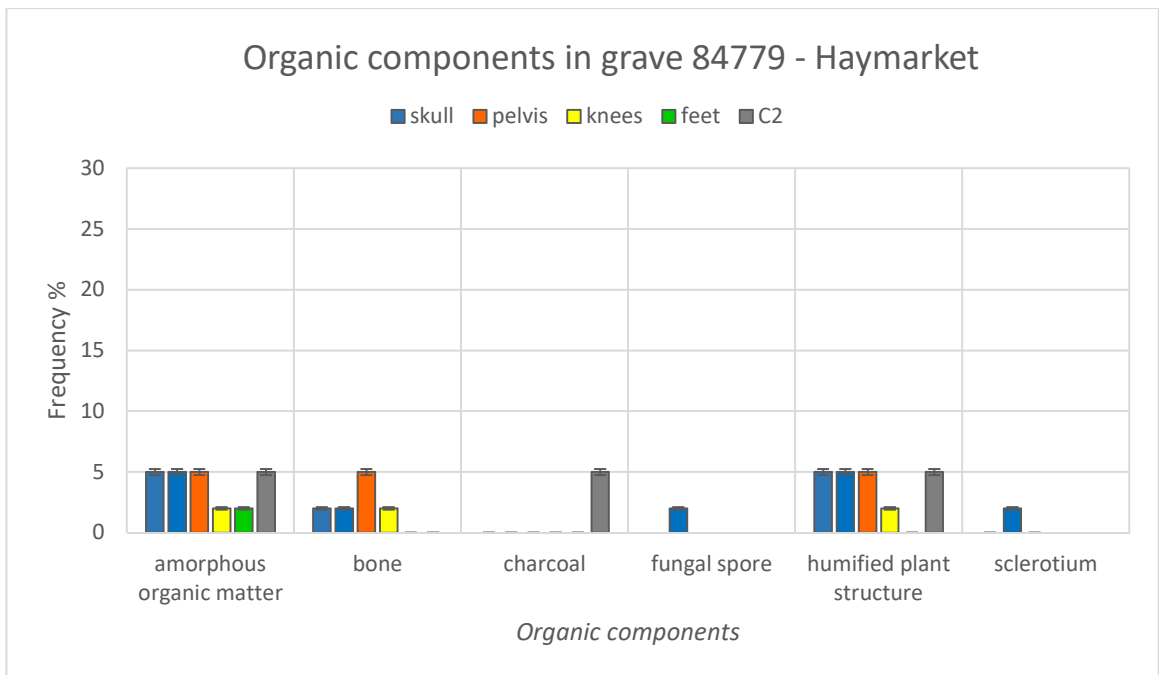
Figure 5.70: Frequency of mineral components in relation to their anatomical location within grave 84779. Amorphous organic matter was few in all of the samples, while humified plant structures were not observed in the area of the feet.

PEDOFEATURES AND ANTHROPOGENIC MATERIAL

The main pedofeatures and anthropogenic materialidentified in grave 84779 were: brick fragments, coatings of amorphous phosphate and $CaCO_3$ crystals, Fe/Mn nodules, infillings of clay, amorphous phosphates, vivianite and worm-derived calcium carbonate granules (Figure 5.71).
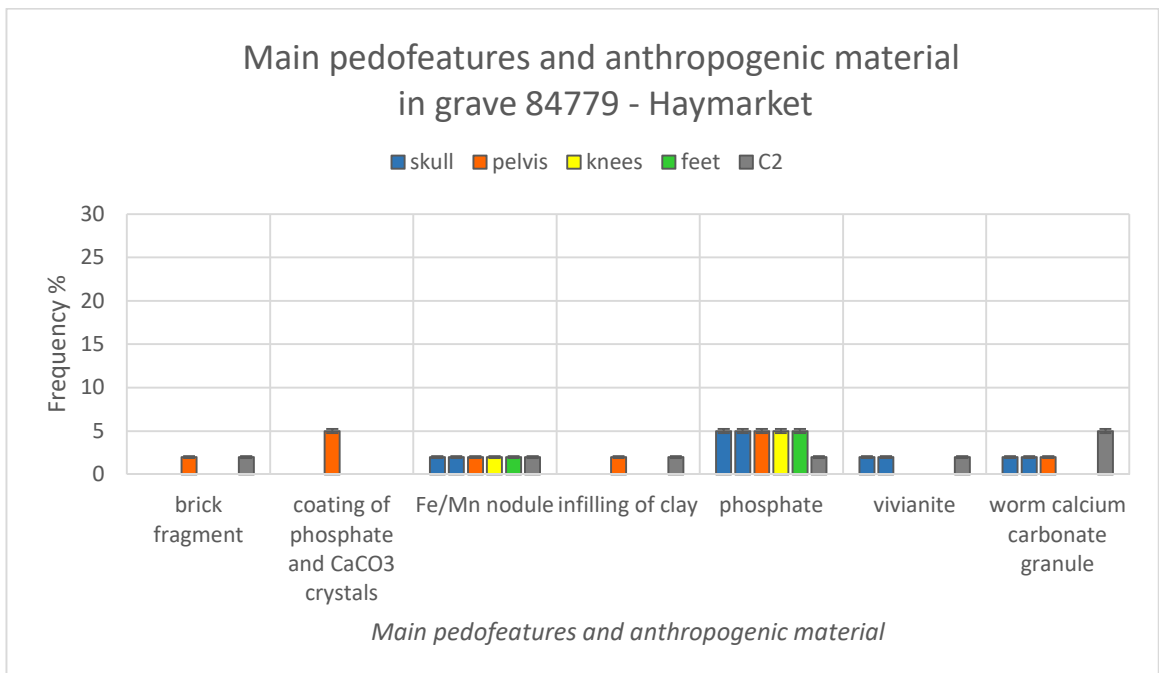
Figure 5.71: Frequency of the main pedofeatures and anthropogenic material in relation to their anatomical location within grave 84779. Amorphous phosphate was present in all of the samples, while vivianite was very few in the areas of the skull and C2. Worm-derived calcium carbonate granules were more frequent in the control than within the layer containing the skeleton.

Few amorphous phosphates were detected in the area surrounding the skeleton (5%), while very few were in the control C2 (2%) (Figure 5.79.a). In the area of the skull, phosphates occurred mainly as coating around voids and they were associated with small crystals of vivianite. Particularly in slide 1044, it was possible to distinguish between amorphous phosphatic coatings with vivianite inclusions and phosphatic coatings formed by sub-rounded or rounded fan-like crystals (100-150 μm). The latter were yellow in PPL, like the amorphous ones, but they had green or isotropic colour in XPL and crystallitic b-fabric (Figure 5.79.e-f-g-h). Some amorphous phosphates from the same slide appeared as impregnations or nodules with granular and coalescent internal sector, formed by very small spherules (2-5 μm). In the area of the pelvis, phosphates were mainly impregnations and inclusions within the groundmass. The coarse fragment of bone, mentioned above, had coatings (40-200 μm of thickness) of amorphous phosphates embedded with secondary $CaCO_3$ crystals around the trabeculae of the trabecular structure. Association between amorphous phosphates and secondary $CaCO_3$ occurred more rarely, as impregnations within the groundmass, in the areas of knees and control C2.

Vivianite (2%) developed in the area of the skull within amorphous phosphates (Figure 5.80.b,g) or as sub-rounded radial crystals within the groundmass (200-300 μm). The latter was also present in the control, but was smaller in size (20-160 μm).

Fe/Mn nodules were very few in all of the samples, and exhibited different size ranges: 50-250 μm in the areas of the skull, pelvis and control and 50-400 μm in the areas of knees and feet. Brick fragments (1450 μm - 1 cm) and limpid or dusty clay infillings in voids (150-300 μm of thickness in the area of the pelvis and 140-450 μm in the control) were detected in the areas of the pelvis and control (2%). Worm-derived calcium carbonate granules were mainly visible in the control C2 (5%) and very few in the areas of the skull and pelvis (2%). They had sub-rounded shape, size between 100-1100 μm, and were more weathered in the area of the skull than the other samples (Figure 5.81.e-g).

GRAVE 84851

ELEMENTS OF FABRIC AND PEDS

The fabric in grave 84851 was characterized by porphyric c/f related distribution and poor sorting. The fine material was brown in PPL and yellow/brown in XPL, with dotted limpidity and speckled or crystallitic b-fabric. The abundance of fine material was between 40-60% in all of the samples, except in the level *z* horizon at the feet, where it was between 30-50%. Granular peds were observed in all of the samples and they were more abundant in the level *z* than level *y*. The former

was distinguished by 5-10% of peds in the areas of the skull and pelvis and 20-30% in the area of the feet, while the latter had between 2-5% of peds in all of the samples. Granules were very fine to fine in size, unaccommodated and strongly developed.

VOIDS

Three types of void were observed in grave 84851: channels, modified complex voids and packing voids (Figure 5.72). Channels were frequent (15%) in the areas of the skull (level *y*), pelvis and feet (level *y*); very frequent in the level *z* of the area of the feet (25%) and common in the level *z* of the area of the skull (8%). Modified complex voids were frequent in the areas of the skull (level *z*) and pelvis (15%) and common in the level *y* of the areas of the skull and in the samples from the area of the feet (8%). Packing voids were few in all of the samples (5%).

Figure 5.72: Abundance of different types of void in relation to their anatomical location within grave 84851. Channels and modified complex voids were common or frequent in all of the samples.

MINERAL COMPONENTS

Mineral components identified in grave 84851 were: chert, mica, quartz and quartzite (Figure 5.73). Quartz (50-1500 μm) was frequent in all of the samples (15%) and very frequent in the level *z* of the area of the feet, while quartzite (500-4000 μm) was few represented (2-5%). Mica (5-300 μm) was very few in all the areas. Fragments of chert (140 μm – 2.5 cm) were detected in the area of the skull (5-8%) and level *y* of the feet (5%).
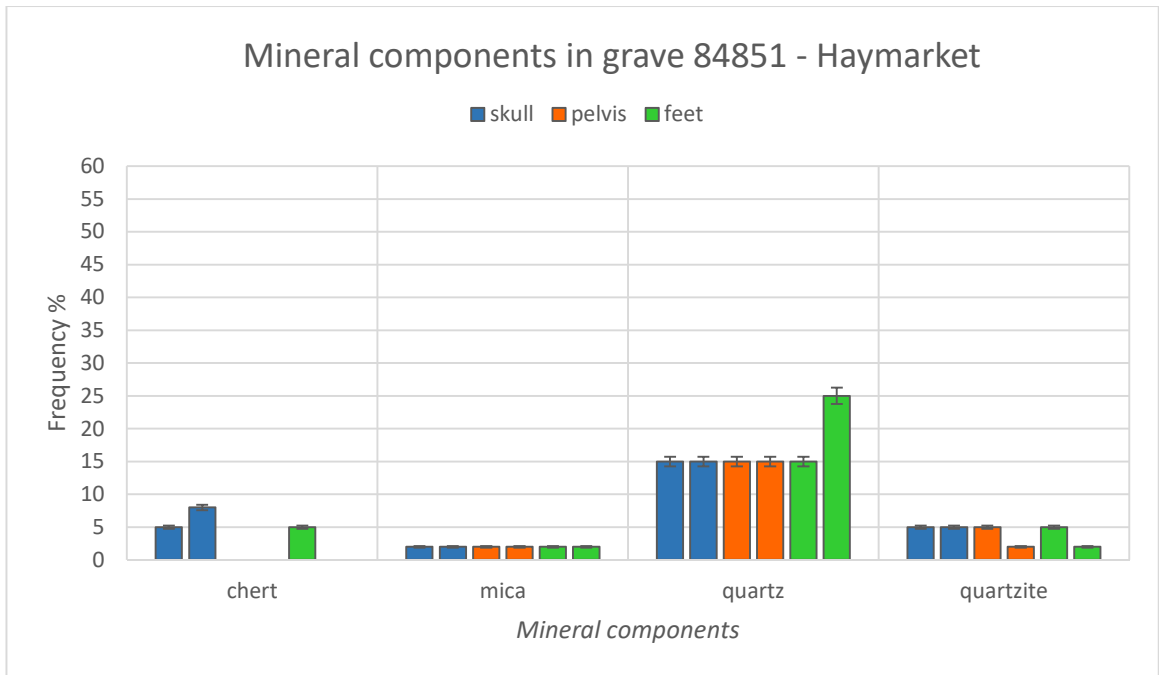
Figure 5.73: Frequency of mineral components in relation to their anatomical location within grave 84851. Quartz was frequent in all of the samples.

ORGANIC COMPONENTS

Five types of organic component were observed in grave 84851: amorphous organic matter, bone fragments, charcoal, humified plant structures and sclerotia (Figure 5.74).
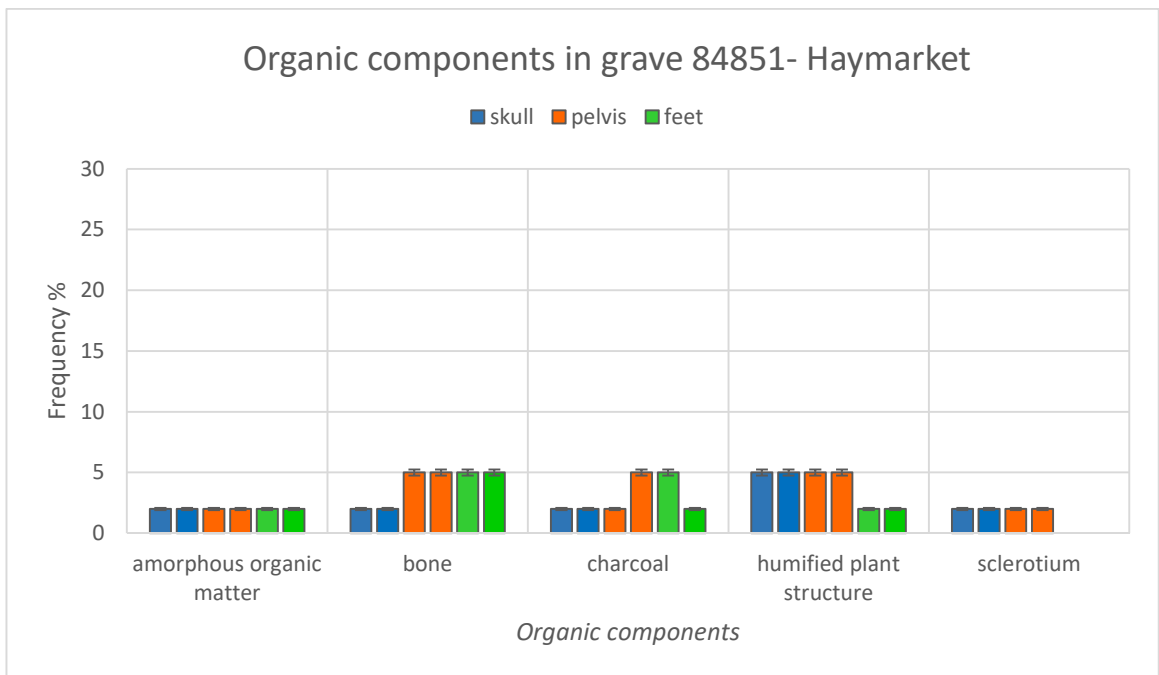
Figure 5.74: Frequency of organic components in relation to their anatomical location within grave 84851. Bone fragments were more frequent in the areas of the pelvis and feet, while humified plant structures were more frequent in the areas of the skull and pelvis.

Amorphous organic matter was very few in all of the samples (2%), while humified plant structures were slightly more abundant in the areas of the skull and pelvis (5%). In particular, coarse fragments from level *z* of the area of the skull were identified as angiosperm wood by the characteristic structure with vessels (Figure 5.78.e). Similarly to the fragment of grave 84779 (Figure 5.78.c-d), it could be identified as Populus sp. or Salix sp. Bone fragments were very few in the area of the skull (2%) and few in the areas of the pelvis and feet (5%). They were light yellow in PPL and with differing degrees of weathering. A coarse fragment from level *z* of the area of the pelvis (3000 μm) had grey maculae within the structure, white background colour and low first order birefringence; the maculae were grey beige and opaque in XPL. Fragments of charcoal were few (5%) in the areas of the pelvis (*z*) and feet (*y*) and very few in the other samples (2%). Very few sclerotia (20-150 μm) were identified in the areas of the skull and pelvis.

PEDOFEATURES

Five main pedofeatures were identified in grave 84851: brown organic coatings, dusty quasicoatings of fine material, Fe/Mn nodules, vivianite and worm-derived calcium carbonate granules (Figure 5.75).
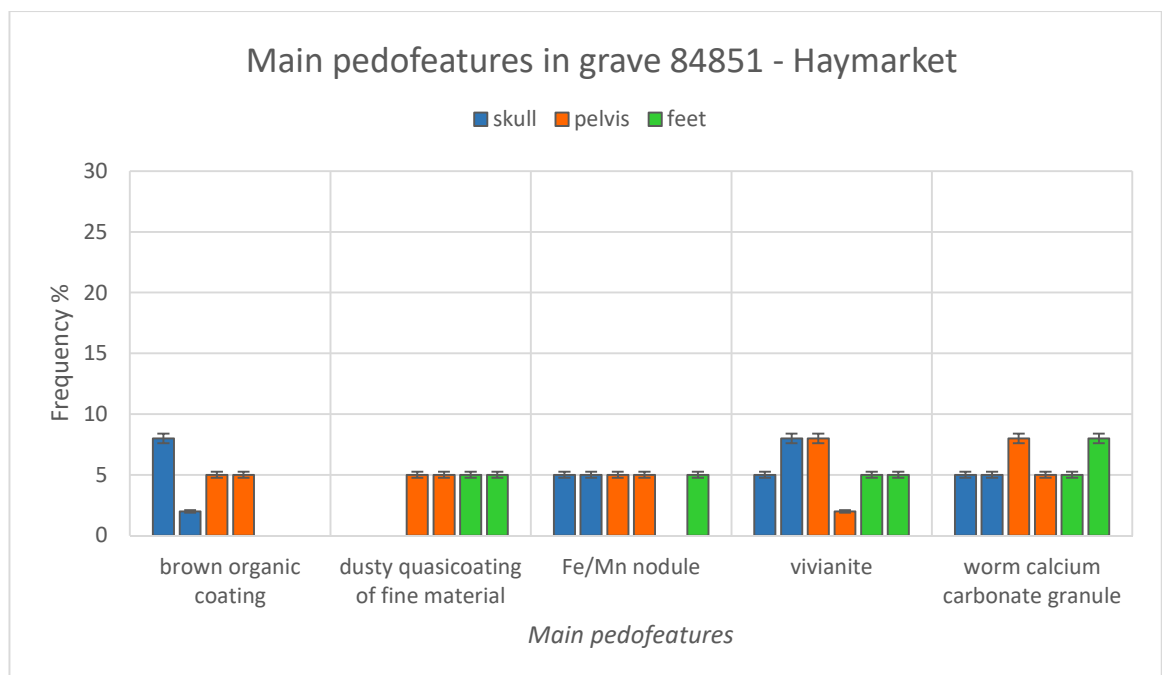
Figure 5.75: Frequency of the main pedofeatures in relation to their anatomical location within grave 84851. Vivianite was present in all of the samples, as well as worm-derived calcium carbonate granules.

Vivianite was common (8%) in the areas of the skull (*z*) and pelvis (*y*); few in the rest of the samples (2-5%) (Figure 5.80.c-d). It was characterized by well developed radial crystals (300-1400 μm) and occurred as intergrowths within the groundmass, with sub-rounded or sub-angular shape. In very few cases, vivianite had coatings of radial crystals of $CaCO_3$. In slide 1087 vivianite crystals

developed as infillings within a humified plant fragment. Fe/Mn nodules were identified in all of the samples (5%), except for level *y* of the area of the feet. Dusty quasicoatings of fine material around channels, with parallel striated b-fabric, were observed in the areas of the pelvis and feet (5%). Brown organic coatings around voids (5-45 µm of thickness) were present in the areas of the skull (2-8%) and pelvis (5%). They were partially weathered, dark brown in PPL and isotropic in XPL. Worm-derived calcium carbonate granules were few in the areas of the skull, pelvis (*z*) and feet (*y*) and more abundant in the other samples (8%). Their size was between 100-1100 µm, sub-rounded shape and more weathered in the level *y* of the area of the pelvis (Figure 5.81.h).

ADDITIONAL SLIDES

Other graves from Haymarket were sampled by the InterArChive team, but they were not chosen for this research. However, some additional slides were examined to observe the frequency and relationship of particular pedofeatures including amorphous phosphates, vivianite and worm-derived calcium carbonate granules (Figure 5.76). Amorphous phosphates were recorded in the areas of the skull (5%) and pelvis (2%) of grave 84863, in the area of the skull (2%) of grave 84332, in the control C2 (2%) of grave 84859, in the areas of the skull (5%), hands (5%) and feet (2%) of grave 83015 and in the areas of the pelvis (5%) and feet (2%) of grave 84579. They were associated with vivianite in graves 84863 (area of the skull) and 84579 (areas of the pelvis and feet). They were absent in grave 84859. Vivianite was identified in the area of the skull in grave 84863 (2%), in the areas of the skull (5%), pelvis (8-15%) and feet (5-8%) in grave 84579 and in the areas of the skull (2-5%), pelvis (5-8%) and feet (5-8%) in grave 84859.

Worm-derived calcium carbonate granules were present in all of the slides (2-8%), except in the area of the skull in grave 84332, the areas of the skull and hands in grave 83015 and the area of the feet in grave 84579. Worm granules seemed to coexist with vivianite.

The following figures were selected as representative of the features described in Section 5.2.3:

- Figure 5.77: bone fragments;
- Figure 5.78: organic components and voids;
- Figure 5.79: phosphates;
- Figure 5.80: vivianite;
- Figure 5.81: secondary $CaCO_3$ crystals.
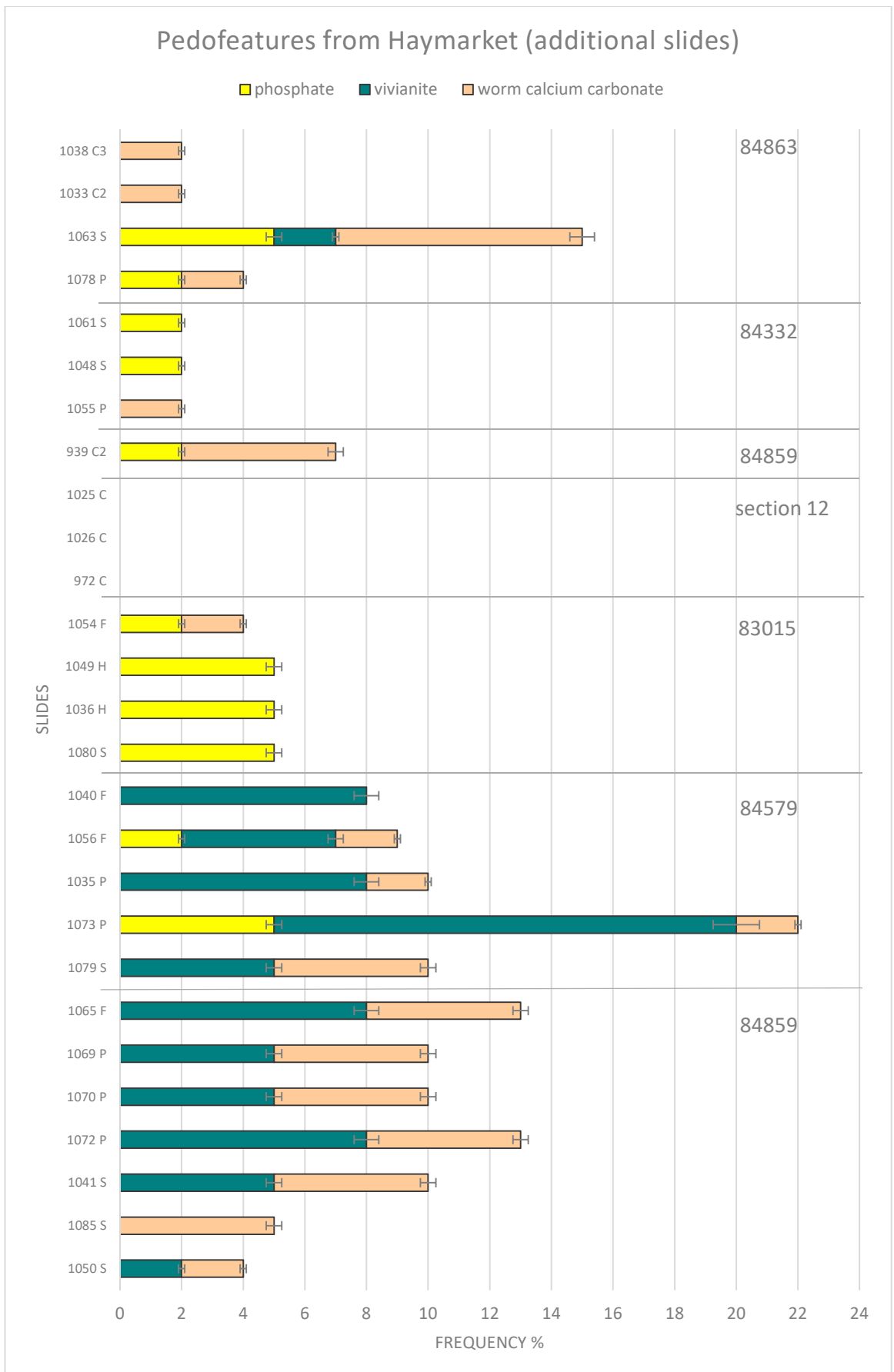
Figure 5.76: Frequency of the main pedofeatures in the additional slides from Haymarket. On the right, the numbers of the graves. On the left, the number of the slides: S=skull, P=pelvis, F=feet, H=hand, C=control.
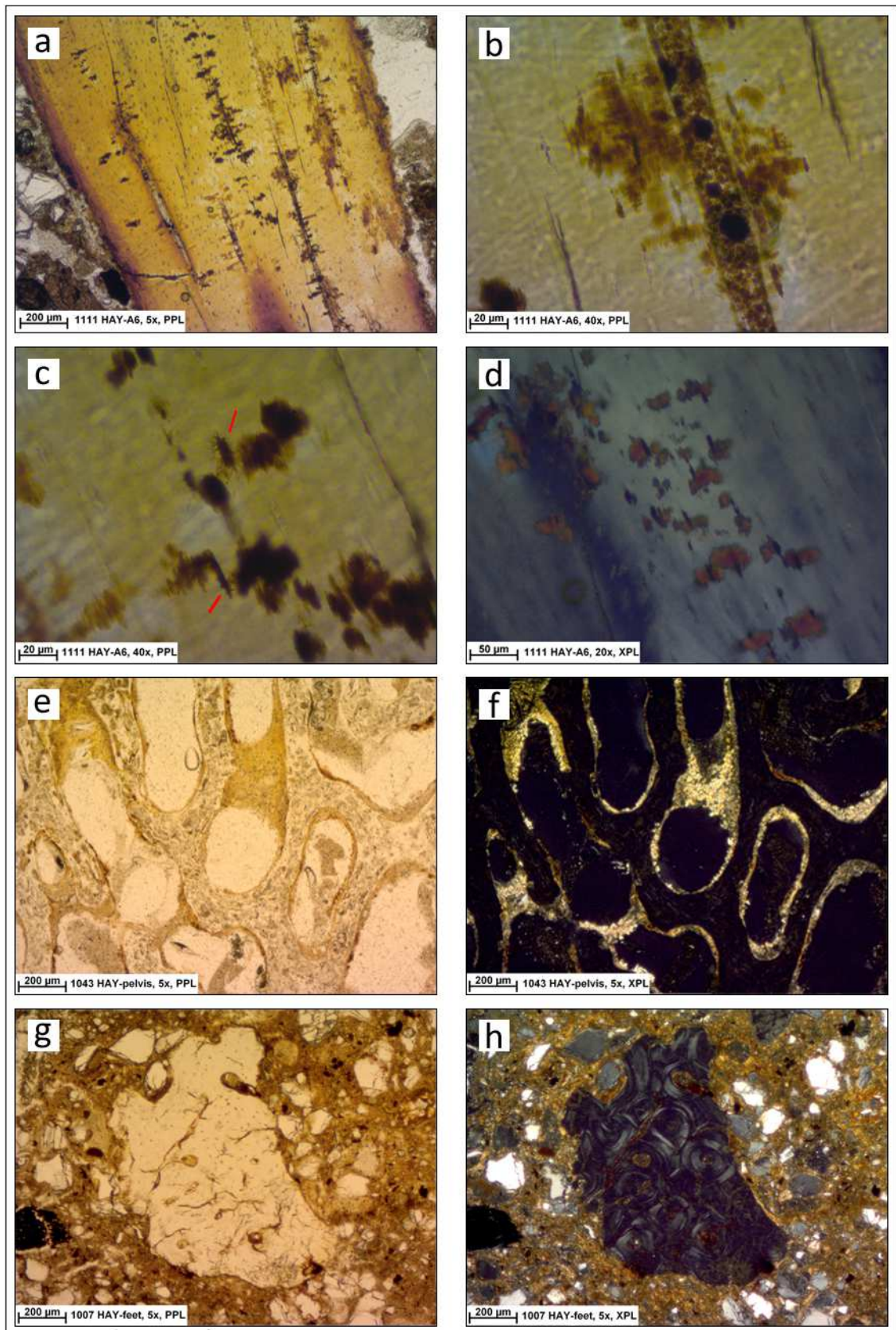
Figure 5.77: Bone fragments in Haymarket. a) fragment of bone with black stain from the area of knees in grave 83012; b) detail of the brown granular infilling in the crack of the bone from the area of knees in grave 83012; c) detail of the black stains, some with very fine definition (red arrows), from the area of knees in grave 83012; d) detail of black stains in XPL from the area of knees in grave 83012; e-f) fragment of weathered bone with crystallitic coating from the area of the pelvis in grave 84779 in PPL (e) and XPL (f); g-h) fragment of bone partially weathered from the area of the feet in grave 84700 in PPL (g) and XPL (h).

160
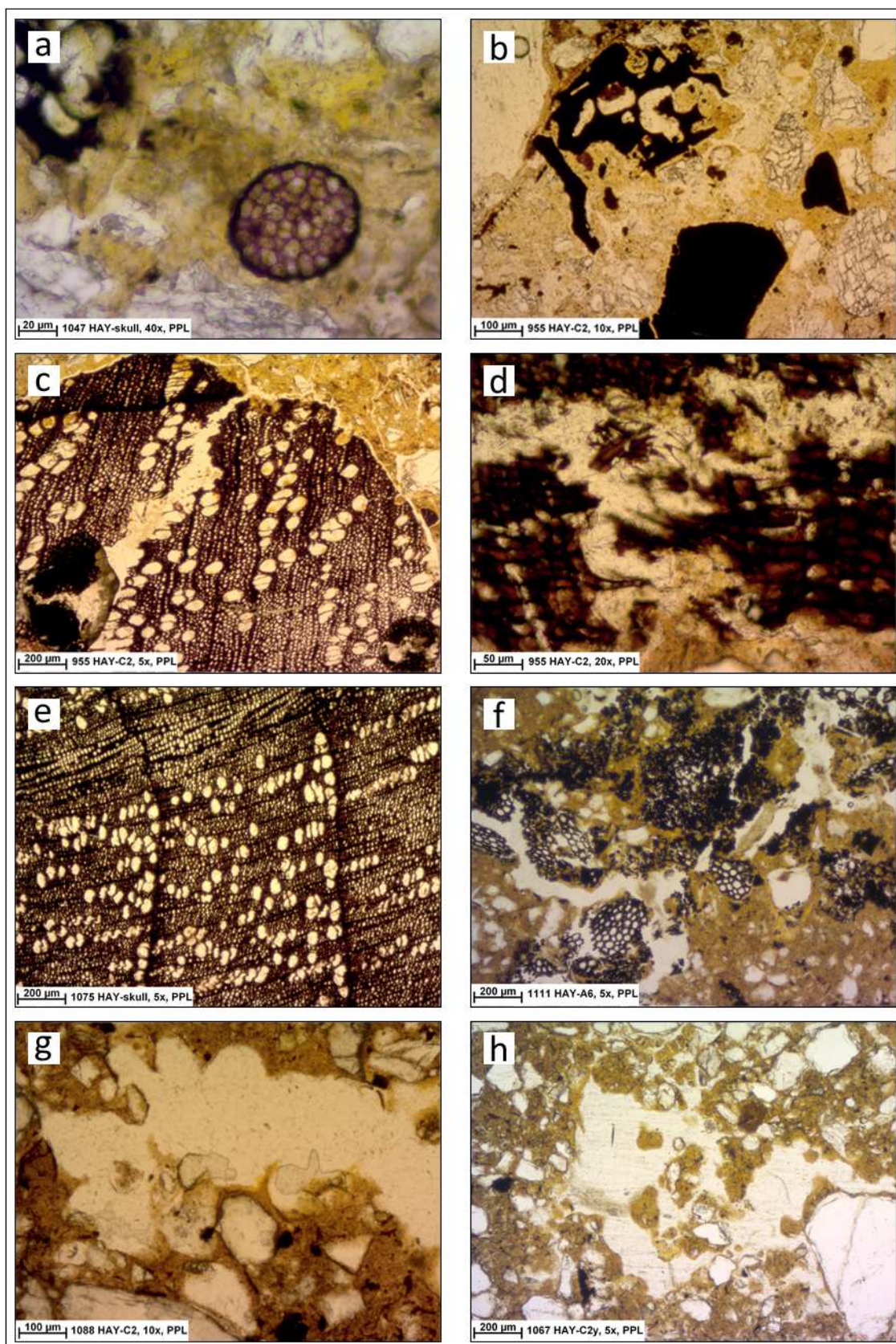
Figure 5.78: Organic components and voids in Haymarket. a) sclerotium from the area of the skull in grave 84779; b) fragments of charcoal from the control C2 in grave 84779; c) fragment of angiosperm wood crossed by a biological channel from the control C2 in grave 84779; d) detail of the weathered area of the angiosperm wood; e) fragment of well preserved angiosperm wood from the area of the skull in grave 84851; f) partially weathered humified plant structure from the area of knees in grave 83012; g) modified complex void from the area o control C2 in grave 84700; h) modified complex void from the control C2 in grave 83012.
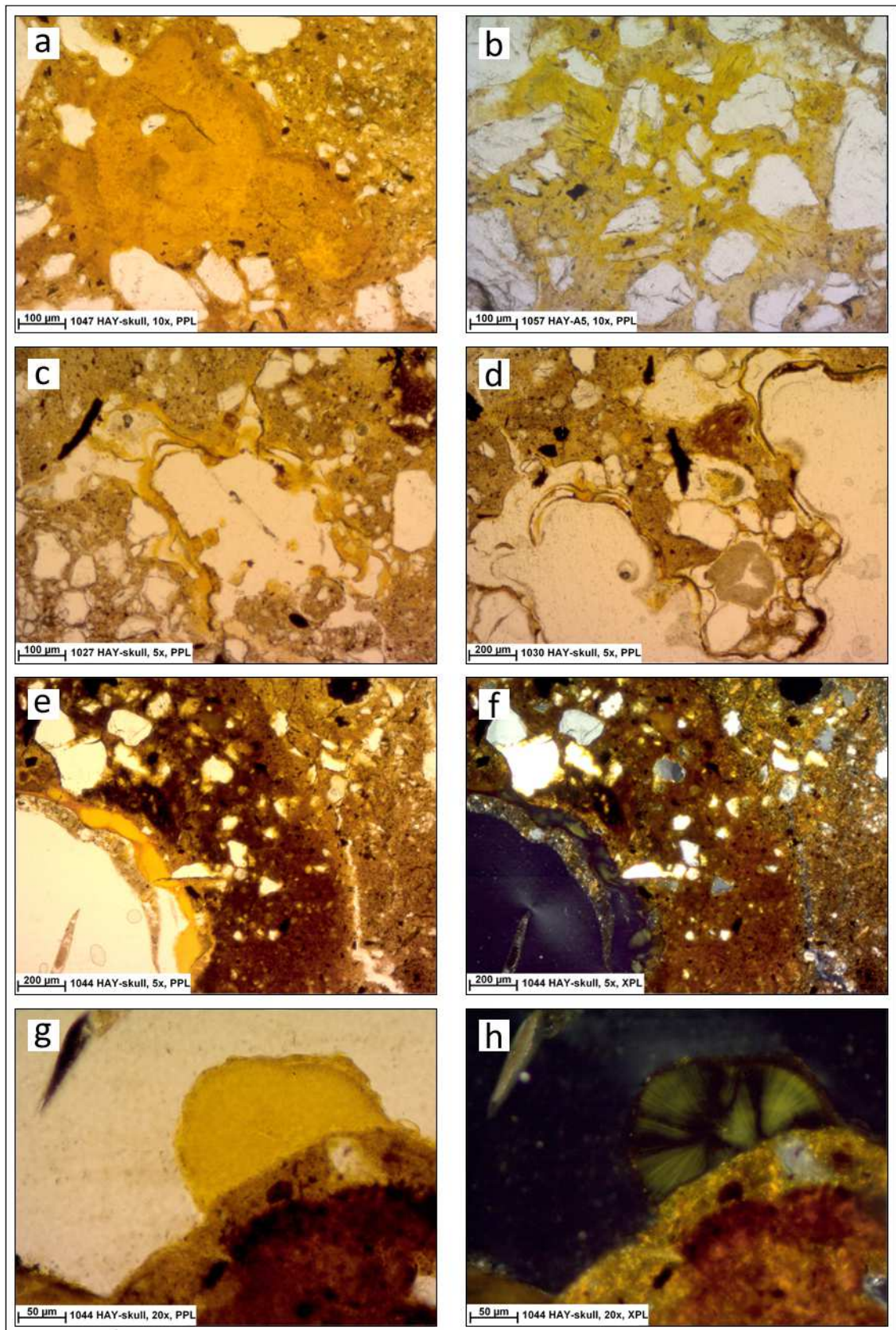
Figure 5.79: Phosphates in Haymarket. a) amorphous phosphate from the area of the skull in grave 84779; b) amorphous phosphatic impregnation including mineral grains from the area of sample A5 in grave 83012; c-d) coatings around voids of pellicular amorphous phosphates from the area of the skull in grave 84700; e-f) coating around void of phosphate yellow in PPL (e) and with radial green b-fabric in XPL (f) from the area of the skull in grave 84779; g-h) detail of the sub-rounded phosphate nodule with radial structure and green colour in XPL and radial b-fabric in the area of the skull in grave 84779 in PPL (g) and XPL (h).
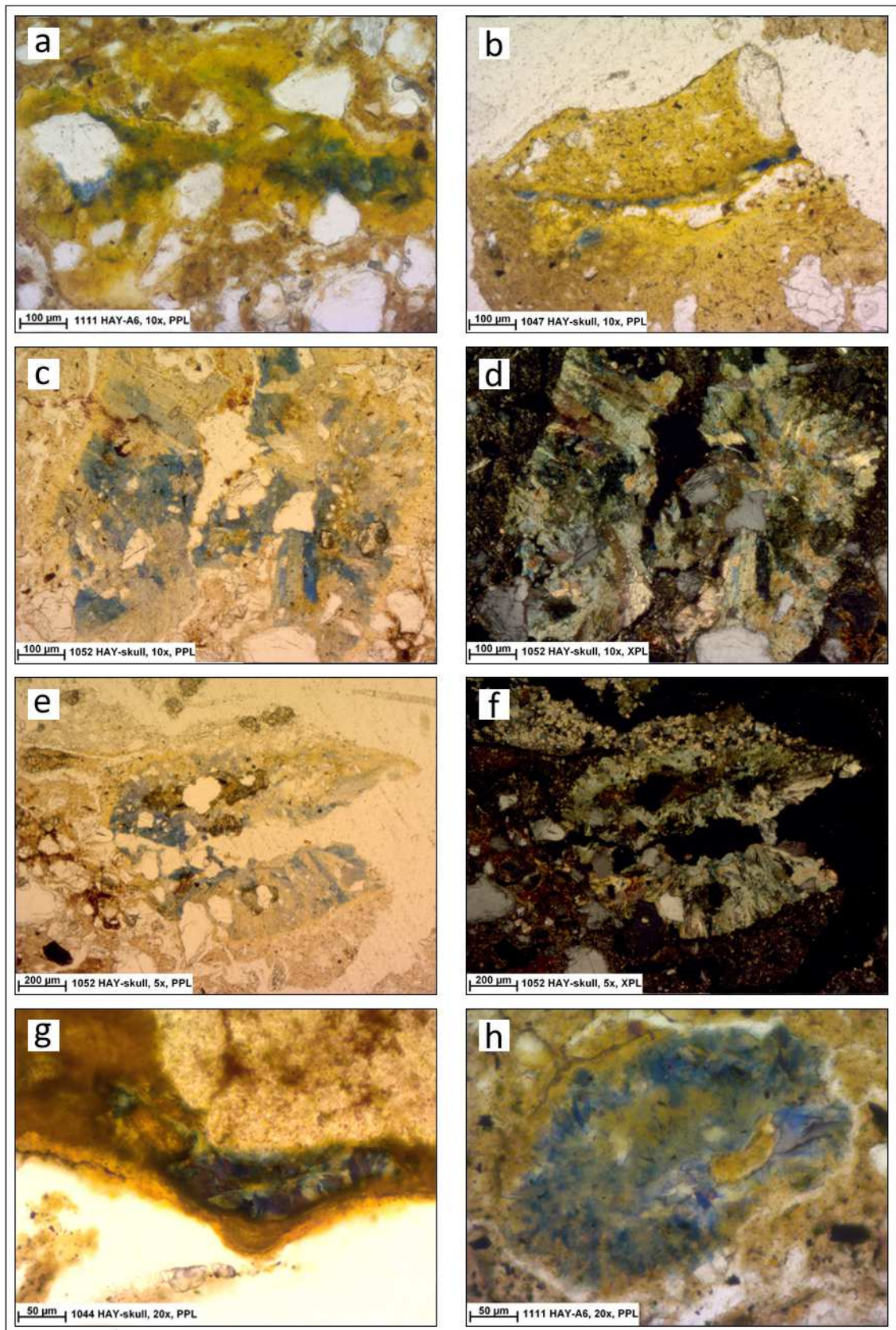
Figure 5.80: Vivianite in Haymarket. a) amorphous phosphate with some blue/green areas for the presence of small crystals of vivianite from the area of the knees in grave 83012; b) amorphous phosphate with a green/blue line of small crystals of vivianite from the area of the skull in grave 84779; c-d) vivianite from the area of the skull in grave 84851 in PPL (c) and XPL (d); e-f) vivianite from the area of the skull in grave 84851 in PPL (e) and XPL (f); g) small crystals of vivianite within an amorphous phosphatic coating from the area of the skull in grave 84779; h) sub-rounded vivianite from the area of knees in grave 83012.

163
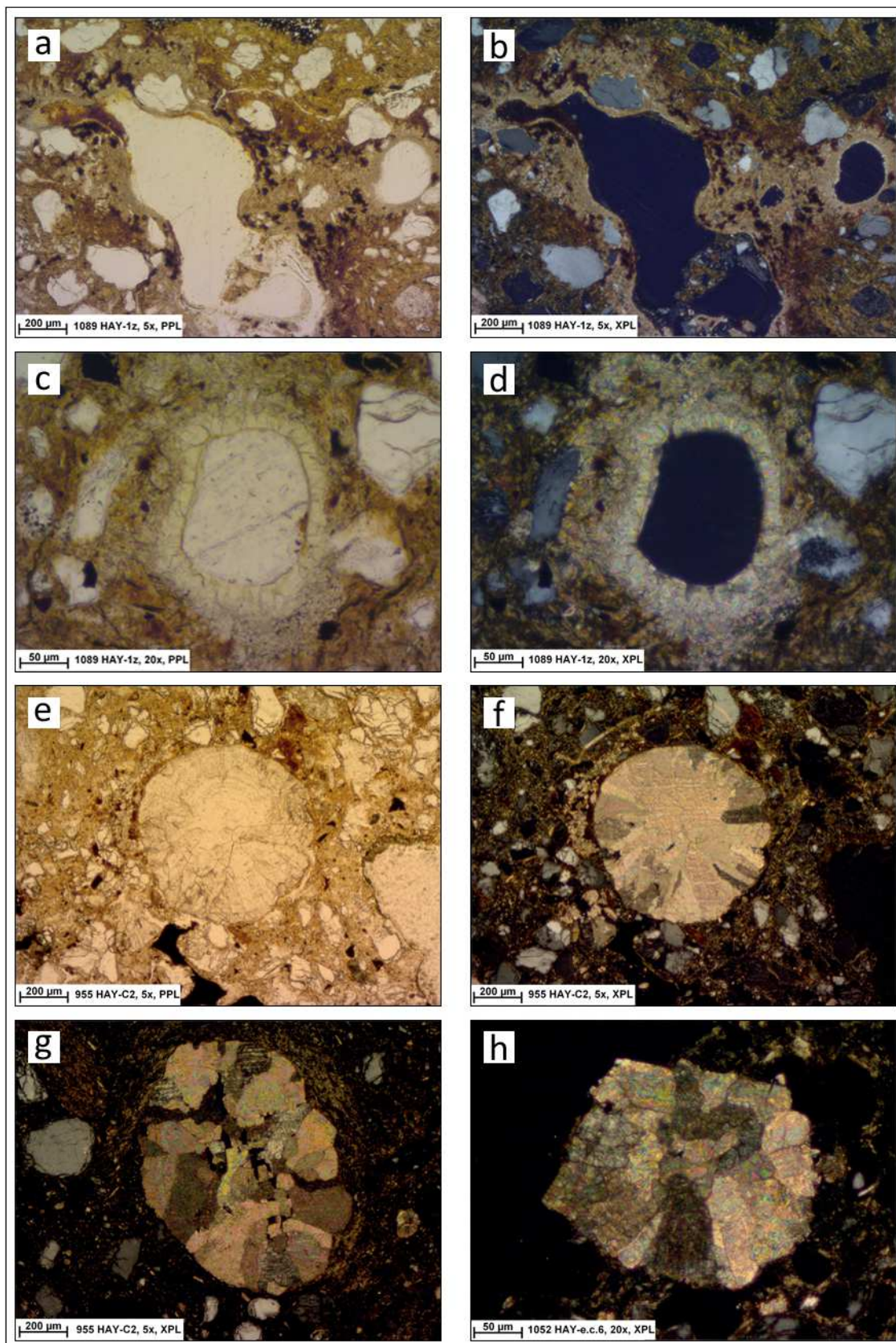
Figure 5.81: Secondary CaCO₃ crystals and worm-derived calcium carbonate granules in Haymarket. a-b) coating of small crystals of CaCO₃ and Mn nodules around void from the area of the skull (z) in grave 83012 in PPL (a) and XPL (b); c-d) coating of CaCO3 around void from the area of the skull (z) in grave 83012 in PPL (c) and XPL (d); e-f) worm-derived calcium carbonate granule from the control C2 in grave 84779 in PPL (e) and XPL (f); g) worm-derived calcium carbonate granule from the control C2 in grave 84779 in XPL; h) worm-derived calcium carbonate granule from the area of the skull in grave 84851 in XPL.

5.3 BORGHAREN (NL). Merovingian cemetery, 5th-8th C AD

Traces of a Roman villa and a Merovingian cemetery were discovered in Borgharen, near Maastricht (NL), between 1995 and 1999 (Figure 5.82). The site was designated as a National Heritage Site in 2008 and since then a research project has been developed by the Dutch Cultural Heritage Agency and the University of Amsterdam (Lauwerier and Müller 2011, 9). Aims of the project were to: study of the graves, including analysis of skeletal remains through histological and DNA investigations, examination of the grave goods, such as metals and flint, and investigation of the soil context through XRF analysis. In addition, evaluations of the Roman pottery, paintings, tiles and mortar composition were performed and new methods and techniques were applied in order to conduct experimental analysis. The InterArChive team was involved in this field and laboratory testing, contributing with its methodology in the study of one of the graves in 2009.
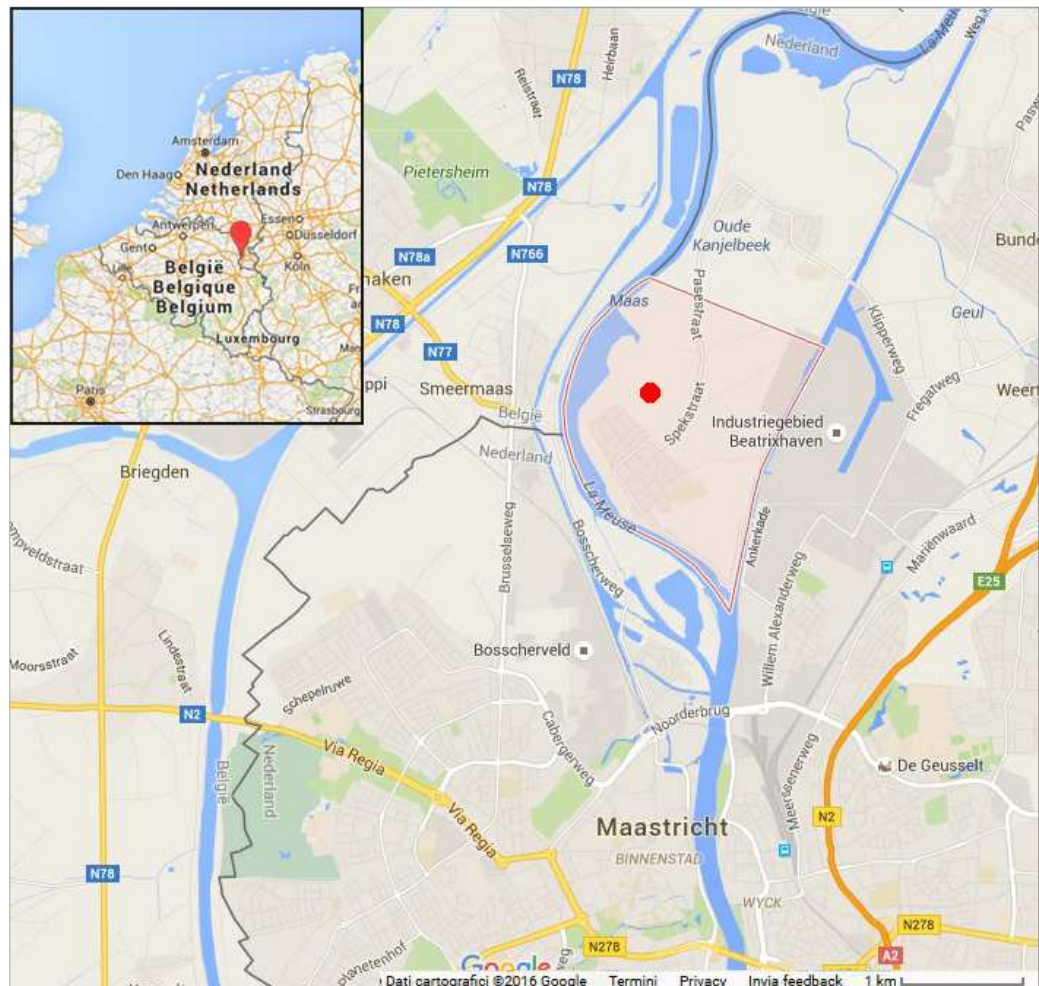
Figure 5.82: Map of Netherlands and location of Borgharen in the area of Maastricht. Graphically modified from Google Maps ©2016.

5.3.1 THE SITE

Borgharen is located on the eastern bank of river Meuse, in the southern Limburg. The landscape is characterized by plateau, terrace and slopes composed mainly by gravel, formed during the cooler stages of Pleistocene and caused by erosion (Figure 5.83). Furthermore, the presence of glacial wind and the absence of plant cover favoured the accumulation of cover sand and loess. The climate improvement at the end of the Pleistocene and during the Holocene, and the consequent fluctuation of temperature, conditioned the development of the Meuse and its meanders, contributing to the deposition of clay and silt sediments (De Groot et al. 2011, 13).
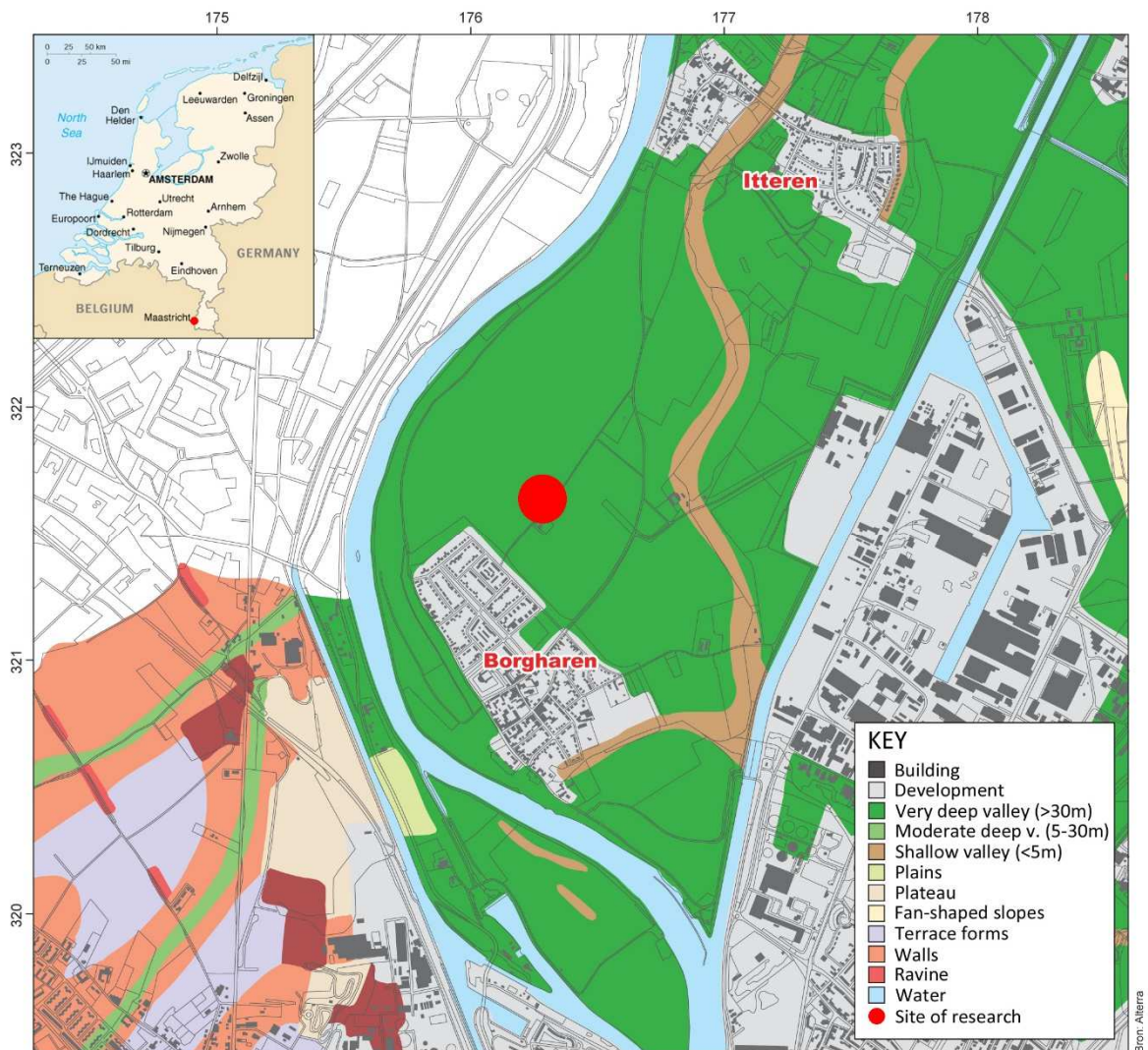
Figure 5. 83: *Geomorphological map of the area surrounding Borgharen. Plateaux, slopes and terraces are visible on the west side of the river, while the green are is the one mostly characterized by clay and silt sediments. The cemetery was indicated with the red dot, in the fields outside the town of Borgharen. The map was graphically modified from Lauwerier and Müller (2011, 12).*

Several villas were situated in South Limburg during the Roman period. That in Borgharen belonged to the Maastricht *vicus,* an important market for agricultural and artisan products produced by the villas of the surrounding area (De Groot et al. 2011, 13). Between 6th-7th C AD, during the Merovingian period, the *vicus* increased rapidly in importance. In the following centuries it experienced an equally rapid decline to become a poorly populated area (De Groot et al. 2011, 15). The Merovingian cemetery in Borgharen, discovered between 2008 and 2009 and in 2012 (Figure 5.84), contained twenty-five graves, including male and female adults, sub-adults and two horses, all oriented northeast – southwest. Grave 15, indicated in red in Figure 5.84, was selected for micromorphological analysis.
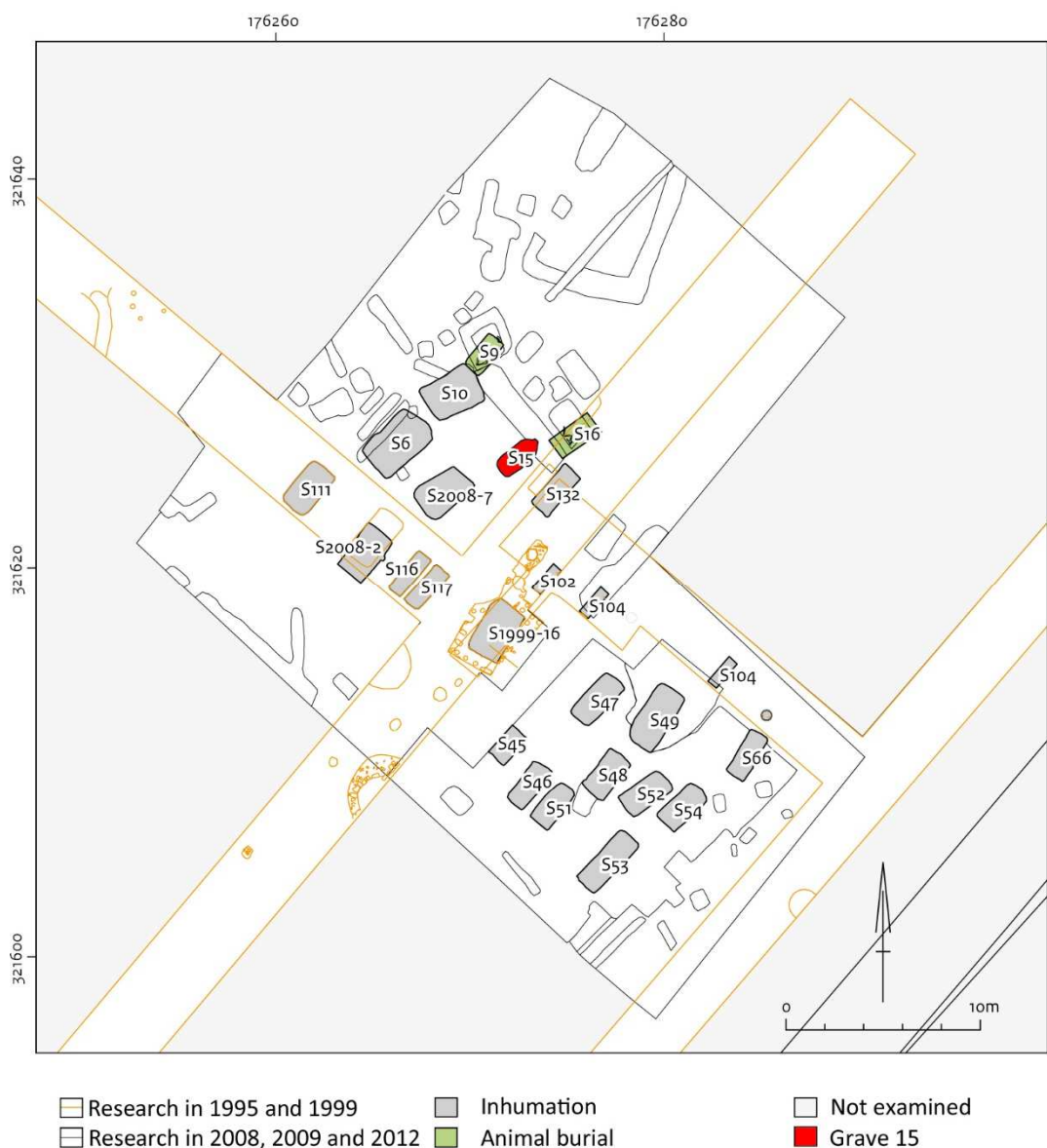
Figure 5.84: Plan of the Merovingian cemetery of Borgharen. The inhumations are highlighted in grey and the two horse burials in green. Grave 15, analysed in this research, is indicated in red. The plan was graphically modified from Lauwerier and De Kort (2014, 23).

5.3.2 GRAVE 15

Grave 15 (Table 5.3) contained the skeleton of a woman 156.8 cm tall, around 44-53 years old (Panhuysen 2001, 84). The burial was dated to the 7th C AD, on the base of two silver earrings, composed of two conical parts riveted together and with a moulded decoration of silver beads, typical of that period. This archaeological interpretation was confirmed by radiocarbon dating of the handle of a knife (Kars and Van Os 2001, 97). The burial plane was 44.29 m a.s.l. and it was 40 cm deep. The shape was oval, the orientation was northeast – southwest, and the dimensions were 2.1 x 1.1 m. Fine sand was at the bottom of the pit and the skeleton was laid directly on this level (Müller and Smal 2011, 55). Traces of wooden coffin were not observed. Some Roman nails were found, although no evidence confirmed whether they came from a coffin or from a different layer. The location of the skeletal remains, however, indicated that the corpse was placed in a container: the pelvis appeared turned beyond the original space occupied by the body, the femur turned away, the knees turned outward and the skull rolled. Such observations have been interpreted by the excavators as indicators of body decomposition in unconfined space, where bone displacement would have been possible, concluding that the body was buried in a wooden coffin (Müller and Smal 2011, 55).

The grave was disturbed by a secondary interment, which caused a displacement of the bones of the right foot. The second burial contained skeletal remains of two children and few pieces of pottery. DNA analysis indicated that the children were the sons of the buried woman (Müller and Smal 2001, 56). The interpretation of archaeologists was that the children died before the mother and were buried in another grave. When the mother died and her body was already skeletonized, the grave was reopened and the disarticulated bones of the children were placed at the feet of the mother (Panhuysen 2015).

Fragments of various materials and grave goods were found in the fill of the grave. In the layer above the remains several pieces of metallic slag and some fragment of tiles were recovered. In the resting plane, more numerous fragments of tiles were found in the area of chest, legs and feet. Two big fragments of animal bone were located over the ribs and metallic scraps were in the area of the legs and feet. Moreover, as mentioned earlier, some nails, a pair of earrings and pieces of pottery derived from the second burial (Müller and Smal 2011, 60-61).

GRAVE	DATE	TYPE	SKELETON INFORMATION and grave-goods	SOIL TYPE	CLIMATE
15	Merovingian, 7th C AD	Wooden coffin	Female adult; 44-53 years old; Grave disturbed by a second interment in the area of the feet; Grave-goods: pieces of metallic slags, tiles and animal bones, nails, a pair of earrings	Sandy	Temperate oceanic

Table 5. 3: Summary of the available information regarding the grave in Borgharen.

Six undisturbed soils samples were collected in the area of the grave. The presence of gravels made sampling difficult hence, except for the controls where the sediment was softer and poorer in coarse mineral components, they were smaller than usual. The slides from the skull, pelvis and hands were not easy to study because of the presence of numerous scratches and patches of dirty resin from the slide processing (Appendix 1.5). Figure 5.85 shows the location of samples in relation to their anatomical position, the code of the slides and includes mosaics. Control C1 was taken from the layer above the burial. The exact position is unknown, so it was not included in the picture of the grave. For better readability, the photograph of the grave has been elaborated with a digitized drawing from the archaeologists (Müller and Smal 2011, 60). The mosaics, with details and indication of some of the features noted in Section 5.4.3, are provided in the Supplementary data (folder "Mosaics").
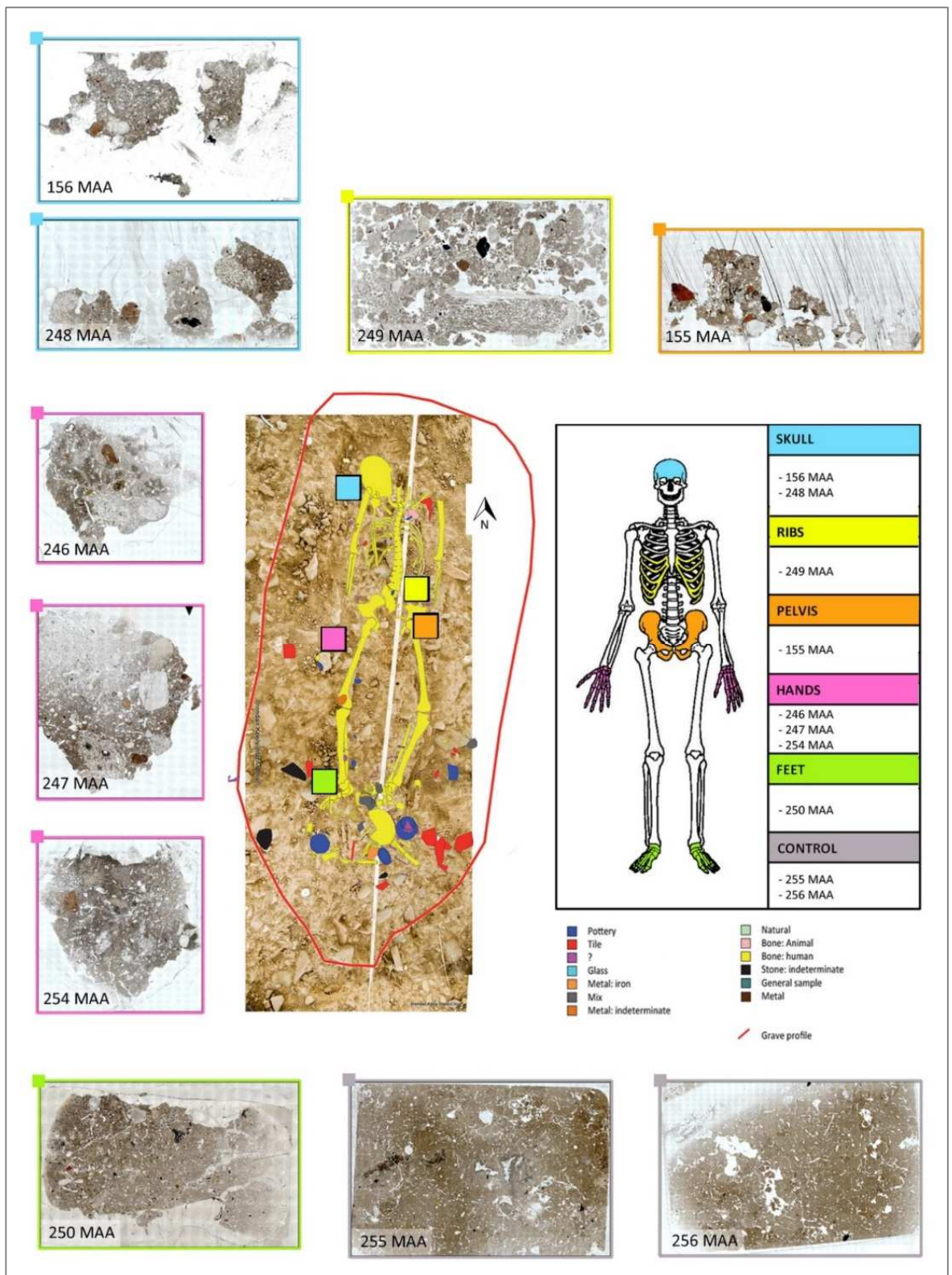
Figure 5.85: Grave 15. At the centre, elaboration of the photograph of the grave and the digitized drawing from the archaeologist, with the addition of the samples location. The red line shows the limit of the burial, while the skeleton is highlighted in yellow. Fragments of tiles (red), pottery (blue), metal (orange), stone (black) and other materials in lower quantities are observable around and above the skeleton. On the right, list of slides in relation to their anatomical location. Left, top and bottom, mosaics of the slides. See the text for descriptions.

5.3.3 MICROMORPHOLOGICAL RESULTS

ELEMENTS OF FABRIC AND PEDS

Slides from grave 15 were characterized by porphyric c/f related distribution and were poorly sorted. 30% of the sample from the area of ribs was distinguished by enaulic c/f related distribution and moderate sorting. The fine material abundance was variable: 20% in the sample from feet; 30% in the sample from hand, ribs and pelvis; 40% in the sample from skull and 70% in the control sample. The aspect of the fine material was different between the samples located within the backfill of the grave and the control sample. In the first case, the fine material was characterized by dotted limpidity, speckled b-fabric, yellowish to reddish brown or brown colour in PPL and XPL. In the second case, it was characterized by dotted limpidity, crystallitic b-fabric for the presence of micrite, light brown colour in PPL and pink/beige colour in XPL. Samples from the areas of the skull, pelvis, hand and feet contained unaccommodated and strong developed coarse aggregates (between 8 and 12 mm), internally organized in smaller peds. These peds were granular in shape, very fine or fine in size, generally unaccommodated and with weak or moderate development (Figures 5.86 and 5.92.a).
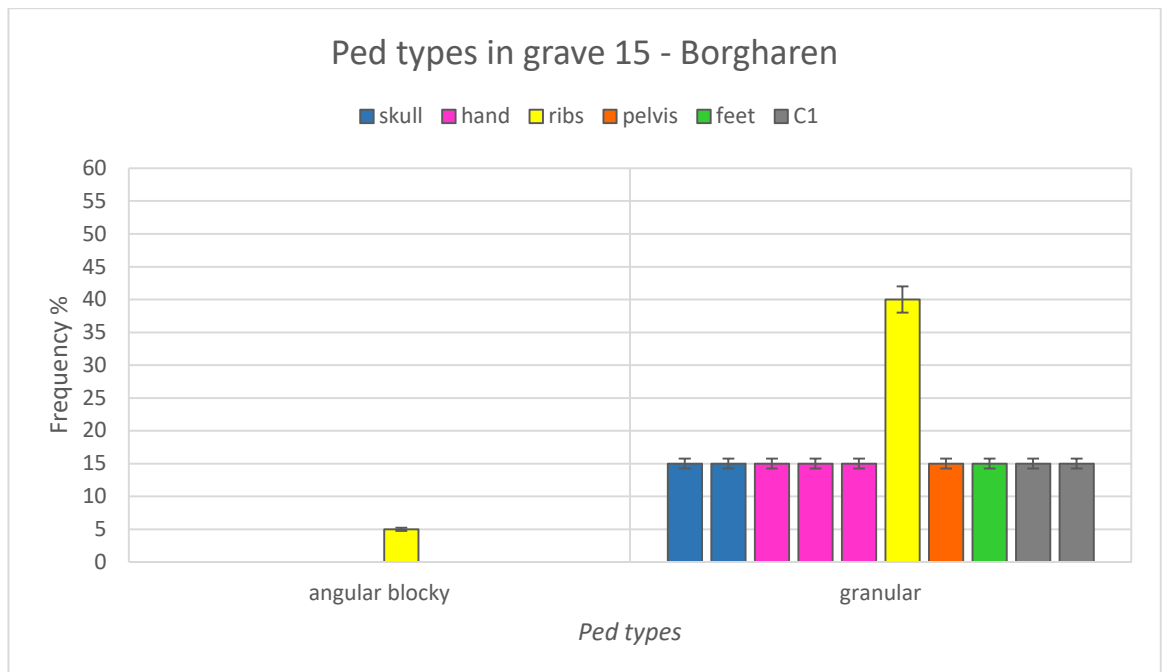
Figure 5.86: Abundance of different type of peds in relation to their anatomical location within grave 15. Granular peds were common in all of the samples (15%) and they reached 40% in the area of ribs, conferring a highly separated granular microstructure. Few angular blocky peds (5%) were detected in the area of ribs.

Ped abundance was between 10-20% except for the slide from the area of ribs which was characterized by more abundant granular peds (30-50%) with the same properties: very fine and unaccommodated, but with a higher level of development, conferring the aspect of highly separated granular microstructure. In the left corner of the same slide, a few peds (2-5%) were angular-blocky in shape, accommodated and moderately developed (Figure 5.92.b). Control samples appeared more compact, without the presence of coarse aggregates such as the ones in the areas of the skull, pelvis and hands. The microstructure was chamber/channel, thus dominated by these type of voids. It comprised two type of peds: Type A represented 20% of the slide and was the same material as the backfill of the grave and the other samples. Their aspect was fine in size, unaccommodated and weak to strongly developed. These peds looked embedded within a different type of fine material, not very well aggregated (10-20%). This second type of ped (type B) was very fine to fine in size, unaccommodated to partially accommodated and with weak to moderate development. Thus, the diversity from the first type was mainly based on the fine material aspect (Figure 5.92.c-d).

VOIDS

Samples from grave 15 were characterized by four types of void: chamber, channel, modified complex and packing (Figure 5.87).
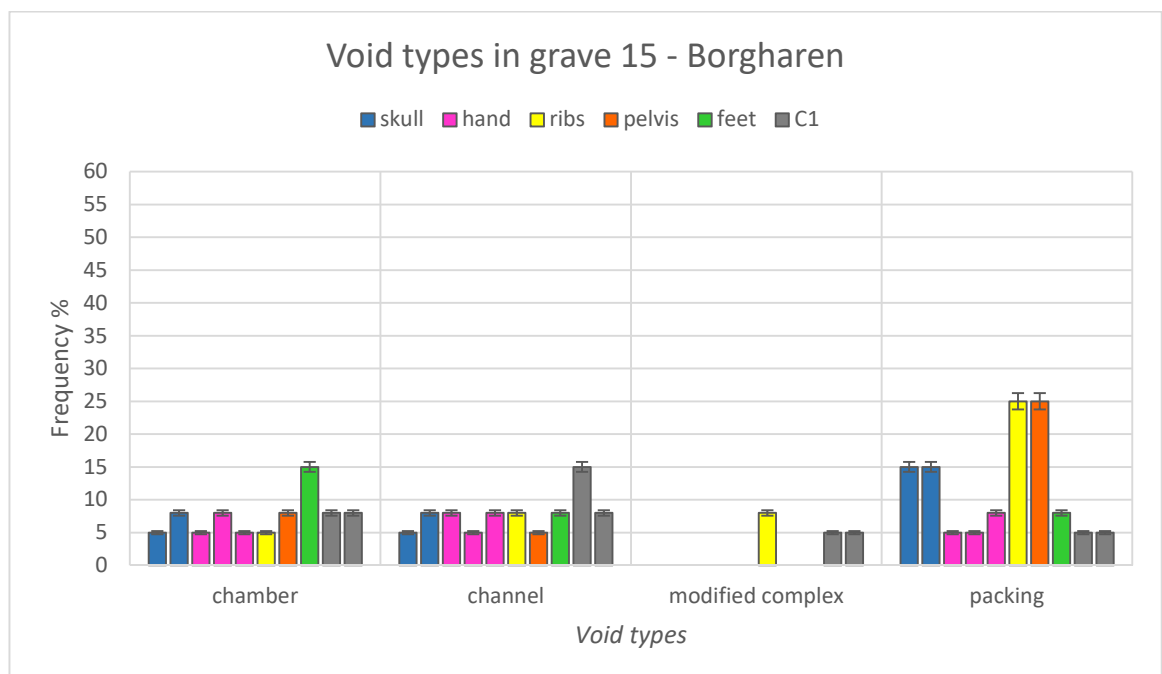
Figure 5.87: Abundance of different types of void in relation to their anatomical location within grave 15. Chambers, channels and packing voids were the most common, with percentages between 5-15%. In addition, packing voids reached 25% in the area of ribs and pelvis. Modified complex voids were detected only in the area of the ribs and in the control samples.

Chambers and channels were observed in all of the samples, with abundances between 5-15%. Chambers were more abundant in the sample from the feet and channels in the control. In this sample, channels were very thin, highly interconnected and with chambers between them, conferring a different microstructure to the other samples. Modified complex voids appeared in the control sample, around 5%, and in the area of the ribs, around 8%. In this last case, modified complex voids were located within the infilling of the coarse fragment of bone. Here there were also channels and a perfect round chamber (Figure 5.92.e-g). Packing voids were the most common in all of the samples, reaching 15% in the area of the skull and 25% in the areas of the ribs and pelvis. Walls of chambers and channels were smooth or undulating, while packing voids had undulating and rough surfaces. Modified complex voids were distinguished from chambers by the typical walls having curved and pointed surfaces.

MINERAL COMPONENTS

Coarse mineral components were present in different abundances in the samples (Figure 5.88): 40% from the area of the skull and hand, 20% from the area of ribs and pelvis, 60% from the area of the feet, 10% in the micritic area of control and 30% in the peds of type A.
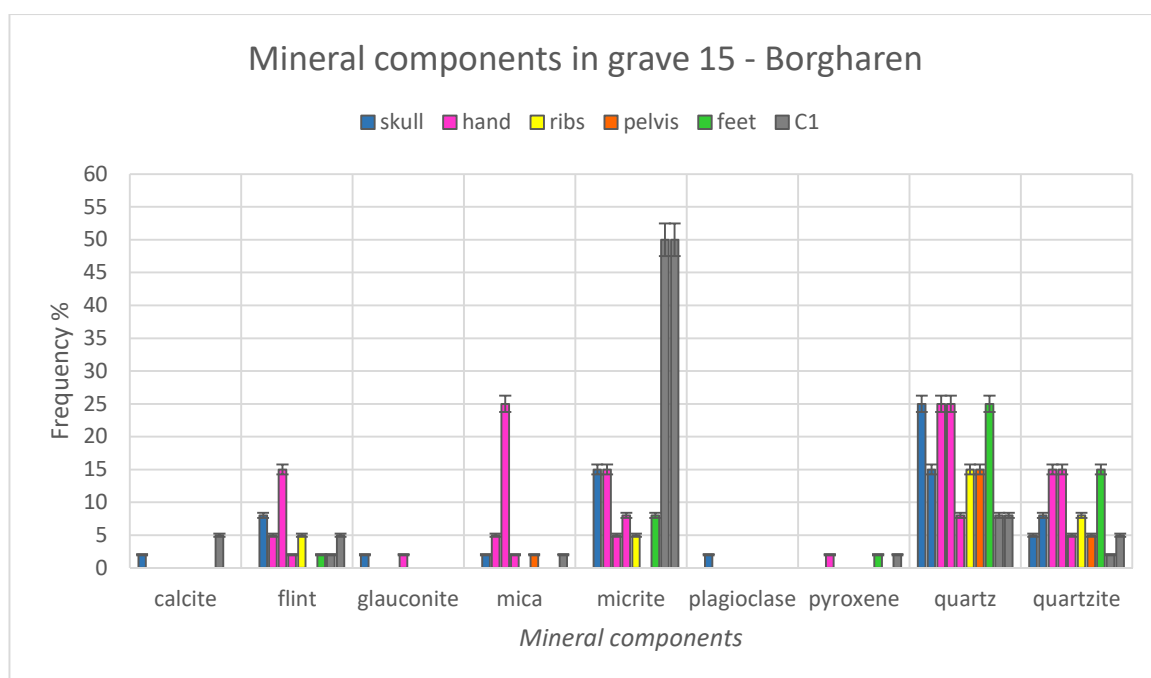
Figure 5.88: Frequency of different types of mineral component in relation to their anatomical location within grave 15. Quartz and quartzite fragments were frequent in all of the slides, between 2-25%. Flint and mica were quite common, between 2-25%, while calcite fragments, glauconite, plagioclase and pyroxene were rare. Micrite was included in this graph, despite the fact it was not a coarse component, to show the difference of it between the sediment within the grave (5-15%) and the one above it (50%).

The most common mineral was quartz, present in all of the samples, reaching 25% in the areas of the skull, hand and feet. Quartz was generally angular/sub-angular in shape, with some example of

sub-rounded shapes and partial weathering. Fragments of quartzite were present in all of the samples, with lower frequency. Quartzite looked weathered in most of the cases. Other minerals were flint, mica and very few examples of calcite fragments, glauconite, plagioclase and pyroxene. All these minerals had sub-angular/sub-rounded shape and were partially weathered or weathered. Glauconite was always sub-rounded/rounded and between 50-100 μm. The graph in Figure 5.88 also includes micrite, even though it was not part of the coarse fraction. It was included to examine the difference in abundance levels between the control and the areas within the grave. Micrite was absent in the area of the pelvis and between 5-15% in the other locations next to the remains. The sediment above the grave, in which the control sample was taken, was very different from the backfill, containing mostly micrite in the fine fraction.

ORGANIC COMPONENTS

Organic components were not abundant in grave 15, with levels never higher than 5% except in the case of the sample from the area of ribs, which contained coarse fragments of bone (3500 μm ca.). Organic components mostly comprised amorphous organic matter, bone fragments, charcoal fragments, humified plant structure, roots and one case sclerotia (Figure 5.89).
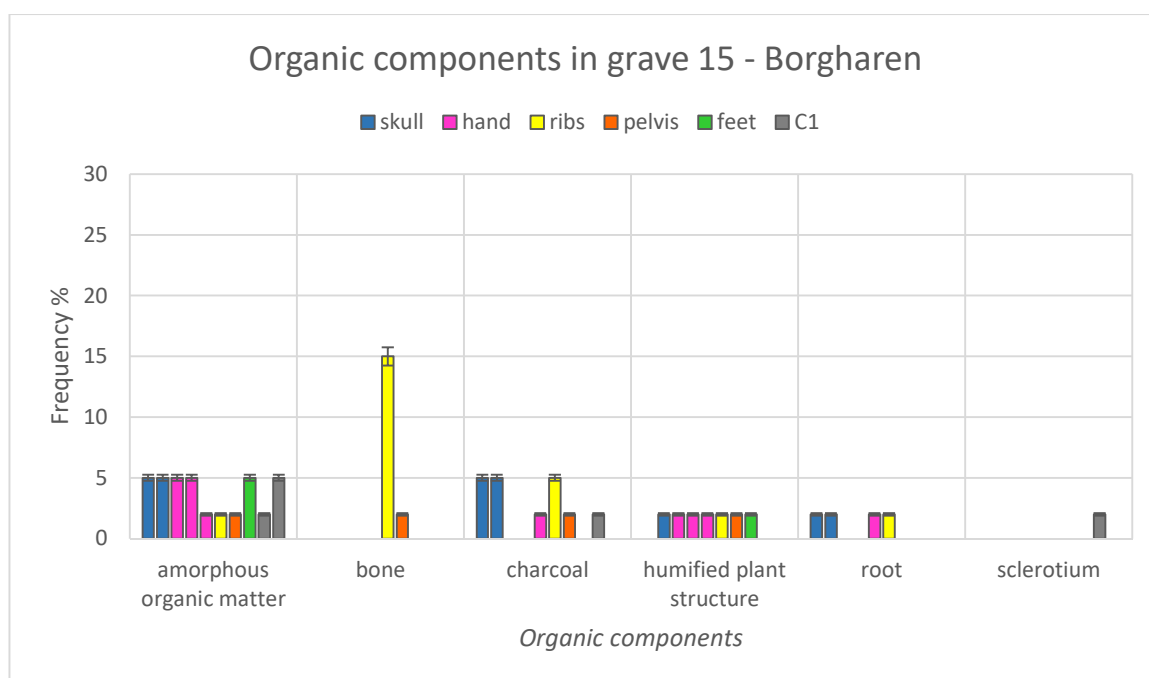
Figure 5.89: Frequency of organic components in relation to their anatomical location within grave 15. Amorphous organic matter and humified plant structures were the most common (2-5% in each sample). A coarse fragment of bone was identified in the area of the ribs (15%). Other components were charcoal, root and sclerotia.

Amorphous organic matter was characterized by fine black fragments, between 50-500 μm, scattered within the fine material. Bone fragments were observed only in the area of ribs and pelvis. The coarse fragment from the area of ribs had trabecular structure filled by loose discontinuous

infilling of fine material. The colour in PPL was light yellow and there were some longitudinal fractures. The structure was well preserved and the haversian canals were visible. The colour in XPL was grey/black with high third order birefringence (Figure 5.93.a-b). Charcoal fragments were observed in the areas of the skull and ribs (5%) and hand, pelvis and control (2%). Their sizes were between 200-2000 µm, the shape angular or sub-angular, and the surfaces smooth or undulating and partially weathered. Humified plant structures were diffuse in most of the samples, but with percentages around 2%. They were identified as fragments of angiosperm wood for the presence of vessels (Figure 5.93.c). Roots in channels were not fresh, light brown in PPL and white in XPL (Figure 5.93.d). They were present in the areas of the grave related to the skull, hands and ribs (2%). One single example of sclerotium was detected from the control sample: 100-200 µm, purple in PPL and isotropic in XPL and not weathered.

PEDOFEATURES AND ANTHROPOGENIC MATERIAL

The main pedofeatures and anthropogenic material in grave 15 were: loose discontinuous infillings, brick fragments, Fe/Mn nodules, coatings of fine material, micrite coatings, a worm-derived calcium carbonate granule and vivianite (Figure 5.90). Three types of loose discontinuous infillings were detected in the slides. The first was represented by loose discontinuous infillings of material in voids; the material being the same as the fine material of the matrix. This type of infilling was observed in the area of the skull (2%), in the area of the hands (8%) and in the area of the feet (25%). The second type was represented by the same material, but within the coarse fragment of bone from the area of ribs (15%). Here the infilling was reworked, as indicated by the modified complex voids. The third type was represented by the infilling of soil micro-fauna faecal pellets within the voids, only documented in the areas of the hands and control (25%) (Figure 5.93.f).

Brick fragments were common in most of the samples (5%), red in PPL and XPL and partially weathered. In one case, from the area of the hand, the fragment had a micritic layer attached to it, identified as remaining of the mortar. The fragments were identified as brick because of the rubified colour in XPL, caused by their firing, by the inclusion of mineral grains and the parallel orientation of pores, which had the shape of vesicles (Elsen 2006; Macphail and Goldberg 2010; Emami et al. 2016).

Fe/Mn nodules were observed in the areas of the skull, hand, ribs and pelvis (5%); they were more frequent in the sample next to the feet (8%) and less frequent in the control sample (2%). The dimensions were between 50-500 µm, reddish brown in PPL and red/dark brown in XPL.

Coatings of fine material around mineral grains were in the areas of the skull, pelvis (5%) and hand (8%). Micrite coatings, and rarely hypocoatings, were mostly in the area of the hand (8%) with few examples in the area of the skull and pelvis (2%). The coatings developed around circular sections

of channels, the shape was sub-rounded, the surface smooth and the colour white/pink in PPL and pink/green in XPL. The b-fabric was parallel striated or crossed striated (Figure 5.93.e). Very few examples of worm-derived calcium carbonate granules came from the control sample. The shape was sub-rounded, the surface smooth and the internal structure characterized by radial crystals of calcite. The colour was pink/grey in PPL and XPL, with crystallitic b-fabric.

Two examples of vivianite were found in the samples from the hand and pelvis. In both cases the nodules were small (200-500 µm), sub-angular, pleochroic, yellow/green in PPL and yellow/blue in XPL (Figure 5.93.g). Exceptional pedofeatures were identified in the samples. A fragment of dark brown material (500 µm) came from the area of ribs. It was internally characterized by vesicles and the shape was sub-rounded. The colour in XPL was reddish brown and the b-fabric was undifferentiated (Figure 5.93.h). A concentric nodule (1000 µm) from the area of the feet: the shape was rounded and the nodule was included mineral grains oriented in circular disposition. The colour was brown in the central layer and yellow (PPL) and isotropic (XPL) in the external one. Speckled b-fabric was observed in the zone in between the two layers.
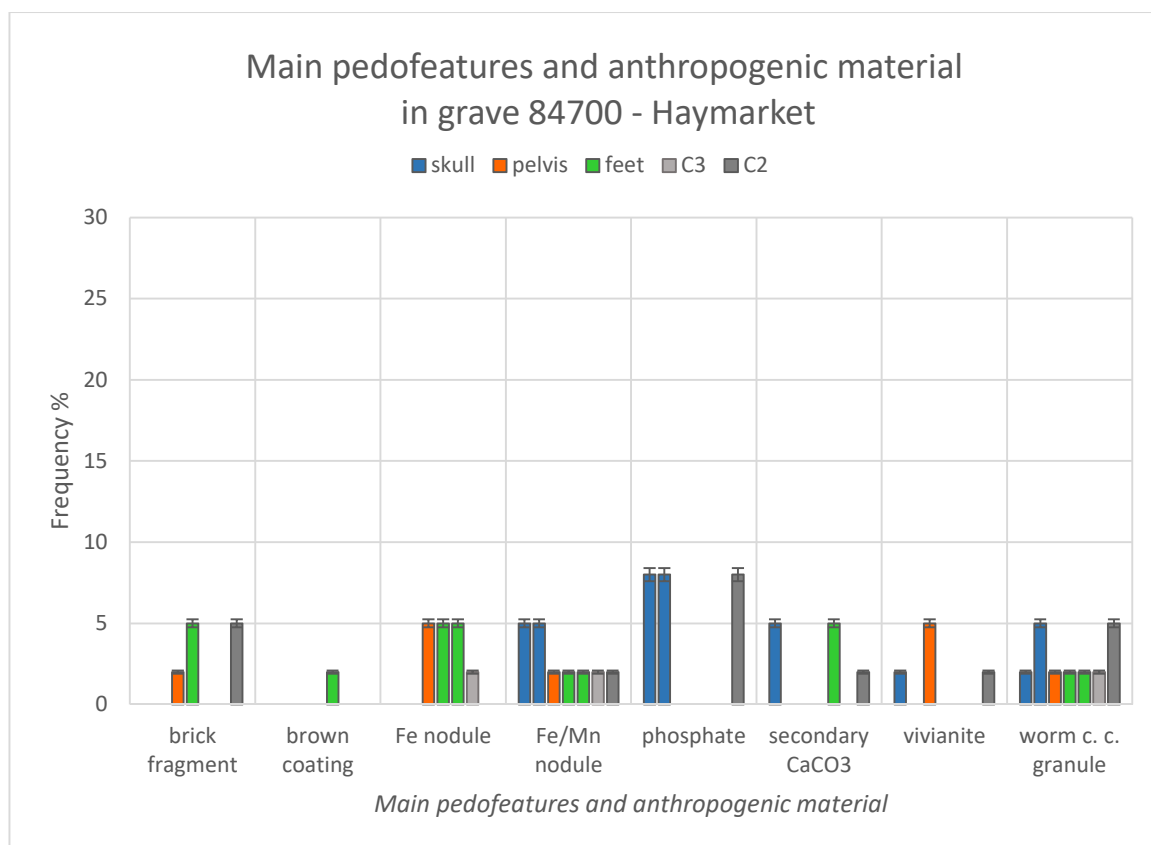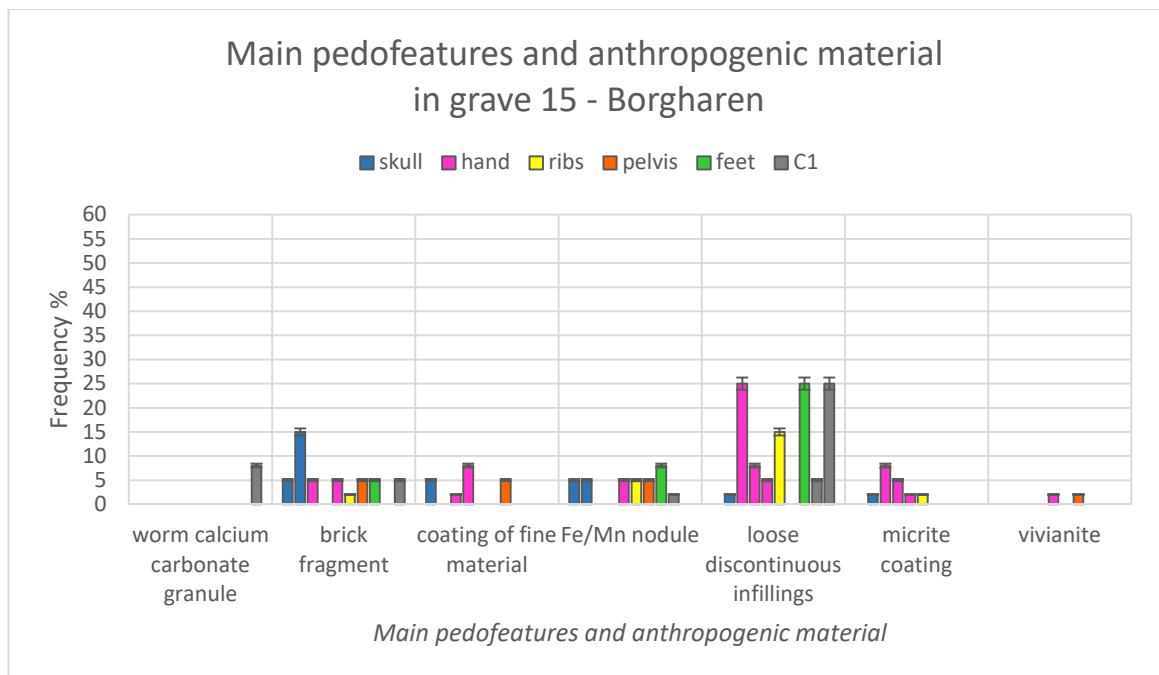

Figure 5.90: Frequency of the main pedofeatures and anthropogenic material in relation to their anatomical location within grave 15. Loose discontinuous infilling within voids was most common (5-25%), followed by brick fragments (5-15%) and Fe/Mn nodules (2-8%). Micrite coatings were detected in the areas of the skull, hands and pelvis; while coatings of fine material around mineral grains were observed in the areas of the skull, hands and pelvis. Two nodules of vivianite were found in the areas of hand and pelvis. One worm-derived calcium carbonate granule came from the control sample.

5.3.4 SEM-EDS RESULTS

SEM-EDS analysis was performed to detect potential differences in chemical composition in the fine material among the anatomical locations. Between four and eight spectra were analysed in each slides (Appendix 1.6) and the weight (%) of the different chemical components was recorded. In the control, two groups of spectra were taken. One group of measurements in the peds of type A and the other in the micritic fine material of type B.

The data were normalized and are elaborated in a box-plot to provide an overview of the differences and similarities (Figure 5.91). The values of O and C were excluded owing to their distortion resulting from the presence of the resin in which the blocks were impregnated. In addition, elements having all spectra with values lower than 1% were excluded. The fine material gave very similar compositions in all of the samples from the grave fill. Generally, higher percentages of Si were related to lower percentages of Al. Levels of K were similar in all of the slides and were very low. Fe was more abundant in the area of the skull and it decreased from the skull to the feet and to the control. Ca was the only element presenting a difference in abundance between the sediment of the grave and the layer in which the control sample was taken. Levels of Ca were constant and low in the areas next to the skeleton (0.2-1.1%) and slightly higher in the area of the feet (0.4-2%). Ca was higher in the control sample in both type of peds: 1-5% in the type A and 5-7% in the type B.

The following figures were selected as representative of the features described in Section 5.4.3:

- Figure 5.92: fabric and voids;

- Figure 5.93: organic components and pedofeatures (micritic coating, soil micro-fauna faecal pellets infilling, vivianite and undetected pedofeature).
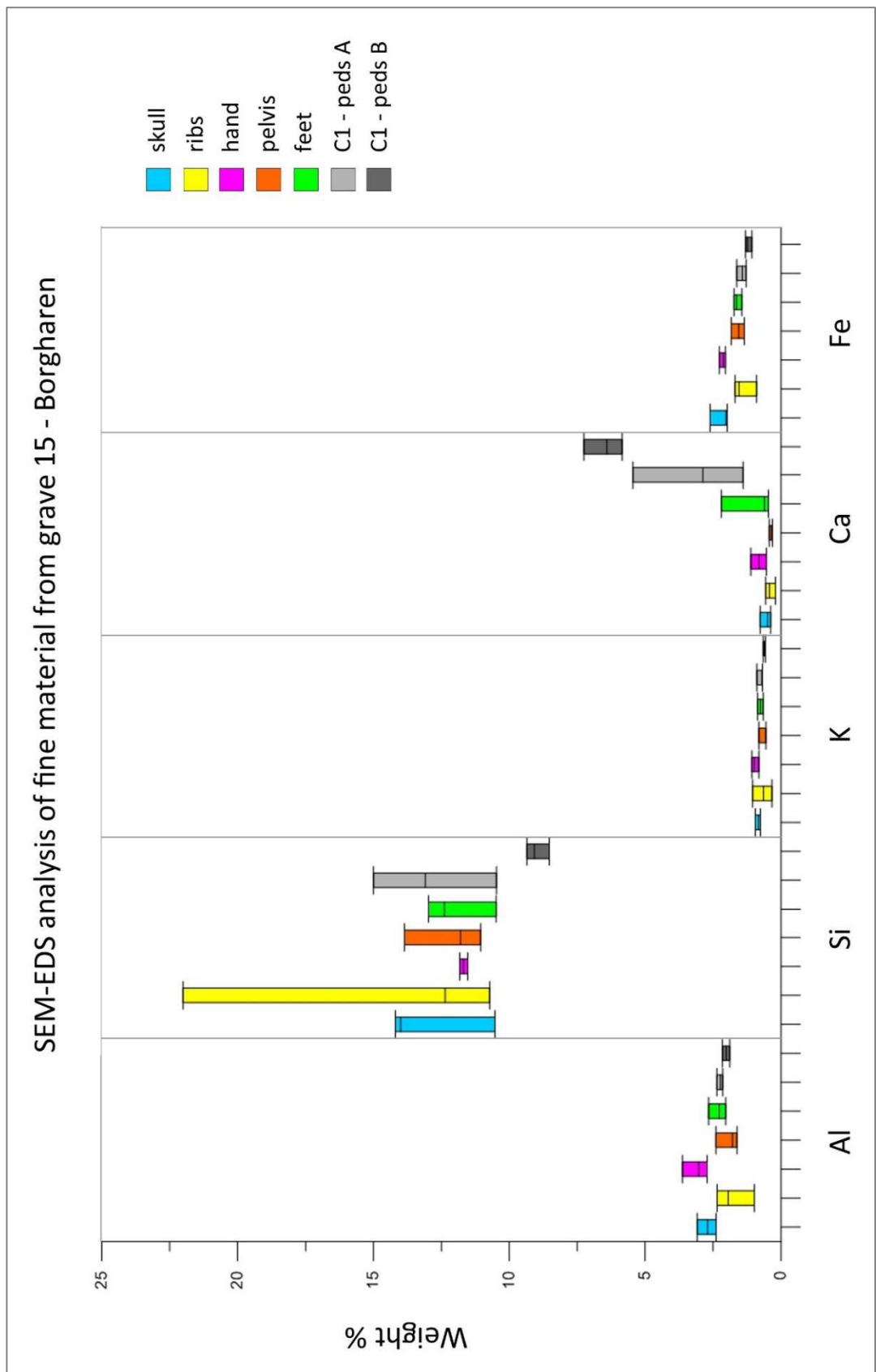
Figure 5.91: Box-plot showing the results of SEM-EDS analysis on fine material in grave 15 among their anatomical locations. The data were normalized and the values of O and C were excluded. In addition, chemical components with values less than 1% were excluded. The percentage of the chemical components (Al, Si, K and Fe) were similar in all of the samples. Fe was higher in the area of the skull. Ca percentages were different in the areas next to the skeleton from the control sample, where they were higher in both the type of peds.
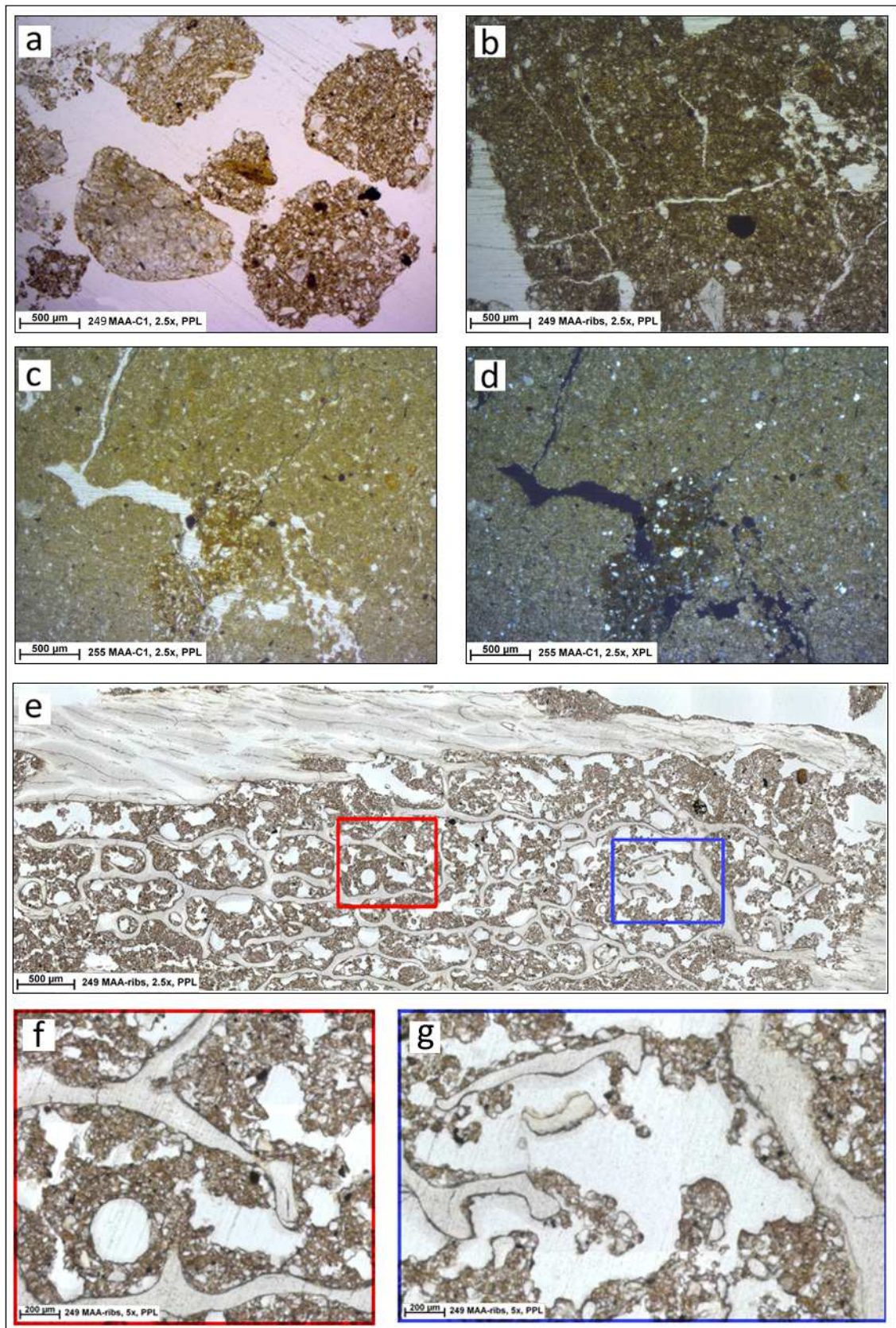
Figure 5.92: Fabric and voids in grave 395. a) granular peds from control C1; b) angular peds from the area of the ribs; c-d) peds type A and B from control C1 in PPL (c) and XPL (d) ; e) bone from the area of the ribs with infilling of fine material and modified complex voids; g) detail of modified complex void and round chamber from the area of the ribs; h) detail of modified complex void from the area of ribs.

179
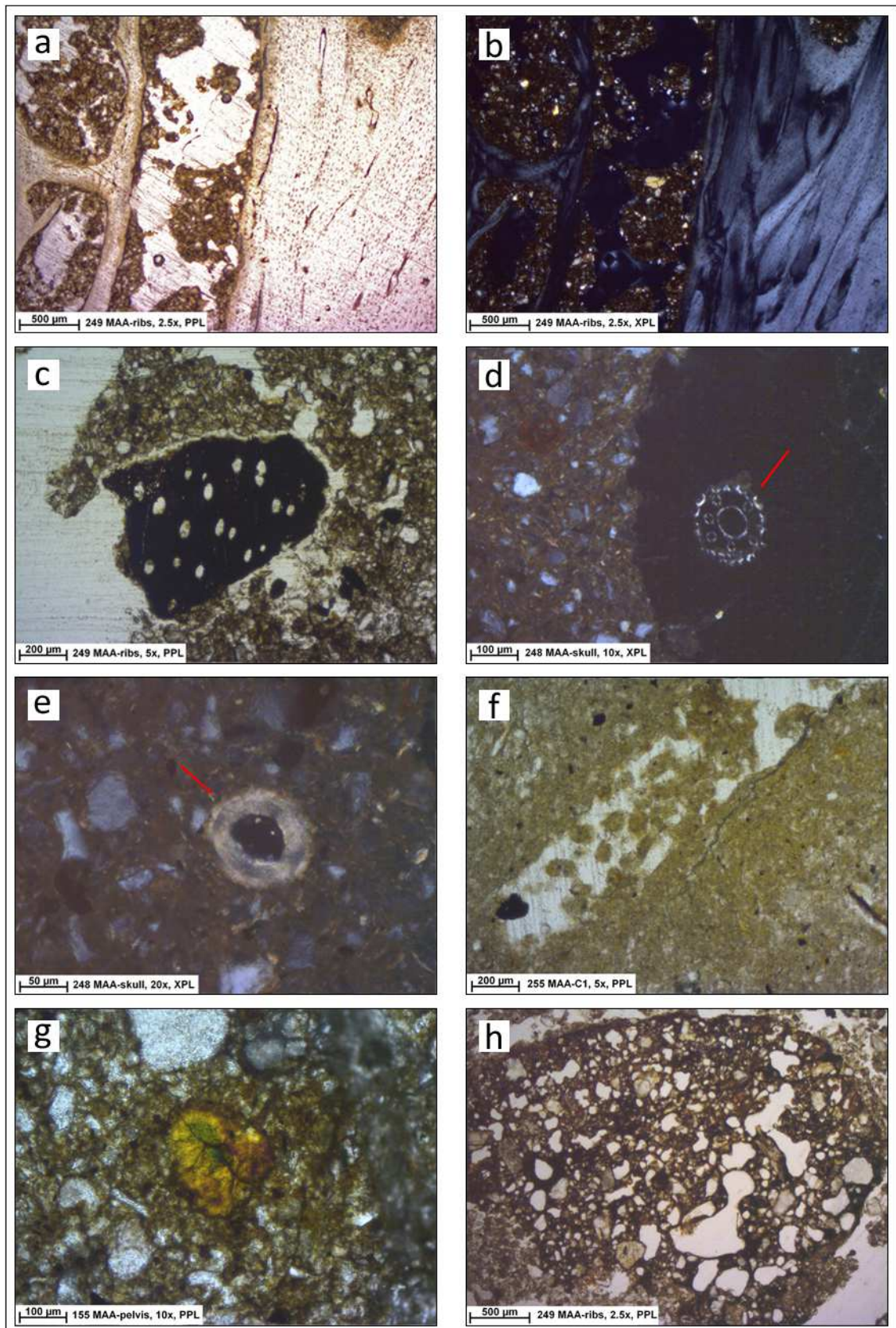
Figure 5.93: Organic components and pedofeatures in grave 395. a-b) bone fragment from the area of ribs in PPL(a) and XPL(b); c) humified plant structure from the area of ribs; d) section of root (red arrow) from the area of the skull (XPL); e) micritic coating (red arrow) from the area of the skull (XPL); f) infilling of soil micro-fauna faecal pellets in channel from the control C1; g) vivianite from the area of the pelvis; h) dark brown material with internal vescicles.

5.4 ROSSIO DO CARMO (PT). Muslim cemetery, 10ᵗʰ-13ᵗʰ C AD

The necropolis of Rossio do Carmo was discovered in the village of Mértola, in the South of Portugal, in the 1970s (Figure 5.94). The excavation was conducted between 1981-1990 and from 2000. The InterArChive team was involved in the sampling of the graves in 2009 and the results one of these burials are presented in this research.
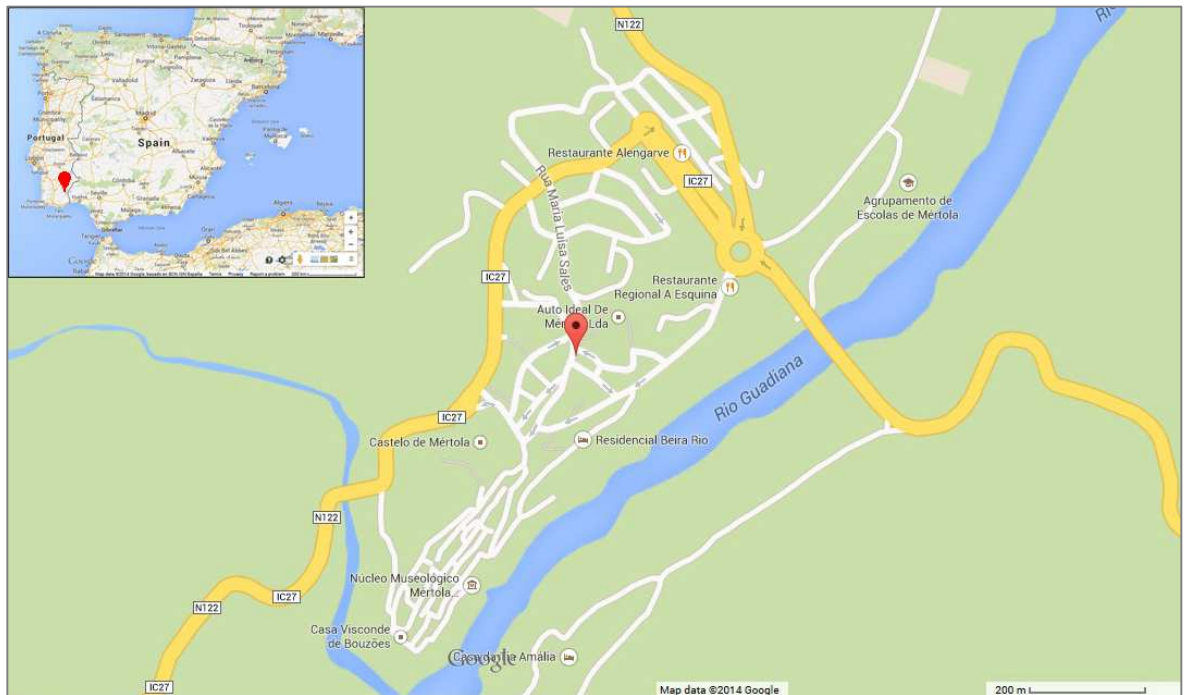
Figure 5.94: Map with the location of Rossio do Carmo in the village of Mértola, Portugal. Graphically modified from Google Maps ©2014.

5.4.1 THE SITE

Mértola is located in the geological formation of the Iberian Pyrite Belt (IPB), which is arranged in an arc about 240 km long and 35 km wide in the South-West of the Iberian Peninsula. IPB was a volcanogenic area rich in sulfides for which it was mined for more than 5000 years (Tornos et al. 2009). The stratigraphy of the Iberian Pyrite Belt includes (from the bottom up):

- Phyllite –Quartzite Group: slates and sandstones, up to 2000 m thick. Phyllite is a foliated metamorphic rock created from slates by metamorphism, leading to a preferred orientation of a very fine grained mica (Tornos et al. 2009);
- Volcano Sedimentary Complex of basalt to rhyolite, between 0 and 1300 m thick (Tornos et al. 2009);

- Culm Group (up to 3000 m thick): composed of flysch, a sedimentary rock of marine origin (Tornos et al. 2009).

Mértola was included in the Phyllite-Quartzite Group. The village of *Myrtilis,* as a fluvial port, was important during the Roman Empire as an agricultural and mineral exporting centre. The village maintained its active status during the Islamic period, with the name of *Martula*, but it started to fall into decline after the conquest in 1238 by the Christians (Le Bars 2005). Several cemeteries were discovered in the area of Mértula, as shown in Figure 5.95:
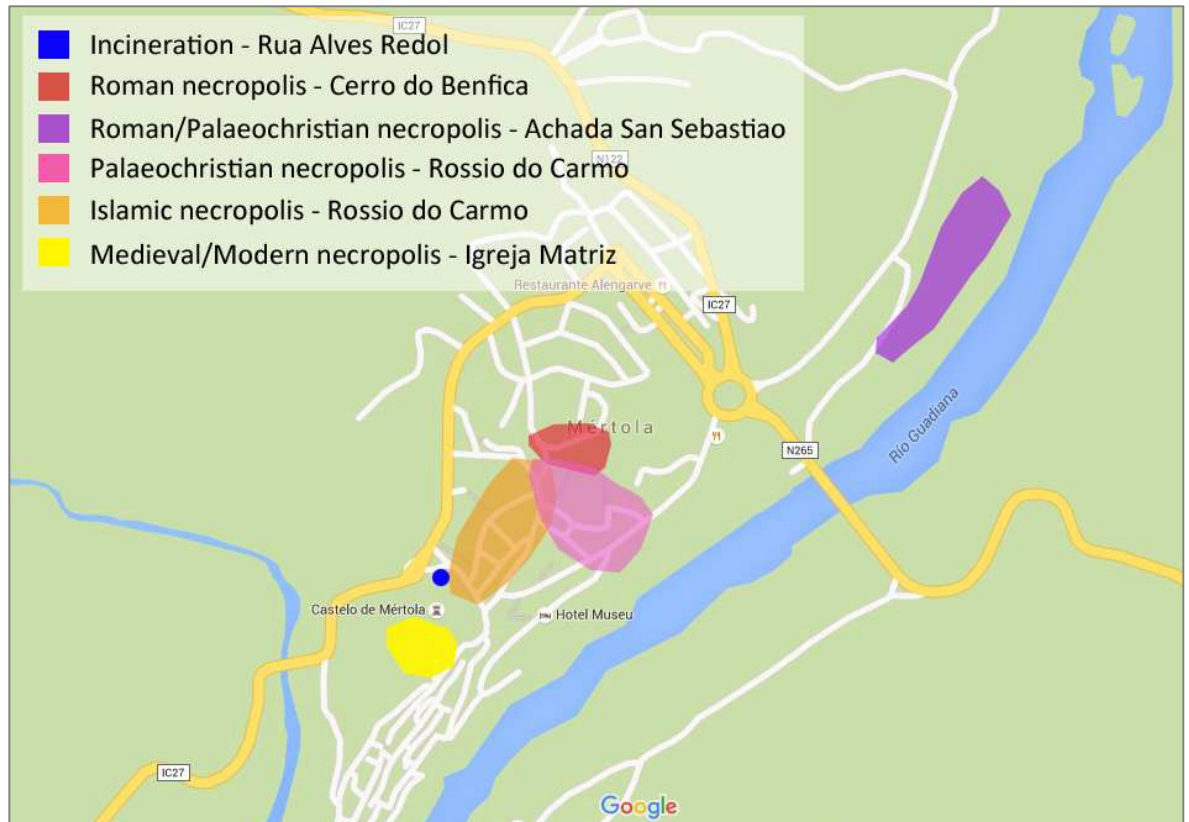
Figure 5.95: Plan of the village of Mértola with the location of the cemeteries: area of incineration (blue), Roman necropolis (red), Roman/Palaeochristian necropolis (violet), Palaeochristian necropolis (pink), Islamic necropolis (orange), and Medieval/Modern necropolis (yellow). Graphically modified from Google Maps ©2014.

The site of Rossio do Carmo was situated along the side of a hill, at 60 m a.s.l., and two cemeteries, one Palaeochristian associated with a basilica and one Islamic, were partially overlapping. The Palaeochristian cemetery was dated between 6th and 8th c. It was located on the South-East side of the hill and included ca. one hundred graves. The skeletons were in prone position, with the skulls turned to the west. No traces of coffin were found and the graves were directly excavated into the bedrock and covered with plates of schist (Le Bars 2005).

The Muslim cemetery was dated to 10th-13th C AD. It was located on the South side of the hill. Graves were excavated in the soil or into the bedrock and traces of coffin were not found. The soil over the bedrock was not deep and the site was damaged by natural erosion and works associated with the development of the village. These issues influenced the preservation of bones (Le Bars 2005). The Palaeochristian graves were respected and not disturbed by the Muslim ones (Le Bars 2005). The Islamic burials in Rossio do Carmo presented features which were characteristics of other Muslim graves in the Iberian Peninsula (Le Bars 2005):

- cemetery along the way of one of the main entrances to the village, on the side of a hill;
- location of the cemetery in an area already used in the past;
- inhumation in soil or rock without a coffin and generally covered by plaques of schist;
- usage of a sheet around the body, suggested by the effect of soil compaction around the skeleton;
- SW/N – N/E orientation of the burials;
- orientation of the skulls toward S or SW, with the face looking in the direction of Mecca;
- skeletons turned on the right side;
- absence of grave goods but presence of a few fragments of pottery.

During the excavation of the burials, no macroscopic difference was apparent between graves covered by schist and graves just filled by sediment. The skeletal remains were articulated in both cases (Le Bars 2005). Thus, it was possible to presume that the graves were filled with sediment during the burial ritual.

Four graves were sampled by the *InterArChive* project in 2009: graves 387, 390, 395 and 398. Grave 395 was selected for this research (Table 5.4 and Figure 5.96), whereas the other three graves were excluded because they were characterized by incomplete sampling of only the controls (graves 390 and 398) or samples from the area of the skull and control (grave 387).

GRAVE	DATE	TYPE	SKELETON INFORMATION and grave-goods	SOIL TYPE	CLIMATE
395	Muslim, 10th-13th C AD	No coffin; Plates of schist surrounded and covered the burial; The bottom of the grave was excavated in the rock	Male adult; 25-35 years old; Skeleton on his right side	Sandy loam; thin layer of sediment, rich of coarse material	Temperate Mediterranean

Table 5. 4: Summary of the available information regarding the grave in Rossio di Carmo.

5.4.2 GRAVE 395

Grave 395 (Figure 5.96) was dated between 10th-13th C AD, by the typology of deposition and the context of the Muslim cemetery. The skeleton was a male adult, 25-35 years old, placed without coffin on his right side. According to the photographical documentation, this skeleton had better preservation than the other three. Plates of schist surrounded and covered the burial.

The layer of sediment in which the skeleton was contained was thin and rich of coarse material. In addition, the skeleton rested directly on the rock surface. For this reasons, the sampling was reported to be difficult. Consequently, the samples were smaller than usual size and were partially disturbed. Considering the mosaics shown in Figure 5.96, it was possible to infer that samples from the area of the pelvis and controls were undisturbed, while samples from the area of the skull and feet had some zones undisturbed and other completely disintegrated. This point was taken into consideration during the analysis of samples.
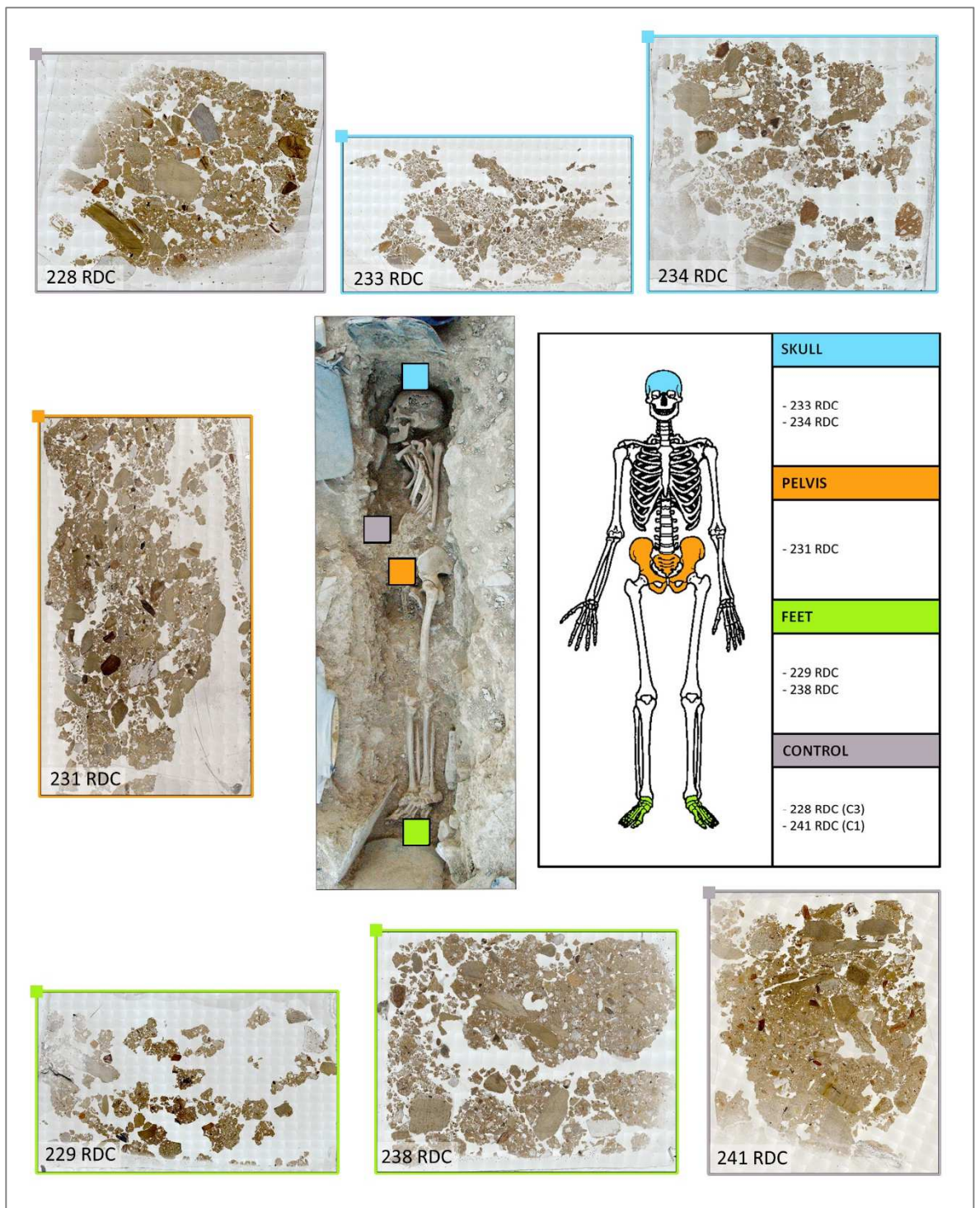
Figure 5.96: Grave 395. In the centre, photograph of the grave and location of the samples. On the right, list of the slides in relation to their anatomical location. On the top, left and bottom, mosaics of the slides. See the text for descriptions.

5.4.3 MICROMORPHOLOGICAL RESULTS

ELEMENTS OF FABRIC AND PEDS

Sediments in grave 395 were characterized by porphyric c/f related distribution and poor sorting. The fine material was greenish yellow brown in PPL and orange-brown in XPL, with dotted limpidity, crystallitic and speckled b-fabric. Fine material was more abundant in the control samples (30-50% in C1 and 30% in C3) and decreased from the areas of the feet (20-30%) and pelvis (20-30%) to the area of the skull (15%). Peds were granular, very fine to coarse, unaccommodated and well developed. In the samples from the areas of the skull and feet they were highly separated and mostly caused by bad preservation of the block after the sampling.

VOIDS

Four types of void were identified in grave 395: chambers, channels, modified complex and packing (Figure 5.97).

Packing voids were the most abundant, principally in the areas of the skull and feet. These are the most disturbed samples, as already mentioned, and it was impossible to distinguish the original packing voids from those formed after sampling. Chambers, channels and modified complex voids were observed within preserved peds. Possibly, their abundance was initially higher and some of them they did not survive. Chambers were detected in the areas of the pelvis (2%), feet (2%) and C3 (5%). Channel voids were more abundant: 2% in the areas of the skull and feet; 5% in the area of the pelvis and 8% in C3 and C1.

Modified complex voids were most evident, characterized by curved and pointed surfaces. They were common in the areas of the pelvis (15%) and feet (5-15%), less common in C3 (8%) and few in the areas of the skull and C1 (5%). Some of these voids interrupted fine material coatings and fragment of rock (Figure 5.101).

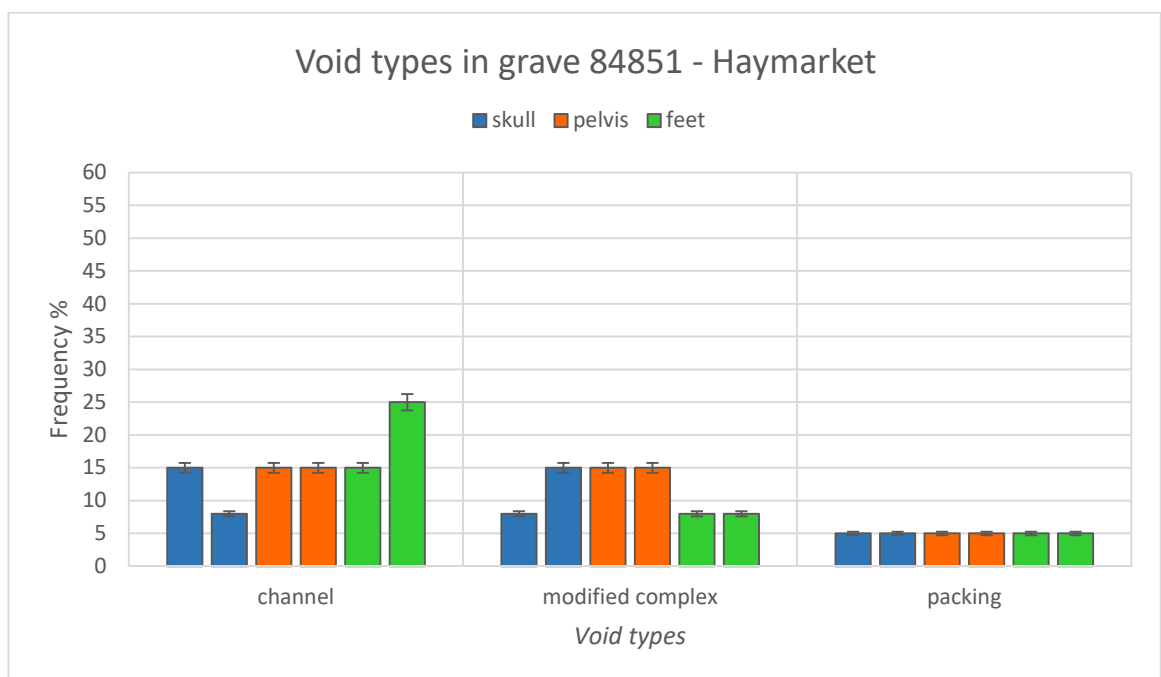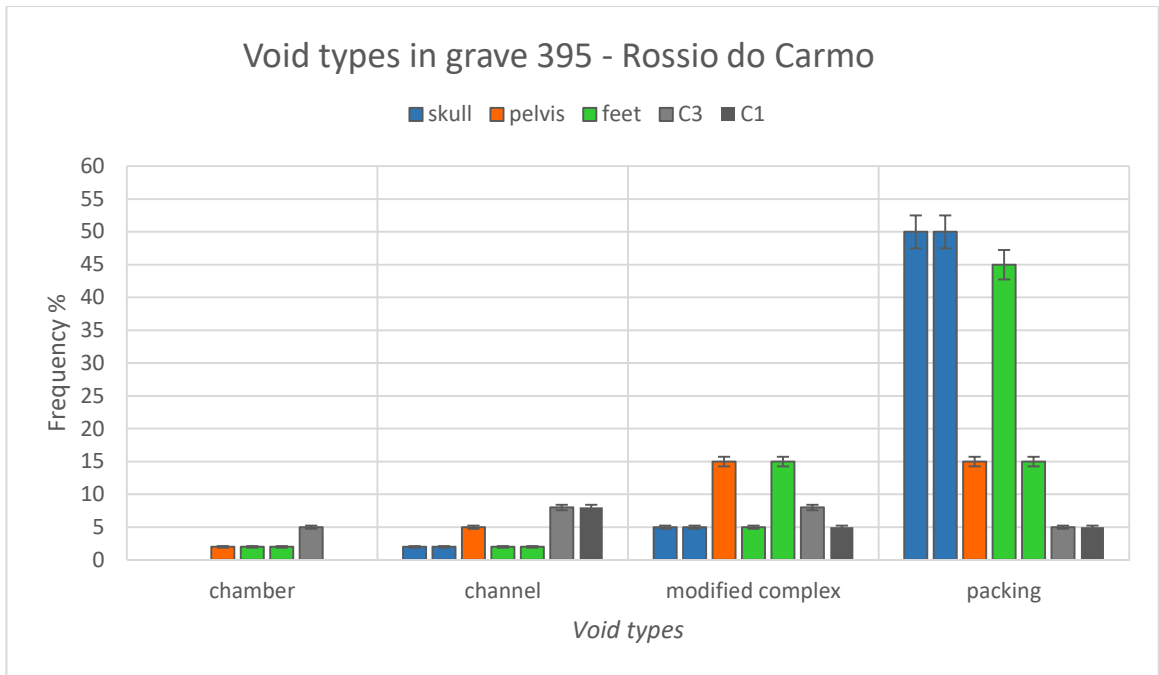*Figure 5.97: Abundance of different types of void in relation to their anatomical location within grave 395. Packing voids were dominant in the areas of the skull and feet, but they mostly originated after sampling. Modified complex voids were common in the areas of the pelvis and feet.*

MINERAL COMPONENTS

Six main types of mineral component were observed in grave 395: mica, plagioclase, pyroxene, quartz, quartzite fragments and schist (Figure 5.98).
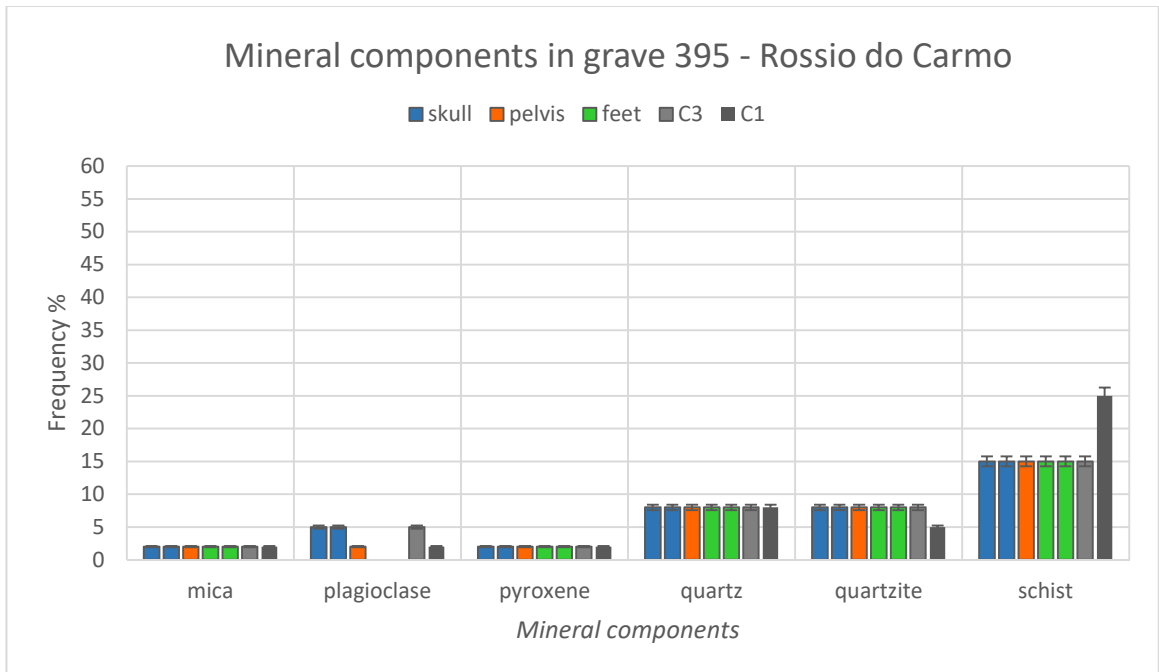
Figure 5.98: Frequency of mineral components in relation to their anatomical location within grave 395. Schist was more common than quartz and quartzite.

Schist was the most frequent component (15%), especially in the control C1 (25%). In the latter, sub-angular fragments were horizontally oriented and parallel to each other in the upper layer of the sample. Quartz and quartzite fragments were common in all of the slides (5-8%), while few grains of pyroxene and mica were observed (2%). Plagioclase was identified in the areas of the skull (5%), pelvis (2%), C3 (5%) and C1 (2%). All the mineral grains were between 50-700 μm in size and were angular or sub-angular.

ORGANIC COMPONENTS

Organic components were not frequent in grave 395. Five types were identified: amorphous organic matter, bone fragments, fungal spores, humified plant structures and sclerotia (Figure 5.99).
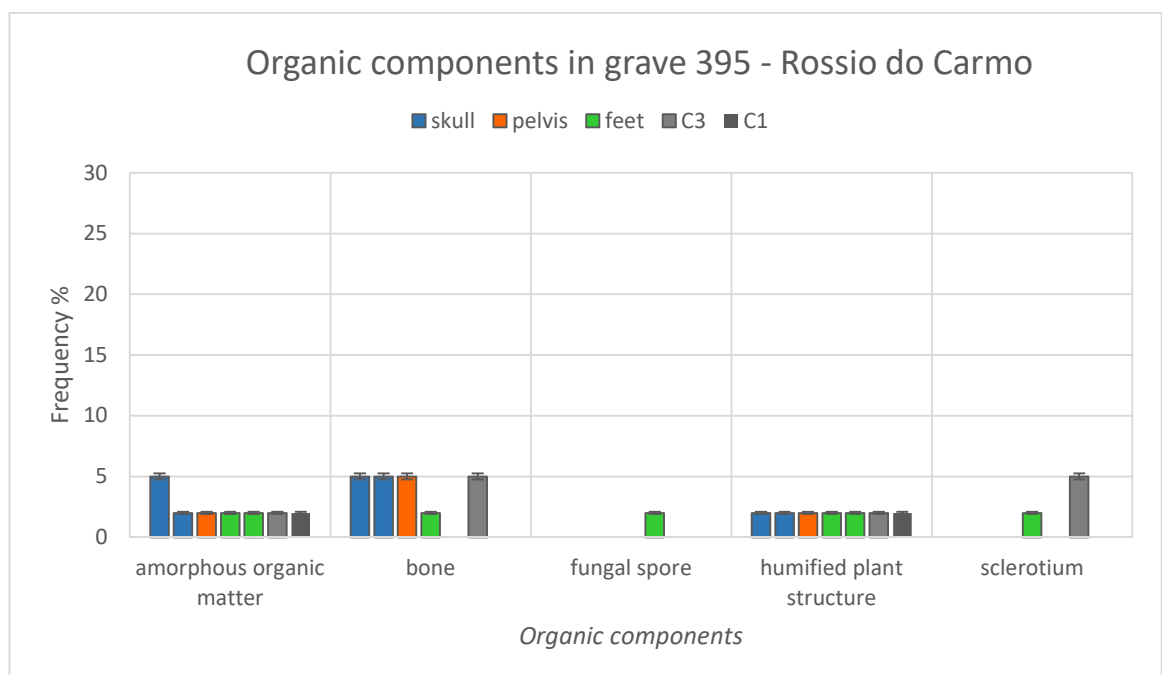
Figure 5.99: Frequency of mineral components in relation to their anatomical location within grave 395. Amorphous organic matter and humified plant structures were observed in all of the samples.

Amorphous organic matter comprised finely comminuted fragments of black matter embedded in the fine material. The size was generally between 20-100 μm, the shape was angular or sub-angular and the colour black in PPL and XPL. The organic matter was more frequent in the area of the skull (2-5%), where some fragments were coarser (500 μm). In the other areas, the percentage of amorphous organic matter was around 2%. Bone fragments were few in the areas of the skull, pelvis and C3 (5%), very few in the areas of the feet (2%) and absent in the C1. Bone was partially weathered, light yellow in PPL and with first order birefringence. The histological structure was still visible, though some fragments were weathered by channels and black stains (Figure 5.102.a-d). Very few fungal spores were observed in the areas of the feet (2%). Sclerotia (Figure 5.102.e-f) were very few in the same area (2%) and few in the C3 (5%), concentrated in the top right of the slide.

Fragments of humified plant structures were present in all of the slides, around 2%. They had different degrees of preservation, though it was noted that the brownish colour was weak/absent and they were mostly fragmented (Figure 5.102.g-h).

PEDOFEATURES AND ANTHROPOGENIC MATERIAL

Five main types of pedofeature and anthropogenic material were detected in grave 395: black redox impregnation, brick fragments, coatings of fine material around mineral grains, dusty clay coatings around voids and Fe/Mn nodules (Figure 5.100).
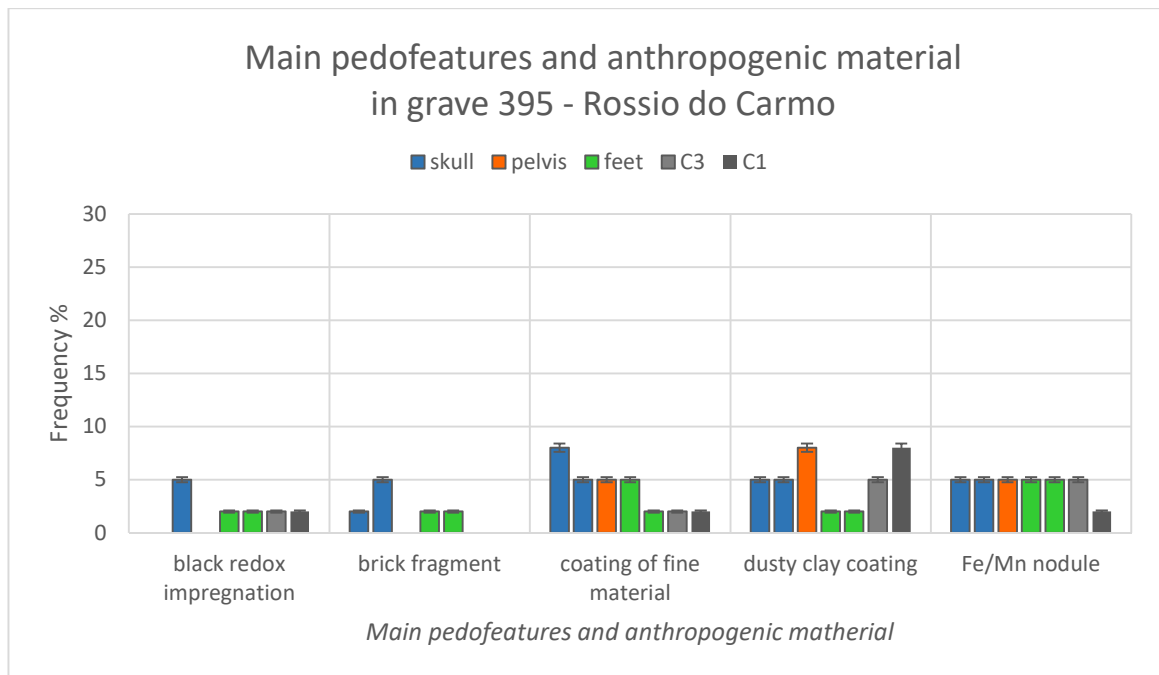
Figure 5.100: Frequency of the main pedofeatures and anthropogenic material in relation to their anatomical location within grave 395. Black redox impregnation, brick fragments and coating of fine material were more common in the area of the skull. Dusty clay coatings were more abundant in the area of the pelvis and control C1. Fe/Mn nodules were few in all of the samples.

Coatings of fine material around coarse components, generally mineral grains but less often organic matter, were mostly detected in the area of the skull (5-8%), followed by the area of the pelvis (5%), the area of the feet (2-5%) and the controls (2%). The fine material was the same as the matrix and the coating was thick 20-250 µm. The shape was commonly sub-rounded, but also sub-angular. Dusty clay coatings around voids were common in the areas of the pelvis and C1 (8%), few in the areas of the skull and C3 (5%) and very few in the area of the feet (2%). Their thickness was between 30-200 µm, the surface was smooth and different layers were observed. The b-fabric was parallel striated. Few Fe/Mn nodules were found in all of the samples (5%; 2% in C1). Their size increased from the area of the skull (50-500 µm) to the area of the feet (50-1200 µm) and decreased from the skeleton level to the C3 and C1 (50-500 µm). Black redox impregnations were few (2-5%) in all areas

other than the pelvis. The size was between 250-750 μm and they had rough surfaces and occasionally had a more reddish colour. Sub-rounded brick fragments (>500 μm) were contained in the samples from the areas of the skull (5-8%) and pelvis (2%).

The following figures were selected as representative of the features described in Section 5.3.3:

- Figure 5.101: voids;

- Figure 5.102: organic components.
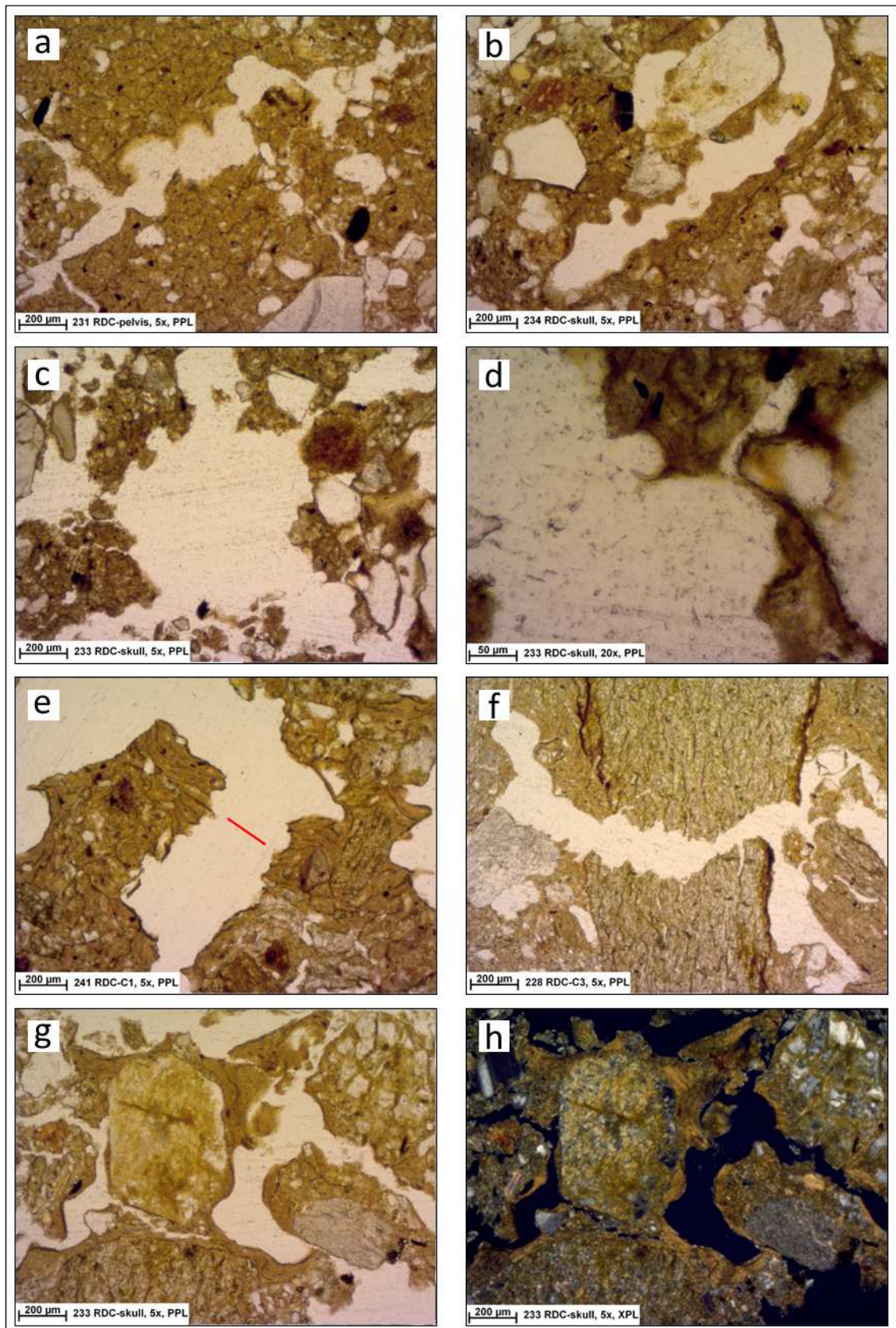
Figure 5.101: Voids in Rossio do Carmo. a) modified complex void from the area of the pelvis in grave 395; b) modified complex void from the area of the skull in grave 395; c) modified complex void from the area of the skull in grave 395; d) detail of figure (c); e) coating of fine material broken by modified complex void (red line) from the control C1 in grave 395; f) fragment of schist broken by modified complex void from the control C3 in grave 395; g-h) coating of fine material with parallel striated b-fabric around voids in grave 395 in PPL (g) and XPL (h).
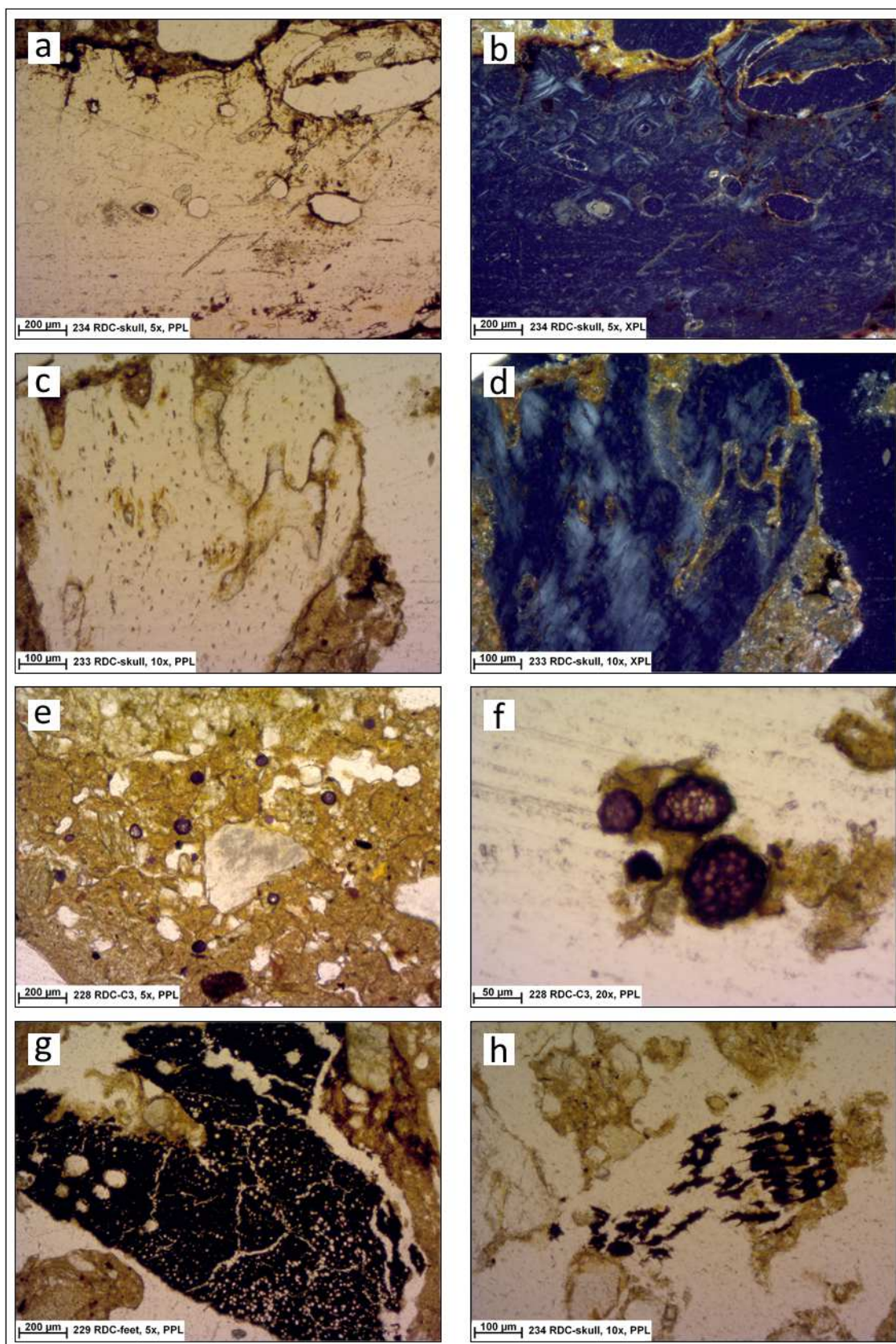
Figure 5.102: Organic components in Rossio do Carmo. a-b) bone fragment with black stains from the area of the skull in grave 395 in PPL (a) and XPL (b); c-d) fragment of partially weathered bone from the area of the skull in grave 395 in PPL (c) and XPL (d); f-g) sclerotia from the control C3 in grave 395; g) partially weathered humified plant structure from the area of the feet in grave 395, h) weathered humified plant structure from the area of the skull in grave 395.

5.5 PILL'E MATTA (IT). Punic and Roman cemetery, 4th-3rd C BC and 2nd-5th C AD

Pill'e Matta is the name of an industrial district of Quartucciu (Figure 5.103), a built-up area near Cagliari (IT), where in 2000 the Soprintendenza per i Beni Archeologici of Cagliari, in collaboration with the Quartucciu municipality, started the excavation of a Punic-Roman necropolis. The site has considerable importance for the presence of intact graves with abundant grave goods (Salvi 2005b, 19). The InterArChive team was involved in the sampling of the graves in 2009 and the results of four of these burials are presented in this research.
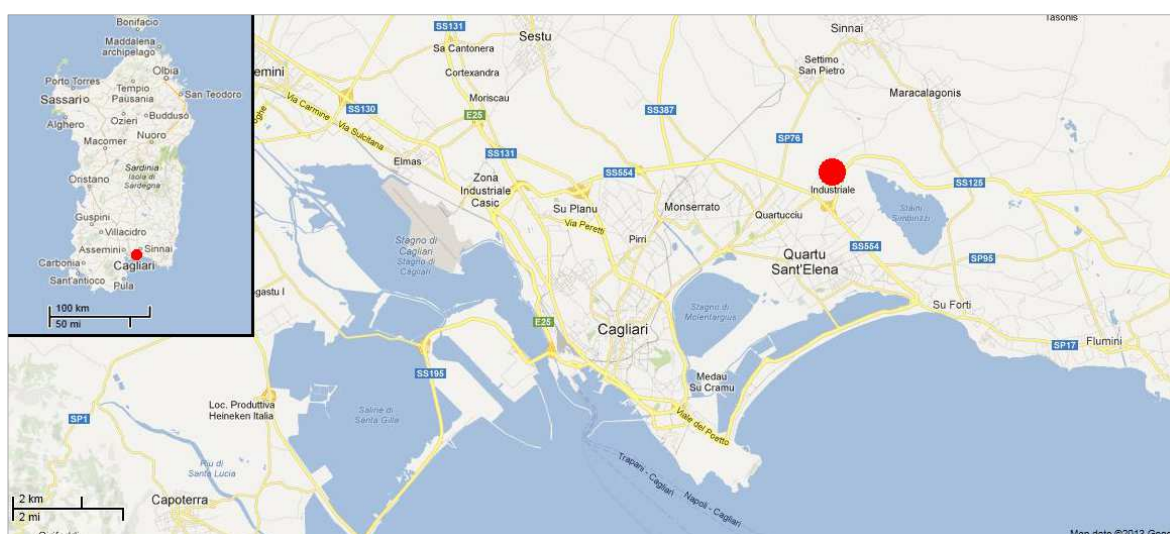
Figure 5.103: Map of Sardinia and the location of Pill'e Matta (red dot) in the area of Quartucciu. Graphically modified from Google Maps ©2013.

5.5.1 THE SITE

The area of the necropolis was situated in the southern Campidano, a plain extending from the Gulf of Cagliari to the Gulf of Oristano. The Campidano formed during the Pliocene, filling a pre-existing basin called Fossa Sarda; the plain was a site of intense anthropic occupation from Prehistory. The Fossa Sarda was formed by the creation of deep NNE-SSW faults and segregation of two blocks during the separation of the Sardinian Corsican Massif from the European continent in the Oligocene-Miocene. This movement induced intense volcanic activity with andesite, rhyolite, trachyte, tuff and ignimbrite products and contributed to the Miocene sea transgression. At this stage, marine and fluvial-lacustrine deposits formed in the submerged areas. During continental phases, the deposition of fluvial-torrential sediments originated the Formazione di Samassi, contributing to a drop of the Campidano, which reached the current aspect during the Quaternary (Matta 2005, 25-27).

The necropolis was situated in the Miocene stone substratum, which defined the depth of most graves (Matta 2005, 26). In the area of Cagliari, the stratigraphic sequence of this substratum, from the top to the bottom, was:

- Italian compact limestone (Lithothamnium or Pietra Forte);

- soft granular limestone (Tramezzario);

- arenaceous marly limestone (Pietra Cantone);

- quartz clays, more or less marly, with calcareous or clay cement (Arenarie di Pirri);

- grey clays and basal marl, more or less fossiliferous *(*Argille di Fangario).

Miocene limestone sediments, however, were absent in Pill'e Matta (Matta 2005, 27-28).

The continental Pliocenic Formazione di Samassi was visible on the eastern side of Campidano and was formed by:

- coarse sandstone, more or less cemented, inserted with thin conglomeratic lens;

- reddish brown clayey silt;

- light brown marly detrial limestone;

- conglomerates with pebbles of hard marl, predominantly of Miocene age.

In Pill'e Matta, the Formazione di Samassi was gradually deposited above the Arenarie di Pirri (Figure 5.104). The marly sediments are characterized by the presence of sandy and coarse lenses, transported by intense fluvio-torrential activities. Coarse lenses are also present in the sandstone deposits, where they are less sorted and less subrounded. In addition, the sandstones deposits are locally intercalated with brown terrigenous materials, which constitute the upper level of the eastern area of the necropolis. In the past, the different degrees of cementation of the limestone and sandstone facilitated the construction of chamber graves, utilizing the more compact layers for the vault. However, the presence of coarse lenses and the terrigenous levels caused the subsequent collapse. The coarse lenses were absent in the western area and it was possible that similar geomorphological differences influenced the use of the necropolis over time (Matta 2005, 30).

The archaeological site was discovered during the construction of a road, whose route divided the necropolis into two sectors (Figure 5.105). The East sector was characterized by a top brown level, subdivided into an uppermost layer of backfill a layer of humus mixed by ploughing, and a light brown marl layer. The graves were cut into the lower levels of the Formazione di Samassi, up to 2 m of depth from the highest level of non-altered sediments. In the West sector, the graves were deeper, following the marl substratum (Secci 2005, 33-36).
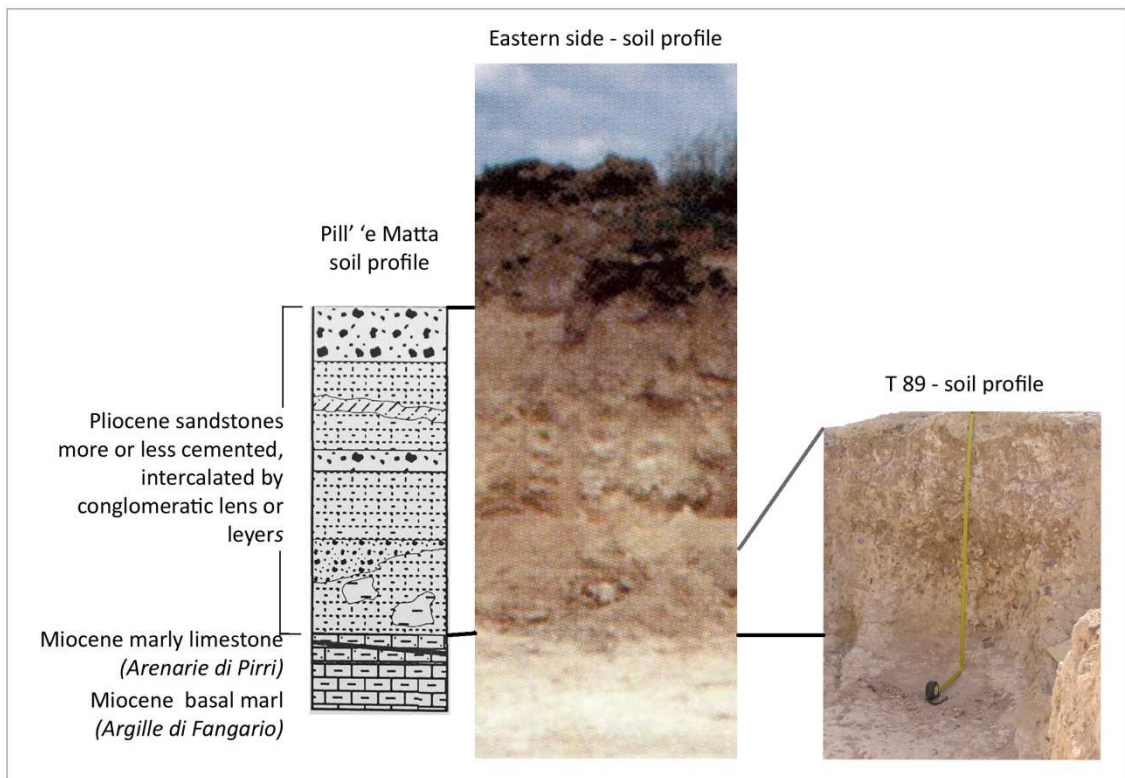
Figure 5.104: Stratigraphic correlation between the soil profile of the Eastern side of Pill'e Matta (left), drawn and photographed by the archaeologists (Salvi 2005) and the soil profile from Grave 89 (right), photographed by the InterArChive team. At the bottom, the Miocene substratum formed the base for the graves. At the top, the Pliocene sandstone, intercalated by lens or layers and containing the vault of the chambers.

Figure 5.105: Photograph (left) and plan (right) of the site of Pill'e Matta in 2005. The chamber tombs of the W sector are visible only in the plan, because the area was not excavated at the time of the photograph. The graves sampled by the InterArChive team were located in the areas highlighted by the two circles of the photograph: yellow for the Punic and red for the Roman. These graves do not appear in the plan, because they were sampled in 2009, while the plan was made in 2005. Graphically modified from Salvi (2005).

The necropolis was in use during 4th C BC - 5th C AD (Figure 5.106). The most ancient graves were Punic (Salvi 2005b, 21). The chambers comprised rectangular pits, flanked along the longer side by niches. The corpse was placed in the niche, while the grave goods where co-located in the niche

195

and covered with an amphora *a siluro* (i.e. cylindrical with conical ends). This particular typology found a direct comparison with the Ras Zébib necropolis, in Capo Bon, Tunisia (Salvi 2005a, 188). During 2nd C BC - 1st C AD incineration was the dominant ritual in Pill' 'e Matta; in particular, the archaeologists found indication of *Bustum*, a practice where the body was burned and buried in the same place. During 2nd - 3rd C AD two different types of graves were in use in the necropolis. The first and less common was *alla cappuccina* grave: the corpse was placed in rectangular pits covered by tiles, which were arranged as a sort of roof. The second type consisted of a chamber grave: subrectangular pit with one or two niches excavated along the two long sides of the pit. The bodies and grave goods were placed into the niches, which were sealed with tiles oriented perpendicular to the floor (Salvi 2005b, 21). This type of grave was used exclusively during 3rd - 5th C AD and was characterized by richer and more abundant grave goods, testifying well developed trading between Sardinia and Africa and the prosperity of the population (Salvi 2005a, 188-189).
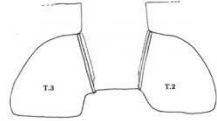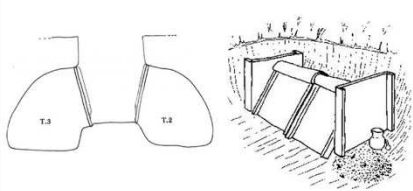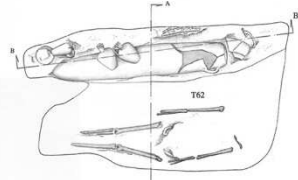
		PERIOD	GRAVE TYPE	EXAMPLE
AD	5th c. / 4th c.	ROMAN IMPERIAL AGE	Subrectangular pit with one or two niches along the long sides. One corpse was placed for each niche closed by tiles.	
AD	3rd c. / 2nd c.	ROMAN IMPERIAL AGE	Subrectangular pit with one or two niches along the long sides. One corpse was placed for each niche, closed by tiles. For a brief period: grave *alla cappuccina*, where the body was covered by tiles organized as a roof	
BC	1st c. / 1st c. / 2nd c.	FIRST ROMAN IMPERIAL AGE ROMAN REPUBLIC AGE	Incineration ritual in urn	
BC	3rd c. / 4th c.	PUNIC	Rectangular pit with a niche along one of the long sides, where the corpse was placed. The niche was closed by an amphora *a siluro*	

Figure 5.106: Summary of the different typology of graves in Pill'e Matta during 4th C BC - 5th C AD. The drawings of the examples are from Salvi (2005) and www.archeovercelli.it ('alla cappuccina' grave and incineration urn).

The presence of many intact chamber graves permitted the reconstruction of the main aspects of the burial and funeral rituals performed in Pill'e Matta. First, the rectangular pit and the niche were dig with flat picks, whose print were still visible in the corner of the graves. Secondly, the body was placed directly on the niche floor, supine, the head pointed to West and the arms along the body or on the abdomen. The clothes were typically roman, though the recoveries of buckles from 4th c. testify the use of dresses held by a belt. Red colour on the bones in Punic graves suggests the presence of coloured cloth around the corpse (Salvi 2005a, 188). Jewels in bronze were worn and coins were probably placed inside a cloth bag. Ceramic and glass grave goods were placed after the body was laid in position, above it or near head, feet or on the internal side of the niche. No remains of animals, shellfish or seed were found. Finally, a plate with one or more oil-lamps always lit, evidenced by traces of burning, were set in the chamber (Secci 2005, 190-191). The ritual did not include backfill or covering of the body. Thus, the sediments found in the graves were from post-depositional processes. Such processes may have been gradual, with the infiltration of material from the tiles, or rapid with the collapse of the vault. In the latter case it was possible to detect if the collapse was more or less recent, considering the compactness or the lack of consistency of the sediment inside the grave. Large tiles, or an amphora during Punic period, were placed side by side to close the recess (Pittoni 2009, 387), and the rectangular pit between the two hollows was filled with the surrounding debris. During the archaeological excavations it was observed that the sediments filling the pit were coloured differently to the sandstone of the chamber tombs (Secci 2005, 33).

Several bones from different graves presented unusual damage, mostly on the skull and on larger long bone shafts: round holes, irregular bone destruction and areas characterized by irregular etching. The origin was attributed to the activity of a specie of bee-wasp, *Hymenoptera helictidae.* Some larvae and adults of this species were present on the site. In addition, similar holes and tunnels were observed in the internal walls of the chambers and in the soil above the burial. The behaviour of these bee-wasps is to dig galleries in the ground and built cells, where larvae grow (Pittoni 2009).

5.5.2 THE GRAVES

Four graves were selected for this research (Table 5.5):

- Punic: 238;

- Roman: 237, 268, US2680.

GRAVE	DATE	TYPE	SKELETON INFORMATION and grave-goods	SOIL TYPE	CLIMATE
238	Punic, 4th-3rd C BC	Chamber, closed by an amphora *a siluro*	Supine, well preserved	Limestone and sandstone	Temperate Mediterranean
237	Roman, 2nd-5th C AD	Chamber, closed by tiles	Scarcely preserved	Limestone and sandstone	Temperate Mediterranean
268	Roman, 2nd-5th C AD	Chamber, closed by tiles	N/A	Limestone and sandstone	Temperate Mediterranean
US2680	Roman, 2nd-5th C AD	Chamber, closed by tiles	N/A	Limestone and sandstone	Temperate Mediterranean

Table 5. 5: Summary of the available information regarding the graves in Pill'e Matta.

Four loose samples from the soil profile of grave 89 (Figure 5.104) were observed in the absence of a C1 control, which could not be collected as undisturbed soil. One control from grave 238 was collected as C1, but possibly it was intended as C2 or C3. Hence, it was exclusively for grave 238. Despite the InterArChive sampling strategy illustrated in Chapter 3.1, much of the information related to the graves was not recorded owing to the sampling taking place prior to the commencement of the project. Only pictures from graves 237 and 238 were taken and information from the archaeologists was lost at early stage of the project and impossible to retrieve owing to changes in personnel associated with the site (Chapter 3, Table 3.2). The exact location of the tins was not recorded, so this information was missing for the graves without photographs; the orientation (up) was missing in 6 samples and for only three samples was it noted which side was in contact with the bones. The manufacture of the slides was good though three samples were cut in the wrong direction, parallel to the resting plane (Appendix 1.5).

GRAVE 238

Grave 238 was dated to the Punic period, during 4th C BC - 3rd C BC. The skeletal remains were in good condition (Figure 5.107).
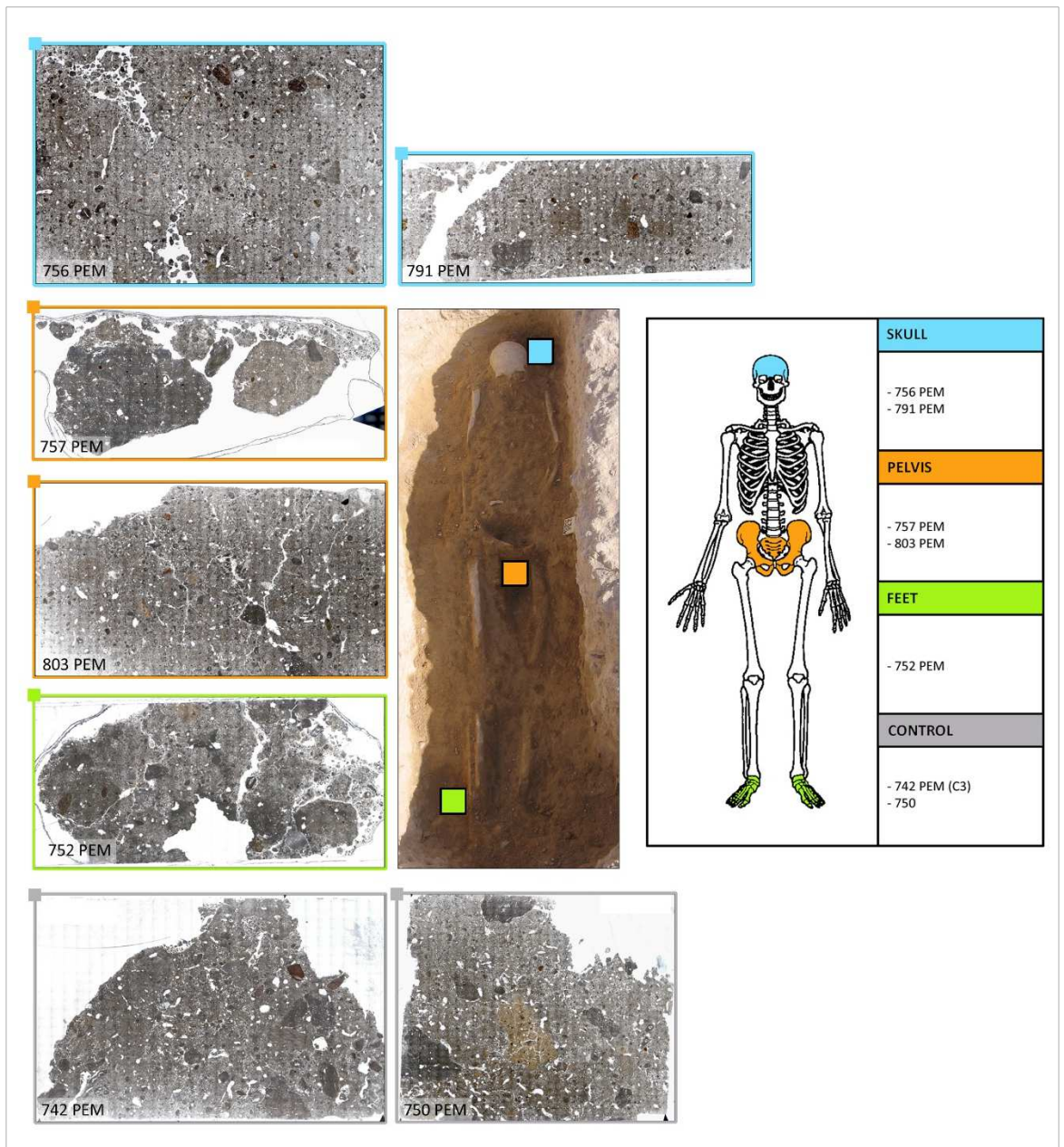
Figure 5.107: Grave 238. In the middle, photograph of the grave and location of the samples. The samples are represented as square and not rectangular, because they were not collected with Kubiena tins, but with containers of different shape. On the right, list of the slides in relation to their anatomical location. On the left and around the photograph, mosaics of the slides. See the text for descriptions.

GRAVE 237

Grave 237 was dated to the Roman period, generically during 2nd-5th C AD in the absence of information from the archaeologists (Figure 5.108).
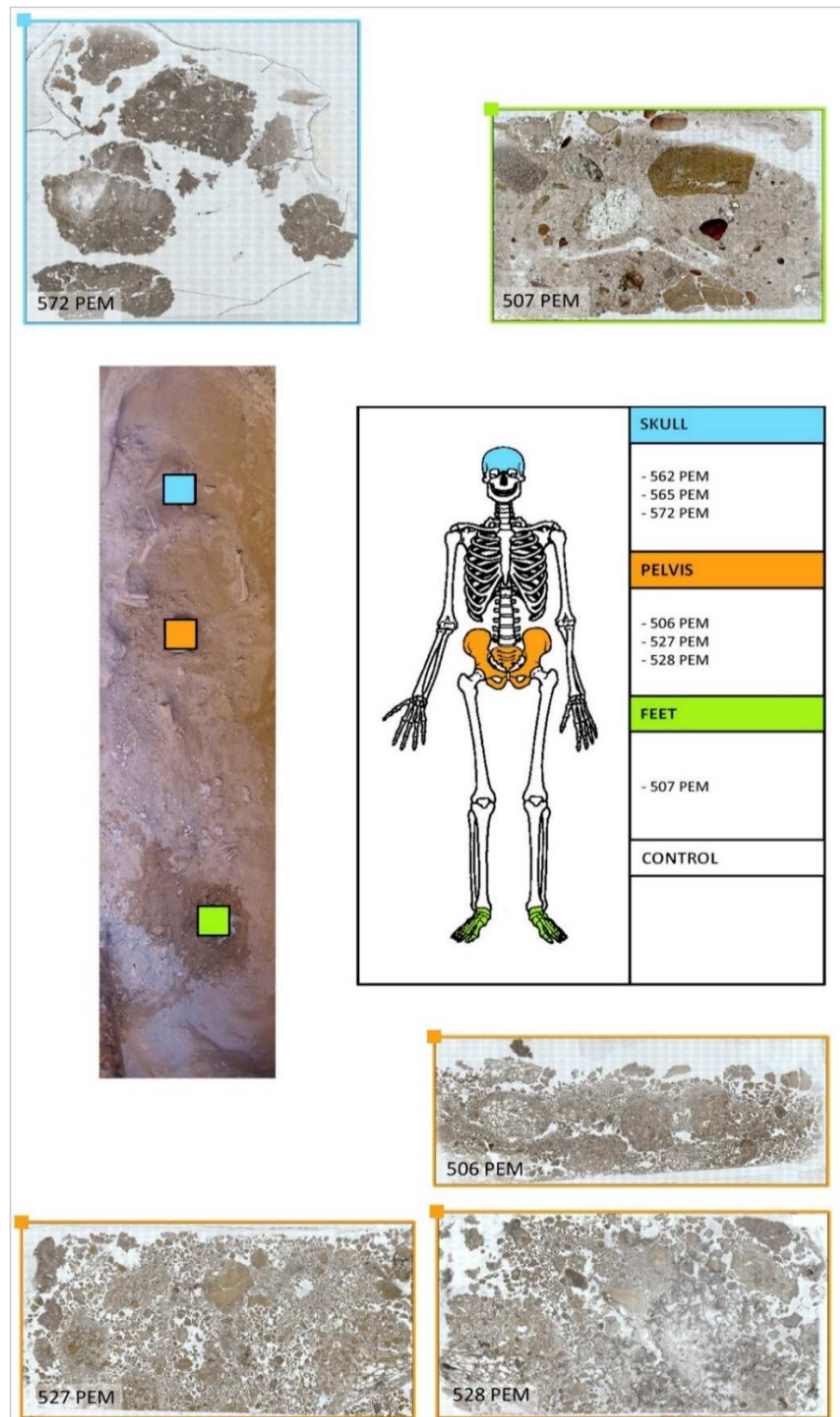
Figure 5.108: Grave 237. On the left, photograph of the grave and location of the samples. The samples were represented as square and not rectangular because they were not collected with Kubiena tins, but with containers of different shape. On the right, list of the slides in relation to their anatomical location. On the top and bottom, mosaics of the slides. Slides 562 and 562 were not digitized, because they were mounted on a glass too small to fit in the arms of the stage of the AxioScope. See the text for descriptions.

GRAVE 268

Grave 268 was dated to the Roman period, generically during 2nd-5th C AD in the absence of information from the archaeologists (Figure 5.109).
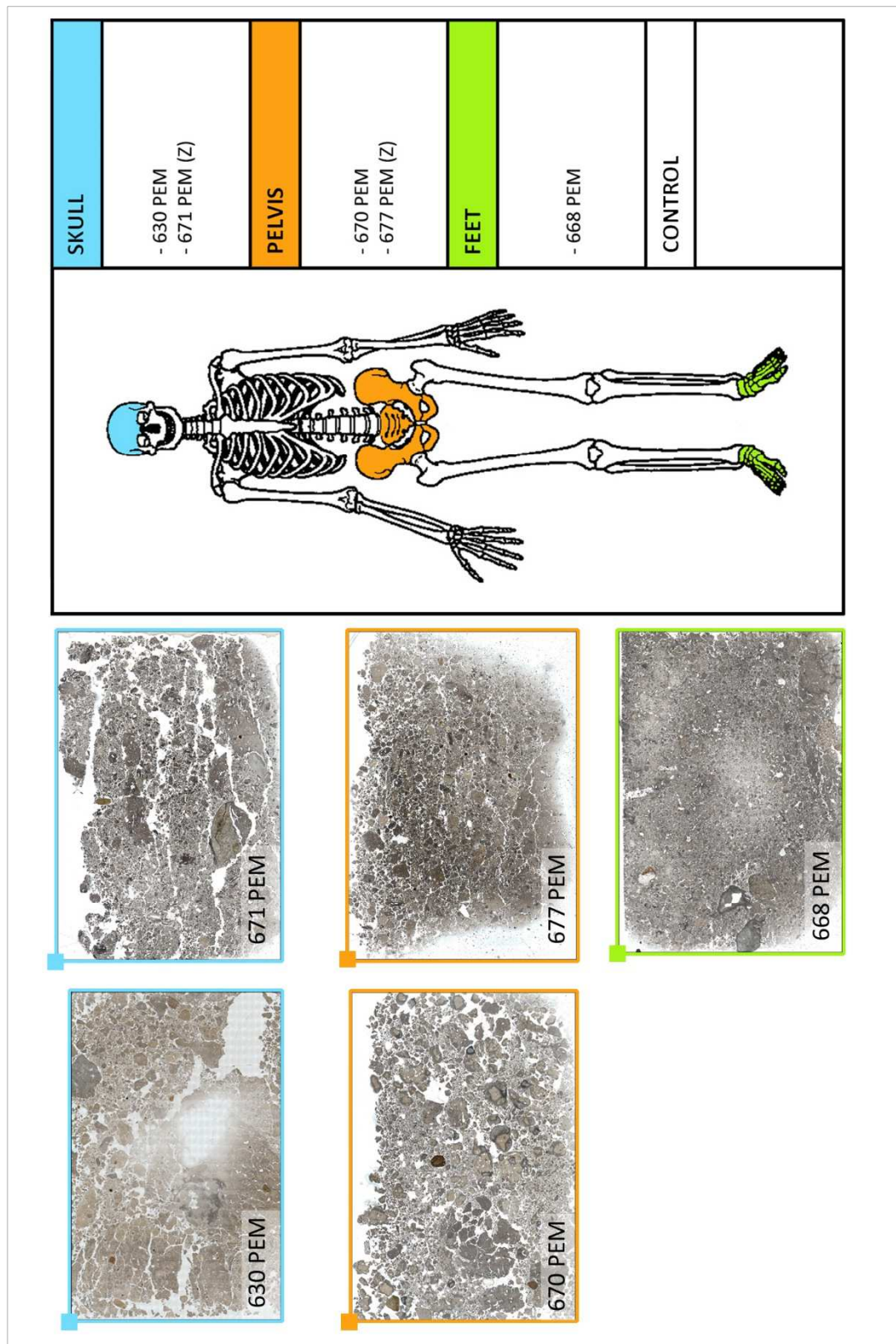
Figure 5.109: Grave 268. Photographs were not taken for this grave. On the right, list of the slides in relation to their anatomical location. On the left, mosaics of the slides. See the text for descriptions.

GRAVE US2680

Grave US2680 was dated to the Roman period, generically during 2nd-5th C AD in the absence of information from the archaeologists (Figure 5.110).
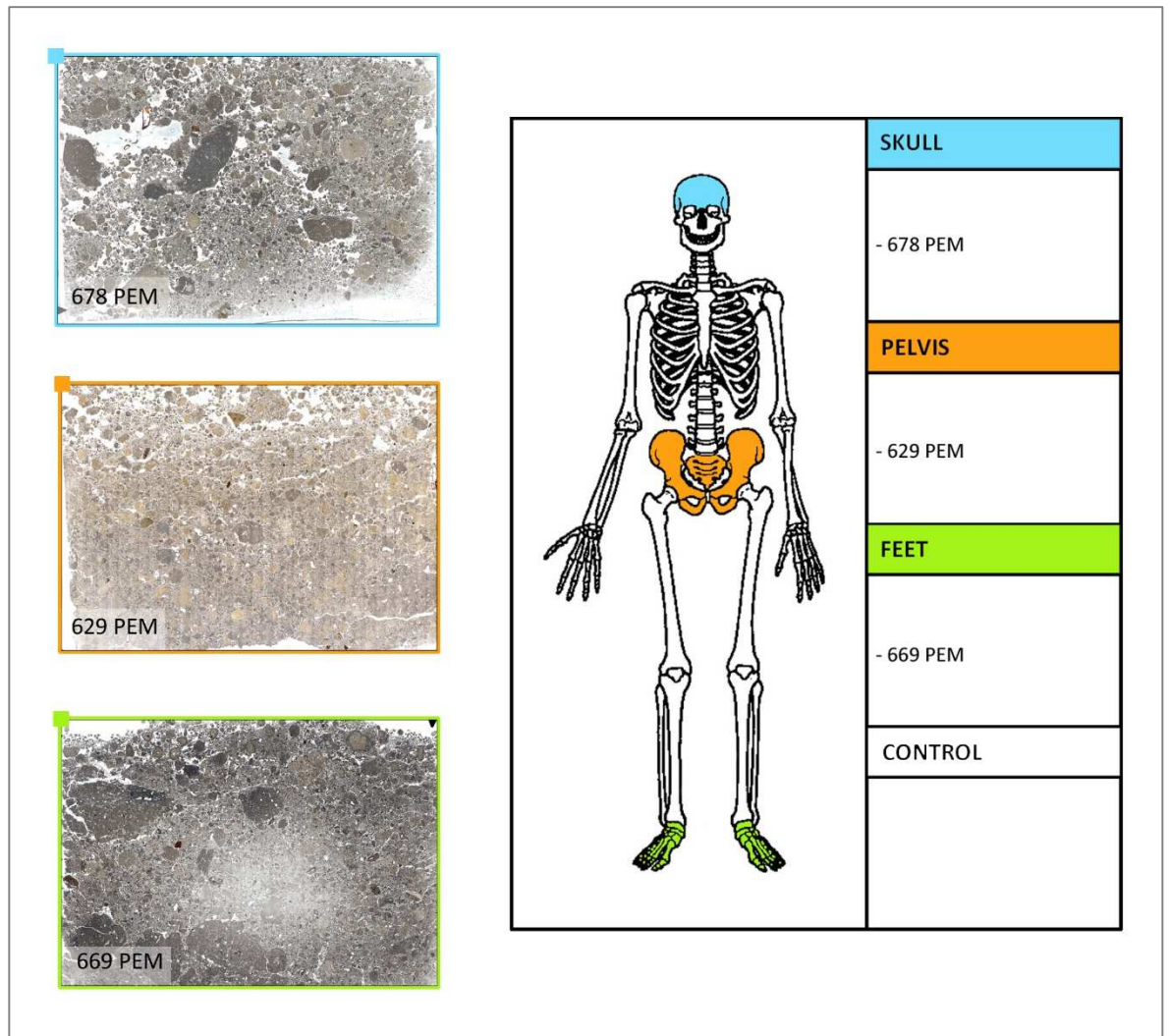
Figure 5.110: Grave US2680. No photographs were taken for this grave. On the right, list of the slides in relation to their anatomical location. On the left, mosaics of the slides. See the text for descriptions.

CONTROL C1

Five slides were made from four loose samples and they were analysed with the microscope, to check the variability of the materials and pedofeatures. Void and ped arrangements were not recorded, because of the nature of the samples. Their location was recorded in the field, so it was possible to correlate the samples to the soil profile of grave 89 (Figure 5.111).
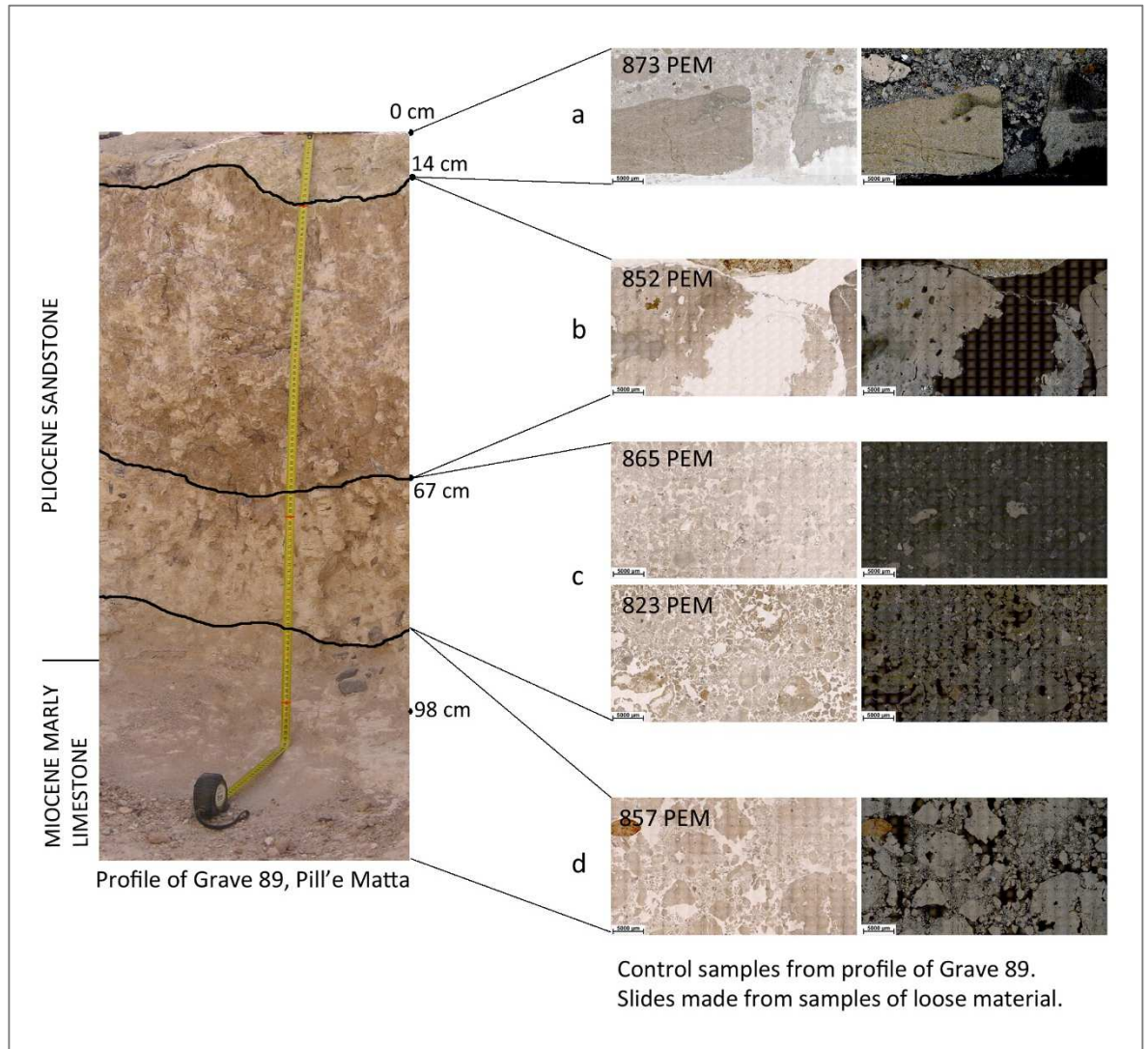
Figure 5.111: Correlation between the soil profile of grave 89 (left) and the slides made from the loose samples of the same profile (right). Slide 857 came from the Miocene marly limestone; slides 823, 865 and 852 from two different layers of Pliocene sandstone and slide 873 from the top of the profile. See the text for descriptions.

5.5.3 MICROMORPHOLOGICAL RESULTS

GRAVE 238

ELEMENTS OF FABRIC AND PEDS

All samples from grave 238 had porphyric c/f related distribution and they were poorly sorted. The characteristics of the fine material were constant among the anatomical locations and in the control samples: limpidity was opaque, the colour light greyish brown in PPL and yellow/beige in XPL, with crystallitic or undifferentiated b-fabric. The abundance of fine material was between 50-60%. The peds were granular, ultrafine in size and unaccommodated. They had strong development in the areas of the skull, strong/weak in the area of the pelvis, moderate/ weak in the area of the feet and C1 and weak in the control C3. It was probable that the development of peds decreased from the area of the skull to the area of the feet and to the controls. Samples from the areas of the pelvis contained two granular aggregates of type B, observed in the Roman graves (below "elements of fabric and peds" of graves 237, 268 and US2680). These peds were distinguished because of different characteristics: well sorted, still porphyric but with higher amount of fine material, masked limpidity, light greyish yellow colour in PPL and grey in XPL; same crystallitic b-fabric.

VOIDS

Four types of void observed in grave 238: chamber, channel, crack and packing (Figure 5.112).
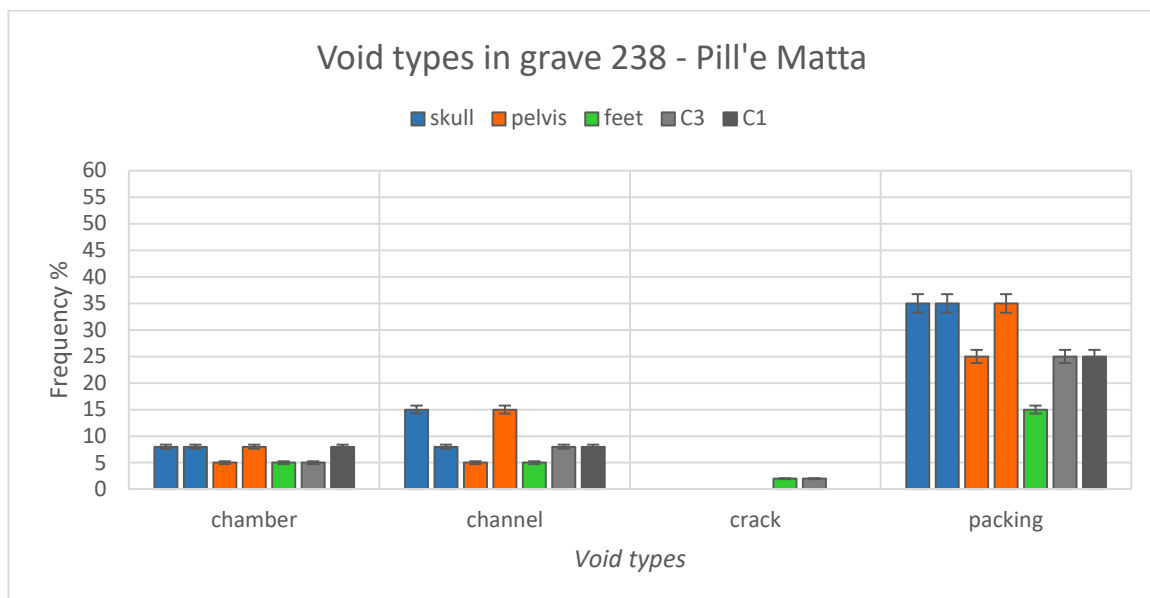
Figure 5.112: Abundance of different types of void in relation to their anatomical location within grave 238. Packing voids were dominant.

Chambers, channels and packing were present in all of the samples, but packing voids were more abundant (15-35%). Cracks, instead, appeared in low percentage (2%) in the area of the feet and control C3. Significant differences were not observed among the anatomical locations, but samples from the areas of the skull and pelvis were slightly more porous than the area of the feet and controls. Chambers and channels had smooth or undulating surfaces, while packing voids were undulating or rough.

MINERAL COMPONENTS

The samples had low abundances of mineral components, between 10-15%. Six types were observed in the slides and their frequency was constant through all of the samples (Figure 5.113). Quartz grains were the most frequent (8%), followed by quartzite fragments and rubified rock fragments (5%). Calcite rock fragments never exceeded 2% and only a few grains of plagioclase were detected in the areas of the pelvis and feet. The minerals had a partially weathered aspect. Examples of foraminifera were also identified within the sediment (5%).
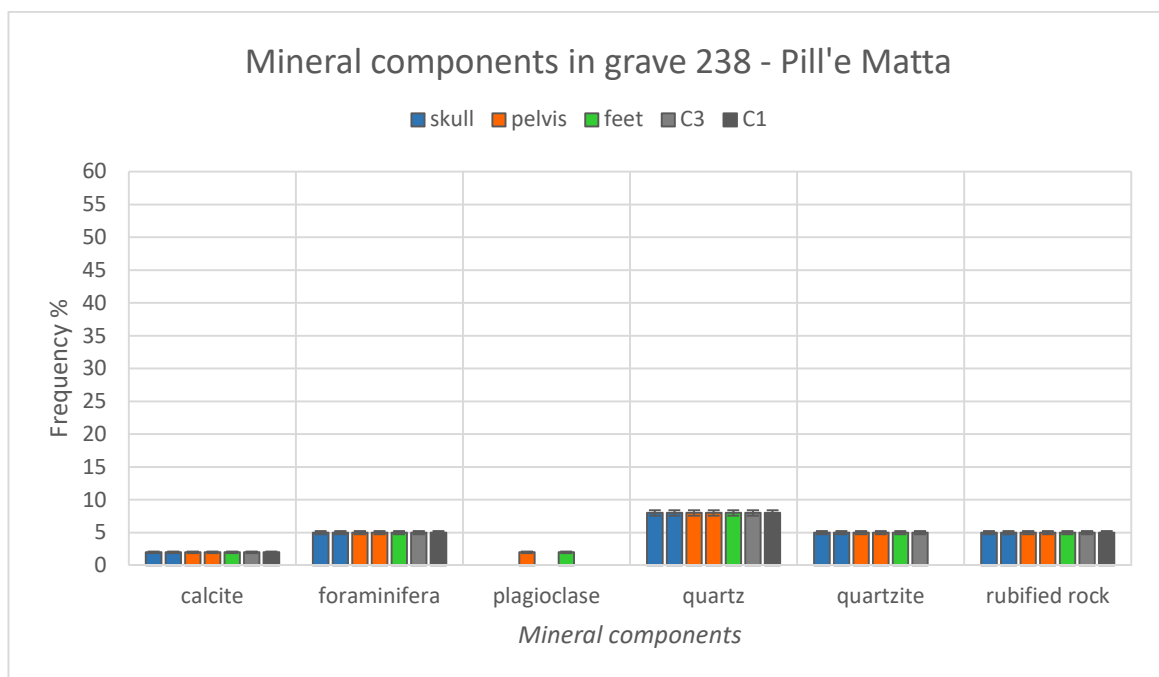
Figure 5.113: Frequency of mineral components in relation to their anatomical location within grave 238. Quartz was the most common mineral.

ORGANIC COMPONENTS

Very few organic components were preserved in grave 238 (Figure 5.114): bone fragments, fungi, humified plant structures and roots. Fresh roots were the most common (2-5%), present in all anatomical locations, especially in the areas of the skull and C1. They had yellow or orange colour in PPL and reddish brown in PPL (Figure 5.131.f). Despite the fresh look caused by the colour, many

roots were weathered, though still preserving the cellular structure. Fragment of bones (5%) and humified plant structures (2%) were observed in the area of the pelvis. The coarser fragment of bone was weathered, with the presence of several fractures, dense complete infillings of micrite within the structure and low levels of staining. The colour was light yellow in PPL and low order grey birefringent in XPL, the birefringence was first order, but still visible. Fungal presence was detected in the areas of the skull and pelvis (2%). The former was characterized by hyphae and spores within voids. The hyphae were very straight, with shorter hyphae orthogonal to the main structure, purple/brown in PPL and isotropic in XPL and not weathered. Some grey granular masses, composed by very fine ovoid cells (3 μm ca.), enveloped some intersections of hyphae as if they were the nucleus of the structure (Figure 5.132.b-d). The spores were very small, ca. 10 μm, ovoid in shape and with rough surface (Figure 5.132.a). The colour was dark brown/black in PPL and isotropic in XPL. Hyphae and spores were located in the same voids, next to each other, so they were probably part of the same type of fungus. In the area of the pelvis, instead, fungal bodies of *Ulocladium sp*. were identified within a void in the top of slide 757. Their main structure was conical, pointed and the surface was rough. The colour was dark purple in PPL and purple or isotropic in XPL (Figure 5.132.e-h).
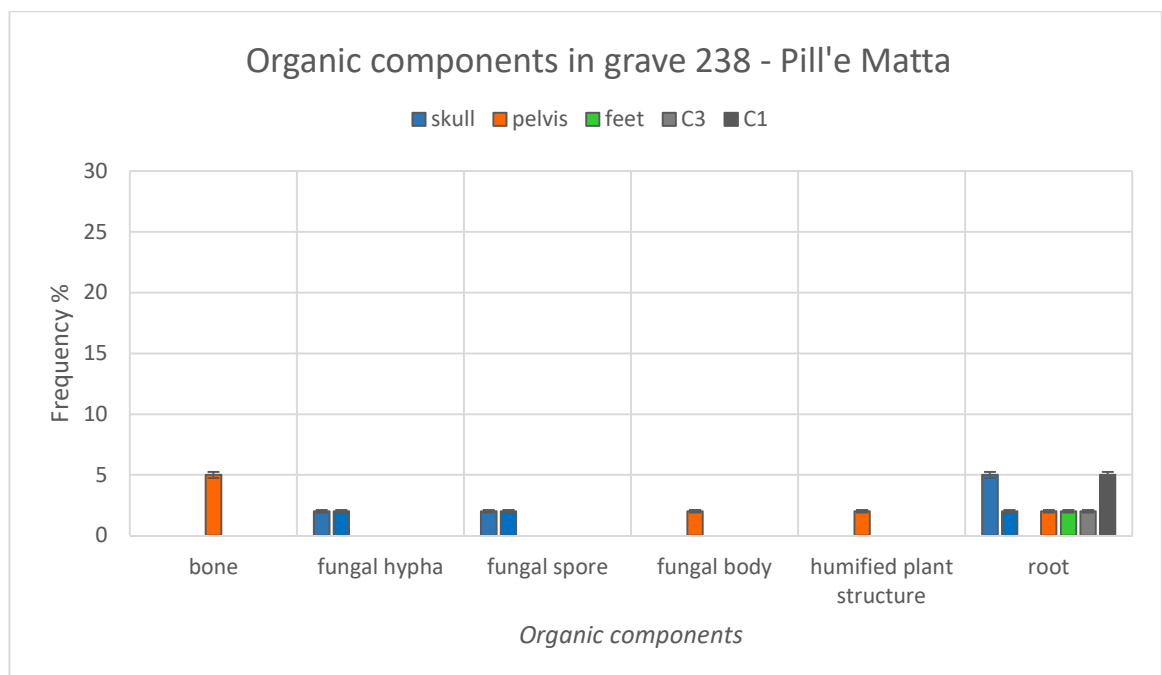
Figure 5.114: Frequency of organic components in relation to their anatomical location within grave 238. Fungal remains were observed in the areas of the skull and pelvis.

PEDOFEATURES

Five main types of pedofeature were observed in grave 238 (Figure 5.115): dendritic Mn nodules, soil micro-fauna faecal pellets, Fe/Mn nodules, infillings of calcified filaments and micritic hypocoatings. All the pedofeatures were of abundances between 2-8%.
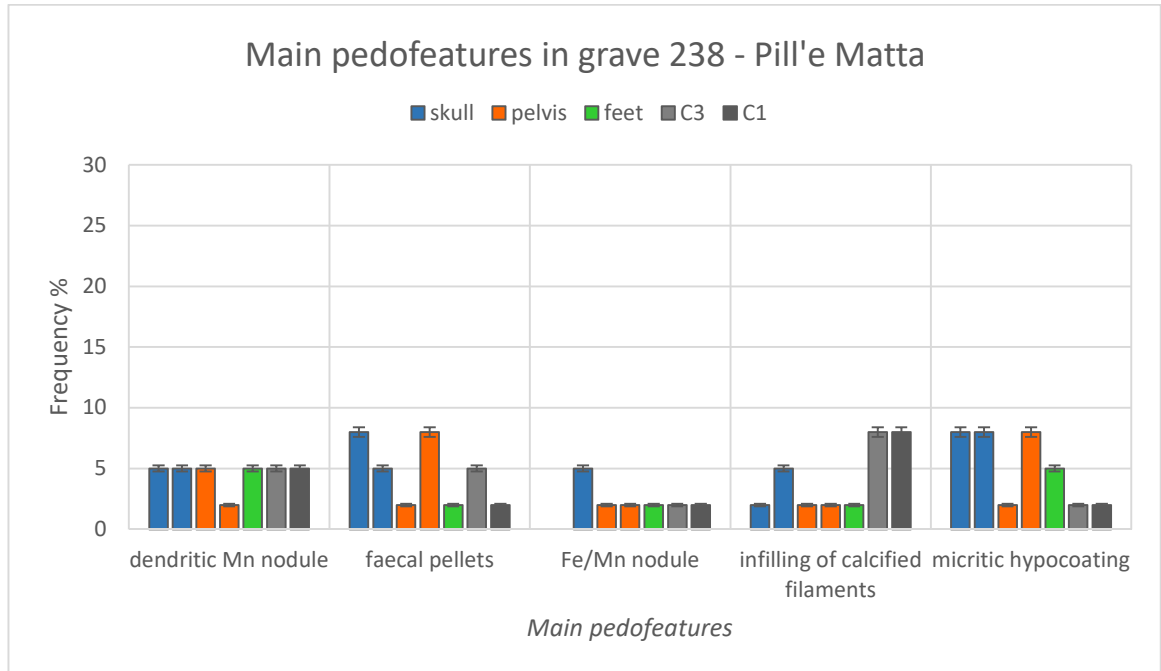
Figure 5.115: Frequency of the main pedofeatures in relation to their anatomical location within grave 238. Soil micro-fauna faecal pellets were observed in all of the samples, especially in the areas of the skull and pelvis.

Dendritic Mn nodules were present within the fine material in all of the samples. Their sizes were between 100-1000 µm, the shape sub-rounded, the surface was rough and the colour was black in PPL and XPL. In a few cases, in the area of the feet, they appeared as external quasicoatings around voids. Fe/Mn nodules between 50-200 µm were observed in all of the samples. They were sub-angular or sub-rounded, not weathered, red/brown colour in PPL and red or isotropic in XPL, undifferentiated b-fabric. Micritic hypocoatings were characterized by a depleted dense micritic hypocoating with undifferentiated b-fabric around a chamber. In some cases an external hypocoating, still micritic but not depleted, with crystallitic b-fabric, developed around the first one. In addition, quite often, loose discontinuous infillings of very fine micritic and crystallitic granules were within the chamber. They were identified in all of the samples, but they were more frequent in the areas of the skull and pelvis (8%). Their size was between 500-2000 µm.

Loose discontinuous infillings of calcified filaments within voids were few in all of the samples (2-5 %), but more abundant in the control samples (8%). The filaments were very fine and exhibited many intersections; in a few cases they nearly filled the void completely. They were difficult to

detect in PPL, because of their white/light grey colour, but the high third order birefringence crystallitic b-fabric and the white colour in XPL made their recognition immediate (Figure 5.133.c-d). Loose discontinuous infillings of sub-rectangular and rounded granules were identified as mite faecal pellets (Figure 5.133.e-h). They were present in all of the samples, especially in the areas of the skull and pelvis (8%). The dimensions of single sub-rectangular pellets were generally 50 x 120 µm, while the diameter of the round pellets was 50 µm. The last ones have been identified as the horizontal section of the sub-rectangular pellets. The faecal pellets appeared not weathered, often parallel to each other, and composed of grey micritic fine material and orange organic matter. Depending on the proportions of these two, the pellets were more grey or more orange and with more or less crystallitic b-fabric. In rare cases, small fragments of organic matter, possibly roots, were detectable in relation with the faecal pellets.

GRAVE 237

ELEMENTS OF FABRIC AND PEDS

Samples from grave 237 were composed of three different materials, A, B and C. Material A was dominant in the area of the skull (95-85%) and less frequent in the areas of the pelvis and feet (10-30%). It was characterized by porphyric related distribution and poor/moderate sorting. The fine material was light greyish brown in PPL and yellow/beige in XPL, with opaque limpidity and crystallitic or undifferentiated b-fabric. The peds were granular and very fine to fine, unaccommodated or partially accommodated and their development was variable, from weak to strong. Material B was infrequent in the area of the skull (5-15%) and pelvis (5%), but more abundant in the area of the feet (25-30%). It was characterized by porphyric related distribution and moderate sorting. The fine material was light greyish yellow in PPL and grey in XPL, with masked limpidity and crystallitic b-fabric. The peds were granular, ultrafine to very fine, unaccommodated and their development was strong. Material C was not present in the area of the skull, but dominant in the area of the pelvis (75-85%) and frequent in the area of the feet (40-50%). It was characterized by fine monic c/f related distribution and perfect sorting. The fine material was light yellowish beige in PPL and XPL, with limpid limpidity and very fine crystallitic b-fabric (Figure 5.130.c-d). The peds were granular, very fine to medium, with angular (Figure 5.130.g) or sub-rounded shapes, were partially accommodated or unaccommodated and with strong development. Small zones from the area of the pelvis were apedal (10-20%).

VOIDS

Five types of void were observed in grave 237: chamber, channel, crack, packing and vugh (Figure 5.116). Packing voids were the most abundant voids in all of the samples (40-50%). Chambers and channels were more common in the area of the skull (8-25%), making this area more porous than the others. Cracks appeared only within Material C, in the areas of the pelvis (5%) and feet (15%). Vughs were rare and only in the area of the skull (5%) and feet (2%). It seemed that the origin of vughs was related to the production of the slides and the possible separation of coarse fragments during the grinding.
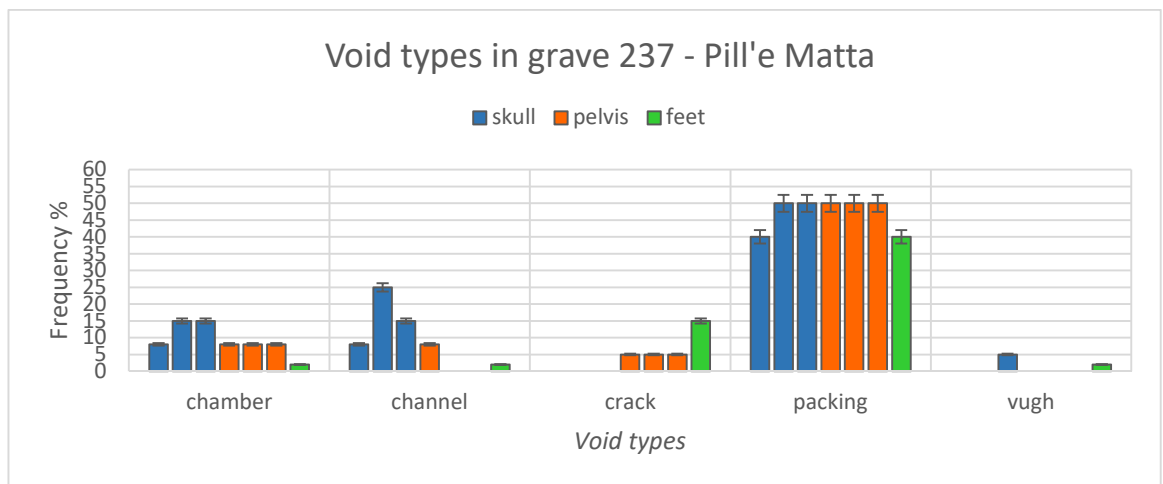
Figure 5.116: Abundances of different types of void in relation to their anatomical location within grave 237. Packing voids were dominant.

MINERAL COMPONENTS

Mineral components were not abundant in grave 237 (Figure 5.117).
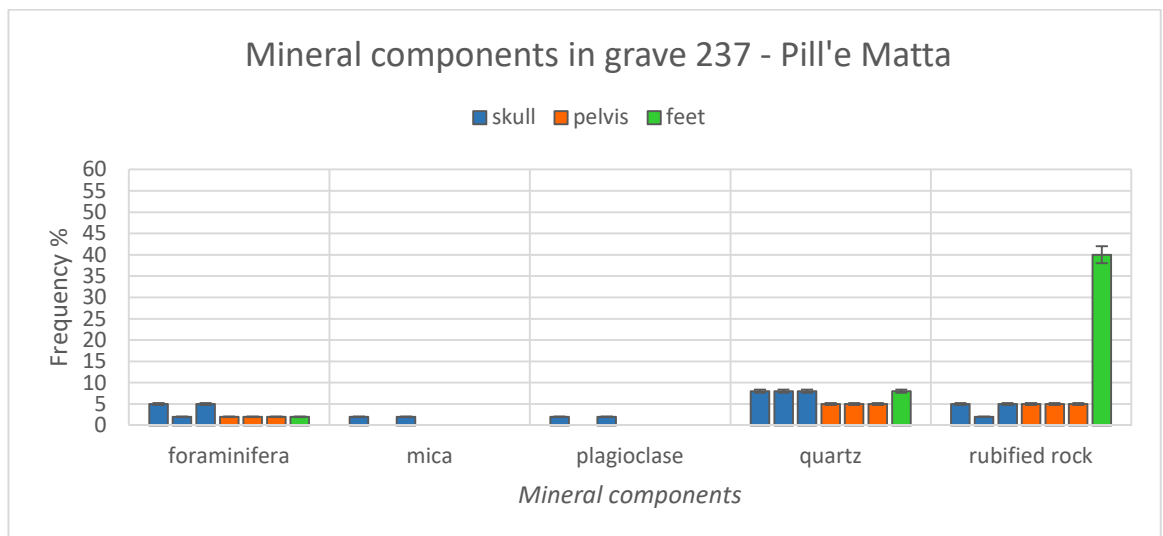
Figure 5.117: Frequency of mineral components in relation to their anatomical location within grave 237. Quartz was common in all of the samples and rubified rock was dominant in the area of the feet.

Quartz was common in all of the samples, between 5-8%. Fragments of rubified rock were observed in all of the samples too (2-5%) and they were very frequent and coarser (>2000 μm) in the area of the feet. Very few partially weathered grains of mica and plagioclase were identified in the area of the skull (2%). Foraminifera were detected in all of the samples between 2-5%.

ORGANIC COMPONENTS

Six organic components were identified in grave 237: amorphous organic matter, bone fragments, charcoal, humified plant structures, roots and shell remains (Figure 5.118).
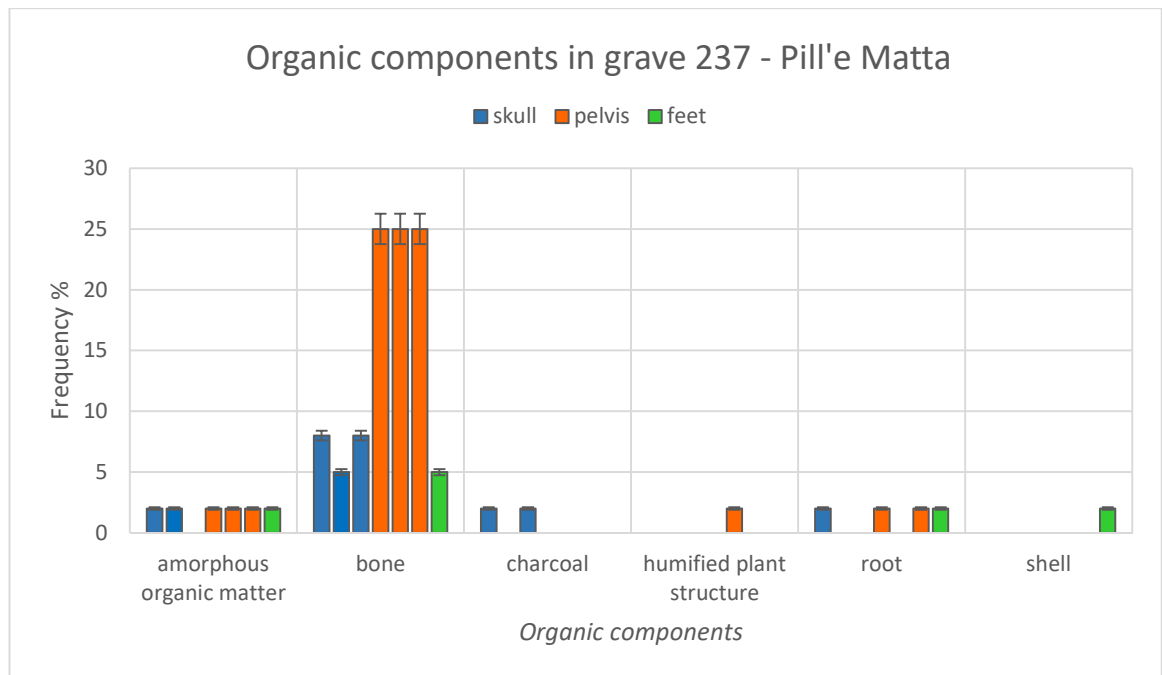
Figure 5.118: Frequency of organic components in relation to their anatomical location within grave 237. Bone fragments were frequent in the area of the pelvis.

Bones were the most common organic remains in all areas, especially in the area of the pelvis, where there were several fragments between 200-2000 μm. The bone was trabecular with sub-rounded voids partially filled with coatings of fine material (type C) and loose discontinuous infillings of the same material. The bone was highly weathered: the colour was light beige/grey in PPL and low order grey birefringent in XPL; no birefringence was visible and the beige colour in XPL suggested that the bone could have been partially phosphatized. The histological structure was corrupted and cracks and black stains occurred (Figure 5.131.a-b).

Low amounts of amorphous organic matter were embedded within the fine material (2%) of the grave, while very few fragments of charcoal were detected in the area of the skull and fragments of humified plant structure in the area of the pelvis. Few traces of fresh roots, red colour in PPL and brown or isotropic in XPL were found in all anatomical locations. Finally, an oval shell (500-2000 μm), partially cracked, was observed in the area of the feet.

PEDOFEATURES

Six types of pedofeature were observed in grave 237: coatings of fine material around mineral components, dendritic Mn nodules, soil micro-fauna faecal pellets, Fe/Mn nodules, loose discontinuous infilling and micritic hypocoatings (Figure 5.119).
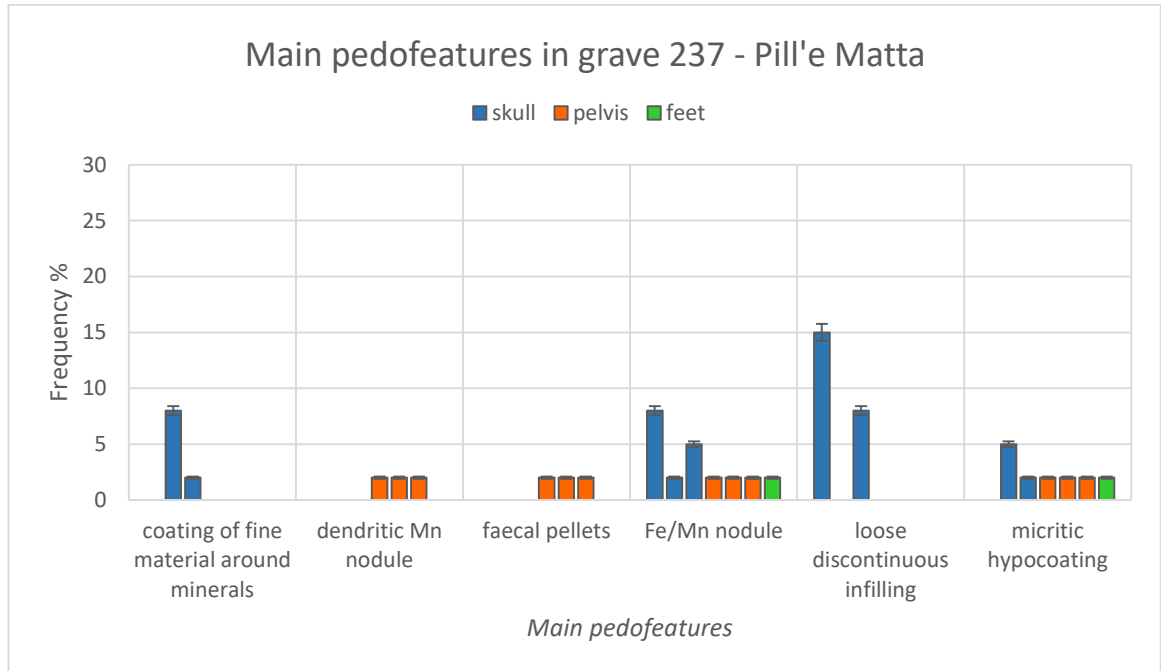
Figure 5.119: Frequency of the main pedofeatures in relation to their anatomical location within grave 237. Soil micro-fauna faecal pellets were present only in the area of the pelvis.

Dendritic Mn nodules appeared with the same characteristics described in the pedofeatures of grave 238 (see above). However, their frequency was lower (2%) and only in the area of the pelvis. Fe/Mn nodules, except for few cases, were smaller than 50 μm and subrounded in shape. They were present in all of the slides (2%) with higher frequency in the area of the skull (5-8%), where they reached coarser dimensions, between 50-500 μm.

Micritic hypocoating had the same aspect of the ones in grave 238 (see above), but they were less frequent: 2% in the areas of the pelvis and feet, 8% in the area of the skull. Coatings of fine material around mineral grains or peds were identified in the area of the skull (2-8%). The fine material was usually of type A around peds of type B. Different types of coatings were the ones mentioned above in the organic components section. It was common to observe coatings of fine material (type C) within the pores of bones from the areas of the pelvis and feet. Loose discontinuous infillings of very fine granules of material A characterized the area of the skull (8-15%). Different loose discontinuous infillings were particular to the area of the pelvis. Sub-rectangular and rounded soil micro-fauna faecal pellets between 50-200 μm, as the ones in grave 237, were identified in some channels and chambers (2%).

GRAVE 268

ELEMENTS OF FABRIC AND PEDS

Samples from grave 268 were composed of Materials A and B. Material A was dominant in the area of the skull (80-95%) and heel (90-95%). It was characterized by porphyric distribution and poor sorting. The fine material was light greyish brown in PPL and yellow/beige in XPL, with opaque limpidity and crystallitic b-fabric. Peds were granular, ultrafine/fine in size, unaccommodated or partially accommodated and with moderate to strong development. Materials A and B were heterogeneous in the area of the pelvis. Material B was characterized by porphyric c/f related distribution and it was well sorted. The fine material was light greyish yellow in PPL and grey in XPL, with masked limpidity and crystallitic b-fabric. The peds were granular, ultrafine to medium, unaccommodated and strongly developed.

VOIDS

Five types of void were observed in grave 268: chambers, channels, cracks, packings and planes (Figure 5.120).
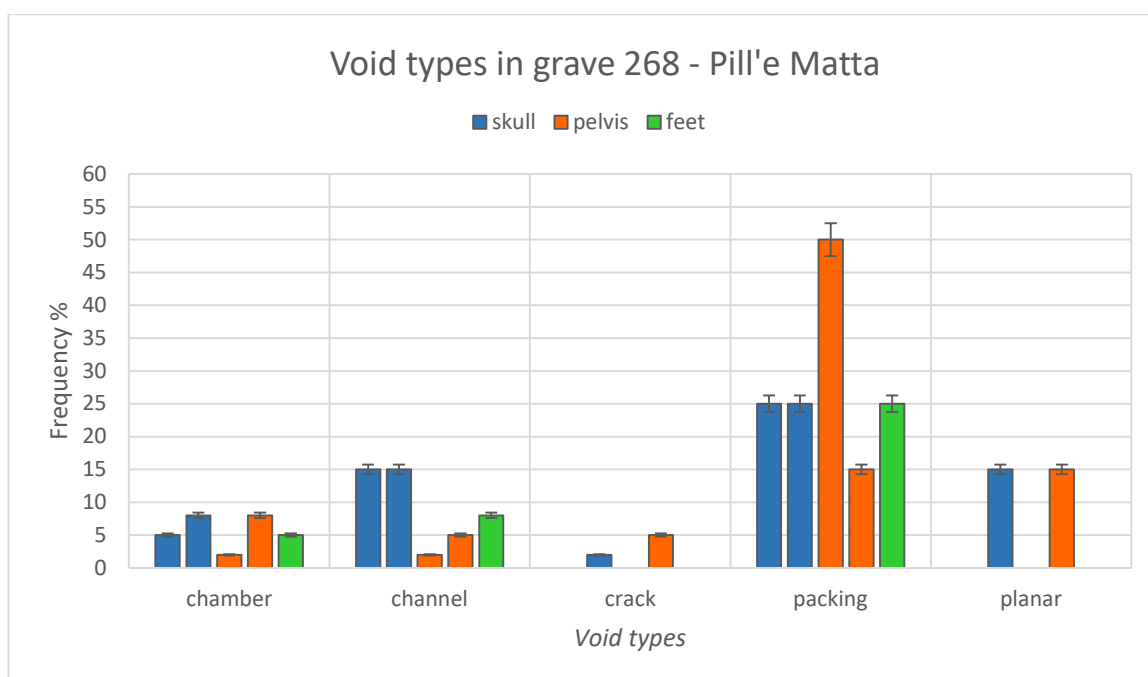
Figure 5.120: Abundances of different types of void in relation to their anatomical location within grave 268. Packing voids were the most frequent, especially in the area of the pelvis.

Chambers were equally distributed in all anatomical locations (2-8%). Channels were more abundant in the area of the skull (15%), while crack appeared only in the area of the skull (2%) and pelvis (5%). Packing voids were the most common (15-25%), mainly in the area of the pelvis (50%). Planar voids were detected in slide 671 from the area of the skull and slide 677 from the area of the pelvis. Both the slides came from samples collected in level *z*, under the skeleton. The thin planes

created a moderately separated platy microstructure, which raised an immediate interest during the first stage of analysis. Additional information concerning the method of sampling adopted for some of the bulk in Pill'e Matta (pouring water on the sediment, testified by some pictures) and about the transportation of the samples, suggests that these planes should be considered to result from sampling and post sampling processes.

MINERAL COMPONENTS

Five main types of mineral component were identified in grave 268: foraminifera, plagioclase, quartz, quartzite rock fragments and rubified rock fragments (Figure 5.121). Foraminifera were equally represented in all of the samples (2%). Plagioclase was detected in the areas of the skull and pelvis (2%), while quartz was present in all of the slides (5%). Very few fragments of quartzite were present in this grave (2%) and rubified rock fragment were slightly more frequent: 2% in the area of the pelvis, 5% in the area of the skull and 8% in the areas of the feet.
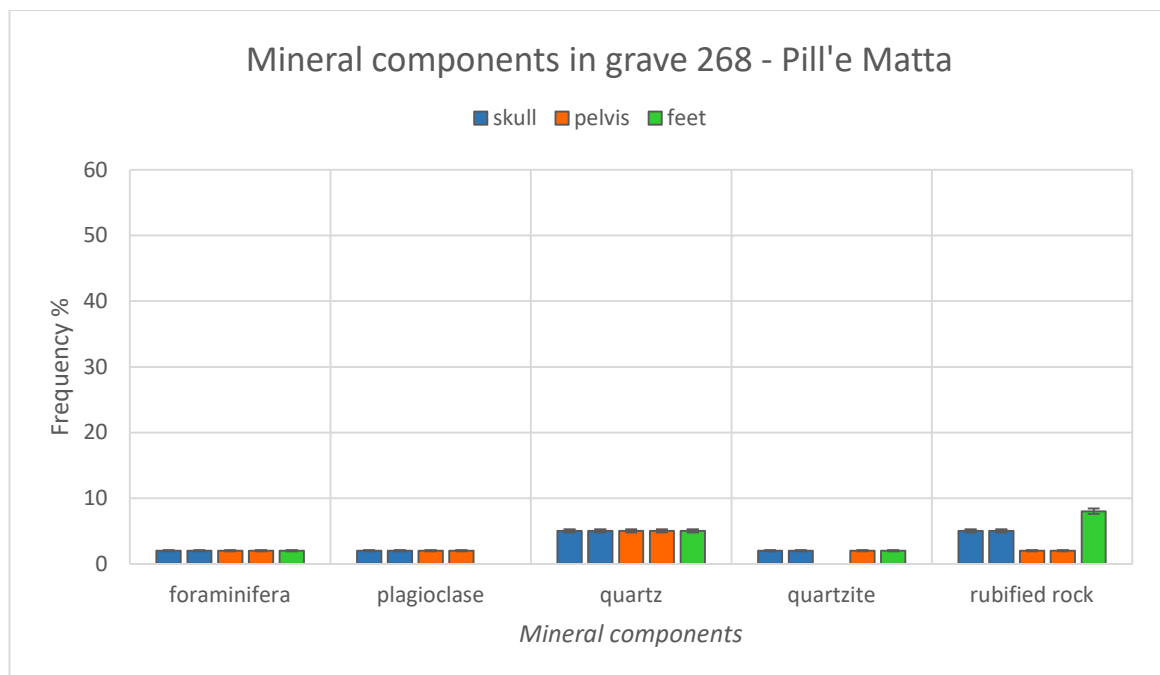
Figure 5.121: Frequency of mineral components in relation to their anatomical location within grave 268. Mineral components were included between 2-5% and the quartz was the most common mineral.

ORGANIC COMPONENTS

Grave 268 was very poor in organic components (Figure 5.122). Partially weathered roots were observed in all of the samples (2%), except for the one collected under the skeleton. Very few fragments of charcoal were present in the area of the skull (2%) and very few humified plant structures were observed in the area of the pelvis (2%). Few examples of ovoid shell were found in the areas of the pelvis and feet. Bone fragments (5%) came from the samples collected under the

skeleton (skull and pelvis). The fragments were relatively small (100-1000 µm), with several cracks, but still light yellow in PPL, with birefringence and without stains (Figure 5.131.c-d).
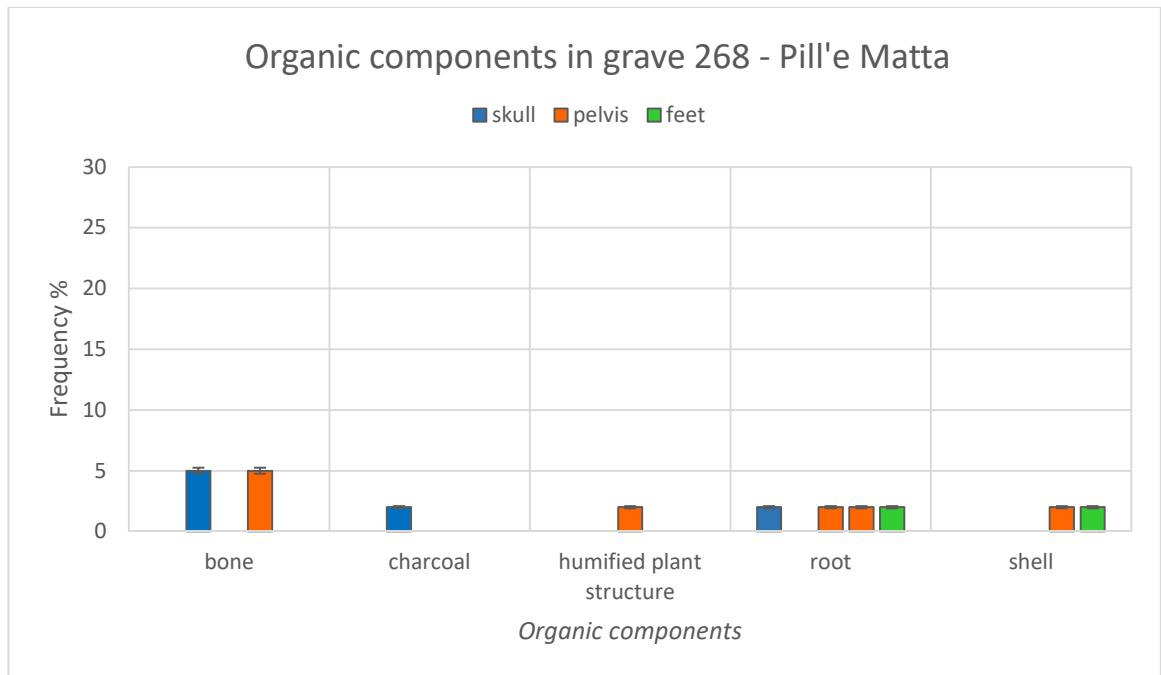
Figure 5.122: Frequency of organic components in relation to their anatomical location within grave 268. Organic components were few represented.

PEDOFEATURES

Five main pedofeatures were observed in grave 268: coatings of fine material around mineral components, dendritic Mn nodules, soil micro-fauna faecal pellets, Fe/Mn nodules and micritic hypocoatings (Figure 5.123). Dendritic Mn nodules had the same characteristics of the ones described in graves 238 and 237. They were present in all of the samples, between 2-5%. Fe nodules were detected in all of the samples with low amounts (2%). Their size was included between 50-200 µm, most similar to the nodules in grave 238. Micritic hypocoatings were the same as those described in the previous graves. Their frequency was 5% in the area of the feet, while there was a difference between samples taken in the *y* or *z* levels. In the level of the bones (*y*), the depletion hypocoatings were very few (2%), while in the level under the skeleton they increased to 8%, both in skull and pelvis area (Figure 5.133.a-b). Coatings of fine material around mineral grains and peds of material B were observed in the area under the skull (5%) and in the area of the pelvis (2% level *y*; 15% level *z*). Soil micro-fauna faecal pellets were identified in the sample from under the pelvis (5%). Their size was 50-120 µm, sub-angular or rounded in shape, light greyish brown in PPL, grey/brown in XPL and with crystallitic or undifferentiated b-fabric.
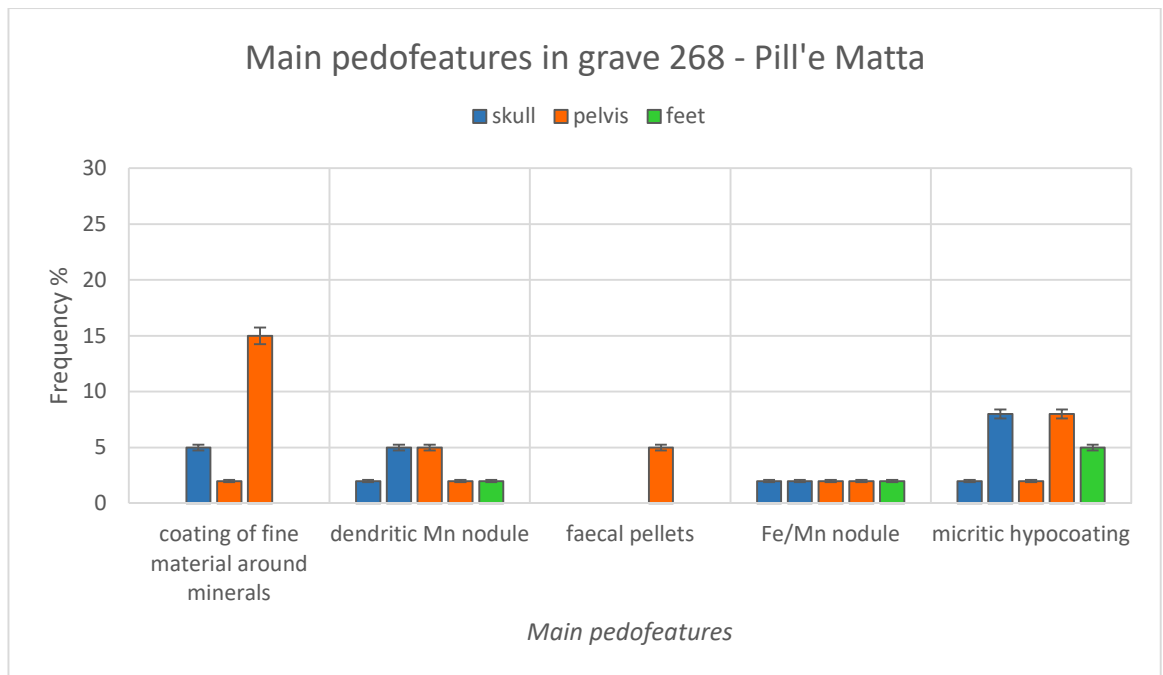
Figure 5.123: Frequency of the main pedofeatures in relation to their anatomical location within grave 268. Soil micro-fauna faecal pellets were found only in the area of the pelvis.

GRAVE US2680

ELEMENTS OF FABRIC AND PEDS

Samples from grave US2680 were composed of Materials A and B (Figure 5.130.a-b). Material A was dominant in all anatomical locations (70-90%). It was characterized by porphyric c/f related distribution and poor sorting. The fine material was light greyish brown in PPL and yellow/beige in XPL, with opaque limpidity and crystallitic B-fabric. The peds were granular, very fine to medium, unaccommodated and weak to strong developed. Material B, less abundant, was porphyric c/f related distributed and moderately sorted. The fine material was light greyish yellow in PPL and grey in XPL, with masked limpidity and crystallitic b-fabric. Peds were granular, very fine to medium, unaccommodated and moderate to strong developed (Figure 5.130.e-f).

VOIDS

Six types of void were observed in the samples: chambers, channels, cracks, packing, planar and vughs (Figure 5.124). The most abundant were packing voids (40%) in all the areas, followed by channels (8-15%) and cracks (5-8%). Chambers were very few in the area of the skull and feet (2%), as were vughs (2-5%). The planar voids were considered to be formed during sampling or post sampling processes, for the same reasons explained for grave 268.
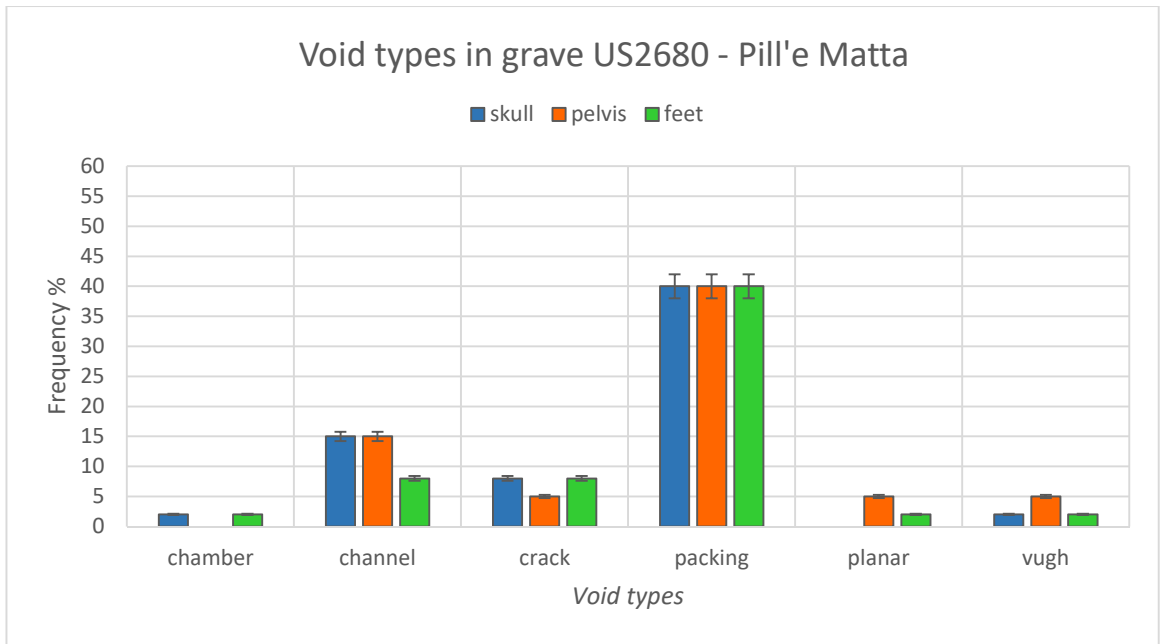
Figure 5.124: Abundances of different types of void in relation to their anatomical location within grave US2680. Packing voids were the most frequent.

MINERAL COMPONENTS

Mineral components were not frequent, though a few more types were detected in this grave: calcite, foraminifera, plagioclase, pyroxene, quartz, quartzite and rubified rock fragments (Figure 5.125).
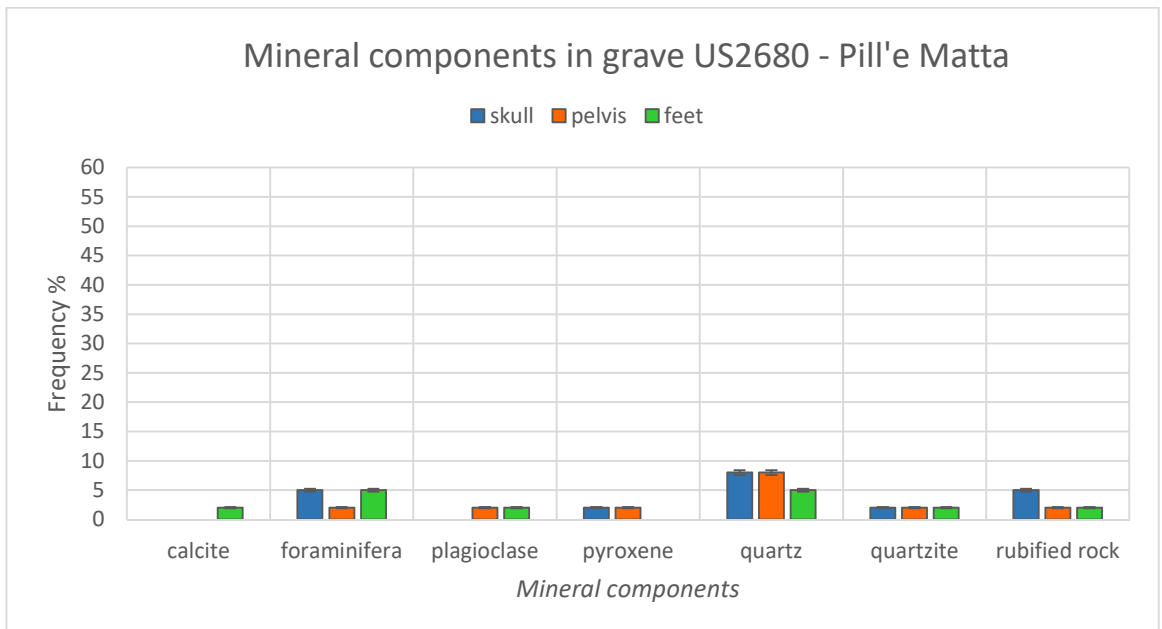
Figure 5.125: Frequency of mineral components in relation to their anatomical location. Quartz was slightly more abundant than the other minerals.

Quartz was the most frequent mineral (5-8%), while quartzite fragments were very few (2%). Pyroxene grains were observed in the skull and pelvis areas (2%), plagioclase grains in the areas of the pelvis and feet (2%) and calcite fragments in the location of the feet (2%). Rubified rock fragments were more frequent in the sample of the skull (5%) and fewer in the area of the pelvis and feet (2%).

ORGANIC COMPONENTS

Grave US2680 had very few organic components (Figure 5.126). Small bone fragments (50-500 µm) were present in the area of the feet (2%), fragments of charcoal (2%) in the areas of the pelvis, while sections of weathered roots (Figure 5.131.e) were sporadic in all their anatomical locations (5-8%).
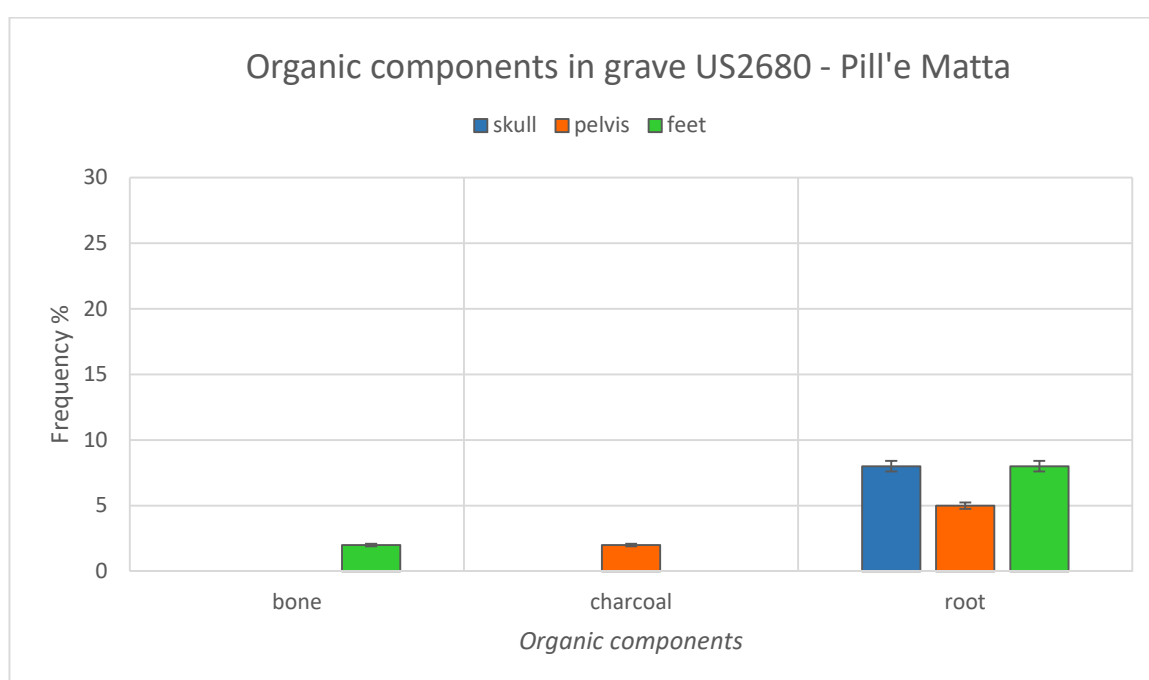
Figure 5.126: Frequency of organic components in relation to their anatomical location within grave US2680.

PEDOFEATURES

Five types of pedofeature were detected in grave US2680: coatings of fine material around mineral grains or peds, dendritic Mn nodules, soil micro-fauna faecal pellets, Fe/Mn nodules and micritic hypocoatings (Figure 5.127).

Dendritic Mn nodules were constantly abundant in all of the samples (8%), while Fe nodules were more frequent and coarser in the area of the skull (5%; 50-300 µm) than the areas of the pelvis and feet (2%; 50-100 µm). Micritic hypocoatings were only present in the area of the skull and feet (5%). Coatings of fine material were more abundant in the area of the pelvis (15% against 5% in the area

of the feet and 8% in the area of the skull). Soil micro-fauna faecal pellets were observed in the areas of the skull and pelvis (5%). The first were smaller than usual, between 20-50 μm, rounded in shape, brown in PPL and brown or isotropic in XPL, without b-fabric. They were located within weathered reddish brown roots (Figure 5.131.g-h). The second were of the same type as in the previous graves: 50-120 μm, sub-angular/sub-rounded in shape, light greyish brown in PPL and grey/beige in XPL, with crystallitic or undifferentiated b-fabric.
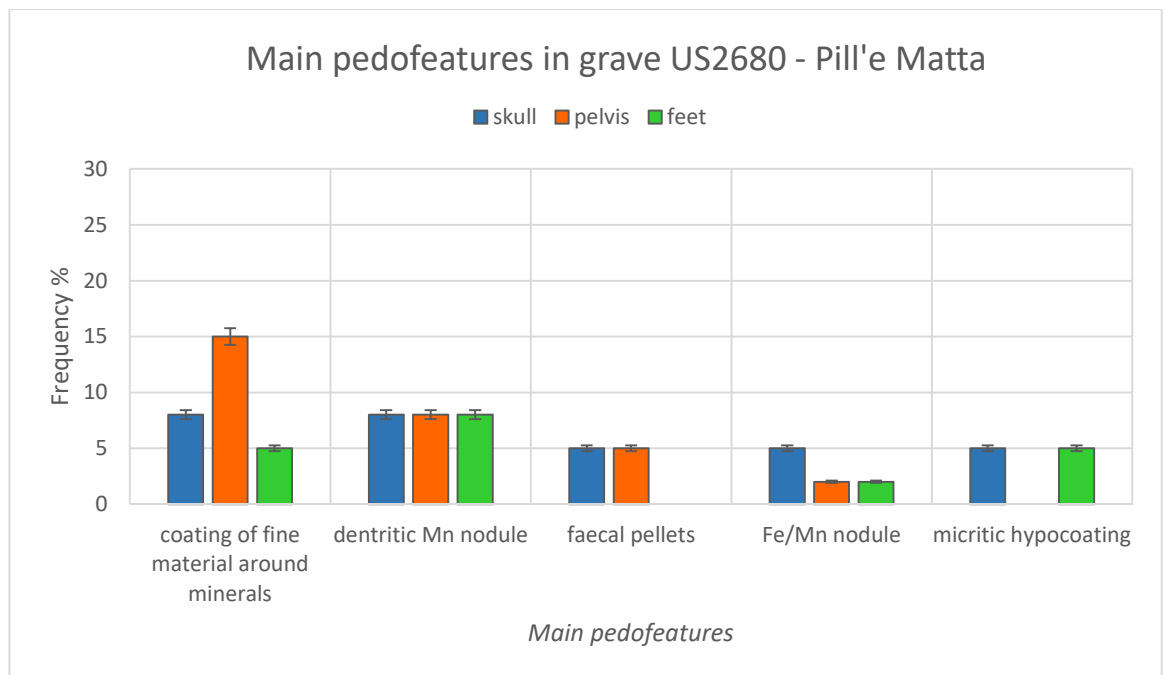
Figure 5.127: Frequency of the main pedofeatures in relation to their anatomical location within grave US2680. Soil micro-fauna faecal pellets were observed in the areas of the skull and pelvis.

CONTROLS C1

Voids were not recorded in the analysis of the following slides, because the samples were made of loose material. Consequently, the original shapes of voids were not preserved.

C1 a (0-14 cm from the top of soil profile): two materials A (40%) and B (20%) characterized this layer. 40% of the slide was represented by coarse material. Both A and B were porphyric c/f related distributed and poorly sorted. Fine material in A was light greyish brown in PPL and yellow/beige in XPL, with opaque limpidity and crystallitic b-fabric. Fine material in B was light greyish yellow in PPL and grey in XPL, with masked limpidity and crystallitic b-fabric. Granular peds were distinctive of both materials. Their shape was angular for the coarser peds and sub-angular or sub-rounded for the smaller ones. Some granules were composed of both materials. Their size was variable, because the sediment was fragile and the sample was composed by disturbed loose material. No pedofeatures were observed in this sample.

C1 b (14-17 cm from the top of soil profile): material A characterized this layer. It had c/f related distribution and was poorly sorted. The fine material was light greyish brown in PPL and yellow/beige in XPL, with opaque limpidity and crystallitic b-fabric. The peds were granular, from angular to sub-rounded; also in this case the size changed considerably owing to the fragility of the sediment. Micritic hypocoatings (2%) around voids were observed. Their size was between 500-2000 µm, sub-rounded, with undulating surface and not weathered.

C1 c (67-88 cm from the top of soil profile): materials A (35-45%) and B (55-65%) characterized this layer. Both materials had porphyric c/f related distribution and poor sorting. Fine material in A was light greyish brown in PPL and yellow/beige in XPL, with opaque limpidity and crystallitic b-fabric. Fine material in B was light greyish yellow in PPL and grey in XPL, with masked limpidity and crystallitic b-fabric. Granular peds had angular shape, the coarser ones being sub-angular to sub-rounded. Some granules were composed of both materials. The size of peds, also in this case, was variable owing to the fragility of the sample. Dendritic Mn nodules were detected in both materials, while very few loose discontinuous infillings of calcified filaments in voids were identified only in material B.

C1 d (88-98 cm from the top of soil profile – bottom of the grave): materials A (98%) and B (2%) characterized this layer. Both materials had porphyric c/f related distribution and poor sorting. Fine material in A was light greyish brown in PPL and yellow/beige in XPL, with opaque limpidity and crystallitic b-fabric. Fine material in B was light greyish yellow in PPL and grey in XPL, with masked limpidity and crystallitic b-fabric. Granular peds had angular shape, the coarser ones being sub-angular to sub-rounded. Dendritic Mn nodules, loose discontinuous infilling of calcified filaments in voids and micritic hypocoatings around voids were detected in material A.

5.5.4 SEM-EDS RESULTS

Graves 238 and 237 were the only two having photographic documentation. From Figures 5.107 and 5.108, it was observed that the skeleton in grave 238 was well preserved, while that in grave 237 was highly fragmented and nearly disappeared. SEM-EDS analysis was applied to the fine material of these two graves to investigate if differences were apparent. In addition, SEM-EDS analysis was conducted on micritic hypocoatings from graves 237, 238 and 268, in order to better characterize the different layers of this common pedofeature. The layers were distinct in external, internal and infilling within the void. The external layer had lighter colour under petrographic microscope and was less bright under SEM. On the contrary, the internal layer was darker under petrographic microscope and brighter under SEM (Section 6.4.6). The infilling, if present, was generally more crystallitic. Measurements were taken at distinct points and weight (%) of chemical components was recorded. The data presented in the box-plots were not normalized and the measurements of O and C were omitted, because they are affected by the presence of the resin used to impregnate the blocks. The data were thus overestimated, but this choice was preferred to the one of underestimating them, to have clear visibility of the components. Na, Mg, Al, Si, K, Ca and Fe were considered as they showed more variability and higher concentrations. Components with less than 0.1% weight were excluded.

Analysis of fine material did not show any significant differences between the two graves and among the various anatomical locations (Figure 5.128). Although the median of the box-plots indicated variability within the same chemical component, the upper and lower extremes, as well as the upper and lower quartiles were included in the same ranges. Si and Ca were the most abundant components, followed by Al, Fe and K. Only traces of Mg and Na were recorded. The same variability was recorded in the micritic hypocoatings (Figure 5.129). In particular, the levels of Ca did not show differences between the internal and external layers, as would have been expected in micritic depleted pedofeatures. The median of the internal layer was at 14%, while the one of the external layer was 20%. However, the upper and lower extremes of the internal layer overlapped the ones of the external layer. Accordingly, the denomination of micritic hypocoating for this pedofeatures could have been incorrect. The discussion about this interpretation is developed in Chapter 6.

The following figures were selected as representative of the features described in Section 5.5.3:

- Figure 5.130: fine material and peds;

- Figure 5.131: organic components;

- Figure 5.132: fungal activity;

- Figure 5.133: pedofeatures (micritic hypocoatings, infillings of calcified filaments and infillings of soil micro-fauna faecal pellets).
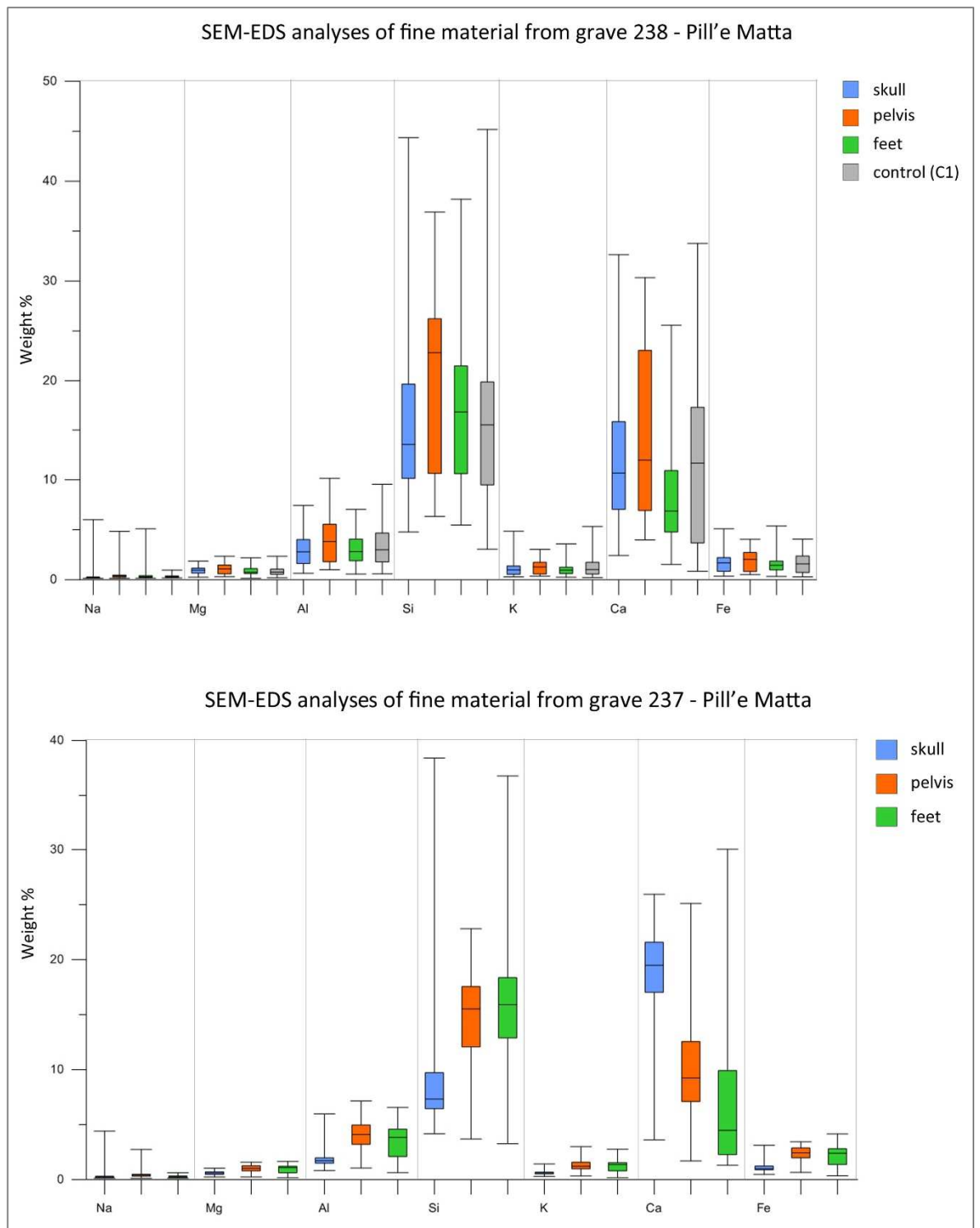
Figure 5.128: Box-plots showing the results of SEM-EDS analyses of fine material in graves 238 and 237.
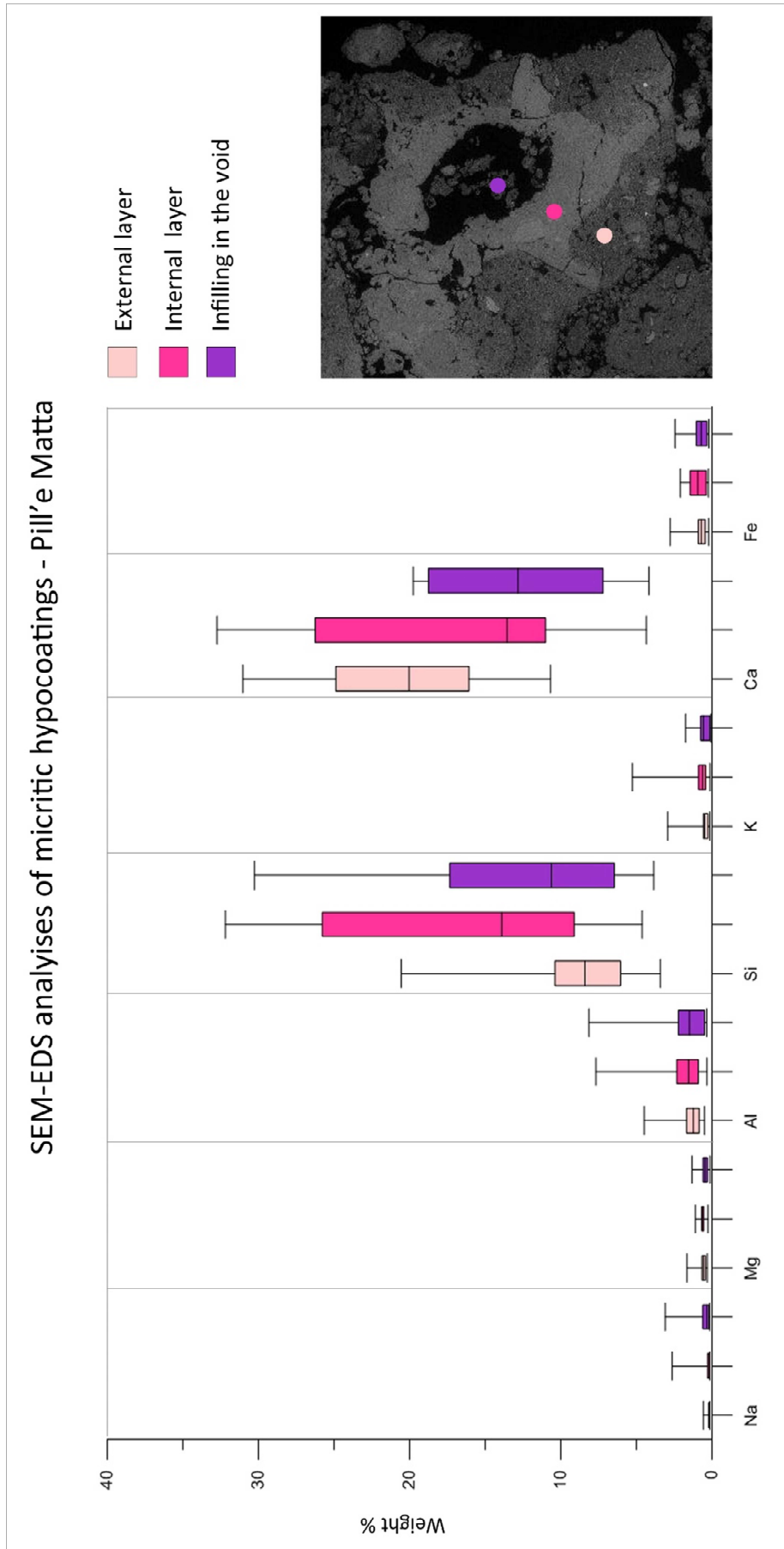
Figure 5.129: Box-plot showing the results of SEM-EDS analyses on micritic hypocoatings. On the right, an example of the pedofeature. The picture was taken under SEM and a difference in colour between the two layers was visible.
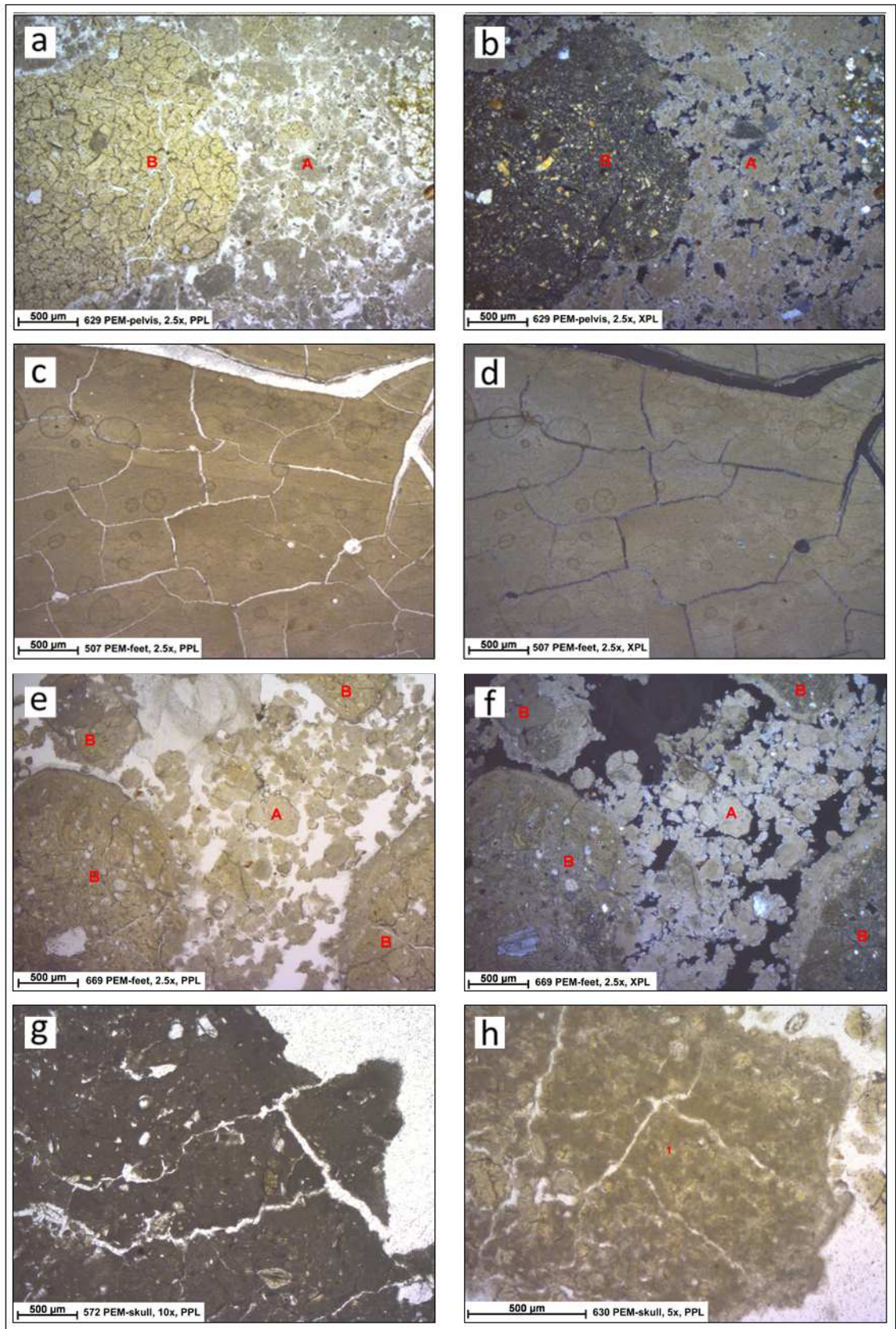
Figure 5.130: Fine material and peds in Pill'e Matta. a-b) fine material of types A and B from the area of the pelvis in grave US2680 in PPL (a) and XPL (b); c-d) fine material of type C from the area of the feet in grave 237 in PPL (c) and XPL (d); e-f) granular peds from the area of the feet in grave US2680 in PPL (e) and XPL (f); g) angular peds from the area of the skull in grave 237; h) angular peds from the area of the skull in grave 268.

223
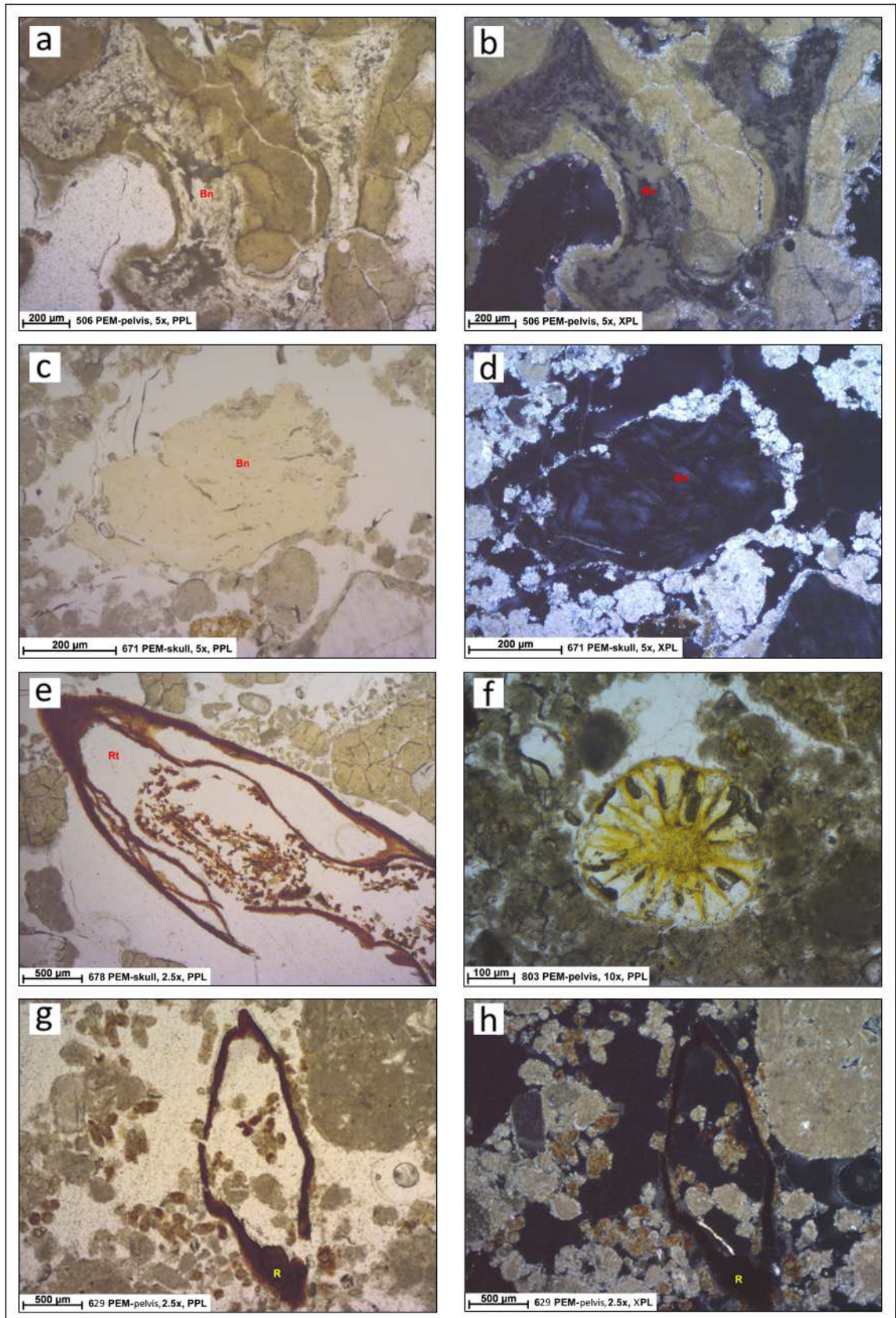
Figure 5.131: Organic components in Pill'e Matta. a-b) weathered bone (Bn) from the area of the pelvis in grave 237 in PPL (a) and XPL (b); c-d) partially weathered bone (Bn) from the area of the skull in grave 268 in PPL (c) and XPL (d); e) partially weathered root (Rt) from the area of the skull in grave US2680; f) fresh root from the area of the pelvis in grave 238; g-h) partially weathered root (R) with soil micro-fauna faecal pellets from the area of the pelvis in grave US2680 in PPL (g) and XPL (h).
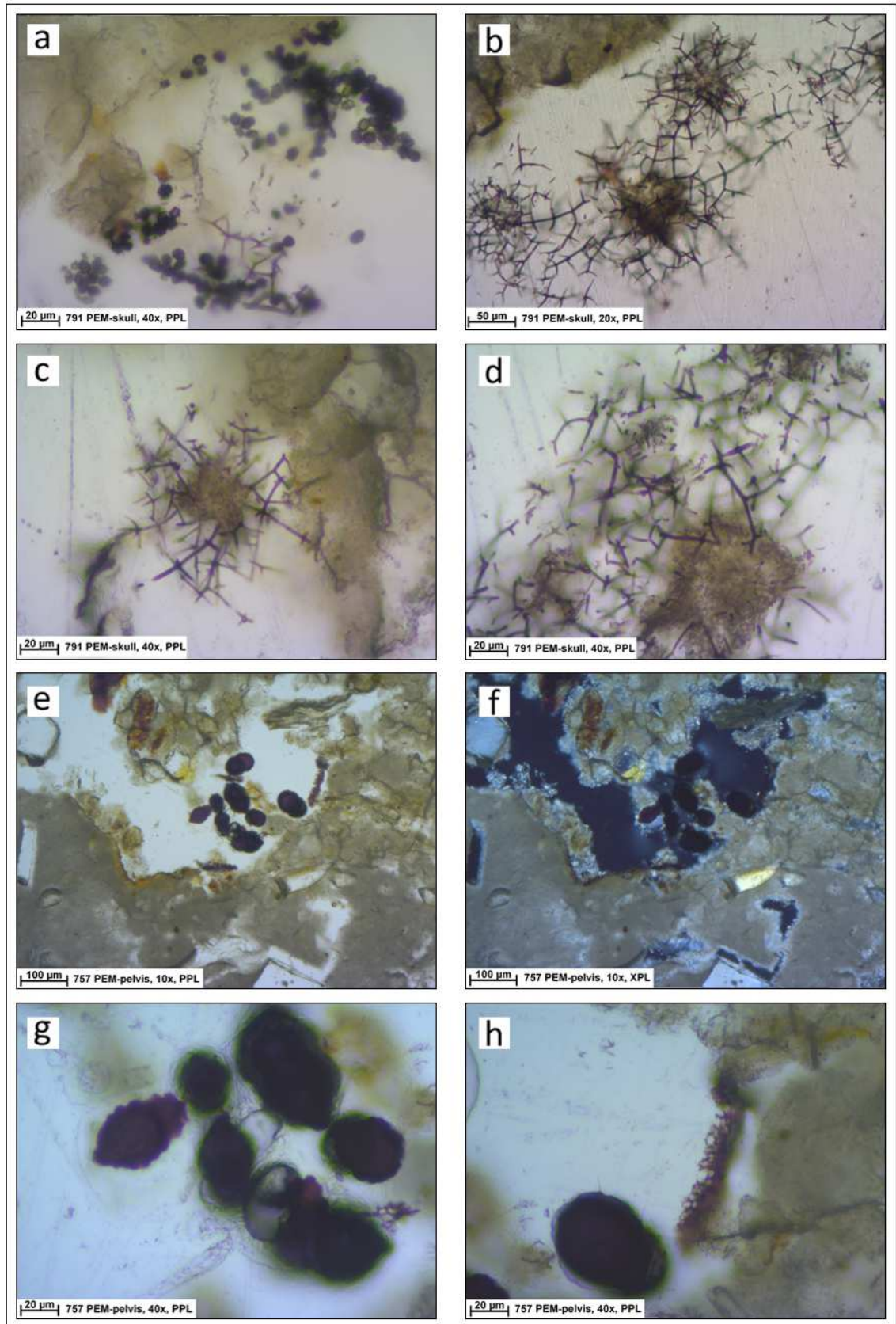
Figure 5.132: Fungal remains in Pill'e Matta. a) fungal spores from the area of the skull in grave 238; b-c-d) fungal hyphae and spores from the area of the skull in grave 238; e-f) Ulocladium from the area of the pelvis in grave 238 in PPL (e) and XPL (f); g-h) details of the anatomy of Ulocladium.
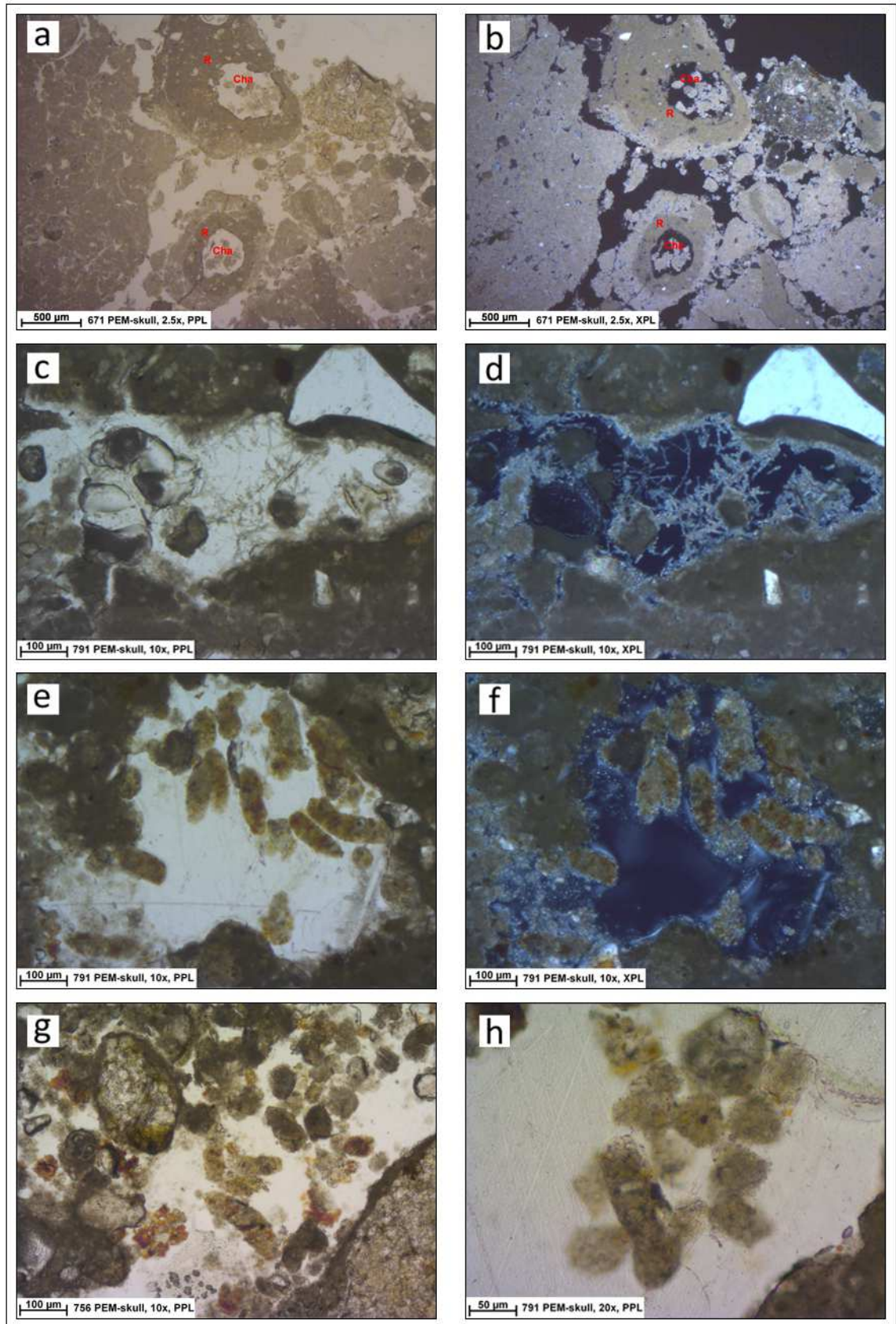
Figure 5.133: Pedofeatures in Pill'e Matta. a-b) micritic hypocoatings (R= hypocoating, Cha= chamber with infilling) from the area of the skull in grave 268 in PPL (a) and XPL (b); c-d) loose discontinuous infilling of calcified filaments in voids from the area of the skull in grave 238 in PPL (c) and XPL (d); e-f) infilling of soil micro-fauna faecal pellets in void from the area of the skull in grave 238 in PPL (e) and XPL (f); g-h) infilling of soil micro-fauna faecal pellets from the area of the skull in grave 238.

226

5.6 EXPERIMENTAL PIGLET BURIALS (UK). 2009-2013

Experimental burials of ten stillborn piglets were accomplished in 2009 in five different locations of Yorkshire (Figure 5.134) and the skeletons of these piglets were exhumed during the summers of 2012 and 2013 by the InterArChive team. The aim of the experiment was to provide reference samples, to compare with the ones from the archaeological sites investigated in the InterArChive project. The locations encompassed different soil contexts and the piglets were buried with or without coffin and with different grave fill, to expand the range of possible results and correspondence with archaeological graves. The list of the piglets, the type of soil of the site and the type of matrix used to fill the grave are indicated in Appendix 1.2.
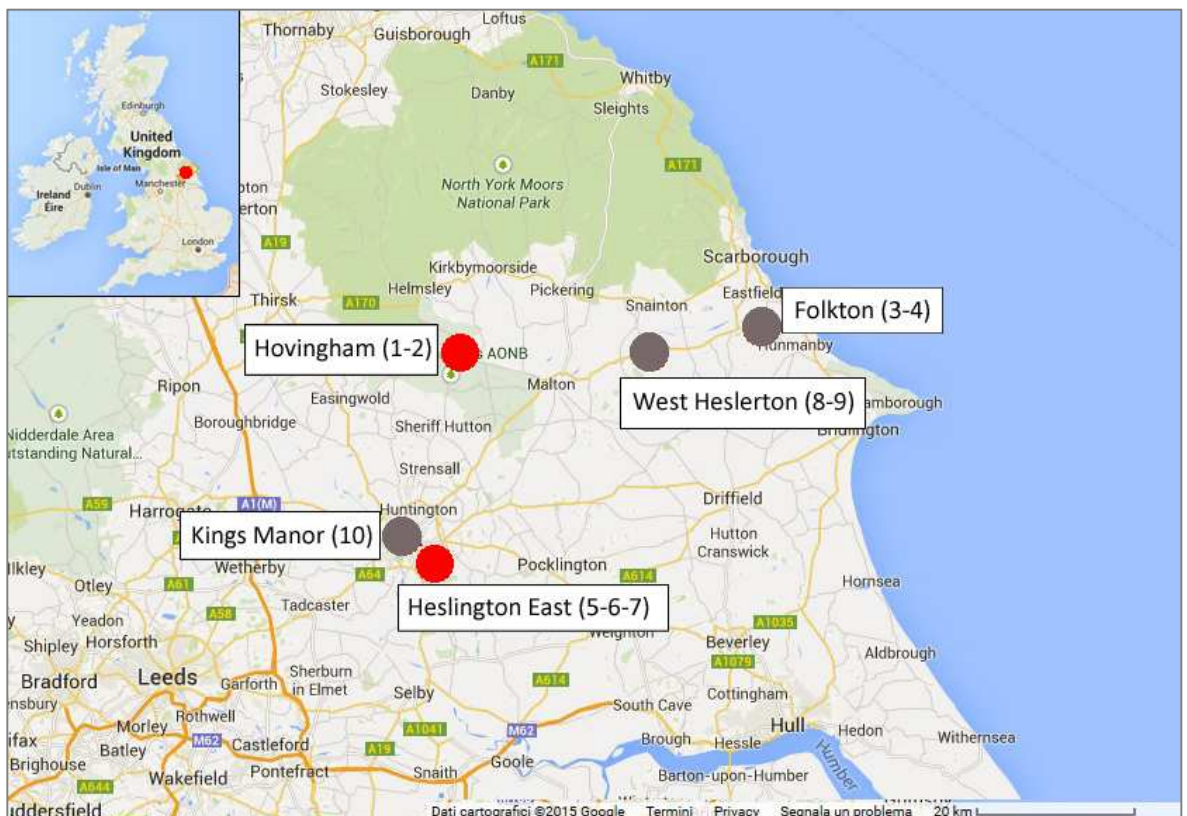
Figure 5.134: Map with the locations of the experimental burials. Piglets 1 and 2 in Hovingham; piglets 3 and 4 in Folkton; piglets 5-6-7 in Heslington East (York), piglets 8-9 in West Heslerton and piglet 10 in Kings Manor (York). The locations of the piglets analysed in this research (2, 6 and 7) are highlighted in red.

5.6.1 THE BURIALS

Piglets 2 from Hovingham and 6 and 7 from Heslington East were investigated in this research (Table 5.6). Piglet 2 (Figure 5.135) was buried in a coffin in a pit dug into a dark brown organic rich sediment, lined with plywood and filled with imported limestone. The coffin comprised a box made of plywood and filled with the same limestone. The coffin was located at ca. 30-40 cm from the top of the pit.

Piglets 6 (Figure 5.136) and 7 (Figure 5.137) were placed next to each other in local soil and divided by a sheet of plywood. Piglet 6 was placed in contact with the soil, while piglet 7 was buried in a coffin, which was filled by local soil to simulate the natural situation occurring when sediments penetrated the casket. The burials were located in the area next to the archaeological site of Heslington East, on the south-east of the city of York, frequented from Bronze Age to Iron Age. The northern corner of the site was characterized by a glacial moraine, from which a smooth slope developed (O'Connor et al. 2011). The piglets were buried in the higher part of the slope, location not more precisely defined. The subsoil parent material was composed of glaciofluvial silts, sands and gravels with water channels developed along the moraine. Thus, the local soil was frequently waterlogged (O'Connor et al. 2011). The burials were accompanied by organic materials, placed next to or inside the piglets:

- one muslin bag in the stomach, containing: rolled oats (25 g), desiccated coconut (25 g), dried clementine peel (5 g), dried apple peel (~2 g), ground ginger (1 teaspoon), ground cinnamon (1 level teaspoon) and red kidney beans (25 g);
- one muslin bag close to the mouth, containing: florets of cloves (60 g), amber leaf tobacco (5 g) and beeswax (5 g);
- one wicker small basket in the burial of piglet 2;
- human head hair placed around the neck;
- leather boots on back feet of piglets 6 and 7.

Piglets 2, 6 and 7, at the moment of the excavation, were skeletonized with little evidence of preservation of the skin, but presence of a hard and fragile crust. Empty spaces were left by the decomposition of the body. Remains of partially preserved basket and fibres were detected and sampled for the organic chemistry analysis (not part of this research).

Despite the precise recording of all of the information on the location of the Kubiena tins during the sampling, the orientation of all of the samples from piglet 6 and of two samples from piglet 7 were irretrievably lost by the technician during the preparation of the slides (see table in Appendix 1.5).

EXPERIMENTAL BURIAL	DATE	TYPE	SKELETON INFORMATION and grave-goods	SOIL TYPE	CLIMATE
2	2009-2012	Wooden coffin	At the moment of the burial: Muslin bag in the stomach (rolled oats, desiccated coconut, dried clementine peel, dried apple peel, ground ginger, ground cinnamon and red kidney beans); Muslin bag close to the mouth (cloves, amber leaf tobacco and beeswax); Wicker small basket; Human head hair.	Imported limestone inside and outside the coffin; Dark brown organic rich sediment on the top	Temperate oceanic
6	2009-2012	Without coffin	At the moment of the burial: Muslin bag in the stomach (same content of Piglets 2 and 7); Muslin bag close to the mouth (same content of Piglets 2 and 7); Human head hair; Leather boots on back feet.	Sandy clay, water-logged	Temperate oceanic
7	2009-2012	Wooden coffin	At the moment of the burial: Muslin bag in the stomach (same content of Piglets 2 and 6); Muslin bag close to the mouth (same content of Piglets 2 and 6); Human head hair; Leather boots on back feet.	Sandy clay (inside and outside the coffin), water-logged	Temperate oceanic

Table 5. 6: Summary of the information regarding the experimental burials of piglets.

PIGLET BURIAL 2
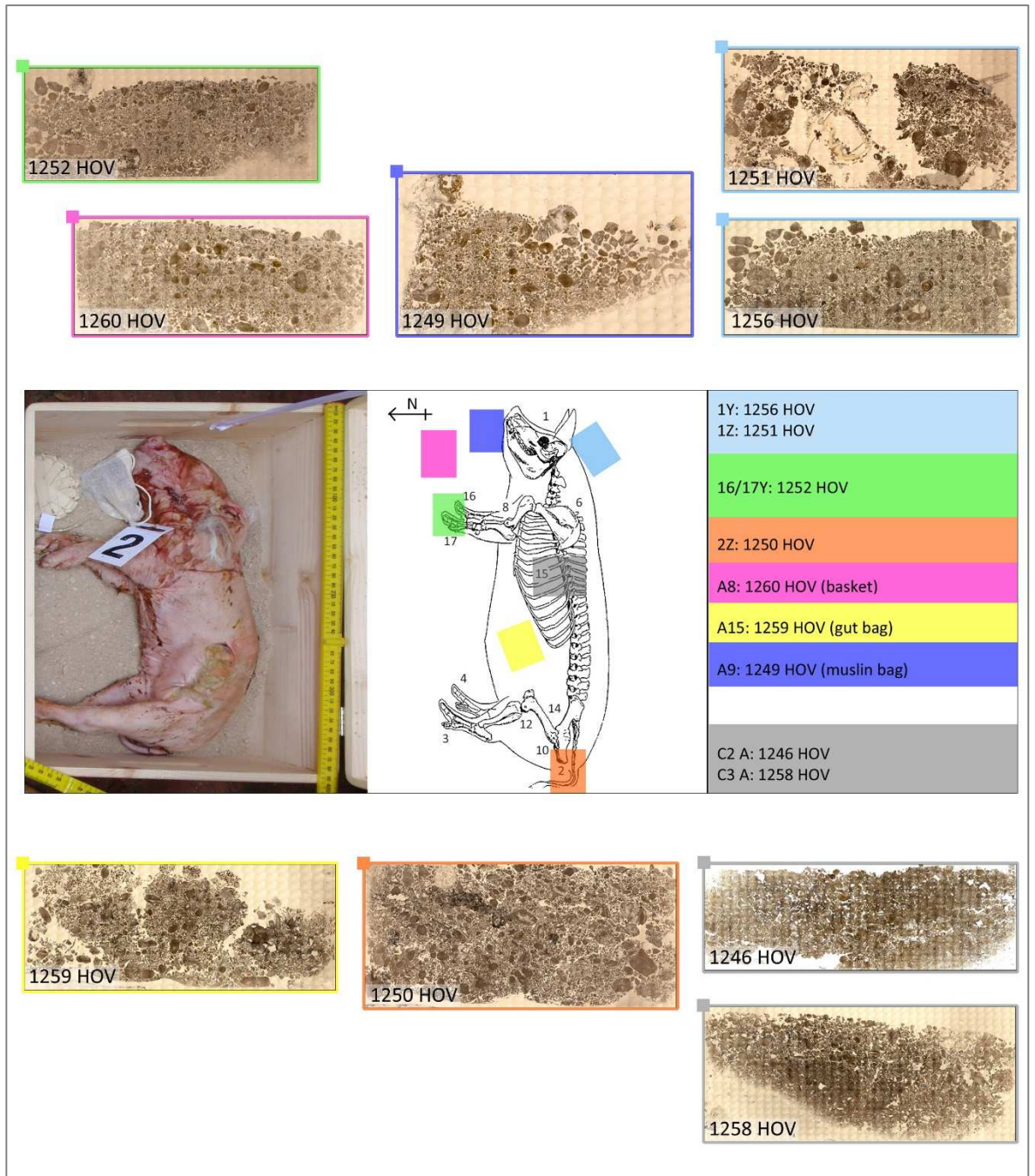
Figure 5.135: Piglet burial 2. In the centre, photograph of the piglet before the burial and list of the slides in relation to their anatomical location. On the top and bottom, mosaics of the slides. See the text for descriptions.
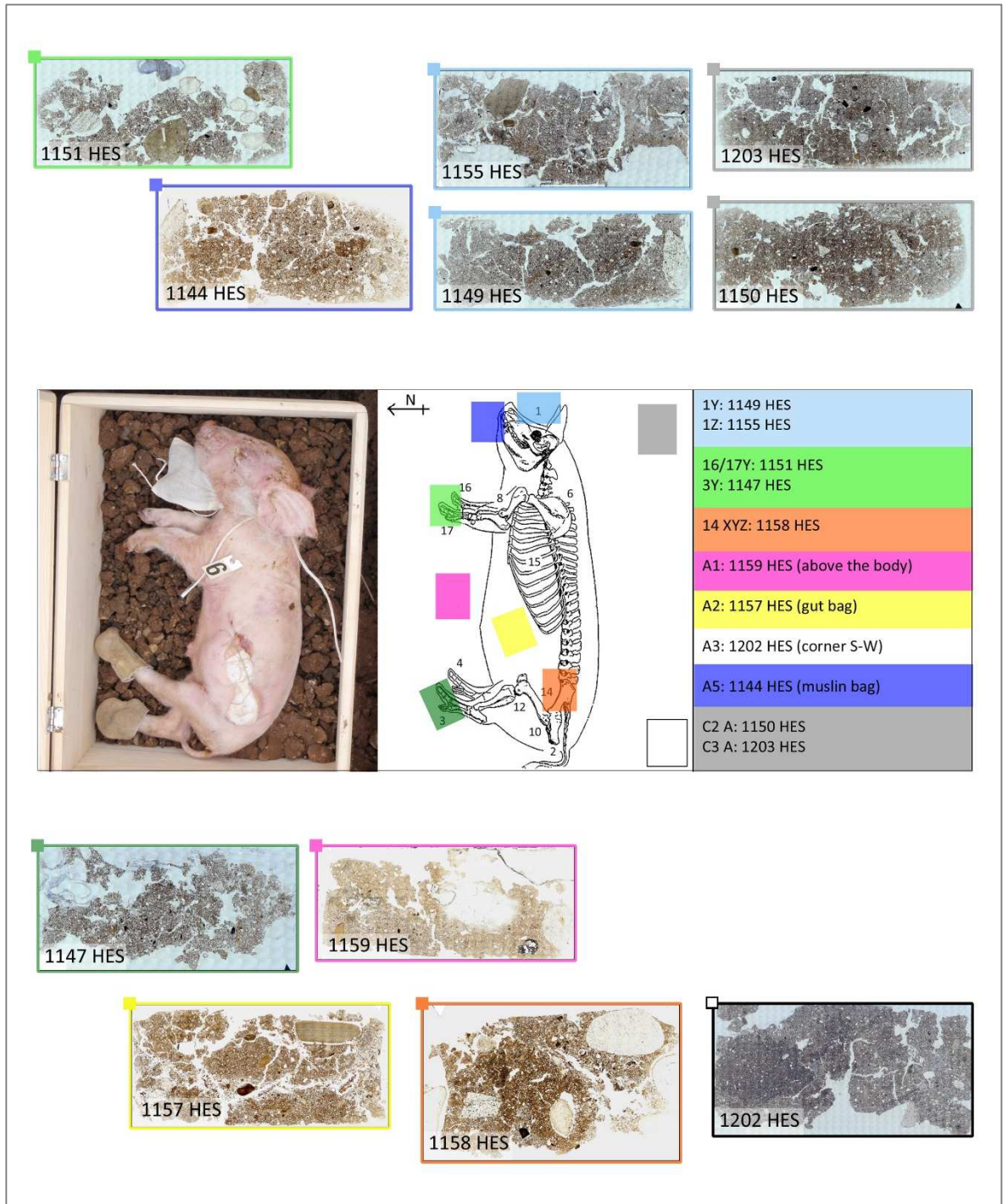
Figure 5.136: Piglet burial 6. In the centre, photograph of the piglet before the burial and list of the slides in relation to their anatomical location. On the top and bottom, mosaics of the slides. See the text for descriptions.
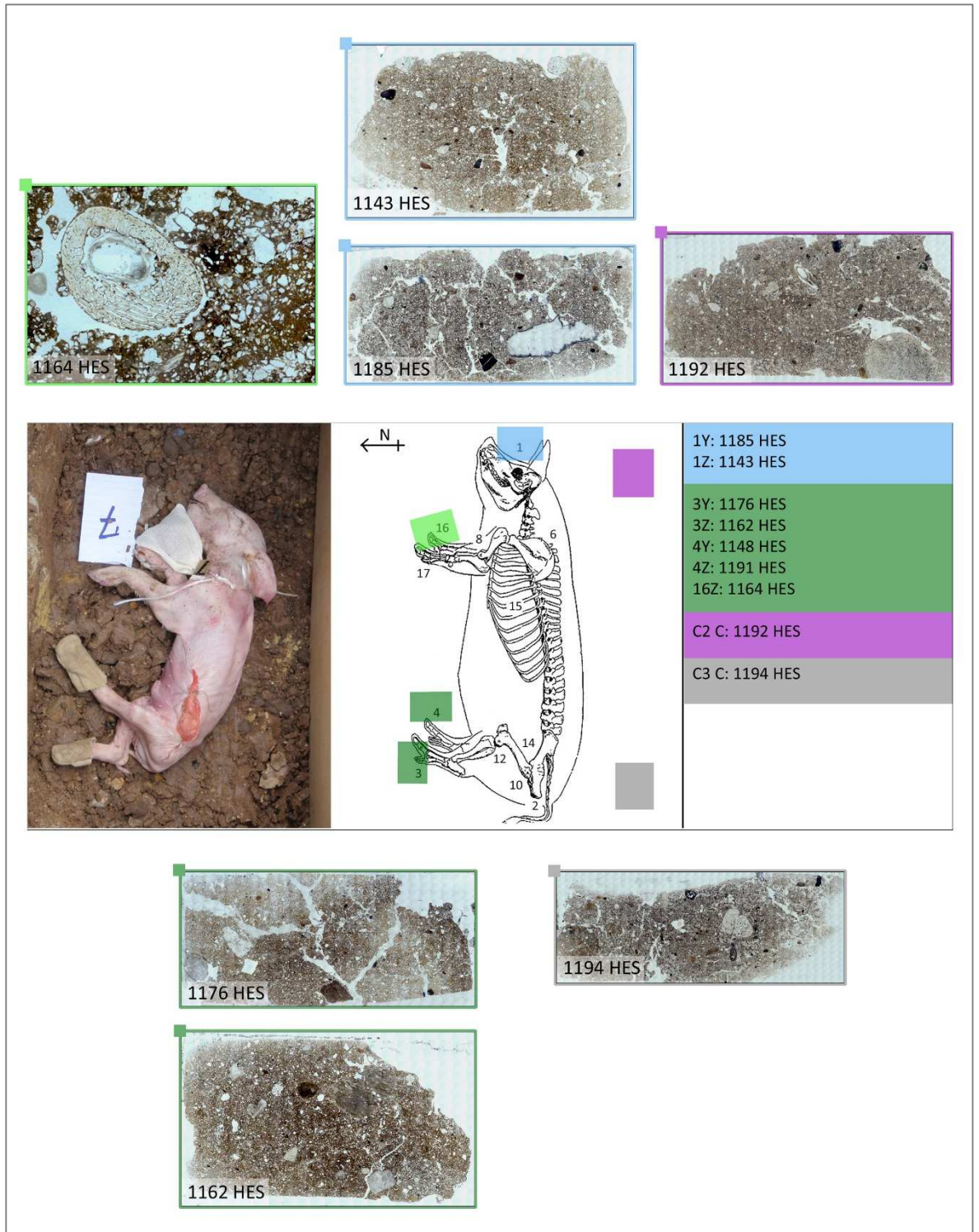
Figure 5.137: Piglet burial 7. In the centre, photograph of the piglet before the burial and list of the slides in relation to their anatomical location. On the top and bottom, mosaics of the slides. See the text for descriptions.

5.6.2 MICROMORPHOLOGICAL RESULTS

PIGLET BURIAL 2

ELEMENTS OF FABRIC AND PEDS

Fabric in burial 2 was characterized by fine monic or open space porphyric c/f relate distribution and well sorting. Fine material was highly represented in all the areas around the skeleton (65-80%) and more abundant in the controls (75-90%). The colour was light grey in PPL and beige/pink/green in XPL, with limpid or dotted limpidity and crystallitic b-fabric. The peds were granular, occupying more than 50% of the slides, very fine to fine in size, unaccommodated and strong developed. Peds in control C3 A were less developed and they looked as though they were fused together.

VOIDS

Two types of void were observed in piglet burial 2: packing and vughs (Figure 5.138). Packing voids were abundant in all of the samples (25%) and less represented in the controls (15% in C3 A and 8% in C2 A). By contrast, very few vughs were detect in control C2 A (5%).
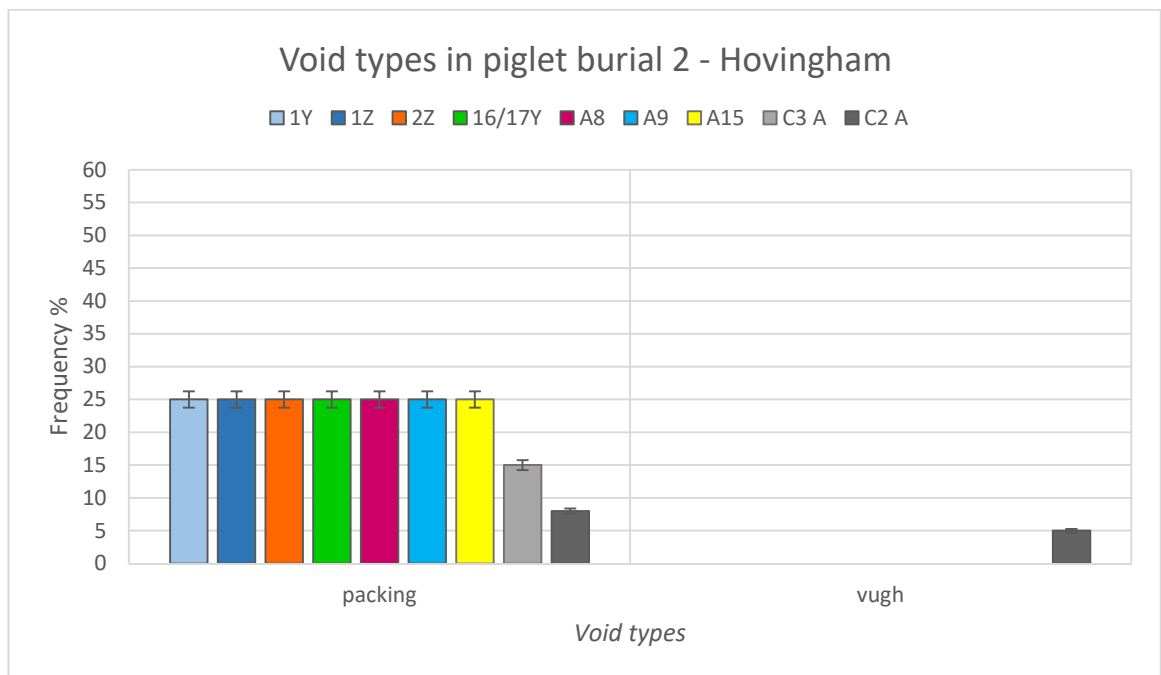
Figure 5.138: Abundances of different types of void in relation to their anatomical location within piglet burial 2. Packing voids were nearly exclusive.

MINERAL COMPONENTS

Quartz was the only coarse-grained mineral component (5%), between 100-300 μm and sub-angular in shape, excluding the carbonate of the limestone (Figure 5.139).
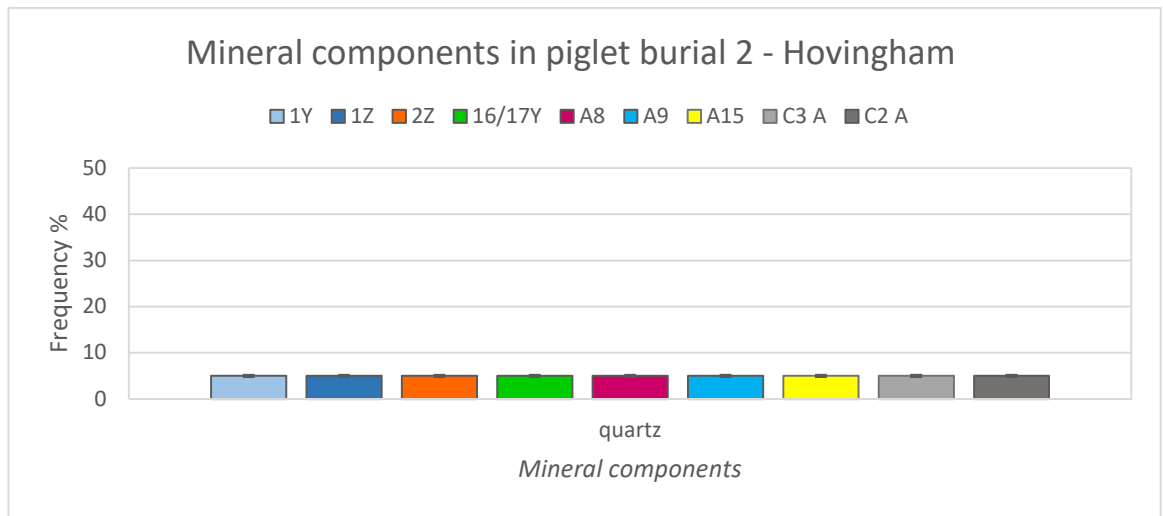
Figure 5.139: Frequency of mineral components in relation to their anatomical location within piglet burial 2. Quartz was the only mineral component.

ORGANIC COMPONENTS

Nine types of organic component were identified in piglet burial 2: bone fragments, fungal hyphae, fungal spores, humified plant structures, roots, sclerotia, seeds and teeth (Figure 5.140).
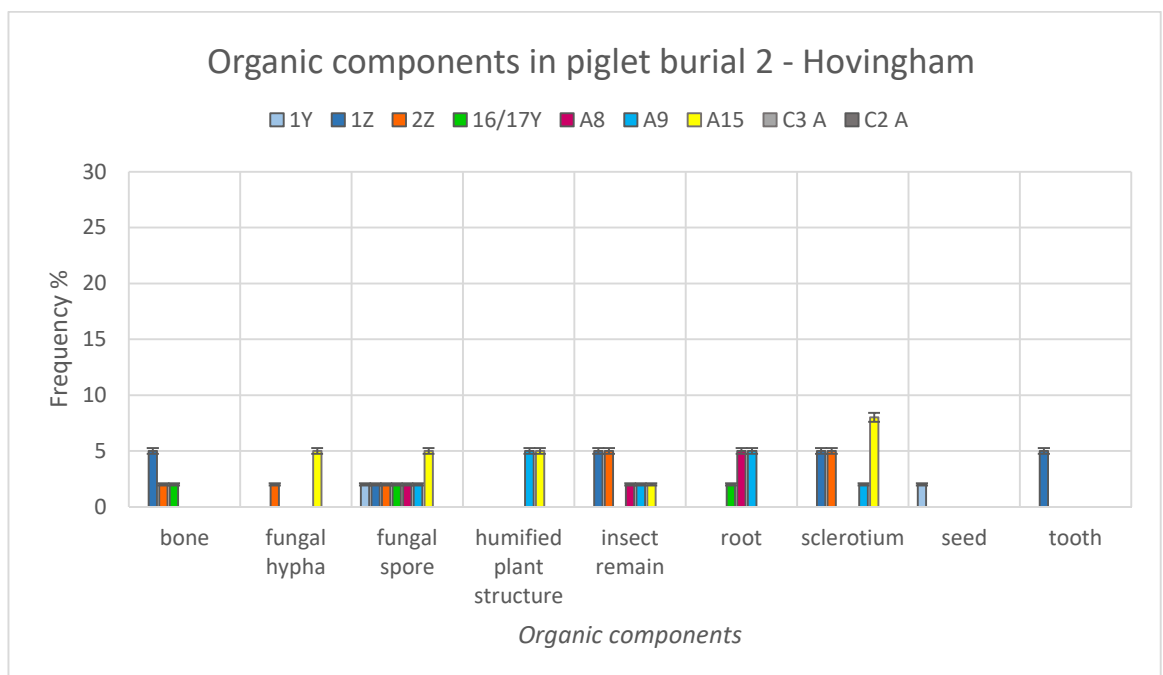
Figure 5.140: Frequency of organic components in relation to their anatomical location within piglet burial 2. Fungal activity, insect remains, plant and bones fragments were documented.

Bone fragments were few (5%) in the area of the skull (*z*) and very few in the areas of the pelvis and feet (2%) (Figure 5.150.a-b, e-f). They were partially weathered, light yellow in PPL and low order grey birefringent in XPL. The trabecular bone fragments from the areas of the pelvis and feet were infilled by soil micro-fauna faecal pellets. One tooth, partially weathered and surrounded by faecal pellets, was observed in the area of the skull (*z*) (Figure 5.150.c-d). Humified plant structures were present in the areas of the muslin bags from the snout and gut (5%). They were weathered, brown or yellow in PPL and isotropic or high order white birefringent in XPL. Fragments of roots were observed in the areas of the feet (2%), basket and muslin bag (5%). They were orange or light yellow in PPL and isotropic or high order white birefringent in XPL. One single seed (400 μm) was detected in the area of the skull (*y*). It was sub-rounded, with rough surface and light brown colour in PPL and XPL.

Fungal activity was detected in all of the samples except the controls. Few fungal hyphae were identified in the areas of the pelvis (2%) and gut bag (5%) (Figure 5.151.g-h). Sclerotia (40-250 μm) were present in the areas of the skull (*z*) and pelvis (5%), muslin bag (2%) and gut bag (8%). Fungal spores were very few in all of the samples and more abundant in the area of the gut bag (5%). Each spore had dimension between 7-8 μm, brownish purple colour in PPL, sub-rounded shape with a depression in the middle. They were aggregated together and sometimes closed by a fungal body with circular shape; in a couple of cases the external structure of this body was preserved and appeared as a sporangium (Figure 5.151.a-d). Spores in the areas of the pelvis had different shape, still sub-rounded but with a pointed extremity. They formed small aggregates of 40 μm, similar to conidia (Figure 5.151.e-f).

Few insect remains were observed in the areas of the skull (*z*) and pelvis (5%) and very few in the areas of muslin and gut bags and basket (2%). From the areas of the skull, basket, and muslin bag, long elongated subrounded shapes, yellow and brown in PPL, with spines were noticed (Figure 5.152.a). From the area of the pelvis, brown fragmented parts of insect, difficult to identify, the remains of an insect type C (see below the description in burial 6) and the section of the head (600 μm) of what possibly was a fly were identified (Figure 5.151.b). From the area of the gut bag, other fragmented remains that were present were difficult to interpret (Figure 5.151.c,g-h).

PEDOFEATURES AND ANTHROPOGENIC MATERIAL

The main pedofeatures and anthropogenic material identified in burial 2 were: clay infillings, brown soil micro-fauna faecal pellets, grey soil micro-fauna faecal pellets, hairs, Fe nodules, Fe/Mn nodules and infillings of brown fine material (Figure 5.141).

Fe nodules (3-20 μm) were present in all of the samples (5%), except for control C3 C, were very few Fe/Mn nodules were observed. Dusty clay infilling and infillings of brown fine material within

the groundmass were observed in controls. The first were yellow/orange in PPL and yellow/black in XPL, with speckled b-fabric (Figure 5.155.g-h), while the second were brown in PPL, brown or isotropic in XPL and undifferentiated.

Soil micro-fauna faecal pellets were frequent (15%) in the areas of the skull (*z*), pelvis and gut bag; while they were few (5%) in the area of the feet. Two different types of pellets were identified. The first one was rounded or sub-rounded, brown in PPL and dark brown or isotropic in XPL. The size was between 30-50 µm and the b-fabric was crystallitic owing to the presence of micrite. They did not look weathered, but coalescent in some cases. The second type was rounded or sub-rounded, brownish grey in PPL and brown/pink/green in XPL. The size was 25-80 µm and the b-fabric was crystallitic (Figure 5.154.e-f). They were not weathered. Remains of hair were observed in the areas of the skull (*y*), pelvis, gut bag and control C3 A (2-5%). They were 40-50 µm thick, white in PPL and white/yellow in XPL, with parallel striated b-fabric. In the area of the pelvis, two parallel fragments of hairs were attached to an amorphous light brown aggregate with irregular and elongated shape and rough surface (Figure 5.150.a-b). In the same area, few hairs were visible across their horizontal section.
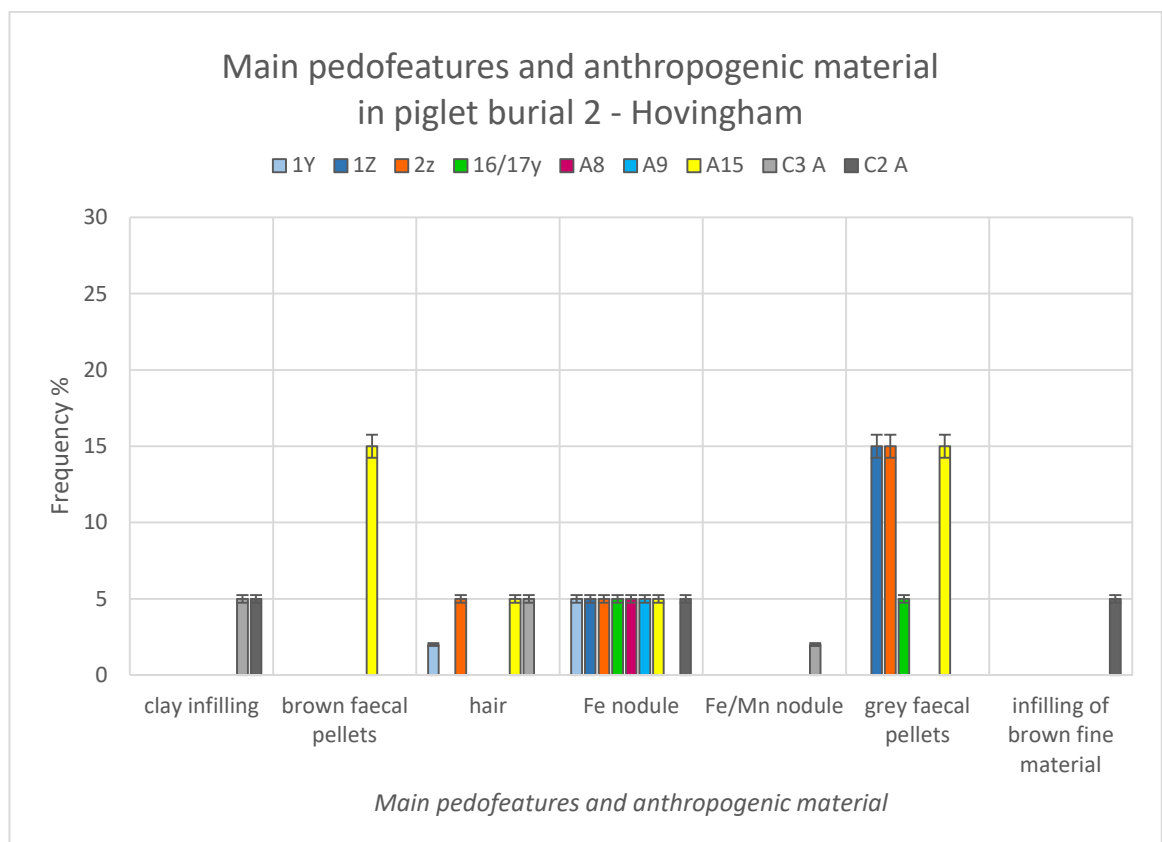
Figure 5.141: Frequency of the main pedofeatures and anthropogenic material in relation to their anatomical location within piglet burial 2. Two types of soil micro-fauna faecal pellets and fragments of hairs were identified.

PIGLET BURIAL 6

ELEMENTS OF FABRIC AND PEDS

The fabric was characterized by porphyric c/f related distribution and poor or moderate sorting. It was single or close porphyric in the areas of the skull, feet, gut bag, snout bag, C3A and C2A, while it was single or double porphyric in the other samples. Fine material was brown in PPL and reddish brown in XPL, with dotted limpidity and speckled b-fabric. Granular peds were present in all of the samples, except for level *z* in the area of the skull and sample A1. They were very abundant in the level *y* in the area of the skull (30-50%), fine to very fine in size, partially accommodated and moderately developed. In the rest of the burial, peds were very few (2-5%), very fine or fine in size, unaccommodated and strongly developed.

VOIDS

Three types of void were observed in burial 6: channels, modified complex voids and packing voids (Figure 5.142).
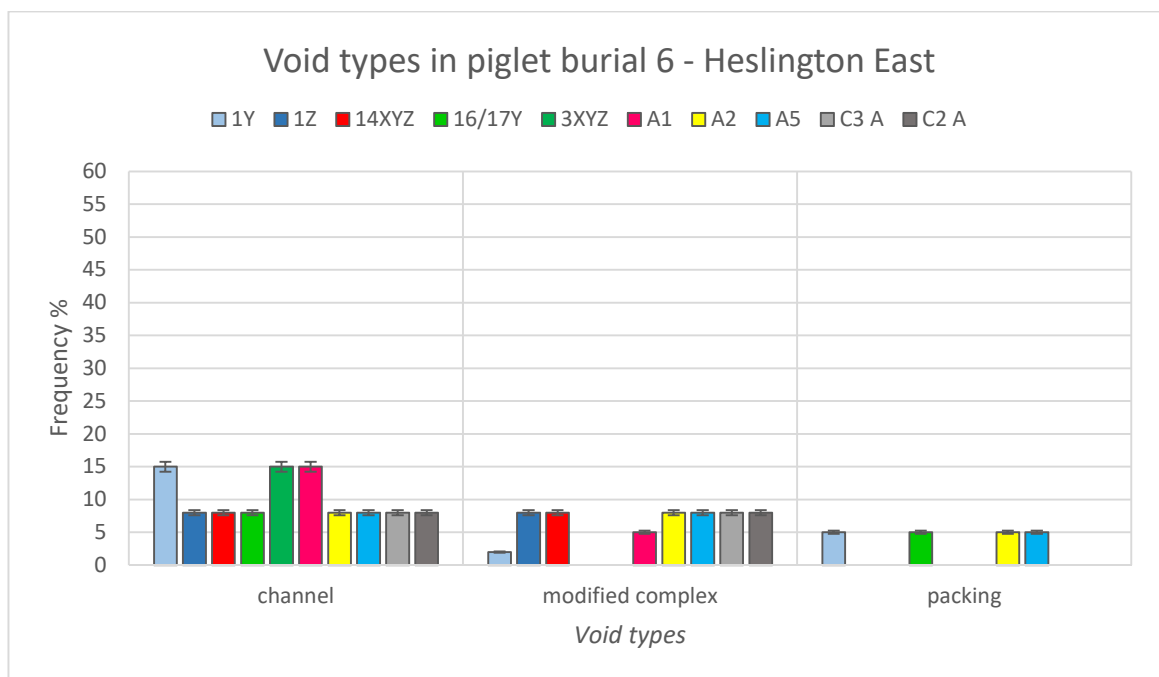
Figure 5.142: Abundances of different types of void in relation to their anatomical location within piglet burial 6. Channels were the most frequent.

Channels were present in all of the samples. They were frequent (15%) in the area of the skull (*y*), back feet and above the skeletal remains (A1) in common with all the other samples (8%). Modified complex voids were very few (2%) in the area of the skull (*y*), few in A1 and common in all the other samples, except for the area of the feet where they were not detected. Few packing voids (5%) were observed in the area of the skull (*y*), front feet, area of the gut bag (A2) and area of the snout bag (A5).

MINERAL COMPONENTS

Mineral components identified in burial 6 were: calcite, chert, plagioclase, quartz and quartzite (Figure 5.143).
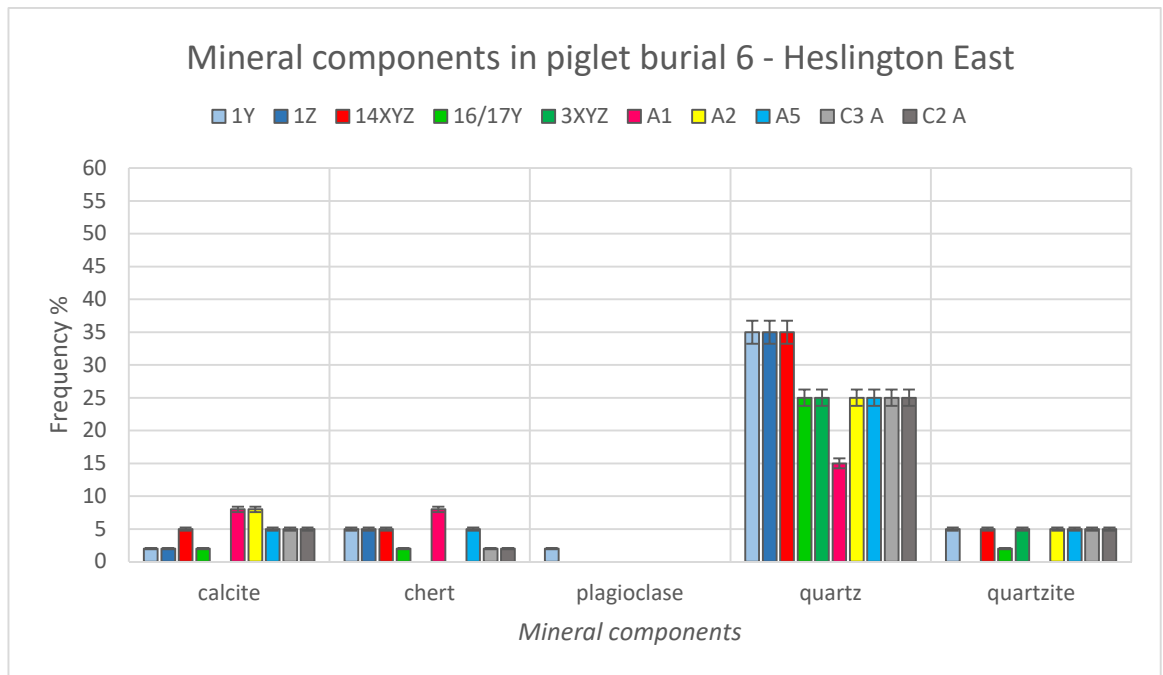
Figure 5.143: Frequency of mineral components in relation to their anatomical location within piglet burial 6. Quartz was the most frequent component.

Quartz was very frequent in all of the samples (15-35%). Quartzite, calcite and chert were few and not present in all of the samples (2-8%). Plagioclase was identified only in the area of the skull (*y*).

ORGANIC COMPONENTS

Several organic components were identified in burial 6: bone fragments, charcoal, fungal spores, humified plant structures, insect remains, roots, sclerotia, seeds and worm remains (Figure 5.144). Bone fragments were common in the areas of the pelvis and front feet (8%), common in the area of snout bag (5%) and very few (2%) in the area of the skull (*z*). They were partially weathered in the first two samples, light yellow in PPL and low order grey birefringent in XPL, with some black stains; their size was between 5-7 mm. In the area of snout bag and skull, they were instead not weathered, yellow in PPL and high order grey birefringent in XPL; their size was between 170-1200 μm (Figure 5.150.h). Charcoal fragments (100-1500 μm) were few in most of the samples and partially weathered.

Fungal activity was visible in the area of back feet with traces of fungal spores (7-9 μm), subrounded, purple in PPL and isotropic in XPL. Sclerotia (80-150 μm) were present in the areas of front feet, gut bag and snout bag (2%). Humified plant structures were found in the areas of front feet (2%), gut bag (5%) and snout bag (2%). They were partially weathered, brown, dark brown or white in PPL

238

and isotropic or high order white birefringent in XPL. The fragment from the area of gut bag was 1 cm in size and weathered. It was composed of amorphous and rough yellowish brown bands and amorphous dark brown zones, which were connected through white segments whose cellular structure was still visible. In addition, round yellowish brown soil micro-fauna faecal pellets (25-33 μm) filled some of the empty areas.

Fragments of roots (200-2000 μm) were observed in the areas of the skull (*y*), back feet and C3A (2%). They were weathered, light yellow in PPL and grey/white in XPL in the regions adjacent to the skeleton, while they were partially weathered, light brown in PPL and isotropic in XPL in control C3A. Seeds with triangular shape (670-950 μm) were present in the areas of the pelvis, back front feet, gut bag and C3A (2%). They were comprised an external layer, orange-brown in PPL and red in XPL, 20-22 μm thick, and an internal area, not always present, white in colour and with cellular structure evident.

A possible fragment of nematode was observed in sample C2A. It was 23-25 μm thick, brown in PPL and isotropic in XPL. Parallel internal lines resembled the setae of worms (Figure 5.153.6). Insect remains were common in the area of the muslin bag (8%), few in the areas skull (*z*), pelvis, front feet, A1 (5%) and very few in the areas of back feet and C2A (2%). They were all partially weathered, having missing parts or only the external part preserved. Three types were identified, A, B and C. Type A (1500 μm) had sub-rounded shape, thick black exoskeleton (50-150 μm) and internal yellowish brown articulated structure. It was noticed in the area of the pelvis (Figure 5.152.e-f). Type B (1400-2000 μm) comprised the remains of elongated structures with spines (2-50 μm), brown in PPL and isotropic in XPL (Figure 5.152.d-f). It was identified in the area of the pelvis and above the skeletal remains (A1). Type C (700-2000 μm) had ovoid shape, with undulating surface. Generally, the only visible part was the external brown layer (1-10 μm thick), while in very few cases the internal structures, characterized by brown spines and yellow brown areas with round cells, were preserved. Type C was more common than the others and it was observed in the areas of the skull (*z*), feet, muslin bag and control C2A (Figure 5.153.a,c-d).
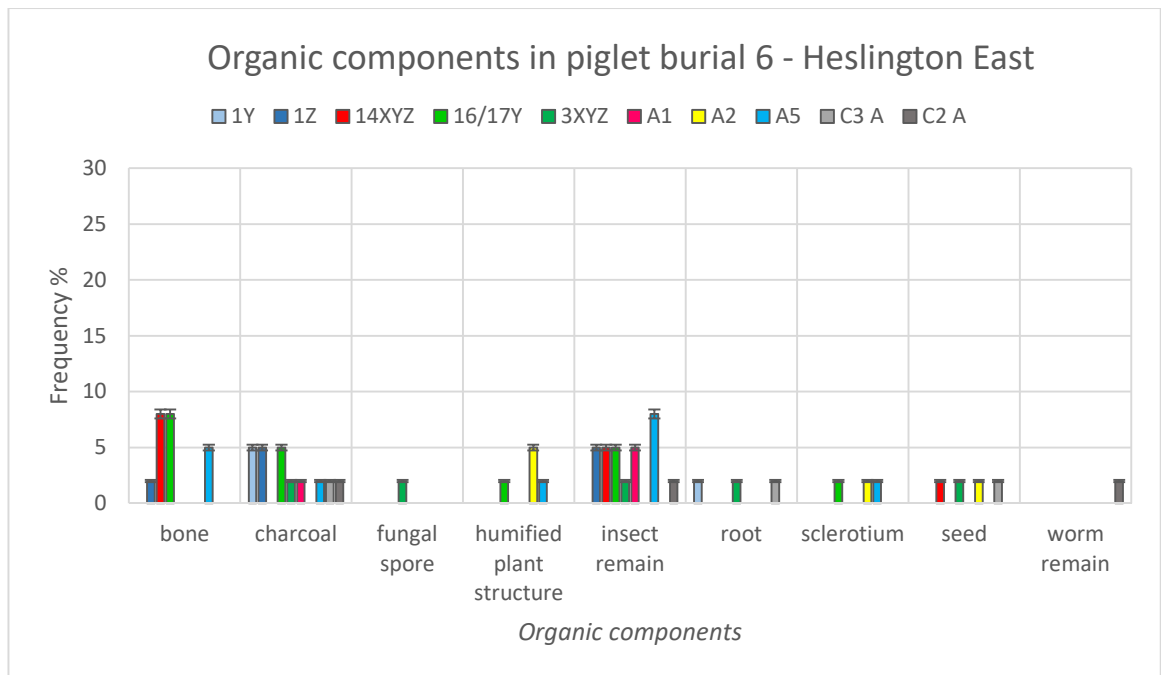
Figure 5.144: Frequency of organic components in relation to their anatomical location within grave 6. Insect remains were present in most of the samples.

PEDOFEATURES AND ANTHROPOGENIC MATERIAL

Six main pedofeatures and anthropogenic material were detected in burial 6: beeswax remains, soil micro-fauna faecal pellets, Fe/Mn nodules, fibres from the muslin bag, redox impregnations and vivianite (Figure 5.145).

Vivianite was common in the area of the pelvis (8%), few in the areas of the skull (*z*) and snout bag (5%), and very few in the areas of front feet, gut bag and control C2A (2%). In all those samples, it had sub-rounded or rounded shape, size between 100-380 μm and radial crystals yellow, blue and green in PPL and yellow, blue, green and pink in XPL. In a few cases vivianite was surrounded by a thin layer coating of amorphous phosphate (Figure 5.155.a-b). In the area of the snout bag, vivianite had sub-angular and irregular shape and it was intergrown with the groundmass, enclosing mineral grains. The colours in XPL were less intense than for the vivianite with sub-rounded shape (Figure 5.155.c-d).

Redox impregnations were few in the control C3A (5%) and very few in the area of the skull (*y*) and control C2A (2%). They were reddish brown in the area of the skull and black in the controls. Fe/Mn nodules were few (5%) in most of the samples and common in the control C3 (8%). Their size was between 50-1000 μm. A possible remain of beeswax (1200 μm) was observed in the area of the snout bag. The fragment was partially weathered, greyish brown in PPL and brown or isotropic in XPL, without b-fabric. It had sub-rounded shape, rough surface and internal vughs. Acrylic fibres

from the string of the muslin bag were identified in the area of the snout bag (5%). They were very well preserved, with crystallitic b-fabric and low interference colours (grey, pink and white). Each single fibre measured 13-15 μm in thickness and formed a cord of thickness 200-300 μm.
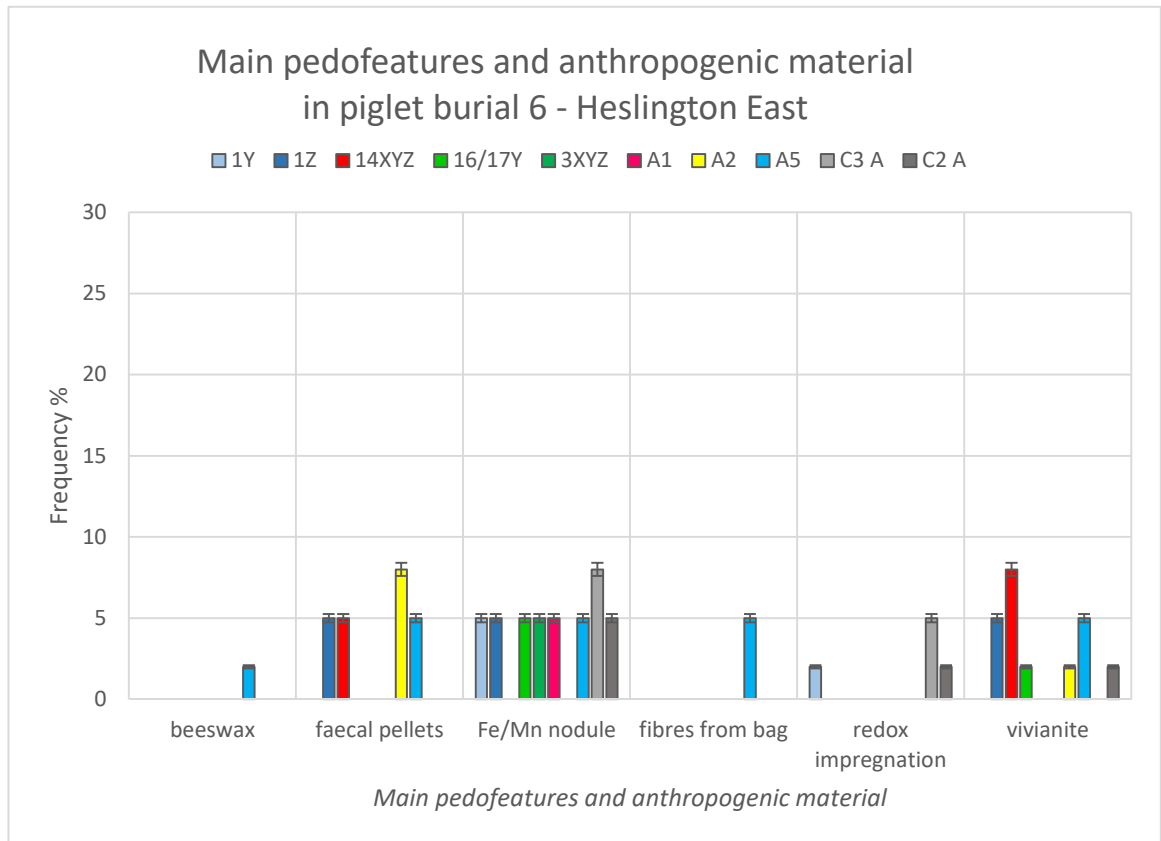
Figure 5.145: Frequency of the main pedofeatures and anthropogenic material in relation to their anatomical location within piglet burial 6. Soil micro-fauna faecal pellets and vivianite were detected in some of the samples.

Soil micro-fauna faecal pellets were common in the area of the gut bag (8%) and few in the area of the skull (*z*), pelvis and snout bag (5%). Three types of pellets were identified, D, E and F. Type D had sub-angular shape with sub-rounded section, size between 110-190 μm in length and 55-75 μm in section, brown colour in PPL and reddish brown in XPL, with crystallitic b-fabric. This type was present in the areas of the skull and pelvis. Type E had sub-rounded shape, size between 75-170 μm, brown colour in PPL and brown/yellow in XPL, with crystallitic b-fabric. This type was present in the areas of the snout bag and pelvis (Figure 5.154.c-d). Type F had sub-rounded shape, size between 25-33 μm, light brown colour in PPL and isotropic in XPL, without b-fabric. This type was present in the area of the gut bag, within the humified plant structure described in the organic component section (Figure 5.154.a-b).

PIGLET BURIAL 7

ELEMENTS OF FABRIC AND PEDS

The fabric was characterized by single or close porphyric c/f related distribution and moderate sorting. Fine material was brown in PPL and orange/brown in XPL, with dotted limpidity and speckled b-fabric. Fine material in sample 1Z was lighter in colour and with speckled or crystallitic b-fabric. The abundance of fine material was between 20-60%. Very few granular peds (2%) were observed in the areas of the skull and feet (*y*). They were very fine in size, unaccommodated and strongly developed.

VOIDS

Two types of void were observed in burial 7: channels and modified complex voids (Figure 5.146).
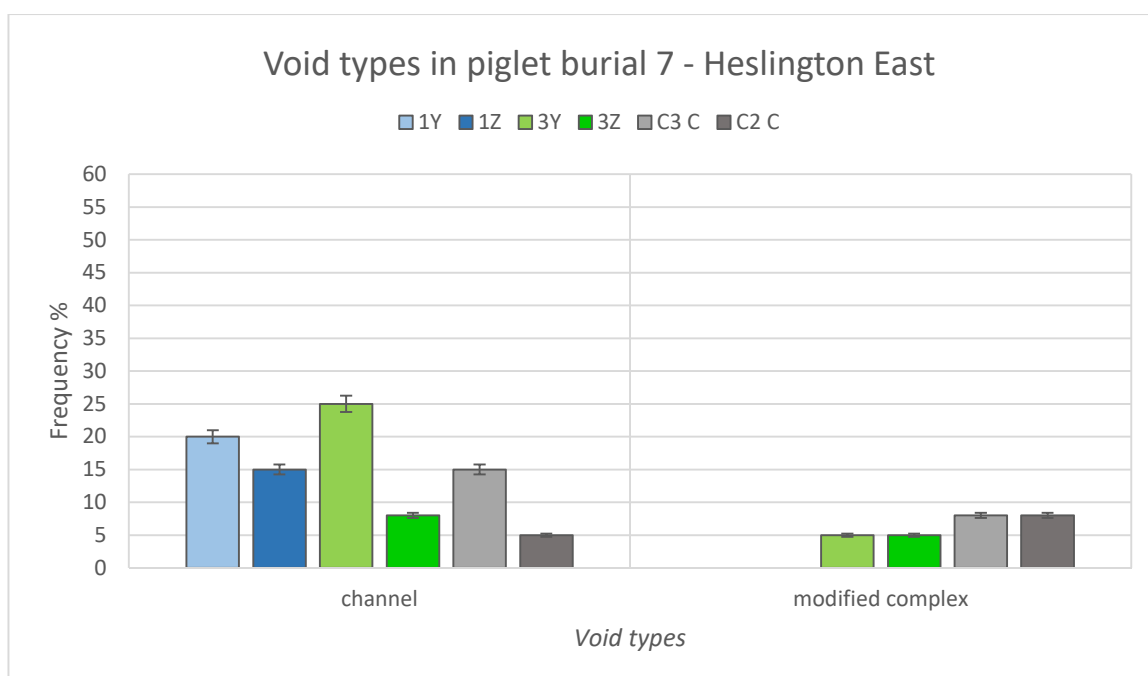
Figure 5.146: Abundances of different types of void in relation to their anatomical location within piglet burial 7. Channels and modified complex voids were identified.

Channels were very frequent in levels *y* of the feet (25%) and skull (20%), frequent in the areas of the skull (*z*) and C3 C (15%), few in the level *z* of the feet (5%) and very few in the control C2 C (2%). Modified complex voids were absent in the area of the skull, few in the area of the feet (5%) and common in the controls (8%).

MINERAL COMPONENTS

Mineral components identified in burial 7 were: calcite, flint, quartz and quartzite (Figure 5.147). Quartz was dominant in all of the samples (25-55%), while quartzite and calcite were few (2-8%). Flint was observed only in the area of the skull (2%). Mineral grains were mainly unweathered.
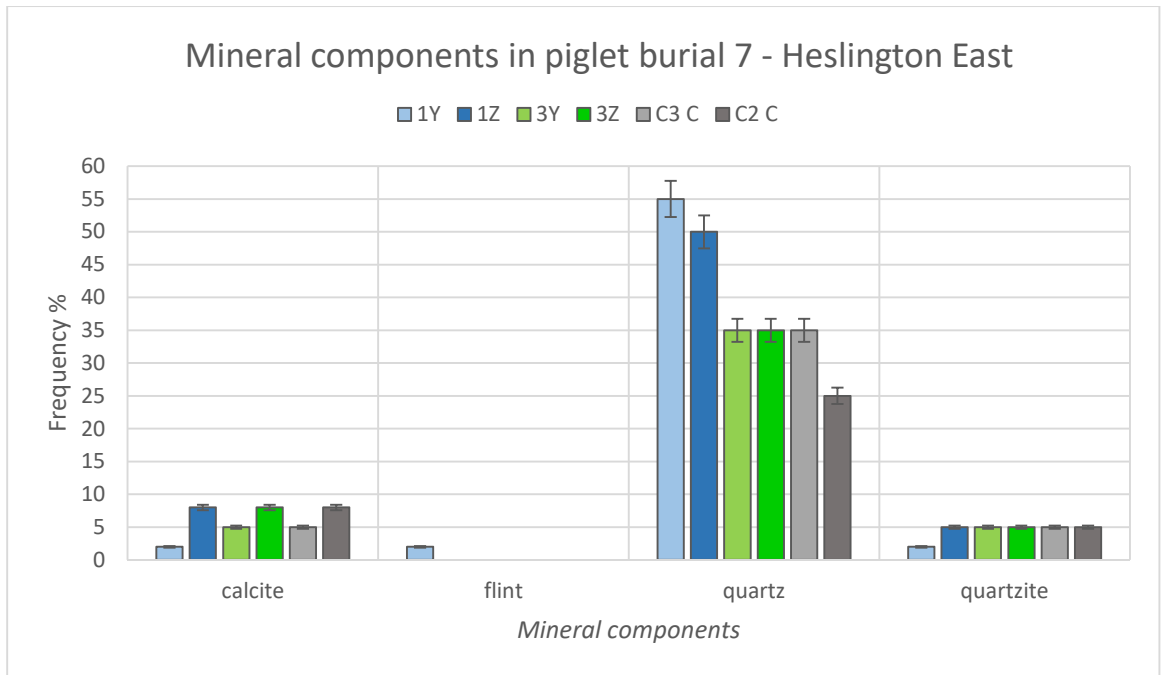
Figure 5.147: Frequency of mineral components in relation to their anatomical location within piglet burial 7. Quartz was the most frequent component.

ORGANIC COMPONENTS

Organic components identified in burial 7 were: bone fragments, charcoal, humified plant structures, insect remains, roots, sclerotia, seeds and worm remains (Figure 5.148).
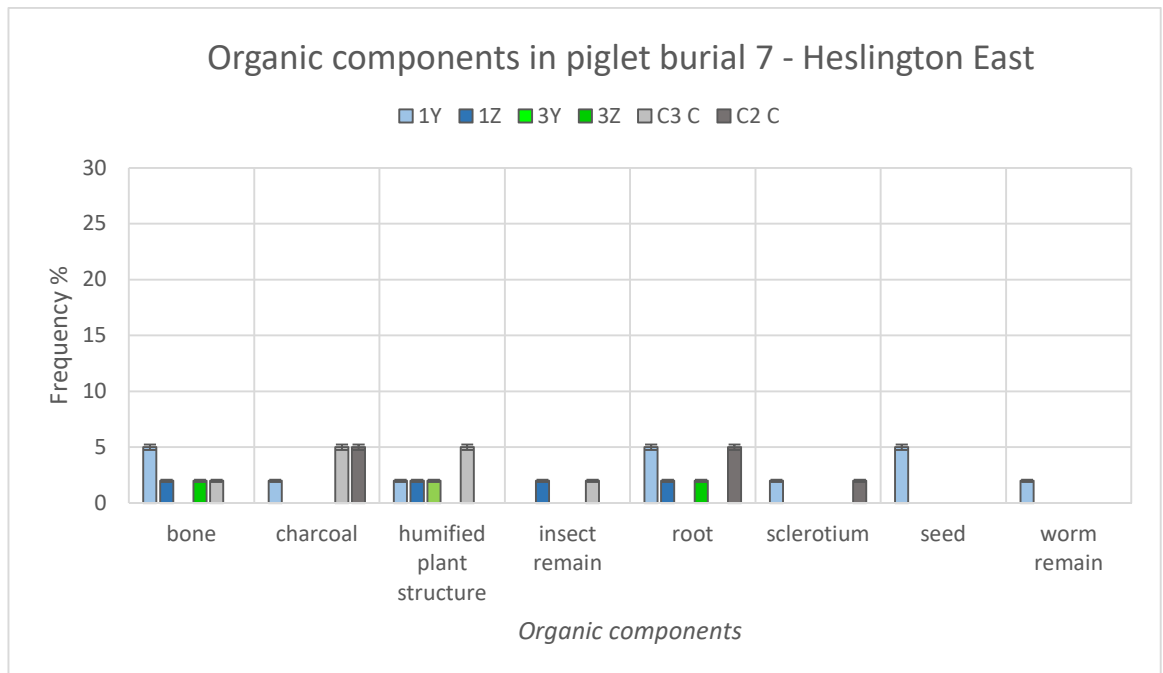
Figure 5.148: Frequency of organic components in relation to their anatomical location within piglet burial 7. Very few insect remains were observed.

Bone fragments were very few in level *z* in the areas of the skull and feet and in the control C3 C (2%) and slightly more abundant in the level *y* in the area of the skull. They had sub rounded or rounded shape, size between 300-1000 μm and thickness between 5-6 μm. The colour was yellow in PPL and yellow or isotropic in XPL and they were not weathered (Figure 5.150.g). Charcoal fragments were present in the areas of controls (5%) and in level Y from the area of the skull (2%). They were partially weathered and the size was between 350-5000 μm.

Humified plant structures were few in the control C3 (5%) and very few in the areas of the skull and feet (*y*) (2%). They were partially weathered, some of them crossed by biological channels. Roots were few in level *y* from the area of the skull and in the control C2 C (5%) and very few in level *z* from the areas of the skull and feet (2%). They were orange in PPL and isotropic in XPL. Few triangular seeds (5%), like the ones observed in burial 6, were identified in the area of the skull (*y*). Very few sclerotia (2%) were observed in the areas of the skull (*y*) and control C2 C. They were sub-rounded, not weathered and the size was between 150-200 μm.

One possible worm remain was identified in the area of the skull (*y*). It was 1300 μm long, 93-110 μm thick, brown in PPL and isotropic in XPL. It had internal segmentation, as the possible worm observed in burial 6, but was more weathered (Figure 5.153.h). Very few insect remains (2%) were detected in burial 7: type A was present in both samples, while type C was observed only in the area of the skull (*z*) (Figure 5.153.b). Insects remains of type B were not found.

PEDOFEATURES AND ANTHROPOGENIC MATERIAL

Five main pedofeatures and anthropogenic material were detected in burial 7: beeswax remains, soil micro-fauna faecal pellets, Fe/Mn nodules, secondary $CaCO_3$ crystals and vivianite (Figure 5.149). Vivianite was rare: only one, with sub-rounded shape and 165 μm in diameter, was noticed in the area of the feet (*z*). Fe/Mn nodules were present in all of the samples (2-5%), especially in the area of the skull (*y*). Secondary $CaCO_3$ impregnations within fine material were common in the area of the skull (8%) and few in the areas of the feet (*z*) and control C3 C (5%). The crystals had sizes between 3-20 μm, greyish pink colour in PPL and pink/green in XPL (Figure 5.155.e-f). Few fragments of beeswax (2-5%) were identified in the areas of the skull (*y*) and feet (*z*). Different to burial 6, they were characterized by internal grey needle-shaped crystals. Soil micro-fauna faecal pellets were common in the control C2 C (8%). Two different types were distinguished within the same root. The first was associated with type D of burial 6: sub-angular shape, size between 60-70 μm and 32-37 μm in section, light brown colour in PPL and brown in XPL, crystallitic b-fabric (Figure 5.154.g-h). The second was similar to type E of the same burial: sub-rounded shape, rough surface, size between 50-60 μm, brown colour in PPL and isotropic in XPL, without b-fabric.
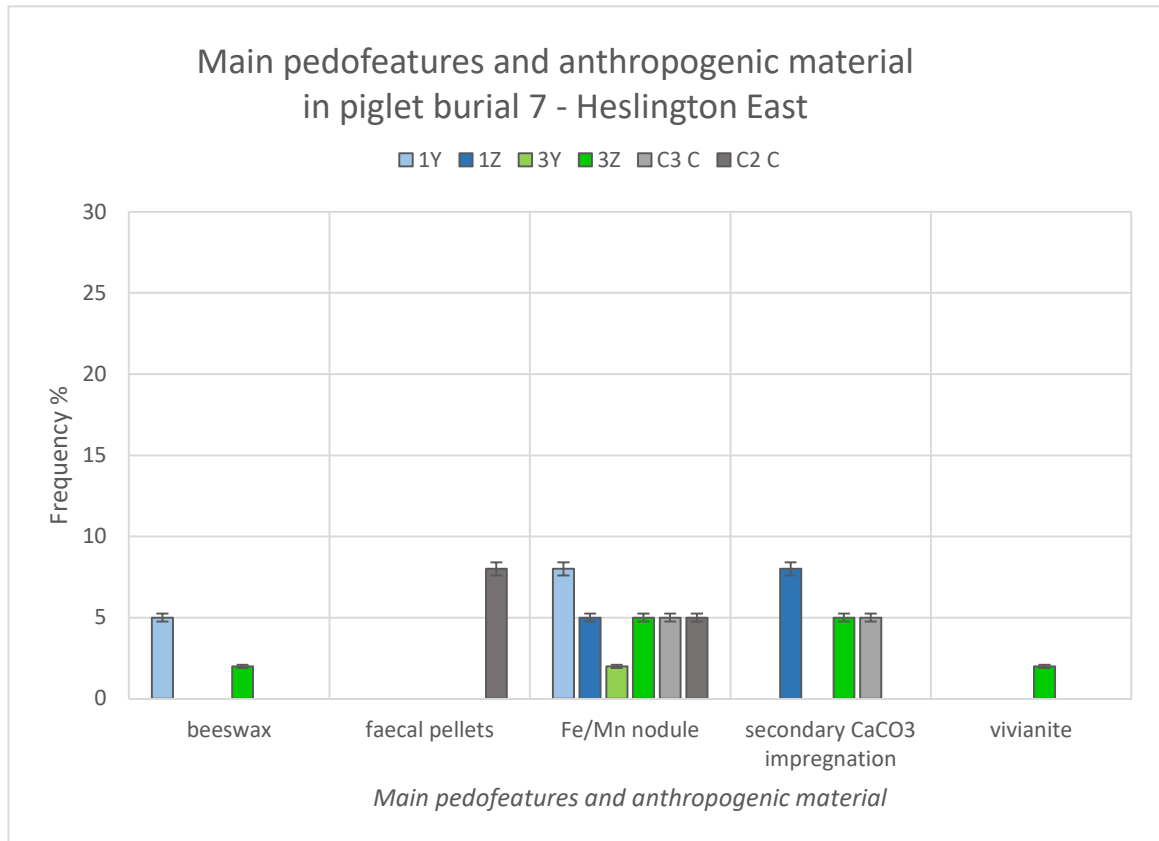
Figure 5.149: Frequency of the main pedofeatures and anthropogenic material in relation to their anatomical location within piglet burial 7. Faecal pellets were noticed only in the control C2.

The following figures were selected as representative of the features described in Section 5.6.2:

- Figure 5.150: hairs and bone fragments;

- Figure 5.151: fungal activity;

- Figure 5.152: remains of insects type B;

- Figure 5.153: remains of insects type A, C and possible worm;

- Figure 5.154: soil micro-fauna faecal pellets of types D, E and F;

- Figure 5.155: pedofeatures (vivianite, secondary CaCO$_3$ crystals and fine material infillings).

Figures of fabric fibres were not included, because they were part of the synthetic fibre cords of the muslin bag. These fibres were very well preserved and, because of their composition, they were not useful reference for the material from the archaeological graves.
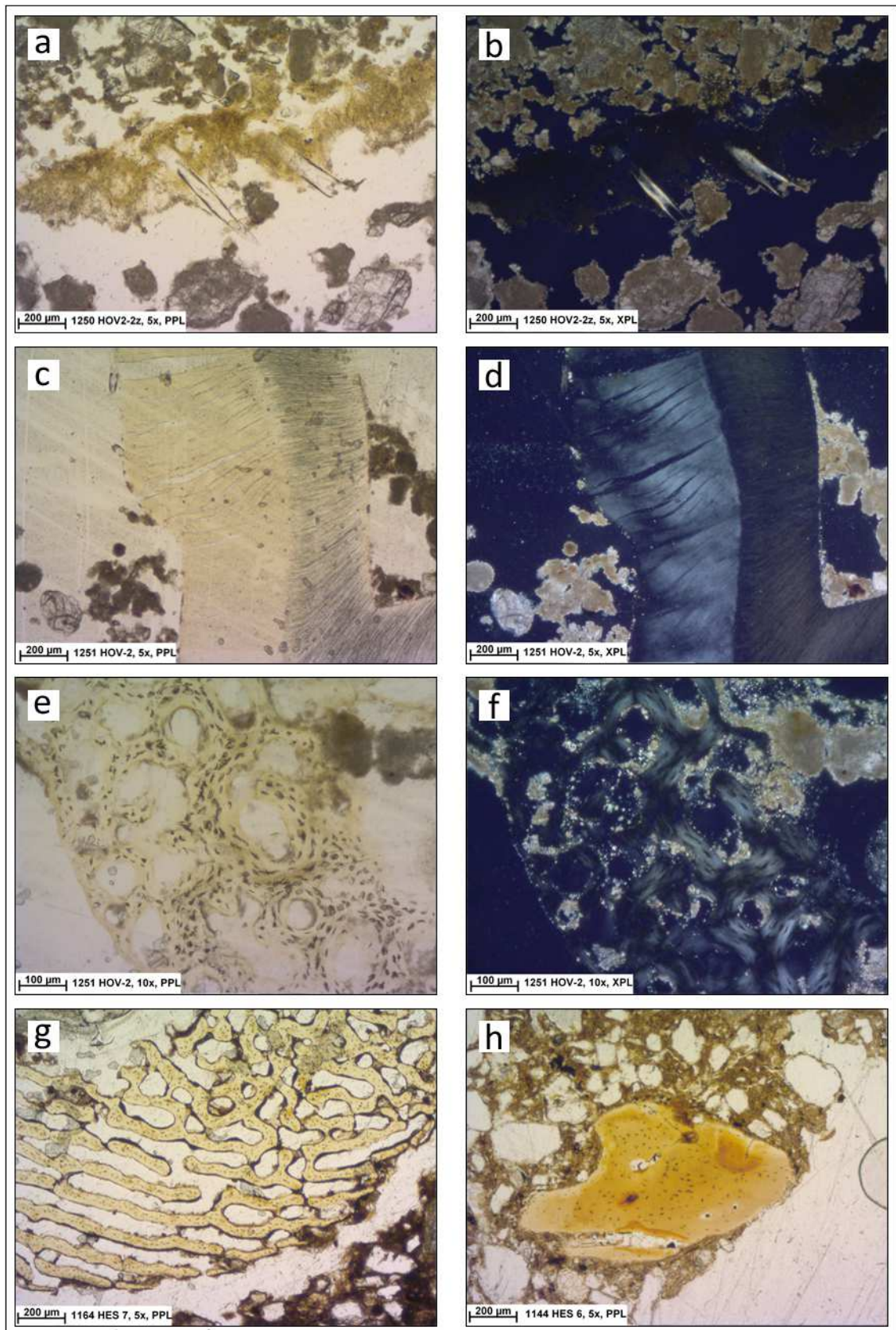
Figure 5.150: Hairs and bone fragments in piglet burials. a-b) fragments of hairs attached to a yellow phosphatic material from the area of the pelvis in burial 2 in PPL (a) and XPL (b); c-d) fragment of tooth and infilling of soil micro-fauna faecal pellets from the area of the skull in burial 2 in PPL (c) and XPL (d); e-f) fragment of partially weathered bone from the area of the skull in burial 2 in PPL (e) and XPL (f); g) fragment of bone from the area of front feet in burial 7; h) fragment of bone from the area of snout bag in burial 6.
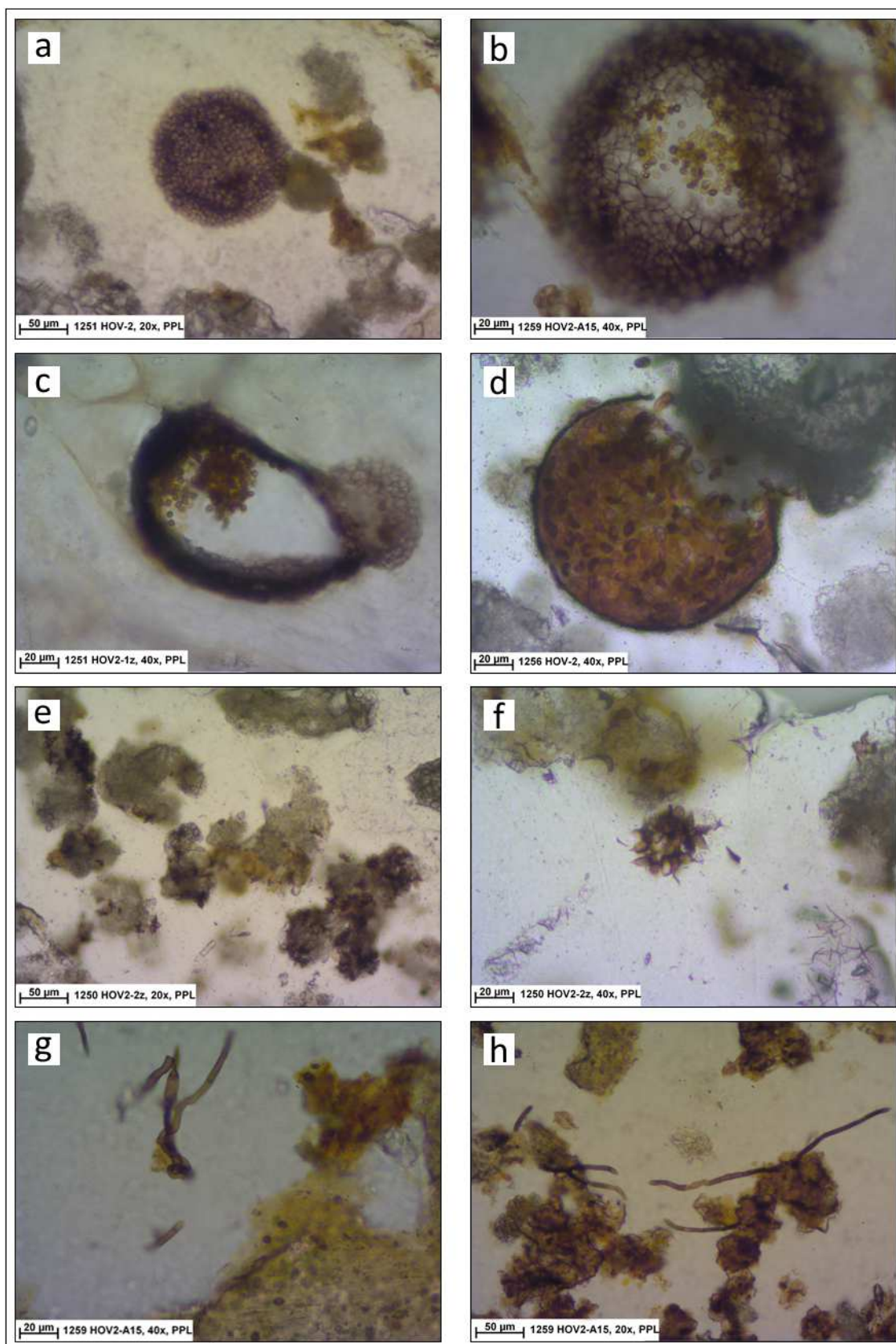
Figure 5.151: Fungal remains in piglet burials. a-b-c-d) spherical and spongy bodies containing sub-rounded spores, from the area of the skull in burial 2 (a-b-c), from the area of gut bag in burial 2 (b); e-f) subrounded spores with one pointed extremity from the area of the pelvis in burial 2; g-h) fungal hyphae, some associated with soil micro-fauna faecal pellets (h), from the area of gut bag in burial 2.
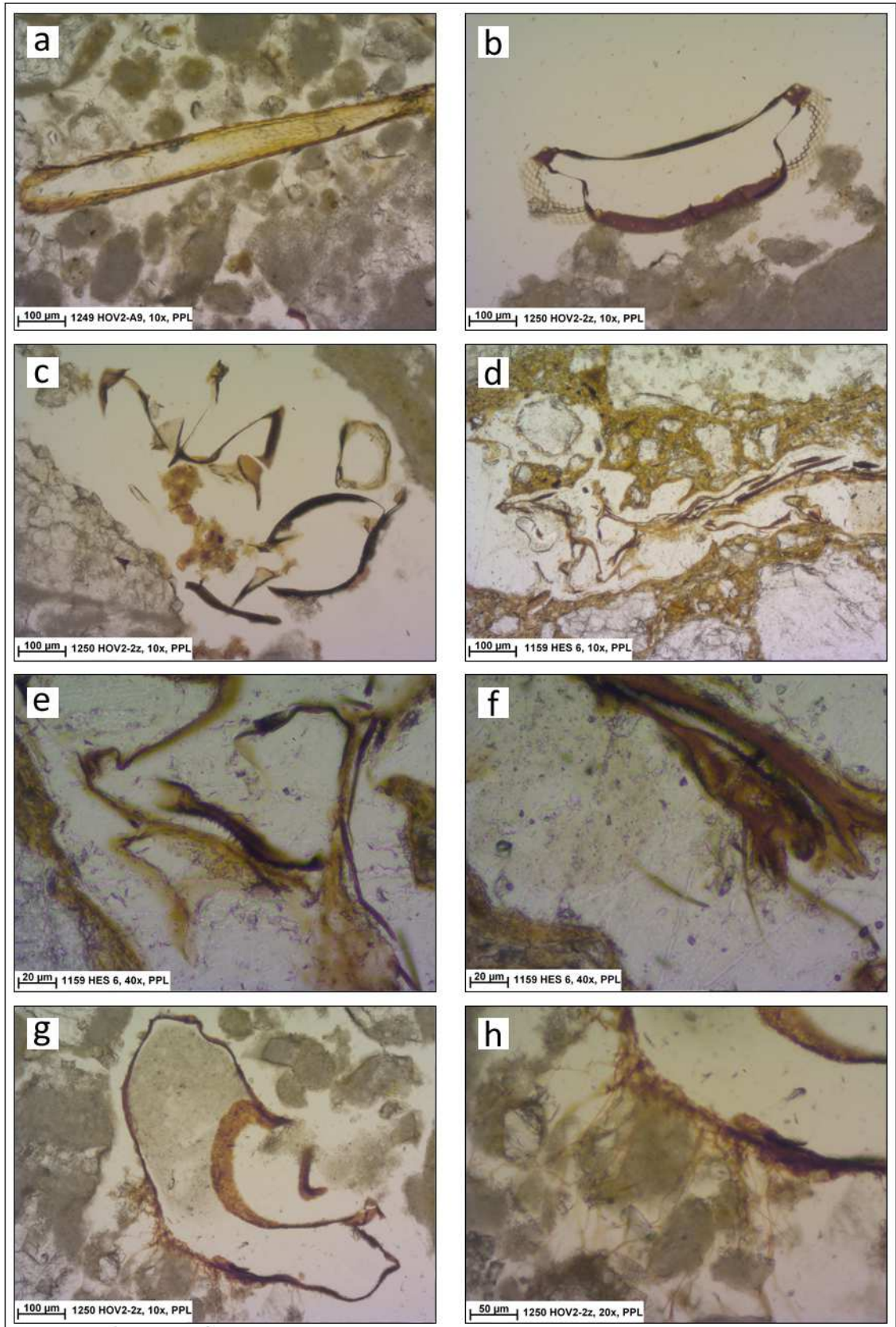
Figure 5.152: Remains of insect type B in piglet burials. a) from the area of the snout bag in burial 2; b-c-g-h) from the area of the pelvis in burial 2; d-e-f) from the area of sample A1, above the skeletal remains, in burial 6; (e) and (f) are details of (d).
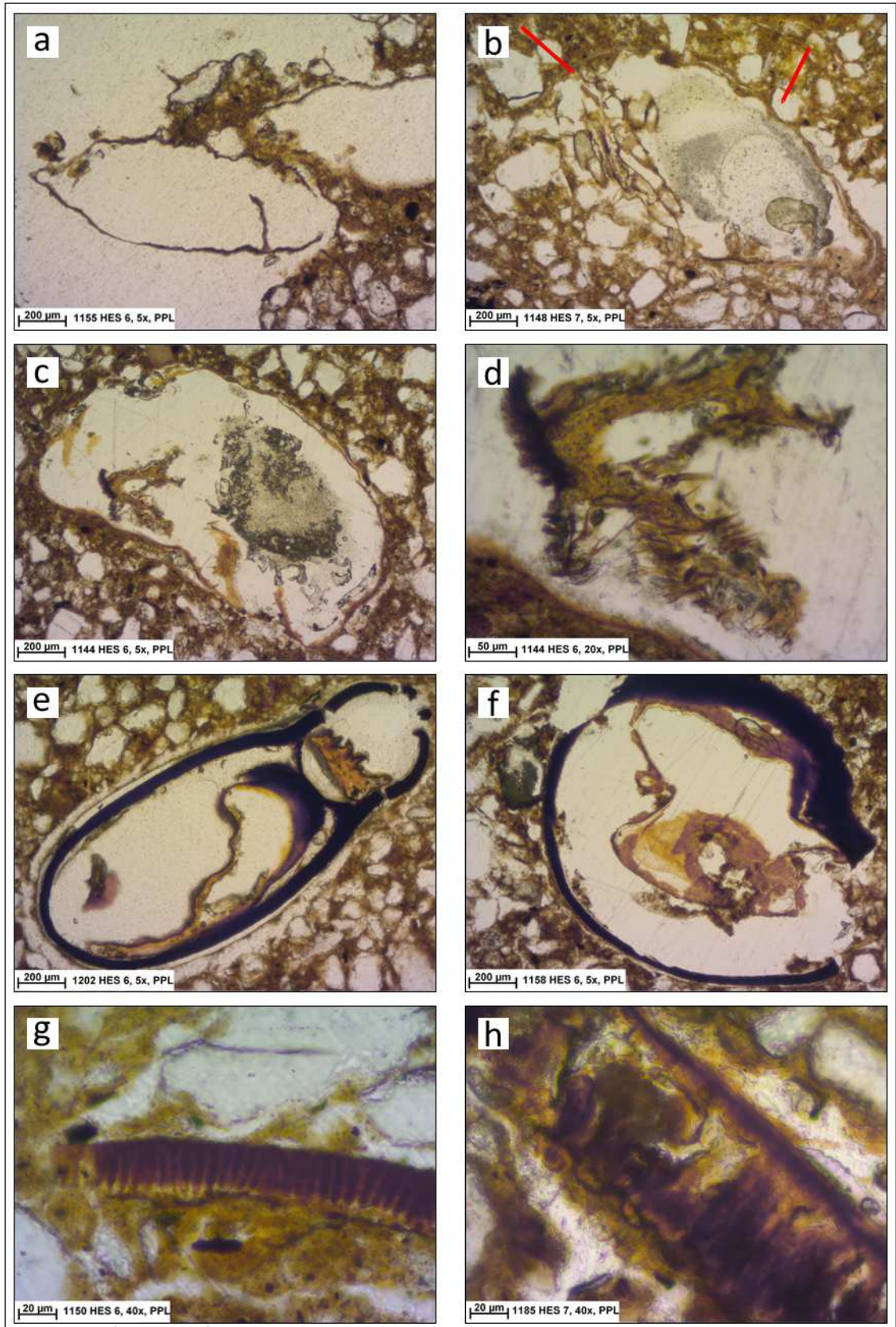
Figure 5.153: Remains of insects of type A, C and possible worm in piglet burials. Type C: a) from the area of the skull in burial 6; b) from the area of the feet in burial 7; c-d) from the area of snout bag in burial 6. Type A: e) from the area in the S-W corner of the coffin in burial 6; f) from the area of the pelvis in burial 6. Possible fragments of nematodes: g) from the control C2 in burial 6; h) from the area of the skull in burial 7.
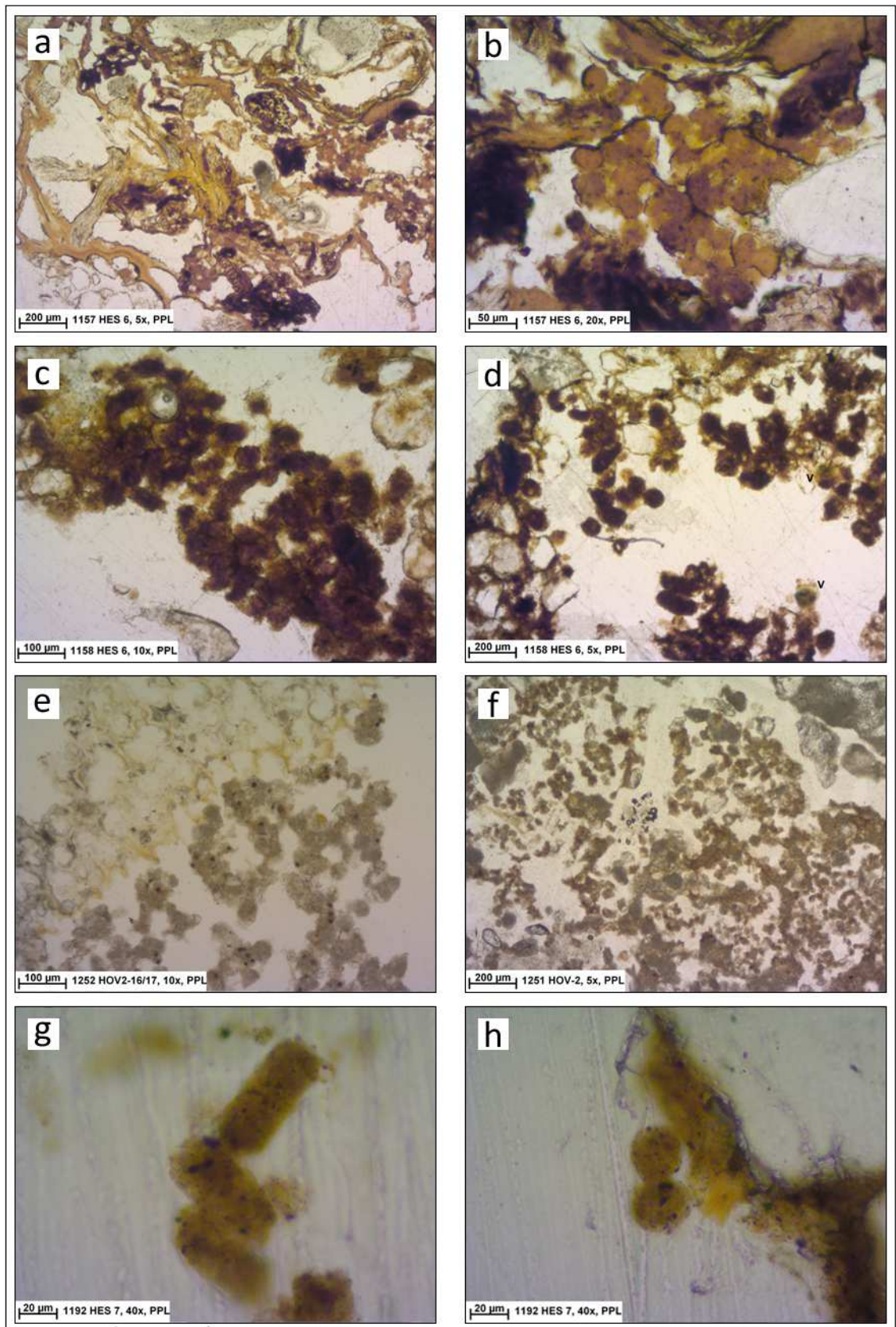
Figure 5.154: Soil micro-fauna faecal pellets of types D, E and F in piglet burials. a-b) type F within weathered organic matter from the area of the gut bag in burial 6; c-d) type E from the area of the pelvis in burial 6; e-f) type D from the area of the feet (e) and skull (f) in burial 2; g-h) type D from the control C2 C in burial 7.
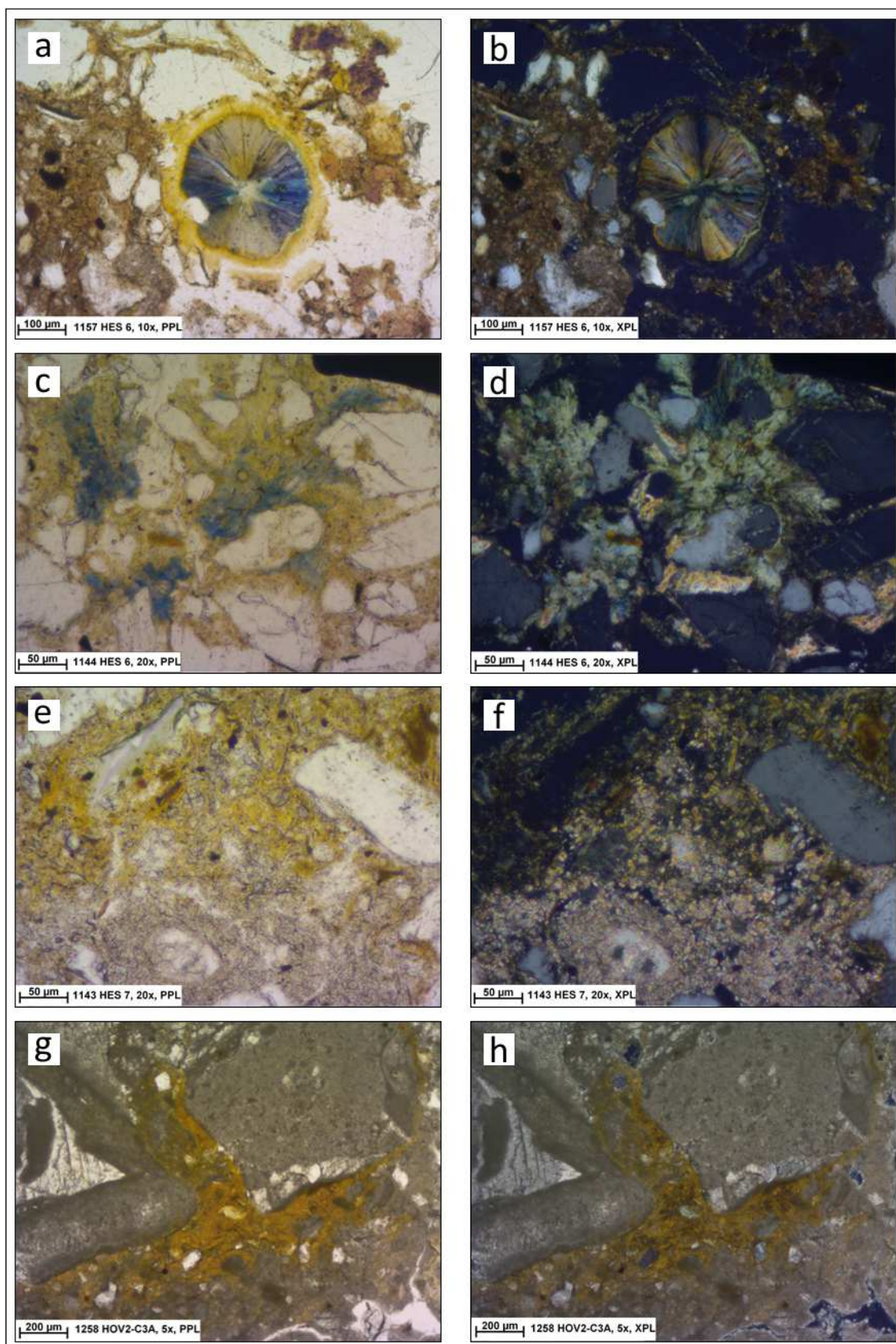
Figure 5.155: Pedofeatures in piglet burials. a-b) sub-rounded crystal of vivianite with phosphatic coating from the area of gut bag in burial 6 in PPL (a) and XPL (b); c-d) vivianite inter-grown within the groundmass in the area of the snout bag in piglet 6; e-f) secondary $CaCO_3$ impregnation in the area of the skull in burial 7 in PPL (e) and XPL (f); g-h) fine material infilling in the control C3A in burial 2 in PPL (g) and XPL (h).

Chapter 6. DISCUSSION

The results of this research, presented in Chapters 4 and 5, are discussed in this chapter. The discussion is organized focusing on the main features observed and recorded by micromorphological analysis, integrated with the image analysis and SEM-EDS data. Interpretations relating to the different case studies are considered throughout the chapter. The correlation of particular features among the graves and the final comparison and overview of the case studies are presented in Chapter 7.

The archaeological sites studied in this research were characterized by different types of burial, soil, climate and natural and anthropic post-depositional processes, illustrated in Figure 1.1 and Table 1.1 (Chapter 1). Thus, differences in the sediments and their microstructure occurring in the graves were observed in the slides.

Six of the graves from Hungate were characterized by wooden coffins, while information on grave 54931/54909 was not available (Chapter 5, Section 5.1.2). Since reports from YAT showed that not all of the graves in Hungate had wooden coffin, micromorphological observations on grave 54931/54909 were applied to identify possible traces that could be linked to the presence or absence of a coffin. The main post-depositional processes in Hungate included water-logged conditions, presence of a refuse dump and use of the area for industrial activities (Chapter 5, Section 5.1.1).

Information regarding the graves of Haymarket was not available (Chapter 5, Section 5.2.2), thus, it is unknown if the corpses were deposited within coffins or in contact with the soil. During the Middle Age in England, the use of wooden coffins was testified since the 7th C AD. However, coffins could be replaced by wooden boards located over the graves, as discovered in the cemeteries in Fishergate, York (Daniell 1997, 163). This author did not have direct information of the graves in Haymarket having only participated in the sampling of two graves, both of which were excluded from this research. Photographs were not taken during the sampling of the graves that are included in this study (Chapter 5, Section 5.2.2). Thus, the observation of micromorphological features was used to advance suggestions concerning the presence or absence of a coffin. The site of Haymarket was rarely affected by water-logged conditions, because it was located in a higher position than Hungate (Chapter 5, Section 5.2.1).

The grave from Borgharen was characterized by a wooden coffin and it was reopened in the past for the addition of two sub-adult individuals, already skeletonized and disarticulated (Chapter 5, Section 5.3.2). However, the samples were collected in the area of the grave not directly affected

by the reopening, because this second interment was not of interest for the aims of this project, considering that the decomposition occurred in a different place, while this project looked at the interaction between corpse decomposition and soil. Hence, this limited the opportunity to investigate the full processes that influenced the grave, as developed in the research of Karkanas et al. (2012) and considered in the project of Aspöck (2011) (Chapter 2, Section 2.5), which could be extended to similar situations in the future. The area of Borgharen was subjected to agricultural activities in modern and contemporary times (Chapter 5, Section 5.3).

The grave from Rossio do Carmo was covered and surrounded by schist, without the use of a wooden coffin. According to Islamic practices, the shroud that wraps the corpse has to be in contact with the ground (Petersen 2013, 246). The schist slabs were not placed at the bottom of the grave and coffin was not utilized. In addition, the grave was cut into the bedrock surface and only a few centimetres of sediments existed between the rock and the skeleton (B. Keely and D. Brothwell, personal communication). Possibly, when the corpse was buried, the pit was immediately covered with soil, because the bones were found in articulation (anatomically connected) at the time of excavation (Chapter 5, Section 5.4.1). It could be suggested that the use of a shroud around the corpse could have maintained the bones in articulation, while the burial was progressively filled by the loose sediment filtering between the schist plates. However, in Islamic practice, graves were generally backfilled after the placement of the corpse and sometimes with the addition of organic materials, such as palm fronds (Petersen 2013, 249). The location of the grave on a slope, the aridity of the area and the development of the village had negatively influenced the preservation of the grave, especially of its sediment.

Information from Pill'e Matta was not always complete, especially regarding the possible collapse of the vaults. The chambers were not backfilled and the sediments on the skeletons could have been produced by the collapse of the vault or by infiltration of material from the space between the tiles, which were placed to seal the niches (Chapter 5, Section 5.5.1). The absence of stratigraphic data and samples from the area of the backfill outside the chambers limited the discussion and interpretation of post-depositional processes. The area of Pill'e Matta was part of an industrial zone in contemporary times and the archaeological site was partially disturbed by the construction of a road.

6.1 ELEMENTS OF FABRIC, PEDS AND MINERAL COMPONENTS

6.1.1 PROCESSES OF BACKFILLING

According to the different types of grave and to macroscopic observations made during studies of archaeothanatology (Duday 2009), the sediments within the burial space could originate through different processes:

- contemporary backfilling during the deposition of the remains: the sediment derives from the surrounding material. It could be part of the same layer in which the burial is excavated, or from the layers above or in the proximity of the grave. In this situation, the corpse is immediately covered by soil;
- gradual backfilling post-burial: translocation of material from the layers above or sideways into the grave as a consequence of the progressive breaching of the coffin. The corpse is gradually in contact with the soil, possibly as early as during the phases of decomposition and, subsequently, of skeletonization;
- rapid backfilling post-burial: filling of the burial space caused by rapid breach of the coffin or collapse of the vault. The sediments come from the layers above the grave. It is plausible that, in this case, the corpse, which requires from 3 to 10 years minimum to decompose (Carter and Tibbett 2008), is already skeletonized when contact with the soil occurs. Decomposition of a wooden coffin could require a long time, especially in waterlogged and anaerobic environments, which could aid the preservation of organic components. In the case of Pill'e Matta, the cemetery was likely subjected to maintenance during its use and the collapse of vaults could be related to a stage in which the corpse was already skeletonized.

It is conceivable that the graves from each case study could have been subjected to more than one single process (Table 6.2). The graves with wooden coffins in Hungate could have had gradual or rapid post-burial backfilling. As consequence, the body would have started decomposing in an empty and slightly aerobic environment (Forbes 2008, 215-216; Chapter 2, Section 2.4.4). In the case of Haymarket, in the absence of macroscopic data, all three processes were considered plausible. The grave from Rossio Do Carmo was probably partially filled at the same time as the deposition of the corpse. However, some material could have been translocated over time through the space between the schist plates. The grave from Borgharen, as with Hungate, could have been subjected to gradual or rapid post-burial backfilling. The last process could have occurred along with the reopening of the grave in the past. Pill'e Matta was possibly characterized by gradual backfilling, consisting of slow detachment of the vault and/or translocation of the material from the side of the chamber, and/or by rapid backfilling caused by the rupture of the vault.

SITE	CONTEMPORARY BACKFILLING	GRADUAL POST-BURIAL BACKFILLING	RAPID POST-BURIAL BACKFILLING
Hungate		✓	✓
Haymarket	✓	✓	✓
Rossio do Carmo	✓	✓	
Borgharen		✓	✓
Pill'e Matta		✓	✓

Table 6.1: Possible backfilling processes occurring in the graves. The tick indicates which process is considered plausible on the basis of macroscopic data.

It is difficult, or rather impossible, to establish when the gradual and the rapid post-burial backfilling may have occurred, especially in the case of coffins where the decay of the wood could be influenced by different variables and occurred with different rates (Dent et al. 2004). In addition, post-depositional processes could modify the original microstructure and complicate the interpretation of the fill (Bertran and Texier 1999). However, understanding of the type of backfill, contemporary to the grave, gradual or rapid post-burial, was attempted in this research.

6.1.2 MICROSTRUCTURE OF THE SEDIMENTS PRODUCED BY BACKFILLING

The backfill of a grave is generally composed of material located in the proximity and/or in the same layers in which the grave was cut. Thus, these sediments comprise a mix of parent soil, rock fragments and locally produced debris from human activities (Karkanas et al. 2012). Sedimentary structures may sometimes be formed during the backfilling, through processes such as gravitational sorting or clustering of coarse fragments. These structures are irregularly distributed and found in lenticular shapes, being created by discontinuous processes such as shovelling and dumping. These characteristics are typical of mass wasting processes and related debris deposits (Karkanas et al. 2012). These processes generally create sediments without stratification, albeit in the case of the debris deposits, the sediment is composed of loose minerals and rock fragments, alternated with fine material. The components are poorly sorted granules and heterogeneous material, which move rapidly under gravitation (Bertran and Texier 1999; Mücher et al. 2010, 44-45). In the case of chamber tomb fillings, the particles move, depending on the height to which the debris is thrown, and they stop in areas characterized by particles of the same size, creating a type of sorting (Karkanas et al. 2012). However, the dominant processes in the case of the backfill of graves produces highly unsorted and unstratified deposits (Karkanas et al. 2012).

These types of microstructure were well represented in the sites of Hungate, Haymarket and, to a lesser extent, Borgharen and Rossio do Carmo (Mosaics, Supplementary Data). In Hungate, some samples were mostly homogeneous and sandy, while others were heterogeneous and richer in fine

material. Graves 51349/51351, 52253 and to some extent graves 54296 and 54931/54909, were mainly composed of sand. Few areas with higher amount of fine material appeared as pedorelicts or fragments of sedimentary crusts. Graves 51350/51364 and 53700, in part, 54296 and 54931/54909 were more porous and the fine material was more abundant, surrounding the pores or heterogeneously mixing with the mineral grains. Grave 54077 was more porous and the fine material was more abundant in the area of the skull, which was the only sample available for the area of the skeleton. The C2 was mostly sandy and the C3 was characterized by clusters of quartz and surrounded by monic fine material. In the presence of stratification, micromorphological examination revealed that the top of the slide was always richer in fine material (the area of the feet in grave 52253; the areas of the pelvis in graves 53700 and 54296; the areas of the skull and pelvis in grave 54931/54909). This layering occurred in both types of fabric: mostly sandy or with higher amount of fine material. The transition between the two fabrics was generally gradual. In the slides of grave 54931/54909, the two fabrics were quite distinctive and the amount of the fine material in the top layer was significantly higher. In Haymarket, the sediments were less sandy than Hungate, having a higher proportion of fine material. Most of the samples were characterized by intensively mixed and heterogeneous microstructures, with unsorted coarse components. In these cases, the samples were more porous. Fragments of pedorelicts and sedimentary crusts, mainly composed of fine material, were numerous and randomly distributed. Few samples were characterized by semi-homogeneous microstructures, frequently having the fine material light in colour. However, it seemed that, in a few cases, this type of fabric was caused by imperfect manufacture of the slides, which produced an extreme thinning and loss of some materials. The intense sampling in grave 83012 offered the opportunity to demonstrate that semi-homogeneous and heterogeneous microstructures could co-exist in the same grave. Samples from the areas of the knees and feet in grave 84779 were characterized by sorted mineral clusters, very similar to the c/f related distribution observed in the C3 of grave 54077 in Hungate.

According to the interpretation of Karkanas et al. (2012), it seems that the sediments of Haymarket, intensively mixed and inclusive of pedorelicts and sedimentary crusts, were formed by rapid backfilling. This observation could suggest the absence of coffin and the immediate filling of the burials by shovelling. The second possibility is the rapid breach of the coffin or wooden board, with fast descending movement of the sediments from the layers above the grave, still preserving the microstructure of the shovelling process or increasing the mixing. In the case of Hungate, the heterogeneous samples were better sorted than the Haymarket ones, but equally composed by mixed material and, considering the presence of the coffin, they could have been formed by its rapid rupture. The top layers of fine material could have been formed at a later time, with translocation of fine particles from the higher layers. In the case of grave 54931/54909, the top

layer could have originated through a different process, creating a very distinctive layer high in fine material. The process could have related to the presence of water within the void space of the burial, causing the suspension of the fine particles and, in a dryer phase, to their accumulation in the top layer (Bertran and Texier 1999). If rapid backfill is characterized by unsorted and heterogeneous deposits (Karkanas et al. 2012), it is feasible that slow backfill could be characterized by more homogeneous and sorted material. Thus, the presence of homogeneous sandy sediments in Hungate could be associated with slow translocation of the components over time. According to these observations, the presence of a coffin and its slow rupture seems plausible in the case of grave 54931/54909. The interpretation of backfills in grave 54077 is more difficult, due to the lack of samples from the areas of the pelvis and feet. Possibly, the wooden coffin breached firstly in the area of the skull, favouring the entrance of mixed fills. The cut of a cesspit next to this area of the grave could have caused the rupture of the coffin. By contrast, the sandy fill of the controls, collected above the area of the feet, would represent a slower rupture of the coffin. Hence, the clustering of quartz in the C3 could be originated by sedimentary processes influenced by the presence of the coffin.

Two factors could suggest the need to partly modify these interpretations. The first is that the sandy sediments within the burial space were not caused by a slow and selective backfilling, but by the fact that the grave itself was excavated in a mostly sandy layer. Hungate was frequently flooded and this could have caused the deposition of sandy sediments and the removal of fine materials from the site, or the deposition of fine material in a lower flood-plain, with the decrease in the energy of the water (Courty et al. 1989, 86-88). Hence Haymarket, which was situated a few meters above the level of Hungate, was not affected by these processes and the fills were less sandy. The second factor is that the fine material present in the fill and located around the pores could have been introduced or re-managed by biological activities, which took place after the burial (Section 6.3). This aspect can also be testified by the presence of clusters of mineral grains, especially in Haymarket, whose shape resembles the features produced by earthworm activities, rather than sedimentary processes (Section 6.3.3). However, independently of post-depositional biological activities, the data seem to confirm that some graves were affected by rapid breach of the coffin whereas others were not. A study concerning the soil pressure above graves proved that soil vertical pressure increases with the augment of the depth of burial and with the decrease of the grain size (McGowan and Prangnell 2015). Sediments of sand size grains trap more air and are consequently lighter, while sediments with fine material and waterlogged conditions have no air and present a solid mass, which weighs on the coffin. In addition, backfills characterized by random mixtures of sediments and irregular sorting attracts more moisture into the voids, contributing to the weakening of the coffin and to the increase of the weight on it (McGowan and Pragnell 2015). These

observations seem to confirm the interpretation of rapid backfilling or rapid breach of the coffin in the graves of Hungate and Haymarket which were characterized by heterogeneous and unsorted sediments, as well as slow breach of the coffin in the graves of Hungate characterized by sandy backfills. The sandy deposit could have originated within the coffin by slow translocation or by the fact that the surrounding deposit was mainly sand. Both interpretations are in accordance with slow decomposition of the coffin.

Unfortunately, interpretation of the processes of backfilling was limited by the absence of macroscopic information such as stratigraphy, depth of the graves and location within the archaeological deposit, and microscopic information such as intense sampling of controls to explore the differences with the surrounding sediments. However, a few other considerations could be proposed. Figure 5.54 (Chapter 5, Section 5.2.1) shows that Haymarket is of higher elevation a.s.l. than Hungate. In addition, it is known that the archaeological levels below the cemetery of Haymarket and the deposit of Hungate were probably in association (Reeves 2013). Hence, an attempt was formulated to derive approximate locations of the graves in the area of Hungate. It was considered possible that the graves with sandy sediments were situated in the lower deposit, in the proximity of the River Foss. This interpretation could be supported by: the presence of sediments with mostly sandy fraction, caused by processes of erosion, transportation and deposition by the river (Courty et al. 1989, 86-88); the more frequent episodes of flooding and water-logged conditions in the proximity of the river, favouring slow decay of the coffin by anaerobic conditions and associated with less intense soil pressure by the sandy fabric. By contrast, the graves characterized by heterogeneous sediments in Hungate could have had thicker deposit above them, the sediments not being eroded by the river. This aspect, associated with higher frequencies of fine material and porosity, would have created more pressure above the graves and consequently led to more rapid decay of the coffin. In the case of Haymarket, the deposit above the graves was possibly thinner than the one in Hungate, because of the location of the former on the top of a slope (Figure 5.54). The probable lower thickness of the deposit, in addition to still presenting water-logged conditions and clay rich sediments, would have created greater pressure over the graves than the one exercised by the sandy fills, but probably less intense than the one affecting the graves with mixed sediments from Hungate. Considering this, it is conceivable that this pressure was not sufficient to create a rapid collapse of the coffin. Hence, this observation combined with the fact that the burial sediments showed microstructures typical of rapid filling, may suggest that the corpses in Haymarket were buried without coffins. The only pictures available of Haymarket (graves 83015 and 84579, not analysed in this research) showed two skeletons with bones, including patellae, metacarpals, metatarsals and phalanges, in perfect anatomical relationship. These data indicate decomposition in soil without a coffin (Duday 2009, 38-40) and

this interpretation could be considered also for the other graves of the cemetery. It would be interesting to validate these observations through direct comparison with macroscopic data from the excavations.

In most cases, samples from Rossio do Carmo and Borgharen were partially disturbed and influenced by post-sampling factors (Chapter 5, Sections 5.3.2 and 5.4.2). However, it was possible to observe that sediments in Rossio do Carmo contained poorly sorted coarse components, while sediments in Borgharen were more sorted and denser. In the first case, the cause could be attributed to the immediate backfilling after the placement of the corpse, without sorting the coarse components. In the second case, the microstructure could be attributed to slower translocations of coarse components, contemporaneous to the progressive decay of the coffin. The control in Borgharen, collected under the plough horizon, comprised micritic sediment including small aggregates of the same material as the grave fill. It seemed that the layer above the fill of the grave was reworked, causing the introduction of small aggregates from the lower layers. These inclusions, associated with compact and apedal microstructures and micritic fabric, could indicate repeated tillage practices causing translocation of soil material. Thus, processes such as mixing and inversion, with a lateral transport, could cause consequent displacement of the features from their original location. The high content of micrite in the sediment could be explained by irrigation activities related to the tillage and evaporation of the water, causing precipitation of the carbonate (Kooistra et al. 1990, 38; Adderley et al. 2010, 571). This interpretation is in accordance with the use of the area as agricultural land till nowadays (De Groot et al. 2011, 13-15).

In the geoarchaeological analysis of Mycenaean chambers, Karkanas et al. (2012) identified features relating to the collapse of the vaults. The layer of collapse was characterized by chaotic loose filling, composed of cobbles and boulders, followed by fine laminated brown sediment. In some cases, the laminae were disturbed by fragments of sorted minerals inside dense brown fine-grained sediment. The collapse of the vault caused a depression, which was filled with sediments produced during the erosion of the top-soil by rain washing (Karkanas et al. 2012). The laminated sediment was capped by brown clay aggregates coming from the standing walls of the chamber (Karkanas et al. 2012).

In Pill'e Matta, laminae were not identified and the filling of sediments from the top soil was not observed. It seems possible that the filling of the graves occurred through slow depositional processes of fragmentation of the vaults. Materials A and B (Chapter 5, Section 5.5.3) were observed in all of the samples from the backfill and all of the loose samples from the soil profile of grave 89. Thus, these materials were not diagnostic to the precise location of the graves within the soil profile, but they confirmed that the fills were formed from materials of the chamber walls. The sediment filling the pit, having different composition and colours from the limestone and sandstone (Secci 2005, 33), was not present in the slides, except for the area of the feet in grave 237. Coarse

259

and unsorted minerals were dominant in the sample and were mixed with Materials A and B. It seems reasonable that infiltrations from the tiled side of the chamber contributed to the formation of the deposit in this area of the grave. By contrast, the presence of the pit did not contribute to the backfilling in the other areas of grave 237 and of graves 238, 268 and US2680. Very few coarse sub-angular aggregates, from the area of the feet in grave US2680 and from the area of the skull in grave 268, were characterized by several parallel planar voids. These feature seemed to be associated with the voids identified in some of the clasts in the Mycenaean chambers and attributed to the detachment from the rock surface by the activity of digging (Karkanas et al. 2012). Thus, they could be traces of the anthropic processes of excavation of the chambers in Pill'e Matta, made with flat picks (Salvi 2005, 188), before the deposition of the corpse. Unfortunately, additional interpretations were not possible due of the absence of undisturbed soil samples from the soil profile, control samples from the fills of the lateral pit and from surrounding sediments, and stratigraphic data.

In the experimental burials of piglets, the sediments surrounding the skeletons were produced by contemporary backfilling of the burials. The coffins (piglets 7 and 2) were filled at the same time as the burial, simulating the situations in the archaeological graves in which the skeletons were in contact with the sediment because of rapid breach of the coffin (Chapter 5, Section 5.6.1). The samples from Heslington East were characterized by mixed materials and poorly sorted components, supporting the interpretation of these microstructures as resulting from rapid backfilling. It would have been interesting to observe the effects of gradual translocation of sediments, corresponding to the progressively degradation of the coffins. However, the length of the experiment, which lasted 3 years, was too brief to observe significant decay of the coffins, even if they had been left empty to enhance the effect of soil pressure from the top layers. Although considerations could have been developed on the fabric microstructure in the situation of rapid weathering of the coffins, the experiments would have implied the use of empty coffins and their placement at greater depth. Further interpretations would have benefitted from the collection of samples of the sediments used for backfilling, before burying the piglets. The coffin of piglet 2 and the area above it were filled with clean imported limestone, limiting observations on the process of backfilling, which was originated by dumping of sorted material, without the opportunity of mixing it with other sediments. In addition, samples of limestone were not taken before the use of it in the burial.

6.1.3 PEDALITY OF THE BACKFILLS

Peds were not common within the burial sediments and their presence was mostly related to the type of soils. Aggregation was favoured in limestone and sandstone deposits and limited in wet soils, in accordance with the fact that the degree of pedality and ped separation is usually strong in

dry conditions and weak in wet soils (Kovda and Mermut 2010, 111). Granular peds were identified in: grave 53700 in Hungate, mostly in the area of the skull, grave 15 in Borgharen, especially in the area of the ribs (Figure 5.93), graves 237, 238, 268 and US2680 in Pill'e Matta (Figure 5.130) and, with lower frequency, in the piglet burial 6. Granular peds are generally formed by activities of soil biota, such as fauna and roots (FitzPatrick 1993, 124-125) or by rapid desiccation of the soil (Kovda and Mermut 2010, 110). The aspect of the peds and their association with biological features (Section 6.3) supported the former interpretation for the peds in Hungate, Borgharen and Piglet 6. By contrast, in the case of Pill'e Matta, rapid desiccation appeared to be the main cause of ped formation, consistent with the location of the graves in the temperate Mediterranean zone with very hot summers, and encouraged by the friable texture of the limestone and sandstone, which formed the deposit. In the grave 237, the separation between the peds was higher in the areas of the skull and pelvis, while peds were closer together and finer in size in the area of the feet, showing more compaction of the fabric microstructure. This increasing of density could be explained by less exposure of the sediment in the area of the feet, maybe caused by the infilling from the lateral pit, affecting the same area. Granules in grave 238 were weakly developed and separated, with consequently dense fabric microstructure. Possibly, this grave was more protected from moisture evaporation. Peds in graves 268 and US2680 were highly separated in the area of the skull and progressively more compact in the areas of the pelvis and feet. In these cases, skeletal regions could have influenced the retention of moisture and compaction of the soil differently to each other. Granular peds were common in grave 395 in Rossio do Carmo, but most of them were formed by sampling and post-sampling factors. Hence, it was difficult to make a distinction with the original peds. Piglet burial 2 had granular microstructure, because of the shape of the imported limestone granules. However, development of peds after the backfilling was not observed, except for very fine granules consisting of soil micro-fauna faecal pellets (Section 6.3.3). By contrast, the sediment in the controls presented denser microstructure, with increase of compaction of the limestone granules from C3 to C2, possibly due to the higher moisture content caused by the percolation of groundwater from the above layer.

Sub-angular peds were less frequent than granules and they were identified in: the area of the ribs in grave 15 in Borgharen (Figure 5.92.b), the areas of the skull in graves 237 and 268 in Pill'e Matta (Figure 5.130.g-h; different from the ones caused by flat picks) and the piglet burials 6 and 7. These types of ped are formed by wetting and drying phases, influencing the expansion and shrinking of the clay fraction of the sediment (FitzPatrick 1993, 118-119). In Pill'e Matta, the sub-angular peds were observed only in the area of the skulls, where there was higher separation between the granules. Sub-angular and angular peds were observed in some of the samples from Haymarket, where their morphology and position at the top of the slide, led to them being considered to be

products of post-sampling processes, such as drying of the sample. Most of the samples from Haymarket and Hungate were apedal. It has been documented that, in hydromorphic conditions such as the ones of these sites, the soil is subjected to decreases in aggregate stability and porosity (Stoops and Schaefer 2010, 73-74).

6.1.4 FINE MATERIAL AND COARSE MINERAL SORTING

The presence and characteristics of fine material and coarse minerals were dependent on factors such as the type of soils and environmental conditions, as well as the post depositional processes (Mosaics, Supplementary Data). The sediments in Hungate, Haymarket, Borgharen and Heslington East were mostly brown with dotted limpidity, due to the presence of fine fragments of organic matter, and with speckled b-fabric due to oriented clay particles. In Hungate, the fine material was more yellow in some areas owing to the presence of amorphous phosphates and more red or black in other areas as a result of redoximorphic conditions. The sediments in Haymarket were mostly brown due to their proximity to the top soil, while red/black areas, caused by redoximorphic conditions, were less frequent than in Hungate. The backfill sediment in Rossio do Carmo was lighter in colour, greenish yellow/brown due to the paucity of organic matter, which still had role in the dotted limpidity, and contained a very fine fraction of schist. The latter influenced the b-fabric, conferring crystallitic aspect to some areas. Sediments in Pill'e Matta and Hovingham were grey beige in colour due to the presence of calcium carbonate, with crystallitic b-fabric for the micritic fraction. The limpidity was dotted in the piglet burial 2 owing to the presence of organic matter and opaque or masked in Pill'e Matta, due to the calcium carbonate and insignificant amorphous organic matter content.

The most abundant mineral in Hungate, Haymarket, Borgharen and Heslington East was quartz, which is the most frequent primary mineral occurring in soils and is extremely resistant to weathering (FitzPatrick 1993, 87). Thus, its concentration in the fills demonstrated that soil weathering was advanced. Other minerals, such as plagioclase, biotite and muscovite, present with very low frequencies, confirmed the advanced weathering of the soil. Plagioclase is generally common in recent sediments and absent in moderately or strongly weathered soils (FitzPatrick 1993, 84). Biotite is susceptible to environmental conditions: weathering by hydration and exfoliation in a first phase and changing to secondary minerals, such as goethite, in a second phase (FitzPatrick 1993, 62). Muscovite weathers by hydration and exfoliation, producing several single laminae, which persist in the soil (FitzPatrick 1993, 83). These minerals were present in few cases and with frequency lower than 2%. In the buried sediments of Rossio do Carmo, schist was the most frequent mineral component, followed by quartz. The presence of coarse fragments of schist was mostly caused by the superficial fragmentation of the surrounding rock and the slabs covering the grave. Hence, fragments of schist were mostly angular or sub-angular in shape. In Hovingham, few

grains of quartz were present in all of the samples, being included as a component in the imported limestone. In Pill'e Matta, the sediments were characterized by low coarse mineral fraction, because of the original composition of the sandstone. An abnormal increase of the coarse mineral fraction was observed in the area of the feet in the grave 237, where the contribution from the fill outside the chamber was identified in the process of backfilling.

Variability in the size of quartz was not observed between the samples of each grave, except for the cases of clustering in the C3 in the grave 54077 in Hungate and in the areas of the feet and knees in the grave 84779 in Haymarket. These three cases represented a proper segregation, possibly produced by earthworm activity, of the smallest grains of quartz. The other mineral types behaved in the same way of quartz. The grains showed angular, sub-angular and sub-rounded shapes. Coarser fragments, such as the quartzite, were mostly sub-rounded. Thus, the origin of the coarse mineral fraction was attributed to the local soils, with low effects of transportation documented by the sub-rounded surfaces, especially visible on the coarser grains. To appreciate the causes, information regarding the processes of formation of the soils in the different archaeological sites would be essential. Hence, only in the cases of Hungate and Borgharen is it possible to suggest that the sub-rounded grains were transported by the rivers Foss and Meuse. At the time of the cutting of the graves, the sediments were mixed during the backfilling of the burials. No changes were observed between the Roman graves and the Anglo-Scandinavian one from Hungate. Observations were conducted on the quartz fraction of the fills, to detect possible movement and segregation of this type of mineral within the graves. Quartz was chosen for the analysis as it was the most frequent and well represented mineral in all of the sites. In all of the graves in Hungate, except for grave 54077, the quartz grains were more frequent in the area of the skeletal remains, progressively decreasing from the skeleton to the C3 and to the C2. Within the area of the skeleton, the grains were more frequent in the areas of the skull and pelvis, decreasing in the region of the feet. The same tendency was observed in Borgharen and in the piglet burials 6 and 7. In grave 54077, the quartz grains were more frequent in C2 and equally frequent in the area of the skull and in C3. Control C2 was mainly composed of quartz, with low amounts of fine material. In the grave in Rossio do Carmo, quartz grains were more frequent in the area of the skeleton, without distinction between the anatomical regions, and less frequent in the control. In the graves of Pill'e Matta, the quartz was more abundant in the area of the skull or equally represented in all of the areas around the skeletons. Similarly, in the piglet burial 2, quartz was equally distributed. The same situation was observed in the graves of Haymarket, except for grave 83012. In this grave, the quartz grains were more frequent in the areas of skull, C3 and C2 and less frequent in the area of pelvis and in the surrounding samples. These data seemed to demonstrate that in sandy soils, such as Hungate, Heslington East and Borgharen, the quartz grains progressively translocated from

the top layers to the area of the burials. Most importantly, the grains were stopped and held in the proximity of the skeleton, especially in the area of the skull and partially in the area of the pelvis. This was well illustrated in the samples of the piglet burials 6 and 7: the quartz content was higher in the samples closed to the skeletons, but less in the ones more distant, even if collected in the same layer. Hence, the role of bones, especially the ones with wide surfaces such as skull and pelvis, to retain mineral seemed evident. By contrast, in Pill'e Matta the frequency of the quartz was low. and the backfill originated differently, inhibiting the possible process of translocation in the chamber tombs. As result, the quartz was mainly equally distributed. Furthermore, it seemed reasonable that the low frequency of the grains, as in the piglet burial 2, did not offer the opportunity to detect considerable changes in the distribution. The situation of Haymarket was quite different. The cause could be identified in the difference of the backfilling processes. According to the interpretation exposed in Section 6.1.2, the graves in Haymarket were potentially without coffin and the backfilling was contemporary to the inhumation. In these circumstances, the mineral grains would have been less subjected to downward translocation, because no empty spaces were available, except for limited areas left free by the decomposition of the corpse. Moreover, it could be suggested that, the corpse being in direct contact with the soil, it could have been more affected by faunal activity. As consequence, the mineral grains, if accumulated in the proximity of the corpse, would have been more easily dispersed. The application of the same investigation to different archaeological sites, affected by various and certain backfilling processes, could be useful to scrutinize and test these considerations.

6.2 VOIDS AND POROSITY

When a burial is made, the sediment of the backfill is typically looser than the surrounding soil and its porosity is greater. The oxygen is captured closed to the coffin, decreasing upward to the top surface for the completion of the backfilling (Dent et al. 2004). When backfilling is complete, soil compaction processes can take place, favoured by water percolation due to infiltration of rainfall. Ground water favours the addition of oxygen from the surface with downward movement (Dent et al. 2004). Further changes in porosity can be produced by faunal activity and processes of pedality or compaction. The presence of the corpse itself, which goes through different stages of decomposition (Chapter2, Section 2.4.4), influences the formation and movement of gases and fluids within the burial soil. Carbon dioxide, methane, hydrogen sulfide, ammonia, cadaverine and putrescine are dissipated upwards from the human remains, the gases competing for space with oxygen and limiting its downward movement (Dent et al. 2004). Few studies have investigated these aspects and, for the first time in this research, the changes of porosity within the burial sediments were examined by image analysis and micromorphology of voids. The attempt was to

identify the possible changes, their relations to the burial characteristics, anatomical locations and to the origin of the voids. It is important to specify that the lack of one or all of the controls from some graves limited this examination.

6.2.1 VARIANCE OF THE POROSITY WITHIN THE GRAVES

The frequency of porosity within the graves was variable between the sites and within the sites themselves (Chapter 4, Section 4.4). However, some consistencies were observed. The data utilized are provided in Appendix 2.9. Three different trends in the changes of porosity within the burial sediments were identified. In the first case, the porosity was higher in the C2 (or C3) and decreased in the C1 (or C2), C3 and in the area of the skeleton. The graves 51349/51351 and 52253 in Hungate showed this trend. Both graves were characterized by not deep backfilling, according to the previous interpretations (Section 6.1.2). In the second case, the porosity was lower in the C3 and increased in the C2 and in the area of the skeleton, as shown in graves 51350/51364 and 54296 in Hungate and 84700 in Haymarket, suggested to be characterized by rapid backfilling. In the third case, the porosity was progressively higher from C2 to the area of the skeleton. This variance was observed in graves 84779 in Haymarket and 15 in Borgharen. Only one control was available in both situations, hence the porosity in C3 was not known and the investigation was limited. The possible cause of these different trends in porosity seem to be related to the presence/absence of a coffin. In the case of slow decay of the coffin, the presence of the wood could have slowed the downward movement of soil particles and, according to the interpretation of Dent et al. (2004), oxygen from the surface and the upward movement of the decomposition gases from the area of the corpse, creating an area with higher porosity in the C2 (or C3, depending on the exact location of the collection of the sample in relation to the coffin, by then decomposed). However, the major role should have been played by the soil fauna. The slow breakdown of the coffin could have attracted the soil fauna for longer periods, favouring the increase of voids in its proximity. By contrast, in the case of the rapid decay of the coffin, or absence of it, it could be suggested that the fine and coarse materials of the fill would have reached and filled more rapidly the area above the corpse (C3). Hence, the corpse, if still not decomposed, would have presented a barrier to the downward translocation of the material. The subsequent decomposition of the corpse would have created gases and more pores in the area of the skeleton, possibly limited in their upward movement by the compaction of C3. The role of the coffin, as obstruction to the downward movement of water and soil particles, and possibly to the upward movement of the gases of decomposition (Dent et al. 2004) was evident in the experimental burials. When excavated, these coffins were still preserved, so the exact location of C3 in relation to the coffins was known. In piglets 2 and 7, the porosity was higher in the sediment under the lid of the coffin, increasing in the areas surrounding the skeletons. The C2, collected just above the lid, was lower in porosity, corresponding to the area in which the

material translocated and stopped. In accordance with the interpretation suggested for rapid backfilling, the grave 83012 in Haymarket had lower porosity in C3 than C2. The pore frequency in grave 395 of Rossio do Carmo was higher in the C3 and lower in the C1 and the area of the skeleton. Considering the observations discussed above, this trend should be typical of slow backfilling. However, the grave was probably filled immediately after the deposition of the corpse (this chapter) and, according to Islamic funeral rules, it was probably covered with organic materials, before the closuring by slabs of schist. If this happened, the organic matter would have attracted more soil fauna and it would explain the increase of porosity in the proximity of the slabs. In addition, the presence of the cover with schist may have aided the preservation of the original porosity.

6.2.2 ORIGINS OF THE VOIDS

The changes in porosity were observed also within the area of the skeleton, by the image analysis technique (Chapter 4, Section 4.4; Appendix 2.9), following four different patterns: increasing from the area of the skull to the area of the feet, decreasing from the area of the skull to the area of the feet, increasing from the areas of the skull and feet to the area of the pelvis and, finally, decreasing from the areas of the skull and feet to the area of the pelvis (Figure 4.9, Chapter 4). The same variation was observed in graves from different sites and fills. Different types of backfilling surely influenced the porosity. However, further changes in porosity were probably produced after the deposition of the corpse. Most commonly, graves were more porous in the area of the pelvis (9 graves), followed by the area of the skull (6 graves) and the area of the feet (1 grave). Several possible explanations were considered: the higher production of gases in the pelvis during the decomposition of the intestines and abdomen, the presence of more organic matter in the pelvis and skull available for the soil fauna, the chance of better preservation of the fabric microstructure in the proximity of these bones, characterized by wider surfaces, as demonstrated by the segregation of mineral grains (Section 6.1.4)

The main voids observed in the graves were: chambers, channels, modified complex voids, packing voids and planar voids. Chambers have round or oval shape and smooth walls; more rarely, they are irregularly shaped. When isolated, they can be the product of non-social fauna, such as beetles and earthworms which do not live communally, as enlargement for deposition of materials or refuge. When organized in complex associations with channels, they are the product of social fauna, such as ants and termites, and their galleries serve for food production and temperature regulation (Stoops 2003, 64-65; Kooistra and Pulleman 2010, 404-405). Channels are tubular smooth voids, commonly uniform over their length, which can be straight, curved or convoluted in shape. Their transversal section can be perfectly round or sub-rounded. They can be produced by different types of worm, termites or by roots. Channels produced by fauna are less regular in shape and their walls are characterized by irregular compressed zones (Stoops 2003, 64-64; Kooistra and Pulleman 2010,

402-403). Chambers and channels are identified as primary voids, formed by pressure on the soil material, digging and removal of loose material or consumption (Babel et al. 1990, 18). Modified complex voids are characterized by irregular shapes, composed by curved and pointed wall surfaces. They are produced by small mesofauna, such as *Acarina*, *Collembola* and *Enchytraeidae*, which enlarge primary voids by consumption of bacteria, algae, fungi and fine-grained soil material situated on the void walls (Babel et al. 1990, 19-20; Kooistra and Pulleman 2010, 405). Packing voids results from the loose organization of the soil components. They are equant or elongated in shape and highly interconnected, possibly originated by biological activities (FitzPatrick 1993, 124-125) or rapid desiccation of the soil (Kovda and Mermut 2010, 110), as space between granular peds. Packing voids can also be formed as secondary voids between coarse-grained soil components when the fine material is depleted (Kooistra and Pulleman 2010, 405). Finally, planar voids are flat voids, with rough or smooth walls and sharp points, often with sub-horizontal or oblique orientation. They form by shrinkage, cracking or slipping (FitzPatrick 1993, 116; Stoops 2003, 65; Kovda and Mermut 2010, 111).

Chambers, channels and modified complex voids (Figures 5.78.g, 5.92-e-g and 5.101) were mostly observed in the area of the skeleton, but they were also present in the C1, while packing voids were more common in the controls. However, in some graves, such as 237, 268 and US2680 in Pill'e Matta, packing voids were frequent in the areas surrounding the skeletal remains. In addition, strong differences and correlations between the types of voids and the increasing of porosity in specific areas were not observed. Thus, it was sensible to affirm that voids in the graves were subjected to the activities of backfilling, followed by biological activities, peds formation, shrinking and cracking processes and possibly by the production of gases from the decomposition of the body. However, the work of Dent (2004) is one of the few reference for the formation and movement of gases. Thus, the origin of voids by the production of gases, remains a hypothesis in this research. Finally, the morphological characteristics of the anatomical regions of skull and pelvis substantially contributed to the preservation and/or generation of the voids.

6.3 ORGANIC COMPONENTS AND BIOLOGICAL ACTIVITIES

Different processes of backfilling and environmental conditions seemed to influence the rate of decay of the coffin, which had a role in the decomposition of the corpse. When the body is directly placed into the soil, the rate of decomposition reduces (Carter and Tibbett 2008, 41-42), while the presence of coffin can favour a more rapid decay owing to the temporary availability of oxygen (Dent et al. 2004). Fungi and bacteria are mostly aerobic and they are the first to be attracted from the release of ammonia during the putrefaction of the cadaver (Carter and Tibbett 2008, 37). Hence,

these organisms are intensively involved in the consumption of the organic matter, which includes soft tissues of the corpse, organic materials deposited into and around the grave and the wooden coffin itself. In addition to fungi and bacteria, several types of meso- and macrofauna are responsible for the decomposition of the corpse (Dadour and Harvey 2008, 109-117). It is difficult to appreciate the traces of soil flora and fauna during the excavations and to identify the organic remains by macroscopic observation, while microscopic analyses allow the recognition of fine-size fragments of organic matter, even in sediments affected by intense human activity and diagenetic processes (Courty et al. 1989, 140; Goldberg et al. 1994; Matthews 2010). The features related to soil organisms and organic matter detected in the burial sediments included biological voids (see above), fragments of organic matter at different stages of decomposition, fragments of bones, roots, fungi, insect remains, soil micro-fauna faecal pellets and worm-derived calcium carbonate granules. The last two features are described in this section for their relation to the faunal activities, even if they were identified and catalogued as pedofeatures.

6.3.1 HUMIFIED PLANT STRUCTURES, AMORPHOUS ORGANIC MATTER AND ROOTS

Humified plant structures and amorphous organic matter were the most common organic remains found in the burial sediments. Different stages of alteration of the tissue residues were documented, from the browning to the compaction and comminution. Living tissues are generally colourless in thin section and they turn yellow, brown or red in colour in the first stage of alteration, called browning, caused by the formation of polymers corresponding to humic substances (Babel et al. 1990, 4). This stage induces weak/medium chemical changes and nearly no structural changes. Two related stages are blackening and bleaching. In the former, the tissue becomes dark brown to black without changes in the cells structure. It is more common in sediments affected by water-logged. The latter sees the disappearance of the brown structures formed during the browning. It is caused by basidiomycetes, which are similar to white rot fungi. Frequently, the plant tissues are deformed by swelling and shrinking or passage through the gut of saprophagus animals. Structure and colours remain unchanged during the phase of fragmentation or comminution by animals. Intense chemical and structural changes are produced by the phases of maceration, liquefaction and disappearance (Babel et al. 1990, 4-6). In the amorphous organic matter, the cell wall structures are not well recognizable. Lignin-rich tissue, such as wood are a large part of most plants. They have thick cell walls and they are commonly observed as residues, more resistant to decomposition. Decomposition of plant residues results in the formation of organic fine material (Stolt and Lindbo 2010, 373-374). This may be subdivided into cells and cell tissues, amorphous organic matter and punctuations (Stolt and Lindbo 2010, 373-374). The lignin-rich material shows first-order interference colours (roots).

Humified plant structures were observed in all of the graves with percentages around 5%, with some exceptions. These structures were scarce in Pill'e Matta, due to the environmental conditions which did not favour their preservation. Better preservation occurred in waterlogged or partially waterlogged sites, such as Hungate, Haymarket and piglet burials 6 and 7. In some cases, the humified fragments preserved the original structures and it was possible to observe that the coarser fragments were derived by angiosperm or gymnosperm wood. The area of the skull in grave 54077 was characterized by abundant fragments of gymnosperm wood (Figures 5.41.c-d and 5.78.c-f). These fragments were embedded within amorphous phosphatic areas and associated to vivianite, which testify reducing condition and consequently good preservation of the organic matter (Section 6.4.2; Figure 5.42.a-d). In the same sample, it was possible to appreciate different phases of decomposition of the wood (Figure 5.42.e-h). In addition, few other fragments of organic matter of different origin, one calcined and one burned bone fragments were observed in the same samples. These materials were possibly introduced in the area of the skull by the cesspit present in the proximity of the grave. A peculiar round feature was noted in the area of the skull in grave 53700 (Figure 5.41.g-h). The morphology of the feature was similar to the antheridium of an alga and comparable examples are the antheridia from the *Characeae* family. The presence of algae in Hungate would be perfectly conceivable, because of the intense presence of water. This alga could have been introduced in the grave during the deposition of the corpse.

Roots were only present in Borgharen, Pill'e Matta and in the piglet burials. Their presence seems to be related to environmental conditions and, possibly, to the depth of the grave within the soil profile. In Borgharen, the roots were represented by more or less fresh fragments and micritic coatings (Section 6.4.6). Their presence seems related to limited depth of the grave and traces of tillage in the C1. In Pill'e Matta some fresh roots were observed (Figure 5.131.e-f). However, they were mostly decomposed by mites, which ate through the root depositing their faecal material and leaving the bark and the epidermidis to be decomposed by fungi and bacteria (FitzPatrick 1993, 165; Figure 5.131.g-h). The absence of roots in waterlogged or partially waterlogged sediments is related to the necessity of oxygen for the respiration of the roots. When the aeration is in deficit due to saturated soils, the limiting root growth occurs (Babel et al. 1990, 16-17).

Fragments of charcoal were absent in Rossio do Carmo, nearly absent in Hungate, rare in Pill'e Matta and more abundant in Borgharen and Haymarket (Figure 5.78.b). Charcoal results from the incomplete combustion of vegetation, generally burned at the surface or burned off-site and applied to the soil with ash. Coarser fragments can preserve their original cell structure (Stolt and Lindbo 2010, 376). The higher frequency of charcoal in the sites of Borgharen and Haymarket, could be associated to the anthropic activities occurred in the sites and its incorporation through bioturbation. However, their frequency was too limited to assert further interpretation.

6.3.2 BONE FRAGMENTS

Bone fragments were common in all of the sites, testifying the weathering of the skeleton in different environments. The most common post-mortem alterations occurring on the bones are caused by root action, insects or rodents. By contrast, microbial and chemical degradation can influence the interiors of the bones as well as their surfaces causing the fragility of the bones. In addition, the water contents of buried bones and surrounding sediments plays an important role in their integrity, because the bone minerals are vulnerable to the dissolution in soil water (Turner-Walker 2008). As soil pH decreases, the destruction of osseous materials increases (Gordon and Buikstra 1981). In water-logged environments, the bones are well preserved until the stabilisation of the water table. Hence, wetting and drying phases increases in the porosity of the bones and decreases their preservation. On the opposite, bones buried in well-drained soils do not saturate and they became susceptible to leaching (Turner-Walker 2008). The first and second cases can be associated with Hungate and Haymarket, the third to Pill'e Matta. The SEM-EDS analyses on the fine material in Pill'e Matta did not show any significant difference relating to the decomposition of the bone. The fragmentation of the bones was mechanical and attributable to the increase of leaching. Bacteria destruction of the bone tissues is related to the putrefactive stage, while fungal alteration may occur at any time during burial. These types of destruction can be identified by four morphologies: linear longitudinal, budded, lamellate and weld tunnelling (Jans et al. 2004). Some fragments of bones from the case studies showed black stains and tunnelling, but generally the fragments were too small to appreciate and identify these alterations (Figures 5.41.e-f, 5.77.g-h, 5.102.a-d and 5.131.a-d). However, in the area of the knees in grave 83012, a coarse fragment of bone showed interesting granular infillings in the fractures and black stains in the osteons (Figure 5.77.a-d). These features were identified as bitumen, according to the chemical analyses done on the sample from the same area (B. Keely, personal communication). The presence of bitumen was attributed to the post-depositional event of the service trench cutting across the grave.

6.3.3 INSECT REMAINS AND PRODUCTS

Insect remains were observed in the piglet burials, while insect products were detected both in the archaeological sites and in the piglet burials. Insect remains in thin sections can be observed when there is the presence of resistant remnants into the soil and of chitin in the insect exoskeletons (Kooistra and Pulleman 2010, 401). The preservation of insect remains depends on anaerobic conditions, in either wet or dry environments. Examples from archaeological graves were represented by the fly puparia from the Arikara burials in South Dakota (Gilbert and Bass 1967) and the beetles from the lead-lined stone sarcophagus of Archbishop Greenfield in York Minster (Panagiotakopulu and Buckland 2012). The fly fauna within graves possibly derives from oviposition onto the body whilst it was laid out prior to burial (Panagiotakopulu and Buckland 2012). This

situation was peculiar of piglet burial 2, were several flies were found under the coffin lid. It is presumed that the eggs were deposited into the carcass of the piglet before the burying and that, when the process of pupation completed, the newborn flies were trapped within the coffin. These flies were identified as fungus gnats (Sciaridae) which live on living plants, rotten wood and plant litter (Shin et al. 2013). Remains of flies (head, legs and wings) were observed in the same burial (Figure 5.152). Chitinous exuvia of fly pupae were observed also in piglets 6 and 7, also suggesting the oviposition before burial in these cases (Figure 5.153.a-d). The presence of fly pupae within graves has been used in the past to date the season of the burial (Gilbert and Bass 1967). Other fragments of insects were observed in piglet burial 6 and they were identified as oribatid mites (Figure 5.153.e-f), on the base of the morphologies showed in Woolley (1970). Oribatid mites are the most abundant soil arthropods. They feed on litter and some species have fungal feeding preferences, particularly for dark pigmented fungi, such as *Ulocladium* (Mitchell and Parkinson 1976; Schneider and Maraun 2005; Renker et al. 2005). It is interesting to notice that the faecal pellets of mites in Pill'e Matta were mostly concentrated in the area of the skull, where the *Ulocladium* was present (Figure 5.132.e-h).

Insect remains did not preserve in the archaeological graves, probably for the environmental conditions and their fragility. However, faunal activity was testified by the presence of soil micro-fauna faecal pellets and worm-derived calcium carbonate granules.

Faecal pellets identification was based on Bullock et al. (1985, 134), FitzPatrick (1993, 139-141), Kooistra and Pulleman (2010, 406) for the excrements produced by mites and FitzPatrick (1993, 139) for the excrements produced by enchytraeids. The first were circular or tubular excrements, observed within the roots in Pill'e Matta and in piglet burial 7 (Figure 5.153.e-h and 5.154.g-h). The second were circular and present in bigger aggregation. They were observed in piglet burial 2 and 6 (Figure 5.154.a-f). It seems that, particularly in the case of faecal pellets produced by enchytraeids, the colour and composition of the pellets were subordinated to the material available. In the presence of high quantities of organic matter, the faecal pellets were mostly brown in colour and composed by fine and organic material (piglet burial 6; Figure 5.154.a-d), while in the presence of lower quantities of organic matter, the faecal pellets were mostly grey and composed by fine mineral components (piglet burial 2; Figure 5.154.e-f). In the case of Pill'e Matta, most of the faecal pellets were composed by mixture of organic and mineral components.

Clusters of sand grains, present in Hungate and Haymarket, are generally considered the result of earthworm activities, caused by the redistribution or the transport of the grains during their movement within the soil (FitzPatrick 1993, 141-142). Earthworms produce also calcium carbonate in the form of 0.1-2.5 mm large granules. These are aggregates of individual calcite crystals arranged in radial, parallel or random pattern depending partly on the earthworm species (Canti 1998; Canti

2003; Canti and Piearce 2003; Canti 2009; Durand et al. 2010, 170-171) . The granules are produced within special glands closed to the mouth. These glands take the form of two or three pairs of pouches attached to the oesophagus. The pouches contain white calcium carbonate either in the form of a paste or as solid granules, which are released into the gut and pass out with the casting. Some granules are found in the subsoil, but most occur in the uppermost layers with general progressive decrease occurring with depth. The recycling and destruction of granules may occur by predator digestion, defecation or by dissolution (Canti 1998; Canti 2003; Canti and Piearce 2003; Canti 2009; Durand et al. 2010, 170-171). Earthworm granules were observed in Haymarket (Figure 5.81.e-h). According to the explanation above, they were more frequent in the controls. However, they were present also in the area surrounding the skeletal remains. The presence of earthworms in Haymarket confirms that the site was rarely water-logged, because earthworms are very sensitive to the changes in humidity and temperature and they avoid watered soils (Canti 2009).

6.3.4 FUNGI

Fungi play the role of decomposer of dead organic matter, including litter, faecal material and dead organisms (FitzPatrick 1993, 218). They have been observed in different types of environments, although they are more common in the topsoil and they are inhibited in anaerobic and reducing environment (FitzPatrick 1993, 221). Fungal activity within the graves was identified by the presence of sclerotia, fungal hyphae, fungal spores and fungal bodies. Fungi were more frequent in grave 238 in Pill'e Matta, graves 53700 and 54931/54909 in Hungate, Rossio do Carmo and in the piglet burials 2 and 6.

Sclerotia are rounded bodies developed from an initial cluster or knot of hyphae (Ritz and Young, 2004). They were the most common fungal indicator in the sites (Figure 5.102.f), probably because they can survive long periods and in adverse environments (Ritz and Young, 2004). Filamentous fungi were also present in the sites (Figure 5.151.g-h). The presence of hyphae is an effective adaptation to life of fungi into the soil, absorbing nutrients from the substratum (Ritz and Young, 2004). Fungi with peculiar characteristics were observed in the piglet burials and Pill'e Matta, but their identification was not possible (Figures 5.132.a-d and 5.151.b-f). In the case of grave 238 in Pill'e Matta, the dark fungal bodies were identified as *Ulocladium* (Figure 5.132.e-h). This genus represents anamorphic fungi, mostly found as saprobes on plant material and in the soil. The species of *Ulocladium* are characterized by conidia ovoid in shape with a pointed basal end and rounded apex. The *Ulocladium* is tolerant to fluctuating humidity (Andersen and Hollensted 2008; Runa et al. 2009).

6.4 PEDOFEATURES

Differences in post-depositional processes, climate, soil and grave types influenced the presence and frequency of pedofeatures within the grave sediments. Some pedofeatures were observed in more than one case study, while others were specifically related to a single archaeological site. The following discussion involves the main pedofeatures detected within the graves that were significant for the interpretation of the burying and post-burying processes. Pedofeatures related to faunal activity are discuss in Section 6.3. The main pedofeatures were: redoximorphic pedofeatures, goethite, amorphous phosphates, vivianite, secondary radial crystals, spherulites, clay and fine material coatings, secondary $CaCO_3$ pedofeatures and anthropogenic materials.

6.4.1 REDOXIMORPHIC PEDOFEATURES

Redoximorphic pedofeatures are associated with the presence of water within the soil, originating by the reduction, translocation and oxidation of Fe and Mn compounds during water saturation and desaturation (Bouma et al. 1990, 265-266; Lindbo et al. 2010, 129). During the phase of reduction, Fe and Mn oxides are removed from the particles of the soil. This happens in case of soil saturation, anaerobic conditions or presence of sufficient organic matter and microorganisms, and temperature above 5° C to permit biological activity (Lindbo et al. 2010, 129). Eh and pH of the soil solution play an important role in the reduction of oxides. The first phase does not leave any trace in the soil and concerns the reduction of oxygen (O_2) and its depletion, creating anaerobic conditions, and the reduction of nitrate (NO^-_3) to nitrogen gas (N_2). In the second phase the reduction of Mn (Mn^{4+} or Mn^{3+} to Mn^{2+}) takes place, followed by the reduction of Fe (Fe^{3+} to Fe^{2+}). These reduced forms are highly soluble and the Fe/Mn oxides dissolve off the soil particles, leaving a grey colour in the soil and developing redox depletion features (Bouma et al. 1990, 266-267; Lindbo et al. 2010, 130). Consequent to the Fe and Mn reduction is the destabilization of soil particles, which are dispersed during the water saturation events. Reduced Fe and Mn in solution move into oxidizing environments: Fe oxidizes precipitates first, followed by the Mn. These elements accumulate on the soil particles or peds surfaces, even in anaerobic soils, when aerobic conditions occur. Examples are air-filled channels, entrapped air in intrapedal voids or aerobic water within peds with few organic matter (Lindbo et al. 2010, 131). Morphological characteristics of redoximorphic features are influenced by the movement of water and air through the soil, the duration of water saturation and anaerobic conditions and the presence or absence of organic matter (Lindbo et al. 2010, 136). Redoximorphic pedofeatures are described as intrusive, impregnative and depleted. In the intrusive, oxidized Fe and Mn accumulate as coating or infilling; in the impregnative they accumulate as nodule, hypo- or quasicoating; in the depleted, the oxidized Fe and Mn have been removed (Lindbo et al. 2010, 132-135). Differences in the colour and morphology of redoximorphic pedofeatures are related to the duration of water saturation (Lindbo

et al. 2010, 129). In case of brief saturation or absence of it, Fe/Mn and Fe nodules are formed, when the dissolve oxygen is consumed rapidly by organic matter decomposing microorganisms. If the saturation persists several days, the Fe/Mn hypocoatings occur. With the duration of water-logged conditions, the impregnative pedofeatures increase and the depletion-related pedofeature are observed (Hseu and Chen, 1996; Lindbo et al. 2010, 136-137). The depleated redoximorphic pedofeatures appear as areas where the Fe/Mn oxides and/or clay have been removed, due to the mobilization of these elements. They have grey colouration and they are often associated to Fe or Mn oxide quasicoatings (Lindbo et al. 2010, 135-136).

Fe/Mn nodules were detected in all of the graves. They were the only types of redoximorphic feature observed in Pill'e Matta, in graves 84700, 87779 and 84851 in Haymarket and piglet burials 2 and 7. In the case of Pill'e Matta, higher frequency of Fe/Mn nodules were observed in the areas of the skull, possibly influenced by the major quantity of organic matter in this area of the corpse and by the shape of the skull itself, which could have aided the preservation of the nodules. Considering that piglet 7 was placed in partially waterlogged sediments, the absence of redoximorphic pedofeatures related to long periods of water saturation could have been caused by the presence of the coffin. During the three years of burying, the coffin did not breach and it seems possible that it preserved the piglet from the effects of water-logged.

By contrast, piglet burial 6, was characterized by redoximorphic impregnative pedofeatures in the area of the skull and in C2 and C3. Hence, the controls represent the oxidizing layers in which Fe and Mn compounds precipitated. Impregnative redoximorphic pedofeatures were observe also in Rossio do Carmo, Hungate and Haymarket (Figure 5.50.e-f). In Rossio do Carmo they were more frequent in the area of the skull, followed by the controls C3 and C1. In Hungate, they were observed in graves 53700, 54296, 52253 and 51349/51351. In the first three graves, Fe and Mn precipitation occurred in the areas surrounding the skeleton and in the controls, while in grave 51359/51351 these pedofeatures were detected only in the controls. Impregnative redoximorphic pedofeatures were not observed in grave 51350/51364 and 54931/54909. In Haymarket, they were observed in graves 84851 and 83012. The latter was characterized by higher frequency of impregnations in the C2, progressively decreasing in the C3 and in the areas under the pelvis and the knees.

Depletion-related pedofeatures, indicating long periods of saturation (Lindbo et al. 2010, 136-137), were identified in grave 54077 of Hungate. Control C2 was grey in colour and it was crossed by vertical voids with oxidized hypocoatings and infillings of very fine Fe nodules.

According to these data, it is possible to conclude that the presence or absence of coffin influenced the presence and location of redoximorphic pedofeatures which form after few days of water

saturation (Hseu and Chen, 1996; Lindbo et al. 2010, 136-137). In the graves of Hungate, Haymarket, Rossio do Carmo and the experimental burials 6 and 7, it seems that impregnations occurred within the area of the skeleton, if the coffin was not present or rapidly decomposed, while they were absent or present only in the controls, especially C2, if the coffin was still present and it slowly breached. Hence, this seems a further proof of the role of the coffin as barrier for the downward movement of fluids and soil particles. The clearest example was offered by grave 54077, where the depleted redoximorphic pedofeatures indicated that the water had stagnated in this area for long periods. This sample was collected above the coffin and, considering the observations discussed in the previous sections, it is plausible that the coffin represented a barrier to the downward movement of water.

In addition to these redoximorphic pedofeatures, dendritic Mn nodules were frequently observed in the graves and loose controls from Pill'e Matta. These nodules were probably originated by bulk of Mn produced from continental weathering, during the formation of the limestone and sandstone in the ocean (Morgenstein and Felsher 1971). Hence, their presence was not related to the burying activity or to post-depositional processes.

6.4.2 GOETHITE

Fan-like crystals of goethite were observed only in the area of the skull in grave 51350/51364 (Figure 5.51.a-d). Goethite (α-FeO·OH) is mainly a product of weathering and recrystallization, generally forming as coatings or grains within the soil (FitzPatrick 1993, 70). Goethite can be a secondary product of biotite, which was present only in this grave. The location of the crystals within soil pores in the area of the skull indicated that it was formed as secondary product into the grave (Stoops et al. 1990, 10) and the multi-layered coatings composed of fan-like aggregates were indicators of very wet soil horizons (Stoops and Delvigne 1990). Goethite is related to the presence of reducing and oxidizing conditions, being predominant in intense oxidizing environments (Lindbo et al. 2010, 137). Considering the characteristics of the goethite, in addition to the fact that impregnative redoximorphic pedofeatures were not observed in this grave, it seems possible to suggest that grave 51350/51364 was affected by water-logged conditions, but a more oxidizing phase occurred and favoured the formation of goethite.

6.4.3 AMORPHOUS PHOSPHATES, VIVIANITE AND RADIAL CRYSTALS

Phosphorous is an important chemical marker and the presence of organic phosphorus is the first indicator of human occupation. Soil phosphorous can be increased by the introduction of guano, animal dung, coprolite, bones and human waste (Schlezinger 2000; Karkanas and Goldberg 2010). Phosphates were observed in Hungate, Haymarket, piglet burials 6 and 7 and, with lower frequency, in Borgharen. Amorphous phosphates were mainly present in Hungate and in few cases in

Haymarket. Radial crystals were observed only in Hungate, while vivianite was present in all of the sites mentioned above.

In Hungate, amorphous phosphates were observed in all of the graves (Figure 5.46.a-h), except for graves 51349/51351 and 52253 (Table 6.2). They were located within the area of the skeleton and in the controls. They occurred as coatings around voids, infillings, nodules or impregnation within the groundmass. The origin of these pedofeature, in accordance with their morphology, seems to be related to the use of the area as refuse dump in 16th C AD (Macnab 1999, as cited in Evans 2007). In addition, the percolation of the phosphates could have been favoured by the movement of the levels of groundwater. Possibly, the presence of the graves and the decomposition of skeletal remains and coffin had a role in the presence of the amorphous phosphates, but it is difficult to understand to what extent. The presence of few nodules, sometimes with radial structure, could be related to the alteration of the vivianite and, consequently, to the presence of the skeleton (see below). In the case of the organic matter and crystals of vivianite embedded in amorphous phosphates, in grave 54077, the influence of both cesspit and organic matter within the grave seems conceivable. In addition, amorphous phosphates were frequent in the additional slides, independently by the location of the samples. Few amorphous phosphates were present in graves 83012, 84700 and 84779 (Figure 5.79.a-d), often in association with vivianite. In this case, their presence could be related to the partial alteration of vivianite during oxidizing phases. Consideration regarding possible influences by the city dump were not possible, because the author did not know the extent of it.

Vivianite crystals were observed in Hungate, Haymarket, Borgharen, piglet burials 6 and 7 (Table 6.2). Vivianite is a pedogenic hydrate iron phosphate mineral ($Fe_3(PO_4)_2 \cdot 8H_2O$), which occurs as amorphous mass or crystals. When fresh and unoxidized, vivianite is colourless or slightly grey, while when it is expose to air, the Fe^{2+} in the crystals is replaced by Fe^{3+}, maintaining the crystals structure and assuming bluish to greenish colours (Stoops and Delvigne 1990; McGowan and Pragnell 2006). The vivianite forms under mildly reducing conditions and under high concentrations of available iron and phosphates ions (Lemos et al 2007). It transforms in isotropic yellowish substance through complete oxidation (Stoops and Delvigne 1990). The vivianite has been identified in many archaeological contexts, especially in association with human and animals remains (Mann et al. 1998; Thali et al. 2011).

In Hungate, the vivianite was observed in graves 53700, 54077, 54931/54909, 54296 and 51349/51351 (Figure 5.47.a-h). It was always associated to the skeletal remains and, in grave 51349/51351, it was observed in the C3. In graves 54296 and 54077, radial crystals of vivianite occurred within amorphous phosphatic areas, which could be interpreted as the phases of alteration of the vivianite (Figure 5.47.a-f). In Haymarket, the vivianite was observed in all of the

graves (Figure 5.79.g-h), except for grave 83012. It was always associated to the location of the skeletal remains and in one case to the C2. The crystals were more frequent and coarser than the ones in Hungate. The intense presence of vivianite in Haymarket, which was not regularly waterlogged, could be explained by the fact that vivianite requires only mildly reducing conditions to crystalize. In Borgharen, two nodules of vivianite were found in the areas of the hands and pelvis (Figure 5.93.g). In the piglet burials, vivianite was very frequent in the piglet 6 and rare in pig 7. Crystals were characterized mainly by round shape, radial arrangement and out-ring of amorphous phosphates (Figure 5.155.a-d). In piglet burial 6 the vivianite was more abundant in the areas of the skull, pelvis and in the two bags containing organic matter. The piglet was placed into the ground without coffin and the higher frequency of vivianite seems to indicate that it was more exposed to water-logged conditions. By contrast, piglet 7 was placed within the coffin, which stayed preserved for three years. The vivianite was observed only in the area of the feet, indicating that the coffin operated as barrier to the movement of groundwater.

In the graves 51349/51351, 52253, 54296 and 54931/54909 from Hungate, infillings of secondary radial crystals were observed within voids (Table 6.2). These features were characterized by coarse spherulites with crossed b-fabric, which were similar to calcite at the first look. However, their colour was more yellow and their morphological appearance was not convincing. Their morphology was very similar to leucophosphite spherulites (Figure 5.49.a-h). The leucophosphite is an Al phosphate mineral containing iron and potassium, mainly present in severely altered anthropogenic sediments, indicating that the apatite in the sediment is not stable and mainly dissolved (Karkanas and Goldberg 2010, 525-526). The leucophosphite can be formed by intense diagenesis of bone, ash and charcoal and it has been found in cave deposits (Simmons 1964; Karkanas 1999). SEM-EDS analyses on the samples from Hungate were not executed, because this interpretation was recent in this research. However, the interpretation of this feature as leucophosphite seems well supported by the micromorphological characteristics. In Hungate, the leucophosphite was observed only in the areas of the skull (graves indicated above) and in the C3 and C2 of grave 51349/51351. Hence, it could be possibly related to an intense diagenesis of the skulls, combined with the percolation of amorphous phosphates from the layers above the graves.

	GRAVE	TYPE	SOIL TYPE	CLIMATE	AMORPHOUS PHOSPHATE	VIVIANITE	LEUCOPHOSPHITE
HUNGATE	51350/51364	Wooden coffin; Cesspit	Sandy clay; Water-logged	Temperate oceanic	Yes	No	No
	51349/51351	Wooden coffin			No	Yes	Yes
	52253	Wooden coffin			No	No	Yes
	54077	Wooden coffin			Yes	Yes	No
	54296	Wooden coffin			Yes	Yes	Yes
	54931/54909	N/A			Yes	Yes	Yes
	53700	Wooden coffin			Yes	Yes	No
HAYMARKET	83012	No coffin/ wooden plank	Sandy clay; Rarely water-logged	Temperate oceanic	Yes	No	No
	84700				Yes	Yes	No
	84779				Yes	Yes	No
	84851				No	Yes	No
BORGHAREN	15	Wooden coffin	Sandy; No water-logged	Temperate oceanic	No	Yes	No
EXPERIMENTAL BURIAL	2	Wooden coffin	Limestone	Temperate oceanic	No	No	No
	6	No coffin	Sandy clay, water-logged	Temperate oceanic	No	Yes	No
	7	Wooden coffin	Sandy clay; water-logged	Temperate oceanic	No	Yes	No

Table 6. 2: Summary of the information related to the presence of phosphates (amorphous phosphates, vivianite and leucophosphite) in the graves.

6.4.4 SPHERULITES

Yellow and orange spherulites were observed in Hungate, in the graves 51349/51351, 51350/51364, 52253 and 54296. The spherulites were 5-20 µm in size and, in the case of orange spherulites, they were characterized by crossed b-fabric. For the characteristics of size, shape and b-fabric, they were very similar to the calcitic spherulites produced in the gut of different animals, particularly herbivores, and recorded in layers of burned dung in most of the Mediterranean caves, frequented during the Neolithic (Canti 1997; Canti 1998; Boschian 2001; Boschian and Ghislandi 2011). However, their colour and their presence into the graves discouraged this interpretation (Table 6.3).

SEM-EDS analyses showed that spherulites were mainly composed by Fe, Si and Ca. These data, in addition to literature evidences (Pye et al. 1990; Driese et al. 2010; Ludvigson et al. 2013), suggested the interpretation of this feature as siderite ($FeCO_3$). Siderite is a carbonate pedogenic mineral, characteristic of wet and persistent saturated soils, often in association with vivianite and more rarely with goethite (Sapota et al. 2006; Lemos et al. 2007). It occurs as small crystallites or spherulitic aggregates in the groundmass or as pore infillings (Stoops and Delvigne 1990). In archaeological sites, it has been observed in floor deposits (Gebhardt and Langohr 1999; Milek 2012).

MORPHOLOGICAL CHARACTERISTICS	CaCO₃ SPHERULITES (from dung)	SIDERITE SPHERULITES (from post-depositional processes)	
SIZE	5-15 µm	5-20 µm	
PPL COLOUR	Transparent	Orange	Yellow
XPL COLOUR	First order white/pink	First order reddish orange	Dark brown/ Isotropic
B-FABRIC	Extinction cross	Extinction cross	Amorphous
AGGREGATION	Homogeneously distributed in the groundmass	Aggregated in pore spaces or in the groundmass	

Table 6. 3: Main characteristics of the calcitic spherulites, produced in the gut of herbivores, and the sideritic ones, produced in reducing-oxidizing conditions.

In Hungate, siderite occurred as loose continuous or discontinuous infillings, quasicoatings and aggregates within the soil particles, sometimes intergrown with radial crystals of vivianite (Figures 5.43, 5.44 and 5.45). In grave 51349/51351, siderite was present in the area of the skull, controls C3 and C2 and more frequently in the areas of the feet and chest located between the feet. In these last two areas and in the C3, siderite was associated with vivianite. In graves 52253 and 54296, siderite was only present in the areas of the skull. In grave 51350/51364, siderite was observed in all of the areas surrounding the skeleton and in C3. The controls were taken in few graves and it

was not possible to have a complete sampling from all of the graves, but it seems reasonable to suggest that siderite formed within the sediments surrounding the skeleton and it was excluded from the upper layers of the backfill. The association of siderite with vivianite, and rarely with goethite, was confirmed in the analysis of the additional slides. Among the graves mentioned above, siderite was associated with goethite only in the case of grave 51350/51364. This grave had not evidence of vivianite and, most importantly, was the only one characterized by the presence of both yellow and orange spherulites. These two types of spherulites were both present in the areas of the skull, pelvis and feet. In one case, they surrounded the same pore. No yellow spherulites were observed in the C3. SEM-EDS analyses showed differences in the amount of Fe and Ca between the two types of siderite, with significant lower quantity of these two components in the yellow spherulites. Particularly, the lower amount of Fe was detected in the middle of the spherulites. This difference appeared in the SEM as an external highly reflective outer ring and an opaque centre. In addition, these two different layers were visible in thin sections, with high contrast at their junction (Figure 5.43.g-h). The interpretation of this differentiation between the two types of spherulites seems not easy to understand.

Siderite forms as mineral transparent in colour in reducing conditions, where it stays stable, in neutral to basic solutions. It can precipitate from weakly acid solution only if the concentration of dissolved iron is abnormally high (Lemos et al. 2007). Consequently to the phases of oxidation and weathering, the siderite assumes brownish colours. Specifically, its weathering produces brown goethitic substances (Stoops and Delvigne 1990). It seems possible to suggest that, in the grave 51350/51364, siderite formed during a phase of reducing environment, possibly caused by the presence of the decomposing corpse. During a first stage of oxidation, the siderite assumed orange colour, maintaining its crystallitic structure. The presence of goethite fan-like crystals in the area of the skull (Figure 5.51.a-d) testified a second and more intense phase of oxidation and hydration, in which goethite precipitated and some of the spherulites mainly weathered, producing goethitic substances and losing their crystallitic structure. The role of the cesspit in the weathering process is unknown. Surely, it influenced the translocation of some of the spherulites from the area of the pelvis to the area of the feet. Hence, layered coatings of fine material and very fine spherulites were found in the trabecular fragments of bone in the area of the feet (Figure 5.45).

6.4.5 CLAY AND FINE MATERIAL COATINGS

Coatings of clay and fine material were observed around pores in Hungate, Haymarket, Rossio do Carmo, Pill'e Matta and piglet burial 2. As explained in Section 6.4.1, clay movement is favoured by reducing conditions and stagnation of water, due to removal of Fe and Mn oxides. The formation of coatings is related to the clay eluviation/illuviation processes, generally originated by the vertical

translocation of fine clay, suspended in percolating soil water. The clay is deposited when the infiltration of the suspension stops (Kühn et al. 2010).

Very thick clay coatings occupied the lowest part of large pores in the samples of grave 54077 (Figure 5.50.a-b). Clusters of quartz and high content of fine material characterized the C3, while Fe hypocoating/coatings and depleted areas were typical in the C2. The area of the skull was near a cesspit. These data seem to indicate that the grave was affected by quite intense water-logged conditions, which produced a reducing environment in the C2 and the translocation of the fine material through the C3 to the area of the skull. The coffin could have played the role of barrier to the water movement, contributing to the segregation of quartz in the C3. It is possible that the cesspit contributed to the translocation of fine material. In grave 51350/51364, clay quasicoatings were present in the areas of the pelvis and feet, testifying the translocation of fine soil particles in these areas of the skeleton. In the area of the skull, concentration of fine material was represented by textural pedofeatures, such as impregnation, but coatings were not observed. It seems possible that the translocation was favoured by the presence of the cesspit on the right side of the grave, influencing only a part of the grave (areas of the pelvis and feet). In grave 51349/51351, clay coatings were present in all of the samples, except for C1 (5.50.c-d). They were more abundant in the areas of the pelvis and feet. These coatings could be originated by the movement of fluids from the C2 to the area of the skeleton and from the area of the skull to the areas of the feet. Clay coatings were observed also in the other graves of Hungate, supporting the interpretation of translocation of fine material favoured by reducing conditions.

In Haymarket, clay coatings were observed only in graves 87779 and 84851. The limited frequency of these pedofeatures could be explained by the lower water-logged conditions and absence of the coffin, which would have favoured the preservation of the pores. In Rossio do Carmo, coatings of fine material and dusty clay coatings were observed in all of the samples, especially in the areas of the skull and pelvis (Figure 5.101.g-h). These features, in association with the presence of black redoximorphic features, mainly in the area of the skull, and Fe/Mn nodules indicated the presence of reducing conditions, with consequent suspension and translocation of the fine material. It is known that the climate in Rossio do Carmo is hot, the geographical area is subjected to desertification and that the soil above the cemetery was partially eroded. Hence, the presence of these features, related to reducing conditions, could not be caused by the surrounding environment. Thus, the higher frequency of these pedofeatures in the areas of the skull and pelvis seems to indicate that they were directly related to reducing conditions formed during the decomposition of the body. In addition, the coatings could also be originated by the translocation of fine material from the less stable and eroded layer of the top surface above the grave.

Clay coatings of fine material within the trabecular structure of the bone were observed in the area of the pelvis in grave US2680, where possibly the structure of the bone trapped and preserved the movement of soil particles (Figure 5.131.a-b). The site is located in a hot environment and the reducing conditions caused by the corpse decomposition could have caused the movement of soil particles. In the other graves of Pill'e Matta, the fine material coatings were mostly around mineral grains and, consequently, had different origin. They indicated the movement of these minerals, probably for the slow deposition from the vault. Infillings of clay and brown fine material were observed in piglet burial 2. The first were present in the two controls C2 and C3, while the second one only in the C2. They indicated translocation of material from the topsoil. The finer-size material was able to go deeper, reaching the C3. Hence, the wooden coffin worked as a barrier for the translocation of the materials.

6.4.6 SECONDARY CaCO$_3$ PEDOFEATURES

Secondary CaCO$_3$ pedofeatures were observed in Haymarket, Borgharen, Pill'e Matta and piglet burial 7. In Pill'e Matta, two types of secondary CaCO$_3$ pedofeatures were detected. The first one was represented by micritic hypocoatings around pores of the limestone and sandstone sediments. These hypocoatings were characterized by change of colour around the pores, being more grey than the surrounding fine material in PPL, and by less intense micritic b-fabric in XPL (Figure 5.133.a-b). It was supposed that the hypocoatings were the result of depletion in the fine material. However, SEM-EDS analyses showed that there was no appreciable difference in the composition of the two layers (Figure 5.129). The interpretation of micritic depletion hypocoatings was consequently discarded. Difference in colour and absence of bi-refringence could be explained by a dense recrystallization of the area surrounding the pore space, which would affect the morphological aspect of the fine material. The smaller particle size around the pores produced darker colouration of this layer in PPL. On the contrary, this recrystallization, because of its higher density, appeared as an area of higher and brighter contrast with the SEM (Section 5.5.4). Intense evapotranspiration, and consequent recrystallization of the calcium carbonate, forming a harder crust, are processes well documented in sediments affected by very hot climates (Sehgal and Stoops 1972; Kemp 1995; Alonso-Zarza 1999) and, as the ones identified in the chamber tombs of Mycenae (Karkanas 2012), they could represent fossilized root imprints. In addition, these pedofeatures were observed in all of the samples of Pill'e Matta and in the controls of loose sediments. Therefore, they were not interpreted as features related to the presence of the grave, but as characteristics of the sediments.

The second pedofeature observed in Pill'e Matta, and exclusively in grave 238, was represented by the infillings of calcified filaments in pore spaces (Figure 5.133.c-d). In the literature, this pedofeature is also called needle fibre calcite or pseudo-mycelium and it is identified as calcified

filaments encrusting mycelial growth of fungal hyphae. Calcified filaments have a biogenic origin, caused by the precipitation of carbonate crystals on the mucilaginous sheath of the hyphae during their respiration (Loisy et al. 1999; Bajnóczi and Kovacs-Kis 2006; Cailleau et al. 2009a; Cailleau et al. 2009b). When the fungus dies, the carbonate tubes remains after the decomposition of the organic tissue (Durand et al. 2010, 169-170). These calcifications were more abundant in the area of the skull and in controls C1 and C3, and less present in the areas of the pelvis and feet. It was interesting to observe that the location of the more frequent calcified filaments corresponded to the location the dark pigmented fungi, in the area of the skull. This observation supported the identification of calcified filaments in Pill'e Matta as biogenic. In addition, the exclusivity of this pedofeature and of the fungi in grave 238, could indicate different sub-environments between the chamber tombs. Grave 238 was located in a different area of the site, far away from the other three graves and, possibly, the presence of fungi, dead or alive, was an indicator of higher humidity. The conditions of the skeletal remains were known only for graves 237 and 238. The first appeared very weathered and fragmented, while the seconds were quite well preserved. The suggestion is that higher contents of humidity in grave 238 limited the fragmentation of the bones. It would be interesting to verify this hypothesis with the comparison of other graves from the same site.

In Borgharen, few micritic hypocoatings and coatings of $CaCO_3$ were observed around round pores, mostly in the areas of the skull, vertebrae and hands (Figure 5.93.e). This type of pedofeature can be related to the percolation of carbonate along the pores and/or the rapid precipitation of calcium carbonate due to root metabolism (Durand et al. 2010, 158). Control C1 was characterized by micritic b-fabric (Figure 5.92.c-d), possibly caused by the practice of tillage, as explained in Section 6.1.2. Thus, the percolation and crystallisation of the micrite along channel roots seems very conceivable in this grave. In Haymarket, micritic hypocoatings, coatings and infillings of $CaCO_3$ were observed in most of the samples of grave 83102, especially in the area of the skull; in grave 84700, in the areas of the skull and feet; and in grave 87779 in the area of the pelvis, associated with amorphous phosphate (Figure 5.81.a-d). The availability of calcium carbonate in these sediments was testify by the presence of worm-derived calcium granules (Figure 5.81.e-h) and part of the percolated calcite could have been supplied by the dissolution of the calcium granules. In Hungate, no traces of secondary $CaCO_3$ were observed, possibly due to water-logged conditions or scarce presence of roots. Piglet burials 7 was characterized by the presence of secondary $CaCO_3$ in the areas of the skull, feet and C3, while it was absent in the piglet burial 6. The two piglets were buried in the same sediments and piglet 7 was placed in the coffin, which was filled with the surrounding soil. The presence of $CaCO_3$ could be related to the casual inclusion of fresh roots in the backfill within the coffin, and consequent precipitation of the calcium carbonate with the death of the

roots. The presence of the coffin, which was thought to have preserved the piglet from intense water-logged conditions, probably preserved the dissolution of the CaCO$_3$.

6.4.7 ANTHROPOGENIC MATERIAL

Anthropogenic materials were observed in the backfills of Borgharen and Rossio do Carmo. In Borgharen, brick fragments, sometimes coated by mortars, were the most common, followed by few fragments of other materials, possibly of metal origin for the morphological characteristics. Archaeological information from the excavation reported the presence of several fragments of materials dispersed around the skeleton. This presence, both at macroscopic and microscopic levels, occurred only in Borgharen and it could be an indicator of the process of grave reopening, causing disturbance of the grave goods and dispersion of small fragments. In addition, the archaeological substrata may have influenced the deposit: fragments of plaster and mortar were common in the Roman and Medieval urban sites (Macphail and Goldberg 2010, 611). Borgharen was located in the proximity of a Roman villa and, similarly, the cemetery of Rossio do Carmo was superimposed to a Palaeochristian necropolis. Hence, the sediments used for the backfilling could have been affected by previous anthropic activities. However, in the case of Borgharen, the presence of metals fragments could be directly related to the presence of the grave goods and to their disturbance.

Chapter 7. CONCLUSIONS

The aim of this research was to detect and understand the changes that occurred in the burial sediments over time and their relationship to the presence of the grave and to natural and anthropic post-depositional processes. A further objective was to assess how soil composition and climatic conditions influenced the burial sediments. The rationale and the hypotheses investigated in this research were presented in Chapter 1. Chapter 2 reviewed the main micromorphological and sedimentary studies applied to burials (Section 2.1.2) and the research context of micromorphology (Section 2.1), archaeothanatology and forensic science (Section 2.2), providing basic concepts on soils (Section 2.2.3) and corpse decomposition (Section 2.2.4). The end of the chapter revised the methodologies applied in this research (Section 2.3). The specific application of these methodologies and the analysed materials were discussed in Chapter 3; the image analysis method and its experimental application were described in detail in Chapter 4. The results of image analysis were described in Chapter 4 (Section 4.4) and Appendix 2.9. The information regarding the case studies and the graves, the micromorphological results and the SEM-EDS results were presented in Chapter 5. The comparison between all of the microscopic results and the macroscopic evidences was discussed in Chapter 6, focusing on morphology of the microstructure (Section 6.1), soil porosity (Section 6.2), organic components and biological activities (Section 6.3), pedofeatures and anthropogenic material (Section 6.4). The aim of the discussion was to identify markers which could testify the presence or absence of coffin at microscopic level and post-depositional processes occurred in the graves. The discussion in Chapter 6 highlighted similarities and differences among the sites.

Chapter 7 focuses attention to observations and conclusions on the case studies, based on the discussion of data in Chapter 6. The first part of Chapter 7 provides answers to the first and second rationale of this research (Section 7.1-7.7). The second part reviews observations in relation to the third rationale (Section 7.8).

7.1 HUNGATE

The cemetery of Hungate was located in the centre of York (UK), encompassing Roman and Anglo-Scandinavian burials (Chapter 5, Section 5.1). The area of Hungate developed on a natural slope (Figure 5.2) and it was affected by periodical flooding, influencing the sediments with water-logged conditions (Chapter 5, Section 5.1.1). During time the area was: a civilian settlement (Roman period); a trade zone (the Anglo-Scandinavian period); part of the construction of a ditch and

consequently flooded (11th C AD; Figure 5.3); filled with refuse and river silts (Late Medieval age); occupied by a church and a cemetery (13th C AD); used as public refuse dump (16th C AD); developed for heavy industry (18th C AD) (Hall 1996, 39-40; Macnab 1999, as cited in Evans 2007; Chapter 5, Section 5.1.1). All or some of these activities possibly operated as post-depositional factors influencing the environment of the graves. The burials were characterized by wooden coffin (grave 54931/54909 unknown) and the sediments were sandy clay, in temperate Oceanic climate (Tables 1.1 and 5.1).

7.1.1 GRAVE 51350/51364 (Roman)

Grave 51350/51364 was adjacent to a cesspit. Traces of wooden coffin were found during the excavation. The backfill material was sandy clay and silt with a firm consistency and mottle mid orange, light yellowish brown and mid grey colours. Pebbles and charcoal fragments were occasionally present. Evidence of bioturbation were observed in the layer above the grave for agricultural activities (Chapter 5, Section 5.1.2 and Figure 5.4).

According to the interpretation presented in Chapter 6, this grave was characterized by rapid breaching of the coffin. The microstructure was heterogeneous, rich in fine material and quite porous (Section 6.1.2). The level of porosity was higher in the area of the skeleton and in the C2 than in the C3, indicating that the coffin was affected by rapid decay (Section 6.2.1). It was observed that the frequency of quartz grains was higher in the area of the skeletal remains and decreased to C3 and C2, showing progressive translocation of mineral components from the top layers to the area of the skeleton, where the grains were entrapped (Section 6.1.4). The author of this research did not know the location of this grave within the cemetery, but the composition of the groundmass seemed to suggest a relatively distant setting from the river (Section 6.1.2). Microscopic evidences indicating the presence of water-logged conditions were: apedal microstructure (Section 6.1.3); absence of roots and biological activities (Sections 6.3.1 and 6.3.3), except for few modified complex voids; clay quasicoatings and clay textural impregnation (Section 6.4.5); Fe/Mn nodules (Section 6.4.1) and siderite (Section 6.4.4). The location of redoximorphic pedofeatures, such as Fe/Mn nodules, indicated that the coffin breached rapidly. Their formation was caused by the interaction of corpse decomposition within the coffin and water-logged conditions (Section 6.4.1). The high content of organic matter from the corpse and the coffin, combined with intense water-logged conditions and consequently intense reducing environment, supported the formation of siderite spherulites in all of the samples (the mid orange colour observed during the excavation; Section 6.4.4). The grave was influenced by the presence of a cesspit, located in the proximity of the area of skull and pelvis, partially cutting the backfill (Chapter 5, Figure 5.4). The excavation of the cesspit in the past caused the release of fluids and oxygen within the grave. The fluids were documented by amorphous phosphatic coatings around the pores wall in the C2, located in

proximity of the cesspit. Furthermore, this observation indicated that the amorphous phosphates were not originated within the grave (Section 6.4.3). The increase of oxygen in the grave context was identified by the presence of weathered spherulites of siderite and goethite fan-like crystals. Some spherulites became brownish in colour and loosed the cross b-fabric, for intense oxidation and hydration (Section 6.4.4). Goethitic substances were produced by this alteration and they crystallized in the area of the skull as fan-like crystals on the pores walls (Section 6.4.2). Furthermore, some spherulites of siderite were transported within the trabecular structure of the bones of the feet by fluids of the cesspit. This movement of cesspit fluids was testified also by impregnative clay pedofeatures in the area of the skull and clay quasicoatings in the areas of the pelvis and feet (Section 6.4.5). The strong oxidizing condition likely inhibited the formation of vivianite.

7.1.2 GRAVE 51349/51351 (Roman)

Traces of wooden coffin were found during the excavation and the skeleton condition was poor. Several grave goods in copper, jet and iron were preserved. The backfill was mid grey, soft and silty, probably containing hydrocarbon from a 20th C AD petrol station and exhibited stain from the coffin (Chapter 5, Section 5.1.2 and Figure 5.5).

The coffin was affected by slow breaching. Consequently, the microstructure was homogeneous, mostly sandy and low porous (Section 6.1.2). The porosity was higher in the C2 and decreased in the C1, C3 and skeleton, showing that the presence of coffin slowed the downward movement of soil particles (Section 6.2.1). It was observed that the frequency of quartz grains was higher in the area of the skeletal remains and decreased to C3 and C2, showing a progressive translocation of mineral components from the top layers to the area of the skeleton, where the grains were entrapped (Section 6.1.4). The author of this research did not know the location of this grave within the cemetery, but the composition of the groundmass seemed to suggest a setting in proximity of the river (Section 6.1.2). The decomposition of the corpse, the slow breaching of the coffin and the water-logged conditions promoted intense reducing conditions, attested by Fe/Mn nodules (Section 6.4.1) and clay coatings of fine material (Section 6.4.5) in all of the samples, and redoximorphic impregnative pedofeatures (Section 6.4.1) in the controls. These strong reducing environments supported the formation of spherulites of siderite (Section 6.4.4) in all of the samples and vivianite (Section 6.4.3) in the area surrounding the skeleton. The skeleton was poorly preserved and microscopic evidences were represented by crystals of leucophosphite in C3 and C2 (Section 6.4.3).

7.1.3 GRAVE 52253 (Roman)

Traces of wooden coffin were found during the excavation. The skeleton of a juvenile individual was poorly preserved. The layer below the cut comprised clayey sand of brownish orange colour and was highly compacted. Occasional charcoal flecks and pebbles were present. Fragments of other pot remains were found (Chapter 5, Section 5.1.2 and Figure 5.6).

The coffin was affected by slow breaching. Consequently, the microstructure was homogeneous, mostly sandy and low porous. The porosity was higher in the C2 and decreased in the C1, C3 and in the area of the skeleton (Section 6.2.1). Considering the characteristics of the groundmass, the grave was possibly located in proximity of the river (Section 6.1.2). Movement of soil particles from the layers above the grave was testify by higher contents of quartz grains in the area of the skeleton than in the controls (Section 6.1.4). The decomposition of the corpse, the slow breaching of the coffin and the water-logged conditions produced reducing environment and consequent formation of Fe/Mn nodules and redoximorphic impregnative pedofeatures in all of the samples (Section 6.4.1), and clay infillings in the areas of skull and pelvis (Section 6.4.5). Quite intense reducing conditions permitted the formation of spherulites of siderite in the area of the skull (Section 6.4.4). The skeleton was poorly preserved and microscopic evidences were represented by crystals of leucophosphite in the area of the skull (Section 6.4.3).

7.1.4 GRAVE 54077 (Roman)

The skull side of the grave was in proximity of a cesspit. Traces of wooden coffin were found during the excavation. The skeleton of a child was poorly preserved. The layer below the skeleton was composed of firm mid brownish grey silty sand. A section of the deposit was friable, containing clay, and it was described as remains of the coffin. Moderate iron stains and a band of friable grey clay were present, while charcoal fragments and subangular pebbles were occasional (Chapter 5, Section 5.1.2 and Figure 5.7).

The coffin was affected by rapid breaching in the area of the skull and slow breaching in the area of the feet (Section 6.1.2). The rapid breaching was likely caused by the excavation of the cesspit in proximity of the grave (Figure 5.7). The microstructure in the area of the skull was heterogeneous and highly porous. At the same time, the slow decomposition of the coffin under the C2 caused long periods of water saturation above the lid, identified by depletion redoximorphic pedofeature (Section 6.4.1). The cut of the cesspit introduced fragments of calcined and rubified bones and white plant structures in the backfill. Thick coatings of fine material around voids and amorphous phosphates testified the movement of fluids from the cesspit into the grave (Section 6.4.5). The presence of reducing condition for the corpse decomposition and water-logged sediment, indicated by Fe/Mn nodules and redoximorphic impregnative pedofeatures, promoted the preservation of

fragments from the coffin, which were embedded in amorphous phosphates and vivianite crystals. The microscopic analysis suggested the identification as gymnosperm wood (Section 6.3.1). On the opposite, the skeletal remains were poorly preserved and microscopic observations indicated the formation of leucophosphite crystals for instability of apatite (Section 6.4.3).

7.1.5 GRAVE 54296 (Roman)

Traces of wooden coffin were found during the excavation. The skeletal remains were well preserved. Hobnail shoes were found in the area of the feet. The layer below the skeleton was friable and composed of mid grey brown silty sand (Chapter 5, Section 5.1.2 and Figure 5.8).

The coffin was affected by rapid breaching and consequent heterogeneous, mixed and poorly sorted microstructure (Section 6.1.2). Movement of soil particles from the layers above the grave was testify by higher contents of quartz grains in the area of the skeleton than in the controls (Section 6.1.4). The decomposition of the corpse, the rapid breaching of the coffin and the water-logged conditions produced reducing environment and consequent formation of Fe/Mn nodules and redoximorphic impregnative pedofeatures in all of the samples (Section 6.4.1). Quite intense reducing conditions permitted the formation of spherulites of siderite and vivianite crystals in the area of the skull (Sections 6.4.3 and 6.4.4). Vivianite occurred within areas of amorphous phosphate, which presumable represented phases of oxidation of the crystals. Amorphous phosphates were present also in the other samples from the area of the skull and in the C3, indicating possible origin for percolation from the above layers. Despite the archaeological evidence of well-preserved bones, leucophosphite crystals were identified in the area of the skull.

7.1.6 GRAVE 54931/54909 (Roman)

No information was available for this grave (Chapter 5, Section 5.1.2 and Figure 5.9).

The decomposition of the coffin was slow and the microstructure of the backfill was characterized by homogeneous, sandy and low porous sediments (Section 6.1.2). The frequency of quartz grains decreased from the area of the skeletal to the C2, indicating downward translocation of soil particles and their segregation in the area of the bones (Section 6.1.4). The decomposition of the corpse and the slow breaching of the coffin produced reducing conditions, documented by Fe/Mn nodules (Section 6.4.1), limpid clay coatings and clay impregnations (Section 6.4.5). The reducing conditions were not too strong (redoximorphic impregnations were absent and fungi were active in the areas of skull and pelvis), but sufficiently favourable for the formation of vivianite (Section 6.4.1). Amorphous phosphates originated from the layers above the grave, as suggested by the higher frequency of these phosphates in the C2. However, the presence of amorphous phosphates possibly influenced the formation of leucophosphite in the area of the skull and C2. The author of

this research did not have information regarding the skeleton, but it seemed probable that the bones were poorly preserved and the apatite in the sediment was mainly dissolved (Section 6.4.3).

7.1.7 GRAVE 53700 (Anglo-Scandinavian)

Traces of wooden coffin were found during the excavation (chest, pelvis and feet). The skeleton was well preserved. Eight large stones surrounded the burial (Chapter 5, Section 5.1.2 and Figure 5.10).

The decomposition of the coffin was rapid and the microstructure of the backfill was characterized by heterogeneous, mixed and unsorted sediments (Section 6.1.2). Figure 5.10 shows good anatomical connection of the bones at the moment of excavation, supporting the interpretation of decomposition in contact with soil since the first stages. The decomposition of the corpse and the rapid breaching of the coffin produced reducing conditions, documented by Fe/Mn nodules, redoximorphic impregnative pedofeature (Section 6.4.1) and clay coatings (Section 6.4.5) in the area of the skeleton. However, the reducing environment was mild and the activities of fungi and roots were not inhibited (Section 6.3.1). Furthermore, the presence of roots indicated that the grave was not intensively water-logged. As consequence, only few crystals of vivianite formed in the area of the pelvis (Section 6.4.1) and siderite was not recorded. The lower water-logged conditions of this grave could indicate that the grave was located in higher position a.s.l. This observation seemed reasonable, considering that the Anglo-Scandinavian burials were successive to the Roman cemetery. High content of phosphates was originated by percolation of the same from the above layers (Section 6.4.3).

7.1.8 INTRA-GRAVES CONCLUSIONS

The interaction among grave type, soil type, post-depositional processes and climate contributed to define the story of each grave, their similarities and differences, as illustrated in Figure 7.1. Two main distinctions in the group of graves were based on the type of microstructure and its significance. It seems plausible to distinguish graves characterized by slow breaching of the coffin from the ones with rapid breaching of the coffin. In the first case (graves 51349/51351, 52253 and, partially, 54296 and 54931/54909) the microstructure was homogeneous, sandy and mostly apedal; the porosity was higher in C2 and C3 than in the area of the skeleton. In the second case (graves 51350/51364, 53700 and, partially, 54296 and 54931/54909) the microstructure was heterogeneous, richer in fine material and mostly apedal; the porosity was higher in the area of the skeleton. The different rate of coffin decomposition seemed to be caused by different spatial location of the graves within the cemetery (Section 6.1.2). Downward translocation of soil particles was recorded by differences in porosity (see above) and segregation of quartz grains in the area of the skeleton (Section 6.1.4). The graves were affected by reducing conditions, promoted by the

decomposition of the corpse and by the water-logged sediments (clay coatings). It seemed that the intensity of water-logged and the slow/rapid breaching of the coffin affected the concentration and location of redoximorphic pedofeatures, siderite and vivianite. In case of slow breaching of the coffin, the redox impregnations were more frequent in the controls. On the opposite, in case of rapid breaching of the coffin, the redox impregnations were more frequent in the area surrounding the skeleton. Vivianite and siderite formed consequently to the decomposition of the corpse in reducing environment and they were generally located in proximity of the skeleton. Intense oxidising phases caused the weathering of vivianite, turning in amorphous phosphate, and the weathering of siderite, transforming in goethitic material. Amorphous phosphates were often identified in the controls, indicating their main origin from the layers above the graves, as consequence of the use of the site as refuse dump in the past. Leucophosphite crystals were generally associated to intense weathering of bones and instability of apatite in the sediments. The reducing conditions were mild in the Anglo-Scandinavian grave, possibly indicating that the grave was located in higher position a.s.l. This observation seemed reasonable, considering that the Anglo-Scandinavian burials were successive to the Roman cemetery.
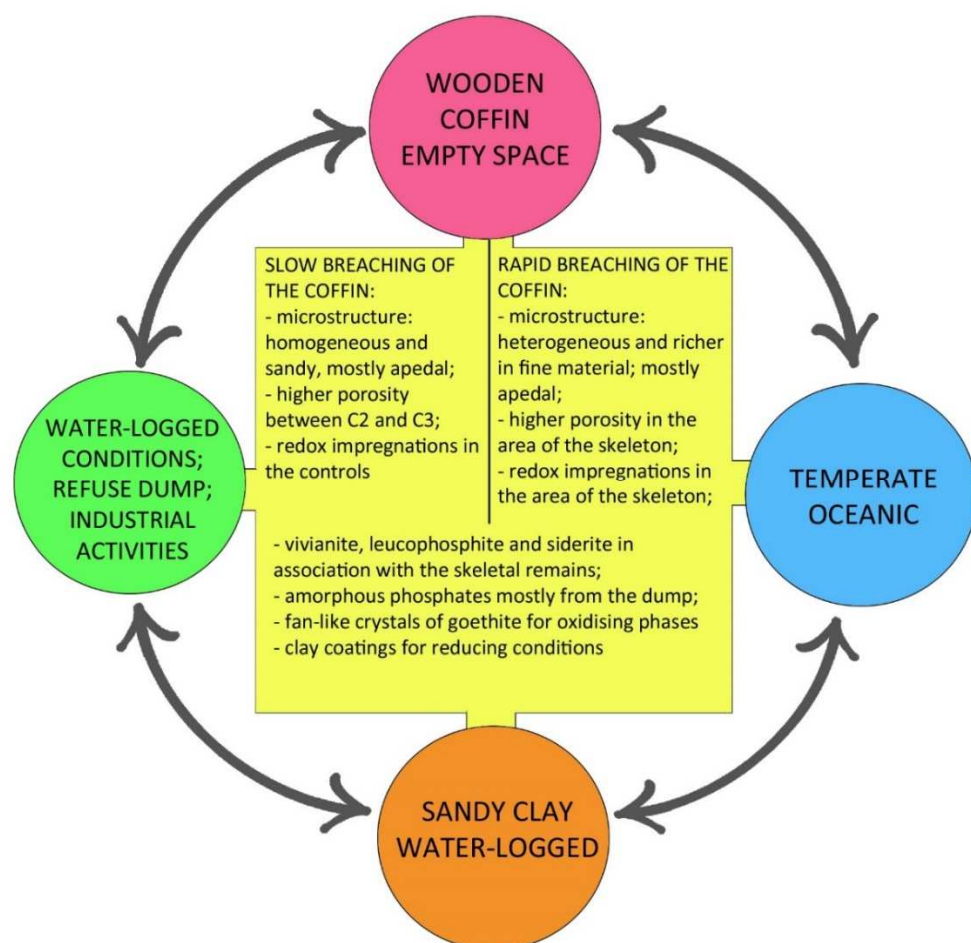
Figure 7. 1: Main microscopic observations on graves from Hungate, related to the grave type, soil type, post-depositional processes and climate.

7.2 HAYMARKET

The Medieval cemetery of Haymarket was located in the centre of York (UK), on the highest part of the slope in proximity to Hungate (Figure 5.54). The site was rarely water-logged (Chapter 5, Section 5.2). The graves investigated were part of the graveyard of All Saints Church (11th-16th C AD), which was demolished in the 16th-18th C AD (Reeves 2013). The area was occupied by buildings in recent times. These activities possibly operated as post-depositional factors influencing the environment of the graves. The burials were characterized by possible deposition of the corpse without coffin or covered with a wooden plank, sandy clay sediments, in temperate Oceanic climate (Tables 1.1 and 5.2).

7.2.1 GRAVE 83012 (Medieval)

The only information available for this grave was that it was disturbed by a service trench cut and the feet were missing (Chapter 5, Section 5.2.2 and Figure 5.55).

The decomposition of the corpse occurred within the soil without coffin or covered by a wooden plank. Microscopic indicators were: heterogeneous and intensively mixed microstructure, with unsorted coarse components (Section 6.1.2), and porosity lower in C3 than C2 (Section 6.2.1). The grave was probably not very deep, considering the brown colour for the inclusion of organic matter from the top soil (Section 6.1.4) and the presence of worm calcium carbonate granules, especially in the controls (Section 6.3.3). This last feature indicated that the grave was rarely water-logged, because earthworms are very sensitive to the changes in humidity and temperature and they avoid watered soils (Section 6.3.3). However, reducing condition and anaerobic environment were dominant and limited the activity of roots, fungi and mesofauna, only rarely present in C2 (Section 6.3). Thus, humified plant structures were commonly preserved for the anaerobic conditions and the few impact of biological activity (Section 6.3.1). The reducing conditions promoted by the decomposition of the corpse and the absence of the coffin influenced the distribution of Fe/Mn nodules and redoximorphic impregnative pedofeatures in the area surrounding the skeleton and in the controls (Section 6.4.1). Reducing conditions, occasional movement of ground water and presence of organic matter in sandy soil facilitated the formation of vivianite in the backfill. The presence of vivianite in a not regularly water-logged sediment could be explained by the fact that vivianite requires only mildly reducing conditions to crystalize (Section 6.4.3). Indications of oxidizing phases were documented by the presence of amorphous phosphates surrounding the vivianite crystals, as weathering product (Section 6.4.3). The presence of secondary $CaCO_3$ infillings and impregnations in all of the samples testified the dissolution, percolation and secondary crystallization of calcite with in the soil from the top layers and confirmed the absence of coffin, which would have operated as barrier to this percolation. Microscopic evidenced of the trench cut

were found in the fragments of bones from the area of the knees: granular infillings in the fractures and black stains of bitumen in the osteons of bone (Section 6.3.2).

7.2.2 GRAVE 84700 (Medieval)

The only information available for this grave was that the skeleton had the hands under the pelvis and the skull was turn to left (Chapter 5, Section 5.2.2 and Figure 5.57).

The decomposition of the corpse occurred within the soil without coffin or covered by a wooden plank. Microscopic indicators were: heterogeneous and intensively mixed microstructure, with unsorted coarse components (Section 6.1.2), and porosity lower in C3 than C2 (Section 6.2.1). The grave was probably not very deep and possibly in higher position a.s.l than grave 83012, considering the brown colour for the inclusion of organic matter from the top soil (Section 6.1.4) and the presence of worm calcium carbonate granules in all of the samples (Section 6.3.3). The more frequent presence of worms within the backfill could be consequent to oxidizing phases, as suggested by higher frequency of sclerotia and modified complex voids, in comparison to grave 83012. However, reducing condition and anaerobic environment were likely dominant and limited the activity of roots (Section 6.3), promoting the preservation of humified plant structures, amorphous organic matter and charcoal fragments (Section 6.3.1). The reducing conditions supported by the decomposition of the corpse and the absence of the coffin influenced the distribution of Fe/Mn nodules in all of the samples, especially in the area of the skull. Redoximorphic impregnative pedofeatures were not observed, recommending the interpretation of more intense or frequent oxidizing phases within the backfill (Section 6.4.1). Reducing conditions, occasional movement of ground water and presence of organic matter in sandy soil facilitated the formation of vivianite in the backfill, forming in mildly reducing conditions (Section 6.4.3). Amorphous phosphates were present in the area of the skull and C2. Vivianite was present in the same areas and the amorphous phosphates were probably produced by the alteration of vivianite during oxidizing phases (Section 6.4.3). The frequency of bone fragments seemed caused by the absence of coffin, as protection of the remains, and by the alternation of oxidizing and reducing conditions. The presence of secondary $CaCO_3$ infillings and impregnations in the area of the skeleton and in C2 testified the dissolution, percolation and secondary crystallization of calcite with in the soil from the top layers and confirmed the absence of coffin, which would have operated as barrier to this percolation.

7.2.3 GRAVE 84779 (Medieval)

The sediment of the backfill was clay rich, while the one outside the grave was friable and sandy. Substantial amounts of white roots matter with long root hairs were found around the feet.

Fragments of charcoal were observed in the area of the skull (Chapter 5, Section 5.2.2 and Figure 5.58).

The decomposition of the corpse occurred within the soil without coffin or covered by a wooden plank. Microscopic indicators were: heterogeneous and intensively mixed microstructure, with unsorted coarse components (Section 6.1.2), and porosity lower in C3 than C2 (Section 6.2.1). The grave was probably not very deep and possibly at the same level of grave 84700, considering the brown colour for the inclusion of organic matter from the top soil (Section 6.1.4) and the presence of worm calcium carbonate granules in all of the samples (Section 6.3.3). The more frequent presence of worms within the backfill could be consequent to oxidizing phases, as suggested by the presence of sclerotia in the area of the skull and modified complex voids. However, reducing condition and anaerobic environment were present and limited the activity of roots and mesofauna (Section 6.3), promoting the preservation of humified plant structures, amorphous organic matter and charcoal fragments (Section 6.3.1). The reducing conditions supported by the decomposition of the corpse and the absence of the coffin influenced the distribution of Fe/Mn nodules in all of the samples. However, these conditions were less intense than graves 83012 and 84700, as showed by lower frequency of the Fe/Mn nodules and absence of redoximorphic impregnative pedofeatures (Section 6.4.1). Reducing conditions, occasional movement of ground water and presence of organic matter in sandy soil facilitated the formation of vivianite in the backfill, forming in mildly reducing conditions (Section 6.4.3). Higher frequency of amorphous phosphates in all of the samples seemed consequent to more frequent oxidizing phases and to alteration of vivianite (Section 6.4.3). However, some of the amorphous phosphates could be percolated by the layers above the grave, as indicated by the coatings of amorphous phosphates and secondary $CaCO_3$ crystals in the area of the pelvis.

7.2.4 GRAVE 84851 (Medieval)

The only information available for this grave was that the skeleton of a sub-adult or infant had the hands under the pelvis (Chapter 5, Section 5.2.2 and Figure 5.59).

The decomposition of the corpse occurred within the soil without coffin or covered by a wooden plank. Microscopic indicators were: heterogeneous and intensively mixed microstructure, with unsorted coarse components (Section 6.1.2), and porosity lower in C3 than C2 (Section 6.2.1). The grave was probably not very deep and possibly at the same level of graves 84700 and 84779, considering the brown colour for the inclusion of organic matter from the top soil (Section 6.1.4) and the presence of worm calcium carbonate granules in all of the samples (Section 6.3.3). The more frequent presence of worms within the backfill could be consequent to oxidizing phases, as suggested by the presence of sclerotia in the areas of the skull and pelvis and modified complex

voids. However, reducing condition and anaerobic environment were present and limited the activity of roots and mesofauna (Section 6.3), promoting the preservation of humified plant structures, amorphous organic matter and charcoal fragments (Section 6.3.1). The reducing conditions supported by the decomposition of the corpse and the absence of the coffin influenced the distribution of Fe/Mn nodules in all of the samples. However, these conditions were less intense than graves 83012 and 84700, and more similar to grave 84779, as showed by lower frequency of the Fe/Mn nodules and absence of redoximorphic impregnative pedofeatures (Section 6.4.1). Reducing conditions, occasional movement of ground water and presence of organic matter in sandy soil facilitated the formation of vivianite in the backfill, which was more abundant in this grave than the others (Section 6.4.3). The absence of secondary $CaCO_3$ crystals and amorphous phosphates, in addition to the presence of dusty quasicoatings of fine material, suggested the interpretation of more stable relation between reducing and oxidizing conditions, without extremes (Sections 6.4.3, 6.4.5 and 6.4.6).

7.2.5 INTRA-GRAVES CONCLUSIONS

The interaction among grave type, soil type, post-depositional processes and climate contributed to define the story of each grave, their similarities and differences, as illustrated in Figure 7.2. The heterogeneous and unsorted microstructure, in addition to the increase of porosity in the C3, indicated that the corpses were buried within the soil without coffin, or with a wooden plank which rapidly breached. All of the graves were affected by reducing conditions alternated to quite intense oxidizing phases. The first were caused by decomposition of the corpse and rare water-logged stages. The second were probably related to the depth of the grave. According to this interpretation and to the frequency of features, grave 83012 was the deepest, followed by graves 84700, 84779 and 84851. Reducing phases were characterized by the formation of Fe/Mn nodules, redoximorphic impregnative pedofeatures (only in grave 83012), vivianite crystals and coatings of fine material around voids. In this context the biological activity was limited and the preservation of organic matter was supported. Oxidizing phases were characterized by presence of worm calcium carbonate granules, sclerotia, amorphous phosphates as oxidised products of vivianite and secondary crystallisation of $CaCO_3$.
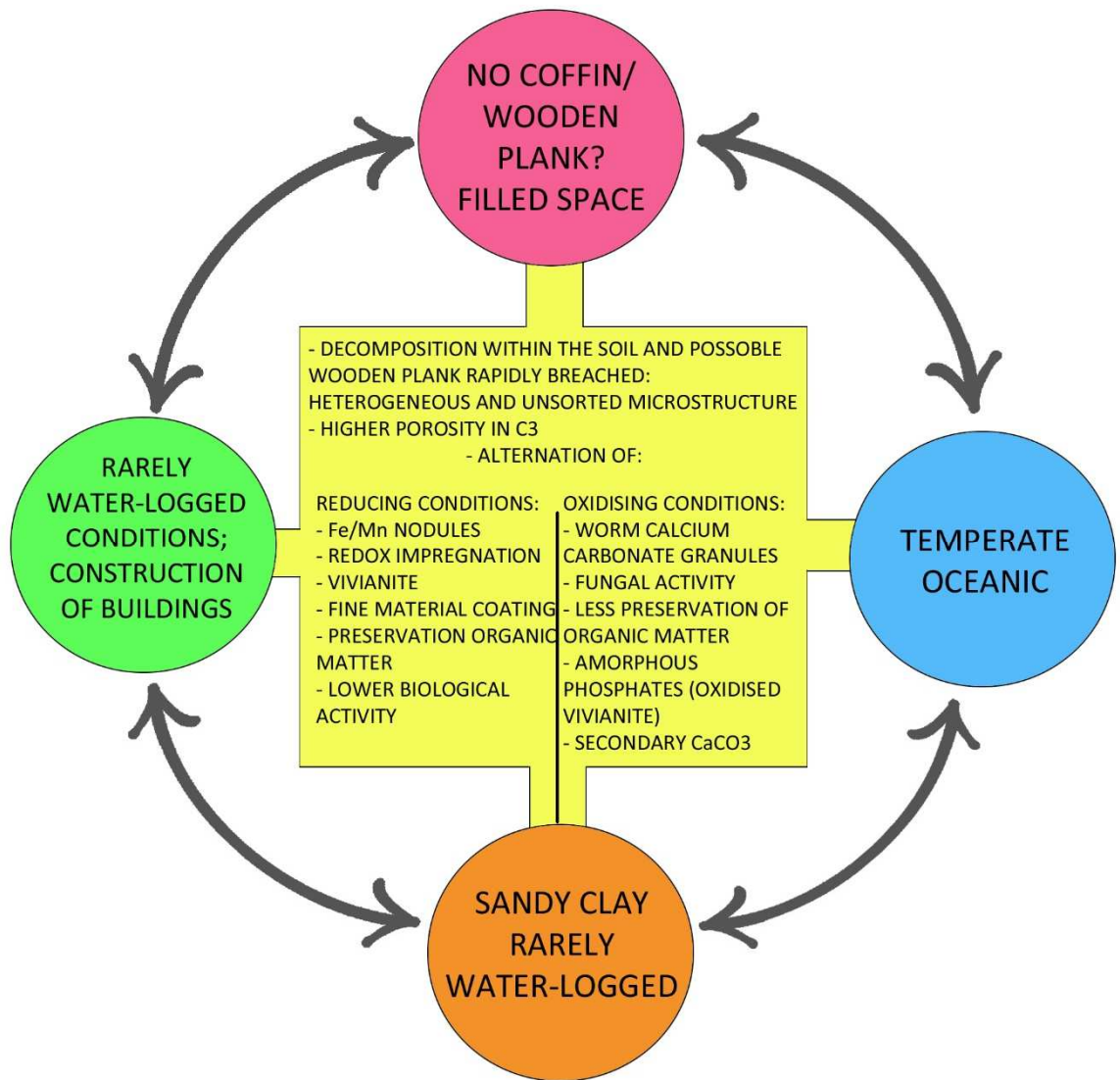
Figure 7. 2: Main microscopic observations on graves from Haymarket, related to the grave type, soil type, post-depositional processes and climate.

7.3 BORGHAREN

The Merovingian cemetery of Borgharen was located on the eastern bank of River Meuse, near Maastricht (NL) (Figure 5.82). A Roman *villa* occupied the same area before the construction of the cemetery. From the 8th C AD, this area became poorly populated and it was used for agricultural practices until recent times (De Groot et al. 2011, 13-15; Chapter 5, Section 5.3.1). All or some of these activities possibly operated as post-depositional factors influencing the environment of the graves. The burial was characterized by wooden coffin and the sediment was sandy, in temperate Oceanic climate (Tables 1.1 and 5.3).

7.3.1 GRAVE 15 (Medieval)

Traces of wooden coffin were found during the excavation. The skeleton was of a woman and various materials and grave goods were found in the filling. The grave was disturbed by a secondary interment in the area of the feet (Chapter 5, Section 5.3.2 and Figure 5.94).

Evidences from the microstructure indicated that the grave was characterized by slow breaching of the coffin, with slow translocation of coarse components, higher porosity in the area of the skeleton and segregation of mineral grains in the areas of skull and pelvis (Section 6.1.2; 6.1.4 and 6.2.1). The second interment affected the microstructure of the infill. Loose discontinuous infillings of material from the groundmass in voids and sub-angular peds seemed to represent the remaining trace of this disturbance (Section 6.1.3). Brick fragments and other unidentified materials, possibly of metal origin (Figure 5.93.h), could be related to the post-depositional process of reopening of the grave, causing disturbance of the grave goods and dispersion of small fragments (Section 6.4.7). Microscopic evidences, such as presence of worm calcium carbonate granules and micritic microstructure of the controls, indicated that the grave was not deep (40 cm, Chapter 5, Section 5.3.2). The C1 was collected under the plough horizon and it comprised micritic sediment including small aggregates of the same soil as the grave infill. It seemed that the layer above the grave was reworked, causing the inclusion of small aggregates from the lower layers. Furthermore, the micritic fabric and the apedal microstructure seemed related to the practice of irrigation related to tillage (Section 6.1.2; Chapter 5, Section 5.4.1). The micritic coatings around pores in the area surrounding the skeletal remains indicated the percolation of carbonate along the pores from the level of C1 and the rapid precipitation of calcium carbonate caused by root metabolism (Section 6.4.6). Thus, the level of C1 and partially the area surrounding the skeleton were affected by the agricultural activities on site. The presence of charcoal indicated that the sediment of the backfill derived from the surrounding area, which was intensively affected by anthropic activities (Section 6.3.1). The shallow depth of the grave seemed to facilitate the presence of mesofauna, particularly in the area of the ribs and C1, documented by modified complex voids and loose discontinuous infillings within the trabecular structure of the bone in the area of the ribs (Figure 5.92.e-g). The decomposition of the corpse within the coffin produced reducing conditions, attested by the presence of Fe/Mn nodules in the area surrounding the skeletal remains (Section 6.4.1), few crystals of vivianite in the area of hands and pelvis (Section 6.4.3) and coatings of fine material around the pores (Section 6.4.5), despite the absence of water-logged conditions.

The interaction among grave type, soil type, post-depositional processes and climate contributed to define the story of the grave, as illustrated in Figure 7.3. The sandy soil, the presence of slow breached coffin and the oceanic climate seemed to contribute to the formation of vivianite crystals. Anthropic post-depositional processes, such as the reopening of the grave and the agricultural

practices, combined with the shallow depth of the grave, influenced the microscopic morphology of the backfill.

Figure 7. 3: Main microscopic observations on the grave from Borgharen, related to the grave type, soil type, post-depositional processes and climate.

7.4 ROSSIO DO CARMO

The Moorish cemetery of Rossio do Carmo was located in the village of Mértola (PT) (Figure 5.94), in the geological Phyllite-Quartzite Group (Tornos et al. 2009; Chapter 5, Section 5.4.1). The cemetery was situated along the South-East side of a hill and overlapped a Palaeochristian cemetery. No traces of coffin were found and the graves were directly excavated into the bedrock and covered with plates of schist (Le Bars 2005). The soil over the bedrock was not deep and the site was damaged by natural erosion and works associated with the development of the village (Le Bars 2005). All or some of these activities possibly operated as post-depositional factors influencing

the environment of the graves. The sediment was sandy loam, in temperate Mediterranean climate (Tables 1.1 and 5.4).

7.4.1 GRAVE 395 (Islamic - Moorish)

The skeleton was a male adult, placed without coffin on his right side. Plates of schist surrounded and covered the burial. The layer of sediment in which the skeleton was contained was thin and rich of coarse material and the skeleton rested directly on the rock surface (Chapter 5, Section 5.4.2 and Figure 5.84).

The grave contained poorly sorted coarse components, caused by immediate backfilling after the placement of the corpse (Section 6.1.2). The granular peds were mostly formed by sampling and post-sampling factors (Section 6.1.3). The porosity was higher in C3 and lower in C1 and in the area of the skeleton, indicating slow infill during time. However, the grave was probably immediately filled after the deposition of the corpse, because the bones were found in articulation (Chapter 5, Section 5.4.1). The higher content of voids in C3 was possibly caused by the decomposition of the organic materials introduced in the grave at the moment of burying, according to the Islamic funeral rules (Le Bars 2005). The organic remains consisted in low quantities of amorphous organic matter and humified plant structures. The organic matter would have attracted more soil fauna in the C3 layer and the presence of schist slabs on the top of the grave could have preserved the original porosity (Section 6.2.2). The biological activity was documented by frequent modified complex voids and, especially in the C3, by fungal remains, confirming an intense activity in the C3 layer. The decomposition of the corpse and, in addition of the organic remains, produced reducing environment within the grave, testified by Fe/Mn nodules, more abundant in the area of the skeleton and C3 than the C2. Redoximorphic impregnative pedofeatures in the grave indicated that these reducing conditions created by the decomposition were quite intense, possibly for the higher content of organic materials. Thus, the hot climate and the dry conditions of the soil could not be the responsible factors for these redoximorphic pedofeatures (Section 6.4.1). The redoximorphic impregnations were more abundant in the area of the skull. It seemed reasonable that this area was more humid, because of the proximity of the skull to the rock surface, facilitating the formation of redoximorphic pedofeatures (Figure 5.84). Furthermore, coatings of fine material around voids were common in the area of the skull and present in the other samples, mostly in the areas surrounding the skeleton, indicating the presence of reducing conditions, with consequent suspension and translocation of the fine material (Section 6.4.5). The presence of brick fragments indicated that the sediments used to fill the grave came from the surrounding area, which was intensively affected by anthropic activities (Section 6.4.7).

The interaction among grave type, soil type, post-depositional processes and climate contributed to define the story of the grave, as illustrated in Figure 7.4. Grave 395 showed that, despite the Mediterranean climate and the dry aspect of the soil, reducing conditions occurred within the grave. The microscopic evidences indicated that this mild reducing environment was originated by the decomposition of the body and the organic matter, probably related to the phase of putrefaction (Section 2.2.4). The high quantity of organic matter attracted micro-, mesofauna and fungi; the porosity was possibly preserved by the schist slates.
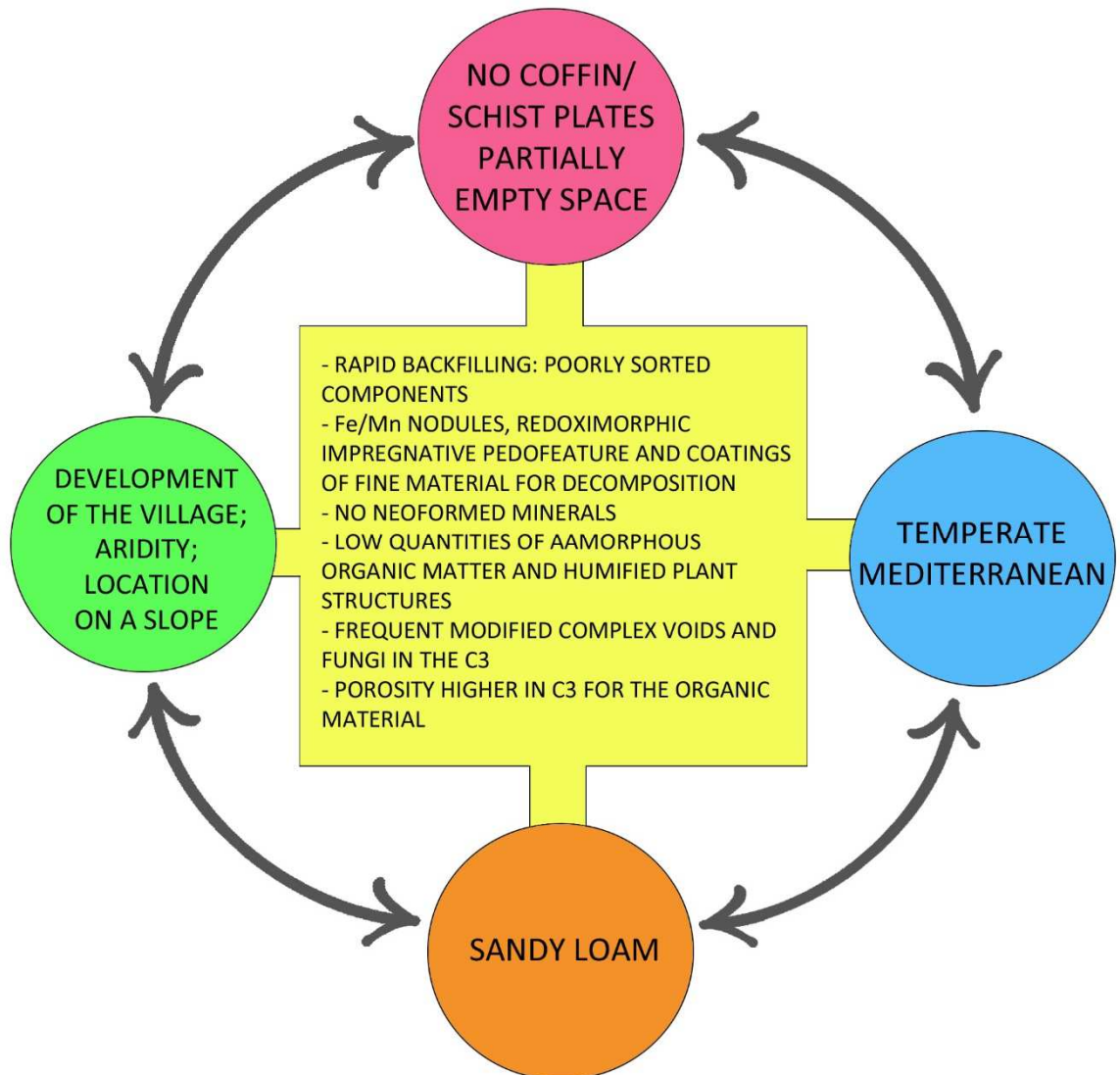
Figure 7. 4: Main microscopic observations on the grave from Rossio do Carmo, related to the grave type, soil type, post-depositional processes and climate.

7.5 PILL'E MATTA

The necropolis of Pill'e Matta was located in the industrial area of Cagliari, Italy (Figure 5.103), in the geological formation of Campidano (Matta 2005, 25-27; Chapter 5, Section 5.5.1). The necropolis was in use during 4th C BC - 5th C AD (Figure 5.106) and the most ancient graves were Punic (Salvi 2005b, 21). The graves were characterized by chambers excavated in the bedrock, and closed with tiles (Roman period) or amphorae *a siluro* (Punic period) (Figure 5.106). The ritual did not include backfill or covering of the body. Thus, the sediments found in the graves were from post-depositional processes (Pittoni 2009, 387). The site was affected by industrial activities and the construction of a road only in recent times (Chapter 5). These activities possibly operated as post-depositional factors influencing the environment of the graves. The sediment was limestone and sandstone, in temperate Mediterranean climate (Tables 1.1 and 5.5).

7.5.1 GRAVE 238 (Punic)

The only information available for this grave was that the skeletal remains were in good conditions. The grave was located in an area separated from the Roman graves (Chapter 5, Section 5.5.2, Figures 5.105 and 5.107).

The decomposition of the corpse occurred in empty space, progressively filled by sediment produced by slow fragmentation of the chamber vault (Section 6.1.2). The presence of micritic hypocoatings and dentritic Mn nodules in the infill, observed in the samples from the soil profile of the site (Chapter 5, Figure 5.111), confirmed the origin of the sediment from the vault walls (Sections 6.1.2, 6.4.1 and 6.4.6). This process of infill inhibited the process of translocation of minerals grains, which were equally distributed around the skeleton (Section 6.1.4). The decomposition of the body produced reducing conditions, identified by Fe/Mn nodules and absent in the soil profile (Section 6.4.1). However, the complete skeletonization of the corpse occurred in oxidizing environment, which permitted the activity of roots, mites and fungi, feeding on the organic remains. Fragments of roots were common in all of the samples and they were mostly consumed by mites, whose traces were identified by the type of faecal pellets produced (Section 6.3.1). Mites feed on litter and they have fungal feeding preferences, particularly for dark pigmented fungi such as *Ulocladium*, which was identified in the same grave, in addition to sclerotia and fungal hyphae (Sections 6.3.3 and 6.3.4). This intense biological activity and the aridity of the site did not preserve organic matter (only one small fragment of humified plant structure; Section 6.3.1). The good preservation of the bones, despite the climatic conditions and the well-drained soil, was caused by the content of humidity in the grave. This environmental condition was documented by the presence of: *Ulocladium*, which is tolerant to fluctuation of humidity; needle-fibre calcite in the pores, which are calcified filaments encrusting mycelial growth of fungal hyphae

(Section 6.4.6); weakly development of the granular peds and dense fabric microstructure. The level of humidity was most likely influenced by the location of the grave within the site.

7.5.2 GRAVE 237 (Roman)

The only information available for this grave was that the skeletal remains were scarcely preserved (Chapter 5, Section 5.5.2 and Figure 5.108).

The decomposition of the corpse occurred in empty space, progressively filled by sediment produced by slow fragmentation of the chamber vault (Section 6.1.2). The presence of micritic hypocoatings and dentritic Mn nodules in the infill, observed in the samples from the soil profile of the site (Chapter 5, Figure 5.111), confirmed the origin of the sediment from the vault walls (Sections 6.1.2, 6.4.1 and 6.4.6). Infiltration from the tiled side of the chamber contributed to the formation of the deposit in the area of the feet, where coarse and unsorted minerals were observed and aggregation of peds was more compact (Sections 6.1.2 and 6.1.3). Furthermore, the material from the pit (Chapter 6, Section 5.5.1) with smaller dimensions reached the area of the skull. This post-depositional process of translocation was identified by coatings of fine material around mineral grains and loose discontinuous infilling of groundmass material within the voids (Section 6.4.5). The decomposition of the corpse produced reducing conditions, more intense in the area of the skull, documented by the presence of Fe/Mn nodules, absent in the soil profile, and coatings of fine material in the trabecular structure of the bone in the area of pelvis (Sections 6.4.1 and 6.4.5). However, the complete skeletonization of the corpse occurred in oxidizing environment, which permitted the activity of roots and mites, as in grave 238. The biological activity seemed less intense than grave 238, because of low presence of roots and faecal pellets and slightly higher content of organic matter (Sections 6.3.1 and 6.3.3). The poor preservation of the skeletal remains seemed to be caused by the low moisture content in the grave and well-drained sediment, identified by high separation of the peds for rapid dessication (Section 6.1.3), absence of fungi and needle-fibre calcitic infillings. Thus, this dry environment caused leaching of bones. Several fragments of bones were identified in the samples and mostly in the area of the pelvis, where they appeared intensively weathered (Figure 5.131.a-b; Section 6.3.2).

7.5.3 GRAVE 268 (Roman)

No information was available for this grave (Chapter 5, Section 5.5.2 and Figure 5.109).

The decomposition of the corpse occurred in empty space, progressively filled by sediment produced by slow fragmentation of the chamber vault (Section 6.1.2). The presence of micritic hypocoatings and dentritic Mn nodules in the infill, observed in the samples from the soil profile of the site (Chapter 5, Figure 5.111), confirmed the origin of the sediment from the vault walls

(Sections 6.1.2, 6.4.1 and 6.4.6). However, some mineral grains with coating of fine material indicated translocation of fine material, possibly from the tiled side of the chamber (Section 6.4.5). The decomposition of the body produced reducing conditions, identified by Fe/Mn nodules and absent in the soil profile (Section 6.4.1). However, the complete skeletonization of the corpse occurred in oxidizing environment, which permitted the activity of roots and mites (faecal pellets) feeding on organic remains (Sections 6.3.1 and 6.3.3). The environment conditions of the grave seemed arid, suggested by the presence of several bone fragments, highly separated peds, absence of fungi and absence of needle-fibre calcitic infillings. However, the skeletal regions influenced the retention of moisture and compaction, showing more compact fabric microstructure in the area of the pelvis (Section 6.1.3).

7.5.4 GRAVE US2680 (Roman)

No information was available for this grave (Chapter 5, Section 5.5.2 and Figure 5.110).

The decomposition of the corpse occurred in empty space, progressively filled by sediment produced by slow fragmentation of the chamber vault (Section 6.1.2). The presence of micritic hypocoatings and dentric Mn nodules in the infill, observed in the samples from the soil profile of the site (Chapter 5, Figure 5.111), confirmed the origin of the sediment from the vault walls (Sections 6.1.2, 6.4.1 and 6.4.6). However, some mineral grains with coating of fine material indicated translocation of fine material, possibly from the tiled side of the chamber (Section 6.4.5). The decomposition of the body produced reducing conditions identified by Fe/Mn nodules and absent in the soil profile (Section 6.4.1). However, the complete skeletonization of the corpse occurred in oxidizing environment, which permitted the activity of roots and mites (faecal pellets) feeding on organic remains (Sections 6.3.1 and 6.3.3). The environment conditions of the grave seemed partially arid, suggested by the presence of few bone fragments, highly separated peds, absence of fungi and absence of needle-fibre calcitic infillings. However, the skeletal regions influenced the retention of moisture and compaction, showing more compact fabric microstructure in the area of the pelvis (Section 6.1.3).

7.5.5 INTRA-GRAVES CONCLUSIONS

The interaction among grave type, soil type, post-depositional processes and climate contributed to define the story of each grave, their similarities and differences, as illustrated in Figure 7.5. The formation of the sediment within the chamber was similar in each grave. The only difference was the inclusion of coarse material in grave 237 and few mineral grains in grave 268 and US2680, originated by the translocation of sediment from the pit. It seemed possible that this communality was caused by the more aridity of these sediments, compared to the ones of grave 238, whose aggregation was more firm. However, the explanation could be possibly linked to differences in the

burying practice between Punic and Roman period. The different location of the graves within the site influenced the preservation of the bones and the biological activity within the chambers. The Punic grave (238) was situated in a more humid area, while the Roman graves were affected by more intense dry conditions. However, in both cases the decomposition of the corpse produced reducing conditions.
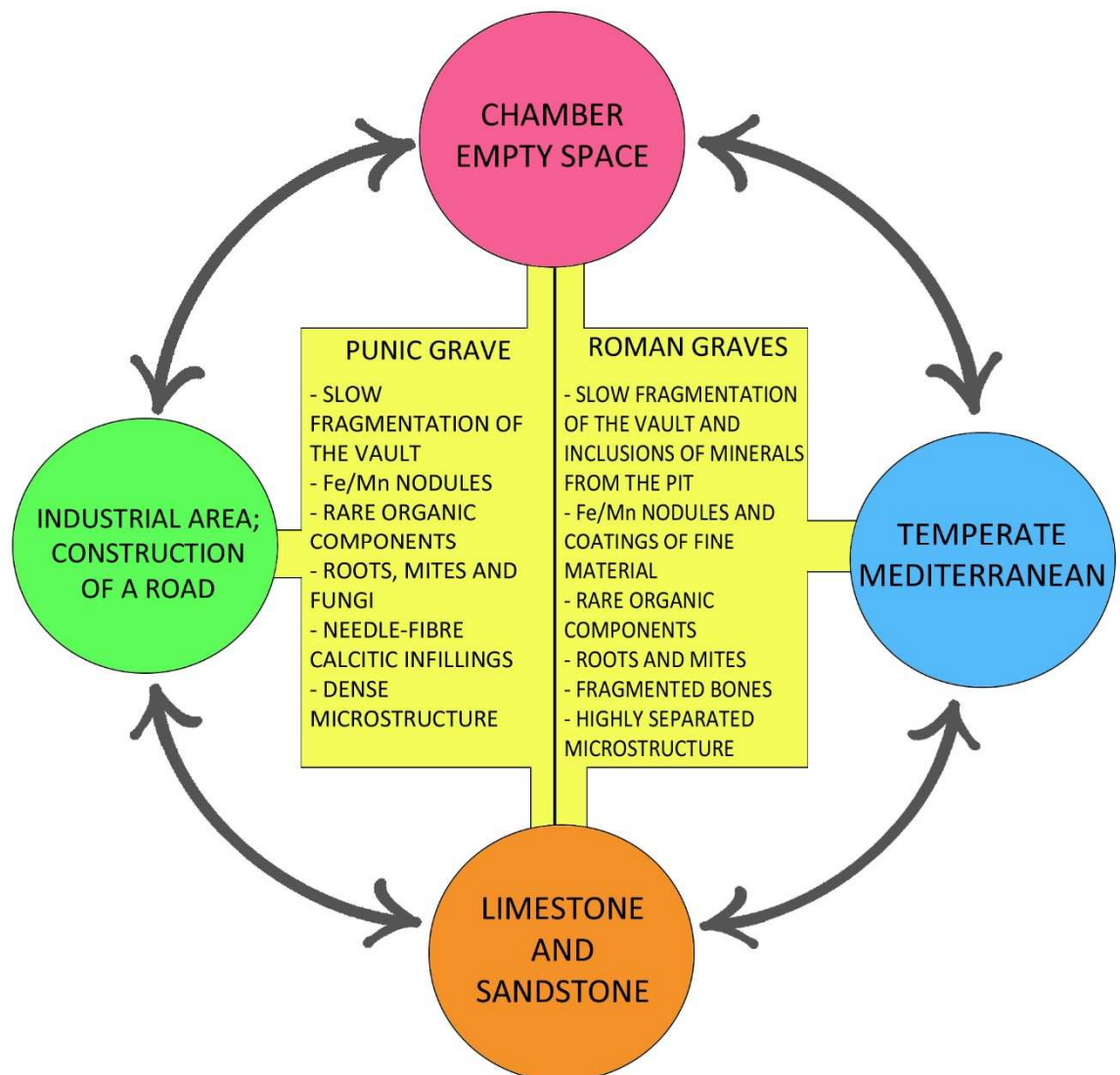
Figure 7. 5: Main microscopic observations on graves from Pill'e Matta, related to the grave type, soil type, post-depositional processes and climate.

7.6 EXPERIMENTAL PIGLET BURIALS

The experimental burials of ten stillborn piglets were located in different locations of Yorkshire (Figure 5.134); they were excavated in 2009 and exhumed during the summer months of 2012 and 2013. The locations encompassed different soil contexts and the piglets were buried with or without coffin and with different grave fill, to expand the range of possible results and

correspondence with archaeological graves (Chapter 5, Section 5.6). Piglet burial 2 was in wooden coffin in limestone sediments; piglet burial 6 was without coffin in sandy clay and water-logged sediments; piglet burial 7 was in wooden coffin in sandy clay and water-logged sediments. All of the burials were excavated in temperate Oceanic climate zone (Tables 1.1 and 5.6).

7.6.1 PIGLET BURIAL 2 (2009-2012)

Piglet 2 was buried in a coffin in a pit dug into a dark brown organic rich sediment, lined with plywood and filled with imported limestone. The coffin was located at ca. 30-40 cm from the top of the pit. Two muslin bags containing organic material were placed in proximity of the mouth and in the stomach (Chapter 5, Section 5.6.1 and Figure 5.135).

The lid of the coffin stopped the percolation of ground water from the top soil to the burial. Infillings of clay and organic rich fine material were observed only in the controls above the lid, indicating movement of fine soil particles through fluids (Section 6.4.5). In addition, a change to major compaction of the microstructure of the imported limestone was recorded in the C2, as consequence of partial dissolution and recrystallization of the calcium carbonate for the percolating water and higher moisture content (Section 6.1.3). The low frequency of quartz in the limestone did not permit further observation on translocation and segregation of mineral grains (Section 6.1.4). Data on change of porosity indicated that the soil particles stopped above the lid, causing less porosity in the C2 (Section 6.2.1). Inside the coffin, higher frequency of pores was observed in the samples with higher content of organic matter at the moment of burying: the areas of the skull and pelvis, and the two muslin bags (Section 6.2.1). Biological activities from mesofauna and fungi were possibly responsible for this porosity, in addition to the cavity left by the decomposition of the soft tissues, observed during the excavation (Section 6.2.2). Enchytraeids, fungus gnats and fungi were the main responsible for the consumption of the organic matter within the coffin. The first were identified by the presence of faecal pellets (Section 6.3.3). The second were found in high content under the lid and, with less frequency, in the samples. The eggs of the fungus gnats were presumably deposed in the carcass of the piglet before the burying and, when the process of pupation completed, the newborn flies stayed trapped within the coffin (Section 6.3.3). The fungi proliferated inside the coffin, but not outside, feeding on the piglet remains (Section 6.3.4). However, few soft remains partially preserved and few piglet hairs were found attached to a fragment of phosphatized skin. The formation of very small Fe and Fe/Mn nodules was possibly induced by the slightly reducing environment produced by the decomposition of the piglet (Section 6.4.1).

7.6.2 PIGLET BURIAL 6 (2009-2012)

Piglet 6 was buried without coffin in sandy clay sediments, frequently water-logged. Two muslin bags containing organic material were placed in proximity of the mouth and in the stomach (Chapter 5, Section 5.6.1 and Figure 5.136).

The decomposition of the piglet contributed to the creation of reducing environment surrounding the remains, testified by the presence of Fe/Mn nodules in most of all the samples, and facilitated by the water-logged conditions of the site, which were represented by redoximorphic impregnative pedofeatures in the controls (Section 6.4.1). Oxidizing phases occurred and affected also the area surrounding the piglet remains, probably because of the absence of coffin. These phases were represented by the precipitation of Fe and Mn compounds in the controls (Section 6.4.1) and by the formation of an amorphous phosphatic out-ring on the vivianite crystals (Section 6.4.3). The decomposition in water-logged soil permitted the formation of vivianite, especially in the areas with higher content of organic remains (Section 6.4.3). These remains and the absence of coffin attracted insects, whose fragments were identified as orbatid mites and fly pupae. Mesofauna, fungi and roots were more likely attracted during the oxidizing phases (Section 6.3.3). The biological activity was identified also by the formation of modified complex voids and channels, mostly in the areas with higher frequency of porosity (Section 6.2.2). The role of the bones to retain the mineral soil particles was well documented (Section 6.1.4).

7.6.3 PIGLET BURIAL 7 (2009-2012)

Piglet 7 was buried with wooden coffin next to piglet 6, but divided by a sheet of plywood. The coffin was filled with local soil, which was mainly sandy clay and water-logged. Two muslin bags containing organic material were placed in proximity of the mouth and in the stomach (Chapter 5, Section 5.6.1 and Figure 5.137).

The decomposition of the piglet contributed to the formation of reducing environment surrounding the remains, testified by the presence of Fe/Mn nodules in all of the samples, and it was facilitated by the water-logged conditions of the site (Section 6.4.1). However, it seemed that the coffin preserved the area of the skeleton from the movement of groundwater, because only one crystal of vivianite formed in the burial (Section 6.4.3) and $CaCO_3$ impregnative pedofeatures preserved from dissolution within the coffin (Section 6.4.6). The role of the coffin as barrier was documented also by the change of porosity in the soil. The porosity was higher in the sediment under the lid of the coffin, increasing in the areas surrounding the skeleton. The C2, collected above the lid was lower in porosity, corresponding to the area in which the material translocated and stopped. Thus, oxidizing conditions took place within the coffin and permitted the activity of fungi and mesofauna (insect remains and modified complex voids). The insect remains were mostly chitinous exuvia of

fly pupae, suggesting their origin from oviposition before burial. At the same time, the presence of the coffin limited the activity of the mesofauna in the areas surrounding the piglet. Higher frequency of modified complex voids and mesofauna faecal pellets occurred only in the controls, especially in the less deep layer (Section 6.3.3). The presence of these decomposers and the oxidizing phases within the coffin did not preserved high contents of organic remains (Section 6.3.1).

7.6.4 INTRA-BURIALS CONCLUSIONS

The interaction among burial type, soil type, post-depositional processes and climate contributed to define the story of each burial, their similarities and differences, as illustrated in Figures 7.6 and 7.7. The role of the coffin as barrier to the downward movement of soil particles was well documented in piglets 2 and 7, demonstrating that this movement was a post-depositional process not interconnected with the type of soil. Furthermore, the coffin influenced the movement of the ground water within the burial and the formation of pedofeatures, such as vivianite and $CaCO_3$ infillings or impregnations. Thus, in the same site, with the same environmental conditions, the coffin was an important factor affecting the decomposition of the piglets. The formation of vivianite occurred in water-logged sandy sediments, but not in partially dry limestone, even if in the same climatic conditions. Insect remains were preserved, because of the short period of burying. However, mesofauna and fungi were mostly present in oxidizing conditions (piglet 2) and their lower presence in piglets 6 and 7 was resulting from oxidizing phases in mostly reducing environment. Their activity was limited by the presence of the coffin and their presence was inversely proportional to the preservation of organic remains.
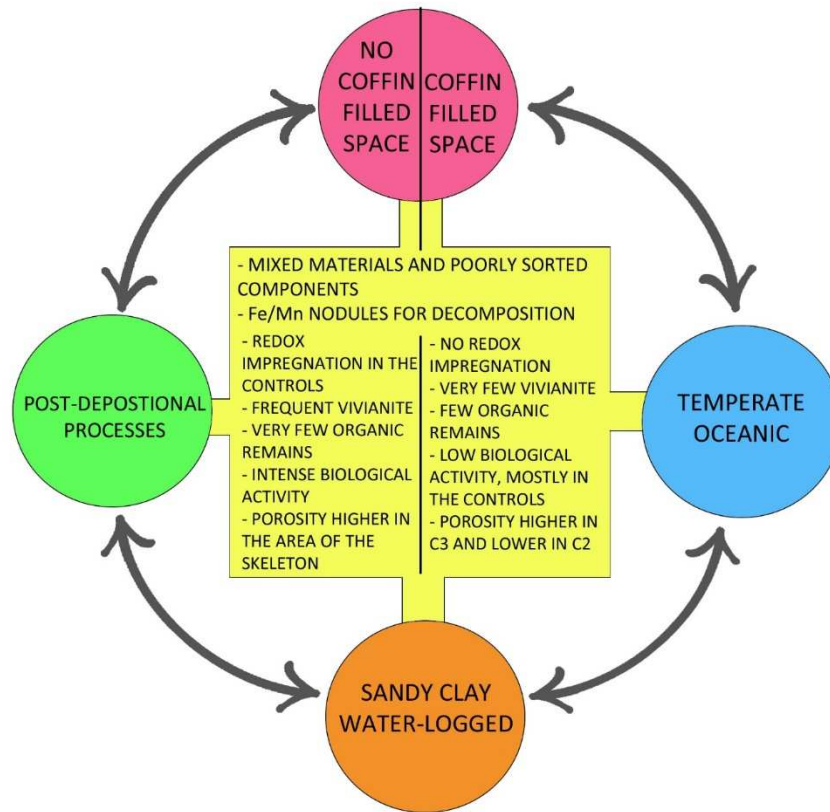
Figure 7. 6: Main microscopic observations on experimental burials 6 and 7 from Heslington East, related to the grave type, soil type, post-depositional processes and climate.
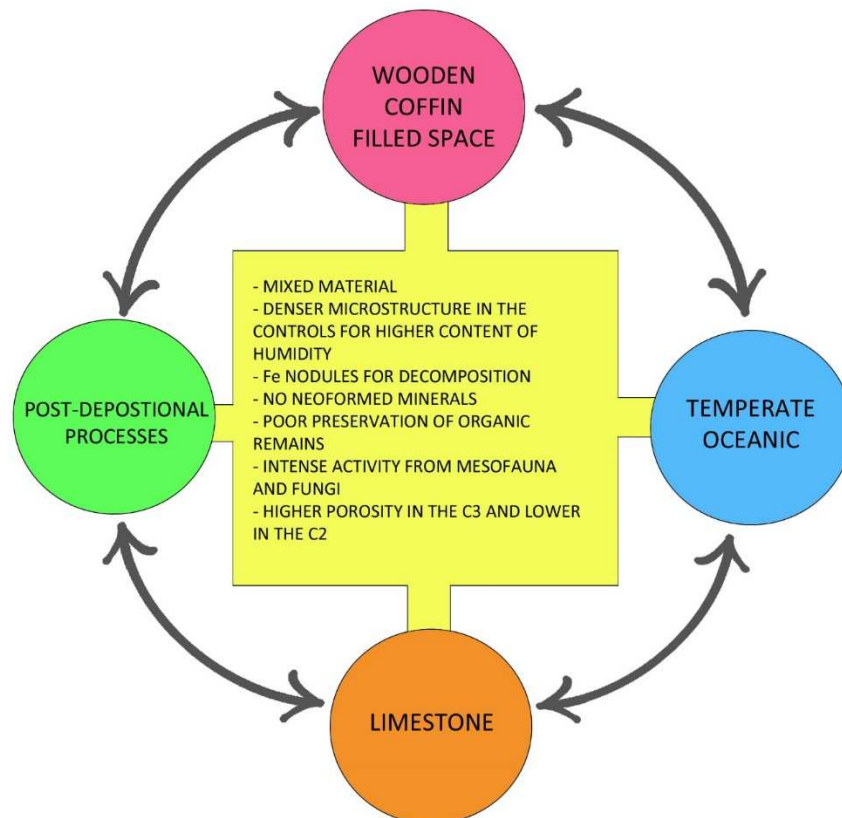
Figure 7. 7: Main microscopic observations on experimental burial 2 from Hovingham, related to the grave type, soil type, post-depositional processes and climate.

7.7 INTRA-SITES CONCLUSIONS

7.7.1 FIRST RATIONALE

Results showed that corpse decomposition within soil produced characteristic microstructures and features according to the type of grave, soil and climate. Figure 7.8 illustrates differences and similarities among the case studies, related to the presence of pedofeatures and organic components. The first rationale of this research was to identify possible features produced by the decomposition of the corpse within the soil and how the nature of such features differed among different environments and soil types.

- Products from the interaction of corpse decomposition and surrounding sediment.

Vivianite formed in sandy soils in reducing conditions produced by the decomposition of the corpse and organic matter. Vivianite was more frequent in the site of Haymarket, which was rarely water-logged and characterized by mild reducing conditions. Vivianite was very scarce in absence of water-logged sediments, such as Borgharen. According to the results from the experimental piglet burials (6 and 7), it seems that the presence of coffin had the major role in the formation of vivianite. At the same water-logged influences, vivianite crystals were more abundant in the area surrounding piglet 6, directly deposed in the soil. Thus, the same difference was observed between Hungate and Haymarket and the absence of coffin in this last site promoted the increase of formation of vivianite. In conclusion, vivianite is produced by the interaction of corpse decomposition and surrounding sediments when the sediments are water-logged or rarely water-logged and reducing conditions occur in the grave. It is promoted by the absence of coffin.

Amorphous phosphates were observed in Hungate and Haymarket. The high frequency of this pedofeature in Hungate and its presence in the controls suggested that their origin was attributable to the use of the site as refuse dump in 16th C AD. The absence of amorphous phosphates in the experimental burials from Heslington reinforced this interpretation. In the case of Haymarket, very few amorphous phosphates were observed in association with vivianite crystals. The same pedofeature was identified in the piglet burials from Heslington. In this case, the amorphous phosphates were produced by weathering of vivianite for oxidising conditions. It seems reasonable to distinguish between the two types of amorphous phosphates and only the phosphates associated to vivianite should be considered products of the decomposition of the corpse within the soil.

Leucophosphite was observed only in Hungate. This pedofeature indicates intense alteration of bones and instability of apatite and if forms in strong reducing conditions, associated with skeletal remains.
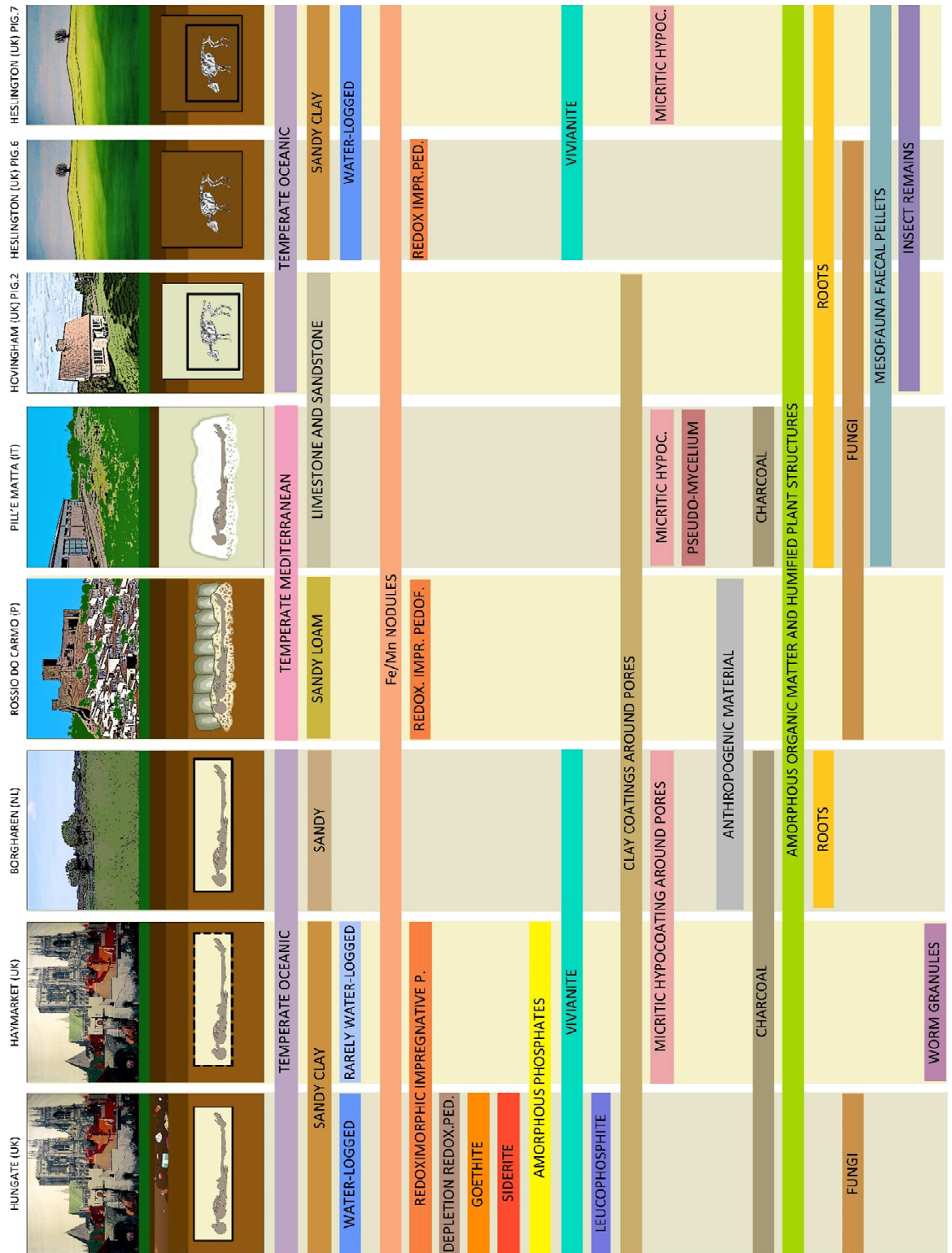
Figure 7. 8: differences and similarities among the case studies, related to the presence of pedofeatures and organic components.

Siderite occurred in the form of spherulites. The formation of this pedofeature was conditional to the decomposition of the corpse (it was recorded only in the areas of the skeleton) and strong reducing conditions. Thus, it was observed in Hungate.

- Secondary products related to environmental conditions of the grave

The decomposition of the body within the soil always produced mild reducing conditions, testified by Fe/Mn nodules in the area surrounding the skeleton. In case of water-logged or rarely water-logged sediments, the reducing conditions were stronger and documented by redoximorphic impregnative pedofeatures. In case of slow breaching of the coffin, the redox impregnations were more frequent in the controls. On the opposite, in case of rapid breaching of the coffin, the redox impregnations were more frequent in the area surrounding the skeleton. Redoximorphic impregnations were observed in Hungate, Haymarket, Rossio do Carmo and piglet burial 6.

Secondary $CaCO_3$ crystals were observed in hot environment, produced by the evapotranspiration and recrystallization of calcium carbonate or, generally, in not water-logged sediments, by the dissolution, percolation and recrystallization of calcium carbonate in the soil. These pedofeatures were more related to post-depositional processes, such as movement of ground water (Haymarket) and agricultural practices (Borgharen).

Needle-fibre calcitic infillings (pseudo-mycelium) indicated variation in the contents of moisture in the chambers of Pill'e Matta. Their presence only occurred in Mediterranean environments and limestone sediments.

- preservation of bone fragments and difference of preservation in different contexts.

Bones were poorly preserved in arid conditions, for leaching of the bone structure (Pill'e Matta), and in intense water-logged conditions (Hungate). In the case of Hungate, poor preservation of skeletons was associated to slow breaching of the coffin. It seemed that the decomposition within the soil from the first stage favoured the preservation of the bones.

- preservation of organic components from the graves.

Organic components were rarely preserved in any type of environment. The best conditions occurred in the site of Haymarket, where reducing conditions alternated to oxidising phases, and in the grave 54077 of Hungate, possibly because the fragments of coffin were embedded in the phosphatic substances derived from the cesspit. Mediterranean climate and well-drain soils represented the less favourable conditions.

- biological activity during and after the corpse decomposition.

Biological activity was inhibited in water-logged sediments; thus it was well documented in well-drained soils. Mesofauna activities were represented by modified complex voids, faecal pellets and, in the case of the piglet burials, insect remains. The presence of fungi and mesofauna faecal pellets in the areas surrounding the skeleton indicated that these organisms were attracted by the decomposition of the corpse.

7.7.2 SECOND RATIONALE

The second rationale of this research concerned the understanding of the processes forming the grave infill, the movement of soil particles and fluids in the grave and the role of the coffin and corpse decomposition in this movement. Homogeneous and well sorted microstructure was identified as product of slow breaching of the coffin and slow translocation of the components over time. Heterogeneous and unsorted microstructure was identified as the product of rapid breaching of the coffin or absence of the coffin, formed by the rapid translocation of the soil components or by activity of shovelling. The analysis of the frequency of quartz grains within the infill indicated downward translocation of the grains with higher concentration and segregation in the areas of skull and pelvis. The variance of porosity within the grave was affected by the presence/absence of the coffin. In the case of slow decay of the coffin, the presence of wood slowed the downward movement of soil particles, creating an area with less porosity above the coffin lid (C2 less porous, C3 more porous). In case of rapid decay of the coffin or absence of it, soil particles reached and filled more rapidly the area above the corpse (C3 less porous).

7.7.3 INVESTIGATED HYPOTHESES

Specific hypotheses were investigated in this research:

1) the movement of soil particles and fluids, the fabric microstructure and the soil porosity change according to the presence or absence of coffin.

As illustrated above, the presence of coffin, which slowly breaches, can be indicated by an increase of porosity in C3 and decrease in C2. Thus, the lid of the coffin has the role of barrier to the movement of soil particles and fluids. The microstructure is homogeneous and well sorted. The absence of coffin, or the rapid breaching of it, can be indicated by a decrease of porosity in C3, because there are no barriers to the downward movement of the soil particles. The microstructure is heterogeneous and unsorted.

2) in presence of coffin, the fabric microstructure changes according to rapid or slow breaching of the coffin.

The microstructure is homogeneous, well sorted and generally less porous in case of slow breaching of the coffin. The microstructure is heterogeneous, unsorted and generally porous in case of rapid breaching of the coffin.

3) moving soil particles are entrapped in some anatomical locations of the skeleton.

The analysis of frequency of quartz grains showed higher contents in the areas of skull and pelvis, in all of the graves. This analysis demonstrated that the quartz grains progressively translocate from the top layers to the area of the burials. Once reached the area of the skeleton, the grains are stopped and held in the areas of the skull and the pelvis, because characterized by wider surfaces.

4) the decomposition of a corpse within the soil promotes the formation of specific indicators.

Vivianite forms in sandy soils in reducing conditions produced by the decomposition of the corpse and organic matter. Leucophosphite forms in sandy and water-logged soils, in reducing conditions and associated to poorly preserved bones. Siderite forms in water-logged sediments and strong reducing conditions. Fe/Mn nodules form in all the types of sediment and redoximorphic impregnative pedofeatures form only when stronger reducing conditions occur.

5) the frequency of these indicators changes according to the presence or absence of coffin.

Vivianite preferably forms in absence of coffin. In case of slow breaching of the coffin, the redox impregnations are more frequent in the controls. In case of rapid breaching of the coffin or absence of it, the redox impregnations are more frequent in the area surrounding the skeleton.

6) the type and frequency of these indicators change according to the type of soil and climate.

These indicators are mostly related to sandy soils, water-logged or rarely water-logged conditions and cold-humid climate. Indicators for warmer climate and well-drained soils were not identified.

7) traces of micro- and mesofauna are detectable even if the corpse skeletonized within the soil and they can increase the information related to the environment.

The main traces are modified complex voids, faecal pellets, worm calcium carbonate granules and fragments of insect remains. The morphology of the faecal pellets can inform about the species of the fauna attracted from the corpse. The presence of worm calcium carbonate granules informs about the levels of water table in sediment. Fragments of body remains preserve in recent burials and progressively decompose. Traces of biological activity can generally inform about oxidising conditions.

8) organic components could preserve and give information regarding coffin and other materials.

Organic components rarely preserve. Coarser fragments of wood, interpreted as part of the decomposed coffin, allow the identification of the family (Gymnosperm or Angiosperm) and, if well preserved, of the species of wood.

7.8 CONSIDERATIONS ON THE PROTOCOL OF THE INTERARCHIVE PROJECT AND ON FUTURE APPLICATIONS (THIRD RATIONALE)

The third rationale was the validation of the methods of sampling and analysis applied to burial sediments and their possible application in future studies by different groups of workers. The method of undisturbed soil sampling, already tested in different archaeological environments by previous studies (Courty 1989, 40-42; Vepraskas 1990, 9-13; Goldberg and Macphail 2003), was applied for the first time to burial sediments. It was standardized for all of the graves, collecting the samples in the same anatomical locations and in the layers above the skeleton (Chapter 3, Section 3.1). According to the results of this research, it is possible to confirm that the locations of the samples provided useful information regarding the corpse decomposition within the soil:

- the sample collected in the regions of skull, pelvis and feet allowed to monitor variations in the area of the skeleton. These variations could relate to: movement of soil particles and the segregation of mineral grains, biological activity within the grave and preservation of the organic remains, presence of indicators of decomposition;
- the samples collected as control C3, C2 and C1 permitted the reconstruction of information regarding the presence or absence of coffin (morphology of microstructure, porosity, redoximorphic pedofeature), the rate of coffin breaching, the rate of backfill and the movement of soil particles within the burial sediments.

The strategy of sampling was appropriate to the burial context and provided useful information regarding the burial environment. However, the documentation of the grave stratigraphy and the annotation of the exact position of the samples within the grave, which were missing in the InterArChive protocol, are considered very important by the author of this research. Thus, several pictures of the grave and of the samples in detail, as well as schematic drawings of the samples within the section, should be taken during the process of sampling. During this research, it was observed that the best results and interpretations could be performed on graves fully sampled. Hence, it is important to predetermine the selection of the graves, excluding the ones having problematic situations, which would prevent complete sampling (e.g. exclusion of the feet). The sampling of all the three controls is relevant for the interpretations regarding the presence of coffin and the type of backfill. Considering the type of results obtained in this research, it is evident that some geological contexts provide more information, for examples sandy soils and water-logged or

partially water-logged conditions. This aspect should be considered in relation to the hypothesis investigated in the research. The second aim of the project was the production of information which could increase the knowledge of the processes related to the burials and which were not detectable at macroscopic analysis. According to the results of this research, this aim seems fully achieved:

- the microscopic analysis of the burial sediments allowed the identification of post-depositional processes and environmental conditions;
- it was possible to define the presence of coffin, even in absence of macroscopic remains, on the base of the characteristics of the microstructure and presence of pedofeatures;
- indicators of corpse decomposition were identified for specific type of soils;
- biological activity offered information of phases of oxidizing conditions, changes in humidity and preservation of bones.

The third aim of the InterArChive project was to create a method applicable to other funerary contexts by different groups of research. The standardize sampling makes this method applicable to any burial context, which can be archaeological or forensic. Furthermore, the innovative application of micromorphology provides information regarding the burial environment, the practices of burying and the post-depositional processes which would remain undetected at macroscopic analysis. This information can be used by the archaeologists to have a complete understanding of the burial and of the cemetery, combining the results with macroscopic data. The presence of indicators, such as vivianite, leucophosphite and siderite, could permit the identification of a burial context in difficult situation, when the skeletal remains completely weathered or were removed. Thus, the analysis of the backfill could provide information related to phases of reopening of the graves in archaeological context or disapparence of the corpse in forensic case.

In conclusion this research highlighted the microscopic processes occurring within the burial and showed that corpse decomposition within the soil produced characteristic microstructures and features according to the type of soil and climate. This information could be used to implement the knowledge of archaeological cemeteries or to support forensic researches.

APPENDIX 1

1.1 ARCHAEOLOGICAL SITES SAMPLED BY THE INTERARCHIVE PROJECT

List of the archaeological sites sampled by the InterArChive team between 2009 and 2012. The sites are listed according to their chronology. The sites selected and analysed in this research are in bold, while the sites utilized for the image analysis experiment are in italics.

NAME OF THE SITE	LOCATION	HISTORICAL PERIOD
Çatalhöyük	Konya, TR	Neolithic
Tel Quarassa	SYR	Neolithic
Al Khiday	Hillat Al Khiday, SUD	Neolithic/Mesolithic
Gannì	Cagliari, IT	Chalcolithic
Cashel	Cúl na Móna, IR	Early Bronze Age (bog body)
La Compaene	Basly, FR	Bronze Age
Thessaloniki	Salonikki, GR	Iron Age/Roman
Heslington East	York, UK	Iron Age/Roman
Pill'e Matta	Cagliari, IT	Punic-Roman
Tharros	Oristano, IT	Roman
Velletri	Rome, IT	Roman
Driffield Terrace	York, UK	Roman
Hungate	York, UK	Roman/Anglo-Scandinavian
Hofstadir	IS	Viking/Medieval
Borgharen	Maastricht, NL	Merovingian
Mechelen	Antwerp, B	Medieval
St Peter's Church of Thaon	Calvados, FR	Medieval
Constitution Street	Edinburgh, UK	Medieval
St Catherine's Church	Eindhoven, NL	Medieval
Sintra	Lisbon, P	Medieval
Rossio do Carmo	Mertola, P	Medieval
Sedgeford	Norfolk, UK	Medieval
Bamburgh	Northumberland, UK	Medieval
Sala	Vastmaal, S	Medieval
Haymarket	York, UK	Medieval
Syningthwaite Priory	Yorkshire, UK	Medieval
Ridgeway	Dorset, UK	Medieval (mass grave)
St Thomas Church	Osbaldwick, UK	Medieval/Modern
Middembeemster	Beemster, NL	Post Medieval/Modern
Fewston	Yorkshire, UK	Post Medieval/Modern
Fromelles	Calais, FR	First World War (mass grave)

1.2 LIST OF THE EXPERIMENTAL BURIALS OF PIGLETS

List of the experimental burials of stillborn piglets, their location, the type of soil in which the burials were excavated and the type of matrix used to fill the coffin. The piglets analysed in this research are in bolt.

PIGLET	SITE	SOIL	MATRIX
1	Hovingham		Coffin Imported sand fill
2	**Hovingham**	Imported limestone	Coffin Imported limestone fill
3	Folkton	Peat bog	Coffin Local soil
4	Folkton	Peat bog	Local soil
5	Heslington East	Sandy-clay soil	Base of sand
6	**Heslington East**	Sandy-clay soil	Coffin Local soil
7	**Heslington East**	Sandy-clay soil	Local soil
8	West Heslerton	Sand, near sand and gravel quarry	Local soil
9	West Heslerton	Sand, near sand and gravel quarry	Coffin, Local soil
10	King's Manor	Urban	Local soil

1.3 SKELETON SAMPLING RECORD SHEET FOR HUMAN BURIALS

Skeleton Sampling Record sheet elaborated by the InterArChive project for geoarchaeological and chemical sampling of human burials.

1.4 SKELETON SAMPLING RECORD SHEET FOR PIGLET BURIALS

Skeleton Sampling Record sheet elaborated by the InterArChive project for geoarchaeological and chemical sampling of experimental piglet burials.

Additional samples *(cont)*:

A5 | C ☐ | ....
MM ☐ | ....

A6 | C ☐ | ....
MM ☐ | ....

A7 | C ☐ | ....
MM ☐ | ....

A8 | C ☐ | ....
MM ☐ | ....

A9 | C ☐ | ....
MM ☐ | ....

A10 | C ☐ | ....
MM ☐ | ....

A11 | C ☐ | ....
MM ☐ | ....

A12 | C ☐ | ....
MM ☐ | ....

A13 | C ☐ | ....
MM ☐ | ....

A14 | C ☐ | ....
MM ☐ | ....

A15 | C ☐ | ....
MM ☐ | ....

A16 | C ☐ | ....
MM ☐ | ....

A17 | C ☐ | ....
MM ☐ | ....

A18 | C ☐ | ....
MM ☐ | ....

A19 | C ☐ | ....
MM ☐ | ....

A20 | C ☐ | ....
MM ☐ | ....

A21 | C ☐ | ....
MM ☐ | ....

Comments *(cont)*:
....
....
....
....
....
....
....
....
....
....
....
....
....
....
....
....

A22 | C ☐ | ....
MM ☐ | ....

A23 | C ☐ | ....
MM ☐ | ....

A24 | C ☐ | ....
MM ☐ | ....

A25 | C ☐ | ....
MM ☐ | ....

A26 | C ☐ | ....
MM ☐ | ....

A27 | C ☐ | ....
MM ☐ | ....

A28 | C ☐ | ....
MM ☐ | ....

1.5 LIST OF THE SLIDES ANALYSED AND THEIR RECORDED INFORMATIONS

List of all of the slides analysed by micromorphology, with ticks indicating the information recorded: accurate location of the sample (for example which was the exact position of the tin in relation to the skeleton, generally visible through a picture or a sketch), orientation of the slide (* indicates that the up orientation was specified, but the slide was erroneously cut parallel to the skeleton resting plane), relation with the bones (which side of the sample was in contact with the bones) and quality of the manufacture of the slide (0= less than 50% of the slide was visible and analyzable; 1= more than 50% of the slide was visible; 2= 100% of the slide was visible. Only in the case of Rossio Do Carmo, the value 0 referred to the sample as disturbed).

SITE	GRAVE	SLIDE	ACCURATE LOCATION	ORIENTATION (UP)	RELATION WITH THE BONES	MANUFACTURE OF THE SLIDE
Hungate	51349/51351	318	✓	✓	✓	2
		320	✓	✓	N/A	2
		323	✓	✓	N/A	2
		333	✓		✓	1
		344	✓	✓	✓	1
		357	✓	✓	N/A	2
		358	✓	✓	N/A	2
		359	✓	✓	✓	2
		366	✓	✓	N/A	2
		368	✓	✓	✓	2
		404	✓	✓	✓	2
	51350/51364	170	✓	✓	N/A	2
		171	✓	✓	N/A	1
		173	✓	✓	N/A	2
		174	✓	✓	N/A	2
		177	✓	✓	✓	1
	52253	319	N/A	✓	N/A	1
		350	N/A	✓	N/A	2
		354	N/A	✓	✓	1
		355	N/A	✓	✓	2
		356	N/A	✓	✓	2
		369	N/A	✓	✓	1
		388	N/A	✓	✓	2
		395	N/A	✓	N/A	2
	53700	587	N/A	✓	N/A	2
		656	✓	✓	✓	2
		682	✓	✓	✓	2

SITE	GRAVE	SLIDE	ACCURATE LOCATION	ORIENTATION (UP)	RELATION WITH THE BONES	MANUFACTURE OF THE SLIDE
		797	✓	✓	✓	2
		815	✓	✓	✓	2
		878	✓	✓	N/A	1
	54077	586	✓	✓	N/A	1
		590	✓	✓	N/A	2
		657	✓	✓	✓	2
		683	✓	✓	✓	2
	54296	575	N/A	✓	N/A	2
		664	✓	✓	✓	2
		665	✓	✓	✓	2
		690	✓	✓	✓	2
		691	✓	✓	✓	1
		798	✓	✓	✓	2
		799	✓	✓	✓	2
		827	N/A	✓	N/A	2
	54931/54909	560	N/A	✓	N/A	2
		573	N/A	✓	✓	2
		576	N/A	✓	✓	2
		604	N/A	✓	✓	2
		605	N/A	✓	✓	2
Haymarket	83012	1034	N/A	✓	N/A	1
		1045	N/A	✓	✓	2
		1053	N/A	✓	✓	2
		1057	N/A	✓	N/A	2
		1067	N/A	✓	✓	1
		1077	N/A	N/A	✓	1
		1081	N/A	✓	N/A	0
		1082	N/A	N/A	✓	1
		1083	N/A	✓	N/A	1
		1089	N/A	✓	✓	2
		1090	N/A	✓	N/A	2
		1108	N/A	✓	N/A	2
		1110	N/A	✓	✓	2
		1111	N/A	✓	N/A	2
		1211	N/A	✓	✓	1
		1213	N/A	✓	✓	2
		1221	N/A	✓	N/A	2
	84700	1007	N/A	✓	✓	2
		1018	N/A	✓	✓	1
		1027	N/A	✓	✓	1

SITE	GRAVE	SLIDE	ACCURATE LOCATION	ORIENTATION (UP)	RELATION WITH THE BONES	MANUFACTURE OF THE SLIDE
		1030	N/A	✓	✓	1
		1074	N/A	✓	N/A	1
		1086	N/A	✓	N/A	1
		1088	N/A	✓	N/A	2
	84779	940	N/A	✓	✓	2
		955	N/A	✓	N/A	1
		1043	N/A	✓*	N/A	0
		1044	N/A	✓	✓	2
		1047	N/A	✓	✓	1
		1062	N/A	✓	✓	1
	84851	1016	N/A	✓	✓	1
		1052	N/A	✓	✓	1
		1064	N/A	✓*	✓	2
		1071	N/A	✓	✓	1
		1075	N/A	✓	✓	1
		1087	N/A	✓*	✓	0
Rossio do Carmo	395	228	N/A	✓	N/A	2
		229	N/A	✓	N/A	0
		231	N/A	✓	N/A	2
		233	N/A	✓	N/A	0
		234	N/A	✓	✓	0
		238	N/A	✓	✓	1
		241	N/A	✓	N/A	2
Borgharen	15	155	N/A	✓	N/A	1
		156	N/A	✓	N/A	0
		246	N/A	N/A	N/A	0
		247	N/A	N/A	N/A	0
		248	N/A	✓	N/A	1
		249	N/A	N/A	N/A	2
		250	N/A	N/A	N/A	1
		254	N/A	N/A	N/A	0
		255	N/A	✓	N/A	2
		256	N/A	✓	N/A	1
Pill'e Matta	237	506	N/A	✓	N/A	2
		507	N/A	✓	N/A	1
		527	N/A	✓*	N/A	2
		528	N/A	✓*	N/A	0
		562	N/A	N/A	N/A	1
		565	N/A	N/A	N/A	1

SITE	GRAVE	SLIDE	ACCURATE LOCATION	ORIENTATION (UP)	RELATION WITH THE BONES	MANUFACTURE OF THE SLIDE
		572	N/A	N/A	N/A	1
	238	742	N/A	N/A	N/A	2
		750	N/A	N/A	N/A	2
		752	N/A	✓	✓	1
		756	N/A	✓*	✓	1
		757	N/A	✓	N/A	1
		791	N/A	✓	✓	2
		803	N/A	✓	N/A	2
	268	630	N/A	✓	N/A	1
		668	N/A	✓	N/A	1
		670	N/A	✓	N/A	2
		671	N/A	✓	N/A	2
		677	N/A	✓	N/A	2
	2680	629	N/A	N/A	N/A	2
		669	N/A	✓	N/A	1
		678	N/A	✓	N/A	2
Heslington East	6	1144	✓	N/A	N/A	2
		1147	✓	N/A	N/A	1
		1149	✓	N/A	N/A	2
		1150	✓	N/A	N/A	2
		1151	✓	N/A	N/A	2
		1155	✓	N/A	N/A	1
		1157	✓	N/A	N/A	1
		1158	✓	N/A	N/A	2
		1159	✓	N/A	N/A	0
		1203	✓	N/A	N/A	2
	7	1143	✓	N/A	N/A	2
		1162	✓	✓*	N/A	2
		1176	✓	✓	N/A	2
		1185	✓	N/A	N/A	1
		1192	✓	✓	N/A	2
		1194	✓	✓	N/A	2
Hovingham	2	1246	✓	✓	N/A	2
		1249	✓	✓	N/A	2
		1250	✓	✓	N/A	2
		1251	✓	✓	N/A	2
		1252	✓	✓	N/A	2
		1256	✓	✓	N/A	2
		1258	✓	✓	N/A	2

SITE	GRAVE	SLIDE	MOSAIC	MICROMORPHOLOGY	MICROMORPHOLOGY ONLY FREQUENCY OF PEDOFEATURES	IMAGE ANALYSIS	SEM EDS
		1259	✓	✓		2	
		1260	✓	✓		2	

1.6. LIST OF THE SLIDES ANALYSED AND THE METHODS APPLIED

List of all of the slides analysed and the methods applied, with ticks indicating which methods were applied to each slide.

SITE	GRAVE	SLIDE	MOSAIC	MICROMORPHOLOGY	MICROMORPHOLOGY ONLY FREQUENCY OF PEDOFEATURES	IMAGE ANALYSIS	SEM EDS
HUNGATE	51349/ 51351	318	✓	✓			
		320	✓	✓		✓	
		323	✓	✓			
		333	✓	✓			
		344	✓	✓			
		357	✓	✓		✓	
		358	✓	✓		✓	
		359	✓	✓			
		366	✓	✓		✓	
		368	✓	✓		✓	
		404	✓	✓		✓	
	51350/ 51364	170	✓	✓		✓	
		171	✓	✓		✓	
		173	✓	✓		✓	✓
		174	✓	✓		✓	✓
		177	✓	✓		✓	✓
	52253	319	✓	✓		✓	
		350	✓	✓		✓	
		354	✓	✓			
		355	✓	✓		✓	
		356	✓	✓			
		369	✓	✓		✓	
		388	✓	✓			
		395	✓	✓		✓	
	53700	587	✓	✓			
		656	✓	✓		✓	✓
		682	✓	✓			
		797	✓	✓		✓	

SITE	GRAVE	SLIDE	MOSAIC	MICROMORPHOLOGY	MICROMORPHOLOGY ONLY FREQUENCY OF PEDOFEATURES	IMAGE ANALYSIS	SEM EDS
		815	✓	✓			✓
		878	✓	✓			✓
	54077	586	✓	✓		✓	
		590	✓	✓		✓	
		657	✓	✓		✓	
		683	✓	✓			
	54264	655			✓		
		659			✓		
		661			✓		
		685			✓		
		687			✓		
	54273	618			✓		
		650			✓		
		662			✓		
		663			✓		
		688			✓		
		689			✓		
		810			✓		
	54292	610			✓		
	54296	575	✓	✓		✓	
		664	✓	✓		✓	
		665	✓	✓		✓	
		690	✓	✓			
		691	✓	✓			
		798	✓	✓			
		799	✓	✓		✓	
		827	✓	✓		✓	
	54341	544			✓		
		549			✓		
		550			✓		
		553			✓		
		554			✓		
		564			✓		
		568			✓		
		832			✓		
		834			✓		
		838			✓		
		839			✓		

SITE	GRAVE	SLIDE	MOSAIC	MICROMORPHOLOGY	MICROMORPHOLOGY ONLY FREQUENCY OF PEDOFEATURES	IMAGE ANALYSIS	SEM EDS
	54342	540			✓		
		541			✓		
		548			✓		
		828			✓		
		829			✓		
		835			✓		
		837			✓		
	54349	538			✓		
		543			✓		
		545			✓		
		551			✓		
		592			✓		
		735			✓		
		830			✓		
	54851	719			✓		
	54898	535			✓		
		539			✓		
		557			✓		
		566			✓		
		608			✓		
		632			✓		
		633			✓		
	54908	556			✓		
		577			✓		
		591			✓		
		598			✓		
		603			✓		
	54931/ 54909	560	✓	✓			
		573	✓	✓			
		576	✓	✓			
		604	✓	✓			
		605	✓	✓			
HAYMARKET	83012	1034	✓	✓		✓	
		1045	✓	✓		✓	
		1053	✓	✓		✓	
		1057	✓	✓		✓	
		1067	✓	✓		✓	
		1077	✓	✓		✓	

SITE	GRAVE	SLIDE	MOSAIC	MICROMORPHOLOGY	MICROMORPHOLOGY ONLY FREQUENCY OF PEDOFEATURES	IMAGE ANALYSIS	SEM EDS
		1081	✓	✓		✓	
		1082	✓	✓		✓	
		1083	✓	✓		✓	
		1089	✓	✓		✓	
		1090	✓	✓		✓	
		1108	✓	✓		✓	
		1110	✓	✓		✓	
		1111	✓	✓		✓	
		1211	✓	✓		✓	
		1213	✓	✓		✓	
		1221	✓	✓		✓	
	83015	1036			✓		
		1049			✓		
		1054			✓		
		1080			✓		
	84332	1048			✓		
		1055			✓		
		1061			✓		
	84579	1035			✓		
		1040			✓		
		1056			✓		
		1073			✓		
		1079			✓		
	84700	1007	✓	✓			
		1018	✓	✓		✓	
		1027	✓	✓			
		1030	✓	✓		✓	
		1074	✓	✓		✓	
		1086	✓	✓		✓	
		1088	✓	✓		✓	
	84779	940	✓	✓			
		955	✓	✓		✓	
		1043	✓	✓		✓	
		1044	✓	✓		✓	
		1047	✓	✓			
		1062	✓	✓		✓	
	84851	998	✓			✓	
		1016	✓	✓			
		1052	✓	✓		✓	

SITE	GRAVE	SLIDE	MOSAIC	MICROMORPHOLOGY	MICROMORPHOLOGY ONLY FREQUENCY OF PEDOFEATURES	IMAGE ANALYSIS	SEM EDS
		1064	✓	✓		✓	
		1071	✓	✓		✓	
		1075	✓	✓		✓	
		1087	✓	✓		✓	
	84859	1041			✓		
		1050			✓		
		1065			✓		
		1069			✓		
		1070			✓		
		1072			✓		
		1085			✓		
	84863	1033			✓		
		1038			✓		
		1063			✓		
		1078			✓		
	84895	939			✓		
	Section 12	972			✓		
		1025			✓		
		1026			✓		
ROSSIO DO CARMO	395	228	✓	✓		✓	
		229	✓	✓			
		231	✓	✓		✓	
		233	✓	✓			
		234	✓	✓		✓	
		238	✓	✓		✓	
		241	✓	✓		✓	
BORGHAREN	15	155	✓	✓		✓	✓
		156	✓	✓		✓	✓
		246	✓	✓			
		247	✓	✓			
		248	✓	✓			
		249	✓	✓			✓
		250	✓	✓		✓	✓
		254	✓	✓			✓
		255	✓	✓		✓	
		256	✓	✓			✓
PILL'E MATTA	237	506	✓	✓			✓
		507	✓	✓		✓	✓
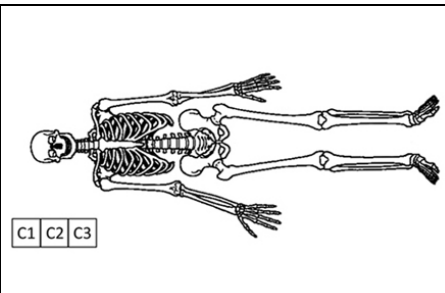
SITE	GRAVE	SLIDE	MOSAIC	MICROMORPHOLOGY	MICROMORPHOLOGY ONLY FREQUENCY OF PEDOFEATURES	IMAGE ANALYSIS	SEM EDS
		527	✓	✓		✓	
		528	✓	✓			
		562	✓	✓			
		565	✓	✓			
		572	✓	✓		✓	✓
	238	742	✓	✓		✓	
		750	✓	✓			✓
		752	✓	✓		✓	✓
		756	✓	✓			
		757	✓	✓			✓
		791	✓	✓		✓	✓
		803	✓	✓		✓	
	268	630	✓	✓		✓	
		668	✓	✓		✓	
		670	✓	✓		✓	
		671	✓	✓			✓
		677	✓	✓			
	2680	629	✓	✓		✓	
		669	✓	✓		✓	
		678	✓	✓		✓	
	Soil profile	823	✓	✓			
		852	✓	✓			
		857	✓	✓			
		865	✓	✓			
		873	✓	✓			
HESLINGTON EAST (piglets)	6	1122	✓		✓	✓	
		1144	✓	✓		✓	
		1147	✓	✓		✓	
		1149	✓	✓		✓	
		1150	✓	✓		✓	
		1151	✓	✓		✓	
		1155	✓	✓		✓	
		1157	✓	✓		✓	
		1158	✓	✓		✓	
		1159	✓	✓		✓	
		1202	✓		✓	✓	
		1203	✓	✓		✓	
	7	1143	✓	✓		✓	

SITE	GRAVE	SLIDE	MOSAIC	MICROMORPHOLOGY	MICROMORPHOLOGY ONLY FREQUENCY OF PEDOFEATURES	IMAGE ANALYSIS	SEM EDS
		1148	✓		✓	✓	
		1162	✓	✓		✓	
		1164	✓		✓	✓	
		1176	✓	✓		✓	
		1185	✓	✓		✓	
		1191	✓		✓	✓	
		1192	✓	✓		✓	
		1194	✓	✓		✓	
HOVINGHAM	2	1246	✓	✓		✓	
		1249	✓	✓		✓	
		1250	✓	✓		✓	
		1251	✓	✓		✓	
		1252	✓	✓		✓	
		1256	✓	✓		✓	
		1258	✓	✓		✓	
		1259	✓	✓		✓	
		1260	✓	✓		✓	
THESSALONIKI	157	133				✓	
		138				✓	
		143				✓	
ST. THOMAS CHURCH (Osbaldwick)	6	479				✓	
		480				✓	
		493				✓	
CATALHÖYÜK	18666	450				✓	
		494				✓	
		500				✓	
		580				✓	
		611				✓	
HESLINGTON EAST	713	188				✓	
		190				✓	
		199				✓	
		200				✓	
EDINBURGH (Constitution Street)	1046	26				✓	
		27				✓	
AL KHIDAY	150	376				✓	
		382				✓	

SITE	GRAVE	SLIDE	MOSAIC	MICROMORPHOLOGY	MICROMORPHOLOGY ONLY FREQUENCY OF PEDOFEATURES	IMAGE ANALYSIS	SEM EDS
		391				✓	
SALA	5914	887				✓	
		907				✓	
		995				✓	
		996				✓	
HOFSTADIR	117	581				✓	
		619				✓	
		621				✓	
		626				✓	
		850				✓	
SYNINGTH-WAITE PRIORY	3	42				✓	
		70				✓	
		71				✓	
		74				✓	
		265				✓	

1.7 TABLE OF DESCRIPTION FOR MICROMORPHOLOGICAL ANALYSIS

Standardized table for the description and analysis of thin sections, elaborated in this research. The significance of the main descriptive terms is explained in the Glossary.

SLIDE NUMBER	
BODY POSITION	
ORIENTATION	
LOCATION	
SLIDE AREA	
% OF SLIDE	
C/F LIMIT	

C1 C2 C3

ELEMENTS OF FABRIC	SLIDE AREA	C/F REL. DISTRIBUTION	SORTING %	BASIC DISTRIBUTION	BASIC ORIENTATION	REFERRED DISTRIBUTION	REFERRED ORIENTATION
		Chitonic Enaulic Gefuric Monic Porphyric	0 - Unsorted 32 - Poorly sorted 75 - Moderately sorted 92 - Well sorted 100 - Perfectly sorted	Banded Clustered Fan-like Interlaced Linear Random	Bimodal parallel Random Unimodal parallel	Bow-like Concentric Inclined Parallel Perpendicular Radial Random	Bow-like Concentric Inclined Parallel Perpendicular Radial Unferred

FINE MATERIAL	SLIDE AREA	LIMPIDITY	B-FABRIC	ABUNDANCE %	PPL COLOUR	XPL COLOUR
		Clouded Dotted Limpid Masked Opaque Speckled	Crystallitic Speckled Strial Striated Undifferentiated	Voids + fine material + coarse material = 100%	Black Brown to dark brown Greenish to greyish green Grey Red Yellowish brown	

PEDS	SLIDE AREA	TYPE	ABUNDANCE %	SIZE µm	ACCOMODATION	DEVELOPMENT
		Angular-blocky (A-B) Apedal Crumb Granular Lenticular platy Platy Prism Sub-Angular blocky (SA-B)	<2 2-5 5-10 10-20 20-30 30-50 >50 In relation to all the area of the slide.	Tab 5.1 from Bullock (1985, p 42)	Accomodated Partially accommodated Unaccomodated	Moderate Strong Weak

VOIDS	ABUNDANCE %	Voids + fine material + coarse material = 100%				
	SLIDE AREA	TYPE	ABUNDANCE %	SIZE µm	SURFACE	
		Chambers Channels Cracks Modified complex Packing Planes Vesicles Vughs	<2 2-5 5-10 10-20 20-30 30-50 >50 In relation to all the area of the slide.	<50 50-300 300-500 500-1000 1000-2000 2000-5000 >5000	Rough Smooth Undulating	

		ABUNDANCE %	Voids + fine material + coarse material = 100%					

		ABUNDANCE %	**Voids + fine material + coarse material = 100%**					

MINERAL COMPONENTS (COARSE MATERIAL)

SLIDE AREA	TYPE	FREQUENCY %	SIZE µm	SHAPE	WEATHERING	PPL COLOUR	XPL COLOUR
	Calcite Chert Flint Glauconite Mica Micrite Microcline Plagioclase Pyroxene Quartz Quartzite Schist	<2 2-5 5-10 10-20 20-30 30-50 >50 In relation to all the area of slide	<50 50-100 100-200 200-500 500-1000 1000-2000	Angular A Subangular SA Subrounded SR Rounded R Well-rounded WR	Not weathered Partially weathered Weathered		

ORGANIC COMPONENTS (COARSE MATERIAL)

SLIDE AREA	TYPE	FREQUENCY %	SIZE µm	SHAPE	SURFACE	WEATHERING	PPL colour	XPL colour
	Amorphous organic matter Bone Charcoal Fungal hyphae Fungal spore Humified plant structure Piglet hair Piglet tooth Remain of insect Remain of worm Root Rubified plant structure Sclerotia Triangular seed	<2 2-5 5-10 10-20 20-30 30-50 >50 In relation to all the slide	<50 50-100 100-200 200-500 500-1000 1000-2000	Angular A Subangular SA Subrounded SR Rounded R Well-rounded WR	Rough Smooth Undulating	Not weathered Partially weathered Weathered		

PEDOFEATURES AND ANTHROPOGENIC MATERIAL

SLIDE AREA	TYPE	FREQUENCY %	SIZE µm	SHAPE	SURFACE	WEATHERING	PPL colour	XPL colour
	Amorphous phosphate Beeswax Brick fragment Clay coating Clay impregnation Clay infilling Dendritic Mn nodule Fe/Mn nodule Fine material coating Infilling of calcifed filaments Infilling of fine material Leucophosphite Micrite coating/hypo coating Red spherulites	<2 2-5 5-10 10-20 20-30 30-50 >50 In relation to all the area of the slide		Angular A Subangular SA Subrounded SR Rounded R Well-rounded WR	Rough Smooth Undulating	Not weathered Partially weathered Weathered		

	SLIDE AREA	TYPE	DISTRIBUTION	ORIENTATION	B-FABRIC	ID NAME
		Redox impregnation Secondary CaCO3 crystals Soil micro-fauna faecal pellets Vivianite Worm calcium carbonate granule			Crystallitic Speckled Strial Striated Undifferentiated	
NOTES						

APPENDIX 2

2.1 RESULTS OF METHODS A, B, C AND D OF IMAGE ANALYSIS

Results from the experimental Methods A, B and C applied to the measurement of soil porosity on 144 slides from the archaeological sites sampled by the InterArChive project. The table contains information regarding the code of the slides, the site, the grave and the anatomical region of provenience. Results of control method D are inserted in the last column.

SITE	GRAVE	SLIDE	BODY REGION	Method A %	Method B %	Method C %	Method D %
HUNGATE	54077	657	skull	24.63	26.18	20.05	26.72
		590	C3	4.32	3.94	3.17	4.03
		586	C2	15.72	15.53	14.76	12.28
	51350	177	skull	16.6	16.17	12.3	18.66
		173	pelvis	13.3	12.09	10.03	13.22
		174	feet	10.25	10.23	7.69	17.76
		171	C3	10.59	8.79	7.82	14.94
		170	C2	17.42	16.29	13.33	23.94
	53700	797	skull	10.75	10.79	9.49	12.19
		656	pelvis	15.58	16.3	13.94	16.82
	52253	395	skull	2.57	4.84	2.88	3.07
		369	pelvis	13.66	12.1	8.37	16.73
		355	feet	6.93	8.22	6.64	3.6
		350	C2	10.47	9.84	6.56	15.7
		319	C3	19.02	15.32	12.79	17.68
	54296	664	skull	7.33	7.83	6.71	7.24
		665	pelvis	17	17.2	15.38	21.15
		799	feet	22.64	22.62	20.35	23.38
		575	C2	7.34	9.41	6.7	7.59
		827	C3	15.95	15.86	14.83	13.21
	51351	368	skull	20.62	18.56	16.64	17.71
		357	pelvis	14.83	14.18	12.48	13.26
		404	feet	9.79	10.89	6.04	4.66
		320	C1 (7-16cm)	12.65	16.93	13.58	10.3
		358	C1 (27cm)	11.17	14.15	10.37	12.41
		366	C1 (49-58cm)	22.63	20.14	18.07	13.8
HAYMARKET	84779	1044	skull	11.48	11.75	10.7	11.67
		1043	pelvis (z)	33.99	35.86	34.94	36.86
		1062	feet	1.42	2.59	2.46	1.71
		955	C2	5.19	5.17	4.14	1.58

SITE	GRAVE	SLIDE	BODY REGION	Method A %	Method B %	Method C %	Method D %
	84851	1052	skull (y)	17.33	19.67	17.6	18.68
		1071	pelvis (y)	11.24	14.43	12.47	12.39
		998	feet (y)	18.58	17.52	16.72	16.74
		1075	skull (z)	29.72	28.76	27.99	29.99
		1087	pelvis (z)	37.2	39.58	39.17	40.56
		1064	feet (z)	36.14	37.64	36.55	34.89
	84700	1030	skull	18.17	19.73	18.24	18.22
		1086	pelvis	6.36	5.65	4.79	4.65
		1018	feet	14.34	12.03	9.91	12.98
		1074	C3	9.69	10.24	9.4	8.63
		1088	C2	11.59	9.83	8.06	8.69
ROSSIO DO CARMO	395	234	skull	38.59	35.96	33.87	5.82
		231	pelvis	23.03	23.43	22.57	19.10
		238	feet	31.82	30.57	29.65	8.24
		228	C3	25.26	27.41	27.94	25.93
		241	C1	32.43	45.27	43.71	22.10
PILL'E MATTA	237	572	skull	10.86	10.66	10.55	10.51
		527	pelvis	35.45	36.88	36.17	36.16
		507	feet	16.01	14.74	13.95	17.39
	268	630	skull	17.03	19.11	12.84	17.44
		670	pelvis	24.87	25.32	23.53	29.45
		668	feet	15.92	12.67	11.71	13.04
	238	791	skull	6.74	7.3	6.71	7.04
		803	pelvis	9.3	10.85	10.31	9.55
		752	feet	9.79	12.32	11.79	4.51
		742	C3	17.03	17.3	15.82	20.11
	2680	678	skull	40.48	30.95	29.78	35.51
		629	pelvis	16.83	12.53	11.75	16.81
		669	feet	13.41	14.41	10.22	13.37
BORGHAREN		156	skull		19.35	18.48	19.17
		155	pelvis	20.3	21.05	17.98	18.99
		250	feet	11.33	9.02	7.37	10.56
		255	control	19.01	17.06	16.46	15.71
THESSALONIKI	157	138	skull	18.19	19.45	17.94	21.97
		133	pelvis	21.25	21.45	20.68	25.05
		143	foot	21.46	21.3	20.25	22.88
ST THOMAS OSBALDWICK	6	493	skull	23.14	23.35	18.97	32.75
		480	pelvis	6.29	7.75	7.45	10.39
		479	feet	6.2	4.6	3.72	4.41
CATALHÖYÜK	18666	500	skull (z)	5.97	6.34	5.88	12.36
		611	pelvis (z)	13.07	14.27	14.15	20.53
		580	feet (z)	3.95	4.99	4.43	9.31
		450	C3	7.59	8.49	6.92	10.77
		494	C1	11.72	14.91	13.88	22.07

SITE	GRAVE	SLIDE	BODY REGION	Method A %	Method B %	Method C %	Method D %
HESLINGTON EAST	713	199	skull	7.78	5.83	5.05	9.16
		200	feet	18.36	19.12	15.95	27.25
		188	C3	9.22	11.91	10.05	15.87
		190	C2	10.86	10.64	9.94	15.56
EDINBURGH (Constituiton street)	1046	27	skull	23.28	27.54	25.54	18.43
		26	pelvis	22.35	14.11	10.38	21.19
AL KHIDAY	150	391	skull	25.32	21.5	10.79	11.35
		382	feet	13.01	16.34	12.47	13.98
		376	C1	18.45	23.03	18.41	17.74
SALA	5914	995	skull	8.98	9.04	8.73	8.93
		996	pelvis	18.73	19.89	19.6	17.96
		907	feet	2.08	2.59	2.1	3.02
		887	C3	8.09	7.74	7.24	8.1
HOFSTADIR	117	626	skull	9.45	15.22	9.42	25.7
		619	pelvis	9.66	15.82	13.33	27.49
		850	feet	23.65	26.57	23.92	31
		581	C3	17.1	15.96	15.72	16.46
		621	C2	18.48	17.55	14.52	21.45
SYNINGTHWAITE PRIORY	3	42	skull	11.58	9.46	7.77	11.95
		265	pelvis	27.49	25.25	21.23	37.12
		70	feet	16.77	11.4	10.57	15.37
		74	C3	2.91	3.05	2.92	3.48
		71	C2	10.41	8.74	6.47	7.79

2.2 RESULTS OF METHODS E AND D OF IMAGE ANALYSIS

Results from the experimental Methods E and D applied to the measurement of soil porosity on 144 slides from the archaeological sites sampled by the InterArChive project. The table contains information regarding the code of the slides, the site, the grave and the anatomical region of provenience.

SITE	GRAVE	SLIDE	BODY REGION	Method E %	Method D %
HUNGATE	54077	657	skull	28.16	26.22
		590	C3	5.40	5.06
		586	C2	10.74	6.40
	51350	177	skull	23.29	21.53
		173	pelvis	17.54	14.60
		174	feet	18.29	18.37
		171	C3	11.61	10.59
		170	C2	20.78	20.19
	53700	797	skull	16.34	15.78
		656	pelvis	14.78	15.15
	52253	395	skull	6.35	7.53
		369	pelvis	22.21	24.59
		355	feet	8.33	6.01
		350	C2	22.09	17.21
		319	C3	22.19	18.04
	54296	664	skull	11.61	8.71
		665	pelvis	11.06	10.71
		799	feet	32.24	31.40
		575	C2	12.18	6.94
		827	C3	16.53	17.75
	51351	368	skull	14.67	13.46
		357	pelvis	8.55	5.68
		404	feet	8.44	6.99
		320	C1 (7-16cm)	6.58	5.14
		358	C1 (27cm)	12.42	5.05
		366	C1 (49-58cm)	11.16	9.45
HAYMARKET	84779	1044	skull	14.11	14.19
		1043	pelvis (z)	21.96	25.70
		1062	feet	3.69	2.98
		955	C2	6.86	6.21
	84851	1052	skull (y)	14.50	17.50
		1071	pelvis (y)	11.10	9.36
		998	feet (y)	10.89	11.67

SITE	GRAVE	SLIDE	BODY REGION	Method E %	Method D %
		1075	skull (z)	9.85	15.17
		1087	pelvis (z)	31.51	33.51
		1064	feet (z)	29.51	29.99
	84700	1030	skull	11.86	12.79
		1086	pelvis	12.91	13.22
		1018	feet	1.59	2.10
		1074	C3	9.71	10.26
		1088	C2	12.69	13.20
ROSSIO DO CARMO		234	skull	17.67	20.02
		231	pelvis	15.63	16.43
		238	feet	12.61	12.35
		228	C3	27.49	28.00
		241	C1a	23.71	26.35
PILL'E MATTA	237	572	skull	8.39	8.91
		527	pelvis	36.97	36.26
		507	feet	14.22	14.42
	268	630	skull	21.88	18.32
		670	pelvis	33.17	31.71
		668	feet	3.37	4.25
	238	791	skull	5.88	6.32
		803	pelvis	7.59	7.34
		752	feet	6.92	5.89
		742	C3	7.46	10.41
	2680	678	skull	27.73	23.60
		629	pelvis	9.89	9.99
		669	feet	15.68	12.23
BORGHAREN		156	skull	15.05	14.73
		155	pelvis	12.87	13.05
		250	feet	12.68	12.36
		255	control	8.95	8.99
THESSALONIKI	157	138	skull	16.34	14.07
		133	pelvis	15.53	16.60
		143	foot	19.40	15.76
ST THOMAS OSBALDWICK	6	493	skull	23.80	20.12
		480	pelvis	6.25	7.12
		479	feet	4.76	6.11
CATALHÖYÜK	18666	500	skull (z)	7.38	7.26
		611	pelvis (z)	11.59	11.06
		580	feet (z)	3.48	5.04
		450	C3	11.89	11.84
		494	C1	16.09	16.62
HESLINGTON EAST	713	199	skull	8.45	9.59
		200	feet	15.47	18.37
		188	C3	10.89	10.15
		190	C2	19.59	21.01

SITE	GRAVE	SLIDE	BODY REGION	Method E %	Method D %
EDINBURGH (Constitution street)	1046	27	skull	18.56	38.60
		26	pelvis	48.06	34.82
AL KHIDAY	150	391	skull	18.96	19.21
		382	feet	20.20	21.04
		376	C1	22.90	22.12
SALA	5914	995	skull	5.61	6.67
		996	pelvis	3.49	3.21
		907	feet	5.24	6.91
		887	C3	8.16	8.15
HOFSTADIR	117	626	skull	12.53	12.29
		619	pelvis	16.76	17.94
		850	feet	27.73	27.18
		581	C3	7.56	7.99
		621	C2	18.76	18.61
SYNINGTHWAITE PRIORY	3	42	skull	11.17	12.29
		265	pelvis	16.52	17.32
		70	feet	20.12	19.90
		74	C3	2.19	2.62
		71	C2	7.96	9.78

2.3 VARIANCE OF ≥ 3% IN METHOD A

Differences between the results obtained with Method D and Method A. The results with variance
≥ 3% are reported in the table, in decreasing order. The variance of 3% was arbitrarily chosen to
separate accurate (≤ 3%) and not accurate (≥ 3%) results.

SITE	GRAVE	SLIDE	Method A %	Method D %	DIFFERENCE ≥3%
ROSSIO DO CARMO	395	234	38.59	5.82	32.77
ROSSIO DO CARMO	395	238	31.82	8.24	23.58
HOFSTADIR	117	619	9.66	27.49	17.83
HOFSTADIR	117	626	9.45	25.7	16.25
AL KHIDAY	150	391	25.32	11.35	13.97
CATALHÖYÜK	18666	494	11.72	22.07	10.35
ROSSIO DO CARMO	395	241	32.43	22.1	10.33
SYNINGTHWAITE PRIORY	3	265	27.49	37.12	9.63
ST THOMAS CHURCH	6	493	23.14	32.75	9.61
HESLINGTON EAST	713	200	18.36	27.25	8.89
HUNGATE	51351	366	22.63	13.8	8.83
HUNGATE	51350	174	10.25	17.76	7.51
CATALHÖYÜK	18666	611	13.07	20.53	7.46
HOFSTADIR	117	850	23.65	31	7.35
HESLINGTON EAST	713	188	9.22	15.87	6.65
HUNGATE	51350	170	17.42	23.94	6.52
CATALHÖYÜK	18666	500	5.97	12.36	6.39
CATALHÖYÜK	18666	580	3.95	9.31	5.36
PILL'E MATTA	238	752	9.79	4.51	5.28
HUNGATE	52253	350	10.47	15.7	5.23
HUNGATE	51351	404	9.79	4.66	5.13
PILL'E MATTA	2680	678	40.48	35.51	4.97
EDINBURGH	1046	27	23.28	18.43	4.84
HESLINGTON EAST	713	190	10.86	15.56	4.7
PILL'E MATTA	268	670	24.87	29.45	4.58
HUNGATE	51350	171	10.59	14.94	4.35
HUNGATE	54296	665	17	21.15	4.15
ROSSIO DO CARMO	395	231	23.03	19.1	3.93
THESSALONIKI	157	133	21.25	25.05	3.8
THESSALONIKI	157	138	18.19	21.97	3.78
HAYMARKET	84779	955	5.19	1.58	3.61
HUNGATE	54077	586	15.72	12.28	3.44
HAYMARKET	84851	1087	37.2	40.56	3.36
HUNGATE	52253	355	6.93	3.6	3.33
BORGHAREN		255	19.01	15.71	3.3
CATALHÖYÜK	18666	450	7.59	10.77	3.18
PILL'E MATTA	238	742	17.03	20.11	3.08
HUNGATE	52253	369	13.66	16.73	3.07

2.4 VARIANCE OF ≥ 3% IN METHOD B

Differences between the results obtained with Method D and Method B. The results with variance ≥ 3% are reported in the table, in decreasing order. The variance of 3% was arbitrarily chosen to separate accurate (≤ 3%) and not accurate (≥ 3%) results.

SITE	GRAVE	SLIDE	Method B %	Method D %	DIFFERENCE ≥3%
ROSSIO DO CARMO	395	234	35.96	5.82	30.14
ROSSIO DO CARMO	395	241	45.27	22.1	23.17
ROSSIO DO CARMO	395	238	30.57	8.24	22.33
SYNINGTHWAITE PRIORY	3	265	25.25	37.12	11.87
HOFSTADIR	117	619	15.82	27.49	11.67
HOFSTADIR	117	626	15.22	25.7	10.48
AL KHIDAY	150	391	21.5	11.35	10.15
ST THOMAS CHURCH	6	493	23.35	32.75	9.4
EDINBURGH	1046	27	27.54	18.43	9.11
HESLINGTON EAST	713	200	19.12	27.25	8.13
PILL'E MATTA	238	752	12.32	4.51	7.81
HUNGATE	51350	170	16.29	23.94	7.65
HUNGATE	51350	174	10.23	17.76	7.53
CATALHÖYÜK	18666	494	14.91	22.07	7.16
EDINBURGH	1046	26	14.11	21.19	7.08
HUNGATE	51351	320	16.93	10.3	6.63
HUNGATE	51351	366	20.14	13.8	6.34
CATALHÖYÜK	18666	611	14.27	20.53	6.26
HUNGATE	51351	404	10.89	4.66	6.23
HUNGATE	51350	171	8.79	14.94	6.15
CATALHÖYÜK	18666	500	6.34	12.36	6.02
HUNGATE	52253	350	9.84	15.7	5.86
AL KHIDAY	150	376	23.03	17.74	5.29
HESLINGTON EAST	713	190	10.64	15.56	4.92
HUNGATE	52253	369	12.1	16.73	4.63
HUNGATE	52253	355	8.22	3.6	4.62
PILL'E MATTA	2680	678	30.95	35.51	4.56
HOFSTADIR	117	850	26.57	31	4.43
ROSSIO DO CARMO	395	231	23.43	19.1	4.33
CATALHÖYÜK	18666	580	4.99	9.31	4.32
PILL'E MATTA	2680	629	12.53	16.81	4.28
PILL'E MATTA	268	670	25.32	29.45	4.13
SYNINGTHWAITE PRIORY	3	70	11.4	15.37	3.97
HESLINGTON EAST	713	188	11.91	15.87	3.96
HUNGATE	54296	665	17.2	21.15	3.95
HOFSTADIR	117	621	17.55	21.45	3.9
THESSALONIKI	157	133	21.45	25.05	3.6
HAYMARKET	84779	955	5.17	1.58	3.59
HESLINGTON EAST	713	199	5.83	9.16	3.33
HUNGATE	54077	586	15.53	12.28	3.25

2.5 VARIANCE OF ≥ 3% IN METHOD C

Differences between the results obtained with Method D and Method C. The results with variance ≥ 3% are reported in the table, in decreasing order. The variance of 3% was arbitrarily chosen to separate accurate (≤ 3%) and not accurate (≥ 3%) results.

SITE	GRAVE	SLIDE	Method C %	Method D %	DIFFERENCE ≥3%
ROSSIO DO CARMO	395	234	33.87	5.82	28.05
ROSSIO DO CARMO	395	241	43.71	22.1	21.61
ROSSIO DO CARMO	395	238	29.65	8.24	21.41
HOFSTADIR	117	626	9.42	25.7	16.28
SYNINGTHWAITE PRIORY	3	265	21.23	37.12	15.89
HOFSTADIR	117	619	13.33	27.49	14.16
ST THOMAS CHURCH	6	493	18.97	32.75	13.78
HESLINGTON EAST	713	200	15.95	27.25	11.3
EDINBURGH	1046	26	10.38	21.19	10.81
HUNGATE	51350	170	13.33	23.94	10.61
HUNGATE	51350	174	7.69	17.76	10.07
HUNGATE	52253	350	6.56	15.7	9.14
HUNGATE	52253	369	8.37	16.73	8.36
CATALHÖYÜK	18666	494	13.88	22.07	8.19
PILL'E MATTA	238	752	11.79	4.51	7.28
HUNGATE	51350	171	7.82	14.94	7.12
EDINBURGH	1046	27	25.54	18.43	7.11
HOFSTADIR	117	850	23.92	31	7.08
HOFSTADIR	117	621	14.52	21.45	6.93
HUNGATE	54077	657	20.05	26.72	6.67
CATALHÖYÜK	18666	500	5.88	12.36	6.48
CATALHÖYÜK	18666	611	14.15	20.53	6.38
HUNGATE	51350	177	12.3	18.66	6.36
PILL'E MATTA	268	670	23.53	29.45	5.92
HESLINGTON EAST	713	188	10.05	15.87	5.82
HUNGATE	54296	665	15.38	21.15	5.77
PILL'E MATTA	2680	678	29.78	35.51	5.73
HESLINGTON EAST	713	190	9.94	15.56	5.62
PILL'E MATTA	2680	629	11.75	16.81	5.06
HUNGATE	52253	319	12.79	17.68	4.89
CATALHÖYÜK	18666	580	4.43	9.31	4.88
SYNINGTHWAITE PRIORY	3	70	10.57	15.37	4.8
PILL'E MATTA	268	630	12.84	17.44	4.6
THESSALONIKI	157	133	20.68	25.05	4.37
PILL'E MATTA	238	742	15.82	20.11	4.29
HUNGATE	51351	366	18.07	13.8	4.27
SYNINGTHWAITE PRIORY	3	42	7.77	11.95	4.18
HESLINGTON EAST	713	199	5.05	9.16	4.11
THESSALONIKI	157	138	17.94	21.97	4.03

SITE	GRAVE	SLIDE	Method C %	Method D %	DIFFERENCE ≥3%
CATALHÖYÜK	18666	450	6.92	10.77	3.85
ROSSIO DO CARMO	395	231	22.57	19.1	3.47
PILL'E MATTA	237	507	13.95	17.39	3.44
HUNGATE	51351	320	13.58	10.3	3.28
HUNGATE	51350	173	10.03	13.22	3.19
BORGHAREN		250	7.37	10.56	3.19
PILL'E MATTA	2680	669	10.22	13.37	3.15
HAYMARKET	84700	1018	9.91	12.98	3.07
HUNGATE	52253	355	6.64	3.6	3.04
HUNGATE	54296	799	20.35	23.38	3.03

2.6 COMPARISON AMONG THE RESULTS OF METHODS A, B AND C WITH VARIANCE ≥ 3%

List of results from Methods A, B and C with variance ≥ 3%. The slides with this variance in all of the three methods are highlighted in yellow (total of 26).

SLIDE	SITE	GRAVE	Method A	Method C	Method B
255	BORGHAREN		3.3		
26	EDINBURGH	1046		10.81	7.08
27	EDINBURGH	1046	4.84	7.11	9.11
42	SYNINGTHWAITE PRIORY	3		4.18	
70	SYNINGTHWAITE PRIORY	3		4.8	3.97
133	THESSALONIKI	157	3.8	4.37	3.6
138	THESSALONIKI	157	3.78	4.03	
143	THESSALONIKI	157			
170	HUNGATE	51350	6.52	10.61	7.65
171	HUNGATE	51350	4.35	7.12	6.15
173	HUNGATE	51350		3.19	
174	HUNGATE	51350	7.51	10.07	7.53
177	HUNGATE	51350		6.36	
188	HESLINGTON EAST	713	6.65	5.82	3.96
190	HESLINGTON EAST	713	4.7	5.62	4.92
199	HESLINGTON EAST	713		4.11	3.33
200	HESLINGTON EAST	713	8.89	11.3	8.13
231	ROSSIO DO CARMO	395	3.93	3.47	4.33
234	ROSSIO DO CARMO	395	32.77	28.05	30.14
238	ROSSIO DO CARMO	395	23.58	21.41	22.33
241	ROSSIO DO CARMO	395	10.33	21.61	23.17
250	BORGHAREN	15		3.19	
265	SYNINGTHWAITE PRIORY	3	9.63	15.89	11.87
319	HUNGATE	52253		4.89	
320	HUNGATE	51351		3.28	6.63

SLIDE	SITE	GRAVE	Method A	Method C	Method B
350	HUNGATE	52253	5.23	9.14	5.86
355	HUNGATE	52253	3.33	3.04	4.62
358	HUNGATE	51351			
366	HUNGATE	51351	8.83	4.27	6.34
369	HUNGATE	52253	3.07	8.36	4.63
376	AL KHIDAY	150			5.29
391	AL KHIDAY	150	13.97		10.15
404	HUNGATE	51351	5.13		6.23
450	CATALHÖYÜK	18666	3.18	3.85	
493	ST THOMAS CHURCH	6	9.61	13.78	9.4
494	CATALHÖYÜK	18666	10.35	8.19	7.16
500	CATALHÖYÜK	18666	6.39	6.48	6.02
507	PILL'E MATTA	237		3.44	
575	HUNGATE	54296			
580	CATALHÖYÜK	18666	5.36	4.88	4.32
586	HUNGATE	54077	3.44		3.25
611	CATALHÖYÜK	18666	7.46	6.38	6.26
619	HOFSTADIR	117	17.83	14.16	11.67
621	HOFSTADIR	117		6.93	3.9
626	HOFSTADIR	117	16.25	16.28	10.48
629	PILL'E MATTA	2680		5.06	4.28
630	PILL'E MATTA	268		4.6	
657	HUNGATE	54077		6.67	
665	HUNGATE	54296	4.15	5.77	3.95
669	PILL'E MATTA	2680		3.15	
670	PILL'E MATTA	268	4.58	5.92	4.13
678	PILL'E MATTA	2680	4.97	5.73	4.56
742	PILL'E MATTA	238	3.08	4.29	
752	PILL'E MATTA	238	5.28	7.28	7.81
799	HUNGATE	54296		3.03	
850	HOFSTADIR	117	7.35	7.08	4.43
955	HAYMARKET	84779	3.61		3.59
1018	HAYMARKET	84700		3.07	
1043	HAYMARKET	84779			
1052	HAYMARKET	84851			
1075	HAYMARKET	84851			
1087	HAYMARKET	84851	3.36		

2.7 VARIANCE OF ≥ 3% IN METHOD E

Differences between the results obtained with Method D and Method E. The results with variance ≥ 3% are reported in the table, in decreasing order. The variance of 3% was arbitrarily chosen to separate accurate (≤ 3%) and not accurate (≥ 3%) results.

SITE	GRAVE	SLIDE	Method E %	Method D %	DIFFERENCE ≥3%
EDINBURGH	1046	27	18.56	38.6	20.04
EDINBURGH	1046	26	48.06	34.82	13.24
HUNGATE	51351	358	12.42	5.05	7.37
HAYMARKET	84851	1075	9.85	15.17	5.32
HUNGATE	54296	575	12.18	6.94	5.24
HUNGATE	52253	350	22.09	17.21	4.88
HUNGATE	54077	586	10.74	6.4	4.34
HUNGATE	52253	319	22.19	18.04	4.15
PILL'E MATTA	2680	678	27.73	23.6	4.13
HAYMARKET	84779	1043	21.96	25.7	3.74
ST THOMAS OSBALDWICK	6	493	23.8	20.12	3.68
THESSALONIKI	157	143	19.4	15.76	3.64
PILL'E MATTA	268	630	21.88	18.32	3.56
PILL'E MATTA	2680	669	15.68	12.23	3.45
HAYMARKET	84851	1052	14.5	17.5	3

2.8 COMPARISON AMONG THE RESULTS OF METHODS A, B, C AND E WITH VARIANCE ≥ 3%

List of results from Methods A, B, C and E with variance ≥ 3%. The slides with this variance in all of the four methods are highlighted in yellow (total of 4).

SLIDE	SITE	GRAVE	Method A	Method C	Method B	Method E
255	BORGHAREN		3.3			
26	EDINBURGH	1046		10.81	7.08	13.24
27	EDINBURGH	1046	4.84	7.11	9.11	20.04
42	SYNINGTHWAITE PRIORY	3		4.18		
70	SYNINGTHWAITE PRIORY	3		4.8	3.97	
133	THESSALONIKI	157	3.8	4.37	3.6	
138	THESSALONIKI	157	3.78	4.03		
143	THESSALONIKI	157				3.64
170	HUNGATE	51350	6.52	10.61	7.65	
171	HUNGATE	51350	4.35	7.12	6.15	
173	HUNGATE	51350		3.19		
174	HUNGATE	51350	7.51	10.07	7.53	
177	HUNGATE	51350		6.36		
188	HESLINGTON EAST	713	6.65	5.82	3.96	
190	HESLINGTON EAST	713	4.7	5.62	4.92	
199	HESLINGTON EAST	713		4.11	3.33	
200	HESLINGTON EAST	713	8.89	11.3	8.13	
231	ROSSIO DO CARMO	395	3.93	3.47	4.33	
234	ROSSIO DO CARMO	395	32.77	28.05	30.14	
238	ROSSIO DO CARMO	395	23.58	21.41	22.33	
241	ROSSIO DO CARMO	395	10.33	21.61	23.17	
250	BORGHAREN	15		3.19		
265	SYNINGTHWAITE PRIORY	3	9.63	15.89	11.87	
319	HUNGATE	52253		4.89		4.15
320	HUNGATE	51351		3.28	6.63	
350	HUNGATE	52253	5.23	9.14	5.86	4.88
355	HUNGATE	52253	3.33	3.04	4.62	
358	HUNGATE	51351				7.37
366	HUNGATE	51351	8.83	4.27	6.34	
369	HUNGATE	52253	3.07	8.36	4.63	
376	AL KHIDAY	150			5.29	
391	AL KHIDAY	150	13.97		10.15	
404	HUNGATE	51351	5.13		6.23	
450	CATALHÖYÜK	18666	3.18	3.85		
493	ST THOMAS CHURCH	6	9.61	13.78	9.4	3.68
494	CATALHÖYÜK	18666	10.35	8.19	7.16	
500	CATALHÖYÜK	18666	6.39	6.48	6.02	
507	PILL'E MATTA	237		3.44		
575	HUNGATE	54296				5.24
580	CATALHÖYÜK	18666	5.36	4.88	4.32	

SLIDE	SITE	GRAVE	Method A	Method C	Method B	Method E
586	HUNGATE	54077	3.44		3.25	4.34
611	CATALHÖYÜK	18666	7.46	6.38	6.26	
619	HOFSTADIR	117	17.83	14.16	11.67	
621	HOFSTADIR	117		6.93	3.9	
626	HOFSTADIR	117	16.25	16.28	10.48	
629	PILL'E MATTA	2680		5.06	4.28	
630	PILL'E MATTA	268		4.6		3.56
657	HUNGATE	54077		6.67		
665	HUNGATE	54296	4.15	5.77	3.95	
669	PILL'E MATTA	2680		3.15		3.45
670	PILL'E MATTA	268	4.58	5.92	4.13	
678	PILL'E MATTA	2680	4.97	5.73	4.56	4.13
742	PILL'E MATTA	238	3.08	4.29		
752	PILL'E MATTA	238	5.28	7.28	7.81	
799	HUNGATE	54296		3.03		
850	HOFSTADIR	117	7.35	7.08	4.43	
955	HAYMARKET	84779	3.61		3.59	
1018	HAYMARKET	84700		3.07		
1043	HAYMARKET	84779				3.74
1052	HAYMARKET	84851				3
1075	HAYMARKET	84851				5.32
1087	HAYMARKET	84851	3.36			

2.9 RESULTS OF IMAGE ANALYSIS ON THE CASE STUDIES

Results from the Method E of image analysis applied to the measurement of soil porosity on the case studies of Hungate, Haymarket, Borgharen, Rossio do Carmo, Pill'e Matta and the experimental burial of piglets (2, 6 and 7).

SITE	GRAVE	SLIDE	BODY REGION	SOIL POROSITY %
HUNGATE	54077	657	skull	28.16
		590	C3	5.40
		586	C2	10.74
	51350/51364	177	skull	23.29
		173	pelvis	17.54
		174	feet	18.29
		171	C3	11.61
		170	C2	20.78
	53700	797	skull	16.34
		656	pelvis	14.78
	52253	395	skull	6.35
		369	pelvis	22.21
		355	feet	8.33
		350	C2	22.09
		319	C3	22.19
	54296	664	skull	11.61
		665	pelvis	11.06
		799	feet	32.24
		575	C2	12.18
		827	C3	16.53
	51349/51351	368	skull	14.67
		357	pelvis	8.55
		404	feet	8.44
		320	C1 (7-16cm)	6.58
		358	C1 (27cm)	12.42
		366	C1 (49-58cm)	11.16
HAYMARKET	84779	1044	skull	14.11
		1043	pelvis (z)	21.96
		1062	feet	3.69
		955	C2	6.86
	84851	1052	skull (y)	14.50
		1071	pelvis (y)	11.10
		998	feet (y)	10.89
		1075	skull (z)	9.85
		1087	pelvis (z)	31.51
		1064	feet (z)	29.51
	84700	1030	skull	11.86

SITE	GRAVE	SLIDE	BODY REGION	SOIL POROSITY %
		1086	pelvis	12.91
		1018	feet	1.59
		1074	C3	9.71
		1088	C2	12.69
	83012	1053	skull (y)	1.13
		1211	skull (side)	3.11
		1089	skull (z)	3.31
		1213	pelvis (z)	4.27
		1083	A4	7.35
		1057	A5	8.25
		1111	A6	8.45
		1034	A7	3.94
		1090	A8	9.18
		1221	A9	4.86
		1108	A10	2.71
		1081	A11	7.01
		1110	C3 (y)	8.86
		1045	C3 (z)	10.51
		1077	C2 (x)	7.87
		1067	C2 (y)	7.55
		1082	C2 (z)	14.75
ROSSIO DO CARMO	395	234	skull	17.67
		231	pelvis	15.63
		238	feet	12.61
		228	C3	27.49
		241	C1a	23.71
PILL'E MATTA	237	572	skull	8.39
		527	pelvis	36.97
		507	feet	14.22
	268	630	skull	21.88
		670	pelvis	33.17
		668	feet	3.37
	238	791	skull	5.88
		803	pelvis	7.59
		752	feet	6.92
		742	C3	7.46
	2680	678	skull	27.73
		629	pelvis	9.89
		669	feet	15.68
BORGHAREN	15	156	skull	15.05
		155	pelvis	12.87
		250	feet	12.68
		255	control	8.95
PIGLETS	2	1256	1 (y)	21.67
		1251	1 (z)	30.74
		1250	2 (z)	14.80

SITE	GRAVE	SLIDE	BODY REGION	SOIL POROSITY %
		1252	16/17	15.68
		1260	A8	13.45
		1249	A9	14.36
		1259	A15	25.85
		1246	C2 A	13.19
		1258	C3 A	14
	6	1149	1 (y)	10.88
		1155	1 (z)	12.73
		1147	3 (y)	18.40
		1158	14	10.68
		1151	16/17	11.61
		1159	A1	17.65
		1157	A2	16.77
		1202	A3	11.69
		1144	A5	18.25
		1203	C3 A	13.89
		1150	C2 A	9.45
		1122	C0	5.41
	7	1185	1 (y)	8.32
		1143	1 (z)	7.75
		1176	3 (y)	15.29
		1162	3 (z)	2.19
		1148	4 (y)	15.43
		1191	4 (z)	12.59
		1164	16 (z)	3.48
		1194	C3 C	9.61
		1192	C2 C	7.63

GLOSSARY

The following definitions were partially modified from Bullock et al. (1985) and Stoops (2003).

Basic distribution: the distribution of fabric units of the same type with regard to each other. It can be:

- *Random*: fabric units do not follow any order;

- *Clustered*: fabric units occur in groups;

- *Linear*: fabric units are organized in lines;

- *Banded*: fabric units are concentrated in bands;

- *Fan-like*: fabric units are distributed according to a fan-like pattern;

- *Interlaced*: fabric units are interlaced with each other.

Basic orientation: the orientation of fabric units of the same type with regard to each other. It can be described as random, unimodal parallel and bimodal parallel, or by the degree of parallelism (small angle, medium angle, broad angle) or by the quantity of oriented particles (strongly, moderately or weakly expressed).

B-fabric: the origin and patterns of orientation and distribution of interference colours in the fabric. It can be:

- *Undifferentiated*: absence of interference colours;

- *Crystallitic*: presence of small birefringent mineral grains;

- *Speckled*: random arrangement of clay orientation;

- *Striated*: presence of elongated zones or streaks in which the domains show more or less simultaneous extinction.

c/f related distribution: the distribution of individual fabric units in relation to smaller fabric units and associated pores. It can be:

- *Monic*: only large fabric units or small fabric units are present;
- *Gefuric*: braces of smaller fabric units link larger fabric units;
- *Chitonic*: a layer of smaller units covers the large fabric units;
- *Enaulic*: aggregates formed by small units are located in the interstitial spaces between larger units;

- *Porphyric*: the larger fabric units occur in a dense groundmass of smaller units.

Chamber: pore with more or less equidimensional smooth walls, generally interconnected with channels.

Channel: void with tubular shape and smooth walls, uniform in most of the length.

Crystals and crystals intergrowths: single crystals and crystal intergrowths (random, parallel, fanlike, radial and framboids) that are not part of the parent material. They are larger than 20 μm and embedded in the groundmass.

Coating: intrusive pedofeature layering a natural surface of voids, grains or aggregates in the soil.

Hypocoating: matrix pedofeatures referred to a natural surface in the soil and immediately adjoining it.

Impregnation/ impregnative pedofeatures: characterized by a higher concentration of a component, generally in the micromass.

Infilling: void partly or completely filled by soil material or some fraction of it.

Limpidity: the transparency of the fine material. The presence of fine particles influences the aspects of the limpidity, which can be:

- *Limpid:* the particle are absent;
- *Speckled:* presence of clay-size microcontrasted particles;
- *Dotted:* fine silt-size opaque particles;
- *Cloudy:* the particles are white or colourless and very finely dispersed.

Nodule: more or less equidimensional pedofeatures, not related to natural surfaces of voids and not consisting of single crystals or crystals intergrowths. It can be:

- Typic: with undifferentiated fabric;
- Concentric: with a concentric fabric;
-

OIL: oblique incident light

Packing void: void resulting from the loose packing of soil components, which are not accommodated.

Ped: primary particle of the soil aggregating organic and mineral components. It is described according to its shape:

- *Spheroidal*: particles arranged into more or less equant peds, which are bounded by rounded faces and they are not accommodated. The two types are *crumbs* (porous) and *granules* (non porous);
- *Blocky*: particles arranged into more or less equant and angular peds;
- *Plates*: particles arranged into elongate peds. They can be more or less straight plates, wavy plates or lenticular plates;
- *Prisms*: particles arranged into more or less vertically elongated peds.

Pedofeature: discrete fabric units in soil material recognizable from an adjacent material by a difference in concentration in one or more components or by a difference in internal fabric.

Plane: planar and flat void, accommodated or not, smooth or rough.

Pleochroic: a mineral grain showing different colours when rotated in plain polarized light.

PPL: plane polarized light

Quasicoating: matrix pedofeatures referred to a natural surface in the soil but not immediately adjoining the natural surface.

Referred distribution: expresses the distribution of like fabric units with respect to a reference.

Referred orientation: espresses the orientation of like fabric units with respect to a reference.

Soil fabric: related to the organization of the soil. It expresses the spatial arrangements of the soil constituents, their shape, size and frequency.

Sorting: the statistical amount of variation in particles diameters found in a sample.

Vesicle: large voids with smooth and simple walls.

Vugh: irregular void, more or less equidimensional, smooth or rough, normally not interconnected with other voids.

XPL: crossed polarized light.

REFERENCES

Adderley, W. P., Simpson, I. A. and Davidson, D. A. (2002). Colour description and qualification in mosaic images of soil thin sections. Geoderma, 108, pp. 181-195.

Adderley, W. P., Simpson, I. A. and Davidson, D. A. (2006). Historic landscape management: a validation of quantitative soil thin-section analyses. *Journal of Archaeological Science*, 33, pp. 320-334.

Adderley, W. P., Wilson, C. A., Simpson, I. A. and Davidson, D. (2010). Anthropogenic features. In Stoops, G., Marcelino, V. and Mees, F. (Eds.). *Interpretation of micromorphological features of soils and regoliths*. Amsterdam: Elsevier, pp. 569-588.

Alonso-Zarza, A. M. (1999). Initial stages of laminar calcrete formation by roots: examples from the Neogene of central Spain. *Sedimentary Geology*, 126, pp. 177-191.

Andersen, B. and Hollensted, M. (2008). Metabolite production by different Ulocladium species. *International Journal of Food Microbiology*, 126, pp. 172-179.

Angelucci, D. E. (2008). Geoarchaeological insights from a Roman age incineration feature (ustrinum) at Enconsta de Sant'Ana (Lisbon, Portugal). *Journal of Archaeological Science*, 35, pp. 2624-2633.

Aspök, E. (2011). Past 'disturbances' of graves as a source: taphonomy and interpretation of reopened early medieval inhumation graves at Brunn am Gebirge (Austria) and Winnall II (England). *Oxford Journal of Archaeology,* 30 (3), pp. 299-324.

Babel, U., Kooistra, M. J. and Altemuller, H-J. (1990). Organic material and effect of biological activities. In Kooistra (Ed.). *European training course on soil micromorphology. II. Applications to soil micromorphology*. Booklet of the course, pp. 1-23.

Bajnóczi, B. and Kovas-Kis, V. (2006). Origin of pedogenic needle-fiber calcite revealed by micromorphology and stable isotope composition – a case study of a Quaternary paleosol from Hungary. *Chemie der Erde*, 66, pp. 203-212.

Bertran, P. and Texier, J-P. (1999). Facies and microfacies of slope deposits. *Catena*, 35, pp. 99-121.

Boschian, G. (2001). New Data on the Pastoral Use of Caves in Italy. *Quaderni Società Preistoria e Protostoria Friuli-Venezia Giulia*, 8, pp. 63-72.

Boschian, G., Ghislandi, S. (2011). Nuovi dati geoarcheologici sulle grotte Continenza e Maritza. *Il Fucino e le aree limitrofe nell'antichità, Atti del III convegno di Archeologia*. Avezzano, pp. 40-54.

Bouma, J., Fox, C. A. and Miedema, R. (1990). Micromorphology of hydromorphic soils: applications for soil genesis and land evaluation. In Douglas, L. A. (Ed.). *Soil Micromorphology*. Amsterdam: Elsevier, pp. 257-278.

Brady, N. C. (1974). *The nature and properties of soils*. New York: Macmillan Publishing Co., Inc.

Brewer, R. (1972). The basis of interpretation of soil micromorphological data. *Geoderma*, 8, pp. 81-94.

Bruneau, P. M. C., Davidson, D. A. and Grieve, I. C. (2004). An evaluation of image analysis for measuring changes in void space and excremental features on soil thin sections in an upland grassland soil. *Geoderma*, 120, pp. 165-175.

Bryant, R. G. and Davidson, D. (1996). The use of image analysis in the micromorphological study of old cultivated soils: an evaluation based on soils from the Island of Papa Stour, Shetland. *Journal of Archaeological Science*, 23, pp. 811-822.

Bui, E. (1991). Applications of image analysis to soil micromorphology. *Agriculture, Ecosystems and Environment*, 34, pp. 305-313.

Bullock, P., Fedoroff, N., Jongerius, A., Stoops, G., Tursina, T., and Babel, C. (1985). *Handbook for Soil Thin Section Description*. Albrighton: Waine Research Publication.

Cailleau, G., Dadras, M., Abolhassani-D, S., Braissant, O. and Verrecchia, E. P. (2009a). Evidence for an organic origin of pedogenic calcitic nanofibres. *Journal of Crystal Growth*, 311, 2490-2495.

Cailleau, G., Verrecchia, E. P., Braissant, O. and Laurent, E. (2009b). The biogenic origin of needle fibre calcite. *Sedimentology*, 56, pp. 1858-1875.

Canti, M. (1997). An investigation of microscopic calcareous spherulites from herbivore dungs. *Journal of Archaeological Science*, 24, pp. 219-231.

Canti, M. (1998). Origin of calcium carbonate granules found in buried soils and Quaternary deposits. *Boreas*, 27, pp. 275-288.

Canti, M. (1998). The micromorphological identification of faecal spherulites from archaeological and modern materials. *Journal of Archaeological Science*, 25, pp. 435-444.

Canti, M. (2003). Earthworm activity and archaeological stratigraphy: a review of products and processes. *Journal of Archaeological Science*, 30, pp. 135-148.

Canti, M. (2009). Experiments on the origin of ^{13}C in the calcium carbonate granules produced by the earthworm Lumbricus terrestris. *Soil Biology & Biochemistry*, 41, pp. 2588-2592.

Canti, M. and Piearce, T. G. (2003). Morphology and dynamics of calcium carbonate granules produced by different earthworm species. *Pedobiologia*, 47, pp. 511-521.

Carter, D. O. and Tibbett, M. (2008). Cadaver decomposition and soil: processes. In Tibbett, M., Carter, D. O. (Eds). *Soil analysis in forensic taphonomy*. CRC Press, pp. 29-51.

Carter, D. O., Yellowlees, D. and Tibbett, M. (2013). Moisture can be the dominant environmental parameter governing cadaver decomposition in soil. *Forensic Science International*, 200, pp. 60-66.

Catt, J. A. (1990). Paleopedology manual. *Quaternary International. The Journal of the International Union for Quaternary Research*, 6. Pergamon Press.

Courty, M. A., Goldberg, P. and Macphail, R. I. (1989). *Soils and micromorphology in archaeology*. Cambridge University Press.

Courty, M-A. (1992). Soil micromorphology in archaeology. *Proceedings of the British Academy*, 77, pp. 39-59.

Dadour, I. R. and Harvey, M. (2008). The role of invertebrates in terrestrial decomposition: forensic applications. In Tibbett, M., Carter, D. O. (Eds). *Soil analysis in forensic taphonomy*. CRC Press, pp. 109-122.

Daniell, C. (1997). *Death and burial in Medieval England*. London: Routledge.

Davidson, D. A., Carter, S. P. and Quine, T. A. (1992). An evaluation of micromorphology as aid to archaeological interpretation. *Geoarchaeology: An International Journal*, 7 (1), pp.55-65.

De Groot, T., De Kort, J. W., Lauwerier, R. C. G. M., Soeters, G. C., Theunissen, E. M. and Theuws, F. C. W. J (2014). Context. In Lauwerier, R. C. G. M. and De Kort, J. W. (Eds.). *Merovingers in een villa 2. Romeinse villa en Merovingish grafveld Borgharen – Pasestraat. Onderzoek 2012*. Amersfoort: Rijksdienst voor het Cultureel Erfgoed, pp. 15-26.

De Groot, T., Müller, A., Soeters, G. C. and Theuws, F. C. W. J. (2011). Context. In Lauwerier, R. C. G. M., Müller, A. and Smal, D. E. (Eds.). *Merovingers in een villa. Romeinse villa en Merovingisch grafveld Borgharen – Pasestraat. Onderzoek 2008-2009*. Amersfoort: Rijksdienst voor het Cultureel Erfgoed, pp. 13-18.

Dent, B. B., Forbes, S. L. and Stuart, B. H. (2004). Review of human decomposition processes in soil. *Environmental Geology*, 45, pp. 576-585.

Driese, S. G., Ludvigson, G. A., Roberts, J. A., Fowle, D. A., Gonzales, L. A., Smith, J. J., Vulava, V. M. and McKay, L. D. (2010). Micromorphology and stable-isotope geochemistry of historical pedogenic siderite formed in pah-contamined alluvial clay soils, Tennessee, U.S.A. *Journal of Sedimentary Research*, 80, pp. 943-954.

Duchaufour, P. (1998). *Handbook of pedology. Soil, vegetation, environment*. Rotterdam: A.A.Balkema.

Duday, H. (2009). *The archaeology of the dead. Lectures in Archaeothanatology*. Oxford: Oxford Books.

Dupras, T. L., Schultz, J. J., Wheeler, S. M. and Williams, L. J. (2006). *Forensic recovery of human remains.* Taylor & Francis Group.

Durand, N., Monger, H. C. and Canti, M. (2010). Calcium carbonate features. In Stoops, G., Marcelino, V. and Mees, F. (Eds.). *Interpretation of micromorphological features of soils and regoliths*. Amsterdam: Elsevier, pp. 149-194.

Elsen, J. (2006). Microscopy of historic mortars – a review. *Cement and Concrete Research*, 36, pp. 1416-1424.

Emami, M., Sakali, Y., Pritzel, C., Trettin, R. (2016). Deep inside the ceramic texture: A microscopic-chemical approach to the phase transition via partial-sintering processes in ancient ceramic matrices. Journal of Microscopy and Ultrastructure, 4 (1), pp. 11-19.

Ern, S. I. E. and Trombino, L. (2013). Forensic geopedology and micropedology: new indications and lookouts from piglets experimental burials. *Geophysical Research Abstracts*, 15, EGU General Assembly.

Ern, S. I. E., Trombino, L. and Cattaneo C. (2010). Micromorphological aspects of forensic geopedology: can vivianite be a marker of human remains permanence in soil? *Geophysical Research Abstracts*, 12, EGU General Assembly.

Ern, S. I. E., Trombino, L. and Cattaneo C. (2012). Micromorphological aspects of forensic geopedology II: ultramicroscopic vs microscopic characterization of phosphatic impregnations on soil particles in experimental burials. *Geophysical Research Abstract*, 14, EGU General Assembly.

Evans, D. (2007). *Areas A, B and C. Hungate development, York. A report on an archaeological watching brief*. York Archaeological Trust.

Fiedler, S. and Graw, M. (2003). Decomposition of buried corpses, with special references to the formation of adipocere. Naturwissenschaften, The Science of Nature, 90, pp. 291-300.

FitzPatrick, E. A. (1993). *Soil microscopy and micromorphology*. West Sussex: John Wiley & Sons Ltd.

Fitzpatrick, R. W. (2008). Nature, distribution and origin of soil materials in the forensic comparison of soils. In Tibbett, M., Carter, D. O. (Eds). *Soil analysis in forensic taphonomy*. CRC Press, pp. 1-28.

Forbes, S. L. (2008). Decomposition chemistry in a burial environment. In Tibbett, M., Carter, D. O. (Eds). *Soil analysis in forensic taphonomy*. CRC Press, pp. 203-223.

Gebhardt, A. and Langohr, R. (1999). Micromorphological study of construction materials and living floors in the Medieval Motte of Werken (West Flanders, Belgium). *Geoarchaeology: An International Journal*, 14 (7), pp. 595-620.

Gilbert, B. M. and Bass, W. M. (1967). Seasonal dating of burials from the presence of fly pupae. *American Antiquity*, 32 (4), pp. 534-535.

Goldberg, P. and Macphail, R. (2003). Short contribution: strategies and techniques in collecting micromorphology samples. *Geoarchaeology: An International Journal*, 18 (5), pp. 571-578.

Goldberg, P. and Macphail, R. (2006). Practical and theoretical geoarchaeology. Blackwell Science Ltd.

Goldberg, P., Lev-Yadun, S. and Bar-Yosef, O. (1994). Petrographic thin sections of archaeological sediments: a new method for paleobotanical studies. *Geoarchaeology: An International Journal*, 9 (3), pp. 243-257.

Gordon, C. C. and Buikstra, J. E. (1981). Soil pH, bone preservation and sampling bias at mortuary sites. *Society for American Archaeology*, 46 (3), pp. 566-571.

Hall, R. A. (1996). *English Heritage Book of York*. London: B. T. Batsford/English Heritage.

Hseu, Z. Y. and Chen, Z. S. (1996). Saturation, reduction, and redox morphology of seasonally flooded Alfisols in Tawain. *Soil Science Society of American Journal*, 60, pp. 941-949.

Huckleberry, G., Stein, J. K. and Goldberg, P. (2003). Determining the provenience of Kennewick Man skeletal remains through sedimentological analyses. *Journal of Archaeological Science*, 30, pp. 651-665.

Jans, M. M. E., Nielsen-Marsh, C. M., Smith, C. I., Collins, M. J. and Kars, H. (2004). Characterisation of microbial attack on archaeological bone. *Journal of Archaeological Science*, 31, pp. 87-95.

Karkanas, P. (1999). Mineral assemblage in Theopetra, Greece: a framework for understanding diagenesis in a prehistoric cave. *Journal of Archaeological Science*, 26, pp. 1171-1180.

Karkanas, P. and Goldberg, P. (2008). Micromorphology of sediments: deciphering archaeological context. *Israeli Journal of Earth Science*, 56, pp. 63-71.

Karkanas, P. and Goldberg, P. (2010). Phosphatic features. In Stoops, G., Marcelino, V. and Mees, F. (Eds.). *Interpretation of micromorphological features of soils and regoliths*. Amsterdam: Elsevier, pp. 521-541.

Karkanas, P., Dabney, M. K., Smith, R. A. K. and Wright, J. C. (2012). The geoarchaeology of Mycenaean chambers tombs. *Journal of Archaeological Science*, 39, pp. 2722-2732.

Kars, M., Van Os, B. J. H. (2011). Inventarisatie en beschrijving van de anarganische grafvondsten. In Lauwerier, R. C. G. M., Müller, A. and Smal, D. E. (Eds.). *Merovingers in een villa. Romeinse villa en Merovingisch grafveld Borgharen – Pasestraat. Onderzoek 2008-2009*. Amersfoort: Rijksdienst voor het Cultureel Erfgoed, pp. 92-109.

Kemp, R. A. (1995). Distribution and genesis of calcitic pedofeatures within a rapidly aggrading loess-paleosol sequence in China. *Geoderma*, 65, pp. 303-316.

Koistra, M. J. and Pulleman, M. M. (2010). Features related to faunal activity. In Stoops, G., Marcelino, V. and Mees, F. (Eds.). *Interpretation of micromorphological features of soils and regoliths*. Amsterdam: Elsevier, pp. 397-418.

Kooistra, M. J., Tovey, N. K. and Pagliai, M. (1990). Agricultural applications. In Kooistra (Ed.). *European training course on soil micromorphology. II. Applications to soil micromorphology*. Booklet of the course, pp. 1-48.

Kovda, I. and Mermut, A. R. (2010). Vertic features. In Stoops, G., Marcelino, V. and Mees, F. (Eds.). *Interpretation of micromorphological features of soils and regoliths*. Amsterdam: Elsevier, pp. 109-127.

Kühn, P., Aguilar, J. and Miedema, R. (2010). Textural pedofeatures and related horizons. In Stoops, G., Marcelino, V. and Mees, F. (Eds.). *Interpretation of micromorphological features of soils and regoliths*. Amsterdam: Elsevier, pp. 217-250.

Lang, C. (2014). *The hidden archive of historical human inhumations locked within burial soils*. Ph.D. thesis, University of York.

Lauwerier, R. C. G. M. and Müller, A. (2011). Inleiding. In Lauwerier, R. C. G. M., Müller, A. and Smal, D. E. (Eds.). *Merovingers in een villa. Romeinse villa en Merovingisch grafveld Borgharen – Pasestraat. Onderzoek 2008-2009*. Amersfoort: Rijksdienst voor het Cultureel Erfgoed, pp. 9-12.

Le Bars, D. (2005). Étude archeo-antropologique de la nécropole musulmane de Rossio do Carmo, Mértola: Bilan des fouilles anciennes (1981-1990). *Arqueologia Medieval*, May, pp. 233-257.

Lemos, V. P., da Costa, M. L. and Lima Lemos, R. (2007). Vivianite and siderite in lateritic iron crust: an example of bioreduction. *Quimica Nova*, 30 (1), pp. 36-40.

Lindbo, D. L., Stolt, M. H. and Vepraskas, M. J. (2010). Redoximorphic features. In Stoops, G., Marcelino, V. and Mees, F. (Eds.). *Interpretation of micromorphological features of soils and regoliths*. Amsterdam: Elsevier, pp. 129-148.

Loisy, C., Verrecchia, E. P. and Dufour, P. (1999). Microbial origin for pedogenic micrite associated with a carbonate paleosol (Champagne, France). *Sedimentary Geology*, 126, pp. 193-204.

Lowe, A. C., Beresford, D. V., Carter, D. O., Gaspari, F. and O'Brien, R. C. (2013). The effect of soil texture on the degradation of textiles associated with buried bodies. *Forensic Science International*, 213, pp. 331-339.

Ludvigson, G. A., Gonzalez, L. A., Fowle, D. A., Roberts, J., Driese, S. G., Villarreal, M. A., Smith, J. J. and Suarez, M. B. (2013). Paleoclimatic applications and modern process studies of pedogenic siderite. *New frontiers in paleopedology and terrestrial paleoclimatology*, 104, pp. 79-87.

Macphail, R. I. and Goldberg, P. (2010). Archaeological materials. In Stoops, G., Marcelino, V. and Mees, F. (Eds.). *Interpretation of micromorphological features of soils and regoliths*. Amsterdam: Elsevier, pp. 589-622.

Macphail, R. I., Cruise, G. M., Dormor, I. and Reeves, K. (1998). Micromorphological interpretation of a "turf-filled" funerary shaft at St. Albans, United Kingdom. *Geoarchaeology: An International Journal*, 13 (6), pp. 617-644.

Mann, R. W., Feather, M. E., Tumosa, C. S., Holland, T. D. and Schneider, K. N. (1998). A blue encrustation found on skeletal remains of Americans missing in action in Vietnam. *Forensic Science International*, 97, pp. 79-86.

Matta, P. (2005). Inquadramento geo-stratigrafico dell'area archeologica di Pill'e Matta. In Salvi, D. (Ed). *Luce sul tempo. La necropoli di Pill'e Matta, Quartucciu*. Cagliari: Edizioni AM&D, pp. 25-32.

Matthews, W. (2010). Geoarchaeology and taphonomy of plant remains and microarchaeological residues in early urban environments in the Ancient Near East. *Quaternary International*, 214, pp. 98-113.

Matthews, W., French, C. A. I., Lawrence, T., Cutler, D. F. and Jones, M. K. (1997). Microstratigraphic traces of site formation processes and human activities. *World Archaeology*, 29 (2), pp. 281-308.

McGowan, G. and Prangnell, J. (2006). The significance of vivianite in archaeological settings. *Geoarchaeology: An International Journal*, 21, pp. 93-111.

McGowan, G. and Prangnell, J. (2015). A method for calculating soil pressure overlying human burials. *Journal of Archaeological Science*, 53, pp. 12-18.

Milek, K. B. (2012). Floor formation processes and the interpretation of site activity areas: an ethnoarchaeological study of turf buildings at Thverà, northeast Iceland. *Journal of Anthropological Archaeology*, 31, pp. 119-137.

Mitchell, M. J. and Parkinson, D. (1976). Fungal feeding or oribatid mites (Acari: Cryptostigmata) in an Aspen Woodland Soil. *Ecology*, 57 (2), pp. 302-312.

Morgenstein, M. and Felsher, M. (1971). The origin of Manganese nodules: a combined theory with special reference to Palagotinization. *Pacific Science*, 25 (3), pp. 301-307.

Morse, D., Crusoe, D. and Smith, H. G. (1976). Forensic archaeology. *Journal Forensic Science*, 21 (2), pp. 323-332.

Mücher, H., Steijn, H. V. and Kwaad, F. (2010). Colluvial and mass wasting deposits. In Stoops, G., Marcelino, V. and Mees, F. (Eds.). *Interpretation of micromorphological features of soils and regoliths*. Amsterdam: Elsevier, pp. 37-48.

Müller, A. and Smal, D. E. (2011). Spore en structuren. In Lauwerier, R. C. G. M., Müller, A. and Smal, D. E. (Eds.). *Merovingers in een villa. Romeinse villa en Merovingisch grafveld Borgharen – Pasestraat. Onderzoek 2008-2009*. Amersfoort: Rijksdienst voor het Cultureel Erfgoed, pp. 45-69.

Murphy, C. P., Bullock, P. and Biswell, K. J. (1977b). The measurement and characterization of voids in soil thin sections by image analysis. Part II. Applications. *Journal of Soil Science*, 28, 509-518.

Murphy, C. P., Bullock, P. and Turner, R. H. (1977a). The measurement and characterization of voids in soil thin sections by image analysis. Part I. Principles and Techniques. *Journal of Soil Science*, 28, pp. 498-508.

O'Connor, S., Ali, E., Al-Sabah, S., Anwar, D., Bergström, E., Brown, K. A., Buckberry, J., Buckley, S., Collins, M., Denton, J., Dorling, K. M., Dowle, A., Duffey, P., Edwards, H. G. M., Faria, E. C., Gardner, P., Gledhill, A., Heaton, K., Heron, C., Janaway, R., Keely, B. J., King, D., Masinton, A., Penkman, K., Petzold, A., Pickering, M. D., Rumsby, M., Schutkowski, H., Schackleton, K. A., Thomas, J., Thomas-Oates, J., Usai, M-R., Wilson, A. S. and O'Connor, T. (2011). Exceptional preservation of a prehistoric human brain from Heslington, Yorkshire, UK. *Journal of Archaeological Science*, XXX, pp. 1-14.

Panagiotakopulu, E. and Buckland, P. C. (2012). Forensic archaeoentomology – An insect fauna from a burial in York Minster. *Forensic Science International*, 221, pp. 125-130.

Panhuysen, R. G. A. M. (2011). Menselijke resten (macroscopisch). In Lauwerier, R. C. G. M., Müller, A. and Smal, D. E. (Eds.). *Merovingers in een villa. Romeinse villa en Merovingisch grafveld Borgharen – Pasestraat. Onderzoek 2008-2009*. Amersfoort: Rijksdienst voor het Cultureel Erfgoed, pp. 83-84.

Panhuysen, R. G. A. M. (2015). *United in a grave, analysis multiple burials in Late Roman and Merovingian Maastricht.* 22nd Archaeology and Theory Symposium. Mortuary Archaeology: methodology and theory. 22 April 2015, Leiden University.

Petersen, A. (2013). The archeology of death and burial in the Islamic world. In Tarlow, S. and Stutz, L. N. (Eds.). *The archaeology of death and burial*. Oxford University Press, pp. 241-258.

Pickering, M. D., Lang, C., Usai, M-R., Keely, B. J. and Brothwell, D. R. (2014). Appendix 1: Organic residue analysis of soils. In Loe, L., Boyle, A., Webb, H. and Score, D. (Eds.) *"Given to the ground": a Viking Age mass grave on Ridgeway Hill, Weymouth*. Dorset Natural History and Archaeological Society Monograph.

Pittoni, E. (2009). Necropoli of Pill'e Matta Quartucciu (Cagliari, Sardinia): wild bee and solitary wasp activity and bone diagenetic factors. *International Journal of Osteoarchaeology*, 19 (3), pp. 386-396.

Protz, R., Shipitalo, M. J., Mermut, A. R. and Fox, C. A. (1987). Image analysis of soils – Present and Future. *Geoderma*, 40, pp. 115-125.

Pye, K., Dickson, A. D., Schiavon, N., Coleman, M. L. and Cox, M. (1990). Formation of siderite-Mg-calcite-iron sulphide concretions in intertidal marsh and sandflat sediments, north Norfolk, England. *Sedimentology*, 37, pp. 325-343.

Rapp, G. R. and Hill, C. L. (2006). *Geoarchaeology: the earth-science approach to archaeological interpretation*, Yale University Press.

Reeves, B. (2013). Haymarket hostel. *York Archaeological Trust magazine*, 1, pp. 22-23.

Renker, C., Otto, P., Schneider, K., Zimdars, B., Maraun, M. and Buscot, F. (2005). Oribatid mites as potential vectors for soil microfungi: study of mite-associated fungal species. *Microbial Ecology*, 50 (4), pp. 518-528.

Ringrose-Voase, A. J. (1987). A scheme for the quantitative description of soil macrostructure by image analysis. *Journal of Soil Science*, 38, pp. 343-356.

Ringrose-Voase, A. J. and Bullock, P. (1984). The automatic recognition and measurement of soil pore types by image analysis and computer programs. *Journal of Soil Science*, 35, pp. 673-684.

Ritz, K. and Young, I. M. (2004). Interactions between soil structure and fungi. *Mycologist*, 18 (2), pp. 52-59.

Roberts, C. A. (2009). *Human remains in archaeology. A handbook*. York: Practical Handbooks in Archaeology, 19. Council for British Archaeology.

Runa, F., Park, M. S. and Pryor, B. M. (2009). Ulocladium systematics revisited: phylogeny and taxonomic status. *Mycol Progress*, 8, pp. 35-47.

Salvi, D. (2005a). Conclusioni. Le novità derivate dallo scavo. In Salvi, D. (Ed). *Luce sul tempo. La necropoli di Pill'e Matta, Quartucciu*. Cagliari: Edizioni AM&D, pp. 187-202.

Salvi, D. (2005b). I contesti chiusi della necropoli di Pill'e Matta, in Salvi, D. (Ed). *Luce sul tempo. La necropoli di Pill'e Matta, Quartucciu*. Cagliari: Edizioni AM&D, pp. 19-23.

Sapota, T., Aldahan, A. and Al-Aasm, I. S. (2006). Sedimentary facies and climate control on formation of vivianite and siderite microconcretions in sediments of Lake Baikal, Siberia. *Journal of Paleolimnology*, 36, pp. 254-257.

Schaetzl, R. J. and Anderson, S. (2009). *Soils: genesis and geomorphology*. Cambridge University Press.

Schlezinger, D. R. (2000). Organic phosphorous and elemental ratios as indicators of prehistoric human occupation. *Journal of Archaeological Science*, 27, pp. 479-492.

Schneider, K. and Maraun M. (2005). Feeding preferences among dark pigmented fungal taxa ("Dematiacea") indicate limited trophic niche differentiation of oribatid mites (Oribatida, Acari). *Pedobiologia*, 49, pp. 61-67.

Secci, G. (2005*). Indagine sul terreno.* In Salvi, D. (Ed). *Luce sul tempo. La necropoli di Pill'e Matta, Quartucciu.* Cagliari: Edizioni AM&D, pp. 33-37.

Sehgal, J. and Stoops, G. (1972). Pedogenic calcite accumulation in arid and semi-arid regions of the indo-gangetic alluvial plain of Erstwhile Punjab (India) – Their morphology and origin. *Geoderma*, 8, pp. 59-72.

Shin, S., Jung, S., Menzel, F., Heller, K., Lee, H. and Lee, S. (2013). Molecular phylogeny of black fungus gnats (Diptera: Sciaroidea: Sciaridae) and the evolution of larval habitats. *Molecular Phylogenetics and Evolution*, 66, pp. 833-846.

Simmons, G. C. (1964). Leucophosphite, a new occurrence in the quadrilatero Ferrero, Minas Gerais, Brazil. *The American Mineralogist*, 49, pp. 377-386.

Spennemann, D. H. R. and Franke, B. (1995). Archaeological techniques for exhumations: a unique data source for crime scene investigations. *Forensic Science International*, 74, pp. 5-15.

Stolt, M. H. and Lindbo, D. L. (2010). Soil organic matter. In Stoops, G., Marcelino, V. and Mees, F. (Eds.). *Interpretation of micromorphological features of soils and regoliths*. Amsterdam: Elsevier, pp. 369-396.

Stoops, G. (2003). *Guidelines for analysis and description of soil and regolith thin sections*. Madison, Wisconsis, USA: Soil Science Society of America, Inc.

Stoops, G. and Delvigne, J. (1990). Morphology of mineral weathering and neoformation. II neoformations. *International Training Centre for Post-Graduate Soil Scientists*, Ghent Publications, 89, pp. 483-492.

Stoops, G. and Schaefer, C. E. G. R. (2010). Pedoplasmation: formation of soil material. In Stoops, G., Marcelino, V. and Mees, F. (Eds.). *Interpretation of micromorphological features of soils and regoliths*. Amsterdam: Elsevier, pp. 69-79.

Stoops, G., Delvigne, J. and Van der Plas, L. (1990). Parent material, weathering and neoformation. In Kooistra (Ed.). *European training course on soil micromorphology. II. Applications to soil micromorphology*. Booklet of the course, pp. 1-17.

Stoops, G., Marcelino, V. and Mees, F. (2010). *Interpretation of micromorphological features of soils and regolith.* Amsterdam: Elsevier.

Thali, M. J., Lux, B., Losh, S., Rosing, F. W., Hurlimann, J., Feer, P., Dirnhofer, R., Konigsdorfer, U. and Zollinger, U. (2011). "Brenzi" – The blue vivianite man of Switzerland: time since death estimation of an adipocere body. *Forensic Science International*, 211, pp. 34-40.

Thompson, M. L., Singh, P., Corak, S. and Straszheim, W. E. (1992). Cautionary notes for the automated analysis of soil pore-space images. *Geoderma*, 53, pp. 399-415.

Tibbett, M. and Carter, D. O. (2008). *Soil analysis in forensic taphonomy*. CRC Press

Tornos, F., López Pamo, E. and Sánchez España, F.J. (2009). The Iberian Pyrite Belt. In García-Cortés, A. (Ed). *Spanish geological frameworks and geosites. An approach to Spanish geological heritage of international relevance*. Madrid: Instituto Géologico y Minero de España, pp. 56-64.

Toynbee, J. M. C. (1996). *Death and burial in the Roman world*. Baltimore: The Johns Hopkins Press. Roman epithaph: "We are and we were nothing. Look, reader, how swiftly we mortals pass from nothing to nothing".

Turner-Walker, G. (2008). The chemical and microbial degradation of bones and teeth. In Pinhasi, R. and Mays, S. (Eds.). *Advances in human palaeopathology*. John Wiley and Sons, Ltd, pp. 3-29.

Usai, M-R., Brothell, D., Buckley, S., Al-Thour, K. and Canti, M. (2010). Micromorphology of two prehistpric ritual burials from Yemen, and considerations on methodological aspects of sampling the burial matrix – work in progress. *Geophysical Research Abstracts*, 12, EGU General Assembly.

Usai, M-R., Brothwell, D. R., Pickering, M. D., Keely, B. J. and Wilson, C. A. (2014). "Interred with their bones": soil micromorphology and chemistry in the study of human remains. *Antiquity, Project Gallery*, 339 [http://antiquity.ac.uk/projgall/usai339/].

Vepraskas, M. J. (1990). *European training course on soil micromorphology. Vol 1. Introduction to soil micromorphology. Booklet of the course.*

Wilson, C. A., Davidson, D. A. and Cresser, M. S. (2008). Multi-element soil analysis: an assessment of its potential as an aid to archaeological interpretation. *Journal of Archaeological Science*, 35, pp. 412-424.

Wolley, T. A. (1970). Some observations on external anatomy of oribatid mites by the scanning electron microscope. *BioScience*, 20 (23), pp. 1253-1257.

Zangarini, S., Cattaneo, C. and Trombino, L. (2014). Micromorphological aspects of forensic geopedology: time-dependents markers of decomposition and permanence in soil in experimental burials. *Geophysical Research Abstracts*, 16, EGU General Assembly.